

Mahendra Rai · Anatoly Reshetilov
Yulia Plekhanova
Avinash P Ingle *Editors*

Macro, Micro, and Nano-Biosensors

Potential Applications and Possible
Limitations

Macro, Micro, and Nano-Biosensors

Mahendra Rai • Anatoly Reshetilov
Yulia Plekhanova • Avinash P. Ingle
Editors

Macro, Micro, and Nano-Biosensors

Potential Applications and Possible
Limitations

 Springer

Editors

Mahendra Rai
Department of Biotechnology
Sant Gadge Baba Amravati University
Amravati, Maharashtra, India

Yulia Plekhanova
Laboratory of Biosensors
G.K. Skryabin Institute of Biochemistry
and Physiology of Microorganisms
Pushchino Center for Biological Research
of the Russian Academy of Sciences
Pushchino, Moscow Region
Russian Federation

Anatoly Reshetilov
Laboratory of Biosensors
G.K. Skryabin Institute of Biochemistry
and Physiology of Microorganisms
Pushchino Center for Biological Research
of the Russian Academy of Sciences
Pushchino, Moscow Region
Russian Federation

Avinash P. Ingle
Department of Biotechnology
Engineering School of Lorena
University of Sao Paulo
Lorena, SP, Brazil

ISBN 978-3-030-55489-7 ISBN 978-3-030-55490-3 (eBook)
<https://doi.org/10.1007/978-3-030-55490-3>

© Springer Nature Switzerland AG 2021

This work is subject to copyright. All rights are reserved by the Publisher, whether the whole or part of the material is concerned, specifically the rights of translation, reprinting, reuse of illustrations, recitation, broadcasting, reproduction on microfilms or in any other physical way, and transmission or information storage and retrieval, electronic adaptation, computer software, or by similar or dissimilar methodology now known or hereafter developed.

The use of general descriptive names, registered names, trademarks, service marks, etc. in this publication does not imply, even in the absence of a specific statement, that such names are exempt from the relevant protective laws and regulations and therefore free for general use.

The publisher, the authors, and the editors are safe to assume that the advice and information in this book are believed to be true and accurate at the date of publication. Neither the publisher nor the authors or the editors give a warranty, expressed or implied, with respect to the material contained herein or for any errors or omissions that may have been made. The publisher remains neutral with regard to jurisdictional claims in published maps and institutional affiliations.

This Springer imprint is published by the registered company Springer Nature Switzerland AG
The registered company address is: Gewerbestrasse 11, 6330 Cham, Switzerland

Foreword

There is no analytical problem in chemistry, biology, or biotechnology that cannot be solved using an existing or envisioned biosensor. Events in the biosensor world indicate that even unsolved issues too can be expected to be solved in the foreseeable future. The reason is that the biosensor field that originated in the mid-1950s expands unusually rapidly to demonstrate the highest potential – the rate of the assay, its unique character and high accuracy, even its simplicity. This became possible owing to notable progress of not only natural sciences, which make the basis of biosensor detection, but also the development of the technical component, that is, micromechanics and microelectronics. This makes understandable the biosensor ranking – macro-sized biosensors appeared first, then micro-sized devices and now nanodevices.

This book is very topical. It witnesses advances in the biosensor field and contributes to comprehending how the transition from macro- through micro- to nano-biosensors has been made possible. The readers are aware of the appearance of devices that could be attributed to microbiosensors. Those were sensors inserted into contact lenses; miniature electrodes implantable into snails, frogs, and lobsters; biosensors produced by immobilizing graphite paste-coated enzymes applied on human skin surfaces as tattoos. One of the most interesting from the biochemical, microelectrical, and applied points of view was the enzyme fuel cell that represented a microbiosensor with three million single fuel cells. Mention should also be made of point-of-care technologies enabling tests to be done at the bedside. Biosensors for such tests are the most advanced in the sense of miniaturization.

The main idea of the book is that, depending on the addressed problem, different approaches are to be used; macro constructs are to be worked with in some cases, micro and nano in others. Biosensors considered are electrochemical, optical, atomic force microscopy-based; biofuel cells that develop the idea of electrochemical biosensors are intended for a double purpose of cleaning up the environment and working out electrical energy. A broad range of problems is presented to be solved using various analytical approaches; the description of how a biosensor for assaying a certain compound operates may trigger in the reader's mind a novel approach due to a new use of the described technique. The book considers the following topics:

from macro- through micro- to nanosensors; application of biosensors for detection of chemical and biological entities; glucose assays; and biofuel cells and self-powered biosensors for human health. Each topic follows from its significance for human health, for protection of the environment.

Potential readers of the book are scientists from different disciplines including biochemists, biophysicists, physicists, chemists, and biotechnologists dealing with the development of biosensors, research scholars of the universities, and postgraduate students. As the analytical trend of the described models is rather broad, the book can also be expected to be of interest to business-class experts developing and implementing biosensor technologies.

Professor, Corresponding Member
of RAS, Scientific Director
N.M. Emanuel Institute of Biochemical Physics RAS
Moscow, Russia

Sergey D. Varfolomeev

Preface

In the present scenario, two fields of science, that is, biosensors and microelectronics technologies are integrated. As a consequence, a great number of publications have appeared that represent the results of this convergence and are characterized by new types of analytical devices, which feature small size first and foremost. This is how analytical systems have emerged that differ from the existing and traditional devices by their macro-/micro-/nanosize. This is a novel trend in research and development, and there is a need to obtain a high efficiency expressed in reduced consumption of electric energy. It is appealing to develop analytical equipment whose implementation would not require a significant expenditure of valuable biomaterials – enzymes, antibodies/antigens, and microbial and animal cells. Moreover, the existing technologies make it possible to use automation and enable spending a minimal number of steps for fabricating a single item. A combination of biochemical and electronic technologies facilitates devices with strictly controlled characteristics. An important fact is that this combination of technologies makes possible highly efficient production.

It should be noted that classical technology, based on the development and production of macro-sized tangible biosensors, has had and continues to have an enormous positive impact on the development of biosensor technology. Macro-sized biosensors are important for modeling the main principle of measurement. In most cases, the sensors are further advanced as mini-/micro-/nanosensors.

The results of combining the technologies are widely reflected in world literature. If the problem of the convergence is considered in a broader context than the development of biosensors, it should also include the development of drug-targeting systems and microdevices, that is, systems that in one way or another are united with the sensor part. Thus, the recent developments in the application of micro- and nanosystems for drug administration/delivery include a diverse range of biosensors that make use of new nanomaterials and methods. The current challenges include the need to balance the small scale of the devices with the quantities of drugs that are clinically necessary. Nanosensors are inexpensive and developed by using modern electronic technologies that mainly consist of thin-film formation, lithography,

etching, dicing, and packaging; the use of nanomaterials including glass, silicon, plastic, elastomers, and textiles enables producing maximally compact devices.

The chapters in the book reflect the transition from macro- through micro- to nanosensors. The use of biosensors for the detection of biological and chemical objects, features of the determination of glucose, and biofuel cells and self-powered biosensors for human health have been discussed in detail.

This book by eminent researchers presents the recent results in the field of enzymatic, immune, and microbial biosensors. Also highlighted are experimental data on the development of dual-purpose biofuel cells – both devices that generate electric energy and systems that simultaneously clean up the environment from organic contaminants. When considering works in the field of biosensors, significant attention was paid to the use of nanomaterials for modifying working electrodes. Nanomaterials in several cases enable a considerable improvement of analytical systems' parameters. Of interest to the readers will be the projection of the discussed theoretical and experimental materials onto the field of the practical application of modern analytical developments. In many cases, the presented results imply a possibility of using the developed macro-/micro-/nanobiosensor and biofuel-cell models in the field of public health and environment protection/restoration.

The book will be useful for postgraduate students and researchers – biochemists, biophysicists, physicists, chemists, biotechnologists – engaged in the development of biosensors. Moreover, it is also hoped that the book will be helpful to the business-class specialists who are actively engaged in development and implementation of analytical technologies.

Amravati, Maharashtra, India
Pushchino, Moscow Region, Russia
Pushchino, Moscow Region, Russia
Lorena, SP, Brazil

Mahendra Rai
Anatoly Reshetilov
Yulia Plekhanova
Avinash P. Ingle

Contents

Part I Macro-, Micro- and Nanofabrication of Biosensors

1	Macro-, Micro- and Nanosensors Based on Biological/Chemical Materials	3
	Vadim Valer'evich Kashin, Vladimir Vladimirovich Kolesov, Iren Evgenievna Kuznetsova, Eugenio Sergeevich Soldatov, Yulia Victorovna Plekhanova, Sergei Evgenyevich Tarasov, Anna Evgenievna Kitova, Maria Assunta Signore, Avinash P. Ingle, Mahendra Rai, and Anatoly Nikolaevich Reshetilov	
2	Bactericidal, Fungicidal, and Immunomodulating Activities of Nanosurfaces	19
	Sergei Georgievich Ignatov, Pavel V. Slukin, O. V. Kalmantaeva, A. G. Voloshin, Sergey F. Biketov, V. M. Tedikov, O. N. Perovskaya, Galina Nikolaevna Fedjukina, A. S. Kartseva, M. V. Silkina, Victoria Valer'evna Firtstova, Ivan Alekseevich Dyatlov, G. P. Bachurina, S. Yu. Filippovich, and D. V. Shtansky	
3	Enzymatic Tissue Biotests (MAO and AChE Biotests) and Bioindicators	37
	Arkadii Yustianovich Budantsev and Victoria Vladimirovna Roshchina	
4	Is It Possible to Detect Less Than One Bacterial Cell?	57
	Sergei Georgievich Ignatov, A. G. Voloshin, G. P. Bachurina, S. Yu. Filippovich, and Ivan Alekseevich Dyatlov	

Part II The Use of Biosensors for the Detection of Biological and Chemical Objects

- 5 SERS for Bacteria, Viruses, and Protein Biosensing** 75
Ilya N. Kurochkin, Arkadiy V. Eremenko, Evgeniy G. Evtushenko,
Natalia L. Nechaeva, Nikolay N. Durmanov, Rustam R. Guliev,
Ilya A. Ryzhikov, Irina A. Boginskaya, Andrey K. Sarychev,
A. V. Ivanov, and Andrey N. Lagarkov
- 6 Biosensors for Virus Detection** 95
Olga I. Guliy, Boris D. Zaitsev, and Irina A. Borodina
- 7 Specific Immobilization of Rotaviruses for Atomic Force Microscopy Using Langmuir Antibody Films Based on Amphiphilic Polyelectrolytes** 117
Sergei Georgievich Ignatov, S. Yu. Filippovich,
and Ivan Alekseevich Dyatlov
- 8 Fluorometric and SERS Sensor Systems for Diagnostics and Monitoring of Catecholamine-Dependent Diseases** 133
Irina A. Veselova, Maria I. Makedonskaya, Olga E. Eremina,
and Tatiana N. Shekhovtsova
- 9 Enhanced Sensitivity Rapid Tests for the Detection of Sepsis Marker Procalcitonin** 161
Kseniya V. Serebrennikova, Jeanne V. Samsonova,
and Alexander P. Osipov
- 10 Analytical Capabilities of Some Immunosensors for the Determination of Drugs** 177
Elvina Pavlovna Medyantseva, Daniil Vladimirovich Brusnitsyn,
Elvina Rafailovna Gazizullina, and
Herman Constantinovich Budnikov
- 11 Electrochemical DNA Sensors Based on Nanostructured Polymeric Materials for Determination of Antitumor Drugs** 193
Anna Porfireva, Tibor Hianik, and Gennady Evtugyn
- 12 Variants of Amperometric Biosensors in the Determination of Some Mycotoxins: Analytical Capabilities** 213
Elvina Pavlovna Medyantseva, Regina Markovna Beylinson,
Adelina Ildarovna Khaybullina, and
Herman Constantinovich Budnikov
- 13 The New Class of Diagnostic Systems Based on Polyelectrolyte Microcapsules for Urea Detection** 225
Sergey A. Tikhonenko, Alexey V. Dubrovskii, Aleksandr L. Kim,
and Egor V. Musin

14	Bioluminescent Nano- and Micro-biosensing Elements for Detection of Organophosphorus Compounds	239
	Elena Efremenko, Ilya Lyagin, Olga Senko, Olga Maslova, and Nikolay Stepanov	
Part III Features of the Determination of Glucose		
15	Nano- and Microelectrochemical Biosensors for Determining Blood Glucose	265
	Sergei Evgenyevich Tarasov, Yulia Victorovna Plekhanova, Mahendra Rai, and Anatoly Nikolaevich Reshetilov	
16	Microstructured Electrochemical SMBG Biosensor Chip Design Development for Sustainable Mass Production Based on the Strategic Platform Patent Map	285
	Hideaki Nakamura	
Part IV Biofuel Elements and Self- Powered Biosensors for Human Health		
17	Biological Fuel Cells: Applications in Health and Ecology	327
	Ivan Alexeevich Kazarinov and Mariia Olegovna Meshcheryakova	
18	Recent Trends in Fabrication and Applications of Wearable Bioelectronics for Early-Stage Disease Monitoring and Diagnosis	357
	Ramila D. Nagarajan and Ashok K. Sundramoorthy	
19	Self-Powered Biosensors in Medicine and Ecology	383
	Yulia Victorovna Plekhanova, Sergei Evgenyevich Tarasov, Anna Evgenievna Kitova, Mikhail Alexandrovich Gutorov, and Anatoly Nikolaevich Reshetilov	
20	Self-Powered Implantable Biosensors: A Review of Recent Advancements and Future Perspectives	399
	Pavel M. Gotovtsev, Yulia M. Parunova, Christina G. Antipova, Gulfia U. Badranova, Timofei E. Grigoriev, Daniil S. Boljshin, Maria V. Vishnevskaya, Evgeny A. Konov, Ksenia I. Lukanina, Sergei N. Chvalun, and Anatoly Nikolaevich Reshetilov	
	Index	411

Contributors

Christina G. Antipova National Research Centre “Kurchatov Institute”, Moscow, Russia

G. P. Bachurina Bach Institute of Biochemistry, Research Center of Biotechnology of the Russian Academy of Sciences, Moscow, Russia

Gulfia U. Badranova National Research Centre “Kurchatov Institute”, Moscow, Russia

Regina Markovna Beylinson A.M. Butlerov Institute of Chemistry, Kazan Federal University (KFU), Kazan, Russia

Sergey F. Biketov State Research Center for Applied Microbiology and Biotechnology, Obolensk, Moscow Region, Russia

Irina A. Boginskaya Institute of Theoretical and Applied Electrodynamics RAS, Moscow, Russia

Daniil S. Boljshin Physical Faculty, Lomonosov Moscow State University, Moscow, Russia

Irina A. Borodina Kotelnikov Institute of Radio Engineering and Electronics, Russian Academy of Sciences, Saratov, Russia

Daniil Vladimirovich Brusnitsyn A.M. Butlerov Institute of Chemistry, Kazan (Volga region) Federal University (KFU), Kazan, Russia

Arkadii Yustianovich Budantsev Institute of Theoretical and Experimental Biophysics of Russian Academy of Sciences, Pushchino, Russia

Herman Constantinovich Budnikov A.M. Butlerov Institute of Chemistry, Kazan (Volga region) Federal University (KFU), Kazan, Russia

Sergei N. Chvalun National Research Centre “Kurchatov Institute”, Moscow, Russia

Alexey V. Dubrovskii Institute of Theoretical and Experimental Biophysics, Russian Academy of Science, Moscow, Russia

Nikolay N. Durmanov Emanuel Institute of Biochemical Physics RAS, Moscow, Russia

Ivan Alekseevich Dyatlov State Research Center for Applied Microbiology and Biotechnology, Obolensk, Moscow Region, Russia

Elena Efremenko Faculty of Chemistry, Lomonosov Moscow State University, Moscow, Russia

Arkadiy V. Eremenko Emanuel Institute of Biochemical Physics RAS, Moscow, Russia

Olga E. Eremina Department of Chemistry, Lomonosov Moscow State University, Moscow, Russia

Gennady Evtugyn Analytical Chemistry Department, Kazan Federal University, Kazan, Russia

Evgeniy G. Evtushenko Faculty of Chemistry of Lomonosov Moscow State University, Moscow, Russia

Galina Nikolaevna Fedjukina State Research Center for Applied Microbiology and Biotechnology, Obolensk, Moscow Region, Russia

S. Yu. Filippovich Bach Institute of Biochemistry, Research Center of Biotechnology of the Russian Academy of Sciences, Moscow, Russia

Victoria Valer'evna Firtstova State Research Center for Applied Microbiology and Biotechnology, Obolensk, Moscow Region, Russia

Elvina Rafailovna Gazizullina A.M. Butlerov Institute of Chemistry, Kazan (Volga region) Federal University (KFU), Kazan, Russia

Pavel M. Gotovtsev National Research Centre “Kurchatov Institute”, Moscow, Russia

Timofei E. Grigoriev National Research Centre “Kurchatov Institute”, Moscow, Russia

Rustam R. Guliev Emanuel Institute of Biochemical Physics RAS, Moscow, Russia

Olga I. Gulyi Institute of Biochemistry and Physiology of Plants and Microorganisms, Russian Academy of Sciences, Saratov, Russia

Mikhail Alexandrovich Gutorov Gamma-DNA LLC, Territory of Skolkovo Innovation Centre, Moscow, Russia

Tibor Hianik Department of Nuclear Physics and Biophysics, Comenius University, Bratislava, Slovakia

Sergei Georgievich Ignatov State Research Center for Applied Microbiology and Biotechnology, Obolensk, Moscow Region, Russia

Avinash P. Ingle Department of Biotechnology, Engineering School of Lorena, University of São Paulo, Lorena, SP, Brazil

A. V. Ivanov Institute of Theoretical and Applied Electrodynamics RAS, Moscow, Russia

O. V. Kalmantaeva State Research Center for Applied Microbiology and Biotechnology, Obolensk, Moscow Region, Russia

A. S. Kartseva State Research Center for Applied Microbiology and Biotechnology, Obolensk, Moscow Region, Russia

Vadim Valer'evich Kashin FSBIS V.A. Kotelnikov Institute of Radio Engineering and Electronics, Russian Academy of Sciences, Moscow, Russia

Ivan Alexeevich Kazarinov Department of Physical Chemistry, Saratov State University, Saratov, Russia

Adelina Ildarovna Khaybullina A.M. Butlerov Institute of Chemistry, Kazan Federal University (KFU), Kazan, Russia

Aleksandr L. Kim Institute of Theoretical and Experimental Biophysics, Russian Academy of Science, Moscow, Russia

Anna Evgenievna Kitova Laboratory of Biosensors, G.K. Skryabin Institute of Biochemistry and Physiology of Microorganisms, Pushchino Center for Biological Research of the Russian Academy of Sciences, Pushchino, Moscow Region, Russian Federation

Vladimir Vladimirovich Kolesov FSBIS V.A. Kotelnikov Institute of Radio Engineering and Electronics, Russian Academy of Sciences, Moscow, Russia

Evgeny A. Konov National Research Centre “Kurchatov Institute”, Moscow, Russia

Ilya N. Kurochkin Emanuel Institute of Biochemical Physics RAS, Moscow, Russia
Faculty of Chemistry of Lomonosov Moscow State University, Moscow, Russia

Iren Evgenievna Kuznetsova FSBIS V.A. Kotelnikov Institute of Radio Engineering and Electronics, Russian Academy of Sciences, Moscow, Russia

Andrey N. Lagarkov Institute of Theoretical and Applied Electrodynamics RAS, Moscow, Russia

Ksenia I. Lukanina National Research Centre “Kurchatov Institute”, Moscow, Russia

Ilya Lyagin Faculty of Chemistry, Lomonosov Moscow State University, Moscow, Russia

Maria I. Makedonskaya Department of Chemistry, Lomonosov Moscow State University, Moscow, Russia

Olga Maslova Faculty of Chemistry, Lomonosov Moscow State University, Moscow, Russia

Elvina Pavlovna Medyantseva A.M. Butlerov Institute of Chemistry, Kazan (Volga region) Federal University (KFU), Kazan, Russia

Mariia Olegovna Meshcheryakova Department of Physical Chemistry, Saratov State University, Saratov, Russia

Egor V. Musin Institute of Theoretical and Experimental Biophysics, Russian Academy of Science, Moscow, Russia

Ramila D. Nagarajan Department of Chemistry, SRM Research Institute, SRM Institute of Science and Technology, Kattankulathur, Tamil Nadu, India

Hideaki Nakamura Department of Liberal Arts, Tokyo University of Technology, Hachioji, Japan

Natalia L. Nechaeva Emanuel Institute of Biochemical Physics RAS, Moscow, Russia

Alexander P. Osipov Chemistry Faculty, Lomonosov Moscow State University, Moscow, Leninskiye Gory, Russia

Yulia M. Parunova National Research Centre “Kurchatov Institute”, Moscow, Russia

O. N. Perovskaya State Research Center for Applied Microbiology and Biotechnology, Obolensk, Moscow Region, Russia

Yulia Victorovna Plekhanova Laboratory of Biosensors, G.K. Skryabin Institute of Biochemistry and Physiology of Microorganisms, Pushchino Center for Biological Research of the Russian Academy of Sciences, Moscow Region, Russian Federation

Anna Porfireva Analytical Chemistry Department, Kazan Federal University, Kazan, Russia

Mahendra Rai Nanobiotechnology Laboratory, Department of Biotechnology, Sant Gadge Baba Amravati University, Amravati, Maharashtra, India

Anatoly Nikolaevich Reshetilov Laboratory of Biosensors, G.K. Skryabin Institute of Biochemistry and Physiology of Microorganisms, Pushchino Center for Biological Research of the Russian Academy of Sciences, Pushchino, Moscow Region, Russian Federation

Victoria Vladimirovna Roshchina Institute of Cell Biophysics, Federal Research Center, Pushchino Scientific Center for Biological Research of the Russian Academy of Sciences, Pushchino, Russia

Ilya A. Ryzhikov Institute of Theoretical and Applied Electrodynamics RAS, Moscow, Russia

Jeanne V. Samsonova Chemistry Faculty, Lomonosov Moscow State University, Moscow, Leninskiye Gory, Russia

Andrey K. Sarychev Institute of Theoretical and Applied Electrodynamics RAS, Moscow, Russia

Olga Senko Faculty of Chemistry, Lomonosov Moscow State University, Moscow, Russia

Kseniya V. Serebrennikova Chemistry Faculty, Lomonosov Moscow State University, Moscow, Leninskiye Gory, Russia

Tatiana N. Shekhovtsova Department of Chemistry, Lomonosov Moscow State University, Moscow, Russia

D. V. Shtansky National University of Science and Technology “MISIS”, Moscow, Russia

Maria Assunta Signore CNR, Institute for Microelectronics and Microsystems, Lecce, Italy

M. V. Silkina State Research Center for Applied Microbiology and Biotechnology, Obolensk, Moscow Region, Russia

Pavel V. Slukin State Research Center for Applied Microbiology and Biotechnology, Obolensk, Moscow Region, Russia

Eugenii Sergeevich Soldatov Department of Physics, Laboratory of Cryoelectronics, Lomonosov Moscow State University, Moscow, Russia

Nikolay Stepanov Faculty of Chemistry, Lomonosov Moscow State University, Moscow, Russia

Ashok K. Sundramoorthy Department of Chemistry, SRM Research Institute, SRM Institute of Science and Technology, Kattankulathur, Tamil Nadu, India

Sergei Evgenyevich Tarasov Laboratory of Biosensors, G.K. Skryabin Institute of Biochemistry and Physiology of Microorganisms, Pushchino Center for Biological Research of the Russian Academy of Sciences, Pushchino, Moscow Region, Russian Federation

V. M. Tedikov State Research Center for Applied Microbiology and Biotechnology, Obolensk, Moscow Region, Russia

Sergey A. Tikhonenko Institute of Theoretical and Experimental Biophysics, Russian Academy of Science, Moscow, Russia

Irina A. Veselova Department of Chemistry, Lomonosov Moscow State University, Moscow, Russia

Maria V. Vishnevskaya National Research Centre “Kurchatov Institute”, Moscow, Russia

A. G. Voloshin State Research Center for Applied Microbiology and Biotechnology, Obolensk, Moscow Region, Russia

Boris D. Zaitsev Kotelnikov Institute of Radio Engineering and Electronics, Russian Academy of Sciences, Saratov, Russia

Part I
Macro-, Micro- and Nanofabrication
of Biosensors

Chapter 1

Macro-, Micro- and Nanosensors Based on Biological/Chemical Materials



Vadim Valer'evich Kashin, Vladimir Vladimirovich Kolesov, Iren Evgenievna Kuznetsova, Eugenio Sergeevich Soldatov, Yulia Victorovna Plekhanova, Sergei Evgenyevich Tarasov, Anna Evgenievna Kitova, Maria Assunta Signore, Avinash P. Ingle, Mahendra Rai, and Anatoly Nikolaevich Reshetilov

Abstract By their geometric dimensions, biosensors can be arranged into a sequence of macro-, micro- and nanodevices. From this perspective, the present chapter considers mainly electrochemical biosensors and biofuel cells; attention is also paid to other, e.g. chemical, types of sensors that can be prototypes of developed biosensor devices. One of the moving forces of miniaturization is finding conditions when the least amount of material is used. Miniature devices can play the role of biosensors and represent electrodes for biofuel systems. Due to the broad use of the enzyme glucose oxidase (GOD), which acts as a model protein or the base of existing devices, we discuss in detail the planar technology of forming a multichannel nanobiochip based on the immobilized GOD. The prospects of micro/nanostructures are

V. V. Kashin · V. V. Kolesov · I. E. Kuznetsova
FSBIS V.A. Kotelnikov Institute of Radio Engineering and Electronics, Russian Academy of Sciences, Moscow, Russia

E. S. Soldatov
Department of Physics, Laboratory of Cryoelectronics, Lomonosov Moscow State University, Moscow, Russia

Y. V. Plekhanova · S. E. Tarasov · A. E. Kitova · A. N. Reshetilov (✉)
Laboratory of Biosensors, G.K. Skryabin Institute of Biochemistry and Physiology of Microorganisms, Pushchino Center for Biological Research of the Russian Academy of Sciences, Pushchino, Moscow Region, Russian Federation
e-mail: anatol@ibpm.pushchino.ru

M. A. Signore
CNR, Institute for Microelectronics and Microsystems, Lecce, Italy

A. P. Ingle
Department of Biotechnology, Engineering School of Lorena, University of Sao Paulo, Lorena, SP, Brazil

M. Rai
Department of Biotechnology, Sant Gadge Baba Amravati University, Amravati, Maharashtra, India

primarily determined by their miniature size, the feasibility of easy duplication and—in production—a combined application of molecular electronics technology and biochemical methods of manipulations with biological material.

Keywords Macro- · Micro- and nanosensors · Biosensors · Biochip · Multichannel

Nomenclature

FET	pH-sensitive field-effect transistor
GCE	glassy carbon electrode
GOD	glucose oxidase
LB	Langmuir–Blodgett
MWCNTs	multiwalled carbon nanotubes
PEDOT:PSS	poly(3,4-ethylenedioxythiophene) polystyrene sulphonate
PM	purple membranes
PQQ	pyrroloquinolinquinone
rGO	reduced graphene oxide

1.1 Introduction

The miniaturization of analytical systems is paid great attention at present; devices are being developed, in which elements of solid-state electronics and biology are coupled. One of the scientists who first started speaking about the prospects of coupling biological material and solid-state electronic devices was the Japanese Isao Karube. His group coupled the photosensitive protein bacterial rhodopsin with a pH-sensitive field-effect transistor (FET) (Gotoh et al. 1989; Tanabe et al. 1989). The produced device was in effect a photodiode and, in accordance with its functions, it converted the light flux into an electric current. Indisputable achievements of that work include (1) the fabrication of a biological photodiode; (2) demonstration of the possibility of coupling a living material and a solid-state device; (3) the device potentially determining prospects of creating biological systems with a varied parameter, namely, the reaction time. It is well known that the time of the reaction and transition of bacterial rhodopsin from one excited state into another varies from femtoseconds to seconds (Seki et al. 1994). Later, experiments with combinations of a FET and bacterial rhodopsin, as well as combinations of a FET/polymer membrane/photochromic dye spirobenzopyran/urease enzyme were successfully continued (Kazanskaya et al. 1996). Reshetilov et al. (1990) used the amphiphilic properties of purple membranes (PM) from photosensitive bacteria of the genus *Halobacterium* applied on two types of transducers—pH-sensitive glass electrodes and field-effect transistors—using the Langmuir–Blodgett (LB) technique. Upon application of purple membranes, pH electrodes acquired photosensitive properties,

which enabled the use of the proposed method for comparing the photogenerating properties of various rhodopsins. A distinction of this study, carried out using a FET, from that presented in Gotoh et al. (1989) was that not classical LB films but self-assembled structures formed on the surface of an aqueous phase (“out/in”-oriented structures, where “out” and “in” refer to the orientation of purple membranes in bacteria). Owing to their amphiphilicity, the percentage of oriented purple membranes at the water–air interface reaches a high value, which enables a distinct electrochemical signal to be produced upon illumination. Due to the small size of a field-effect transistor and its gate zone, which is units of square micrometres, the FET–PM system can be considered as a microsensor model. Microbiosensors represented by a set of FETs incorporated into an agar medium on which bacterial cells grow can also be considered as miniature devices. The growth of cells initially inoculated into the centre of a Petri dish was accompanied with their propagation in the agar medium in the form of a circle; this was followed by another wave of the same form, etc. pH-sensitive FETs incorporated into the agar medium enabled tracing the change of pH of the medium at the propagation of a wave of growing bacteria via the FET position point (Reshetilov et al. 1992). These authors have shown that depending on the type of the medium on which bacteria grow either oxidation or alkalization is observed. This model of registering the propagation of pH waves could be considered as the use of miniature FET-based pH-sensitive biosensors.

The results of coupling FETs with purple bacteria opened a wide potential in creating optical memory elements for constructing rapid-response optical systems, in which a solid-state converter but not a biological part served as an element that restricted the response. A combination of a FET and a propagating bacterial colony has shown that miniature converters enable making measurements not feasible using standard macrosensors.

Typical examples of nanosized biosensors are analytical systems based on nanoparticles (Kurbanoglu and Ozkan 2018; Li et al. 2019). Nanoparticles can possess efficient catalytic properties, be biocompatible and have a high electrical conductance. These properties enable their use in various types of biosensors, both optical and electrochemical. Such a sensor can be either biological or non-biological. Nanoparticles of gold are used most often due to their high resistance to oxidation, low toxicity and ability to amplify the sensor signal. The application of these particles leads to an increase in the sensitivity and detection limits down to one molecule in the sample (Vigneshvar et al. 2016). Nanoparticles can also act as alternative biorecognition elements (Qi et al. 2018). Possessing electrocatalytic properties, nanoparticles in the sensor may replace enzyme preparations (Hsu et al. 2016; Xu et al. 2019).

This chapter briefly considers achievements in the field of electrochemical-type molecular work of nanobiosensors (molecular nanostructures) based on biological materials, predominantly enzymes; non-biological/chemical types of analysis are also considered. These devices can perform dual functions, i.e. they play the role of biosensors and are electrodes for biofuel cell systems. As an enzyme, glucose oxidase (GOD) is at present singled out; it is being used in research very often and acts as either a model protein or the base of implementable devices. The planar technology of forming a multichannel nanobiochip based on immobilized GOD is presented in sufficient detail. Biosensors in the line-up of macro-/micro-/nanodevices

are considered, like macro- and microdevices can be used to verify various hypotheses and to model a principle, which will then be used in nanosized sensors. The prospects of nanostructures are primarily determined by their miniature size and by the possibility of combining the microelectronics technology and the biological methods of working with biomaterial.

1.2 Macro-/Microdevices

Along with the traditional methods of analysis, biosensors and biofuel cells have become widespread in recent years in clinical diagnostics and foodstuff-quality analysis. The development of industries, medicine, agriculture and other branches of production requires developing reliable methods of qualitative and quantitative analyses of the presence of various substances in water, soil, blood, foodstuffs, etc. To date, most analyses have been delivered to laboratories, but it would be much better if they can be done on the spot of sampling. For this reason, small-sized, fast and reliable biosensors acquire widespread use. Fields of application for these biosensors mainly include clinical diagnostics, assays of foodstuffs and bioprocesses, monitoring of the environment (Scognamiglio et al. 2010). Thus, the development of biosensors and, in particular, their miniaturization is being paid great attention. However, not only micro- and nanosensors are of great interest. Analysis of the literature on the subject often reveals classical studies of macro-sized devices that lay the foundation of biosensor development; frequently, one also comes across research whose authors propose novel interesting and unusual approaches for the development of macro- and microsized biosensors. This chapter presents works predominantly of recent years. The main attention is, certainly, paid to the detection of glucose (as the most in-demand analyte in medical research), the miniature size of devices; analysis of other compounds is also taken into account.

One of the major problems encountered by most investigators is to preserve the activity of biosensor's bioreceptor element for a prolonged period of time. When developing bioanalytical systems, several authors (Decher and Hong 1991; Petrov et al. 2005; Tikhonenko et al. 2014) proposed enzyme immobilization into polyelectrolyte microcapsules for preserving biocatalyst's activity. These capsules protect the biocatalyst from the aggressive impact of the environment, but do not prevent the penetration of biocatalyst's substrate into the capsule (Caruso et al. 2000). The entrapment of the enzyme into the microcapsule makes it possible to preserve the activity of the enzyme in the biosensor at a high level for several months (Reshetilov et al. 2016).

The use of electrochemical sensors can be one of the methods for determining the activity of encapsulated enzymes. Thus, for instance, the activity of GOD can be determined by the amount of hydrogen peroxide that evolved as the result of glucose oxidation. For this purpose, graphite electrodes with incorporated Prussian blue, which catalyses the electrochemical reduction of hydrogen peroxide, can be used (Karyakin 2001). The urease activity can be determined using a pH-sensitive FET by the change of pH due to the digestion of urea under the action of the enzyme

(Chang et al. 2010). Based on such polyelectrolyte microcapsules, Reshetilov et al. (2016, 2019) developed biosensors for the detection of urea and glucose. In one case, the authors used for immobilization the upper layer of the polyelectrolyte coating the capsule, which carried a negative charge and stuck well to the graphite electrode surface owing to Coulomb interaction. In the case of a pH-sensitive FET with the tantalum pentoxide surface, paramagnetic particles of Fe_3O_4 were additionally introduced into the capsule; the bioreceptor was formed using a permanent magnetic field directly on the FET gate. The fabricated biosensors were used for assays of blood, milk and commercially manufactured juices. A high correlation of the data with the standard spectrophotometric method of analysis was shown.

Some studies on the application of nanomaterials in biosensor technology were carried out on glassy carbon measuring electrodes; some other works considered electrode compositions based on screen-printed electrodes containing GOD and multiwalled carbon nanotubes (MWCNTs) immobilized using osmium polymers. Modification of closed multilayer membrane structures, represented by polyelectrolyte microcapsules with the enzyme formed on screen-printed electrodes, by carbon nanotubes makes it possible to change the properties of these closed structures. For instance, Reshetilov et al. (2019) showed that the introduction of MWCNTs into polyelectrolyte microcapsules with GOD formed on screen-printed electrodes reduced the impedance of the bioreceptor layer virtually by two orders of magnitude. Cyclic voltammograms at the modification of multilayer structures were characterized by an increase of current. A composition based on polyelectrolyte capsules was the basis of the receptor element of an amperometric biosensor; inclusion of MWCNTs into the capsules led to increase the sensitivity of the biosensor to glucose and to decrease its limit of detection. Subsequently, these structures can be efficient not only in the development of biosensors but also can be applicable for biofuel cells, which, in turn, would find application in biotechnology, medicine, power engineering and robotic engineering.

Another frequently used nanomaterial is graphene-like thermally expanded graphite having a high surface area and low resistivity. Reshetilov et al. (2015) used this material in combination with microbial membrane fractions. A number of reports revealed the effect of direct electrooxidation of glucose with the participation of PQQ-dependent glucose dehydrogenase immobilized on MWCNTs (MacVittie et al. 2015; Ratautas et al. 2015). Reshetilov et al. (2015) studied the bioelectrocatalytic oxidation of ethanol with the participation of *Gluconobacter oxydans* VKM B-1280 membrane fractions as an electrocatalyst. Using the methods of cyclic voltammetry and chronopotentiometry, it was shown that electrooxidation of ethanol on the bioanode could proceed both in the mode of direct mediator-free electrocatalysis and by the mediator mechanism.

In recent years, many investigators intensively include in their research the conductive polymer poly(3,4-ethylenedioxythiophene) polystyrene sulfonate (PEDOT:PSS). This is due, first and foremost, to the fact that both independently and mainly in combination with other components this polymer adds novel properties to the quality of bioreceptor material—an increase of sensitivity, much exceeding the known value, and stability (Wisitsoraat et al. 2013). In this work, the PEDOT:PSS-containing bioreceptor was a combination of this polymer and

graphene. The authors observed the direct electron transfer at the oxidation of glucose by GOD.

Gotovtsev et al. (2019) considered an important issue of the interaction of PEDOT:PSS with iota-carrageenan and polyvinyl alcohol. The authors produced a biocompatible conductive material without potentially hazardous binding substances. This issue is important for the preparation of bioreceptors for biosensors, including miniature devices. The results of important studies of PEDOT:PSS polymer were reviewed by Shim et al. (2009). The authors have shown the ability to measure glucose using a completely organic electrochemical FET (OECT) in which the channel, source, drain and gate electrodes were made from the conducting polymer PEDOT doped with PSS. The OECT employed a ferrocene mediator to shuttle electrons between the enzyme GOD and a PEDOT:PSS gate electrode. The device can be fabricated using a one-layer patterning process and offers glucose detection down to the micromolar range, consistent with levels occurring in human saliva.

The nanocomposite for the sensor was synthesized by the hydrothermal method.

Jeevanandham et al. (2020) developed non-enzymatic selective sensors for the detection of glucose. The nanocomposite for the sensor was synthesized using a hydrothermal method. The basis of the sensor is nickel oxide coated with molybdenum disulphide. This sensor having the NiO/MoS₂/GCE structure (MoS₂ and GCE, molybdenum sulphite and glassy carbon electrode, respectively) provides for a rapid response (2 s) and a broad linear range with the limit of detection of ~2 μM for glucose. Real sample analysis was also carried out in blood serum with additions of glucose. This NiO/MoS₂ nanocomposite-based sensor can be used for the selective detection of glucose in biological and medical samples. Sundramoorthy et al. (2015) used a composite based on reduced graphene oxide (rGO) and PEDOT:PSS as a sensor for detecting Fe²⁺ and Fe³⁺ ions. The sensor was also useful in determining the oxidation kinetics of Fe²⁺ using hydrogen peroxide and measuring Fe³⁺ by differential pulse voltammetry. The sensor response was not affected by several tested metallic and organic interferences and other components present in commercial iron supplement tablets and wine samples. Thus, the electrode system based on rGO/PEDOT:PSS films is potentially suitable not only for testing the iron content in food, environmental and biological samples but also for various laboratory-scale electrochemical experiments with iron ions.

In another paper, Kumar and Sundramoorthy (2019) proposed an electrochemical biosensor for methyl parathion detection based on single-walled carbon nanotube/glutaraldehyde crosslinked acetylcholinesterase-wrapped bovine serum albumin nanocomposites. This paper shows the possibilities of using a sensor based on carbon nanotubes for the detection of methyl parathion, which is an organophosphorus pesticide. The proposed biosensor exhibited a wide linear range for pesticide target in 100 mM phosphate-buffered saline solution (pH 7.4) from 1×10^{-10} M to 5×10^{-6} M with a limit of detection of 3.75×10^{-11} M.

1.3 Nanodevices

As we mentioned above, the work by Gotoh et al. (1989) that marked the general tendency can be considered to be one of the first descriptions of solid-state electronics (FET)–biological material compositions paving the way to micro- and nanodevices. This direction was supported by other investigators, and in 1999, a new idea was put forward aimed at the miniaturization and creation of combined devices (Sasaki 1999). The study by Gotoh et al. (1989) dealt with the development of a potentiometric sensor, whereas the combination presented by Sasaki (1999) was an amperometric device based on GOD and a biofuel-cell electrode. The device contained 25 microcells (microsensors) of the total size $40 \times 50 \text{ mm}^2$; the developed power was planned to be units of watts.

The work by Kanwal et al. (2014) can be considered as a pioneering research that emerged against the background of the accepted development of the miniaturization ideas. These authors gave the characteristics of the fabricated integrated circuit comprising three million separate biofuel cells based on the monomolecular insertion of GOD and laccase as enzymes providing for the activity of biofuel cell's anode and cathode. The achieved current density was 1 A/cm^2 ; power density 1 W/cm^2 . The presented parameters characterized this integrated circuit as the most powerful of those known by the publication date.

The method of detecting proteins in solution using a nanowire biosensor (Lee et al. 2012; He et al. 2015; Malsagova et al. 2015) is attributed to modern methods. Chips to such biosensors contain nanosized wires (nanowires), which are sensor elements. The nanowire biosensor is attributed to molecular detectors that enable registration of separate biological molecules in their counting mode, which determines a high concentration sensitivity of the analysis. The operating principle of the nanowire biosensor is based on the registration of current flowing through the nanowire. At its adsorption on the surface of the nanowire, a biological molecule changes its surface potential. Thus, the biomolecule is a local “virtual” gate changing the conductivity of the chip's nanowire sensor elements. A biospecific analysis requires nanowires to be functionalized. The most widespread functionalization in biomedical research is that of the sensor element surface using molecular probes—antibodies or aptamers. This forms an antibody–antigen or aptamer–antigen complex on the surface of a nanowire owing to affinity interaction. The event is registered by the electronic system of the nanowire biosensor (Malsagova et al. 2018; Ivanov et al. 2018).

Comparatively recent works considered the electrochemical principle of DNA sequencing. Two bioelectrochemical processes—the emergence of a current pulse and evolution of a proton—were shown to occur during the insertion of a subsequent deoxynucleotide triphosphate by DNA polymerase into the immobilized single-stranded matrix DNA in a respectively designed electrode (Purushothaman et al. 2006; Pourmand et al. 2006). It is important to note that the basis of the developed device was a registering semiconductor matrix, which was, in fact, a set of field-effect transistors; their number in the first model of the sequencer was

1.5 million transistors, each of which contained a measuring cell 10^{-9} microlitres in volume. In light of the considered issue, this type of sensor undoubtedly belongs to nanobiosensors.

It is important to note the results obtained by the group of investigators headed by Gou-Jen Wang. The authors developed a system of nanostructured non-enzymatic biosensors. A thin layer of nickel was applied onto an anodic aluminium oxide surface; the layer was then used to form a 3D matrix from nanostructured polycarbonate (Hsu and Wang 2014; Hsu et al. 2015, 2016). Then a thin layer of gold and gold nanoparticles, which formed an array of nanohemispheres, was applied onto the polycarbonate support. This array contributes to an increase of the electrode working surface and an increase of the sensitivity to glucose, which rises tenfold as compared with a simple gold electrode. The electrode's linear range of detection is within 55 μM to 13.89 mM at a sensitivity of $750 \mu\text{A}\cdot\text{mM}^{-1}\cdot\text{cm}^{-2}$ and the detection limit of 9 μM (Lin and Wang 2018; Lin et al. 2019). It should be noted that the developed system has high glucose detection characteristics, considering its possible high lifetime. The drawback of measurements being carried out only in a 0.1 M solution of NaOH, however, significantly reduces the scope of its application.

In addition to non-enzymatic biosensors, Gou-Jen Wang's group is working on the creation of nanostructured electrochemical biosensors based on 3D sensing elements featuring uniformly deposited gold nanoparticles. Electrochemical impedance spectroscopy was chosen as a measurement method. The authors successfully conducted detections of the dust mite antigen Der p2 (Shen et al. 2017), allergy patient's serum, allergy disease-related gene mutations (SNP and Haplotype), dengue virus-receptor binding (Tung et al. 2016), hepatitis B virus DNA (Chen et al. 2016) and Alzheimer's A β protein.

A common feature of works by Gou-Jen Wang's group is the use of a special membrane of anodic aluminium oxide. This membrane is characterized as a nano-sized porous array of regular hexagonal-shaped cells with straight columnar channels. It is widely used by the authors as a template in fabricating one-dimensional nanomaterials with controllable orientation. In particular, this membrane was used by the authors for work in such directions as the development of gold/nickel coaxial nanorod arrays, nanobiosensors, nanohemispheric nickel array moulds and nanostructure biomaterials (Lee et al. 2015; Peng et al. 2017, 2018).

1.4 Single-Molecule Nanobiosensor

One of the intensively developed directions of biomedicine is biosensorics, including biosensor implantation methods. Significant progress in the development of miniature sensors has been observed in recent years. Consider some details of such devices as exemplified by the use of planar technology and the enzyme GOD (Kashin et al. 2013).

The planar nanostructure of a nanoelectronic transducer is created using the suspended rigid mask technology, methods of standard lithography and reactive ion etching (Steinmann and Weaver 2004). The phototemplate for the system of lead-in and registration electrodes is shown in Fig. 1.1a. The lead-in electrodes converging to the central part of the chip were formed by photolithography. The central part of the chip, representing a system of nanowires, was formed by electron lithography and is shown in Fig. 1.1b. A separate nanowire with a nanogap is shown in Fig. 1.1c. A precision measuring system couples the nanochip with the control computer. The dimensions of these structures imply the possibility of immobilizing on them separate molecules of an enzyme, e.g. GOD.

To fix molecule-sized objects in the measuring nanowires, nanogaps are formed using focus ion beam and electromigration technologies (Park et al. 1999). Kashin et al. (2013) demonstrated immobilization of GOD within a nanogap by crosslinking with glutaraldehyde. Images of immobilized GOD molecules produced by atomic force microscopy are shown in Fig. 1.2.

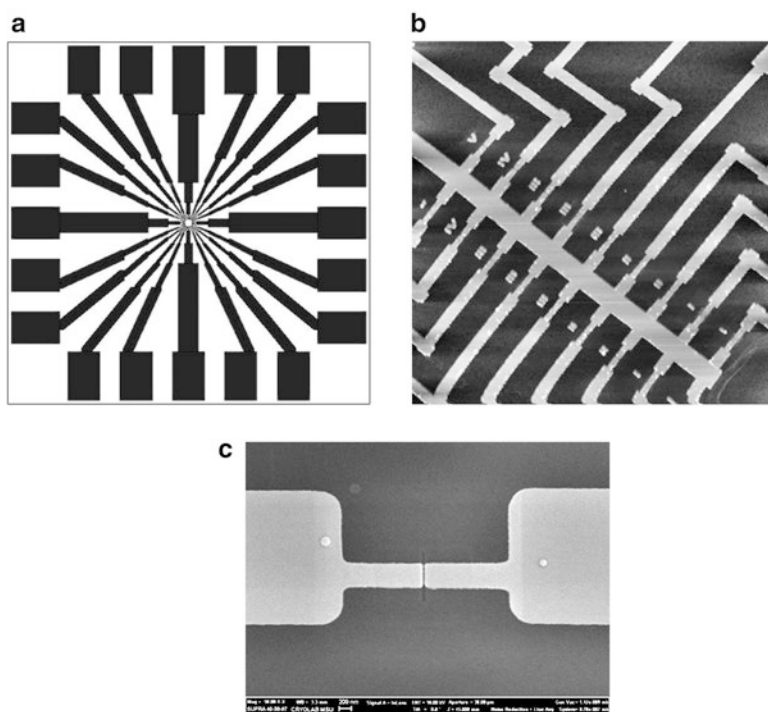


Fig. 1.1 The form of the phototemplate, of the central part of the chip and of a particular nanowire. (a) The phototemplate for the system of lead-in electrodes; (b) the system of nanowires in the central part of the chip; (c) a micrograph of a thin-film nanowire with a nanogap

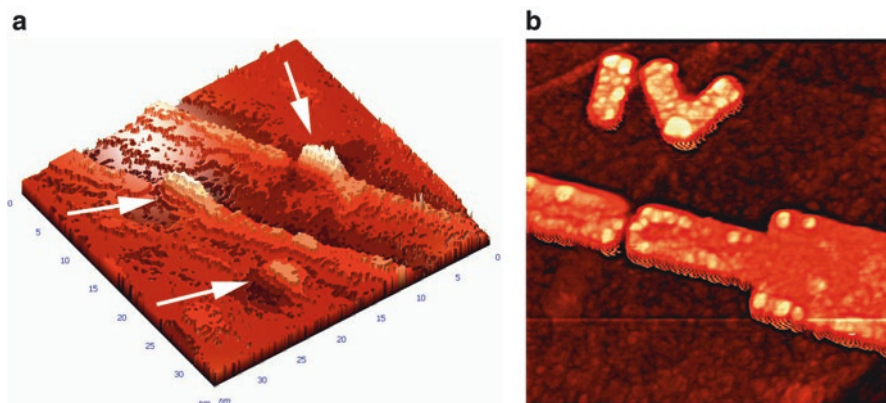


Fig. 1.2 (a) AFM image of single GOD molecules (shown by arrows) on a SiO₂ support (frame size, 35 × 35 nm²); (b) AFM image of a nanogap between gold nanoelectrodes coated with a single molecule-thick enzyme layer (frame size, 2 × 2 μm²)

Cyclic voltammograms for GOD immobilized on such nanostructures are shown in Fig. 1.3a. It is seen that an insignificant ohmic current is registered in the absence of glucose. The addition of glucose at a concentration of 10 mM leads to a significant current caused by the oxidation of the substrate. The presented dependencies are also characteristic of the enzyme immobilized on macrostructures, e.g. on screen-printed electrodes (Plekhanova et al. 2019), where the working electrode area is 7 mm², which emphasizes once again the similarity of macro- and nanostructures. A change in the concentration of the added substrate leads to a graded change of the nanosensor signal (Fig. 1.3b) in the same way as in the case of macroscale sensors. Signals of any size of sensors are evoked by the catalytic activity of the immobilized receptor, in this case, the enzyme GOD. In the case of the presented nanosensor, the direct mediator-free charge transfer was most probably observed; besides, it should be noted that, quite probably, the charge transfer is both from a single molecule and from several molecules that proved to be in the gap zone.

This model can be a prototype for the development of the subsequent series of similar nanodevices bringing them closer to practice.

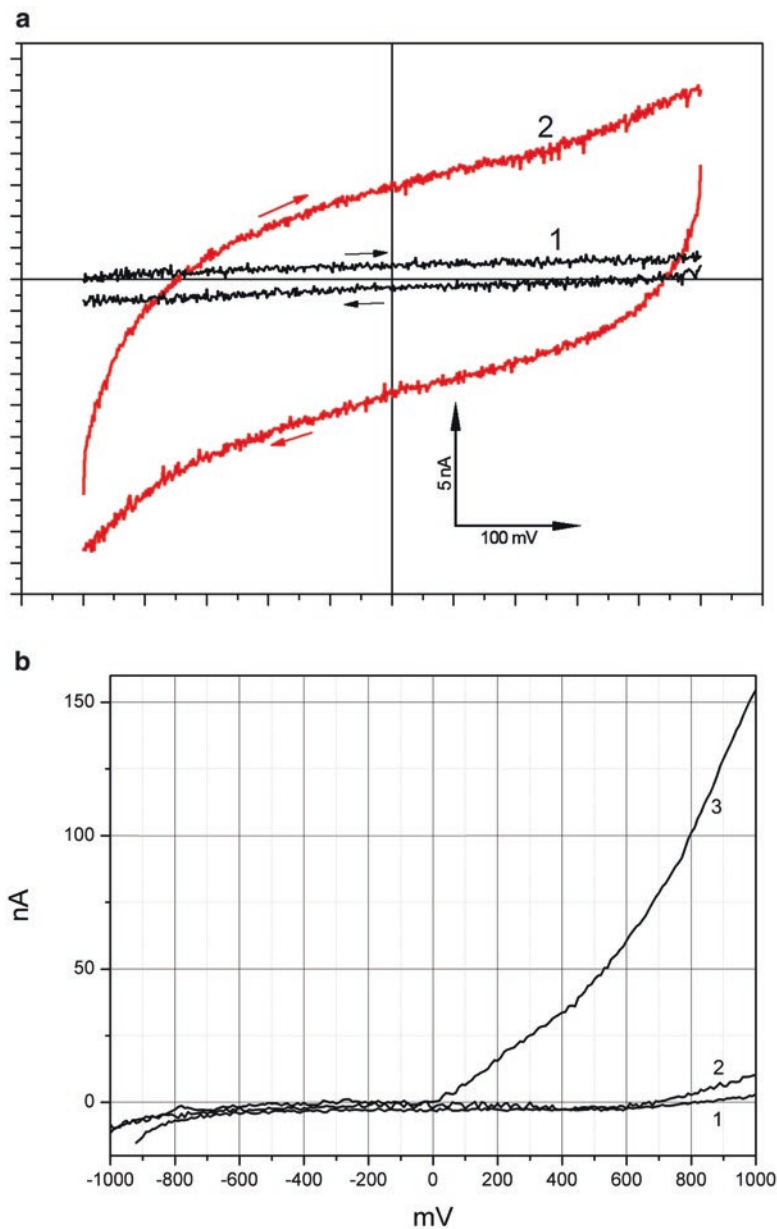


Fig. 1.3 Electronic properties of the nanosensor. (a) Increase of current at the introduction of GOD into the measured solution of substrate. 1, control signal; 2, GOD + glucose, 10 mM. (b) graded dependence of nanosensor responses from substrate concentration (1, 0.2 mM glucose; 2, 1 mM glucose; 3, 6 mM glucose)

1.5 Conclusion and Future Prospects

In the general field of biosensors, the class of electrochemical biosensors is singled out as the most developed. As the authors of any type of biosensors strive for their devices to be miniature, in the field of electrochemical devices, this tendency is of primary significance. This made it rather problematic to write an exhaustive review on the subject combining macro-, micro- and nanobiosensors. Nevertheless, the tendency is there, and some conclusions can already be made. First, it is evident that the miniaturization is achievable when microelectronic and biochemical technologies are combined to develop a device. Further, an evident tendency at present is the use of nanomaterials—nanotubes, graphene materials, etc.—for modification of the bioreceptor element. Undoubtedly, the introduction of novel materials—nanomaterials—into the bioreceptor is accompanied by the verification of their biocompatibility. These tendencies, in our view, represent the main novelty in the field of biosensors and biofuel cells. It would be natural to assume that constructions would be created in the long run to solve biomedical tasks by implanting them into plant and animal organisms.

Acknowledgments The authors are grateful to the Russian Foundation for Basic Research (grants 18-57-7802, 18-29-23042 and 19-58-45011) for financial support.

References

- Caruso F, Trau D, Möhwald H, Renneberg R (2000) Enzyme encapsulation in layer-by-layer engineered polymer multilayer capsules. *Langmuir* 16:1485–1488
- Chang KM, Chang CT, Chan KM (2010) Development of an ion sensitive field effect transistor based urea biosensor with solid state reference systems. *Sensors (Basel)* 10(6):6115–6127. <https://doi.org/10.3390/s100606115>
- Chen CC, Lai ZL, Wang GJ, Wu CY (2016) Polymerase chain reaction-free detection of hepatitis B virus DNA using a nanostructured impedance biosensor. *Biosens Bioelectron* 77:603–608
- Decher G, Hong JD (1991) Buildup of ultrathin multilayer films by a self-assembly process. I: consecutive adsorption of anionic and cationic bipolar amphiphiles on charged surfaces. *Makromol Chem Macromol Symp* 46:321–327
- Gotoh M, Tamiya E, Karube I (1989) Micro FET biosensor using polyvinylbutyral resin membrane. *J Membr Sci* 41:291–303
- Gotovtsev PM, Badranova GU, Zubavichus YV, Chumakov NK, Antipova CG, Kamyshevsky RA, Presniakov MY, Tokaev KV, Grigoriev TE (2019) Electroconductive PEDOT:PSS-based hydrogel prepared by freezing-thawing method. *Heliyon* 5:e02498. <https://doi.org/10.1016/j.heliyon.2019.e02498>
- He J, Zhu J, Gong C, Qi J, Xiao H, Jiang B, Zhao Y (2015) Label-free direct detection of miRNAs with poly-silicon nanowire biosensors. *PLoS One* 10(12):e0145160. <https://doi.org/10.1371/journal.pone.0145160>
- Hsu CW, Wang GJ (2014) Highly sensitive glucose biosensor based on Au–Ni coaxial nanorod array having high aspect ratio. *Biosens Bioelectron* 56:204–209
- Hsu CW, Feng WC, Su FC, Wang GJ (2015) A novel electrochemical glucose biosensor with a silicon nanowire array electrode. *J Electrochem Soc* 162(10):B1–B5

- Hsu CW, Su FC, Peng PY, Young HT, Liao S, Wang GJ (2016) Highly sensitive non-enzymatic electrochemical glucose biosensor using a photolithography fabricated micro/nano hybrid structured electrode. *Sensors Actuators B* 230:559–565
- Ivanov YD, Malsagova KA, Pleshakova TO, Galiullin RA, Kozlov AF, Shumov ID, Ivanova IA, Archakov AI, Popov VP, Latyshev AV, Rudenko KV, Glukhov AV (2018) Ultrasensitive detection of 2,4-dinitrophenol using nanowire biosensor. *J Nanotechnol* 2018:1–6. article ID 9549853, 6 pages
- Jeevanandham G, Jerome R, Murugan N, Preethika M, VEDIAPPAN K, Sundramoorthy AK (2020) Nickel oxide decorated MoS₂ nanosheet-based non-enzymatic sensor for the selective detection of glucose. *RSC Adv* 10(2):643–654. <https://doi.org/10.1039/c9ra09318d>
- Kanwal A, Wang SC, Ying Y, Cohen R, Lakshmanan S, Patlolla A et al (2014) Substantial power density from a discrete nano-scalable biofuel cell. *Electrochem Commun* 39:37–40. <https://doi.org/10.1016/j.elecom.2013.12.010>
- Karyakin AA (2001) Prussian blue and its analogues: electrochemistry and analytical applications. *Electroanalysis* 13(10):813–819
- Kashin VV, Kolesov VV, Krupenin SV, Parshintsev AA, Reshetilov AN, Soldatov ES, Azev VN (2013) Molecular nanobiosensor on the basis of glucose oxydas enzyme. *Radioelectron Nanosyst Inf Technol* 5(2):45–61
- Kazanskaya N, Kukhtin A, Manenkova M, Reshetilov A et al (1996) FET-based sensors with robust photosensitive polymer membranes for detection of ammonium ions and urea. *Biosens Bioelectron* 11(3):253–261
- Kumar THV, Sundramoorthy AK (2019) Electrochemical biosensor for methyl parathion based on single-walled carbon nanotube/glutaraldehyde crosslinked acetylcholinesterase-wrapped bovine serum albumin nanocomposites. *Anal Chim Acta* 1074:131–141
- Kurbanoglu S, Ozkan SA (2018) Electrochemical carbon based nanosensors: a promising tool in pharmaceutical and biomedical analysis. *J Pharm Biomed Anal* 147:439–457
- Lee I, Luo X, Huang J, Cui XT, Yun M (2012) Detection of cardiac biomarkers using single polyaniline nanowire-based conductometric biosensors. *Biosensors* 2(2):205–220. <https://doi.org/10.3390/bios2020205>
- Lee BY, Li CW, Wang GJ (2015) Nanoporous anodic aluminum oxide tube encapsulating a micro-porous chitosan/collagen composite for long-acting drug release. *Biomed Phys Eng Express* 1:045004
- Li Y, Wang Z, Sun L, Liu L, Xu C, Kuang H (2019) Nanoparticle-based sensors for food contaminants. *TrAC Trends Anal Chem* 113:74–83
- Lin YC, Wang GJ (2018) A novel non-enzymatic glucose biosensor with a monolayer of self-assembled gold nanoparticles on a micro hemisphere array. 28th Anniversary World Congress on Biosensors, Miami, FL, USA
- Lin YC, Liao S, Huang T, Wang GJ (2019) A novel biosensor electrode with self-assembled monolayer of gold nanoparticle on a micro hemisphere array. *J Electrochem Soc* 166(6):B349–B354
- MacVittie K, Conlon T, Katz E (2015) A wireless transmission system powered by an enzyme biofuel cell implanted in an orange. *Bioelectrochemistry* 106(A):28–33
- Malsagova KA, Ivanov YD, Pleshakova TO, Kaysheva AL, Shumov ID, Kozlov AF, Archakov AI, Popov VP, Fomin BI, Latyshev AV (2015) A SOI-nanowire biosensor for the multiple detection of D-NFATc1 protein in the serum. *Anal Methods* 7(19):8078–8085. <https://doi.org/10.1039/c5ay01866h>
- Malsagova KA, Pleshakova TO, Galiullin RA, Kaysheva AL, Shumov ID, Ilnitskii MA, Popov VP, Glukhov AV, Archakov AI, Ivanov YD (2018) Ultrasensitive nanowire-based detection of HCVcoreAg in the serum using a microwave generator. *Anal Methods* 10(23):2740–2749
- Park H, Lim AKL, Alivisatos AP (1999) Fabrication of metallic electrodes with nanometer separation with electromigration. *Appl Phys Lett* 35:2–5
- Peng CY, Hsu CW, Li CW, Wang GJ (2017) Using anodic aluminum oxide film and nanoimprint to produce polymer anti-counterfeit labels. *Smart Sci* 5(3):117–122

- Peng CY, Hsu CW, Li CW, Wang PL, Jeng CC, Chang CC, Wang GJ (2018) A flexible photonic crystal material for multiple anti-counterfeiting applications. *ACS Appl Mater Interfaces* 10(11):9858–9864
- Petrov AI, Volodkin DV, Sukhorukov GB (2005) Protein–calcium carbonate coprecipitation: A tool for protein encapsulation. *Biotechnol Prog* 21:918–925
- Plekhanova YV, Tikhonenko SA, Dubrovsky AV, Kim AL, Musin EV, Wang G-J, Kuznetsova IE, Kolesov VV, Reshetilov AN (2019) Comparative study of electrochemical sensors based on enzyme immobilized into polyelectrolyte microcapsules and into chitosan gel. *Anal Sci* 35:1037–1043. <https://doi.org/10.2116/analsci.19P131>
- Pourmand N, Karhanek M, Persson HHJ, Webb CD, Lee TH, Zahradníková A, Davis RW (2006) Direct electrical detection of DNA synthesis. *Proc Natl Acad Sci U S A* 103(17):6466–6470
- Purushothaman S, Toumazou C, Chung-Bei O (2006) Protons and single nucleotide polymorphism detection: a simple use for the ion sensitive field effect transistor. *Sensors Actuators B* 114(2):964–968
- Qi P, Wang J, Wang X, Xu H, Di S, Zhang H, Wang Q, Wang X (2018) Construction of a probe-immobilized molecularly imprinted electrochemical sensor with dual signal amplification of thiol graphene and gold nanoparticles for selective detection of tebuconazole in vegetable and fruit samples. *Electrochim Acta* 274:406–414
- Ratautas D, Marcinkevičiene L, Meškys R, Kulys J (2015) Mediatorless electron transfer in glucose dehydrogenase/laccase system adsorbed on carbon nanotubes. *Electrochim Acta* 174:940–944
- Reshetilov AN, Abramochkina FN, Litvinov EG, Zaitsev SY, Zubov VP (1990) Generation of electrochemical potentials by membranes containing monomolecular films of bacterial rhodopsin. *Zh Anal Khim* 45(7):1022–1025
- Reshetilov AN, Medvinskii AB, Eliseeva TP, Shakhbazian VI, Tsyganov MA, Boronin AM, Ivanitskii GR (1992) Formation of pH-waves caused by expansion of a bacterial population in agar culture media. *Dokl Akad Nauk* 323(5):971–975
- Reshetilov AN, Kitova AE, Kolesov VV, Yaropolov AI (2015) Mediator-free bioelectrocatalytic oxidation of ethanol on an electrode from thermally expanded graphite modified by *Gluconobacter oxydans* membrane fractions. *Electroanalysis* 27(6):1443–1448
- Reshetilov AN, Plekhanova YV, Dubrovskii AV, Tikhonenko SA (2016) Detection of urea using urease and paramagnetic Fe₃O₄ particles incorporated into polyelectrolyte microcapsules. *Process Biochem* 51(2):277–281. <https://doi.org/10.1016/j.procbio.2015.11.028>
- Reshetilov A, Plekhanova Y, Tarasov S, Tikhonenko S, Dubrovsky A, Kim A, Kashin V, Machulin A, Wang G-J, Kolesov V, Kuznetsova I (2019) Bioelectrochemical properties of enzyme-containing multilayer polyelectrolyte microcapsules modified with multiwalled carbon nanotubes. *Membranes* 9:53
- Sasaki S (1999) The development of microfabricated biocatalytic fuel cells. *Trends Biotechnol* 17(2):50–52. [https://doi.org/10.1016/s0167-7799\(98\)01243-8](https://doi.org/10.1016/s0167-7799(98)01243-8)
- Scognamiglio V, Pezzotti G, Pezzotti I, Cano J, Buonasera K, Giannini D, Giardi MT (2010) Biosensors for effective environmental and agrifood protection and commercialization: from research to market. *Microchim Acta* 170:215–225
- Seki A, Kubo I, Sasabe H, Tomioka H (1994) A new anion-sensitive biosensor using an ion-sensitive field effect transistor and a light-driven chloride pump, halorhodopsin. *Appl Biochem Biotechnol* 48(3):205–211
- Shen MC, Lai JC, Hong CY, Wang GJ (2017) Electrochemical aptasensor for detecting Der p2 allergen using polycarbonate-based double-generation gold nanoparticle chip. *Sens Bio-Sens Res* 13:75–80
- Shim NY, Bernards D, Macaya D, DeFranco J, Nikolou M, Owens R, Malliaras G (2009) All-plastic electrochemical transistor for glucose sensing using a ferrocene mediator. *Sensors* 9(12):9896–9902. <https://doi.org/10.3390/s91209896>
- Steinmann P, Weaver JMR (2004) Fabrication of sub-5 nm gaps between metallic electrodes using conventional lithographic techniques. *J Vac Sci Technol B* 22:3178

- Sundramoorthy AK, Premkumar BS, Gunasekaran S (2015) Reduced graphene oxide-poly(3,4-ethylenedioxythiophene) polystyrenesulfonate based dual-selective sensor for iron in different oxidation states. *ACS Sens* 1(2):151–157. <https://doi.org/10.1021/acssensors.5b00172>
- Tanabe K, Hikuma M, Soomi L, Iwasaki Y, Tamiya E, Karube I (1989) Photoresponse of a reconstituted membrane containing bacteriorhodopsin observed by using an ion-selective field effect transistor. *J Biotechnol* 10:127–134
- Tikhonenko SA, Dubrovsky AV, Saburova EA, Shabarchina LI (2014) Polyelectrolyte enzyme-bearing microdiagnostic: a new step in clinical-biochemistry analysis. In: *Physics and chemistry of classical materials: applied research and concepts*, pp 127–138
- Tung YT, Chang CC, Lin YL, Hsieh SL, Wang GJ (2016) Development of double-generation gold nanoparticle chip-based dengue virus detection system combining fluorescence turn-on probes. *Biosens Bioelectron* 77:90–98
- Vigneshvar S, Sudhakumari CC, Senthilkumaran B, Prakash H (2016) Recent advances in biosensor technology for potential applications – an overview. *Front Bioeng Biotechnol* 4:1–9
- Wisitorsaat A, Pakapongpan S, Sriprachuabwong C, Phokharatkul D, Sritongkham P, Lomas T, Tuantranont A (2013) Graphene–PEDOT:PSS on screen printed carbon electrode for enzymatic biosensing. *J Electroanal Chem* 704:208–213
- Xu J, Chen T, Qiao X, Sheng Q, Yue T, Zheng J (2019) The hybrid of gold nanoparticles and Ni(OH)₂ nanosheet for non-enzymatic glucose sensing in food. *Colloids Surf A Physicochem Eng Asp* 561:25–31

Chapter 2

Bactericidal, Fungicidal, and Immunomodulating Activities of Nanosurfaces



Sergei Georgievich Ignatov, Pavel V. Slukin, O. V. Kalmantaeva,
A. G. Voloshin, Sergey F. Biketov, V. M. Tedikov, O. N. Perovskaya,
Galina Nikolaevna Fedjukina, A. S. Kartseva, M. V. Silkina,
Victoria Valer'evna Firtstova, Ivan Alekseevich Dyatlov, G. P. Bachurina,
S. Yu. Filippovich, and D. V. Shtansky

Abstract Nanomodified surfaces are increasingly used as bactericidal and immunomodulatory tools in the transition to personalized medicine and health-saving technologies. Medical device-associated infections account for a large proportion of hospital-acquired infections. The use of biomedical implants significantly increases the risk of infection of the human body. Although microbiological contamination is constantly minimized by modern sterilization procedures, postoperative infections are frequently observed after implant placement. To enhance the bactericidal effect of the implant, surface modification is applied. Bactericidal activity of nanoparticles has been investigated against *Mycobacterium tuberculosis* H37Rv. It was shown that the inhalation of silver nanoparticles stabilized with polyvinylpyrrolidone led not only to a noticeable bactericidal effect but also recovered the balance of the immune system of mice. Implant-related bacterial and fungal infections remain a serious problem that has not been solved yet. Bactericidal activity of different nanosurfaces was studied against clinically isolated bacterial strains. The antifungal activity of nanoparticles' surfaces modified with antibiotics and the immunomodu-

S. G. Ignatov (✉) · P. V. Slukin · O. V. Kalmantaeva · A. G. Voloshin · S. F. Biketov ·
V. M. Tedikov · O. N. Perovskaya · G. N. Fedjukina · A. S. Kartseva · M. V. Silkina ·
V. V. Firtstova · I. A. Dyatlov
State Research Center for Applied Microbiology and Biotechnology,
Obolensk, Moscow Region, Russia
e-mail: ignatov@obolensk.org; firstova@obolensk.org; dyatlov@obolensk.org

G. P. Bachurina · S. Y. Filippovich
Bach Institute of Biochemistry, Research Center of Biotechnology of the Russian Academy
of Sciences, Moscow, Russia
e-mail: syf@inbi.ras.ru

D. V. Shtansky
National University of Science and Technology "MISIS", Moscow, Russia
e-mail: shtansky@shs.misis.ru

lating activity of the samples was evaluated. This chapter provides new insights into understanding and designing of antibacterial, fungicidal, and immunomodulating yet biologically safe surfaces.

Keywords Nanoparticles · Nanosurfaces · Antibacterial activity · Fungicidal activity · Immunomodulation

Nomenclature

7-AAD	7-Aminoactinomycin
BCG	Bacillus Calmette-Guerin
BPL	Bronchopulmonary lavage
CFSE	Carboxyfluorescein
CFUs	Colony-forming units
Con A	Concanavalin A
FBS	Fetal bovine serum
IFN- γ	Interferon gamma
IL-2 α	Interleukin-2 alpha
IL-4	Interleukin-4
MDR	Multidrug-resistant
NP	Nanoparticle
NSS	Normal saline solution
PBS	Phosphate-buffered saline
ROS	Reactive oxygen species
SNP	Silver nanoparticles
SNP-PVP	SNPs stabilized by polyvinylpyrrolidone
TiCaPCON	Ti-Ca-P-C-O-N
TB	Tuberculosis
TNF α	Tumor necrosis factor alpha
XDR	Extensively drug-resistant

2.1 Introduction

Biomedical implants have revolutionized medicine, but they increase the infection risk. Indeed, implant infection is one of the most frequent and severe complications associated with the use of biomaterials. The use of nanomaterials in medical implants was introduced a few decades ago. A comprehensive assessment of the physics of material selection, process optimization, and design/geometry requirements will enable the rapid commercialization of different technologies for medical implant applications (Velu et al. 2020). Implant infection includes complex interac-

tions between the microbial pathogen, the biomaterial, and the host immune response to both. Chronic implant-related bone infections are a major problem in orthopedic and trauma surgery. As numbers of joint replacements are rising, complications such as bone infections also increase. Current treatment options are associated with severe consequences for patients and often fail to eliminate the infection (Seebach and Kubatzky 2019).

The high risk of chronicity for such infections is due to successful evasion strategies of bacteria with biofilm formation being one major mechanism behind bacterial persistence. An important factor in the resistance of pathogens is the formation of biofilms (Donlan and Costerton 2002). Biofilms are considered as a vital structure with bacteria which are incorporated in polymeric matrix. It is generally accepted that in the first stage, planktonic microbial cells adhere to the surface either by physical forces or by bacterial structures. In the second stage, some of the reversibly attached cells remain immobilized and become irreversibly adhered when the attractive forces are greater than repulsive forces (Garrett et al. 2008). The presence of biofilms in bacterial infections can increase the pathogenicity of the bacteria and protects them from being destroyed by external treatment. Biofilms protect the cells from assaults like UV radiation, pH stress, chemical exposure, phagocytosis, dehydration, and others (Gupta et al. 2016). The future of biofilm research relies upon various concerted efforts from scientists of different disciplines to understand the complexity of biofilm formation and device efficient strategy for biofilm inhibition. The presence of a foreign material facilitates biofilm formation and further supports the persistence of an infection. Thus, there is a high interest to clear infections already at the planktonic stage before biofilm transition occurs and to prevent reinfection after antibiotic and surgical treatment (Seebach and Kubatzky 2019). However, novel therapeutic strategies are required to perform this process.

Immune modulation can serve as an additional process and required medical treatment option to restore an effective host response. It is to be hoped that the combination of antibiotic and surgical treatment with immune therapeutic intervention may lead to the successful management of chronic implant-related infections in the future.

Recently, significant advances have been made in the design of implants with antibacterial properties. However, the general weakness of the body and incomplete sterility of the hospitals can lead to severe postoperative infections. Chronic implant-related bone infections are a major problem in orthopedic and trauma-related surgery with severe consequences for the affected patients. As antibiotic resistance increases in general and because most antibiotics have poor effectiveness against biofilm-embedded bacteria in particular, there is a need for alternative and innovative treatment approaches. Recently, the immune system has moved into focus as the key player in infection defense and bone homeostasis, and the targeted modulation of the host response is becoming an emerging field of interest. The presence of foreign material adversely affects the immune system by generating a local immune-compromised environment where spontaneous clearance of planktonic bacteria does not take place.

Therefore, a comprehensive assessment of the bactericidal, fungicidal, and immunomodulatory activities of new complexly organized surfaces is an important task to reduce losses from socially significant diseases. Investigating fundamental interactions between nanoparticles and fungal cells is key in determining the fate and behavior of nanomaterials designed for antimicrobial applications. Fungi are clinically important in the context of bloodstream infections. With the widespread production and use of nanomaterials, the growing exposure of workers and consumers in everyday life raises concern about potential health risks. Currently, nanotechnology has a wide range of applications in biomedical research, industries, and in almost all types of modern technology. The growing applications of nanotechnology in medicine urge scientists to analyze the impact of nanomaterials on human body tissues and the immune system (Seebach and Kubatzky 2019).

It is known that tuberculosis (TB) is socially significant infection in the world. TB is currently a global pandemic that kills approximately 1.3 million people worldwide each year. Although the incidence of TB is decreasing each year, the rate of that decline is not high enough to accomplish the TB Global Strategy for the 2015–2035 period. Tuberculosis (TB), caused by *Mycobacterium tuberculosis*, causes more human deaths in comparison with any other diseases from a single infectious agent (Donnellan and Giardiello 2019). While global rates of incidence of TB have been falling at an average of 2% per year, the incidence of drug-resistant TB remains steady. Multidrug-resistant (MDR) and extensively drug-resistant (XDR) tuberculosis strains began to be detected. Antibiotic-resistant infections were reported to give rise to losses estimated at \$55–70 billion annually in the USA. In Europe, the losses surpassed €1.5 billion annually. From this point of view, bactericidal nanoparticles (NP) are a promising way for anti-TB therapy. Nanotechnology holds great promise to improve human health and is predicted to significantly benefit all human society (Etheridge et al. 2013; Chang et al. 2015; Saravanan et al. 2018). The aim of this chapter is to analyze bactericidal, fungicidal, and immunomodulating activities of nanosurfaces.

2.2 Nanosurfaces Against Pathogens

The discovery of antibiotics in the early twentieth century revolutionized the treatment of bacterial infections, but after several decades of overuse, the evolution of antibiotic-resistant bacteria is a major threat to the practice of modern medicine. Recent studies have reported that bacteria-contaminated surfaces make a significant contribution to the incidence of healthcare-associated infections and that repeated cleaning/disinfection of the contaminated surfaces, which is commonly performed in healthcare facilities, is not always sufficient to remove pathogens. For example, 27% of surfaces in rooms were still contaminated by bacteria after four complete cleaning cycles with disinfectant (Hwang et al. 2020).

The excessive and improper consumption of antibacterials resulted in the emergence of more aggressive microbial strains that do not respond to standard treat-

ments. The disastrous human and economic cost of antibiotic resistance renders the development of new alternative strategies against pathogens (Eleraky et al. 2020).

New approaches to the design of new complex nanosurfaces with the possibility of their subsequent antibacterial modification and explanation of the mechanism of their bactericidal action are a promising direction. Therefore, there is a need for an integrated evaluation of bactericidal, fungicidal, and immunomodulatory activities of new complex-organized surfaces used in implantology. Despite significant advances in materials, science in the design of implants with antibacterial and fungicidal properties, the problem of postoperative infections remains very urgent (Firestein et al. 2018; Sukhorukova et al. 2018; Permyakova et al. 2018). The emergence of multidrug-resistant bacterial strains induced the search and development of new effective bactericidal agents. Various modifications of the implant surface are designed to reduce bacterial and fungal contamination of the surface. Currently, nanomodified surfaces are increasingly used as bactericidal, fungicidal, and immunomodulatory tools in the transition to personalized medicine and health-saving technologies. Medical device-associated infections account for a large proportion of hospital-acquired infections. The use of biomedical implants significantly increases the risk of infection of the human body. Despite the fact that microbiological contamination is constantly minimized by modern sterilization procedures, postoperative infections are constantly observed after implant placement. To enhance the bactericidal and fungicidal effect of the implant, surface modification is applied. Coating TiCaPCON (Ti-Ca-P-C-O-N) was precipitated on a silicon wafer by magnetron sputtering. Pt and Fe particles and their combinations were obtained by implantation of metal ions into the TiCaPCON coating.

2.2.1 *Antibacterial Activity*

Most bactericidal materials consist of different chemical substances, such as nano-sized metals (Marambio-Jones and Hoek 2010; Suresh et al. 2010; Azam et al. 2012), antibiotic agents (Oda et al. 2011; Parhi et al. 2013), and antimicrobial compounds (Condell et al. 2012; Elshaarawy and Janiak 2014). These materials have disadvantages such as short stability, cost, and being harmful to human beings. Recently, microorganisms presenting antimicrobial resistance have become a serious threat, causing approximately 700,000 deaths per year. Additionally, it has been estimated that the number of antimicrobial resistance-related deaths will increase to 10 million by 2050 (Ivanova et al. 2012).

TiCaPCON (Ti, Ca, P, C, O, N – chemical elements) films are very promising bactericidal surfaces. The TiCaPCON samples were placed into the wells of a sterile 24-well culture plate filled with 0.5 mL of normal saline solution (NSS). Sample-free well and a well with NP-free TiCaPCON sample were used as controls. Simultaneously, 0.03 mL of the overnight culture suspension of test strains in NSS was added to all wells with a cell concentration of about 10^4 – 10^5 CFU (colony-forming unit)/mL. The samples were incubated in a thermostat at 37 °C. Aliquots

Table 2.1 Antibacterial activity of samples with implanted Pt and Fe ions into the TiCaPCON evaluated as the number of colony-forming units (CFUs). All samples were active against bacteria cells, especially against *E. coli*

Bacterial strain	CFU (before incubation with samples)	CFU (after incubation with samples for 24 h)
<i>Acinetobacter baumannii</i>	$5 \times 10^5 \pm 2 \times 10^4$	$8 \times 10^2 \pm 7 \times 10^1$
<i>E. coli</i>	$2 \times 10^5 \pm 5 \times 10^4$	0
<i>Enterococcus faecium</i>	$9 \times 10^4 \pm 3 \times 10^3$	$2 \times 10^2 \pm 5 \times 10^1$
<i>Staphylococcus aureus</i>	$2 \times 10^5 \pm 1 \times 10^4$	$3 \times 10^4 \pm 8 \times 10^3$
<i>Staphylococcus epidermidis</i>	$5 \times 10^5 \pm 4 \times 10^4$	$5 \times 10^5 \pm 5 \times 10^5$

were taken for analysis after 24 h incubation. To obtain CFU concentrations, the content of each well was titrated using a serial tenfold bacterial dilution. From each dilution, 0.01 mL of bacterial suspension was put on Petri dishes with a nutrient medium Mueller-Hinton agar, incubated in the thermostat at 37 °C for 24 h, and then the culture titer was counted (Permyakova et al. 2018).

For protection against pathogenic bacteria, it is possible to use probiotic bacteria (Fursova et al. 2012), but nanomodified surfaces are more effective. As you can see in Table 2.1, TiCaPCON samples with implanted Pt and Fe ions demonstrated a pronounced antibacterial effect, especially against *Escherichia coli* cells.

Pt and Fe nanoparticles form nanogalvanic elements after immobilization on the surface. Thus, pathogenic bacteria can be killed by microgalvanic interactions. We have obtained boron-doped TiCaPCON films as a promising alternative to the widely used approach based on the introduction of other famous bactericidal elements, such as Ag, Cu, and Zn (Ponomarev et al. 2019a). Nevertheless, interesting results can be obtained when creating original Ag structures on the surface. Novel samples with patterned surface having the same Ag total coverage area and content, but different surface topography made of periodically spaced Ag/Si pillars, have been analyzed against antibiotic-resistant strain *E. coli*. Samples with the largest pillar heights which had also Ag particles formed between pillars demonstrated the fastest Ag + ion release and, correspondingly, a noticeable antibacterial effect toward antibiotic-resistant hospital *E. coli* strains already after 3 h. All samples showed 100% antibacterial effect after 24 h (Ponomarev et al. 2019b).

2.2.2 Nanoparticles Against Tuberculosis

M. tuberculosis is the causal agent of the pulmonary TB, which is air-transmitted by nasal/oral inhalation of aerosol droplets carrying the pathogen from an active TB patient to a healthy individual usually through coughing or sneezing. Small droplets are able to reach the lower lung and induce formation of a granuloma, which is a host-defensive structure providing a fibrotic physical barrier between the infected and the healthy neighboring tissues. Latently infected individuals represent roughly a quarter of the global population. Tuberculin Skin Test and Interferon-Gamma

Release Assay are commonly used for diagnosis of latently infected individuals. Although they cannot infect a healthy person, *M. tuberculosis* activation occurs in roughly 10% of cases due to recurrent infections or a compromised immune system in the host. The safest and most cost-effective way to fight against infectious diseases is vaccination. TB and other poverty-related and neglected infectious diseases still lack effective vaccines to protect the entire population. Bacillus Calmette-Guerin (BCG), the only licensed vaccine currently in use against TB, was developed 80 years ago which displays an efficacy of 80% or more in children under 4 years old. However, the efficacy of BCG in adolescents and adults is variable, from 0 to 80% depending on the geographical region (Mateos et al. 2020).

The main direction in the treatment of tuberculosis remains antibiotic therapy (Sterling et al. 2020). MDR tuberculosis is defined as infection resistant to the first-line antibiotics, rifampicin and isoniazid. XDR tuberculosis is defined as an infection that is MDR and additionally resistant to at least one drug in both of the two classes used to treat MDR: fluoroquinolones and the second-line injectable drugs (amikacin, capreomycin, or kanamycin) (Wollenberg et al. 2020). The emergence of antibiotic-resistant pathogens of infectious diseases, including pan-resistant isolates (insensitive to all antibiotics from all functional classes), raises questions of further investigation of pathogens and new approaches to fight against them. The relevance of the study of antibiotic-resistant pathogens of infections in humans throughout the world is emphasized by the dynamics of the increase in the number of scientific publications presented on the web-resource PubMed. Scientific studies are devoted to a wide range of problems: the description of clinical cases of infections, the evaluation of antibiotic resistance of strains, the prevalence of epidemically successful clones, and the study of molecular genetic mechanisms of antibiotic resistance and virulence. It has been established that the increase in resistance levels of strains isolated throughout the world is associated with the appearance of new variants and the spread by the horizontal transfer of genetic determinants of resistance. NPs are used to detect the serum antibody responses to dormancy-related antigens of *M. tuberculosis* for the diagnosis of active and latent TB infections (Shi et al. 2020). A recent book *Nanotechnology Based Approaches for Tuberculosis Treatment* discusses multiple nanotechnology-based approaches that may help overcome persisting limitations of conventional and traditional treatments.

Today, several directions are being developed to struggle against TB, including the use of monoclonal antibodies, mycobacteriophages, bacterial vaccines, immunomodulators, and silver nanoparticles (SNP). Since ancient times, silver has been one of the main antimicrobial agents in medicine and used in the treatment of infectious diseases (Nasiruddin et al. 2017). The therapeutic properties of silver have been known for over 2000 years. Currently, the development of nanotechnology has made it possible to create the nanosized particles to fight against TB. The use of silver in the form of NPs makes it possible to reduce the silver concentration by hundreds of times while maintaining the bactericidal properties and to use these drugs in medicine. However, the question of simultaneous assessment of the bactericidal and immunomodulating activity of NP remains open. The goal of this part of work was to study the antimicrobial activity of SNPs against TB and to assess the

immune parameters of experimental animals after exposure to these NP (Kalmantaeva et al. 2020). SNPs were stabilized by a low molecular weight polymer polyvinylpyrrolidone (SNP-PVP). The *M. tuberculosis* H37rv was obtained from the department of collection cultures of the State Research Center for Applied Microbiology and Biotechnology (Obolensk, Russia). The bacterial suspension and SNPs were mixed in a ratio of 1:9. The SNP concentrations of 0.1, 1.0, 10, 25, and 50 $\mu\text{g}/\text{mL}$ were tested. The exposure of SNPs with mycobacteria was 1 h at 37 °C. After incubation, 0.1 mL of each sample was inoculated into Petri dishes with a nutrient medium, Middlebrook 7H11 Agar Base, and cultured at 37°C for 20 days. The colony-forming units (CFUs) were then counted. The number of mycobacterial cells decreased twofold after treatment with SNP-PVP at a concentration of 50 $\mu\text{g}/\text{mL}$. Experimental animals were divided into three groups (two experimental and control), 15 mice of each. The contents and manipulations with animals were carried out in accordance with “Guidelines for the Maintenance and Use of Laboratory Animals” (Institute of Laboratory Animals Resources, Commission on Life Science 1996). Animals of experimental groups were infected with strain *M. tuberculosis* H37Rv by intraperitoneal administration of 0.2 mL of suspension mycobacteria in physiologically buffered solution. Experiments were conducted on mice with a chronic form of TB. Ten days after SNP-PVP inhalation, the animals showed a sharp decrease in organ contamination by pathogens (Kalmantaeva et al. 2020). The course and outcome of TB infection is largely determined by the degree of activation of Th1 lymphocytes and phagocytes (Rajamanickam et al. 2020). A key role in the formation of the cellular immune response in TB infection is assigned to various subpopulations of T lymphocytes: CD4 + –helper T lymphocytes, which regulate the phagocytic and bactericidal activity of macrophages, and CD8 + cytotoxic T lymphocytes, which can have a direct cytotoxic effect on cells infected with mycobacteria. In the group of mice with TB, an increase in the relative number of T lymphocytes was found due to a subpopulation of T helpers and a decrease in the relative number cytotoxic T lymphocytes and B lymphocytes in the spleen. In the group of TB mice after the SNP-PVP treatment, the relative number of T lymphocytes (including T helpers and cytotoxic T lymphocytes) and B lymphocytes in the spleen did not differ from the values of these indicators in the control group. Type-1 T lymphocytes predominantly are formed in mycobacterial infections. Their characteristic features include the production of interferon gamma ($\text{IFN}\gamma$) and tumor necrosis factor alpha ($\text{TNF}\alpha$) cytokines. Both cytokines can better stimulate the antimycobacterial activity of macrophages, which is due to the protective effect of T helpers. The experiments showed that the percentage of $\text{IFN-}\gamma$ -producing T helpers increased twofold in the TB mice as compared to the control. The inhalation of SNP-PVP in TB mice caused a decrease in the relative number of $\text{IFN-}\gamma$ -producing lymphocytes in the spleen. It can be assumed that the decrease in the relative amount of $\text{IFN-}\gamma$ -producing lymphocytes in the spleen of TB mice after the treatment with SNP-PVP was caused by a decrease in the number of *M. tuberculosis* cells. The dynamics of changes in the content of free $\text{IFN-}\gamma$ in the blood serum of TB mice showed a significant increase in the amount of this cytokine on day 7 after the intro-

duction of SNP-PVP. A significant increase in the IFN- β content was also observed in the bronchopulmonary lavage (BPL) of TB mice on the seventh day after the treatment with SNP-PVP compared with the level of this cytokine in controls. Thirty days after the treatment with SNP-PVP, the IFN- γ content was significantly lower in comparison with the level of this cytokine in the group of TB mice. There was significant increase in the content of cytokine in serum and BPL fluid 7 days after the administration of SNP-PVP to TB mice, which coincided in time with a decrease in the number of mycobacteria in the lungs and spleen. Although of SNP-PVP inhalation in TB mice led to an increase in the relative amount of TNF α -producing T helpers in the spleen, the amount of free TNF α in the blood serum and BPL fluid decreased, which indicated a decrease in the level of inflammatory reactions of the body. To better understand the effects of SNP-PVP on the course of chronic TB, we determined the content of the anti-inflammatory cytokine interleukin-4 (IL-4) in the serum and BPL fluid of the experimental animals. A significant increase in the content of free IL-4 in serum and fluid (by six- and 17-fold, respectively) relative to the values of these indicators in the control group was found in group of TB mice. Thirty days after the administration of SNPs in TB mice, there was a decrease in the IL-4 level in the blood serum and the BPL fluid, which did not significantly differ from the IL-4 content in the studied biological fluids of the control group.

Neutrophils are one of the first cells that migrate to the site of TB infection, where they gradually accumulate with the development of the chronic stage of the disease. Human and mouse neutrophils effectively phagocytize mycobacteria and participate in the initiation of the T-cell response and in the formation of granuloma. One of the neutrophil mechanisms of bactericidal action is the production of reactive oxygen species (ROS, oxidative burst) (Németh et al. 2020), the level of which can be measured based on the luminal-dependent chemiluminescence. The study on the group of TB mice found a significant decrease in the level of neutrophil production of ROS (2.7-fold as compared with the control group). In the group of TB mice treated with SNP-PVP, there was a decrease in ROS products relative to the control on 1 and 7 days after the treatment with NP. However, after 30 days, this indicator showed a significant increase (by 2.5-fold) relative to the group of TB mice untreated with SNPs. Inflammation always accompanies an infection and is an essential component of the host's immune defense. However, hyperinflammatory reactions can exacerbate the disease. An increase in the protein concentration in BPL is a signal of pulmonary inflammation, since it reflects alveolar-capillary permeability. This indicator was chosen to assess the level of inflammation in the lungs of experimental animals. TB mice demonstrated a fourfold increase in the fluid protein content as compared to that in the control group. After exposure to SNP-PVP, the amount of protein in the BPL fluid decreased twofold which reflects the decrease of pneumonia.

Finally, the antibacterial activity of SNP-PVP against the strain *M. tuberculosis* H37Rv was studied in vitro and in vivo (an experimental murine model of chronic tuberculosis). It was shown that the SNP-PVP treatment inhibited *M. tuberculosis* growth twofold in vitro. The inhalation of SNP-PVP by infected mice resulted in a twofold decrease in the colonization of the lungs and spleens by *M. tuberculosis*

cells. In infected animals, the quantity of protein in the BPL fluid was reduced by twofold, which indicates a decrease in the inflammatory processes in the lungs. The level of the production of ROS by neutrophils increased, reflecting their bactericidal potential, which was reduced by 2.7-fold before treatment as compared to the control group of animals. After the introduction of SNP, a recovery in the ratio of lymphocyte populations in the spleen and cytokine balance was observed. A decrease in the levels of IFN- γ , TNF α , and IL-4 in the blood serum and BPL fluid in TB mice was observed. Thus, it was shown for the first time that the inhalation of SNP stabilized with PVP led not only to a noticeable bactericidal effect but also recovered the balance of the immune system of mice.

2.2.3 Antifungal Activity

The fungal infections pose a significant health problem with higher mortality from systemic infections than that of bacterial sepsis (with latest estimates of mortality at 10–20%, possibly up to 47%) (Kesarwani et al. 2019). A series of nanomaterials have been developed and proven to exhibit prominent antifungal properties (Chen et al. 2020). Recently, it has been found that graphene oxide silver nanoparticle nanocomposites can suppress the development of hyphae, showing a significant antifungal effect (Chen et al. 2016).

The red bread mold *Neurospora crassa* has long been established as a model system in basic research. It can be very easily genetically manipulated and a wealth of molecular tools and mutants are available. In addition, *N. crassa* is very fast growing and nontoxic. All of these features point to a high potential of this fungus for different applications (Havlik et al. 2017). More detail analysis of antifungal activity has been done for *N. crassa*. The antifungal activity of samples was studied against wild-type strain *wt-987* and *nit-2* (no nitrite and nitrate reductases) and *nit-6* (no nitrite reductase) mutants of *N. crassa* (Fungal Genetics Stock Center, USA). The concentration of conidial suspension (vegetative spores) stored at $-70\text{ }^{\circ}\text{C}$ was 30 mg/mL. 0.3 mL of *N. crassa* spore suspension was dripped onto the surface of a 2% Vogel's agar medium in sterile Petri dishes. The control and antibiotic-loaded UV-sterilized samples were placed face down onto the nutrient medium with a uniformly distributed spore suspension and incubated at $28\text{ }^{\circ}\text{C}$ for 24 h. The degree of antifungal activity was estimated as the diameter of fungal growth inhibition zone around the sample (agar diffusion test) (Sukhorukova et al. 2018). The results of agar diffusion tests of samples against *wt-987 N. crassa* strain and its *nit* and *nit-6* mutants with impaired nitrogen metabolism are presented in Table 2.2. The results indicated that samples with amphotericin B effectively inhibited mycelium growth of all *N. crassa* strains. The fungus is characterized by strong cell walls acting as a barrier against metal ions, which makes their use less effective. Thus, these results clearly demonstrated that TiCaPCON films with implanted Pt and Fe ions and modified with amphotericin B provide innovative hybrid bioconstructions that are equally effective against bacterial and fungal cells.

Table 2.2 Zones of inhibition around TiCaPCON samples with implanted Pt and Fe ions after agar diffusion tests. Pt, Fe-A – samples with implanted Pt and Fe ions and modified with amphotericin B. Control – TiCaPCON samples without amphotericin B. A, amphotericin B disc

Samples	Diameter of growth inhibition zone, mm		
	<i>nit-6 N. crassa</i>	<i>nit-2 N. crassa</i>	<i>wt987 N. crassa</i>
Pt, Fe -A	17–20	15–19	23–24
Control	0	0	0
A	22–23	24	27–28

2.3 Immunology Tests

Assessing how engineered NP could interact with the immune system and more specifically could promote the development immune-toxic effect is still a matter of concern. NP could have an adjuvant effect on the immune system as previously demonstrated for particulate air pollution (Feray et al. 2020). Easy surface modifications of the NPs enable the modulation of the immune system either by evading the immune system to prevent allergic reactions or by enhancing the immunogenic response. During their delivery of payloads, NPs are also involved in interactions with nonspecific biomolecules inside the human body. These interactions are key functional properties of NPs. The surface modification of NPs enables their fabrication with properties that facilitate either their escape from the immune system or increase the immune response to a particular infection. The modulation of the immune response is a unique area of interest in biomedical research, as it can aid in the efficacious treatment of cancer and other immune disorders. However, uncontrolled immune-stimulation can lead to the development of allergic reactions, anaphylaxis, and thrombosis (Muhammad et al. 2020). Experimental in vitro models must be developed to monitor these effects. The challenge is to select the most relevant cells and endpoints using a simple, robust, and representative model. Most of the work regarding NP-induced immunomodulation has been focused on the activation of key immune cells.

Lymphocyte viability was determined using the vital 7-aminoactinomycin D (7-AAD) intercalating DNA dye, which penetrates the cell only when the integrity of the membrane is broken. 7-AAD solution was added to the mononuclear cell suspension (10^6 cells/mL) selected on the density gradient and incubated for 10 min. Samples were analyzed after 15 min staining on a FACSAria III flow cytometer using BD FACSDiva software. The 10^4 cells were analyzed in each sample.

The proliferation of lymphocytes was determined using the carboxyfluorescein (CFSE) dye. Each lymphocyte cell stained with CFSE under the influence of a mitogen is divided into two cells with approximately twofold lower intensity. The more occurred cell divisions (mitoses), the lower the level of luminescence. On the cytometric histogram, CFSE-stained cells are arranged in a series of consecutive peaks with decreasing luminescence intensity. Lymphocytes (10^6 cells/mL) were stained with 5 mM CFSE prior to their cultivation. Cells were incubated in an atmosphere of 5% CO_2 at 37 °C for 10 min. Then 3 mL of cooled RPMI-1640 medium was

added, incubated at 40 °C for 5 min, and then washed twice with cooled RPMI-1640 medium containing 10% fetal bovine serum (FBS). Centrifugation was performed at 400xg for 5–7 min and the supernatants were discarded. The cells were resuspended in RPMI-1640-based complete nutrient medium to their original concentration. Then, the cell suspension was introduced into the wells of a 96-well plate and incubated in 5% CO₂ at 37 °C for 6 days renewing the medium, if necessary. At the end of incubation, the cell suspension was transferred into cytometric tubes and then 1 mL of PBS was added. After centrifugation at 400xg for 5 min, the supernatant was removed, the pellet was resuspended, fixed with 1% formalin solution, and finally analyzed using flow cytometry method.

After separation on a density gradient, lymphocytes were incubated in the presence of Pt- and Fe-implanted TiCaPCON-coated samples in full nutrient medium RPMI 1640 and 5% CO₂ at 37 °C for 2 days. Then the lymphocytes were phenotyped. For this, lymphocyte suspension was stained with monoclonal antibodies: CD3 PerCP-Cy 5.5 (to identify T cells), CD19 PE (B-cells), and CD25 APC and CD 69 FITC (to reveal activation markers on the surface of T and B lymphocytes). Staining was carried out in the dark at 20°C for 20 min. Then the cells were washed in PBS, fixed with formalin solution, and subjected to flow cytometric analysis within 24 h. Previously, antibacterial and immunomodulating activities of silver NP were studied in tuberculosis models on experimental mice (Kalmantaeva et al. 2020). To assess the cytotoxicity of Pt- and Fe-implanted NP, the viability and proliferation of lymphocytes, as well as the expression of activation markers CD69 and CD25 on the lymphocyte surface, were studied. Heparinized blood, diluted twofold with phosphate-buffered saline (PBS) with 2% FBS, was layered on a Histopaque-1077 density gradient in a ratio of 1:1 and centrifuged at 400xg for 30 min at room temperature. The selected opalescent ring was washed twice at 250xg in 10 ml of PBS with 2% PBS. The pellet was resuspended in RPMI 1640 complete nutrient medium containing 10% FBS, 2 mM glutamine, 10 mM HEPES, and 25 μM 2-mercaptoethanol. Cell viability was determined using a trypan blue assay. The concentration of cell suspension was adjusted to 10⁶ cells/ml using an automatic TC20 counter.

The Fe, Ag, and Pt NPs did not significantly change the viability of lymphocytes relative to cells incubated in the medium during the entire analysis period, except for Pt NP, which slightly increased the number of dead cells in the culture after 7 days of incubation (Fig. 2.1).

A comparative analysis of the influence of NPs on the change in the functional activity of lymphocytes showed that in the presence of NPs the level of proliferative activity of lymphocytes does not change. In the presence of Fe and AgNPs, there was a slight decrease in the proliferative activity of lymphocytes induced by concanavalin A (Con A) mitogen. The level of lymphocyte proliferation in the presence of Pt NPs did not significantly differ from that when this indicator of lymphocytes incubated without Pt NP (Fig. 2.2).

The content of CD3 T lymphocytes and CD19+ B lymphocytes in cell cultures incubated in the medium for 48 h was $82.0 \pm 1.95\%$ and $8.7 \pm 1.16\%$, respectively. The presence of NP in the medium did not affect the content of T and B lymphocytes.

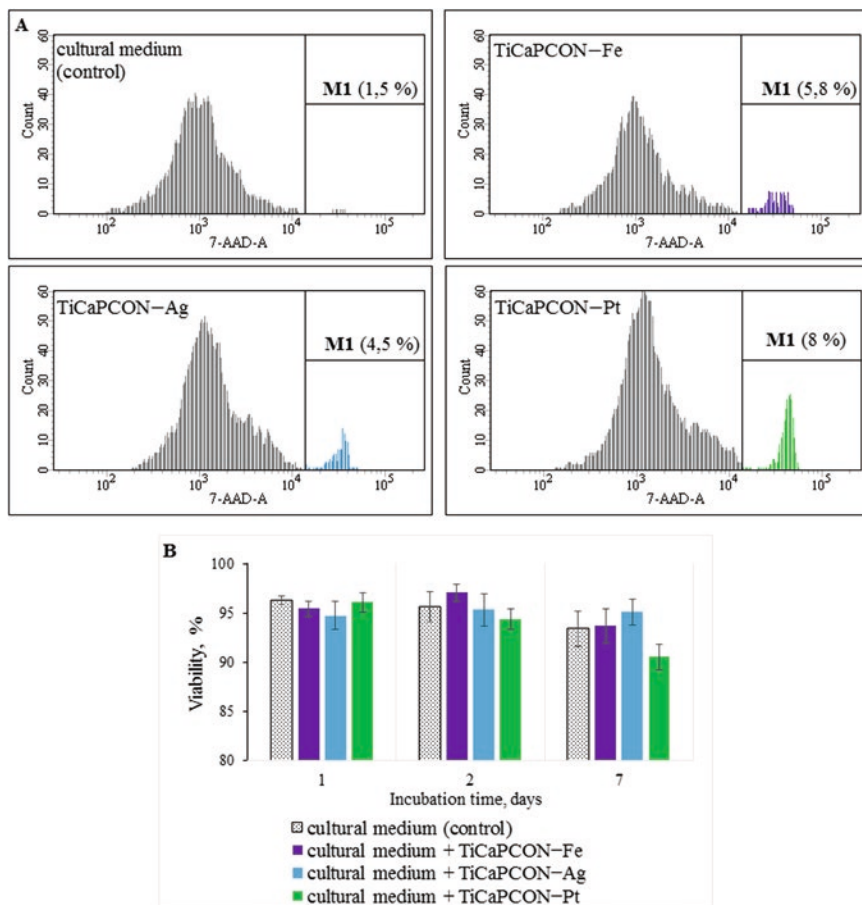


Fig. 2.1 The viability and proliferation of lymphocytes

A – an example of a cytofluorogram reflecting the percentage of dead cells over a 7-day period: control, lymphocytes without the addition of nanoparticles (RPMI); TiCaPCON-Fe, lymphocytes in the presence of Fe nanoparticles; TiCaPCON-Ag, lymphocytes in the presence of Ag nanoparticles; TiCaPCON- Pt, lymphocytes in quantities of Pt nanoparticles; M1, percentage of dead cells
 B – a diagram reflecting cell viability at different times of observation. Data are presented as mean and standard deviation of three conditionally healthy donors

One of the indicators reflecting cell activation is an increase in the expression of activation markers, in particular, a CD69 marker of early activation and CD25, a subunit of the IL-2 α receptor. A comparative analysis of the number of B lymphocytes carrying a CD69 marker on their surface showed that in the presence of Fe and Ag NPs, the content of CD19 + CD69 + cells increases by 1.8- and 1.5-fold, respectively, and when Pt nanoparticles are added, by two- and sevenfold. In addition, under the influence of all nanoparticles, the expression of the CD25 molecule on the surface of B lymphocytes was enhanced (Fig. 2.3).

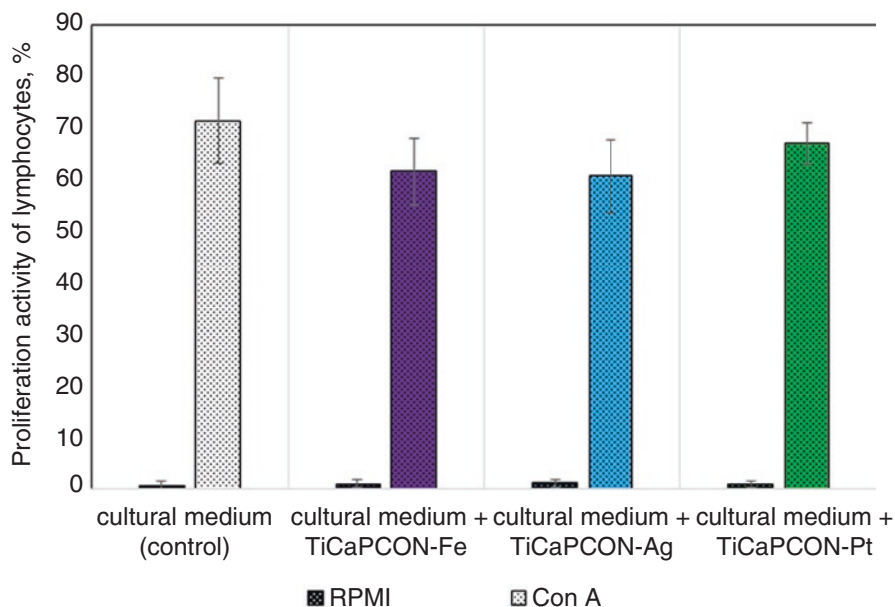


Fig. 2.2 Proliferation of lymphocytes. Assessment of proliferative activity of peripheral blood lymphocytes of donors: RPMI, unstimulated cells; Con A, mitogen-stimulated cells

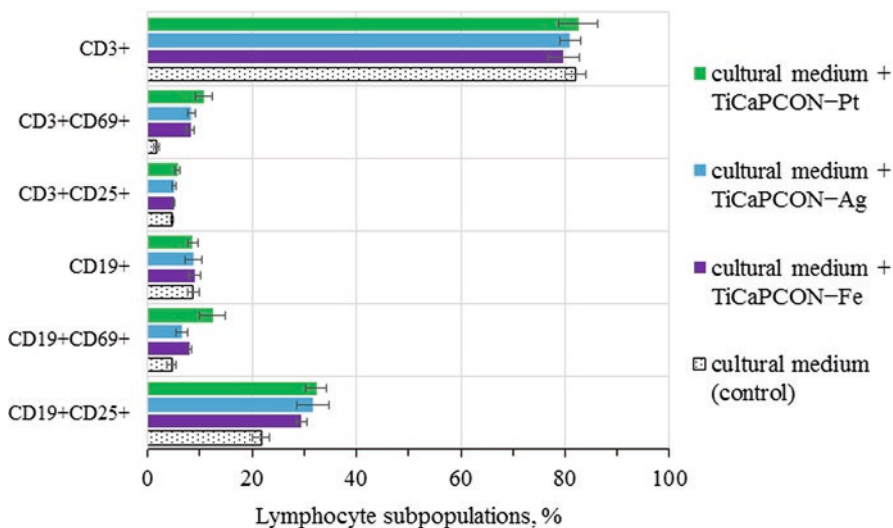


Fig. 2.3 The expression of activation markers CD69 and CD25 on the lymphocyte surface. The effect of Fe, Ag, and Pt nanoparticles on the activation of lymphocytes in vitro reactions. Data are presented as mean and standard deviation of three conditionally healthy donors

In the presence of NP, there was an increase in the marker of early activation of CD69 on the surface of T lymphocytes. The number of T lymphocytes carrying a molecule on the surface of CD25 did not significantly differ between the studied NP.

Thus, all NPs were not toxic to cells (with the exception of Pt NPs, although their cytotoxicity appeared only on the 7th day in cell culture). NP did not affect the proliferative activity of lymphocytes, i.e., there was no nonspecific activation of cells in the presence of NPs, and NP had virtually no effect on the ability of lymphocytes to activate in response to mitogen. Nevertheless, a certain reaction of lymphocytes to NPs can be traced, as evidenced by the increased expression of activation markers on the surface of both B and T lymphocytes.

2.4 Conclusion and Future Perspectives

The application of nanotechnology methods for pharmacological systems suggests that these methods might improve the physicochemical and pharmacological properties of bioactive substances. Various nanomaterials have been explored to improve bactericidal and fungicidal efficiency. Consequently, the search for new antimicrobial agents is a major challenge for modern medicine. The development and fabrication of antibacterial and antifungal yet biocompatible surfaces are still a challenge. Thus investigations will open up new possibilities for the production of cost-effective, scalable, and biologically safe implants with strong bactericidal activity for future applications in the orthopedic field and the field for the struggle against hospital infections.

Acknowledgments The work was supported by Rospotrebnadzor. F.S.Y. was supported by the State Assignment 0104-2019-0024 to Research Center of Biotechnology RAS.

References

- Azam A, Ahmed AS, Oves M, Khan MS, Memic A (2012) Size-dependent antimicrobial properties of CuO nanoparticles against Gram-positive and -negative bacterial strains. *Int J Nanomedicine* 7:3527–3535. <https://doi.org/10.2147/IJN.S29020>
- Chang EH, Harford JB, Eaton MAW, Boisseau PM, Dube A, Hayeshi R, Swai H, Lee DS (2015) Nanomedicine: past, present and future – a global perspective. *Biochem Biophys Res Commun* 468(3):511–517
- Chen JN, Sun L, Cheng Y, Lu ZC, Shao K, Li TT, Hu C, Han H (2016) Graphene oxide-silver nanocomposite: novel agricultural antifungal agent against *Fusarium graminearum* for crop disease prevention. *ACS Appl Mater Interfaces* 8(36):24057–24070. <https://doi.org/10.1021/acsami.6b05730>
- Chen J, Wu L, Lu M, Lu S, Li Z, Ding W (2020) Comparative study on the fungicidal activity of metallic MgO nanoparticles and macroscale MgO against soilborne fungal phytopathogens. *Front Microbiol* 11:365. <https://doi.org/10.3389/fmicb.2020.00365>

- Condell O, Iversen C, Cooney S, Power KA, Walsh C, Burgess C, Fanning S (2012) Efficacy of biocides used in the modern food industry to control salmonella enterica, and links between biocide tolerance and resistance to clinically relevant antimicrobial compounds. *Appl Environ Microbiol* 78(9):3087–3097
- Donlan RM, Costerton JW (2002) Biofilms: Survival mechanisms of clinically relevant microorganisms. *Clin Microbiol Rev* 15:167–193
- Donnellan S, Giardiello M (2019) Nanomedicines towards targeting intracellular Mtb for the treatment of tuberculosis. *Nanomedicine* 4(3). <https://doi.org/10.1002/jin2.61>
- Eleraky NE, Allam A, Hassan SB, Oma MM (2020) Nanomedicine fight against antibacterial resistance: an overview of the recent pharmaceutical innovations. *Pharmaceutics* 12:2. <https://doi.org/10.3390/pharmaceutics12020142>
- Elshaarawy RF, Janiak C (2014) Toward new classes of potent antibiotics: synthesis and antimicrobial activity of novel metallosaldach-imidazolium salts. *Eur J Med Chem* 75:31–42
- Etheridge ML, Campbell SA, Erdman AG, Haynes CL, Wolf SM, McCullough J (2013) The big picture on nanomedicine: the state of investigational and approved nanomedicine products. *Nanomedicine* 9(1):1–14
- Feray A, Szely N, Guillet E, Hullo M, Legrand F-X, Brun E, Pallardy M, Biola-Vidamment A (2020) How to address the adjuvant effects of nanoparticles on the immune system. *Nano* 10:425. <https://doi.org/10.3390/nano10030425>
- Firestein KL, Leybo DV, Steinman AE, Kovalskii AM, Matveev AT, Manakhov AM, Sukhorukova IV, Slukin PV, Fursova NK, Ignatov SG, Golberg DV, Shtansky DV (2018) BN/Ag hybrid nanomaterials with petal-like surfaces as catalysts and antibacterial agents. *Beilstein J Nanotechnol* 9:250–261
- Fursova OV, Potapov VD, Brouckov AV, Pogorelko GV, Griva GI, Fursova NK, Ignatov SG (2012) Probiotic activity of a bacterial strain isolated from ancient permafrost against *Salmonella* infection in mice. *Probiotics Antimicrob Prot* 4:145–153
- Garrett TR, Bhakoo M, Zhang Z (2008) Bacterial adhesion and bio-films on surfaces. *Prog Nat Sci* 18(9):1049–1056
- Gupta P, Sarkar S, Das B, Bhattacharjee S, Tribedi P (2016) Biofilm, pathogenesis and prevention—a journey to break the wall: a review. *Arch Microbiol* 198(1):1–15. <https://doi.org/10.1007/s00203-015-1148-6>
- Havlik D, Brandt U, Bohle K, Fleißner A (2017) Establishment of *Neurospora crassa* as a host for heterologous protein production using a human antibody fragment as a model product. *Microb Cell Factories* 16:128. <https://doi.org/10.1186/s12934-017-0734-5>
- Hwang GB, Huang H, Wu G, Shin J, Kafizas A, Karu K, Du Toit H, Alotaibi AM, Mohammad-Hadi L, Allan E, macRobert AJ, Gavriilidis A, Parkin IP (2020) Photobactericidal activity activated by thiolated gold nanoclusters at low flux levels of white light. *Nat Commun* 11:1207. <https://doi.org/10.1038/s41467-020-15004-6>
- Institute of Laboratory Animals Resources, Commission on Life Sciences, National Research Council (1996) National Academy Press, Washington, 138 p
- Ivanova EP, Hasan WHK, Truong VK, Watson GS, Watson JA, Baulin VA, Pogodin S, Wang JY, Tobin MJ, Löbbe C, Crawford RJ (2012) Natural bactericidal surfaces: mechanical rupture of *Pseudomonas aeruginosa* cells by cicada wings. *Small* 8(16):2489–2494
- Kalmantaeva OV, Firstova VV, Grishchenko NS, Rudnitskaya TI, Potapov VD, Ignatov SG (2020) Antibacterial and immunomodulating activity of silver nanoparticles in tuberculosis models on experimental mice. *Appl Biochem Microbiol* 56:226–232
- Kesarwani V, Kelly HG, Shankar M, Robinson KJ, Kent SJ, Traven A, Corrie SR (2019) Characterization of key bio–nano interactions between organosilica nanoparticles and *Candida albicans*. *ACS Appl Mater Interfaces* 11:34676–34687
- Marambio-Jones C, Hoek EMV (2010) A review of the antibacterial effects of silver nanomaterials and potential implications for human health and the environment. *J Nanopart Res* 12:1531–1551. <https://doi.org/10.1007/s11051-010-9900-y>
- Mateos J, Estévez O, González-Fernández Á et al (2020) Serum proteomics of active tuberculosis patients and contacts reveals unique processes activated during *Mycobacterium tuberculosis* infection. *Sci Rep* 10:3844

- Muhammad Q, Jang Y, Kang SH, Moon J, Kim WJ, Park H (2020) Modulation of immune responses with nanoparticles and reduction of their immunotoxicity. *Biomater Sci*. <https://doi.org/10.1039/C9BM01643K>
- Nasiruddin M, Neyaz K, Das S (2017) Nanotechnology-based approach in tuberculosis treatment. *Tuberc Res Treat* 1–12:4920209. <https://doi.org/10.1155/2017/4920209>
- Németh T, Sperandio M, Mócsai A (2020) Neutrophils as emerging therapeutic targets. *Nat Rev Drug Discov*. <https://doi.org/10.1038/s41573-019-0054-z>
- Oda Y, Kanaoka S, Sato T, Aoshima S, Kuroda K (2011) *Biomacromolecules* 12(10):3581–3591. <https://doi.org/10.1021/bm200780r>
- Parhi AK, Zhang Y, Saionz KW, Pradhan P, Kaul M, Trivedi K, Pilch DS, LaVoie EJ (2013) Antibacterial activity of quinoxalines, quinazolines, and 1,5-naphthyridines. *Bioorg Med Chem Lett* 23(17):4968–4974
- Permyakova ES, Polčák J, Slukin PV, Ignatov SG, Gloushankova NA, Zajíčková L, Shtansky DV, Manakhov AM (2018) Antibacterial biocompatible PCL nanofibers modified by COOH-anhydride plasma polymers and gentamicin immobilization. *Mater Des* 153:60–70
- Ponomarev VA, Sheveiko AN, Sukhorukova IV, Shvindina NV, Manakhov AM, Zhitnyak IY, Gloushankova NA, Fursova NK, Ignatov SG, Permyakova ES, Polčák J, Shtansky DV (2019a) Microstructure, chemical and biological performance of boron-modified TiCaPCON films. *Appl Surface Sci* 465:486–497
- Ponomarev VA, Shvindina NV, Permyakova ES, Slukin PV, Ignatov SG, Sirota B, Voevodin AA, Shtansky DV (2019b) Structure and antibacterial properties of Ag-doped micropattern surfaces produced by photolithography method. *Colloids Surf B: Biointerfaces* 173:719–724
- Rajamanickam A, Munisankar S, Dolla C, Menon PA, Nutman TB, Babu S (2020) Helminth coinfection alters monocyte. Activation, polarization, and function in latent *Mycobacterium tuberculosis* infection. *J Immunol* 204:1274–1286
- Saravanan M, Ramachandran B, Hamed B, Giardiello M (2018) Barriers for the development, translation, and implementation of nanomedicine: an African perspective. *Journal Interdisciplinary Nanomedicine* 3:106–110
- Seebach E, Kubatzky KF (2019) Chronic implant-related bone infections—can immune modulation be a therapeutic strategy? *Front Immunol* 10:1724. <https://doi.org/10.3389/fimmu.2019.01724>
- Shi SD, Hsueh PR, Yang PC, Chou CC (2020) Use of DosR Dormancy Antigens from *Mycobacterium tuberculosis* for Serodiagnosis of Active and Latent Tuberculosis. *ACS Infect Dis* 6:272–280
- Sterling TR, Njie G, Zenner D (2020) Guidelines for the treatment of latent tuberculosis infection: Recommendations from the National Tuberculosis Controllers Association and CDC. *MMWR Recomm Rep* 69(1): 1–1):11
- Sukhorukova IV, Sheveiko AN, Manakhov AM, Zhitnyak IY, Gloushankova NA, Denisenko EA, Filippovich SY, Ignatov SG, Shtansky DV (2018) Synergistic and long-lasting antibacterial effect of antibiotic-loaded TiCaPCON-Ag films against pathogenic bacteria and fungi. *Mater Sci Eng C* 90:289–299
- Suresh DA, Wang PW, Moon J-W, Gu B, Mortensen NP, Alison DP, Joy DC, Phelps TJ, Doktycz MJ (2010) Silver nanocrystallites: biofabrication using *Shewanella oneidensis*, and an evaluation of their comparative toxicity on Gram-negative and Gram-positive bacteria. *Environ Sci Technol* 44(13):5210–5215
- Velu R, Calais T, Jayakumar, Raspall F (2020) A comprehensive review on bio-nanomaterials for medical implants and feasibility studies on fabrication of such implants by additive manufacturing technique. *Materials (Basel)* 13(1):pii: E92. <https://doi.org/10.3390/ma13010092>
- Wollenberg K, Harris M, Gabrielian A, Ciobanu N, Chesov D, Long A, Taaffe J, Hurt D, Rosenthal A, Tartakovsky M, Crudu V (2020) A retrospective genomic analysis of drug-resistant strains of *M. tuberculosis* in a high-burden setting, with an emphasis on comparative diagnostics and reactivation and reinfection status. *BMC Infect Dis* 20:17. <https://doi.org/10.1186/s12879-019-4739-z>

Chapter 3

Enzymatic Tissue Biotests (MAO and AChE Biotests) and Bioindicators



Arkadii Yustianovich Budantsev and Victoria Vladimirovna Roshchina

Abstract A review of results in the development of biosensor systems and biotests using enzyme tissue preparations is presented. Three types of sensory systems are considered:

1. Tissue sections and homogenates of the rat liver, which have high monoamine oxidase activity (MAO, monoamine O₂ oxidoreductase, EC 1.4.3.4). The analytical range for tryptamine, serotonin, tyramine, dopamine, and noradrenaline is 10⁻⁴–10⁻² M. The indicator biotests can be used for the determination of biogenic monoamines in solutions, inhibitors, and promoters of MAO (e.g., for the primary screening of pharmacological compounds affecting the activity of MAO).
2. Tissue samples with high acetylcholinesterase activity (AChE, KΦ 3.1.1.7). The sensitivity of the AChE test for the tested inhibitors is shown to be for eserine and neostigmine ~10⁻⁵ M.
3. Whole plants (apical root meristem, etc). A system for using the Allium test for determining cytostatics in pharmacology and ecology is developed. We studied blocking mitoses in the S-phase of the cell cycle by amethopterin (methotrexate). The developed biotests may be used in the system of primary screening of various natural and artificial compounds in ecology, pharmacology, and biosafety.

Keywords Tissue biotests · MAO biotest · AChE biotest · Root meristem · Allium test · Test bioprobes (plant cells)

A. Y. Budantsev (✉)

Institute of Theoretical and Experimental Biophysics Russian Academy of Sciences, Pushchino, Russia

V. V. Roshchina

Institute of Cell Biophysics, Federal Research Center, Pushchino Scientific Center for Biological Research of Russian Academy of Sciences, Pushchino, Russia

Nomenclature

ACh	Acetylcholine
AChE	Acetylcholine hydrolase
AntiChEs	Anticholinesterase activity
BCh	Butyrylcholine
BChE	Butyrylcholinesterase
ChE	Cholinesterase
DTPDD	2,2-Dithio-bis-(p-phenyleneazo)-bis-(1-oxy-8-chlorine-3,6)-disulfur acid
Fast Red TR	4-Chloro-2-methylbenzenediazonium salt (or 4-chloro-2-methylaniline hydrochloride)
MAO	Monoamine: oxygen oxidoreductase

3.1 Introduction

In 1978, an article by G. Rechnitz entitled “Biochemical Electrode using tissue slice” was published in the journal *Chemical & Engineering News* (v. 56, 9 Okt., h.16). This article was the first to describe the possibility of using sections of mammalian tissue as a biosensor. G. Rechnitz used a system consisting of a thin layer of bovine liver and a purified urease preparation immobilized on the membrane of an ammonia gas-sensitive electrode to determine arginine. In 1979, G. Rechnitz created a “tissue biosensor” using sections of mammalian tissue as a biocatalytic element of an electrochemical biosensor. A few years later, reviews about tissue biosensors were published (Arnold 1986; Terner et al. 1992).

Biosensor devices (electrodes), in which crude enzymes (enzyme preparations) are used in the form of cell populations, tissue sections and immobilized microorganisms, etc., “tissue biosensors,” have a number of advantages and disadvantages.

Among the advantages, the following can be noted: (1) There is no need to carry out complex and expensive procedures for the isolation and purification of enzymes (commercial pure enzymes are extremely expensive). (2) The enzymes (and cofactors) in tissue preparations are in a natural immobilized state, especially in the case of membrane-bound enzymes and in a natural biochemical environment. (3) In the case of using living cells (cell culture) and especially microorganisms, biosensor electrodes can be regenerated by immersing them in a nutrient medium.

These advantages make it possible to develop inexpensive biosensors with a sufficiently long term of use.

However, tissue biosensors have disadvantages: (1) low selectivity due to the presence of a number of impurities in the enzyme preparations that can catalyze side reactions, (2) often slowly working tissue biosensors due mainly to the diffusion of substrates into cells and products of enzymatic activity from cells, and (3) low rate of electrode surface regeneration for the next measurement.

The noted advantages and disadvantages are not absolute, and in each case, the disadvantages do not turn out to be limited when choosing a strategy for developing a tissue biosensor, and the advantages may not be so winning.

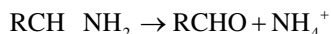
Another group of bioanalytical systems, “tissue bioindicators,” is small-cell, simple animals and lower plants, living cells, and organs of plants and animals that have specific reactions to external physicochemical effects (Budantsev 2012a, b).

This chapter presents the results of studies related to the processing of biosensors, test systems based on tissue pre-preparations of monoamine oxidase (MAO; monoamine:oxygen oxidoreductase, deamination, KF 1.4. 3.4), and acetylcholinesterase (AChE, acetylcholine hydrolase KF 3.1.1.7). Also, the results of a study of some tissue bioindicators have been summarized.

3.2 Tissue Biotests

3.2.1 Tissue Biotest for Monoamines (MAO Biotest)

In various animal tissues, a high activity of monoamine oxidase (MAO; monoamine:oxygen oxidoreductase, deamination, K Φ 1.4. 3.4) was found, that at deamination of catecholamines and indolamines in the aqueous medium connected with the formation of ammonium ions:



MAO is a membrane-bound enzyme of the outer mitochondrial membranes. Many methods have been described for determining the activity of MAO, among which one of the most convenient is associated with determining the concentration of ammonium using an ion-selective ammonium electrode (Meyerson et al. 1978). Another variant of the electrochemical biosensor using purified MAO preparations (and liver mitochondrial homogenate) and a pH electrode allows one to determine millimoles of tyramine, serotonin, and benzylamine (Balcere et al. 1989).

It is known that the animal liver contains high MAO activity (Budantsev and Guryanova 1975); therefore, to develop the MAO biotest, we used slices, homogenate, and rat liver lyophilizate fractions. Slices of rat liver (Wistar line) were prepared in a cryostat at a temperature of 15–20 ° C. The thickness of the slices is 20–50 microns. Cellulose matrices (9 mm in diameter) were used to immobilize the liver and enzyme section.

The MAO activity level in the biotest was determined by Nessler’s reagent (optical density of the reaction product was 400 nm). It was shown that in a biotest with a diameter of 9 mm, the MAO activity (substrate – tryptamine) is 59 ± 2.9 nmol $NH_3/45$ min/biotest or 77 nmol NH_3 /mg protein /45 min. The average protein content in one biotest is about 760 mcg. To analyze the MAO inactivity in the biotest, a color reaction (drop analysis) with nitro blue tetrazolium (HCT) was used (Glenner

and Burthner 1957; Budantsev and Zharikova 1976). Reflectometric measurements were carried out on a special device (Budantsev et al. 1995).

Reflectometry analysis showed that the sensitivity of the biotest for catecholamines (cofamine, tyramine, and norepinephrine) is 5×10^{-4} mol/l and for indolamines (tryptamine and serotonin) $(2-3) \times 10^{-4}$ mol/l. Histamine is not deaminated when using the MAO biotest. Fifty percent MAO activity = test persists for 3 months (Budantsev et al. 1997).

MAO inhibitors are widely used in experimental biology and medicine (Gorkin 1981; Finberg and Yodim 1983; Gorkin and Ovchinnikova 1993). It is known that a number of antidepressants are MAO inhibitors (Pare 1976; Mashkovsky et al. 1983). Various pharmacological, biochemical, and physiological methods are used for the primary pharmacological screening of antidepressants (Mashkovskiy et al. 1983). Table 3.1 shows the results of the measurement of the activity of MAO tests with placebo and some MAO inhibitors. Lyophilized rat liver homogenate was used as an enzyme preparation of MAO.

Figure 3.1 shows the kinetics of the formation of NH_4^+ at deamination of tyramine, dopamine, tryptamine, and serotonin. The substrate activity with respect to the MAO biotest decreases in the following order: tyramine > dopamine > tryptamine > serotonin (Budantsev 1991).

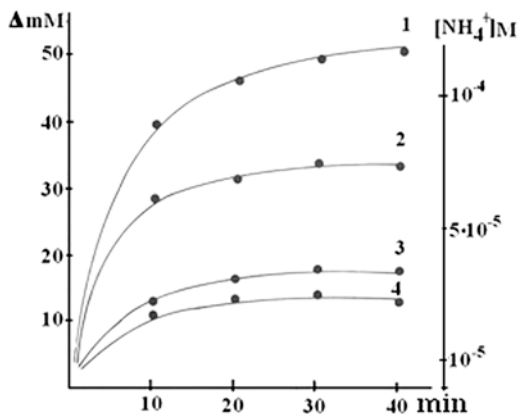
The formation of NH_4^+ linearly depends on the thickness of the section of the liver (tissue mass) in the range 25–125 μm (5–25 mg of tissue) with a 20-min incubation. The nonlinearity observed in the range of 125–200 μm (25–40 mg of tissue)

Table 3.1 Results of the reflectometric measurement of the activity of MAO tests

Substance	Concentration mM	Im	Ie	R
Buffer		$0.80 \pm 0.01(6)$	$0.54 \pm 0.04(8)$	1.49 ± 0.11
NaCl	3.4	$0.83 \pm 0.01(6)$	$0.58 \pm 0.03(8)$	1.43 ± 0.07
KCl	2.7	$0.84 \pm 0.05(2)$	$0.58 \pm 0.07(4)$	1.45 ± 0.19
$\text{CdCl}_2 \cdot 5\text{H}_2\text{O}$	0.7	$0.81 \pm 0.01(2)$	$0.53 \pm 0.03(2)$	1.51 ± 0.08
H_3BO_3	3.2	$0.86 \pm 0.04(2)$	$0.53 \pm 0.02(2)$	1.62 ± 0.09
BaCO_3	1.0	$0.83 \pm 0.02(2)$	$0.44 \pm 0.00(2)$	1.89 ± 0.04
Ficoll	0.5	$0.82 \pm 0.01(2)$	$0.59 \pm 0.04(4)$	1.40 ± 0.09
Heparin	0.2	$0.83 \pm 0.02(2)$	$0.61 \pm 0.07(4)$	1.37 ± 0.20
Ipranioside	0.7	$0.81 \pm 0.01(6)$	$0.77 \pm 0.02(10)$	1.05 ± 0.03
Chlorhilin	0.6	$0.82 \pm 0.05(2)$	$0.76 \pm 0.01(4)$	1.07 ± 0.06
Pargilin	1.0	$0.82 \pm 0.03(2)$	$0.78 \pm 0.02(4)$	1.05 ± 0.04
Nialamide	0.7	$0.81 \pm 0.03(2)$	$0.73 \pm 0.03(4)$	1.12 ± 0.06
CuSO_4	0.8	$0.88 \pm 0.02(2)$	$0.78 \pm 0.01(2)$	1.12 ± 0.04
NH_4OH	2.8	$0.89 \pm 0.02(2)$	$0.75 \pm 0.05(4)$	1.19 ± 0.08
Acridine Orange	0.7	$0.59 \pm 0.01(2)$	$0.75 \pm 0.01(2)$	0.79 ± 0.01
Sodium-dodecyl sulfate	0.7	$0.90 \pm 0.01(2)$	$0.76 \pm 0.03(2)$	1.18 ± 0.04
8-Oxydroxy-quinoline	1.4	$0.79 \pm 0.03(2)$	$0.43 \pm 0.02(2)$	1.82 ± 0.09

Abbreviations: $R = \text{Im} / \text{Ie}$, Where Ie is the reflection value of the biotest after the color reaction of biotest after inhibitors, and Im is the reflection of the pure biotest

Fig. 3.1 Kinetics of the formation of NH_4^+ as a result of deamination of tyramine (1), dopamine (2), tryptamine (3), and serotonin (4)



is apparently associated with an increase in the diffusion barrier for substrates and the release of NH_4^+ ions from the tissue.

The data showed that all the tested main specific MAO inhibitors gave positive results with the MAO test ($K = 1.05$ – 1.12 ; for placebo and buffer, the value $K = 1.43$ – 1.49). In addition, copper sulfate and sodium dodecyl sulfate had an inhibitory effect on MAO activity ($K = 1.12$ and 1.18), which is consistent with the data obtained by modifying the activity of copper ions and solubilization with ionic detergents during MAO purification (Gorkin 1976). The inhibitory effect on the MAO test of hydroxylamine ($K = 1.19$) and acridine orange ($K = 0.79$), with the interaction with MAO cofactor, is well known (Gorkin 1981), although the color with acridine orange changes the spectral properties of MAO test. It did not give a positive result of 8-hydroxyquinoline, the inhibitory effect of which on MAO is well known (Gorkin 1981).

3.2.2 Tissue Biotest for Inhibitors of Acetylcholinesterase (AChE Biotest)

The diameter of the cellulose matrices for AChE biotest is 8 mm. Acetone powder of an electric organ *Electrophorus electricus* (Sigma, E2384), cryostat sections, and lyophilization of the *nuc. caudatus* (rat brain) were used as a tissue source of ACh in biotests (for details of preparation, see Budantsev 2012a).

To determine the AChE activity in the homogenate, the Ellman method was used in modification with an alcohol solution of 5,5'-dithiobis-2-nitrobenzoic acid (DTNB) (Ellman et al. 1961; Gorun et al. 1978).

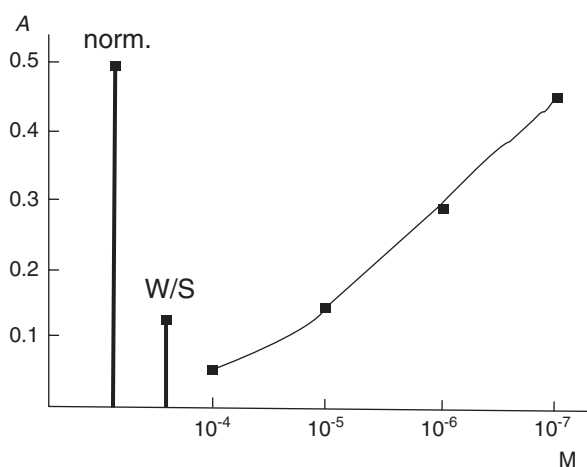
The ferry-ferrocyanide reaction (Karnowsky and Roots 1964) was used for photometric analysis of AChE test ($\lambda = 480$ nm) (Budantsev 1999, 2004; Budantsev and Budantseva 2005).

Table 3.2 The results of a study of the action of inhibitors on AChE activity in a biotest

Experience conditions	$M \pm m$ (n = 9)	% activity**	P
Control incubation	$0.142 \pm 0.004 D_{ci}^*$	100	
Incubation without substrate	$0.047 \pm 0.002 D_{ws}$		<0.01
Ezerin 10^{-4} M	$0.060 \pm 0.003 D_{inh}$	13.7	<0.01
Ezerin, 1×10^{-5} M	0.095 ± 0.005	50.5	<0.01
Ezerin, 1×10^{-6} M	0.151 ± 0.004	109.5	н/д
Neostigmine, 1×10^{-4} M	0.059 ± 0.002	12.63	<0.01
Neostigmine, 1×10^{-5} M	0.066 ± 0.002	20	<0.01
Neostigmine, 1×10^{-6} M	0.104 ± 0.002	60	<0.01

Note: * – reflected coefficient $D^* = \log(S_0 / S_i)$, where S_0 is the “brightness” of the test before the action of the tested compounds and S_i is the “brightness” of the tests after incubation with the test compound (“brightness” values of biotest images on a scale of 256 gray gradations); ** – % activity = $[(D_{inh} - D_{ws}) \times 100] / (D_{ci} - D_{ws})$

Fig. 3.2 The optical density (A) of AChE tests after the action of the inhibitor (MicroReader4 photometer, special tablet). Designations: norm, AChE activity in control; w/s, incubation without substrate; 10^{-4} – 10^{-7} M, the concentration of eserine; the difference between the D values is significant with $P < 0.001$ (except for 10^{-7} M eserine)



Three AChE inhibitors were used: eserine (eserine hemisulfate, Sigma), neostigmine (neostigmine methyl sulfate) in a final concentration of 10^{-6} – 10^{-4} M, and sanguinarine chloride (Sigma, S5890) in a concentration of 10^{-4} – 10^{-3} M. The test results are shown in Table 3.2. The sensitivity of the AChE test for the tested inhibitors is shown to be for eserine and neostigmine 1×10^{-5} M.

The AChE activity in the homogenate of the acetone powder of the tissue of an electric eel organ is $118 \mu\text{mol}$ of thiocholine/min/g of powder. After 3 months of storing the biotests at room temperature, the AChE activity in one matrix was $19.8 \mu\text{mol}$ thiocholine/min, i.e., 70% of the initial activity ($28.3 \mu\text{mol}$ thiocholine/min).

The results of the measurement of AChE activity in microplate photometry are shown in Fig. 3.2. Reliably, you can measure the effect of eserine in the range of 10^{-4} – 10^{-6} M, which coincides with the results given above.

A number of bioassays based on the enzymes AChE and butyrylcholinesterase (BChE) are known. For example, biotests are based on cellulose matrices and puri-

fied AChE from erythrocytes of bovine blood (Fleisher et al. 1955), flounder (Badilevska et al. 1983), and human (Aptukhin et al. 1991). In other embodiments, chemical polymer matrices with AChE preparations from the brain and BChE from blood plasma and from horse blood serum were used (Halamek and Tusarova 1994, etc.). In the above works, various methods of staining the final reaction products were used and mainly a visual assessment of the reaction of biotests to test substances – organophosphorus and carbamate pesticides and medicinal compounds. The detection limit of these compounds varied in the range of 10^{-3} mg/ml– 10^{-8} (10^{-9}) M of phosphorus-organic pesticides (chlorophos, etc.). Comparative characteristics of AChE active biotests and other biosensor systems for the determination of AChE inhibitors, in particular pesticides, are given in several review articles (Evyugin et al. 1999, 2002).

In our experiments, acetone powder of fish electric organs/homogenate of rat brain tissue and cryostat sections from brain regions with high AChE activity (*nuc. caudatus*) was used for the development of biotests. According to our data, using the developed biotests and the used detection method (ferry-ferrocyanide reaction), it is possible to reach the detection limits of AChE inhibitors of the order of 10^{-6} – 10^{-5} M. (Budantsev 2001). The developed biotest and detection system can be used for primary screening of AChE inhibitors and reactivators in pharmacology, ecology, biological resource science, etc. It is necessary to note the simplicity of the technology and low material costs in the manufacture of AChE biotests based on tissue enzyme preparations.

Of interest is the work in which a tablet photometer was used to determine the effect of organophosphorus compounds on the activity of AChE. In one case, the Ellman reaction was carried out directly in the cells of the tablet, and photometric analysis was performed. In other works, in the cells of a standard tablet, “solid solutions” of cholinesterase were prepared using N-phthaloylchitosan, and a tablet test was obtained for 96 samples (Prokopov et al. 1992).

The use of 96-cell tablets and tablet photometers is a convenient and fast way for quantitative photometric analysis of the reactions of chemical tests and biotests made based on paper materials. Proprietary tablet photometers are equipped with the necessary software and tablet scanning systems, which allow not only single-wave but also multi-wave photometric analysis. This will increase the accuracy of the analysis.

3.3 Bioindicator Tests (Plant Tissues)

3.3.1 Bioindicators for Cytostatics (*Allium Test*)

In 1989, a report by the International Commission for Protection against Environmental Mutagens and Carcinogens was published on tests for the detection of mutagenic and carcinogenic chemicals (Guide 1989). Among the recommended

tests, the report contains an *Allium* test, which was first recommended for analysis of cytostatics in 1985 at the suggestion of the Swedish Academy of Sciences (Fiskesj 1985, 1995; Fiskesj and Levan 1993). It was known that cytostatics block the primary growth of *Allium cepa* roots (Truchaut and Deysson 1964; Deysson 1968).

The *Allium* test involves an analysis of the effects of chemical compounds and physical factors on the growth of the roots of *Allium cepa* onions. Currently, the test is widely used to analyze the effects of many harmful environmental factors: organic compounds, heavy metals, radionuclides, etc. (Arambasic et al. 1995; Liu et al. 1995; Sinevits et al. 2009).

Methotrexate

Here we cite as an example the use of the *Allium* test to analyze the effect of methotrexate, a well-known cytostatic agent. Methotrexate is used to treat cancer and autoimmune diseases (Samuilov 2001; Nasonov 2005; Perevodchikova 2005; Nevezhaj et al. 2006).

The experiments were carried on the bulbs of *Allium cepa* of the first year of development (Stuttgart rizen, Holland). Bulbs were germinated for 24 hours in tap water, at a temperature of +24 °C, in the dark, until the appearance of roots 7–10 mm long. Then the bulbs were transplanted into a six (or ten) canal installation, where the main experiments with methotrexate were carried out.

The inhibitory effect of methotrexate is manifested during the first 30 min (concentration 2×10^{-7} M) and persists for several days after washing methotrexate (Table 3.3).

During incubation with roots in the spectra of the incubation solution, changes are observed, apparently indicating metabolic destruction of methotrexate in the process of interaction with the onion root system. Cytological analysis showed that under the influence of methotrexate, the root apex meristem cells undergo strong degenerative changes characteristic of programmed cell death (Budantsev 2013a, b; Budantsev and Kutysenko 2014).

Table 3.3 The effect of different concentrations of methotrexate on root growth

Time of experiments	Control		Methotrexate (M)			
	1 (n = 5)	2 (n = 5)	$2.2 \cdot 10^{-6}$ (n = 5)	$2.2 \cdot 10^{-7}$ (n = 5)	$2.2 \cdot 10^{-8}$ (n = 5)	$2.2 \cdot 10^{-9}$ (n = 5)
0 hour*	13.2 ± 0.5**	15.1 ± 0.3	13.7 ± 0.7	11.8 ± 0.2	14.1 ± 0.2	16.1 ± 0.6
After 28.5 h	27.9 ± 1.7	27.9 ± 1.4	13.5 ± 0.7	14.1 ± 0.3	16.9 ± 1.2	30.7 ± 1.7
After 52.5 h	37.6 ± 1.0	34.2 ± 0.6	13.6 ± 0.3	13.5 ± 0.6	18.9 ± 1.4	41.3 ± 0.7
After 78 h	52.8 ± 1.3	51.0 ± 0.6	11.6 ± 0.4	13.0 ± 0.5	19.5 ± 1.3	51.8 ± 0.7

Note: * – beginning of the experiment; ** – root length in mm; *** – the growth of roots relative to the “zero” time (n is the number of measurements)

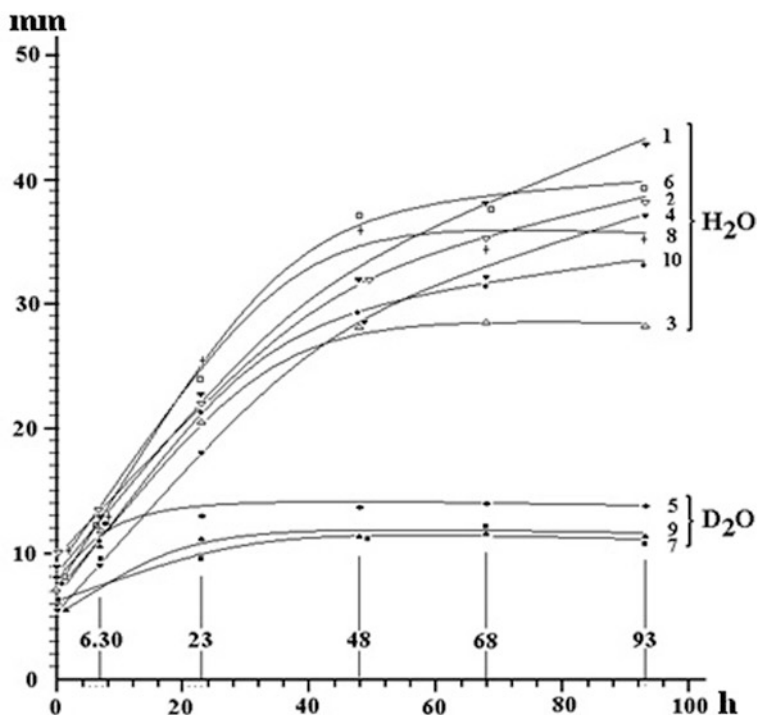


Fig. 3.3 Growth curves of onion roots in “light” and “heavy” water. The ordinate axis is the length of the roots, and the abscissa axis is the growth times

Heavy Water (D₂O)

The root growth curves in H₂O and D₂O are shown in Fig. 3.3. It is seen that in heavy water there is an irreversible halt to root growth. After incubation in heavy water, roots transferred to light water did not resume growth. In addition, the incubation in heavy water stopped the growth of the upper green parts of the plant.

There is evidence that the transfer of some algae and bacteria to heavy water by 70–100% leads to “isotopic suspended animation” with or without growth arrest, but is always accompanied by a change in the dynamics of mitoses (Goldovsky 1961; Roginsky and Shnol 1963). An unambiguous conclusion about the anabiotic nature of stopping root growth in heavy water cannot be drawn from our data, but analysis of the “crushed” samples revealed a strong weakening of mitotic activity in the apex of roots growing in heavy water (Budantsev et al. 2010; Budantsev et al. 2012).

3.3.2 *Living Plant Cells as Bioindicators*

Many living plant cells are used to test various chemical compounds: for example, the famous *Tradescantia* stamen filament cells (a chain of large single cells with high metabolic activity), the epidermis of the succulent onion bulb leaves (cell monolayer), and the double layer of cells – the *Elodea* leaf.

It is known that epidermal cells of succulent bulb leaves are used as a test to determine the toxic effect of herbicides (Beuret and Pont 1987), stamen filaments of *Tradescantia* are highly sensitive to ionizing radiation and heavy metals (Osipova and Shevchenko 1984; Evseeva and Geraskin 2001), and others. Interesting studies were performed in studying the effects of various chemical fixatives on plant hair cells, for example, basal cells from tomato petiole hairs (Mersey and McCully 1978), pumpkin hairs, etc. (Braune et al. 1967).

Elodea Leaf

In recent years, *Elodea* has been widely used as a biotest in the environmental monitoring of water pollution, mainly by heavy metals and radionuclides (Olette et al. 2008; Ipatova and Dmitrieva 2009). We performed a detailed quantitative morphological analysis of both layers of cells and cells of the central vein of the leaf blade (Budantsev and Kornilova 2011; Budantsev 2012b).

Tradescantia Stamen Hair Cells

Tradescantia hair cells have unique properties that respond to various mutagenic effects: radiation, chemical mutagens, mignite fields, etc. (Ichikawa et al. 1969; Evseeva and Geraskin 2001). In connection with this, they are widely used as test objects in radiobiology and ecology (Osipova and Shevchenko 1984, etc.).

The mutagenic effect on the flowers of *Tradescantia* leads to a change in the color of the flower scaffolds, as well as a change in morphological parameters: the appearance of “giant cells”; a change in the direction of hair growth, including bifurcation of the hair (normally the hairs will represent linearly connected cells); a change in the pigment content; the appearance of unpainted cells; etc. Several types of morphological violations of the structure of the hair cells of *Tradescantia* under mutagenic influences were identified (Underbrink et al. 1970) (Fig. 3.4).

Changes in the sequence of arrangement of cells in the hair (bends, branching) and cell sizes are considered as morphological anomalies connected not only with mutations but also with the physiological state of cells (Evseeva and Geraskin 2001).

We have shown high variability in the morphological parameters of cells in three regions of the hair: the basal, middle, and apical parts, which must be taken into account when using these cells as biotests for mutagens (Budantsev et al. 2018; Budantsev 2019a, b).

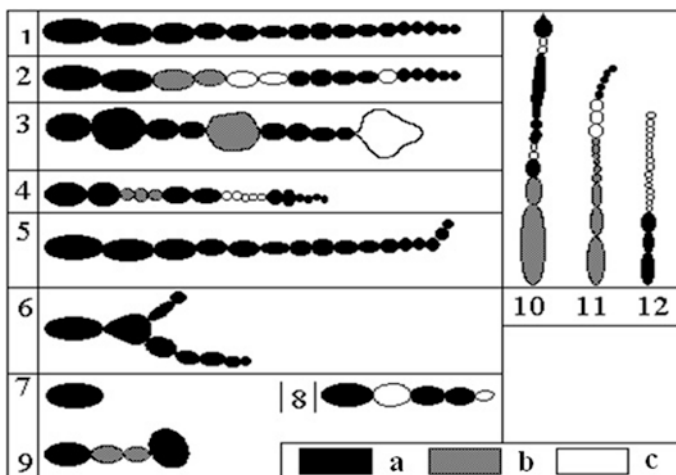


Fig. 3.4 Types of violations in the hairs of stamens of the *Tradescantia*. 1, normal hair; 2, pink and colorless cells; 3, giant cells; 4, dwarf cells; 5, curving hair; 6, branched hair; 7–9, hairs with stunted growth; 10–12, some complex combinations of cell types; (a) blue, (b) pink, (c) colorless hair

3.4 Test Bioprobes for Inhibitors of Cholinesterases

Some similar experiments with coloring on cholinesterase activity were demonstrated on female bract cells of hop *Humulus lupulus* and alga *Chara vulgaris*.

Some authors applied azo dye Fast Red TR salt (4-chloro-2-methylbenzenediazonium salt (or 4-chloro-2-methylaniline hydrochloride)) for determination of spot (band) of ChE reacting with β -naphthyl acetate as substrate in gel electrophoresis (Harris et al. 1962) or bacteria analysis (Kakariari et al. 2000).

For the experiments connected with the observation of ChE activity in algae cells, we used dye Fast Red TR which in the presence colorless α - or β -naphthyl acetate colors in red (Kakariari et al. 2000). All experiments on cholinesterase activity were performed at temperatures 20–22 °C. Samples of the slide flooded in optimal for hydrolytic reaction substrate concentrations (10^{-3} M β -naphthyl acetate (0.05 ml) dissolved in 0.05 M potassium phosphate buffer pH 7.25–7.5. Enzyme activity was estimated by incubation of algae sample with α - or β -naphthyl acetate.

First histochemical research for coloration of ChE in animal cells has been based on the color reactions with some azo compounds (Menten et al. 1944; Nachlas and Seligman 1949). The histochemical staining was also used for plant cells and isolated organelles (Roshchina 2018). The main mechanisms of the dye Fast Red TR salt staining and β -naphthyl acetate as substrate are based on the transfer of the colorless object to red color. Some experiments are done with coloring on ChE of worm planarians that also release the enzyme from the body to river water (Roshchina et al. 2019).

Pretreatment with ChE inhibitors neostigmine and physostigmine (10^{-6} – 10^{-4} M, 20–30 min) shows the inhibition of enzyme activity in the sample. The most complete inhibition of coloring was observed at concentrations 10^{-4} M, as described in the work of Fluck and Jaffe (1974). The images of the cells were analyzed under transmitted light of luminescence microscope Leica DM 6000 B. The absorbance intensity was measured in three to four samples of algae body per one variant. Results are shown graphically as upper horizontal lines on the figure histograms, $P = 0.95$.

Staining with dye Fast Red TR salt for the ChE assay demonstrated the red coloration of algae cells after the exposure with the colorless substrate (Fig. 3.5). The red color is seen in the thick cellular wall and in plasmalemma as well as in excretions in regimes of transmitted light of the microscope. Its appearance was prevented by the cholinesterase inhibitors neostigmine and physostigmine. After the preliminary exposure of the samples with the inhibitors, the evidence of the ChE activity is confirmed by the decrease or lack of coloration like it is illustrated for neostigmine (Fig. 3.5). By spectrophotometer, the changes in the absorbance at 560 nm have been registered on the algae body (Fig. 3.5). Besides the effects with Fast Red TR salt, we stained the samples with DTPDD reagent (named 2,2-dithio-bis-(p-phenyleneazo)-bis-(1-oxy-8-chlorine-3,6)-disulfur acid in form of sodium salt or Red analogue of Ellman reagent) if used acetylthiocholine as a substrate (Roshchina et al. 1994, 2019). Unlike the variant with Fast Red, the blue product formed on the surface of the cells was lesser noticed by the eye under the microscope due to the intensive bluish-green native color of the algae.

Among the species of *Characeae*, the cholinesterase activity was found only in *Nitella* (Dettbarn 1962). Earlier location of the cholinesterase in the plasmalemma of cells from some terrestrial species has demonstrated with electron microscopy (Fluck and Jaffe 1974; Gorska-Brylass and Smolinski 1992) or usual light micros-

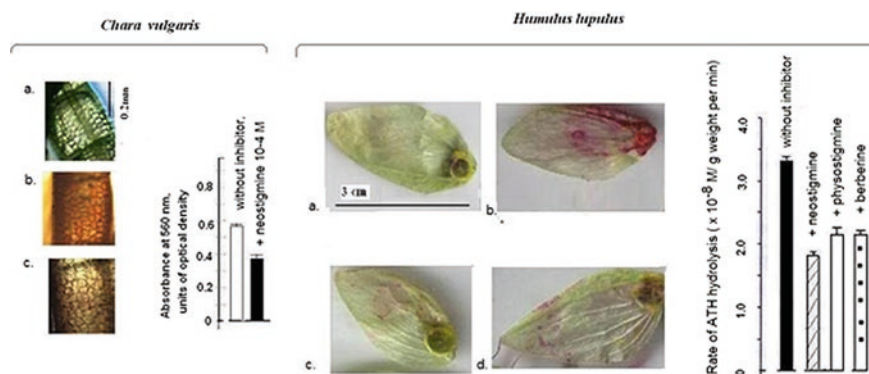


Fig. 3.5 The cellular cholinesterase reactions of algae *Chara vulgaris* and female bract of hop *Humulus lupulus* with Fast Red TR salt. Left, images of the histochemical staining and right – spectrophotometric data. (a) Without any treatment; (b) red color in the reaction with β -naphthyl acetate; (c) or (d) with preliminary treatment 15 min with inhibitors neostigmine and physostigmine 10^{-4} M

copy after vital coloration with azo dyes such as DTPDD (Roshchina et al. 1994; Roshchina 2001). The presence of ChE as a marker of ACh on the surface and excretions of *C. vulgaris* shows the possibility of the algae communications with other water organisms (both animals and plants) which are able to release this neurotransmitter (biomediator).

The recent possible role of plant systems including neurotransmitters such as ACh has been discussed for terrestrial allelopathic relation (Sharma and Gupta 2019). In this way, cells of algae *Chara vulgaris* may serve as a suitable model in ecology for the analysis of contacts between various living inhabitants of water biocenosis due to secretions of neurotransmitters contacting with biosensors such as cholinergic receptors as well as cholinesterase (Roshchina 2019) that directly relates to allelopathic interactions.

We stained the samples with DTPDD reagent (Red analogue of Ellman reagent) if used acetylthiocholine as a substrate (Roshchina et al. 1994, 2019). Unlike the variant with Fast Red, the blue product formed on the surface of the cells was lesser noticed by the eye under the microscope due to the intensive bluish-green native color of the algae. Unlike algae, the cells of female bract of hop demonstrated in equal degree coloring both by Fast Red TR salt and DTPDD reagent. Cells of *Chara* and hop may serve as suitable models for testing various factors on ChE.

The ChE activity is determined in the presence of various natural organic and inorganic compounds, among which are allelochemicals (alkaloids, terpenes, phenols) and reactive oxygen species ozone and peroxides.

Plants release excretions that may influence animal and plant ChE activity. The most significant inhibitory effect was observed for steroidal, bisbenzylisoquinoline, norditerpenoid, and triterpenoid alkaloids (Atta-Ur-Rahman et al. 2000, 2001, 2002, 2004a, b). In the experiments with water extract from horsetail (*Equisetum arvense*) microspores and pollen of *Hippeastrum hybridum* as models having cholinesterase activity, known allelochemicals such as alkaloids berberine, glaucine, sanguinarine, and others inhibited the acetylthiocholine hydrolysis (Budantsev and Roshchina 2004, 2007). However, unlike AChE of eel, maximal inhibition was observed at concentrations 10^{-7} – 10^{-5} M for variants with glaucine (70–75%), but lesser with sanguinarine (30–50%), whereas with berberine, physostigmine, and neostigmine it was not higher, 20–30%. About 20–30% rate of the acetylthiocholine hydrolysis was inhibited by the animal ChE inhibitors such as physostigmine and neostigmine (Augustinsson 1963). Therefore, the activity of microspores with pure ChE was also approximately 20–30%. In drastic inhibition, by glaucine and sanguinarine, the activity of nonspecific esterase also depressed. The main mechanism of the ChE inhibition may be through binding with the anionic center of the enzyme (quarternary nitrogen atom), as shown for protoberberine and benzophenanthridine alkaloids (Ulrichova et al. 1983). The effects of alkaloids were compared with the action of natural inorganic reactive oxygen forms such as ozone and peroxides (Budantsev and Roshchina 2007). Ozone and peroxides (as active oxygen species formed in living cells at normal and at allelopathic relations (Roshchina and Roshchina 2003) decreased the rate of acetylthiocholine hydrolysis by 20–30%.

The sensitivity of the ChE of microspores to allelochemicals analyzed may be also estimated from the comparison of I_{50} (a concentration of the inhibitor, which decreases the rate of the enzyme synthesis by 50% of the control). Among the studied compounds, the highest sensitivity to neostigmine has been observed. The rutin-like phenolic compound, flacosid from *Phellodendron amurense*, also inhibits the cholinesterase activity, at higher concentrations. Organic peroxide *tert*-butyl hydroperoxide and alkaloid physostigmine were equally effective in similar concentrations (Budantsev and Roshchina 2007). To compare the cell sensitivity, pollen grains of *H. hybridum* were most sensitive than vegetative microspores of *E. arvense*, because the effect of inhibitor is observed at lower concentrations.

Sharma and Gupta (2019) did experiments and summarized information for substances with an anticholinesterase activity (antiChEs) in weeds. It has been shown that weeds are rich in inhibitors of ChE both plants and animals. Leaves and roots/tubers of the weeds were tested for the presence of antiChEs. Most weeds tested inhibited AChE from both animal (Eel AChE) and plants (tomato and wheat AChE). From ethanolic extract of roots of 45 weeds analyzed, 12 showed 100% and 27 showed 50% inhibition of the enzyme from the animal source, while methanolic extract of leaves of 30 weeds showed 50% inhibition and 17 weeds showed 100% inhibition of enzyme from the same source. Anticholinesterases from roots of 14 weeds showed 50% inhibition of AChE from wheat and weeds like *Bidens biternata*, *Coronopus didymus*, *Prosopis juliflora*, *Ricinus communis*, *Verbascum chinense*, and *Veronica agrestis* and completely inhibited the enzyme. Leaf extract of 75% of these weeds inhibited the wheat AChE by more than 50%, and 15 weeds caused complete inhibition of the enzyme. The root extract of the weeds tested showed more than 50% inhibition of AChE from tomato leaves. Sharma and Gupta (2007) showed that excretions *Cyperus rotundus* inhibited AChE from animal and plant sources and inhibited germination and seedling growth in wheat and tomato. Many antiChEs from plants like galanthamine (Turi et al. 2014), juglone (Hejl and Koster 2004), pinene, and 1,8-cineole (Savelev et al. 2003) are established allelochemicals.

3.5 Conclusion

Currently, a global problem has been designated under the collective name “bio-safety,” which includes the following main areas.

1. *Environmental issues.* Ecological biomonitoring is a big complex task in identifying, assessing, eliminating, and, most importantly, preventing environmental disasters of anthropogenic nature, natural origin, or associated with mismanagement. The biomonitoring of especially dangerous territories in which there is a chemical production, storage areas for pesticides, including chemical warfare compounds, is of great importance.

2. *Health problems.* Quality control of pharmacological preparations, food products, and physicochemical conditions of work and life of different population groups.
3. *Problems of biological resource science.* Studying the safety of the animal and vegetable raw materials for the production of food additives, perfumes, means of disease prevention, etc.
4. *The fight against terrorism,* especially in cases where chemical agents are used for terrorist acts. The study of the means of forensic analysis of crimes is also of great importance in this direction.

To solve these problems, it is necessary to search and study analytical tools that allow selectively and with high sensitivity to determine various chemical compounds that pose an increased danger to humans: environmental pollution (pesticides, salts of heavy metals, etc.), cytostatics, psychotropic compounds, drugs and narcotic drugs, etc. For these purposes, you can use test methods, whose place in chemical analysis has long been formulated (Zolotov 1997).

A new aspect of the influence on cholinesterase activity connects with the chemical interactions between various organisms – allelopathy. Many plant excretions contain inhibitors of the enzyme, which also are allelochemicals. Weeds enriched in most allelochemicals may act on plant growth through the mechanism of the inhibition of ChE activity.

Biosensor and bioindicator tests represent one of the classes of analytical systems for solving biosafety problems. Tissue biosensors and bioindicators are the simplest tests that can be effectively used for a *primary screening system* for physicochemical effects that threaten biosafety.

References

- Apukhtin V, Bezzubov I, Yu M, Nikolaeva M, Samokish V, Statsevich V (1991) Anticholinesterase pesticide detection matrix action. A.S. 1701749, Bull Inv N 48:4
- Arambasic M, Bjelic S, Subakov G (1995) Acute toxicity of heavy metals (copper, lead, zinc), phenol and sodium on *Allium cepa* L., *Lepidium sativum* L. and *Daphnia magna* St. – comparative investigation and the practical applications. Water Res 29:497–503
- Arnold M (1986) Potentiometric sensors using whole tissue sections. Ion-Sel Electr Rev 8:85–113
- Atta-Ur-Rahman FN, Akhtar F, Choudhary M, Khalid A (2000) New norditerpenoid alkaloids from *Aconitum falconeri*. J Nat Prod 63:1393–1395
- Atta-Ur-Rahman PS, Khalid A, Farooq A, Choudhary M (2001) Acetyl and butyrylcholinesterase-inhibiting triterpenoid alkaloids from *Buxus papillosa*. Phytochemistry 58:963–968
- Atta-Ur-Rahman A, Choudhary M, Tsuda Y, Sener B, Khalid A, Parvez M (2002) New steroidal alkaloids from *Fritillaria imperialis* and their cholinesterase inhibiting activities. Chem Pharm Bull 50:1013–1016
- Atta-Ur-Rahman A, Atia-Tul-Wahab NS, Choudhary I (2004a) New cholinesterase inhibiting bis-benzylisoquinoline alkaloids from *Cocculus pendulus*. Chem Pharm Bull 52:802–806
- Augustinsson KB (1963) Classification and comparative enzymology of the cholinesterases and methods of their determination. In: Cholinesterases and Anticholinesterase Agents. (Ed G.B. Koelle). Handbuch der Experimentale Pharmacologie. Springer-Verlag: Berlin, 15: 89–128

- Atta-ur-Rahman FF, Naem I, Zaheer-ul-Haq NS, Khan N, Khan R, Choudhary M (2004b) New pregnane-type their steroidal alkaloids from *Sarcococca saligna* and cholinesterase inhibitory activity. *Steroids* 69:735–741
- Badilevsku F, Bogoda P, Clobanie O (1983) Paper-indicateur pour la detection de substances organophosphoriques inhibiteurs de cholinesterase. Pat RO 82028, GOI 31/22
- Balcere D, Grinberg B, Prikulis A, Nikolskaya E, Yagodina O (1989) A method for the quantitative determination of biogenic monoamines. *Discover Invention* 40:130 (rus)
- Beuret E, Pont V (1987) Un biotest simple pour mettre en evidence l'action des herbecides sur la membrane plasmique. *Rev Suisse Vitic Arboric Hortic* 19:323–328
- Braune W, Lemman A, Taubert H (1967) Pflanzenantonomisches praktikum, vol 60. VEB Gustav Fischer Verlag, Jena, pp 67–68
- Budantsev A (1991) Biosensor for catecholamines with immobilized MAO in tissue sections. *Analytica Chim Acta* 249:71–76
- Budantsev A (1999) Methods of histochemical analysis of acetylcholinesterase activity (AChE histochemistry for fifty years). *Neurochemistry* 16:103–117
- Budantsev A (2001) Enzymatic biosensors in neurochemistry. *Neurochemistry* 18:75–79
- Budantsev A (2004) Photometric determination of substances in paper matrices using digital recording of images of matrices in transmitted light. *Zhurn Anal Chem* 59:791–795
- Budantsev A (2012a) Bioindication. *Palmarium Academic Publ, Saarbrucken*, 137 p
- Budantsev A (2012b) Elodea “Atlas of leaf micromorphology” State Educational Portal of the Ministry of Education and Science of the Russian Federation Electronic atlas. <http://www.informika>, Single window for access to educational resources
- Budantsev A (2013a) The Allium test: injection of test compounds into the bulb. *Biotech Histochem* 88:323–328
- Budantsev A (2013b) The growth of roots and green leaves of *Allium cepa* L. after the remove different parts of bulb. *Am J Plant Sci* 4:972–975
- Budantsev A (2019a) The effect of the Bowen fixative on the morphology of hair cells of stamens filaments of *Tradescantia* (morphometric analysis). *Cytology* 61:1–5
- Budantsev A (2019b) The effect of formaldehyde and Clark's fixative on the morphology of hair cells of stamens filaments of *Tradescantia* (morphometric analysis). *Cytology* 61:1–6
- Budantsev A, Budantseva T (2005) Photometric analysis of paper tests using microplate photometers. *Zhurn Anal Chem* 60:794–797
- Budantsev A, Guryanova A (1975) Monoamine oxidase Usp. *Mod Biol* 79:184–204
- Budantsev A, Kornilova O (2011) Morphometric analysis of Elodea leaf cells (*Elodea canadensis* Michx.). *Basic Res (rus)* 7:192–195
- Budantsev A, Kutysenko V (2014) Measurement of the dynamics of root growth using the Allium test. *Basic Res (rus)* 6:1393–1396
- Budantsev A, Roshchina V (2004) Testing alkaloids as acetylcholinesterase activity inhibitors. *Farmatsiya (Moscow)* 5:37–39
- Budantsev A, Roshchina V (2007) Chapter 11. Cholinesterase activity as a biosensor reaction for natural allelochemicals: pesticides and pharmaceuticals. In: Roshchina VV, Narwal SS (eds) *Cell diagnostics. Images, biophysical and biochemical processes in allelopathy*. Science Publisher/Taylor and Francis Group, Enfield, Jersey/Plymouth, pp 127–146
- Budantsev A, Zarikova A (1976) On the method of Glenner for the histochemical demonstration of the MAO. *Histochemistry* 48:335–345
- Budantsev A, Zhiromsky V, Kovaleva M, Litvinva E (1995) Reflective photometry of indicator biotests (IBT) for biogenic amines. *Opt Technol* 1:11–15
- Budantsev A, Litvinova E, Kovaleva M (1997) Indicator paper on biogenic amines. *Zhurn Anal Chem* 52:539–542
- Budantsev A, Uversky V, Kutysenko V (2010) Analysis of the metabolites in apical area of *Allium Cepa* roots by high resolution NMR spectroscopy method. *Protein Pept Lett* 17:86–91
- Budantsev A, Molchanov M, Kutysenko V, Ivanitsky G (2012) From fragments to morphogenesis: NMR spectroscopy of metabolites in onion root apex. *Doklady Russ Acad Sci* 442:828–832

- Budantsev A, Demyanov A, Pogorelova M (2018) Micrometric analysis hair cells of stamens filaments *Tradescantia*. *Cytology* 60:653–658
- Dettbarn WD (1962) Acetylcholinesterase activity in *Nitella*. *Nature*. 194: 1175–1176
- Deysson G (1968) Antimitotic substances. *Int Rev Cytol* 24:99–148
- Ellman G, Courtney K, Andres V, Featherstone R (1961) A new rapid colorimetric Determination of acetylcholinesterase activity. *Biochem Pharmacol* 7:88–95
- Evsheeva T, Geraskin S (2001) Combined effect of factors of radiation and non-radiation nature on *tradescantia*. Ural Branch of the Russian Academy of Sciences, Ekaterinburg, p 156
- Evyugin G, Budnikov G, Nikolskaya E (1999) Biosensors for the determination of enzyme inhibitors in the environment. *Success Chem (rus)* 68:1142–1167
- Evyugin G, Budnikov G, Nikolskaya E (2002) Biochemical tests based on stabilization preparations of cholinesterases – new approaches. *J Anal Chem (rus)* 57:1127–1132
- Finberg J, Youdim M (1983) Monoamineoxidase. In: Lajtha A (ed) *Handbook of neurochemistry*, vol 4, 2nd edn, New York/London, pp 293–313
- Fiskesj G (1985) The Allium-test as a standard in environmental monitoring. *Hereditas* 102:99–112
- Fiskesj G (1995) The Allium-test. In: O'Hare S, Atterwill C, Totowa N (eds) *Methods in molecular biology*. Ch. 43. *In vivo* toxicity testing protocols. Humana Press Inc, pp 119–127
- Fiskesj G, Levan A (1993) Evolution of the first ten MEIC chemicals in the Allium test. *ATLA* 21:139–149
- Fleisher J, Spear S, Pope E (1955) Stable cholinesterase preparations at laboratory standards of activity. *Anal Chem* 27:126
- Fluck R, Jaffe M (1974) Cholinesterases from plant tissues VI Distribution and subcellular localization in *Phaseolus aureus* Roxb. *Plant Physiol* 53:752–758
- Glenner G, Burchner H (1957) The histochemical demonstration of monoamine oxidase activity by tetrazolium salts. *Histochem Cytochem* 5:591–602
- Goldovsky A (1961) *Anabiosis*, 1st edn. Science, Leningrad (rus)
- Gorkin V (1976) Monoamine oxidase inhibitors and the transformation oxidases. In: *Monoamine oxidase and its inhibition*, Ciba foundation symposia 39. Elsevier, Amsterdam, pp 61–79
- Gorkin V (1981) *Aminoxidases and their importance in medicine*. Moscow, Medicine (rus)
- Gorkin V, Ovchinnikova L (1993) The aminoxidase system: modern advances in the study of nature, functions and their disorders. *Questions Honey. Chemistry* 39:2–10
- Gorska-Bryllass A, Smolinski DJ (1992) Ultrastructural localization of acetylcholinesterase activity in stomata of *Marchantia polymorpha* L. *Electron Microscopy* 3:439–440
- Gorun V, Proinov I, Baltescu V, Balaban G, Barzu O (1978) Modified Ellman procedure for assay of cholinesterases in crude enzymatic preparations. *Anal Biochem* 86:324–326
- Guide to short-term tests for the detection of mutagenic and carcinogenic chemicals. Hygienic criteria for the state of the environment (1989). Geneva: WHO 51: 212
- Halamek E, Tusarova I (1994) Biosensor for detection of distinguishing between cholinesterase inhibitors. WO 94/05808, C12N 11/12, patent No 02143617
- Harris H, Hopkinson D, Robson E (1962) Two-dimensional electrophoresis of pseudocholinesterase components in normal human serum. *Nature* 196:1296–1297
- Hejl A, Koster K (2004) Juglone disrupts root plasma membrane H⁺-ATPase activity and impairs water uptake, root respiration and growth in Soyabean (*Glycine max*) and Corn (*Zea mays*). *J Chem Eco* 30:453–471
- Ichikawa S, Sparrow A, Thompson K (1969) Morphologically abnormal cells, somatic mutations and loss of reproductive integrity in irradiated *Tradescantia* stamen hairs. *Radiat Bot* 9:195–211
- Ipatova I, Dmitrieva A (2009) Toxicity assessment of heavy metals using higher aquatic plants. *Ecol Syst Devices* 1:59–62 (rus)
- Kakariari E, Georgalaki M, Kalantzopoulos G, Tsakalidou E (2000) Purification and characterization of an intracellular esterase from *Propionibacterium freudenreichii* ssp *freudenreichii* ITG 14. *Lait* 80:491–501
- Karnovsky M, Roots L (1964) A direct colouring method for Cholinesterase. *J Histochem Cytochem* 2:219–221

- Liu D, Jiang W, Wang W, Zhai I (1995) Evolution of metal ion toxicity on root tip cells by the Allium test. *Israel J Plant Sci* 43:125–133
- Mashkovekiy M, Andreeva N, Polezhaev A (1983) *Pharmacology of antidepressants*. Moscow (rus)
- Menten M, Junge J, Green M (1944) A coupling histochemical azo dye test for alkaline phosphatase in the kidney. *J Biol Chem* 153:471–477
- Mersey B, McCully M (1978) Monitoring of the course of fixation of plant cells. *J Microsc* 114:49–76
- Meyerson L, McMurtrey K, Davis V (1978) A rapid and sensitive potentiometric assay for monoamine oxidase using an ammonia-selective electrodes. *Anal Biochem* 86:287–297
- Nachlas M, Seligman A (1949) The histochemical demonstration of esterase. *J Nat Cancer Inst* 9:415–425
- Nasonov E (2005) *Methotrexate. Prospects for use in rheumatology*. Filomatis, Moscow, p 196 (rus)
- Nevozhaj D, Budzynskaya R, Kan'skaya U, Yagello M, Boratyn'skay Y (2006) Modern ideas about the mechanism of antineoplastic action of methotrexate and resistance to it. *Pac Med J* 4:12–16
- Olette R, Couderchet M, Biagianti S, Eullaffroy P (2008) Toxicity and removal of pesticides by selected aquatic plants. *Chemosphere* 70:1414–1421
- Osipova R, Shevchenko V (1984) The use of *Tradescantia* (clones 02 and 4430) in studies of radiation and chemical mutagenesis. *J Gen Biol* 95:226–232 (rus)
- Perevodchikova N (2005) *Handbook an chemotherapy of cancers*. Practical medicine, 2nd edn. Moscow, 698 pp. (rus)
- Prokopov A, Svyatkovsky E, Nikolsky E, Kuzektsova L (1992) A.S. USSR number SU1745769 A1. BI No. 25 (rus)
- Rechnitz G, Arnold M, Meyerhoff M (1979) Bio-selective membrane electrode using slices. *Nature* 278:466–467
- Roginsky S, Shnol S (1963) *Isotopes in biochemistry*, 1st edn. USSR Academy of Sciences, Moscow (rus)
- Roshchina V (2001) Neurotransmitters in plant life. Science Pub L, Enfield, Plymouth, 283 p
- Roshchina V (2018) Cholinesterase in secreting cells and isolated organelles. *Biol Membr* (rus) 35:143–149
- Roshchina V (2019) Tools for microanalysis of the neurotransmitter location in plant cells. In: Ramakrishna A, Roshchina VV (eds) *Neurotransmitters in plants, perspectives and applications*. CRC Press, Boca Raton, pp 135–146
- Roshchina VV, Roshchina VD (2003) *Ozone and plant cell*. Kluwer Academic Press, Dordrecht/Boston/London, 267 pp
- Roshchina V, Melnikova E, Kovaleva L, Spiridonov N (1994) Cholinesterase of pollen grains. *Dokl Biol Sci* 337:424–427
- Roshchina V, Prizova N, Khaibulaeva L (2019) Allelopathy experiments with Chara algae model. Histochemical analysis of the participation of neurotransmitter systems in water inhabitation. *Allelopath J* 46:17–24. <https://doi.org/10.26651/alleleo.j/2019-46-1-1195>
- Samuilov V (2001) Programmed cell death in plants. *Soros Edu J* 10:12–17
- Savelev S, Okello E, Perry N, Wilkins R, Perry E (2003) Synergistic and antagonistic interactions of anticholinesterase terpenoids in *Salvia lavandulaefolia* essential oil. *Pharmacol Biochem Behav* 75:661–668
- Sharma R, Gupta R (2007) *Cyperus rotundus* extract inhibits acetylcholinesterase activity from animal and plants as well as inhibits germination and seedling growth in wheat and tomato. *Life Sci* 80:2389–2392
- Sharma R, Gupta R (2019) Role of acetylcholine system in allelopathy in plants. In: Ramakrishna A, Roshchina VV (eds) *Neurotransmitters in plants. Perspectives and applications*. CRC Press, Boca Raton, pp 243–270

- Sinovets S, Pyatkova S, Kozmin G (2009) Experimental substantiation of the use of the allium test in radioecological monitoring. News of Higher Educational Institutions. Nucl Energy 1:32–38 (rus)
- Terner E, Karube I, Wilson JN. (Eds.) (1992) Biosensors, Translate to Rus., Moscow, p 34
- Truhaut R, Deysson G (1964) Sur les propriétés animitotiques des antifoliques. Recherches à l'aide du test Allium. Biochem Pharmacol 13:1197–1207
- Turi C, Axwik K, Smith A, Jones A, Saxena P, Murch S (2014) Galanthamine, an anticholinesterase drug, effects plant growth and development in *Artemisia tridentata* Nutt. via modulation of auxin and neurotransmitter signalling. Plant Signal Behav 9. <https://doi.org/10.4161/psb.28645>
- Ulrichova J, Walterova D, Preininger V, Slavik J, Lenfeld J, Cushman M, Simanek V (1983) Inhibition of acetylcholinesterase activity by some isquinoline alkaloids. *Planta Medica* 48: 111–115
- Underbrink A, Sparrow L, Sparrow A, Rossi H (1970) Relative biological effectiveness of R- rays and 0.43-MeV monoenergetic neutrons on somatic mutation and loss of reproductive integrity in *Tradescantia* stamen hairs. Radiat Res 44:187–203
- Zolotov Y (1997) Chemical analysis without laboratories: test methods. Her Russ Acad Sci 67:508–513 (rus)
- Pare C (1976) Introduction to clinical aspects of monoamine oxidase inhibitors in the treatment of depression. Monoamine Oxidase and its inhibition. Ciba Foundation Symp, vol 39. Elsevier, Amsterdam, pp 271–296

Chapter 4

Is It Possible to Detect Less Than One Bacterial Cell?



Sergei Georgievich Ignatov, A. G. Voloshin, G. P. Bachurina,
S. Yu. Filippovich, and Ivan Alekseevich Dyatlov

Abstract It is generally accepted that the detection limit of bacterial cells using biosensors is one cell. The present chapter describes the specific visualization of bacterial nanofragments using atomic force microscopy (AFM). The development of new sensitive biosensor methods for the analysis of bacteria is a very important area in biotechnology. AFM is a form of scanning probe microscopy where a cantilever with a very sharp tip is periodically scanned across special surface with immobilized sample. AFM can also be used to measure forces between the tip and sample. The high-resolution imaging of living object is easily possible using AFM. AFM is a powerful, multifunctional imaging platform that allows to visualize and manipulate with biological samples from single molecules to living cells. An artificial nose is unique system for non-contact method for microbial detection. Using this approach, it is possible to detect bacterial “footstep,” even after removing bacteria from the assay medium. These two approaches can be used for detection of less than one bacterial cell.

Keywords Bacteria detection · Fiber-optic sensor · Artificial nose system · Volatile organic components · Atomic force microscopy · Bacterial nanofragments

S. G. Ignatov (✉) · A. G. Voloshin · I. A. Dyatlov
State Research Center for Applied Microbiology and Biotechnology,
Obolensk, Moscow Region, Russia
e-mail: ignatov@obolensk.org; dyatlov@obolensk.org

G. P. Bachurina · S. Y. Filippovich
Bach Institute of Biochemistry, Research Center of Biotechnology of the Russian Academy
of Sciences, Moscow, Russia
e-mail: syf@inbi.ras.ru

Nomenclature

AFM	Atomic force microscopy
CFU	Colony-forming unit
LB	Lysogeny broth
OD	Optical density
VOCs	Volatile organic components

4.1 Introduction

Recently, a computational live bacterial detection system has been developed based on periodical for capturing the coherent microscopy images of bacterial growth inside an agar plate and analysis of these time-lapsed holograms using deep neural networks for rapid detection of bacterial growth and classification of the corresponding species. This system can be used for the rapid detection of bacteria in physiological samples. Using pre-incubation of samples in growth media, this platform achieved a limit of detection of ~ 1 colony-forming unit (CFU)/L within 9 h of total test time (Wang et al. 2020). This automated and cost-effective live bacterial detection system can be changed and used for different applications in microbiology by significantly reducing the detection time and also automating the identification of colonies, without labeling or the need for an expert.

To date, numerous microbiological, chemical, and physical methods are used to identify bacteria. The use of light and electron microscopy helps to obtain visual images for the analysis of the microbial population (Kommnick et al. 2019), and X-ray photoelectron microscopy (Turishchev et al. 2019), infrared microscopy (Shi et al. 2019), contact angle (Pan et al. 2020), and electrophoretic mobility measurement (Kaundal et al. 2020) methods are also commonly used in microbiology. However, most of these methods require special preliminary sample preparation and cannot be used for native analysis. The artificial nose system is interesting for the analysis of pathogenic microorganisms. It avoids direct physical contact with microorganisms and explores only their volatile components. Using this method, it is possible to detect bacteria in samples without contact with bacterial material. Non-contact method for bacteria detection is very important during analysis of the samples with potentially pathogenic bacteria. The principle of bacterial detection is based on the headspace analysis of bacterial volatile organic components (VOCs) by an artificial nose system (Tilocca et al. 2020). Two methods for non-contact bacteria detection have been developed (Stitzel et al. 2002; Voloshin et al. 2010). First includes simple VOC analyzers (thermostatic and for continuous monitoring) developed for the detection of bacteria and fungi by analysis of the headspace of microbial cultures. Method is based on analysis of optical density (OD) spectra of solvent after pumping through the headspace of bacterial and fungal cultures. Principle possibility of using a simple modification of spectrophotometric method was shown for

the fast detection of microorganisms by VOC excreting in or absorbing from surrounding environment. In addition, this method allows to distinguish the *Neurospora crassa* mutants damaged in nitrogen metabolism from wild-type strain. It is obvious that *nit-2* and *nit-6* genes of the fungus are involved in VOC synthesis. The second method is connected with an artificial nose system based on high-density optical biosensor arrays. Porous silica microspheres with an incorporated environmentally sensitive fluorescent dye are employed in high-density sensor arrays to monitor fluorescence changes during sample vapor exposure. Classification accuracies and confusion matrices for experiment with bacteria and media for bacteria cultivation have shown the possibility of using artificial nose system based on fiber-optic system for bacteria identification.

In the recent years, new ways for probing bacterial cells have been opened in microbiology. Within the past 30 years, atomic force microscopy (AFM) has revolutionized the approach which microbiologists use for the study of the bacterial world (Viljoen et al. 2020). AFM is a scanning near-field tool invented in 1986 for nanoscale investigation (Binnig et al. 1986). A bacterial cell has a complex physicochemical structure of protein, lipid, and carbohydrate components. This organization determines its physicochemical interaction with various surfaces in physiological conditions or water. The unique ability of AFM to visualize such interactions in high resolution will help in understanding many microbiological processes. AFM can provide high-resolution images of the bacteria and their tiny organization.

The aim of the present chapter is to discuss the feasibility of determining bacterial traces using an artificial nose system and the possibility of specific determination of bacterial fragments using AFM.

4.2 Method for VOC Analysis of Bacteria and Fungi

Simple modification in a spectrophotometric method was proposed for the rapid detection of microorganisms based on their ability either to excrete or to absorb VOC (Voloshin et al. 2010). This method is based on analysis of OD spectra of solvent after pumping through the headspace of microbial cultures. The method provides the possibility of contactless control for bacterial growth at a concentration above 10^7 cells/ml.

The *Escherichia coli* and *Bacillus thuringiensis* strains were received from the museum of the State Scientific Center for Applied Microbiology and Biotechnology (Obolensk, Moscow Region), and the strains of *N. crassa* supplied by the Fungal Genetics Stock Center (Kansas City, USA) were used for analysis. Similarly, *wild-type (wt)-987 N. crassa* strain and the *nit-2* (defective in both nitrite and nitrate reductases) and the *nit-6* (lacking nitrite reductase) mutants were also used (Voloshin et al. 2010). The bacterial cultures of *E. coli* and *B. thuringiensis* were grown at 37 °C under aerobic conditions on a shaker at 200 rpm. The *N. crassa* mycelia were grown in the darkness at 28 °C with agitation at 200 rpm. In order to analyze VOC, the gaseous mixture from the headspace of the growth cultures of microorganisms

was pumped through 7.5 ml of water or ethyl alcohol, which was used as the solvent, by a Millipore Vacuum Pump 50 for 5 min at 5 l/min flow rate. Time of pumping was 5 min. The Millipore filters were used at the entrance (prior to air access to the flask containing the culture) and at the exit (before the vacuum pump) to prevent cross-contamination with a nonspecific microflora. The inoculated culture medium (LB and Vogel's) served as control. Thermostatic and continuous monitoring VOC analyzers have been developed for the bacteria and fungi determination by analysis of the headspace of microbial cultures (Fig. 4.1). The water or ethyl alcohol extracts of the gaseous mixtures collected from the headspaces of the microorganisms were placed into a 1 cm cuvette, and the OD of these solutions was measured at 210–350 nm (with a step of measurements 10 nm) using Genesys 10 UV-Vis spectrophotometer. Pure solvents were used as blanks.

Three classes of microorganisms were studied using this approach:

- Gram-negative bacteria (*E. coli*)
- Gram-positive bacteria (*B. thuringiensis*)
- Fungus (*N. crassa*)

For all of these microorganisms, the difference in OD spectra has been received in comparison with OD spectra of cultivation media. For bacterial cultivation, LB medium was used. For *N. crassa* cultivation, Vogel medium containing mineral salts, 2% sucrose, and biotin was used. Growth medium was modified – 4 mM ammonium chloride was used as the only source of nitrogen. It has been shown that:

- Minimal bacterial concentration for detection was 10^8 cells/ml
- The difference between OD spectra of bacterial VOCs for died bacteria (treated with NaN_3) and alive bacteria (without NaN_3) was revealed at 190 nm
- *E. coli* cells produced VOCs, which can be detected by our simple analyzer; *S. cirsi* cells could not produce enough VOCs for registration; *B. thuringiensis* cells can utilize VOCs as sources for their growth

An attempt to find the difference between the strains of ascomycete *N. crassa* with normal (*wild type*) and damaged nitrogen (*nit-2* and *nit-6*) metabolism using



Fig. 4.1 Simple system for analysis of microbial VOCs. To increase stability and sensitivity of the method, the flask with the sample has been placed to thermostat at 30 °C (1), and for continuous analysis of VOCs during cultivation, the flask with the sample has been placed to the shaker (2)

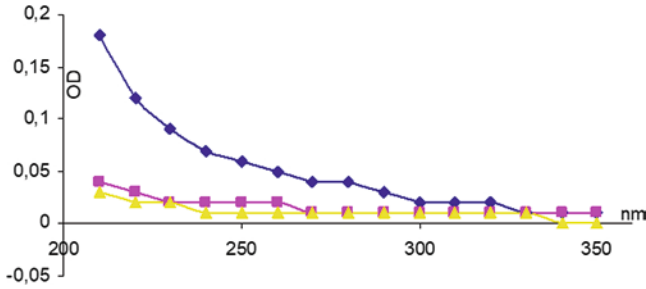


Fig. 4.2 VOCs OD spectra of wild type wt (□) and mutants *nit-2* (◆) and *nit-6* (△) *N. crassa* (24 h growth, 4 mM NH_4Cl as a nitrogen source)

system for analysis of VOC was performed. *nit-2* is a global regulatory gene of *N. crassa* coding nuclear protein positively influencing the expression of more than 100 genes connecting with the nitrogen metabolism of this fungus. *nit-6* is a structural gene of *N. crassa* coding nitrite reductase. Water and ethanol extracts of VOC after growth of submerged culture of different *N. crassa* strains were analyzed. The comparison of water extracts by system for analysis of VOC revealed the difference in OD between *N. crassa* wt strain and mutants with damaged nitrogen metabolism (Fig. 4.2). The OD of VOC water extracts in the range of 210–290 nm from the mycelia of the wt *N. crassa* was significantly higher than that for one of the mutants.

Thus, a significant difference between the wild strain of *N. crassa* and its mutants for nitrogen metabolism using this approach was shown. It can be assumed that this is due to a change in the composition of volatile components in cells with altered nitrogen metabolism.

4.3 Artificial Nose System for VOC Analysis of Bacteria

The second method for contactless bacterial detection uses an artificial nose system based on high-density optical biosensor arrays. An artificial nose is a universal system capable of detecting all kinds of volatile compounds. This method is used in sensory technology to detect and distinguish different bacterial cultures. The artificial nose was able to accurately distinguish between different live strains of bacteria; moreover, it also has ability to differentiate living and dead cells of the same bacterial strains (Stitzel et al. 2002). The detection of VOCs is the subject of growing interest in a wide range of applications, from environmental use to the food or chemical industries. VOC fiber-optic sensors have new benefits compared to standard gas analyzers (Elosua et al. 2006). In the matrices of high-density sensors, porous silica microspheres are used to monitor changes in fluorescence during exposure to sample vapors. Significant differences in signals from different bacteria and culture medium indicate the possibility of using this system to identify microorganisms. An artificial nose based on such sensor matrices is used to evaluate

numerous volatile compounds. Sensor elements consist of silica and polymer spheres (3–5 microns in diameter), which are stained with a special fluorescent dye adsorbed on the surface of the microsphere. These sensors respond to changes in the local polarity of the environment, shifting their fluorescence characteristics, thereby indicating the presence of various VOCs. Arrays of high-density microspheres containing thousands of individual sensor elements and several copies of each type of sensor were performed. By monitoring the temporal fluorescence responses of sensors using a charge-coupled camera, unique samples were recorded that identify individual analyte or characteristics of a complex mixture (Stitzel et al. 2002).

4.4 AFM Analysis of Bacterial Fragments

AFM is a form of scanning probe microscopy where a cantilever with a very sharp tip is periodically scanned across special surface with immobilized sample. AFM can also be used to measure forces between the tip and sample. The high-resolution imaging of living object is very attractive application of AFM. AFM is a powerful, multifunctional imaging platform that allows to visualize and manipulate with biological samples from single molecules to living cells (Dufrêne et al. 2017). The unique ability of AFM to obtain high-resolution images of bacteria and their structures under physiological conditions and without any type of labeling has opened new capabilities in microbiology. Recently, the single-cell-level AFM techniques enabled the quantification of adhesive forces between bacteria and substrate (Mittelviehhaus et al. 2019). Such opportunity opens up new possibilities for the study of bacterial biofilms too. Novel approaches in the fight against infectious diseases are caused by the understanding that the pathogens are organized in biofilms. Bacterial biofilms are structurally organized groups of microorganisms integrated in polymeric matrix which get attached to the biotic and abiotic surfaces. Nearly 80% of bacterial infections are associated with the existing biofilms. Bacterial biofilms are formed by communities that are embedded in a self-produced matrix of extracellular polymeric substances. Importantly, bacteria in biofilms exhibit a set of emergent properties that differ substantially from free-living bacterial cells (Flemming et al. 2016). Thus, understanding the mechanisms about the formation of bacterial biofilms and strategy of their disruption is very important in the fight against pathogens.

Imaging living bacterial cells with AFM is a serious problem. This problem arises from the relatively reduced adsorption forces of most living bacteria to the standard substrates used for AFM (such as glass or mica). Bacterial cells should be immobilized on the special surface before AFM analysis (Allison et al. 2011). Poly-L-lysine or gelatin modifications (Benn et al. 2019) or using cross-linking of carboxyl groups on the surface (Welch et al. 2017) are the most typical immobilization methods used for bacterial cells. There are other methods for immobilization: the physical entrapment of bacterial cells into polycarbonate filters (Andre et al. 2010) or micro-wells (Chen et al. 2014) or the use of specific substrate coatings (Longo

et al. 2013) or polyphenolic proteins (Meyer et al. 2010). The latest advances in AFM provide us with powerful tools to discriminate various types of different bacterial strains on the basis of their size and surface morphology (Soon et al. 2009). However, in the presence of a mixture of bacteria of various types, it is difficult to analyze images for the identification of bacteria. Surface modification of specific antibodies against bacteria leads to stronger binding of bacteria to the substrate and an increase in the sensitivity and specificity of studies (Welch et al. 2017). Immunological methods are widely used in microbiology to identify bacteria due to the high specificity of binding of antibodies to bacterial antigens. Standard methods for immobilizing antibodies to the surface are silanized layers, polymer membranes, and self-assembled monolayers (Ahluwalia et al. 1999). AFM imaging of antigen-antibody interaction is one of the few promising methods that could provide local information in liquids such as molecular conformations and their flexibility and their binding domains (Kominami et al. 2018). Immunoassay methods (radioimmunoassay, enzyme immunoassay, and surface plasmon resonance) are bioanalytical methods in which quantitation of analyte depends on its reaction with specific antibody. Thus, AFM is a powerful tool to detect in vitro antibody-antigen interactions.

For AFM, Gram-negative bacteria, (*E. coli* and *B. thuringiensis*) and their nano-sized fragments have been identified with immobilized films of antibodies on the surface (Dubrovin et al. 2012). For the investigation of specific binding of bacterial fragments with affine surface, the following structure of this surface is proposed: activated mica – protein G – antibody (Dubrovin et al. 2012). Activated glow discharge mica improves adsorption of protein G, which in turn increases the degree of adhesion of antibodies (due to specific binding). For correct choice of initial concentration of protein G, the authors have established experiments for the following values of concentration: 0.1, 0.6, and 3 mg/ml (Fig. 4.3). The thickness of formed protein G layer increases with the increase of the protein concentration in solution. Therefore, author used further the concentration in the range 0.1–0.6 mg/ml, which corresponds to the thickness of the layer up to 1.3 nm.

AFM images of mica surface modified with antibodies both in presence and in absence of protein G are presented in Fig. 4.4. The thickness of the total layer in the second case (Fig. 4.4b) is not the sum of the thicknesses of two layers in control images (Figs. 4.3b and 4.4a) but considerably lower. This is most probably connected with both mechanical action of the cantilever on protein surfaces and with possible redistribution of the layers during their interaction. The ability of surfaces, modified with the antibodies to *E. coli* or *Salmonella* spp., to bind the fragments of *E. coli* cells was visualized using AFM. From the AFM images presented in Fig. 4.5, it is clear that the number of nanofragments adsorbed by the “native” antibodies (i.e., to *E. coli*) is hundreds times higher than those adsorbed by the “alien” antibodies (i.e., to *Salmonella*). During preparation of the samples presented in Fig. 4.5, the exposer time of the surface to the bacterial nanofragments containing suspension was 3 min, and the volume of antigen solution was 5 μ l. The surface ceased effectively adsorbs antigen with concentration 10^7 cells/ml and lower. In order to detect lower concentrations of bacterial cells, the parameters of preparation of the

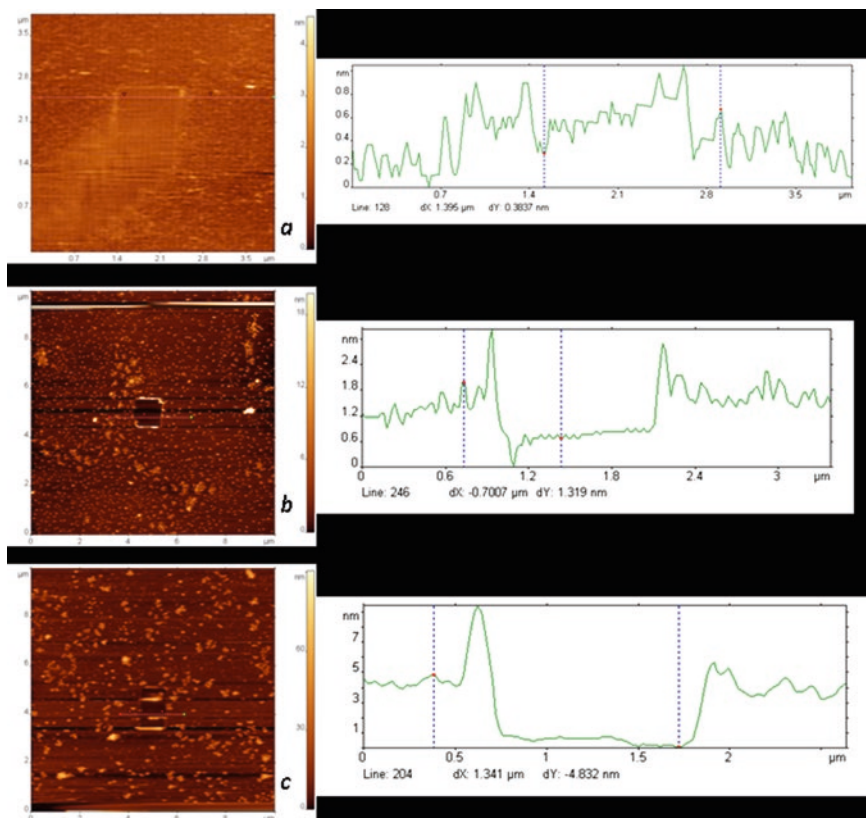


Fig. 4.3 AFM images of protein G layers deposited from the solution with concentration 0.1 (a), 0.6 (b), and 1 (c) mg/ml on a glow discharged modified mica surface

functional surface have to be adjusted. Thus, the procedure of the preparation of the functional surface has been modified as follows: at first freshly cleaved mica is modified in a glow discharge during 60 s (current 0.2 mA), followed by the exposition to a droplet (20 μl) of a protein G solution (0.6 mg/ml). After this, a mica plate is washed for 1 min in the droplet (50 μl) of distilled water and exposed to the antibody solution (0.1–0.2 mg/ml) for 10 min. Then the plate is washed once more for 1 min in water and is dried with a nitrogen flow.

The experiments were conducted with the *E. coli* and *Salmonella* spp. bacterial fragments and their antibodies. To perform the control experiments, authors exposed a mica surface modified with anti-*Salmonella* antibodies to suspension containing the *E. coli* fragments and conversely. In these cross-control experiments, the concentration of the cells in the suspension was made quite high, i.e., in the range of 10^6 – 10^8 cells/ml: in this case the absence of bacterial binding would be more convincing than for smaller concentrations of the bacterial cells. This method of preparation of biofunctional surface allows detecting the fragments of antigens with the

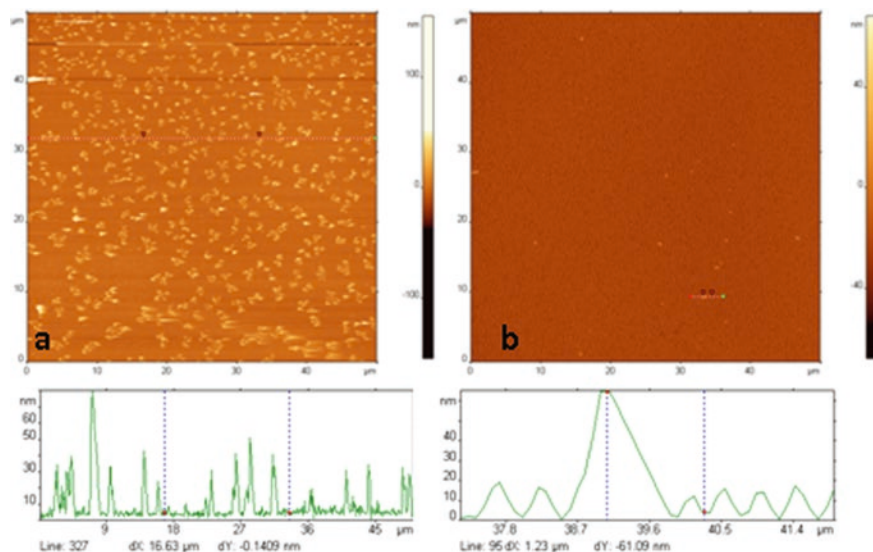


Fig. 4.4 AFM images of a glow discharged modified (0.2 mA, 60 sec) mica surface, (a) exposed to the solution (0.1 mg/ml) of monoclonal antibodies to *E. coli*, (b) exposed successively to the protein G solution (0.1 mg/ml), and then (after washing) to the solution (0.1 mg/ml) of monoclonal antibodies to *E. coli*. Image (b) is reproduced from [3] licensed under CC BY 3.0. Rotaviruses specifically bound to the film of correspondent antibodies formed on the basis of amphiphilic polyelectrolyte. Scan size is $3500 \times 3500 \text{ nm}^2$

concentration at least 10^4 cells/ml. The AFM images of the surfaces exposed to the antigen solution (10^4 cells/ml) are presented in Fig. 4.6. As in the previous experiment (Fig. 4.5), a considerable difference in the number of adsorbed bacterial nano-fragments is observed. Results of the analysis of the AFM images presented in Figs. 4.5 and 4.6 are showed in Figs. 4.7 and 4.8, respectively. The height distribution histograms of those samples, where bacterial fragments were exposed to a functional surface modified with “native” antibodies (Figs. 4.7a and 4.8a), showed a very broad maximum between 30 and 60 nm, whereas the control samples demonstrate the maximums at 20 nm and lower (Figs. 4.7b and 4.8b). After comparing these values with the values of the heights of bacterial fragments on mica, we can assume that in the second case (Figs. 4.7b and 4.8b) different impurity particles (that may present in the solution) rather than bacterial fragments are observed.

In some experiments, the step of surface modification with a protein G was skipped, and the antibodies were deposited directly on an activated mica surface. In Fig. 4.9, the AFM images of a mica surface activated in a glow discharge (current 0.4 mA) during 60 s, modified with the anti-*E. coli* antibodies, and then exposed into suspension containing the *Salmonella* cell fragments (10^7 cells/ml) (a) or to suspension containing the *E. coli* cell fragments (10^6 cells/ml) (b) for 10 min are presented. When the substrate was modified with the protein specific to an antigen (Fig. 4.9b), the AFM images reveal a large number of objects (several hundred per

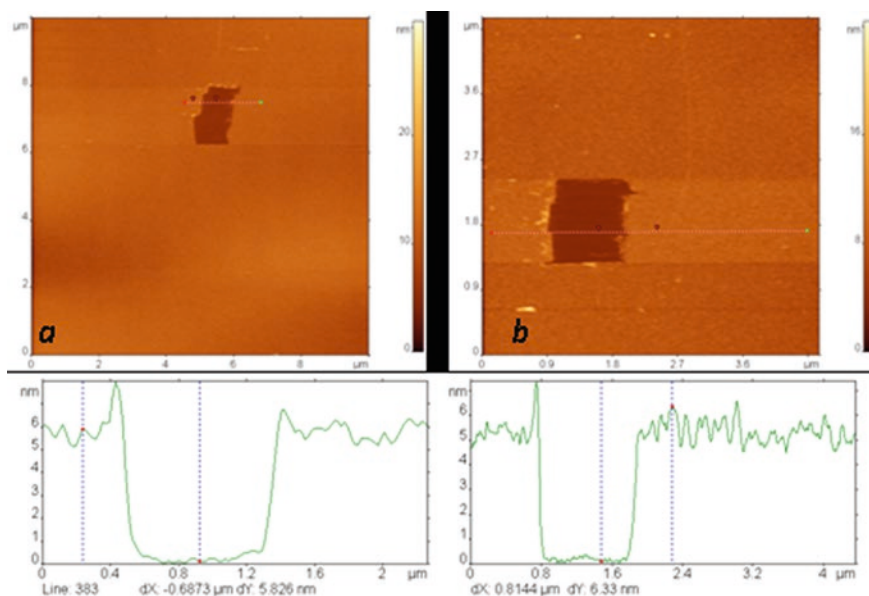


Fig. 4.5 AFM images of the surfaces modified with the antibodies to *E. coli* (a) and *Salmonella* (b) after their exposition to the suspension containing *E. coli* fragments (10^9 cells/ml)

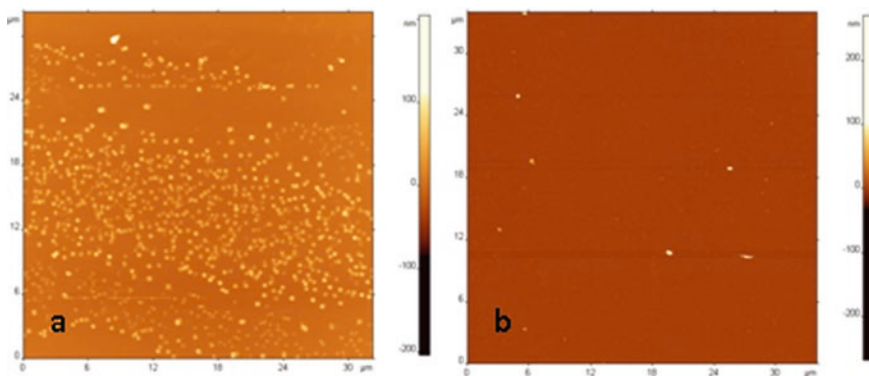


Fig. 4.6 AFM images of the surfaces modified with the antibodies to *E. coli* (a) and to *Salmonella* (b) after their exposition to suspension containing the *E. coli* cell fragments (10^4 cells/ml)

164 μm scan), whereas, for a nonspecific “antigen-antibody” pair, the surface is practically devoid of objects (Fig. 4.9a). The height distribution histogram of the *E. coli* cell fragments obtained from the AFM image in Fig. 4.9b is presented in Fig. 4.9c. The example shown in Fig. 4.9 demonstrates the possibility of the formation of a biofunctional surface without the use of protein G; however, in this case the specific adsorption is less effective, as can be seen from the comparison of the data presented in Fig. 4.9 and, for example, in Fig. 4.6. Lower specific adsorption for the

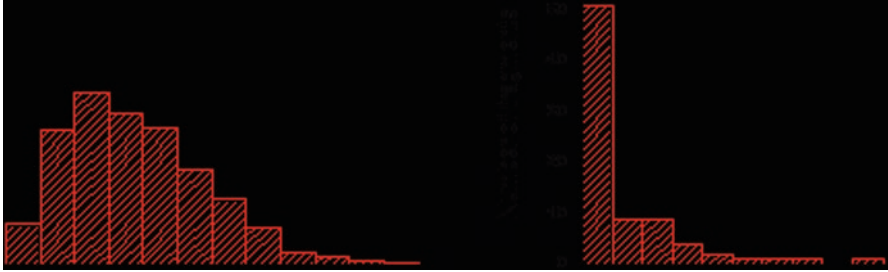


Fig. 4.7 AFM images of protein G layers deposited from the solution with concentration 0.1 (a), 0.6 (b), and 1 (c) mg/ml on a glow discharged modified mica surface. Statistical analysis of the bacterial fragments, presented in Fig. 4.5: the height distribution histograms (bottom) and the probabilities plot (top). (a) and (b) are described in the text

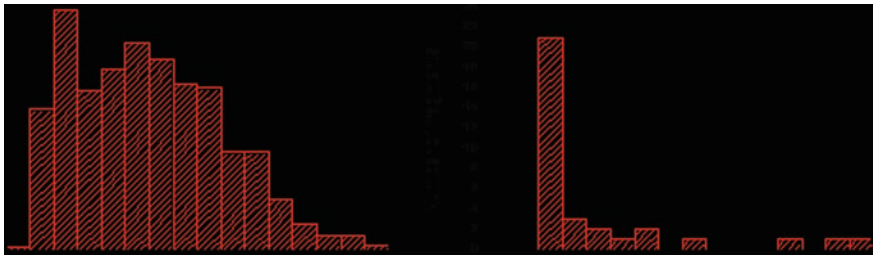


Fig. 4.8 Statistical analysis of the bacterial fragments, presented in Fig. 4.6: the height distribution histograms (bottom) and the probabilities plot (top). (a) and (b) are described in the text

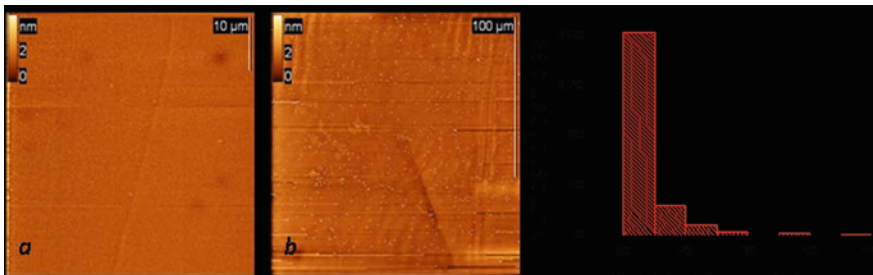


Fig. 4.9 AFM images of a mica surface activated in a glow discharge and modified with the anti-*E. coli* antibodies and then exposed for 10 min to (a) suspension containing the *Salmonella* cell fragments (10^7 cells/ml) and (b) suspension containing the *E. coli* cell fragments (10^6 cells/ml). The height distribution of the particles in the image (b) is presented in (c). The sizes of the AFM images are (a) $50 \times 50 \mu\text{m}^2$ and (b) $164 \times 164 \mu\text{m}^2$

functional surface prepared without the use of the protein G layer may be connected with a spontaneous orientation of the antibodies on a substrate. For the study of the possibility of AFM detection of bacteria taken in small concentrations using affine surfaces, the decreased concentration of antigen in the analyzed suspension was

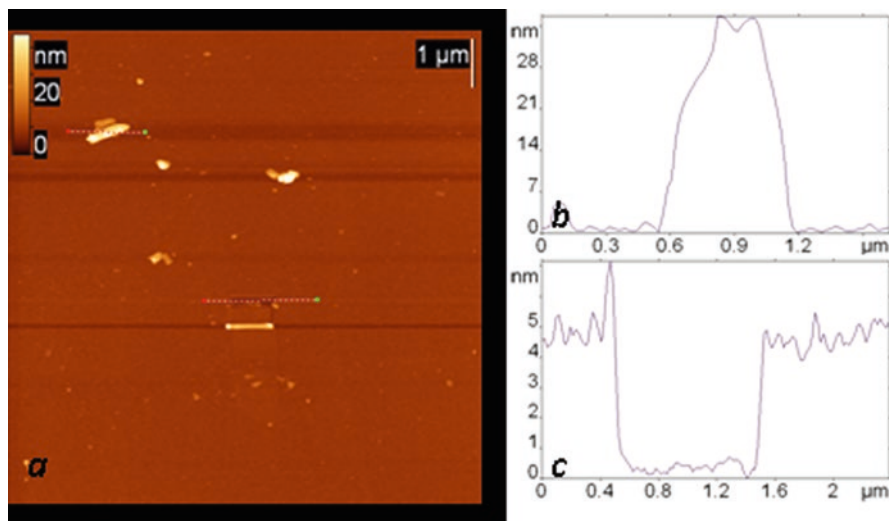


Fig. 4.10 AFM image of a mica surface activated in a glow discharge, modified with a protein G and anti-*E. coli* antibodies, (a) exposed during 10 min to suspension containing the *E. coli* cell fragments (10^2 cells/ml); (b) the cross section along the upper dotted line in the AFM image demonstrating the profile of the bacterial fragment; (c) the cross section along the lower dotted line in the AFM image demonstrating the result of scratching experiment

taken. Figure 4.10 represents the AFM image of a mica surface, activated in a glow discharge, modified with a protein G and the anti-*E. coli* antibodies, and after that exposed for 10 min to the suspension containing the *E. coli* cell fragments (10^2 cells/ml). The AFM image contains particles that may be attributed to the bacterial fragments. Figure 4.10b, c represent the cross sections along the upper and lower dotted lines in the AFM image. The upper cross section demonstrates the profile of the bacterial nanofragments, and the lower one describes the depth of the protein layer on a mica surface (protein G + antibody), whose integrity was disturbed by the AFM cantilever during a scratching experiment.

If to proceed decreasing the concentration of an antigen, its quantity becomes so small that the probability of even specific binding is very low. Therefore, it is necessary to elaborate an additional modification of the method of preparation of bio-functional surfaces with a bound antigen for effective detection of ultralow concentrations of antigen with AFM. For this purpose, it is necessary to increase the efficiency of specific binding and decrease the efficiency of nonspecific binding. To solve this issue, the method of an antigen deposition on a biofunctional surface was modified. Initially, antigen binding was carried out with a surface at the alkaline pH (8.2) and at the temperature $32\text{ }^\circ\text{C}$ that favor specific binding. After that, a washing was performed by the immersion of the substrate in the buffer followed by the rotation in the shaker for 10 min. This rinsing method should increase the efficiency of the removal of nonspecifically bound material from the surface due to additional hydrodynamic flows in the surface proximity.

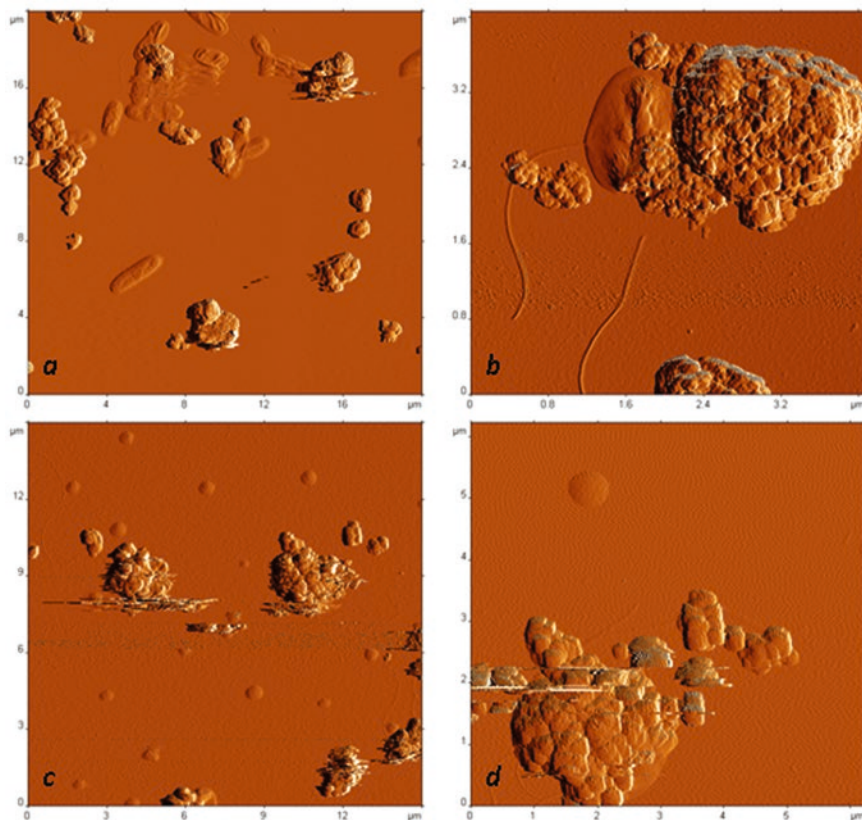


Fig. 4.11 AFM images of (a, b) anti-*E. coli* and (c, d) anti-*Salmonella* modified nanoparticles, incubated for 40 min with (a, b) *E. coli* and (c, d) *Salmonella* cells. The size of the AFM images in (a–d) is 20, 4, 15, and 6.2 μm , respectively

We have also studied binding of antibody-modified magnetic nanoparticles with bacterial cells. The AFM images of the nanoparticles incubated with cells for 40 min are presented in Fig. 4.11. AFM allows the visualization of binding of the nanoparticles with cells.

4.5 Conclusion and Future Perspectives

An attempt to find the difference between the strains of ascomycete *N. crassa* with normal (*wild type*) and damaged nitrogen (*nit-2* and *nit-6*) metabolism by using system for analysis of VOCs) was discussed herewith. *nit-2* is a global regulatory gene of *N. crassa* coding nuclear protein positively influencing the expression of more than 100 genes connecting with nitrogen metabolism of this fungus. *nit-6* is a

structural gene of *N. crassa* coding nitrite reductase. Water and ethanol extracts of VOCs after growth of submerged culture of different *N. crassa* strains were analyzed. The comparison of water extracts by system for analysis of VOC revealed the difference in OD between *N. crassa wt* strain and strains with damaged nitrogen metabolism. It has been shown that using thermostatic and continuous monitoring analyzer, it is possible to distinguish a wild strain and its isogenic mutants in the frame of the same microbiological species. It is possible to consider that nitrogen genes of microorganism participate in producing VOC. The possibility to use AFM to visualize bacterial fragments using specific antibody-antigen (bacterial) immobilization on the surface has been described too. We hope that these approaches will be useful for sensitive detection of pathogens.

Acknowledgments The work was supported by Rospotrebnadzor. F.S.Y. and G.P.B. were supported by the State Assignment 0104-2019-0024 to Research Center of Biotechnology RAS. The authors wish to thank E.V. Dubrovin and D.S. Ignatov for the help.

References

- Ahluwalia A, Basta G, Ricci D, Francesconi R, Domenici C, Grattarola M, Palchetti L, Preininger C, De Rossi D (1999) Langmuir-Blodgett films of antibodies as mediators of endothelial cell adhesion on polyurethanes. *J Biomater Sci Polym* 10(3):295–304
- Allison DP, Sullivan CJ, Mortensen NP, Retterer ST, Doktycz M (2011) Bacterial immobilization for imaging by atomic force microscopy. *J Vis Exp* 10(54):pii: 2880. <https://doi.org/10.3791/2880>
- Andre G, Kulakauskas S, Chapot-Chartier MP, Navet B, Deghorain M, Bernard E, Hols P, Dufrêne YF (2010) Imaging the nanoscale organization of peptidoglycan in living *Lactococcus lactis* cells. *Nat Commun* 1:27. <https://doi.org/10.1038/ncomms1027>
- Benn G, Pyne ALB, Ryadnov MG, Hoogenboom BW (2019) Imaging live bacteria at the nanoscale: comparison of immobilisation strategies. *Analyst* 144(23):6944–6952
- Binnig G, Quate CF, Gerber CH (1986) Atomic force microscopy. *Phys Rev Lett* 56:930–933
- Chen P, Xu L, Liu J, Hol FJ, Keymer JE, Taddei F, Han D, Lindner AB (2014) Nanoscale probing the kinetics of oriented bacterial cell growth using atomic force microscopy. *Small* 10(15):3018–3025
- Dubrovin EV, Fedyukina GN, Kraevsky SV, Ignatyuk TE, Yaminsky I, Ignatov SG (2012) AFM specific identification of bacterial cell fragments on biofunctional surfaces. *Open Microbiol J* 6:22–30
- Dufrêne YF, Ando T, Garcia R, Alsteens D, Martinez-Martin D, Engel A, Gerber C, Müller DJ (2017) Imaging modes of atomic force microscopy for application in molecular and cell biology. *Nat Nanotechnol* 12(4):295–307
- Elosua C, Matias IR, Barriain C, Arregui FJ (2006) Volatile Organic Compound Optical Fiber Sensors: A Review. *Sensors (Basel)* 6(11):1440–1465
- Flemming HC, Wingender J, Szewzyk U, Steinberg P, Rice SA, Kjelleberg S (2016) Biofilms: an emergent form of bacterial life. *Nat Rev Microbiol* 14(9):563–575
- Kaundal S, Deep A, Kaur G, Thakur KG (2020) Molecular and Biochemical Characterization of YeeF/YezG, a Polymorphic Toxin-Immunity Protein Pair From *Bacillus subtilis*. *Front Microbiol* 11:95. <https://doi.org/10.3389/fmicb.2020.00095>
- Kominami H, Kobayashi K, Ido S, Kimiya H, Yamada H (2018) Immunoactivity of self-assembled antibodies investigated by atomic force microscopy. *RSC Adv* 8(51):29378–29384

- Kommnick C, Lepper A, Hensel M (2019) Correlative light and scanning electron microscopy (CLSEM) for analysis of bacterial infection of polarized epithelial cells. *Sci Rep* 9:17079
- Longo G, Rio LM, Trampuz A, Dietler G, Bizzini A, Kasas S (2013) Antibiotic-induced modifications of the stiffness of bacterial membranes. *J Microbiol Methods* 93(2):80–84
- Meyer RL, Zhou X, Tang L, Arpanaei A, Kingshott P, Besenbacher F (2010) Immobilisation of living bacteria for AFM imaging under physiological conditions. *Ultramicroscopy* 110(11):1349–1357
- Mittelviehhaus M, Müller DB, Zambelli T, Vorholt JA (2019) A modular atomic force microscopy approach reveals a large range of hydrophobic adhesion forces among bacterial members of the leaf microbiota. *ISME J* (7):1878–1882
- Pan F, Altenried S, Liu M, Hegemann D, Bülbül E, Moeller J, Schmahl WW, Maniura-Weber K, Ren Q (2020) A nanolayer coating on polydimethylsiloxane surfaces enables mechanistic study of bacterial adhesion influenced by material surface physicochemistry. *Mater Horiz* 7:93–103. <https://doi.org/10.1039/C9MH01191A>
- Shi H, Sun J, Han R, Ding C, Hu F, Yu S (2019) The strategy for correcting interference from water in Fourier transform infrared spectrum based bacterial typing. *Talanta*:120347. <https://doi.org/10.1016/j.talanta.2019.120347>
- Soon RL, Nation RL, Hartley PG, Larson I, Li J (2009) Atomic force microscopy investigation of the morphology and topography of colistin-heteroresistant *Acinetobacter baumannii* strains as a function of growth phase and in response to colistin treatment. *Antimicrob Agents Chemother* 53(12):4979–4986
- Stitzel SE, Albert KJ, Ignatov SG, David R, Walt DR (2002) Artificial nose employing microsphere sensors for detection of volatile organic compounds. *Proc. SPIE* 4575, chemical and biological early warning monitoring for water, food, and ground. <https://doi.org/10.1117/12.456916>.
- Tilocca B, Cao A, Migheli Q (2020) Scent of a killer: microbial volatilome and its role in the biological control of plant pathogens. *Front Microbiol* 11:41. <https://doi.org/10.3389/fmicb.2020.00041>
- Turishchev SY, Marchenko D, Sivakov V, Belikov EA, Chuvenkova OA, Parinova EV, Koyuda D, Chumakov RG, Lebedev AM, Kulikova TV, Berezhnoy AA, Valiakhmedova IV, Praslova NV, Preobrazhenskaya EV, Antipov SS (2019) On the possibility of Photo Emission Electron Microscopy for *E. coli* advanced studies. *Result Phys*. <https://doi.org/10.1016/j.rinp.2019.102821>
- Viljoen A, Foster SJ, Fantner GE, Hobbs JK, Dufrêne YF (2020) Scratching the surface: bacterial cell envelopes at the nanoscale. *Scratching the surface: bacterial cell envelopes at the nanoscale*. *MBio* 11:1. <https://doi.org/10.1128/mBio.03020-19>
- Voloshin AG, Filippovich SY, Bachurina GP, Besaeva SG, Ignatov SG (2010) Spectrophotometric analysis of volatile compounds in microorganisms. *Appl Biochem Microbiol* 46(3):303–306. <https://doi.org/10.1134/S0003683810030099>
- Wang H, Koydemir HC, Qiu Y, Bai B, Zhang Y et al (2020) Early-detection and classification of live bacteria using time-lapse coherent imaging and deep learning. *arXiv:2001.10695 [physics.ins-det]*, 2020.
- Welch NG, Scoble JA, Muir BW, Pigram PJ (2017) Orientation and characterization of immobilized antibodies for improved immunoassays. *Biointerphases* 12(2):02D301. <https://doi.org/10.1116/1.4978435>

Part II
**The Use of Biosensors for the Detection
of Biological and Chemical Objects**

Chapter 5

SERS for Bacteria, Viruses, and Protein Biosensing



Ilya N. Kurochkin, Arkadiy V. Eremenko, Evgeniy G. Evtushenko, Natalia L. Nechaeva, Nikolay N. Durmanov, Rustam R. Guliev, Ilya A. Ryzhikov, Irina A. Boginskaya, Andrey K. Sarychev, A. V. Ivanov, and Andrey N. Lagarkov

Abstract In this chapter, various techniques are reviewed with focus on the identification of complex biological agents such as bacteria, viruses, proteins, and enzymes using SERS-active silver substrates. Biological targets have multiple peculiarities that add to the challenges of the SERS biosensing. In regards to the direct non-labeled sensing of bacteria, it was discovered that all bands in the registered SER spectra were generated by metabolites released from bacterial cells. It undermined the prior notion of non-labeled detection and identification of bacteria based on the presumed spectra of cellular walls. However, it also provides new opportunities for the SERS analysis of bacteria. The SERS measurements of viruses can be performed with SERS-active surfaces or colloidal solutions of silver nanoparticles. However, the use of surfaces requires extensive sample preparation and often lacks sensitivity, while colloidal SERS substrates have another problem—most types of silver nanoparticles are negatively charged and have a poor interaction with likewise predominantly negatively charged virions. Thus, a challenge is posed to develop SERS-ready positively charged silver nanoparticles or use other methods to enforce the non-specific binding of viruses to the silver surfaces. Meanwhile, SER spectra of proteins are nearly impossible to acquire at adequate sensitivity. Thus, non-direct measurements are the only way. SERS provides the most benefits when working with relatively small molecules, so small molecules serving as Raman probes can be

I. N. Kurochkin (✉)

Emanuel Institute of Biochemical Physics RAS, Moscow, Russia

Faculty of Chemistry of Lomonosov Moscow State University, Moscow, Russia

e-mail: ikur@genebee.msu.su

A. V. Eremenko · N. L. Nechaeva · N. N. Durmanov · R. R. Guliev

Emanuel Institute of Biochemical Physics RAS, Moscow, Russia

E. G. Evtushenko

Faculty of Chemistry of Lomonosov Moscow State University, Moscow, Russia

I. A. Ryzhikov · I. A. Boginskaya · A. K. Sarychev · A. V. Ivanov · A. N. Lagarkov

Institute of Theoretical and Applied Electrodynamics RAS, Moscow, Russia

© Springer Nature Switzerland AG 2021

M. Rai et al. (eds.), *Macro, Micro, and Nano-Biosensors*,

https://doi.org/10.1007/978-3-030-55490-3_5

used as an intermediary to produce SER spectra. For enzymes like butyrylcholinesterase, it means measuring SER spectra of substrates and products of the relevant reaction, while for other proteins, specialized techniques must be developed. It can be concluded that biological targets require a case-by-case approach. Prior experiences with direct SERS measurements of highly Raman-active molecules like R6G and others often used in fundamental studies might not be relevant in bioanalytics.

Keywords SERS · bacteria · viruses · proteins · enzymes · biosensing

Nomenclature

4-mPBA	4-mercaptophenylboronic acid
AChE	acetylcholinesterase
AFM	atomic force microscopy
AMP	adenosine monophosphate
BChE	butyrylcholinesterase
CDV	canine distemper virus
EB-PVD	electron beam physical vapor deposition technique
EF	enhancement factor
ELISA	enzyme-linked immunosorbent assay
EW	excitation wavelength
GA	glycated albumin
HSA	human serum albumin
LDA	linear discriminant analysis
LOD	limit of detection
MYXV	myxomatosis virus
PCA	principal component analysis
PCR	polymerase chain reaction
PLS	partial least squares regression
PVX	potato virus X
SEM	scanning electron microscopy
SERS	surface enhanced Raman spectroscopy/scattering
SER	surface enhanced Raman
TCh	thiocholine
TMV	tobacco mosaic virus
TNB	5-thio-2-nitrobenzoate ion
UV	ultraviolet
VERS	volume-enhanced Raman spectroscopy/scattering

5.1 Introduction

Surface-enhanced Raman scattering (SERS) is a powerful analyzing tool providing the high sensitive detection of different types of molecular compounds (Sharma et al. 2012; Sarychev et al. 2019). SERS is promising in clinical diagnostics, which include the cancer detection and imaging, cancer therapy and drug delivery (Pazos et al. 2016; Oseledchik et al. 2016; Litti et al. 2016; Schurmann and Bald 2016; Andreou et al. 2016; Chen et al. 2016b; Chen et al. 2016c; Li et al. 2016a, 2016b; Cheng et al. 2017; Kneipp 2017; Harmsen et al. 2017; Rastinehad 2019), quantitative control of glycated proteins for diabetes detection (Xu et al. 1999; Kiran et al. 2010; Dingari et al. 2012; Barman et al. 2012; Lin et al. 2014), cardiovascular biomarkers for early diagnosis of acute myocardial infarction (Das et al. 2008; Benford et al. 2009; Chon et al. 2014), etc.; in environmental and food safety for real-time monitoring of pathogenic bacteria, pesticides, and toxic molecules (Bodelon et al. 2016; Duan et al. 2016a; Duan et al. 2016b; Yang et al. 2016; Chen et al. 2016a; Zhou et al. 2016; Tian et al. 2016; Liu et al. 2017); for detection of ultra-low quantities of nerve gases, explosive substances, and other hazardous substances (Hakonen et al. 2016; Chen et al. 2017). The basis of the SERS sensing is the generation of several plasmon modes at a metallic surface and further Raman scattering of the plasmons by analyte molecules. The molecules are excited by surface plasmons and generate secondary plasmons which can be significantly enhanced. The radiation coming from these secondary plasmons produces a SERS signal (Brouers et al. 1997). Therefore, in SERS, the dominant contribution to enhancement factor (EF) is the electromagnetic mechanism (Ding et al. 2016) allowing it to reach very high sensitivity. This EF for SERS is evaluated as the fourth power of the intensity of the local electric field (Brouers et al. 1997; Itoh et al. 2017; Ding et al. 2017). Thus, the surface morphology of nanostructured SERS substrates is crucial for achieving high EFs. It is an important point in context of increasing the sensitivity of the biological and chemical sensing. Several groups have already demonstrated EFs from 10^4 to 10^9 for SERS substrates composed of clusters of gold or silver nanoparticles encapsulated in a dielectric matrix (McFarland et al. 2005; Perney et al. 2006; Yan et al. 2009; Fan et al. 2011; Banaee and Crozier 2011; Li et al. 2011; Mattiucci et al. 2012; Huang et al. 2013; Hu et al. 2014; Lee et al. 2014; Zhang et al. 2015). Modern fabrication technologies such as focused ion-beam lithography, electron-beam lithography, X-ray, UV, and interference lithographies allow to produce SERS substrates with an accuracy control over the shape and spatial distribution of nanostructures. However, most of these techniques are still expensive and complicated. A large number of nanostructures such as nanodisks, nanoholes, and nanodimers have been tested and provided high EFs for SERS (Brolo et al. 2004; Lim et al. 2010; Suh and Odom 2013; Barbillon et al. 2019). High EF was also observed in a system of silver microplates resulting from the enhancement of the local electric field in gaps between plates (Nechaeva et al. 2020).

The chemical enhancement strongly depends on local electronic structures of the molecules and the substrate it interacts with as each of their wave functions begins

to overlap (Campion et al. 1995; Kambhampati et al. 1998; Otto 2005). Influence of chemical enhancement is significantly weaker than electromagnetic enhancement. Indeed, the magnitude order of the chemical enhancement is only 10^2 (Jensen et al. 2008; Jahn et al. 2016), but it can play a crucial role in SERS. The maximum convergence of the analyzed molecules with the surface is extremely important.

In this chapter, we have reviewed useful techniques for identification of complex biological agents such as bacteria, viruses, proteins, and enzymes using SERS-active silver substrates.

5.2 Bacteria

Bioanalytical applications of label-free SERS for bacterial cells are fully defined by molecular origin of bacterial spectra. Early research papers on this topic (Picorel et al. 1990; Efrima and Bronk 1998; Zeiri et al. 2002, 2004) have shown that at excitation wavelengths (EWs) of 488 and 514.5 nm, SER spectra of various bacterial species, both Gram-positive and Gram-negative, are almost identical. Moreover, they do not differ from spectra of isolated cell membranes. Bands of oxidized or reduced forms of riboflavin as common components of cell membranes fully dominate in such spectra due to overlap of their extinction band with mentioned EWs, which leads to additional resonant enhancement of riboflavin spectrum. Such molecular origin of bacterial spectra at EWs of 488 and 514.5 nm holds the potential for their detection, but not discrimination of different species.

Pioneering studies on SERS of bacteria with longer EWs, particularly 785 nm, reported (Guzelian et al. 2002; Jarvis and Goodacre 2004; Premasiri et al. 2005) significant distinctive features in spectra of different species and sometimes strains. It has been hypothesized that label-free SERS of bacteria at EW of 785 nm might be used for both detection and identification of bacteria. Unfortunately, for more than 10 years, many attempts to assign observed bands to particular chemical substances were unconvincing as they were focused on single bands, but not the full spectrum (Guzelian et al. 2002; Jarvis and Goodacre 2004; Premasiri et al. 2005; Luo and Lin 2008; Kahraman et al. 2011; Feng et al. 2015; Su et al. 2015; Mosier-Boss 2017). However, it should be noted that adenine and guanine bands were identified in spectra (Guzelian et al. 2002; Luo and Lin 2008; Kahraman et al. 2011; Feng et al. 2015; Su et al. 2015), but their assignment to intracellular RNA/DNA raised questions about lacking bands of pyrimidines (thymine, uracil, and cytosine). Without solid basement of molecular origin, the main aim of the most bioanalytical papers was to demonstrate the ability of SERS to discriminate different species or strains using formal mathematical approach, based on application of principal component analysis (PCA) or similar procedures of dimensionality reduction to spectra, followed by discriminant or cluster analysis (Jarvis and Goodacre 2004; Patel et al. 2008; Sundaram et al. 2013; Mosier-Boss 2017; Witkowska et al. 2018).

Premasiri et al. (2016) decisively demonstrated that SER spectra of 10 various bacterial species at EW of 785 nm using “*in situ* grown, aggregated-Au-nanoparticle-

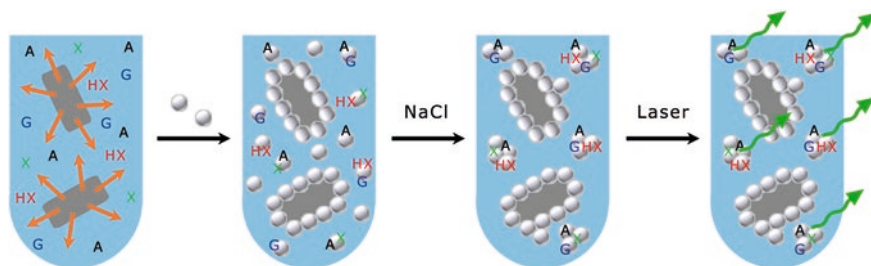


Fig. 5.1 Scheme of SERS acquisition from bacterial suspensions using silver nanoparticles sols as SERS substrates

covered SiO₂ substrate” originated from 6 purine derivatives (adenine, AMP, guanine, hypoxanthine, xanthine, and uric acid). It has been shown that these molecules were not bound to the cell surface, but were secreted by cells into the surrounding solution. Later the applicability of such assignment was confirmed for another type of SERS substrate, a sol of silver nanoparticles, and two EWs: 532 and 785 nm (Durovich et al. 2018). DH5 α strain of *Escherichia coli* was used as a model bacterium; silver nanoparticles were incubated for 1 minute with thoroughly washed *E. coli* suspension followed by sol aggregation with NaCl for SER signal generation (Fig. 5.1). Bacterial SER spectra of a cell suspension batch showed high repeatability on a timescale of 10–20 min. However, during the course of 4 h of cell suspension storage, the overall intensity of spectra increased together with pronounced changes in intensity ratios of some strong bands (e.g., I_{1325}/I_{655}). Even more severe differences in spectra were observed for independently cultivated and harvested cells. Spectrum of the 0.22 mkm filtrate of cell suspension retained all the bands of the original suspension. Moreover, the intensities of these bands were substantially higher for filtrate. Thermal inactivation of cells at +90 °C for 1 h followed by washing resulted in almost complete disappearance of the spectra. They contained only 3 weak bands characteristic of intact bacteria (730, 1325, and 1450 cm⁻¹), the band of phenylalanine (1002 cm⁻¹), and two bands of the amide III (1230–1270 cm⁻¹) and amide I (1640–1680 cm⁻¹). Despite strong variations in spectra, they contained a limited number of bands. All of these bands both for the entire set of spectra or any particular spectrum were in a good agreement with positions and relative intensities of 4 purines: adenine, guanine, hypoxanthine, and xanthine. These substances were gradually released by cells into the surrounding media; their presence was characteristic of viable cells only; the ratio of purines varied both for different batches of the same strand and during 4 h storage in starvation conditions.

This newly revealed molecular origin of bacterial SER spectra at EWs of 532 and 785 nm considerably reshapes the entire bioanalytical area of label-free SERS of bacteria. Indeed, from this point of view, the problem of discrimination of bacterial species and strains is strongly related to dissimilarities in their purines metabolism. On the other hand, the presence of purines might be used as a general bacterial marker for their detection. It also starts a whole new field of SERS application for purine metabolome profiling in bacteria.

5.3 Identification of Animal and Plant Viruses

Viruses represent another type of biological object for SERS measurements. There is an urgent need to develop new rapid methods of virus detection, only further exacerbated by the emergence of new viral diseases, such as novel coronaviruses or new influenza strains (Afrough et al. 2019).

Highly sensitive and express techniques are thus in demand. Nowadays, there are two mutually exclusive types of solutions: highly sensitive techniques (variations of ELISA and PCR) and rapid techniques (such as immune–chromatography strips). The methods with sufficient sensitivity lack the necessary speed, which limits their applications in epidemics control. The rapid techniques mostly lack required sensitivity and cannot detect viruses without prior concentration.

SERS techniques appear to have almost the same limit of detection as ELISA in some cases, such as the SERS detection of porcine circovirus' intact virions (Luo et al. 2013), influenza virus SERS assay (Kukushkin et al. 2019), hepatitis B antigen detection (Kamińska et al. 2015), and many others. Thus, SERS is considered to be one of the most promising approaches to achieve both rapid and sensitive detection of viral pathogens. Non-labeled detection, while harder to achieve, is especially alluring, due to the fact that it enables the detection of multiple different targets as well as new strains without the need for pre-existing antibodies or other selective agents. There are also less requirements for reagents and materials, and no time spent on any specific binding or amplification reaction.

There are several peculiarities associated with viruses in general, that must be taken into consideration before attempting to develop a SERS-based detection and/or identification methods. First of all, viral particles are almost always negatively charged due to low isoelectric point value, which lies around 4 to 5 for most viruses (Michen and Graule 2010). Simultaneously, many viruses are very fragile and stable only at specific pH values, which makes it impossible to reliably alter the charge of virions by adjusting pH of the solution. Most frequently used methods of silver nanoparticles synthesis produce negatively charged particles. Such particles have poor compatibility with negatively charged analytes. Another issue is the shape and size of virions. Most viruses can not fit entirely into hot spots of normal SERS substrates. That means that only surface components of the virions generate SERS signals, and the strength of that signal might be greatly reduced. While some viruses with thread-like shapes might generate strong SERS signals from both exterior and interior components, large spherical viruses might not. Finally, viruses might have empty virions (no nucleic acid inside) or destroyed virions' fragments present in the solution, which further complicates data interpretation.

Taking into consideration the above-mentioned challenges, SERS-active surfaces remain the main focus for label-free SERS-based virus detection. One of the common approaches to solve the problem with the size of various viral particles is the application of nanocavities, which can incorporate the entire virion inside, maximizing the contacts between the virus and the hot spots (Chang et al. 2011; Yan et al. 2017). In fact, the entire internal volume of the nanocavities, depending on

their shape and size, might benefit from the electromagnetic signal enhancement, an effect which is sometimes called VERS (volume-enhanced Raman scattering) (Zhang et al. 2019), and can be used to acquire scattered light from the internal components of the large virions.

In one of our prior works (Durmanov et al. 2018), a SERS substrate with nanocavities was utilized for non-labeled SERS analysis of four viral species—two thin, thread-like non-enveloped plant viruses, and two large spherical enveloped animal viruses. The substrates were fabricated with electron beam physical vapor deposition technique (EB-PVD), achieving porous interwoven surface by altering temperature of the mica substrate and tuning adatom energy levels by altering EB acceleration voltage. EB-PVD, while not exactly precise, is a cheap and readily available method of fabrication. The resulting SERS substrates contained a large amount of nanocavities, 200–300 nm in diameter, as characterized by SEM and AFM methods. The 3-dimensional reconstruction, based on SEM and AFM images, can be seen in Fig. 5.2.

The tobacco mosaic virus (TMV) and the Potato virus X (PVX) are RNA containing plant viruses with a thin unenveloped thread-like capsid. Moreover, the two animal viruses, viz. Canine Distemper virus (CDV) and the rabbit Myxomatosis virus (MYXV), are large, with MYXV being somewhat larger, roughly spherical (CDV) or brick-shaped (MYXV), and enveloped, though their respective envelope-formation mechanisms are different. Also, one is a DNA-containing virus (MYXV), while the other RNA (CDV). The viruses were purified and diluted in the same buffer solution, and then deposited on the SERS-active surface and dried. Raman spectra were collected from the dried spot, containing adsorbed virions. The concentration was about 100 viral particles per the detection zone.

Then the preprocessing was applied: the spectra were trimmed to the region between 1800 cm^{-1} and 400 cm^{-1} , and cosmic spikes were removed by straight line generation; then baseline was corrected, mean buffer spectrum was subtracted from each spectra, and vector normalization was applied. Figure 5.3 represents the averaged spectrum of each virus. For visual contrast, the values are also presented in a heat-map style.

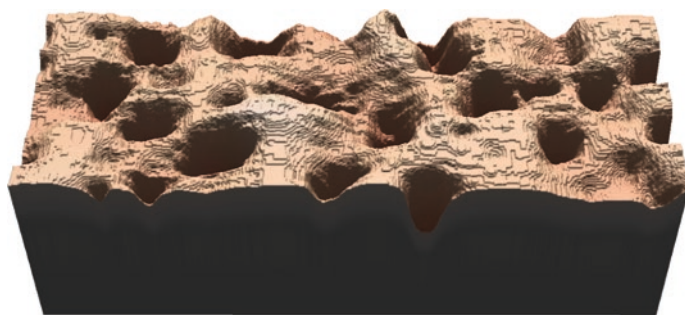


Fig. 5.2 Three-dimensional reconstruction of the SERS-active porous surface, based on SEM and AFM images

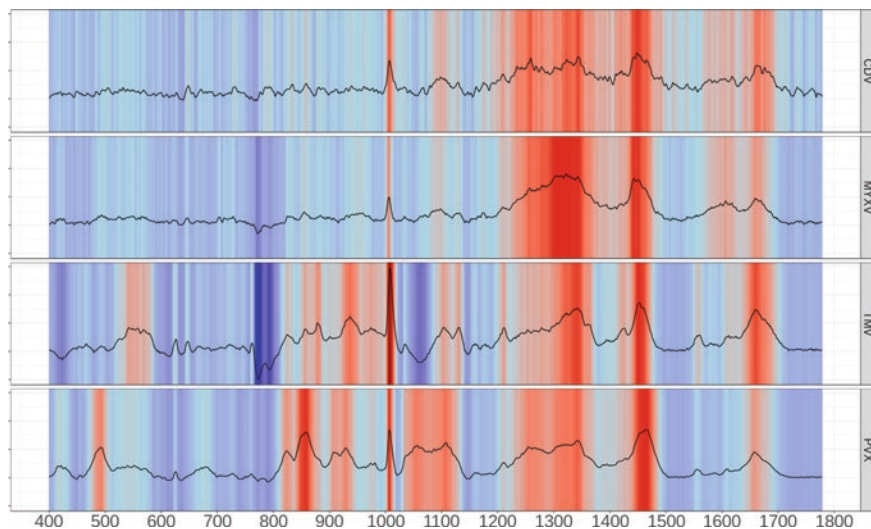


Fig. 5.3 Averaged spectra of each virus (black line). From top to the bottom: CDV, MYXV, TMV, and PVX. Each Raman shift is marked by a colored vertical line. The color of the line reflects the value of the averaged spectrum at the corresponding Raman shift. The values are colored by a gradient from dark red (the highest value within all averaged spectra) to the dark blue (the lowest value)

The expected differences between viruses should be attributed to the variations in their structure and components. And indeed, the areas of interest, as indicated by the heat-map, correspond to the expected differences in chemical properties. The bands of cholesterol and other lipid content, as well as β -sheets typical for membrane proteins (610 , 1067 – 69 , 1098 , 1302 , 1443 , 1448 , 1491 , 1676 , and 1734 cm^{-1}), are present in the spectra of MYXV and CDV, but absent in TMV and PVX, due to their lack of an envelope. Some bands have high influence in all groups: 770 – 800 cm^{-1} , 1006 – 1008 cm^{-1} , 1430 – 1450 cm^{-1} , and 1650 – 1700 cm^{-1} . These might be related to proteins, nucleic acids, and aromatic amino acids. Some bands, like 1103 , 1108 , 1463 cm^{-1} , and others, are more pronounced in the two plant viruses. Presumably, these bands correspond to the nucleic acid components among other things. Since plant viruses have thin thread-like structure, their internal components, namely, RNA, are closer to the silver surface and thus can contribute more to the SERS signal. There are also differences between amino acid composition, seen at ~ 480 cm^{-1} , ~ 850 cm^{-1} , and 1560 cm^{-1} .

The collation of PCA-LDA values, visually observed differences, and expected variation in SERS bands positions points to the conclusion that label-free SERS can indeed support the identification of viruses based on their spectra. The overhaul accuracy of the classification model, trained with the spectra of the viruses, was no less than 99.4%. The main challenge is sensitivity. One of the possible ways to increase it is to use SERS colloids, such as silver nanoparticles. The problem with the charge of the viruses might be overcome by using positively charged aggrega-

tion reagents, which would act as intermediaries between negatively charged nanoparticles and virions. One example of that approach is the use of spermin, which was successfully applied to the nucleic acid SERS measurement (Li et al. 2018). The results for viruses are unclear so far, which opens a whole new field of research.

5.4 Quantitative Enzyme Detection

Since solid SERS-substrate application is limited by diffusion, it is very important to attract the analyte to the surface. Special attraction techniques can include imprinting in complex-shaped pores (Li et al. 2020; Ren et al. 2020), antibodies (Kamińska et al. 2017; Smolsky et al. 2017), or labels (e.g., peptides or low-molecular-weight targeting ligands (Lee et al. 2010; Li et al. 2016a, 2016b), or just utilize covalent bonding to the surface of the substrate (Shan et al. 2018). Here we describe two examples of covalent interaction with the view of analyte attraction.

Butyrylcholinesterase (BChE), or pseudocholinesterase, is a serine hydrolase closely related to acetylcholinesterase (AChE). This enzyme is of high toxicological and pharmacological importance because it hydrolyzes ester-containing drugs and scavenges cholinesterase inhibitors including potent organophosphorus nerve agents (Masson and Lockridge 2010; Lockridge 2015; Lockridge et al. 2016). Decreased BChE level is a diagnostic and prognostic indicator for organophosphate poisoning. BChE activity is associated with obesity (Li et al. 2008; Lima et al. 2013), with insulin resistance and the metabolic syndrome (Valle et al. 2006; Iwasaki et al. 2007), hyperlipidemia (Kálmán et al. 2004), coronary artery disease and hypertension (Alcantara et al. 2002), and the arterial pathology of diabetes mellitus (Vaisi-Raygani et al. 2010). Thus, plasma level of BChE represents an important prognostic marker in the organophosphate exposure biomonitoring and in the diagnostic network of various patient clinical conditions.

One of the most widespread techniques for estimation of the cholinesterase activity is the detection of thiocholine—the product of enzymatic hydrolysis of butyrylthiocholine. Comparing to electrochemical methods (Arduini et al. 2009; Eremenko et al. 2012; Sgobbi et al. 2013; Kurochkin et al. 2014), Raman spectroscopy detection has a number of advantages: since the sample can be dried, the technique is suitable for routine measurements, the experiment can be carried out far away from the special equipment, and it is not necessary to transport blood or plasma samples.

Preparation and characterization of silver SERS-substrate were described by Nechaeva et al. (2018). In this study, silver-containing polymeric paste was applied to a 5-mm thick aluminum block and dried. The surface represents heterogeneous flaked structure with silver particles of various sizes and shapes. Numerous points of contact as well as the variation of the angles of incident light make possible the local enhancement of electromagnetic field, which causes a gain of Raman signal of the analyte.

The silver SERS substrate was used for thiocholine determination. Thiocholine solution was obtained by the enzymatic hydrolysis of butyrylthiocholine chloride according to the Scheme (1). The concentration of produced TCh was determined by Ellman's assay (Ellman et al. 1961). The conversion from the substrate reached 100%. The thiocholine concentration was calculated by the Beer–Lambert–Bouguer law ($\epsilon_{412} = 14.15 \text{ ml}/\mu\text{mol}\cdot\text{cm}$ is the absorption coefficient of 5-thio-2-nitrobenzoate ion (TNB) at 412 nm) (Eyer et al. 2003).

The obtained Raman spectra of thiocholine have several characteristic peaks, the most intensive 773 cm^{-1} can be attributed to CH₃ rocking vibration modes (Liron et al. 2011).

For different concentrations of TCh, the resulting spectra have different intensities of 773 cm^{-1} peak (Fig. 5.4). Therefore, it is possible to plot a calibration curve based on this peak. Each point at this curve represents the average of 10 replicates of TChCl spectra, and zero-point means phosphate buffer. The right axis on this figure demonstrates the PLS-calibration curve of thiocholine, the reference was Ellman's method. It is possible to calculate the limit of detection (LOD) for TCh

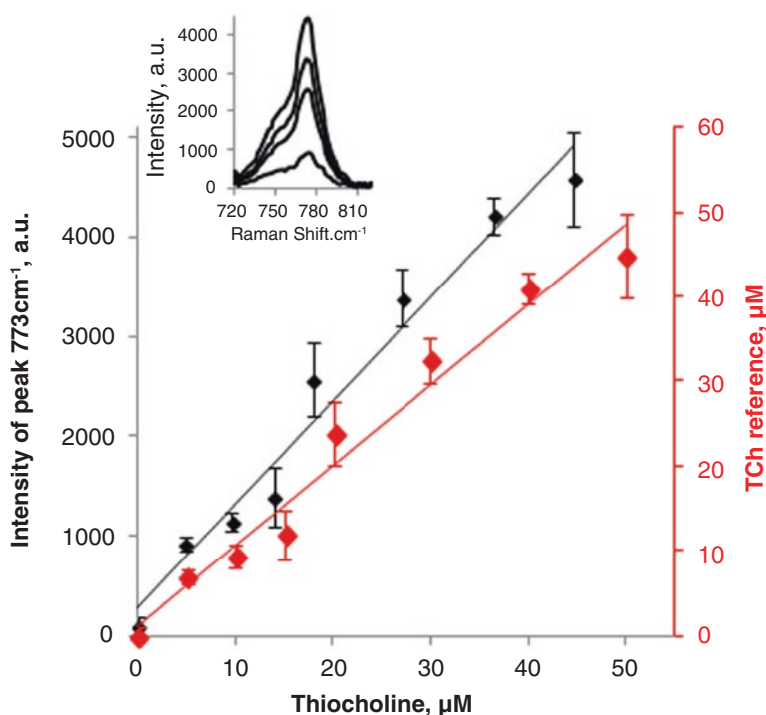
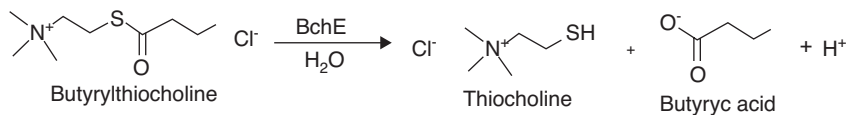


Fig. 5.4 The calibration curve of thiocholine chloride on the silver SERS substrate based on intensity of 773 cm^{-1} peak (black) and PLS-regression plot for the same data (red). The inset shows dependence of 773 cm^{-1} peak intensity from the concentration of TCh, concentrations from the top to the bottom: 50, 30, 20, and $5 \mu\text{M}$



Scheme 5.1 The enzymatic hydrolysis of butyrylthiocholine chloride by butyrylcholinesterase

using a calibration curve. For developed technique, LOD (TCh) is 260 nM and sensitivity is 103.92 intensity units/1 μM .

It was shown that BTCh presence does not affect TCh detection on silver SERS substrate (Nechaeva et al. 2018). This conclusion is very important because thiocholine is the product of enzymatic hydrolysis of butyrylthiocholine (Scheme 5.1). The resulting curve at the end of the enzymatic reaction enables us thiocholine determination (and BChE activity correspondingly) despite the BTCh presence.

Butyrylcholinesterase activity in solution is strongly connected with thiocholine concentration and can be evaluated by measuring TCh. The solutions with high initial BChE activity give intensive Raman spectra because of high concentration of the TCh, and the solutions with low BChE activity contrariwise give low-intensive spectra. As for TCh, BChE calibration curve in the buffer and in human plasma can be created in two ways—by 773 cm^{-1} peak and by PLS regression. The offset for BChE calibration curve in plasma also takes into account initial BChE contained in human plasma. It must be highlighted that the matrix effect does not impact the results of measurements.

Silver SERS substrate can be applied for low-molecular substances determination, for example, thiocholine, for enzymatic activity detection in model systems and in spike solutions with plasma. This technique has a number of undeniable advantages: it is label-free, inexpensive, and has the possibility to routine measurements of hundreds of samples.

5.5 Glycated Human Albumin Biosensing

The SERS substrate described above can be also used for glycated albumin (GA) biosensing. GA level shows the average concentration blood sugars over 2 weeks (Koga et al. 2010). Thus, GA can be considered as a marker for glycemic status (Kohzuma and Koga 2010). The present techniques of GA determination often require antibodies and enzymes and also represent many-step difficult processes. We propose to expand the possible methods of analyzing the content of GA in plasma by using the SERS effect. There are a number of previous studies available which demonstrated the prospective use of SERS method for plasma glucose monitoring (Chen et al. 2011; Sun et al. 2014a, 2014b; Usta et al. 2016; Zhao et al. 2017).

The analysis itself includes silver SERS substrate, described above (Fig. 5.5a), modified with low-molecular-weight SERS label 4-mercaptophenylboronic acid

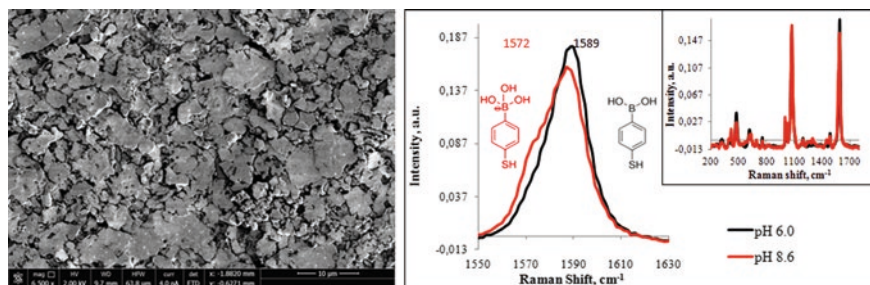


Fig. 5.5 (a) SEM image of silver SERS-substrate surface, (b) comparison of Raman spectra of anionic and molecular form of 4-mPBA

(4-mPBA). This label creates very strong covalent bond Ag–S with silver surface and on the other hand has affinity to *cis*-diols and polyols due to boronic group.

Surface modification of SERS substrate with 4-mPBA helps to produce specific substrate for *cis*-diol and polyols (including glycated proteins). Nechaeva et al. (2020) proposed the use of 4-mPBA-modified silver SERS substrate for one-step GA measuring both in the buffer and human plasma. In this work, selective changes of SERS spectra have been observed due to ionization of 4-mPBA on the surface. The main differences are observed at 416, 470, 999, 1021, 1072, 1572, and 1589 cm^{-1} due to symmetry breaking of a 4-mPBA molecule from nearly C_{2v} to C_s (Sun et al. 2014a, 2014b; Su et al. 2017). An obvious change of 8a (1586 cm^{-1}) and 8b (1573 cm^{-1}) modes is observed (Fig. 5.5b). Peaks demonstrate different areas, maximum position, different total intensity, and intensity of shoulders. All these changes indicate the difference between molecular HS-Ph-B(OH)₂ and anionic HS-Ph-B(OH)₃[−] forms of 4-mPBA.

4-mPBA band amplitude is distributed unevenly on the surface due to the heterogeneous morphology. Maximal Raman signals correspond to the excitation of gap plasmons between silver flakes as it is discussed above.

Silver SERS substrate modified with 4-mPBA was applied for sugars and glycated albumin determination. This technique provides detection of only covalently bonded molecules. To explore minor differences appearing due to glycation, statistical methods were used. Principal component analysis (PCA) was used to distinguish sugar spectra. The main differences that help to distinguish sugar spectra from the control lay in ranges 400–500 cm^{-1} , 950–1100 cm^{-1} , and 1550–1630 cm^{-1} and correspond to 4-mPBA vibrations including in-plane benzene ring breathing mode and totally and non-totally symmetric ring-stretching vibrational modes.

For distinguishing human serum albumin (HSA) and glycated albumin (GA)—proteins with very similar structure—PLS (partial least square) regression was used. First, a model for standard concentrations of mixture HSA + GA was built. GA fraction was 24, 48, 60, 90, and 120 μM , and HSA was used as control (0 μM of GA). Then, using this model for GA, we can predict the value of GA in unknown samples. Plasma from three different healthy donors was examined on the SERS

substrate modified with 4-mPBA. The most significant loadings represent Raman shifts corresponded to 4-mPBA vibrations (ranges 250–450 cm^{-1} , 1000–1100 cm^{-1} , and 1600–1650 cm^{-1}) as in case with sugars. Although human plasma contains different sugars, they don't affect the protein detection. We trained our model on protein spectra, thus we take into account only bands that play a key role in protein distinguishing. Predicted GA values are consistent with independent laboratory values. Thus silver SERS substrate modified with 4-mPBA allows quantitative biosensing of GA in the buffer and human plasma.

This technique requires an extremely low volume of the sample—about 15 μl —to measure 4 replicates. The method simplifies the experimental procedure and can be automated by computer processing of measurements. It also has an important advantage of technical simplicity since our silver-based substrates are easy to manufacture and operate.

5.6 Conclusion

Biological targets often differ from expectations. The revelation about the true nature of the SER spectra of bacteria came after more than a decade of multiple publications in which researchers demonstrated their ability to acquire SER spectra of bacterial cells, and used it to form classification models that successfully identified bacteria down to a strain. However, their results naturally couldn't be reproduced in another lab, since every time the metabolites would be present in slightly differing proportions, and the classification model would have to be formed anew. That long-lasting confusion stemmed from a rigid approach and treating a complex living target like a static chemical reagent. Researchers expected to see the repeat of the same logic they observed when working with classical Raman probes like R6G and others. Viruses proved to be likewise tricky. It remains unknown what viral components actually provide the majority of the SERS signal, and the difficulties associated with the sample preparation render that field of biosensing impractical so far. Colloidal solutions can be an answer to some of those concerns, but also pose a number of new challenges caused by the charge interaction and the presence of various impurities. As for the proteins, non-direct measurements seem to be the main trend since protein molecules usually do not produce strong-enough SERS signals. But non-direct methods cannot be universal and applicable to a large variety of different proteins and have to be developed case-by-case. Thus, in order to create new biosensing techniques, more fundamental studies are a necessity.

Acknowledgments The work was partially supported by Russian Science Foundation Grant (No. 16-14-00209), as well as Ministry of Science and Higher Education (AAAA-A19-119071890024-8—Physicochemical fundamentals of highly sensitive bio-analytical processes and development of new sensing materials; AAAAA19-119110790066-5—Principle development for the creation of an innovative technological solutions “laboratory on a chip”).

References

- Afrough B, Dowall S, Hewson R (2019) Emerging viruses and current strategies for vaccine intervention. *Clin Exp Immunol* 196:157–166. <https://doi.org/10.1111/cei.13295>
- Alcantara VM, Chautard-Freire-Maia EA, Scartezini M, Cerci MSJ, Braun-Prado K, Picheth G (2002) Butyrylcholinesterase activity and risk factors for coronary artery disease. *Scand J Clin Lab Invest* 62:399–404. <https://doi.org/10.1080/00365510260296564>
- Arduni F, Cassisi A, Amine A, Ricci F, Moscone D, Palleschi G (2009) Electrocatalytic oxidation of thiocholine at chemically modified cobalt hexacyanoferrate screen-printed electrodes. *J Electroanal Chem* 626:66–74. <https://doi.org/10.1016/j.jelechem.2008.11.003>
- Andreou C, Neuschmelting V, Tschaharganeh D, Huang C, Oseledchyk A, Iacono P, Karabeber H, Colen R, Mannelli L, Lowe S, Kircher M (2016) Imaging of liver tumors using surface-enhanced Raman scattering nanoparticles. *ACS Nano* 10:5015–5026
- Banaee M, Crozier K (2011) Mixed dimer double resonance substrates for surface-enhanced Raman spectroscopy. *ACS Nano* 5:307–314
- Barbillon G, Ivanov A, Sarychev (2019) A hybrid Au/Si disk-shaped Nanoresonators on gold film for amplified SERS chemical sensing. *Nano* 9:1588
- Barman I, Dingari N, Kang J, Horowitz G, Dasari R, Feld M (2012) Raman spectroscopy- based sensitive and specific detection of glycated hemoglobin. *Anal Chem* 84:2474–2482
- Benford M, Wang M, Kameoka J, Cote G (2009) Detection of cardiac biomarkers exploiting Surface Enhanced Raman scattering (SERS) using a Nanofluidic Channel based biosensor towards coronary point-of-care diagnostics. *Proc SPIE* 7192:719203
- Bodelon G, Montes-Garcia V, Lopez-Puente V, Hill E, Hamon C, Sanz-Ortiz M, Rodal-Cedeira S, Costas C, Celiksoy S, Perez-Juste I, Scarabelli L, La Porta A, Perez-Juste J, Pastoriza-Santos I, Liz-Marzan L (2016) Detection and imaging of quorum sensing in *Pseudomonas aeruginosa* biofilm communities by surface-enhanced resonance Raman scattering. *Nat Mater* 15:1203–1211
- Brolo A, Arctander E, Gordon R, Leathem B, Kavanagh K (2004) Nanohole-enhanced Raman scattering. *Nano Lett* 4:2015–2018
- Brouers F, Blacher S, Lagarkov A, Sarychev A, Gadenne P, Shalaev V (1997) Theory of giant raman scattering from semicontinuous metal films. *Phys Rev B* 55:13234–13245
- Campion A, Ivanecy J, Child C, Foster M (1995) On the mechanism of chemical enhancement in surface-enhanced Raman scattering. *J Am Chem Soc* 117:11807–11808
- Chang CW, Der Liao J, Shiau AL, Yao CK (2011) Non-labeled virus detection using inverted triangular Au nano-cavities arrayed as SERS-active substrate. *Sensors Actuators B Chem*. <https://doi.org/10.1016/j.snb.2011.04.006>
- Chen PC, Wan LS, Ke BB, Xu ZK (2011) Honeycomb-patterned film segregated with phenylboronic acid for glucose sensing. *Langmuir* 27:12597–12605. <https://doi.org/10.1021/la201911f>
- Chen N, Ding P, Shi Y, Jin T, Su Y, Wang H, He Y (2017) Portable and reliable surface-enhanced Raman scattering silicon chip for signal-on detection of trace trinitrotoluene explosive in real systems. *Anal Chem* 89:5072–5078
- Chen J, Huang Y, Kannan P, Zhang L, Lin Z, Zhang J, Chen T, Guo L (2016a) Flexible and adhesive SERS active tape for rapid detection of pesticide residues in fruits and vegetables. *Anal Chem* 88:2149–2155
- Chen Y, Zhang Y, Pan F, Liu J, Wang K, Zhang C, Cheng S, Lu L, Zhang W, Zhang Z, Zhi X, Zhang Q, Alfranca G, de la Fuente J, Chen D, Cui D (2016c) Breath analysis based on surface-enhanced Raman scattering sensors distinguishes early and advanced gastric cancer patients from healthy persons. *ACS Nano* 10:8169–8179
- Chen Y, Ren J, Zhang X, Wu D, Shen A, Hu J (2016b) Alkyne-modulated surface-enhanced Raman scattering-palette for optical interference-free and multiplex cellular imaging. *Anal Chem* 88:6115–6119

- Cheng Z, Choi N, Wang R, Lee S, Moon K, Yoon S, Chen L, Choo J (2017) Simultaneous detection of dual prostate specific antigens using surface-enhanced Raman scattering-based immunoassay for accurate diagnosis of prostate cancer. *ACS Nano* 11:4926–4933
- Chon H, Lee S, Yoon S, Lee E, Chang S, Choo J (2014) SERS-based competitive immunoassay of troponin I and CK-MB markers for early diagnosis of acute myocardial infarction. *Chem Commun* 50:1058–1060
- Das G, Mecarini F, Angelis F, Prasciolu M, Liberale C, Patrini M, Fabrizio E (2008) Attomole (Amol) myoglobin Raman detection from plasmonic nanostructures. *Microelectron Eng* 85:1282–1285
- Ding S-Y, Yi J, Li J-F, Ren B, Wu D-Y, Panneerselvam R, Tian Z-Q (2016) Nanostructure-based plasmon-enhanced Raman spectroscopy for surface analysis of materials. *Nat Rev Mater* 1:16021
- Ding S-Y, You E-M, Tian Z-Q, Moskovits M (2017) Electromagnetic theories of surface-enhanced Raman spectroscopy. *Chem Soc Rev* 46:4042–4076
- Dingari N, Horowitz G, Kang J, Dasari R, Barman I (2012) Raman spectroscopy provides a powerful diagnostic tool for accurate determination of albumin glycation. *PLoS One* 7:e32406
- Duan N, Chang B, Zhang H, Wang Z, Wu S (2016a) Salmonella typhimurium detection using a surface-enhanced Raman scattering-based aptasensor. *Int J Food Microbiol* 218:38–43
- Duan N, Yan Y, Wu S, Wang Z (2016b) Vibrio parahaemolyticus detection aptasensor using surface-enhanced Raman scattering. *Food Control* 63:122–127
- Durmanov NN, Guliev RR, Eremenko AV, Boginskaya IA, Ryzhikov IA, Trifonova EA, Putlyaev EV, Mukhin AN, Kalnov SL, Balandina MV, Tkachuk AP, Gushchin VA, Sarychev AK, Lagarkov AN, Rodionov IA, Gabidullin AR, Kurochkin IN (2018) Non-labeled selective virus detection with novel SERS-active porous silver nanofilms fabricated by Electron beam physical vapor deposition. *Sensors Actuators B Chem*. <https://doi.org/10.1016/j.snb.2017.10.022>
- Durovich EA, Evtushenko EG, Senko OV, Stepanov NA, Efremenko EN, Eremenko AV, Kurochkin IN (2018) Molecular origin of surface-enhanced Raman spectra of E. coli suspensions excited at 532 and 785 nm using silver nanoparticle sols as SERS substrates. *Bull RSMU* 6:25–32
- Ellman GL, Courtney KD, Andres V, Featherstone RM (1961) A new and rapid colorimetric determination of acetylcholinesterase activity. *Biochem Pharmacol* 7:88–95. [https://doi.org/10.1016/0006-2952\(61\)90145-9](https://doi.org/10.1016/0006-2952(61)90145-9)
- Efrima S, Bronk BV (1998) Silver colloids impregnating or coating Bacteria. *J Phys Chem B* 102:5947–5950
- Eremenko AV, Dontsova EA, Nazarov AP, Evtushenko EG, Amitonov SV, Savilov SV, Martynova LF, Lunin VV, Kurochkin IN (2012) Manganese dioxide nanostructures as a novel electrochemical mediator for Thiol sensors. *Electroanalysis* 24:573–580. <https://doi.org/10.1002/elan.201100535>
- Eyer P, Worek F, Kiderlen D, Sinko G, Stuglin A, Simeon-rudolf V, Reiner E (2003) Molar absorption coefficients for the reduced Ellman reagent: reassessment. *Anal Biochem* 312:224–227
- Fan M, Andrade G, Brolo A (2011) A review on the fabrication of substrates for surface enhanced Raman spectroscopy and their applications in analytical chemistry. *Anal Chim Acta* 693:7–25
- Feng J, de la Fuente-Núñez C, Trimble MJ, Xu J, Hancock REW, Lu X (2015) An in situ Raman spectroscopy-based microfluidic “lab-on-a-chip” platform for non-destructive and continuous characterization of Pseudomonas aeruginosa biofilms. *Chem Commun* 51:8966–8969
- Guzelian AA, Sylvia JM, Janni JA, Clauson SL, Spencer KM (2002) SERS of whole-cell bacteria and trace levels of biological molecules. In: Proceedings of the SPIE 4577, vibrational spectroscopy-based sensor systems, (22 February 2002), pp 4511–4577.
- Hakonen A, Rindcevicus T, Schmidt M, Andresson P, Juhlin L, Svedendahl M, Boisen A, Kall M (2016) Detection of nerve gases using surface-enhanced Raman scattering substrates with high droplet adhesion. *Nanoscale* 8:1305–1308
- Harmsen S, Wall M, Huang R, Kircher M (2017) Cancer imaging using surface-enhanced resonance Raman scattering nanoparticles. *Nat Protoc* 12:1400–1414

- Huang J, Zhao Y, Zhang X, He L, Wong T, Chui Y, Zhang W, Lee S (2013) Ordered Ag/Si nanowires Array: wide-range surface-enhanced Raman spectroscopy for reproducible biomolecule detection. *Nano Lett* 13:5039–5045
- Hu F, Lin H, Zhang Z, Liao F, Shao M, Lifshitz Y, Lee S (2014) Smart liquid SERS substrates based on Fe₃O₄/Au nanoparticles with reversibly tunable enhancement factor for practical quantitative detection. *Sci Rep* 4:1–10
- Itoh T, Yamamoto Y, Ozaki Y (2017) Plasmon-enhanced spectroscopy of absorption and spontaneous emissions explained using cavity quantum optics. *Chem Soc Rev* 49:3904–3921
- Iwasaki T, Yoneda M, Nakajima A, Terauchi Y (2007) Serum butyrylcholinesterase is strongly associated with adiposity, the serum lipid profile and insulin resistance. *Intern Med* 46:1633–1639. <https://doi.org/10.2169/internalmedicine.46.0049>
- Jahn M, Patze S, Hidi I, Knipper R, Radu A, Muhliger A, Yuksel S, Peksa V, Weber K, Mayerhofer T, Cialla-May D, Popp J (2016) Plasmonic nanostructures for surface enhanced spectroscopic methods. *Analyst* 141:756–793
- Jarvis RM, Goodacre R (2004) Discrimination of Bacteria using surface-enhanced Raman spectroscopy. *Anal Chem* 76:40–47
- Jensen L, Aikens C, Schatz G (2008) Electronic structure methods for studying surface-enhanced Raman scattering. *Chem Soc Rev* 37:1061–1073
- Kahraman M, Keseröglu K, Çulha M (2011) On sample preparation for surface-enhanced Raman scattering (SERS) of bacteria and the source of spectral features of the spectra. *Appl Spectrosc* 65:500–506
- Kálmán J, Juhász A, Rakonczay Z, Ábrahám G, Zana M, Boda K, Farkas T, Penke B, Janka Z (2004) Increased serum butyrylcholinesterase activity in type IIb hyperlipidaemic patients. *Life Sci* 75:1195–1204. <https://doi.org/10.1016/j.lfs.2004.02.019>
- Kambhampati P, Child C, Foster M, Champion A (1998) On the chemical mechanism of surface enhanced Raman scattering: experiment and theory. *J Chem Phys* 108:5013–5026
- Kamińska A, Winkler K, Kowalska A, Witkowska E, Szymborski T, Janeczka A, Waluk J (2017) SERS-based immunoassay in a microfluidic system for the multiplexed recognition of interleukins from blood plasma: towards Picogram detection. *Sci Rep* 7:1–11. <https://doi.org/10.1038/s41598-017-11152-w>
- Kamińska A, Witkowska E, Winkler K, Dziecielewski I, Weyher JL, Waluk J (2015) Detection of hepatitis B virus antigen from human blood: SERS immunoassay in a microfluidic system. *Biosens Bioelectron*. <https://doi.org/10.1016/j.bios.2014.10.082>
- Kiran M, Itoh T, Yoshida K, Kawashima N, Biju V, Ishikawa M (2010) Selective detection of HbA_{1c} using surface enhanced resonance Raman spectroscopy. *Anal Chem* 82:1342–1348
- Kneipp J (2017) Interrogating cells, tissues, and live animals with new generations of surface-enhanced Raman scattering probes and labels. *ACS Nano* 11:1136–1141
- Koga M, Murai J, Saito H, Kasayama S (2010) Glycated albumin and glycated hemoglobin are influenced differently by endogenous insulin secretion in patients with type 2 diabetes. *Diabetes Care* 33:270–272. <https://doi.org/10.2337/dc09-1002>
- Kohzuma T, Koga M (2010) Lucica GA-L glycated albumin assay kit: a new diagnostic test for diabetes mellitus. *Mol Diagn Ther* 14:49–51. <https://doi.org/10.2165/11317390-000000000-00000>
- Kukushkin VI, Ivanov NM, Novoseltseva AA, Gambaryan AS, Yaminsky IV, Kopylov AM, Zavyalova EG (2019) Highly sensitive detection of influenza virus with SERS aptasensor. *PLoS One* 14:1–14. <https://doi.org/10.1371/journal.pone.0216247>
- Kurochkin IN, Sigolaeva LV, Eremenko AV, Dontsova EA, Gromova MS, Rudakova EV, Makhaeva GF (2014) Layer-by-layer electrochemical biosensors for blood Esterases assay. In: Dishovsky C, Radenkova-Saeva J (eds) *Toxicological problems*. Military Publishing House, Sofia, pp 51–67
- Lee J, Hua B, Park S, Ha M, Lee Y, Fan Z, Ko H (2014) Tailoring surface plasmons of high-density gold nanostar assemblies on metal films for surface-enhanced Raman spectroscopy. *Nanoscale* 6:616–623

- Lee S, Xie J, Chen X (2010) Peptide-based probes for targeted molecular imaging. *Biochemistry* 49:1364–1376. <https://doi.org/10.1021/bi901135x>
- Li W, Ding F, Hu J, Chou S (2011) Three-dimensional cavity nanoantenna coupled plasmonic nanodots for ultrahigh and uniform surface-enhanced Raman scattering over large area. *Opt Express* 19:3925–3936
- Li J, Zhu Z, Zhu B, Ma Y, Lin B, Liu R, Song Y, Lin H, Tu S, Yang C (2016b) Surface-enhanced Raman scattering active plasmonic nanoparticles with ultrasmall interior nanogap for multiplex quantitative detection and cancer cell imaging. *Anal Chem* 88:7828–7836
- Lim D, Jeon K, Kim H, Nam J-M, Suh Y (2010) Nanogop-engineerable Raman-active nanodumbbells for single-molecule detection. *Nat Mater* 9:60–67
- Lin J, Lin J, Huang Z, Lu P, Wang J, Wang X, Chen R (2014) Raman spectroscopy of human hemoglobin for diabetes detection. *J Innov Opt Health Sci* 7:1350051
- Litti L, Amendola V, Toffoli G, Meneghetti M (2016) Detection of low-quantity anticancer drugs by surface-enhanced Raman scattering. *Anal Bioanal Chem* 408:2123–2131
- Liu Y, Zhou H, Hu Z, Yu G, Yang D, Zhao J (2017) Label and label-free based surface-enhanced Raman scattering for pathogen bacteria detection: a review. *Biosens Bioelectron* 94:131–140
- Li B, Duysen EG, Lockridge O (2008) The butyrylcholinesterase knockout mouse is obese on a high-fat diet. *Chem Biol Interact* 175:88–91. <https://doi.org/10.1016/j.cbi.2008.03.009>
- Li H, Wang Y, Li Y, Zhang J, Qiao Y, Wang Q, Che G (2020) Fabrication of pollutant-resistance SERS imprinted sensors based on SiO₂@TiO₂@ag composites for selective detection of pyrethroids in water. *J Phys Chem Solids*. <https://doi.org/10.1016/j.jpss.2019.109254>
- Li M, Banerjee SR, Zheng C, Pomper MG, Barman I (2016a) Ultrahigh affinity Raman probe for targeted live cell imaging of prostate cancer. *Chem Sci* 7:6779–6785. <https://doi.org/10.1039/c6sc01739h>
- Li X, Yang T, Li CS, Song Y, Lou H, Guan D, Jin L (2018) Surface enhanced Raman spectroscopy (SERS) for the multiplex detection of Braf, Kras, and Pik3ca mutations in plasma of colorectal cancer patients. *Theranostics* 8:1678–1689. <https://doi.org/10.7150/thno.22502>
- Lima JK, Leite N, Turek LV, Souza RLR, da Silva Timossi L, Osiecki ACV, Osiecki R, Furtado-Alle L (2013) 1914G variant of BCHE gene associated with enzyme activity, obesity and triglyceride levels. *Gene* 532:24–26. <https://doi.org/10.1016/j.gene.2013.08.068>
- Liron Z, Zifman A, Heleg-Shabtai V (2011) Surface-enhanced Raman scattering detection of cholinesterase inhibitors. *Anal Chim Acta* 703:234–238. <https://doi.org/10.1016/j.aca.2011.07.033>
- Lockridge O (2015) Review of human butyrylcholinesterase structure, function, genetic variants, history of use in the clinic, and potential therapeutic uses. *Pharmacol Ther* 148:34–46. <https://doi.org/10.1016/j.pharmthera.2014.11.011>
- Lockridge O, Norgren RB, Johnson RC, Blake TA (2016) Naturally occurring genetic variants of human acetylcholinesterase and Butyrylcholinesterase and their potential impact on the risk of toxicity from cholinesterase inhibitors. *Chem Res Toxicol* 29:1381–1392. <https://doi.org/10.1021/acs.chemrestox.6b00228>
- Luo Z, Li W, Lu D, Chen K, He Q, Han H, Zou M (2013) A SERS-based immunoassay for porcine circovirus type 2 using multi-branched gold nanoparticles. *Microchim Acta* 180:1501–1507. <https://doi.org/10.1007/s00604-013-1032-5>
- Luo BS, Lin M (2008) A portable Raman system for the identification of foodborne pathogenic Bacteria. *J Rapid Methods Autom Microbiol* 16:238–255
- Masson P, Lockridge O (2010) Butyrylcholinesterase for protection from organophosphorus poisons: catalytic complexities and hysteretic behavior. *Arch Biochem Biophys* 494:107–120. <https://doi.org/10.1016/j.abb.2009.12.005>
- Mattiucci N, D'Aguanno G, Everitt H, Foreman J, Callahan J, Buncick M, Bloemer M (2012) Ultraviolet surface-enhanced Raman scattering at the plasmonic band edge of a metallic grating. *Opt Express* 20:1868–1877
- McFarland A, Young M, Dieringer J, Van Duyne R (2005) Wavelength-scanned surface-enhanced Raman excitation spectroscopy. *J Phys Chem B* 109:11279–11285

- Michen B, Graule T (2010) Isoelectric points of viruses. *J Appl Microbiol* 109:388–397. <https://doi.org/10.1111/j.1365-2672.2010.04663.x>
- Mosier-Boss AP (2017) Review on SERS of Bacteria. *Bios* 7:51
- Nechaeva N, Prokoptkina T, Makhaeva G, Rudakova E, Boltneva N, Dishovsky C, Eremenko A, Kurochkin I (2018) Quantitative butyrylcholinesterase activity detection by surface-enhanced Raman spectroscopy. *Sensors Actuators B Chem* 259:75–82. <https://doi.org/10.1016/j.snb.2017.11.174>
- Nechaeva N, Boginskaya I, Ivanov A, Sarychev A, Eremenko A, Ryzhikov I, Lagarkov A, Kurochkin I (2020) Multiscale flaked silver SERS-substrate for glycosylated human albumin biosensing. *Anal Chim Acta* 1100:250–257
- Oseledchik A, Andreou C, Wall M, Kircher M (2016) Folate-targeted surface-enhanced resonance Raman scattering nanoprobe ratiometry for detection of microscopic ovarian cancer. *ACS Nano* 11:1488–1497
- Otto A (2005) The “chemical” (electronic) contribution to surface-enhanced Raman scattering. *J Raman Spectrosc* 36:497–509
- Patel IS, Premasiri WR, Moir DT, Ziegler LD (2008) Barcoding bacterial cells: a SERS-based methodology for pathogen identification. *J Raman Spectrosc* 39:1660–1672
- Pazos E, Garcia-Algar M, Penas C, Nazarenus M, Torruella A, Pazos-Perez N, Guerrini L, Vazquez M, Garcia-Rico E, Mascarenas J, Alvarez-Puebla R (2016) Surface-enhanced Raman scattering surface selection rules for the proteomic liquid biopsy in real samples: efficient detection of the Oncoprotein c-MYC. *J Am Chem Soc* 138:14206–14209
- Perney N, Baumberg J, Zoorob M, Charlton M, Mahnkopf S, Netti C (2006) Tuning localized plasmons in nanostructured substrates for surface-enhanced Raman scattering. *Opt Express* 14:847–857
- Picorel R, Lu T, Holt RE, Cotton TM, Seibert M (1990) Surface-enhanced resonance Raman scattering (SERRS) spectroscopy of bacterial membranes: the Flavoproteins. In: Baltscheffsky M (ed) *Current research in photosynthesis: proceedings of the VIIIth international conference on photosynthesis*. Stockholm, Sweden, August 6–11, vol 1989. Springer Netherlands, Dordrecht, pp 1867–1870
- Premasiri WR, Lee JC, Sauer-Budge A, Théberge R, Costello CE, Ziegler LD (2016) The biochemical origins of the surface-enhanced Raman spectra of bacteria: a metabolomics profiling by SERS. *Anal Bioanal Chem* 408:4631–4647
- Premasiri WR, Moir DT, Klemperer MS, Krieger N, Jones G, Ziegler LD (2005) Characterization of the surface enhanced Raman scattering (SERS) of Bacteria. *J Phys Chem B* 109:312–320
- Ren X, Yang L, Li Y, Cheshari EC, Li X (2020) The integration of molecular imprinting and surface-enhanced Raman scattering for highly sensitive detection of lysozyme biomarker aided by density functional theory. *Spectrochim Acta – Part A Mol Biomol Spectrosc*. <https://doi.org/10.1016/j.saa.2019.117764>
- Sarychev A, Ivanov A, Lagarkov A, Barbillion G (2019) Light concentration by metal-dielectric micro-resonators for SERS sensing. *Materials* 12:103
- Schurmann R, Bald I (2016) Decomposition of DNA Nucleobases by laser irradiation of gold nanoparticles monitored by surface-enhanced Raman scattering. *J Phys Chem C* 120:3001–3009
- Sgobbi LF, Razzino C a, Rosset IG, Burtoloso ACB, Machado S a S (2013) Electrochemistry and UV-vis spectroscopy of synthetic thiocholine: revisiting the electro-oxidation mechanism. *Electrochim Acta* 112:500–504. <https://doi.org/10.1016/j.electacta.2013.08.143>
- Shan B, Pu Y, Chen Y, Liao M, Li M (2018) Novel SERS labels: rational design, functional integration and biomedical applications. *Coord Chem Rev*. <https://doi.org/10.1016/j.ccr.2018.05.007>
- Sharma B, Frontiera R, Henry A-I, Ringe E, Van Duyne R (2012) SERS: materials, applications, and the future. *Mater Today* 15:16–25
- Smolsky J, Kaur S, Hayashi C, Batra SK, Krasnoslobodtsev AV (2017) Surface-enhanced Raman scattering-based immunoassay technologies for detection of disease biomarkers. *Bios* 7. <https://doi.org/10.3390/bios7010007>

- Su H, Wang Y, Yu Z, Liu Y, Zhang X, Wang X, Sui H, Sun C, Zhao B (2017) Surface-enhanced Raman spectroscopy study on the structure changes of 4-Mercaptophenylboronic acid under different pH conditions. *Spectrochim Acta – Part A Mol Biomol Spectrosc* 185:336–342. <https://doi.org/10.1016/j.saa.2017.05.068>
- Su L, Zhang P, Zheng D, Wang Y, Zhong R (2015) Rapid detection of *Escherichia coli* and *Salmonella typhimurium* by surface-enhanced Raman scattering. *Optoelectron Lett* 11:157–160
- Suh J, Odom T (2013) Nonlinear properties of nanoscale antennas. *Nano Today* 8(5):469–479
- Sun F, Bai T, Zhang L, Ella-Menye J-R, Liu S, Nowinski AK, Jiang S, Yu Q (2014a) Sensitive and fast detection of fructose in complex media via symmetry breaking and signal amplification using surface-enhanced Raman spectroscopy. *Anal Chem* 86:2387–2394. <https://doi.org/10.1021/ac4040983>
- Sun X, Stagon S, Huang H, Chen J, Lei Y (2014b) Functionalized aligned silver nanorod arrays for glucose sensing through surface enhanced Raman 23382–23388. <https://doi.org/10.1039/c4ra02423k>
- Sundaram J, Park B, Hinton A, Lawrence KC, Kwon Y (2013) Detection and differentiation of *Salmonella* serotypes using surface enhanced Raman scattering (SERS) technique. *J Food Meas Charact* 7:1–12
- Tian L, Jiang Q, Liu K, Luan J, Naik R, Singamaneni S (2016) Bacterial nanocellulose- based flexible surface enhanced Raman scattering substrate. *Adv Mater Interfaces* 3:1–8
- Usta DD, Salimi K, Pinar A, Coban İ, Tekinay T, Tuncel A (2016) A Boronate affinity-assisted SERS tag equipped with a Sandwich system for detection of Glycated hemoglobin in the Hemolysate of human erythrocytes. *ACS Appl Mater Interfaces* 8:11934–11944. <https://doi.org/10.1021/acsami.6b00138>
- Vaisi-Raygani A, Rahimi Z, Tavilani H, Pourmotabbed T (2010) Butyrylcholinesterase K variant and the APOE-??4 allele work in synergy to increase the risk of coronary artery disease especially in diabetic patients. *Mol Biol Rep* 37:2083–2091. <https://doi.org/10.1007/s11033-009-9666-4>
- Valle A, O'Connor DT, Taylor P, Zhu G, Montgomery GW, Slagboom PE, Martin NG, Whitfield JB (2006) Butyrylcholinesterase: association with the metabolic syndrome and identification of 2 gene loci affecting activity. *Clin Chem* 52:1014–1020. <https://doi.org/10.1373/clinchem.2005.065052>
- Witkowska E, Korsak D, Kowalska A, Janeczka A, Kamińska A (2018) Strain-level typing and identification of bacteria – a novel approach for SERS active plasmonic nanostructures. *Anal Bioanal Chem* 410:5019–5031
- Xu H, Bjerneld E, Kall M, Borjesson L (1999) Spectroscopy of single hemoglobin molecules by surface enhanced Raman scattering. *Phys Rev Lett* 83:4357–4360
- Yan B, Thubagere A, Premasiri W, Ziegler L, Negro L, Reinhard B (2009) Engineered SERS substrates with multiscale signal enhancement: nanoparticle cluster arrays. *ACS Nano* 3:1190–1202
- Yan Y, Zhang J, Xu P, Miao P (2017) Fabrication of arrayed triangular micro-cavities for SERS substrates using the force modulated indentation process. *RSC Adv* 7:11969–11978. <https://doi.org/10.1039/c6ra28875h>
- Yang T, Zhang Z, Zhao B, Hou R, Kinchla A, Clark J, He L (2016) Real-time and in situ monitoring of pesticide penetration in edible leaves by surface-enhanced Raman scattering mapping. *Anal Chem* 88:5243–5250
- Zhang N, Liu K, Liu Z, Song H, Zeng X, Ji D, Cheney A, Jiang S, Gan Q (2015) Ultrabroadband Metasurface for efficient light trapping and localization: a universal surface-enhanced Raman spectroscopy substrate for “all” excitation wavelengths. *Adv Mater Interfaces* 2:1–7
- Zhang X, Zhang X, Luo C, Liu Z, Chen Y, Dong S, Jiang C, Yang S, Wang F, Xiao X (2019) Volume-enhanced Raman scattering detection of viruses. *Small* 15:1–8. <https://doi.org/10.1002/smll.201805516>

- Zhao L, Huang Q, Liu Y, Wang Q, Wang L, Xiao S, Bi F, Ding J (2017) Boronic acid as glucose-sensitive agent regulates drug delivery for diabetes treatment. *Materials (Basel)* 10:1–14. <https://doi.org/10.3390/ma10020170>
- Zhou Q, Meng G, Wu N, Zhou N, Chen B, Li F, Huang Q (2016) Dipping into a drink: basil-seed supported silver nanoparticles as surface-enhanced Raman scattering substrates for toxic molecule detection. *Sensors Actuators B Chem* 223:447–452
- Zeiri L, Bronk BV, Shabtai Y, Czégé J, Efrima S (2002) Silver metal induced surface enhanced Raman of bacteria. *Colloids Surf A Physicochem Eng Asp* 208:357–362
- Zeiri L, Bronk BV, Shabtai Y, Eichler J, Efrima S (2004) Surface-enhanced Raman spectroscopy as a tool for probing specific biochemical components in Bacteria. *Appl Spectrosc* 58:33–40

Chapter 6

Biosensors for Virus Detection



Olga I. Guliy, Boris D. Zaitsev, and Irina A. Borodina

Abstract Viral infections today remain one of the global problems. Despite the significant number of developed methods for the determination and study of viral particles, their practical use is difficult due to the complexity and a small number of existing measuring instruments. In addition, in a number of devices, there is a high proportion of manual operations that require highly qualified staff. Therefore, the problem of the development of new rapid methods for diagnosing viruses that allow getting accurate results in a short time in automatic mode is urgent. Instrumentation implementation of these methods should ensure high accuracy of measurements. One of the most sought-after areas is the development of fast and sensitive methods for determining viruses based on methods of electrophysical analysis. These methods can significantly reduce the analysis time and simplify the preparation of the investigated materials. The chapter provides a brief overview of modern biosensor methods for the virus's detection.

Keywords Biosensors · Virus detection · Bacteriophages · Electrochemical biosensors · Optical sensors · Acoustic biosensors · Microwave resonator · Cantilever · Antibodies

Nomenclature

Ab	Antibody
Ab-AuNPs	Antibody-conjugated gold nanoparticles
Abs	Antibodies
DNA	Deoxyribonucleic acid
ELISA	Enzyme-linked immunosorbent assay
EO	Electro-optical

O. I. Guliy (✉)

Institute of Biochemistry and Physiology of Plants and Microorganisms, Russian Academy of Sciences, Saratov, Russia

e-mail: guliy_olga@mail.ru

B. D. Zaitsev · I. A. Borodina

Kotelnikov Institute of Radio Engineering and Electronics, Russian Academy of Sciences, Saratov Branch, Saratov, Russia

FITC	Fluorescein isothiocyanate conjugated
GM	Gas membrane
GNPs	Gold nanoparticles
GRS	Giant Raman scattering
HEV	Hepatitis E virus
HIV	Human immunodeficiency viruses
HSV	Human herpes simplex virus type 1
IgG	Immunoglobulin G
LFIA	Lateral flow immunoassay
MMA	Micromagnetic array
MNPs	Magnetic nanoparticles
NP	Nucleoprotein
NS1	Non-structural protein 1
PCR	Polymerase chain reaction
PFU	Plaque-forming units
RNA	Ribonucleic acid
RT-qPCR	Real-time quantitative polymerase chain reaction
SPM	Superparamagnetic
SPR	Surface plasmon resonance
TMBZ	Tetramethylbenzidine
TGEV	Transmissible gastroenteritis virus

6.1 Introduction

Viral infections occupy one of the leading positions among human and animal diseases. Therefore, the diagnosis of viruses is the main strategy for combating viruses and eliminating them.

Various approaches are used to detect and identify viruses, such as microbiological and biochemical tests, genetic engineering, and immunological methods. Existing methods for identifying viral particles can be divided into the following groups:

1. Detection (identification, determination of concentration, size, and other physicochemical properties) of viral particles (virions) and determination of viral infectivity.
2. Determination of viral antigens.
3. Determination of viral nucleic acids (Carter and Saunders 2007).

Despite the significant number of developed methods for detecting viral particles, their practical use is difficult due to the complexity, high cost, and the small number of existing measuring instruments. In addition, in a number of devices, there is a high proportion of manual operations that require highly qualified staff.

For example, traditional methods for identifying viruses have drawbacks, primarily due to insufficient sensitivity (immunofluorescence methods), long duration of analysis, tedious, and lack of the universality of the procedure (culture method). The detection of antibodies to viruses in the serum of patients using enzyme-linked immunosorbent assay (ELISA) is a retrospective method because it does not detect the pathogen itself, but records the body's response to infection. ELISA detection of viral antigens in clinical samples is limited by the lack of sensitivity of the method. The use of immunochemical and serological methods also complicates the high antigenic diversity of some groups of viruses. Traditional methods, due to the limitations listed above, do not allow simultaneous and highly sensitive detection of the main virus groups in clinical samples.

The molecular approaches, including the polymerase chain reaction (PCR) and its various modifications, are widely used in the laboratory diagnosis of viral infections. It should be noted that the real-time PCR is also widely used (Coiras et al. 2004; Syrmis et al. 2004; Templeton et al. 2004). In recent years, such high-tech technology as DNA microarray technology (Lin et al. 2007; Mehlmann et al. 2007; Huguenin et al. 2012; del Pilar Martinez Viedma et al. 2019) has been increasingly used for diagnostics, for example, acute respiratory viral infections. The advantages of molecular methods are high specificity, sensitivity, universality of the procedure, short analysis time, process automation, and the ability to identify several pathogens at once.

Viruses are dispersed and usually exist in various morphological forms, the size of which usually varies from 20 to 900 nm (Passi et al. 2015; Rojek et al. 2017; Shawky et al. 2017). Their intact, mature infectious particles usually consist of certain units of proteins and nucleic acids that self-assemble to form nanoparticle structures called virions. Viral proteins are usually located in the surface layer, called the capsid, and, sometimes, in the outer shell surrounding the inner nucleic acid nucleus. This core of viral nucleic acids can be single or double-stranded (ds), DNA or RNA, one or more linear or circular molecules, ranging in size from several thousand nucleotides to one million base pairs.

Features of the structure and activity of viruses are taken into account when developing methods for their analysis. However, it is important to consider that all viruses evolve rapidly, which is facilitated by the world-wide migration processes that have intensified in recent years. Under these conditions, humanity is increasingly encountering the emergence of new viruses or strains that are well-known but distinguished by increased pathogenicity (e.g., SARS coronavirus, A/H5N1 avian influenza virus). Therefore, a very important area is the development of express methods for determining viruses. One of the most promising tools for detecting viruses is biosensor analysis methods. Instrumentation of these methods should ensure high accuracy of measurements, and measurements should be carried out automatically by mid-level personnel.

An important criterion in the development of new methods for determining viruses is their versatility and the ability to use for various objects. Therefore, the

development of methods for the electrophysical analysis of viral particles occupies one of the leading positions in this direction. The chapter provides a short overview of modern biosensor virus detection methods.

6.2 Biosensor Methods for Virus Detection

Initially, methods of electrophysical analysis were used to study the electrophysical properties of the cell. A systematic study of these issues began in the 30s of the last century, when they began to study one of the electrical characteristics of cells—surface charge. Later, in the 60s, investigations on the study of the dielectric constant and electrical conductivity of tissues, cells, and cellular organelles began to carry out. Recent years have been characterized by an increased interest in the electrical characteristics of not only cells, but also viruses. With the advent of biosensors, the traditional approaches to methods for determining viruses are changing significantly. The development of biosensor virus detection technologies will be extremely useful for the early detection of diseases and the timely provision of medical care (Chandra, 2016).

Biosensors are biochemical-physical systems consisting of two components: a sensitive biological element and a detection system, allowing to record the concentration or activity of various analytes presenting in the sample. The biological element can be catalytic and non-catalytic. Catalytic elements include enzymes and tissues. Non-catalytic elements are receptors and nucleic acids. The detection system can be optical, calorimetric, acoustic, electrical, etc. There is a possibility of combining all these systems, which indicates the possibility of creating a huge number of various biosensor systems (Turner 1987).

Biosensor methods of analysis began to be used to determine glucose by Clark and Lyons in 1960 and have now become an integral part of clinical diagnosis and environmental monitoring (Brooks et al. 1988). Biosensors can significantly reduce the analysis time, due to the relative simplicity of the procedures, and as the published data show, they are quite sensitive and require minimal preliminary processing of the test material. For the detection of viral particles, biosensors with different designs and mechanisms of operation are increasingly being used. The key problem in the development of a biosensor is the process of introducing and fixing the bioreceptor on the surface of the carrier (transducer), that is, an immobilization process that allows the development of a selective, reproducible, sensitive, and stable biosensor (Leca-Bouvier 2010; Moreira 2014).

Therefore, one of the main points for the classification of sensors is to use the immobilization of analysis components on the surface of the sensor or to conduct studies directly in the liquid without immobilizing the analysis components.

Depending on the detection method, the sensors are divided into electrochemical, optical, acoustic, and cantilever sensors for viruses and bacteriophages.

6.2.1 *Electrochemical Biosensors*

Electrochemical biosensors were created with the aim of combining the sensitivity of the electrochemical detector and the specificity of the active layer during antigen–antibody interaction. Electrochemical biosensors include:

- Potentiometric sensors in which the cell potential is measured at zero current;
- Voltametric (or amperometric) sensors, in which the oxidation or reduction current of electroactive particles is measured at applying a given potential difference between the electrodes;
- Conductometric sensors in which the conductivity of the contents of the container is measured using a conductivity bridge (Budnikov 2010; Evtugin 2013).

Combining the principles of voltammetry with immunological reactions allows creating inexpensive and selective analytical devices—amperometric immunosensors, which combine high sensitivity of amperometric detection and the specificity of immune interactions. The immunosensor operation scheme is presented in Fig. 6.1(a).

In biosensors of the electrochemical type, in combination with potentiometric electrodes, enzymes, receptors, microorganism cells, plant and animal tissues, and antibodies labeled with enzymes are used. In combination with amperometric electrodes, the use of enzymes, microorganisms, plant and animal tissues, and antibodies labeled with enzymes is known.

For example, an amperometric immunosensor was developed without the use of labels for the sensitive determination of antibody (Ab) to the Japanese encephalitis B virus. In order to obtain a biosensitive part of the sensor, the antiserum was immobilized to an *o*-phenylenediamine film modified with gold nanoparticles (GNPs) and Prussian blue on the surface of a platinum electrode. The formation of the analytical signal of the sensor is based on a change in the behavior of the mediator—Prussian blue ($\text{Fe}^{2+}/\text{Fe}^{3+}$)—during immunochemical interaction, which was recorded using the method of cyclic voltammetry. The detection limit was 6×10^9 (Ig particles)/Mn. The prospects of using the proposed immunosensor to determine the encephalitis virus in biological samples are shown (Budnikov et al. 2013).

Los et al. (2006) proposed the use of an electrochemical biochip to quickly detect phage infection and the phenomenon of lysogeny. The principle of the method is to capture target molecules (either nucleic acids or proteins) on a chip using a probe that is connected to an enzyme that catalyzes the oxidation–reduction reaction. The electrical signal resulting from this reaction is measured using a microelectrode. Two types of biochips were used in the work: for detecting nucleic acids of bacteriophages (using DNA probes) and for detecting virions (using specific Ab). The authors demonstrated the ability to detect phages M13, P1, T4, and λ in a short time (25–50 min) and in an amount of 10^4 to 10^7 particles/ml.

Using the detection of T7 bacteriophage as an example, the use of a colorimetric immunosensor made on the basis of gold nanoparticles covalently associated with specific antibodies to the T7 bacteriophage was proposed (Lesniewski et al. 2014).

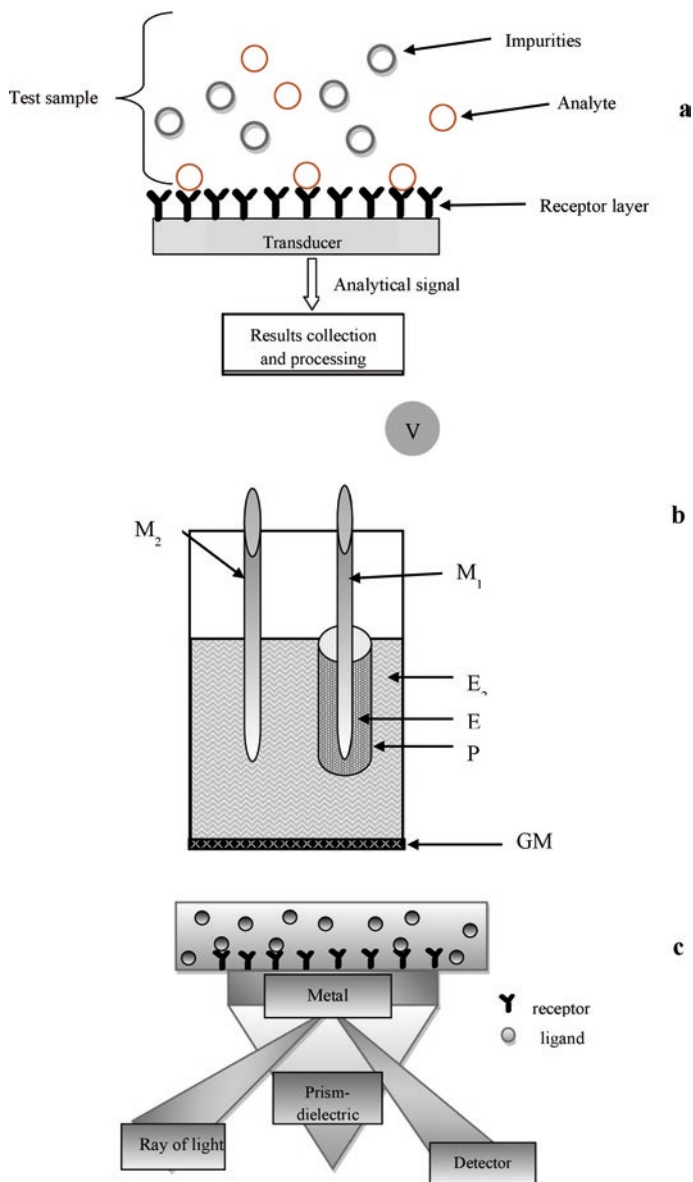


Fig. 6.1 (a) The general scheme of the immunosensor. (b) The structure of the gas-sensitive electrochemical sensor: M_1 and M_2 —internal and external metal electrodes; E_1 and E_2 —internal and external electrolyte; P—porous septum; GM—gas-permeable membrane. (c) Diagram of the SPR biosensor based on a dielectric prism (like Kretschmann scheme)

The described model of the immunosensor, due to the formation of immune complexes of the bacteriophage with Ab and gold nanoparticles, allows us to detect quickly, simply, and selectively the virus. As a result, one can observe a change in the color of the solution from red to purple with the naked eye. At that, the authors conclude that this method can be used to detect almost any virus.

The study by Grabowska et al. (2014) provides data on the use of an electrochemical biosensor (genosensor and immunosensor) for determining the bird flu virus.

A barcode lateral flow immunoassay (LFIA) based on magnetic nanoparticles with a controllable cut-off level was developed for the first time to detect potato virus X in the leaf extracts. To obtain specific conjugates, monoclonal antibodies were covalently immobilized on the magnetic nanoparticles' surface. The application of magnetic concentration leads to a six-fold reduction in the first cut-off level (0.5 ng/mL) in comparison with magnetic LFIA without the concentration stage (Panferov et al. 2017).

The joint use of magnetic nanoparticles (MNPs) and gold nanoparticles (GNPs) double enhancement in a LFIA for potato virus X detection was shown in Razo et al. (2018). The study realizes two types of enhancement: (1) increasing the concentration of analytes in the samples using conjugates of MNPs with specific antibodies and (2) increasing the visibility of the label through MNP aggregation caused by GNPs. The double-enhanced LFIA achieved the highest sensitivity, equal to 0.25 ng/mL and 32 times more sensitivity than the non-enhanced LFIA (detection limit: 8 ng/mL).

Although LFIA has many advantages including speed and ease of use, their sensitivity is limited without specific equipment. Furthermore, their response cannot be enhanced through enzymatic reactions. Owing to these limitations, LFIA has not yet been generally adopted as the standard protocol for in vitro analysis of infectious pathogens. Noh et al. (2019) described a novel pipetting-based immunoassay using a removable magnetic ring-coupled pipette tip. The "magnetic bead-capture antibody-targeted protein complex" was simply purified by pipetting and quantified by enzymatic color development or using a lateral flow system. This pipetting-based immunoassay was applied to detect the nucleoprotein (NP) of the influenza A virus. Using an HP-conjugated monoclonal antibody as a probe, the assay allowed for specific and sensitive detection. Khoris et al. (2020) described an efficient and quick monitoring system for *Hepatitis E virus* (HEV) detection. The advanced platform for immunoassay has been constructed by a nanozyme that constitutes anti-HEV IgG antibody-conjugated gold nanoparticles (Ab-AuNPs) as core and in situ silver deposition on the surface of Ab-AuNPs as outer shell. The virus has been entrapped on the nanocomposites while the silver shell has decomposed back to the silver ions (Ag⁺) by adding a tetramethylbenzidine (TMBZ) and hydrogen peroxide (H₂O₂) which indirectly quantifies the target virus concentration. Most importantly, the sensor performances have been examined in clinically isolated HEV from HEV-infected monkey over a period of 45 days which successfully

correlated with their standard RT-qPCR data, showing the applicability of this immunoassay as a real-time monitoring on the HEV infection.

By using as an example the bacteriophage PhiX17 and *Escherichia coli* WG5 sensitive to this phage, a fast method for detecting viral particles in a sample using a whole-cell biosensor was demonstrated. A biofilm of *Escherichia coli* cells was formed on the surface of the metal electrode. The infection of biofilm cells with a specific bacteriophage leads to their lysis and a change in impedance on the surface of the microelectrode. This change was recorded using impedance spectroscopy. The method is simple and allows to detect bacteriophages as long as there are sensitive cells on the chip (Muñoz-Berbel et al. 2008).

Constant outbreaks of infectious diseases have shown that in some cases there are no quick non-invasive methods for their diagnosis. In modern realities, a patient sometimes cannot detect, for example, the flu virus without assistance. Therefore, in most cases, a person has no idea whether he is infected until certain symptoms appear, and most often this moment comes too late. One example of a virus definition is the so-called “gas-sensitive electrodes.” The principle of their operation is shown in Fig. 6.1 (b). An important structural element of the potentiometric gas-sensitive sensor is the permeable gas membrane (GM), which separates the electrolyte of the “external” half cell from the surrounding atmosphere. The membrane is impervious to the electrolyte, but permeable to molecules of controlled gases. The higher the concentration of such gases in the surrounding atmosphere, the more their molecules penetrate through the GM membrane into the electrolyte and dissolve in it. They can enter into chemical reactions, and this violates the dynamic equilibrium in the near-electrode zone and changes the potential difference between the electrodes. For example, Gouma et al. (2017) created a device resembling a breathalyzer and able to detect the influenza virus in the early stages. The main difference from breathalyzers or household carbon monoxide detectors is the specificity of sensors that detect gas.

The measurement of the amount of heat released during the interaction of the analyte with the bioreceptor material is used in biosensors of the calorimetric type. In this case, the basis of the bioreceptor can serve as enzymes, cells of microorganisms and animals. For a more detailed acquaintance with various types of biosensors, you can refer to the monographs (Turner 1987; Buerk 1993; Harsanyi 2000).

Electrochemical biosensors have advantages over many alternative approaches, in particular, optical sensors, for which the turbidity of the solution or its color can significantly limit the scope of potential applications. The current stage of development of electrochemical biosensors is characterized by an explosive increase in interest in additional factors determining their selectivity and sensitivity. These include modification of the surface of the electrode as a primary signal transducer, and the substrate for the localization of the biochemical receptor. The disadvantages of electrochemical biosensors include sensitivity to radiation, as well as to fluctuations in temperature and pH of the solution.

6.2.2 *Optical Biosensors*

In optical biosensors, the analytical signal is caused not by the chemical interaction of the component being determined with the sensitive element, but by the measured physical parameters—the absorption and reflection of light, the luminescence intensity of the object, etc. The principle of operation of optical biosensors is based on recording changes in the optical properties of the medium: optical density (densitometric biosensors), color (colorimetric biosensors), turbidity (turbidimetric biosensors), medium refractive index (refractometric biosensors), and other properties as a result of the presence of a biological agent. Currently, optical biosensors are most developed, based on a change in the direction of propagation of the light flux passing through an optical fiber or a triangular prism coated with a thin metal film. They are based on the effect of surface plasmon resonance (Deisingh 2003).

Optical biosensors, including planar waveguide sensors, were developed simultaneously with the first electrochemical devices, but for a long time, they did not receive proper attention (Evtugyn 2013). Optical fiber sensors can be divided into two large groups: internal and external sensors. Internal sensors include ones in which the transit time, intensity, or polarization of light propagating along the fiber can be modulated by an external force acting on the fiber. In external sensors, fiber is used primarily as a means of transmitting light to the substance being determined, where the properties of light (intensity, length, wave polarization) are modified, and then the modified light is removed from the measuring element through the fiber (Turner 1987).

Most optosensors are optical fibers modified with various auxiliary chemicals and biocomponents. The optical fiber is a flexible transparent layer (core) of glass (silicon dioxide, plastic) with a refractive index n_1 , coated by the shell with a refractive index n_2 ($n_2 < n_1$). Due to total internal reflection, optical fibers are used as waveguides for light. Optical biosensor fibers can be used in combination with various spectroscopic methods, for example, with fluorescent ones. Chemically and bioluminescent biosensors, as well as electroluminescent sensors, provide very sensitive detection of specific substrates. The only problem existing in the detection of luminescence of a biochemical signal is the achievement of the selectivity of the system due to the numerous light interferences. Optosensors have several advantages, namely: each type of analyte can be determined using appropriate spectrometric methods. At that, there is the possibility of remote monitoring and the implementation of non-invasive formats of biomedical sensors. The widespread use of optical biosensors is also due to the fact that they allow the analysis of very small quantities of substances and can be adapted to the analysis and detection of a large range of various biological and chemical objects (Erickson et al. 2008; Fan et al. 2008). However, some disadvantages make their development difficult. These include interference with ambient light, possible photobleaching of dyes and other auxiliary components, the high optical density of the background, the fluorescence of the fiber, a fairly long measurement time, and the limited availability of accessories.

An optical immunosensor has also been developed to detect the biomarker of non-structural protein 1 (NS1) dengue in clinical samples obtained in the early stages of infection. The principle of operation is based on the determination of the NS1 antigen by immunofluorescence using fluorescein isothiocyanate (FITC) conjugated to an IgG antibody. The sensor is characterized by high reproducibility (relative standard deviation of 2%) and good stability for 21 days at 4 °C with a detection limit of 15 ngmL⁻¹ (Darwish et al. 2018).

The fluorescence method has made great progress in the construction of sensitive sensors, but the background fluorescence of the matrix and photobleaching limit its broad application in clinical diagnosis. Wu et al. (2019) proposed a digital single virus immunoassay for multiplex virus detection by using fluorescent magnetic multifunctional nanospheres as both capture carriers and signal labels. The superparamagnetism and strong magnetic response ability of nanospheres can realize efficient capture and separation of targets without sample pretreatment. Due to their distinguishable fluorescence imaging and photostability, the nanospheres enable single-particle counting for ultrasensitive multiplexed detection. Based on multifunctional nanospheres and digital analysis, a digital single virus immunoassay was proposed for simultaneous detection of H9N2, H1N1, and H7N9 avian influenza virus without complex signal amplification, whose detection limit was 0.02 pg/mL.

The highly efficient detection of the Human herpes simplex virus type 1 (HSV) UL27 gene through the programmed assembly of superparamagnetic (SPM) nanoparticles based on oligonucleotide hybridization was demonstrated (Li et al. 2020). The state of assembly of the SPM nanoparticles was determined by optical signature of the synchronized motion on the beads on a micromagnetic array (MMA). This technique has been used to identify <200 copies of the HSV UL27 gene without amplification in less than 20 min.

In the late 60s of the twentieth century, E. Kretschmann showed the possibility of excitation of surface plasmons by polarized light, which served as an impetus for the development of the method of surface plasmon resonance (SPR). After 10–20 years, using the phenomenon of plasmon resonance, a number of researchers have shown the possibility of using the method to study biological objects, including viruses. The advantage of this technology is the ability to observe almost any intermolecular interactions in real-time, without using special tags (Homola 2006; De Mol and Fischer 2010).

SPR is a phenomenon that occurs at the phase boundary, for example, a glass prism—a metal film. Part of a light passing through a prism and falling at a certain angle on the metal surface propagates in a metal film in the form of a damped electromagnetic wave, which causes collective oscillatory movements of free electrons. The connection of the studied object with the surface of the metal film leads to a change in the dielectric constant and, consequently, to a change in the angle of spatial resonance. The change in the angle of spatial resonance can be monitored in real-time, obtaining information on the kinetics of interactions that occur on the surface of a metal film (Garcia-Aljaro et al. 2008; De Mol and Fischer 2010).

In the majority of biosensor SPRs used today, surface plasmons are excited using a prism scheme, which is widespread due to the simple implementation and the

possibility of using methods with various types of signal modulation (see Fig. 6.1c) (Kretschmann et al. 1968; Kanso et al. 2008; Mamichev et al. 2012).

Biosensors of this type allow the study of a variety of intermolecular ties and affinity. In general, SPR can be attributed to express methods. For example, in the work (Garcia – Aljaro et al. 2008) showed the possibility of detecting bacteriophages of *Escherichia coli* using a two-channel microfluidic SPR sensor in real-time. Biotinylated *Escherichia coli* WG5 cells were applied to a gold film using avidin as a ligand. Bacterial cells immobilized in this way were used as targets for the selective detection of coliphages. After adding bacteriophages isolated from wastewater to this system, their binding to cells was observed. The sensitivity of this method was 10^2 plaque-forming units (PFU/ml), with an incubation time of 120 min.

Biosensors are widely used, the effect of which is based on giant Raman scattering (GRS) (Monzon-Hernandez and Villatoro 2006; Liu 2007). One of the most promising applications of GRS is to study the structural and functional features of various biological molecules, since this method is non-destructive and allows you to quickly obtain information about the chemical and structural properties of biomolecules.

Two methods for detecting biomolecules by means of GRS are most common: homogeneous—the target molecule forms a bond with metal nanoparticles in the solution, which play the role of cattle “amplifiers” (Fig. 6.2 a), and heterogeneous—the solution of the analyzed molecules is placed on the surface with GRS active centers (Fig. 6.2 b). The advantages of the first method are the high reaction rate and the relative ease of implementation, as well as the uniformity and repeatability of the obtained amplification of the GRS signal, since nanoparticles can be synthesized with a high degree of repeatability of their parameters. In such GRS systems, metal nanoparticles with various types of shells (Jackson et al. 2003) and nanorods (Nikoobakht 2003) are often used as GRS-active substrates.

The GRS technique is used for various biochemical analyzes, including immunoassay, the purpose of which is to detect a specific interaction between antibodies and antigens. In Xu et al. (2004), hepatitis B virus antigen was detected by using gold nanoparticles equipped with immunolabels that were adsorbed on a GRS-active silver substrate.

Progress in the use of an electro-optical (EO) sensor for transmissible gastroenteritis virus (TGEV) detection with help of specific antibodies without their immobilisation on the sensor surface was described in Guliy et al. (2020). The EO signal is an information parameter that characterizes the change in the electrical characteristics of suspended particles (viruses) under the influence of an electric field. During the surface interaction of viral particles with antibodies, the surface electrical properties change, which leads to a change in particle polarization, orientation, and optical response. In the method used for the optical recording of interaction effects, the response is used in the form of a change in the attenuation of monochromatic unpolarized light when the virus-specific antibody complexes are oriented. The limit for reliable virus detection is 10^4 virus particles/ml, and the time of analysis is 10–15 min.

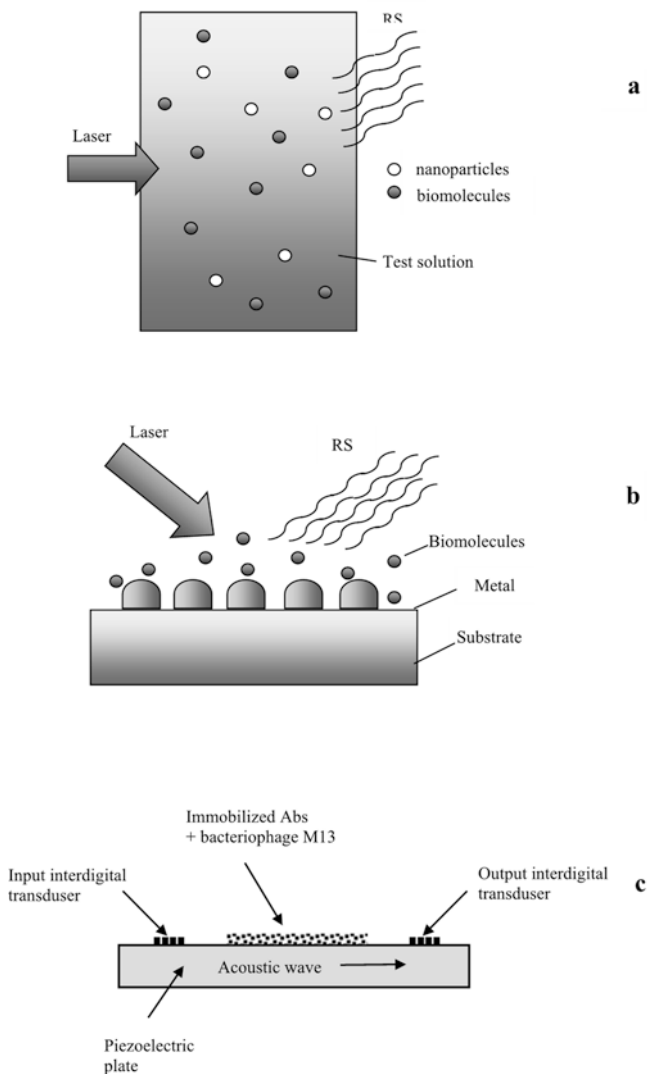


Fig. 6.2 The principle of action of the biosensor for detecting biomolecules by means of giant Raman scattering (GRS). **(a)** the homogeneous variant (the target molecule forms a bond with metal nanoparticles in the solution, which play the role of cattle “amplifiers”) and **(b)** the inhomogeneous variant (the solution of the analyzed molecules is placed on the surface with GRS active centers). **(c)** General scheme of a sensor with an acoustic Love wave

Rossi et al. (2007) demonstrated the possibility of detecting the bacteriophage MS2 using a biosensor based on thin films of nanoporous silicon. Due to the advantages of nanoporous silicon—the simplicity of the technology and extremely high surface area—it is an ideal basis for the manufacture of sensors. Antibodies were immobilized on porous films by covalent bioconjugation and then dye-labeled

bacteriophages MS2 were introduced into the system. During the measurement of fluorescence, the possibility of detecting viral particles in the amount of 2×10^7 PFU/ml was established.

6.2.3 Acoustic Biosensors

Recently, piezoelectric resonators or delay lines with a propagating surface or plate acoustic wave have been widely used to create biosensors. Such biosensors are sensitive to changes in the mechanical or electrical properties of a biological object contacting with the surface of the waveguide. Acoustic biosensors are most often made on the basis of piezoelectric crystals such as quartz, lithium niobate, or lithium tantalate, since they are characterized by high chemical resistance. Acoustic waves excited in a piezoelectric medium may be used for creating a whole family of sensors characterized by high sensitivity, speed of analysis, low cost, and small sizes.

Some methods are based on the use of Abs or membranes as a receptor deposited on the surface of a piezoelectric waveguide or resonator (Ballantine et al. 1997). For example, using the immobilization of the corresponding antiviral antibodies on the surface of a piezoelectric resonator, an immunosensor was developed for the selective detection of herpes viruses in human blood (Koenig and Graetzel 1994), as well as in natural water reservoirs (rivers, sewers, wastewaters) without preliminary processing of the analyzed substrate (Bisoffi et al. 2008).

The work (Uttenthaler et al. 2001; Kurosawa et al. 2006) showed the possibility of detecting bacteriophages by biosensors representing a piezoelectric resonator based on crystalline quartz (SiO_2). The surface of the crystal is coated with antibodies (Abs) specific for the bacteriophage, and in the course of a specific reaction on the surface of the crystal, the resonant frequency of the vibrations changes, which is detected by the biosensor.

Tamarin et al. (2003), using elastic Love waves with horizontal shear polarization in a layered medium, showed the possibility of detecting the bacteriophage M13 in real-time. Initially, irreversible immobilization of Abs specific for bacteriophage M13 was performed on a silicon oxide substrate. Then, an immunoreaction was carried out between the bacteriophage M13 and the immobilized Abs, and the resulting multilayer structure appeared on the surface of the waveguide, leading to a change in the velocity, and attenuation of the Love wave was analyzed. The general scheme of the sensor based on Love waves is shown in Fig. 6.2c. As a control for counting the bacteriophage titer, particles bound to Abs on the surface of the sensor were eluted by changing the pH of the solution. In this case, the number of PFU was evaluated by microbiological methods.

Matatagui et al. (2014) considered the possibility of using a Love-wave immunosensors in combination with a microfluidic chip to determine the bacteriophage M13.

Along with the use of active layers, the possibility of studying biomolecular interactions in solutions in direct contact with the surface of the waveguide was shown. This significantly reduces the time required for detecting the test sample.

For example, a biosensor for detecting endotoxin in various solutions was created on the basis of a resonator with a longitudinal electric field (Muramatsu et al. 1989).

It has been shown that an acoustic sensor with a surface acoustic wave allows to detect the Ebola virus (Baca 2004). The absence of an active layer in the sensor led also to the possibility of its multiple uses. A biosensor based on a piezoelectric resonator with a longitudinal electric field was developed and successfully tested to detect hepatitis B virus (Zhou et al. 2002).

The possibility of using an acoustic biosensor based on lithium tantalate to quickly detect human immunodeficiency viruses (HIV) and differentiation between two different serotypes of HIV-1 and HIV-2 in complex matrices such as human blood has been demonstrated (Bisoffi 2013). This is extremely important for emergency assistance, which requires quick and reliable testing for the presence of blood-borne pathogens.

Piezoelectric resonators with a lateral electric field, in which there is no contact of the material under study with metal electrodes, are very promising for the study of biological objects (Fig. 6.3 a). These resonators are used to study the properties of various liquids, including biological ones. Such a resonator is a piezoelectric plate with two electrodes deposited on one of its side. The test suspension is in contact with the opposite side of the plate. It is known that a change in the viscosity and conductivity of a contacting liquid leads to a change in the characteristics of such a resonator (Zaitsev et al. 2015).

This allows the analysis of biological objects directly in the liquid phase without applying specific Abs to the surface of the resonator. On this basis, the possibility of detecting bacteriophages using specific microbial cells, antibodies, and phage mini-antibodies directly in the liquid phase has been shown (Zaitsev et al. 2012; Guliy et al. 2016a, b; Guliy et al. 2017a; Guliy et al. 2018; Guliy et al. 2019). It was found that the lower limit of detection of bacteriophages was 10^6 phages/ml with an analysis time of ~ 10 min. The degree of change in the characteristics of the resonator depends on the number of phage particles, which opens up prospects for conducting not only a qualitative but also quantitative analysis of bacteriophages. The obtained data showed the possibility of using the value of the real or imaginary part of the electrical impedance at a fixed frequency near the resonance as an analytical signal. Sensor capabilities have been demonstrated for bacteriophages belonging to different taxonomic groups.

For example, filamentous bacteriophage of class I M13K07 belongs to the *Inoviridae* family, and the bacteriophages Φ A1-Sp59b and Φ A1-SR65 correspond to the *Podoviridae* family. A criterion for confident registration of a specific interaction was developed, which consists in the fact that the change in the module of the electrical impedance of the sensor should be at least $\sim 5\%$ when a certain amount of Abs is added to the suspension of bacteriophages. The advantage of a piezoelectric resonator with a lateral electric field is the possibility of its multiple use. This is because the resonator is made of a lithium niobate crystal, which is chemically resistant to almost all chemical compounds. In addition, the surface of the resonator, processed according to the 14th class of purity, does not allow any adsorption. Therefore, after washing the resonator, no trace of the suspension remains on its surface, and

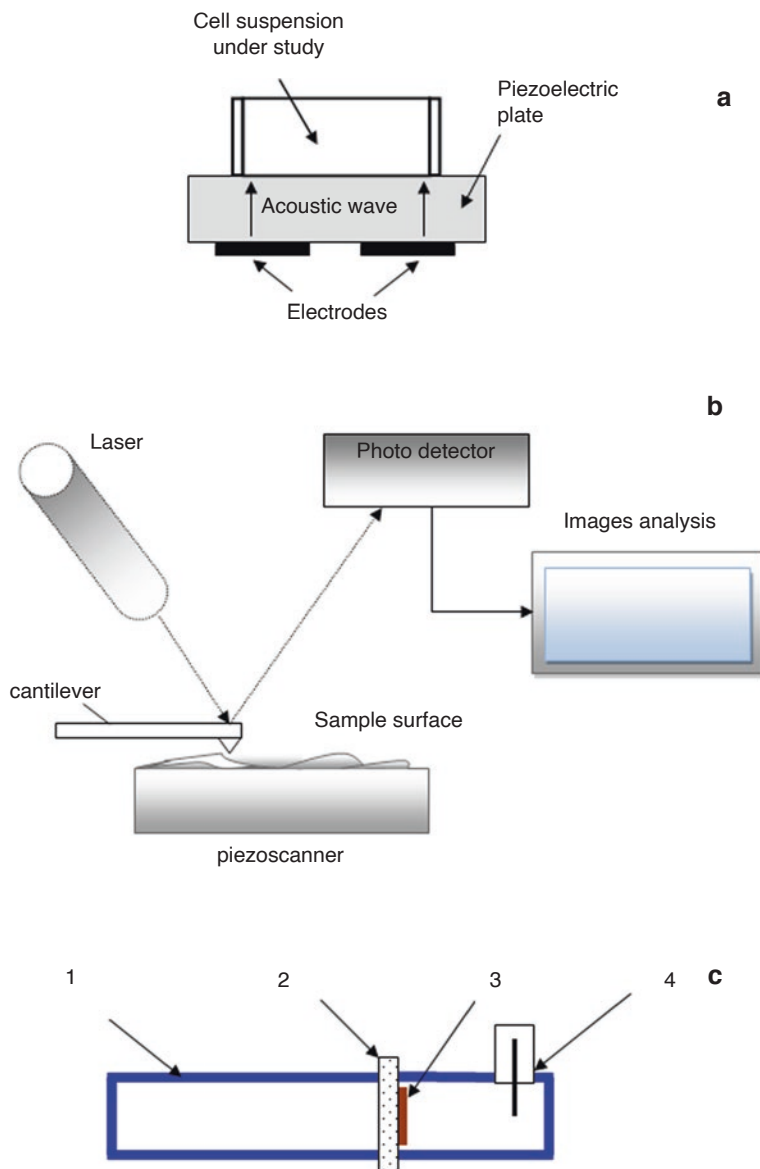


Fig. 6.3 (a) The scheme of an acoustic sensor based on a piezoelectric resonator with a lateral electric field. (b) The general scheme of the cantilever sensor. (c) The scheme of a detecting system based on a microwave resonator: 1—segment of the rectangular waveguide; 2—plate of lithium niobate; 3—sensitive layer with immobilized cells; 4—coaxial waveguide adapter

confirmation of this is the complete restoration of all its characteristics after all experiments.

Obviously, for reliable determination of viral particles, one should select a specific receptor in each case. Currently, specific antibodies immobilized on carriers are most often used to detect viruses. Improvements in this area of research have focused on the development of platforms for immobilizing antibodies, such as micro- or nanochips, in which several agents can be identified in various ways. The development of virus detection technologies is focused on improving the sensitivity, cost-effectiveness, and reusability of the sensor.

Ideally, in order to elicit the most effective response to a virus, a “speed-type” biosensor network is needed to quickly receive an initial warning of the presence, spread, and virality of an infectious agent. To achieve this, it is desirable to use a portable biosensor with high sensitivity and accuracy, which can detect viruses in real-time. Continued research to improve probes and platforms should lead to the creation of effective biosensors that can be used in real samples. In this context, the method of electroacoustic analysis based on a piezoelectric resonator with a lateral electric field has shown the promise of its application for solving the problems of virus detection. Further standardization and automation of the electro-acoustic analysis method will expand the range of its application and use in microbiology, biotechnology, veterinary medicine, medicine, and phage therapy.

6.2.4 Cantilever Biosensors

Compact and autonomous sensors based on microcantilevers integrated into microfluidic chips have prospects for use as personalized diagnostic devices (Vasan et al. 2013; Kolesov et al. 2016). The main element in such a sensor is the cantilever, that is, high-quality mechanical resonator made of a piezoelectric rod of the rectangular cross-section. One end of the rod is mechanically fixed, and the other is mechanically free. Since the length of the rod is significantly greater than its shear dimensions, it is able to perform bending vibrations. When the microprobe moves along the surface of the sample, the spike tip rises and falls, outlining the surface microrelief, similar to the way a gramophone needle slides along a gramophone. At the protruding end of the cantilever (above the spike), there is a mirror area onto which the laser beam is incident and reflected. When the spike lowers and rises on surface irregularities, the reflected beam is deflected, and this deviation is detected by the photodetector. Photodetector data is used in a feedback system that provides a constant pressure force of the tip on the sample. Thus, the cantilever is a high-Q resonator, the resonant frequency of which depends on its effective mass and material stiffness. Figure 6.3 (b) as an example presents the general scheme of a cantilever sensor.

The dynamic mode of operation of cantilever sensors is based on a change in the resonant frequency of the cantilever during a specific interaction of analyte molecules with the receptor layer, which leads to an increase in the mass of the resonator

(Chen et al. 1995; Kolesov et al. 2016). To create a biological multifunctional sensor, you can use a system of cantilevers tuned to various microorganisms and viruses.

In the past few years, the development of biosensors for detecting viruses in the environment has become popular. For example, Timurdogan et al. (2011) described the use of a cantilever biosensor to detect hepatitis A and C viruses in bovine serum. In this case, antibodies specific for hepatitis A and C viruses were immobilized on cantilevers with different resonant frequencies. The detection limit was shown to be 0.1 ng/ml (1.6 pM). Gupta (2004) has shown that the sensitivity of a cantilever to a change in its mass can be quite sufficient for the detection of a single vaccinia virus if a specific sensory layer is not used.

Gorelkin et al. (2015) reported the possibility of detecting duck virus A in a static mode using a cantilever modified with a synthetic glycopolymer containing sialic acid residues. The authors believe that the polymer layer on the surface of the cantilever creates a matrix that increases surface tension due to additional interaction with viral particles. The detection limit in this system was 10^6 virions/ml. The resonant-mode piezoelectric cantilever sensor was used to detect hepatitis C virus helicase with a concentration of 100 pg/ml (Hwang et al. 2007). Helicase is an enzyme responsible for the deployment of viral RNA, and it is specific for this virus. RNA aptamers representing short nucleotide sequences capable of specifically binding an antigen (protein) also were used as a receptor. They can be easily synthesized and are more shelf-stable than antibodies.

Thus, cantilever biosensors provide a promising platform for creating highly sensitive and selective sensor devices. However, under operation in liquids, the cantilever sensor operating in dynamic mode has low sensitivity due to a decrease in the quality factor of bending vibrations. As for sensors operating in static mode, they are highly susceptible to changes in external influences: changes in the flow rate of the analyzed liquid, changes in temperature, etc.

6.2.5 Microwave Resonator for Detecting Bacteriophages

Bacteriophages are an excellent model in developing methods for detecting viruses. Some types of bacteriophages have a wide spectrum of lytic activity and infect only certain strains of one bacterial species, while others are characterized by multiple virulences. Due to receptors located on the cell surface, bacteriophages are recognized and attached only to specific bacterial cells. This principle can be applied to the detection of bacteriophages using biosensor methods. Studies in the field of biosensors have shown that it is advisable to use microbial cells as a biologically sensitive element in sensors. Microorganisms immobilized in various ways on carriers, in combination with an electrophysical sensor, can represent simple, sensitive, high-speed biosensors.

The study by Guliy et al. (2017b) showed the possibility of determining bacteriophages using a detection system based on a microwave resonator operating in the

frequency range 5–8.5 GHz. The circuit of such a resonator is shown in Fig. 6.3 (c). The electrodynamic resonator is a segment of a rectangular microwave waveguide, which is bounded by a short-circuit metal plate on one side. A plate of lithium niobate with a porous polystyrene film containing immobilized cells is set on the other side. When a small amount of a suspension containing bacteriophage specific to immobilized cells was applied to the polystyrene plate, the reflection coefficient of the wave from the resonator changed significantly. The detection limit of such a sensor was 10^6 phages/ml, with an analysis time of about 10 min.

6.3 Conclusion and Future Perspectives

Viral infections still pose a danger to humanity, which stimulates the development of new rapid methods for their detection. There is no doubt that the medical manifestations of the disease, confirmed by biochemical, microbiological, and animal tests, remain the gold standard in clinical diagnostic laboratories. However, the number of methods to obtain information on viral danger is steadily growing. At that, the main requirements for new methods, in addition to high sensitivity, are the ability to analyze a large number of samples in a short time, as well as in “field conditions.”

The use of biosensors for the signal indication of viruses will prevent the spread of viral infection due to fast and timely pro-anti epidemic measures. In general, the biosensor methods for determining viruses can be developing in two directions: with the immobilization of the components of the analysis and without their immobilization. Each of these areas has its own advantages and disadvantages. The main point for all sensors is that the sensors allow to clearly distinguishing between situations when viruses interact with specific reagents from control experiments when this interaction does not occur. The biosensors considered, being highly sensitive to virus detection, allow working with different taxonomic groups. In addition, biosensors allow you to measure in real-time, conduct analysis without the use of markers, and reuse one chip for analysis. They also have high-performance stability and reproducibility of results. Low cost, small sample requirements, and the possibility of miniaturization justify their growing development.

An analysis of the scientific literature on the research and development of technologies in this direction shows the significant potential of acoustic biosensor systems for detecting viruses. Despite the fact that acoustic sensors are used to detect microbial cells, their use for detecting viruses is described very poorly. Acoustic sensors can analyze viruses directly in a liquid without immobilizing analysis components on the surface. This advantage allows for avoiding the procedure for optimizing the process of immobilization and selection of the sensor surface. The acoustic assay constitutes a specific and sensitive alternative to other methods for virus detection. The indisputable advantages of acoustic sensors are simple sample preparation, sensitivity, efficiency, and the possibility of multiple uses. Further

standardization and automation of the electro-acoustic analysis method will expand the range of its application for virus detection.

It should be emphasized that all developed biosensor methods are universal and can be adapted to detect viruses belonging to different groups. In the future, with the development of methods for the specific treatment of viral diseases, test systems developed on the basis of biosensor diagnostics will undoubtedly find application in clinical practice for making a diagnosis and prescribing adequate treatment. Thus, the development of sensor technology for the analysis of viral particles can be used in microbiology, biotechnology, veterinary medicine, medicine, and phage therapy.

Acknowledgments This work was supported in part by the Russian Foundation for Basic Research (grants nos. 19-07-00300 and 19-07-00304).

Conflict of Interest There is no conflict of interest in this chapter.

References

- Ballantine DS, White RM, Martin SJ, Ricco AJ, Zellers ET, Frye GC, Wohltjen H (1997) Acoustic wave sensors: theory, design, and physico-chemical applications. Academic Press, San Diego
- Bisoffi M, Hjelle B, Brown DC, Branch DW, Edwards TL, Brozik SM, Bondu-Hawkins VS, Larson RS (2008) Detection of viral bioagents using a shear horizontal surface acoustic wave biosensor. *Biosens Bioelectron* 23(9):1397–1403
- Bisoffi M, Ra Severns V, Branch DW, Edwards TL, Larson RS (2013) Rapid detection of human immunodeficiency virus types 1 and 2 by use of an improved piezoelectric biosensor. *J Clin Microbiol* 51(6):1685–1691
- Brooks SL, Ashby RE, Turner APF, Calder MR, Clarke DJ (1988) Development of an on-line glucose sensor for fermentation monitoring. *Bios* 3:45–56
- Buerk DG (1993) Biosensors: theory and applications. Technomic Publishing Company
- Budnikov GK, Evtuygin GA, Maistrenko VN (2010) Modified electrodes for voltammetry in chemistry, biology and medicine. M: BINOM. Laboratory of Knowledge
- Budnikov GK, Gkrmonov S.Yu., Medyantseva EP, Evtuygin GL (2013) Chemical safety and monitoring of living systems on the principles of biomimetics: textbook [in Russia].
- Carter J, Saunders V (2007) Virology: principles and applications. Wiley, London. 358 p
- Chen GY, Thundat T, Wachter EA, Warmack RJ (1995) Adsorption induced surface stress and its effects on resonance frequency of microcantilevers. *J. Appl. Phys.* 77(8):3618–3622.
- Darwish NT, Sekaran SD, Alias Y, Khor SM (2018) Immunofluorescence-based biosensor for the determination of dengue virus NS1 in clinical samples. *J Pharm Biomed Anal* 149:591–602. <https://doi.org/10.1016/j.jpba.2017.11.064>
- Deisingh A (2003) Biosensors for microbial detection. *Microbiologist*. 2:30–33.
- De Mol NJ, Fischer MJE (2010) Surface Plasmon resonance. Methods and protocols. Humana Press. LLC, New Jersey
- Erickson D, Mandal S, Yang A, Cordovez B (2008) Nanoscale Optofluidic devices for biomolecular detection. *J. Microfluid Nanofluid* 4:33–52
- Evtuygin G (2013) In: Evtuygin G (ed) Biosensors: essentials. Springer, Berlin
- Fan X, White IM, Shopoua SI, Zhu H, Suter JD, Sun Y (2008) Sensitive optical biosensors for unlabeled targets: a review. *J Anal Chim Acta* 620:8–26
- Chandra P (ed) (2016) Nanobiosensors for personalized and onsite biomedical diagnosis. IET, London

- Garcia-Aljaro C, Munoz-Berbel X, ATA J, Blanch AR, Munoz FX (2008) Surface plasmon resonance assay for real-time monitoring of somatic coliphages in wastewaters. *Appl Environ Microbiol* 74(13):4054–4058
- Coiras MT, Aguilar JC, Garcia ML, Casas I, Pérez-Breña P (2004) Simultaneous detection of four-teen respiratory viruses in clinical specimens by two multiplex reverse transcription nested-PCR assays. *J Med Virol* 72:484–495
- del Pilar Martinez Viedma M, Puri V, Oldfield LM, Shabman RS, Tan GS, Pickett BE (2019) Optimization of qRT-PCR assay for zika virus detection in human serum and urine. *Virus Res* 263:173–178. <https://doi.org/10.1016/j.virusres.2019.01.013>
- Gorelkin PV, Erofeev AS, Kiselev GA, Kolesov DV, Dubrovin EV, Yaminsky IV (2015) Synthetic sialylglycopolymer receptor for virus detection using cantilever-based sensors. *Analyst* 140(17): 6131–6137.
- Gouma PI, Wang L, Simon SR, Stanacevic M (2017) Novel isoprene sensor for a flu virus breath monitor. *Sensors* 17:199. <https://doi.org/10.3390/s17010199>
- Grabowska I, Malecka K, Jarocka U, Radecki J, Radecka H (2014) Electrochemical biosensors for detection of avian influenza virus—current status and future trends. *Acta Biochim Pol* 61(3):471–478
- Guliy OI, Zaytsev BD, Shikhabudinov AM, Teplykh AA, Borodina IA, Pavliy SA, Larionova OS, Fomin AS, Staroverov SA, Dykman LA, Ignatov OV (2016a) Immunodetection of bacteriophages by a piezoelectric resonator with transverse electric field. *Appl Biochem Microbiol* 52(4):457–463
- Guliy OI, Zaitsev BD, Kuznetsova IE, Shikhabudinov AM, Balko AB, Teplykh AA, Staroverov SA, Dykman LA, Makarikhina SS, Ignatov OV (2016b) Application of the method of electro-acoustical analysis for the detection of bacteriophages in a liquid phase. *Biophysics* 61(1):52–58
- Guliy OI, Zaitsev BD, Borodina IA, Fomin AS, Staroverov SA, Dykman LA, Shikhabudinov AM (2017a) Use of mini-antibodies for detection of bacteriophages by the electroacoustic analysis method. *Biophysics* 62(3):373–384
- Guliy OI, Zaitsev BD, Smirnov AV, Karavaeva OA, Borodina IA (2017b) Biosensor for the detection of bacteriophages based on a super-high-frequency resonator. *Appl Biochem Microbiol* 53(6):725–732
- Guliy OI, Zaitsev BD, Borodina IA, Shikhabudinov AM, Staroverov SA, Dykman LA, Fomin AS (2018) Electro-acoustic sensor for the real-time identification of the bacteriophages. *Talanta* 178:743–750
- Guliy OI, Zaitsev BD, Larionova OS, Borodina IA (2019) Virus detection methods and biosensor technologies. *Biophysics* 64(6):892–899. <https://doi.org/10.1134/S0006350919060095>
- Guliy OI, Kanevskiy MV, Fomin AS, Staroverov SA, Bunin VD (2020) Progress in the use of an electro-optical sensor for virus detection. *Opt Commun* 465:125605. <https://doi.org/10.1016/j.optcom.2020.125605>
- Harsanyi G (2000) *Sensors in Biomedical Applications; Fundamentals: Technology & Applications*. Technomic Publishing Company. CRC Press. LLC. N.W. Corporate Blvd., Boca Raton
- Homola J (2006) *Surface plasmon resonance based sensors*. Springer, Berlin
- Huguenin A, Moutte L, Renois F, Lévéque N, Talmud D, Abely M, Nguyen Y, Carrat F, Andreoletti L (2012) Broad respiratory virus detection in infants hospitalized for bronchiolitis by use of a multiplex RT-PCR DNA microarray system. *J Med Virol* 84(6):979–985
- Hwang KS, Lee SM, Eom K, Lee JH, Lee YS, Park JH, Yoon DS, Kim TS (2007) Nanomechanical microcantilever operated in vibration modes with use of RNA aptamer as receptor molecules for label-free detection of HCV helicase. *Biosens Bioelectron* 23(4):459–465
- Jackson JB, Westcott SL, Hirsch LR, West JL, Halas NJ (2003) Controlling the surface enhanced Raman effect via the nanoshell geometry. *J Appl Phys Lett* 82:257–259
- Kanso M, Cuenot S, Louarn G (2008) Sensitivity of optical fiber sensor based on surface Plasmon resonance: modeling and experiments. *Plasmonics* 3:49–57. <https://doi.org/10.1007/s11468-008-9055-1>

- Khoris IM, Chowdhury AD, Li T-C, Suzuki T, Enoch Y, Parkab EY (2020) Advancement of capture immunoassay for real-time monitoring of hepatitis E virus-infected monkey. *Anal Chim Acta.*, Available online 12 February 2020 (article in press. <https://doi.org/10.1016/j.aca.2020.02.020>)
- Koenig B, Graetzel M (1994) A piezoelectric immunosensor for hepatitis viruses. *Anal Chem* 66:341–348
- Kolesov D, Yaminsky IV, Ahmetova A, Sinitsyna O, Meshkov G (2016) Cantilever biosensors for detection of viruses and bacteria. *Nano Industry* 4(66):26–35. <https://doi.org/10.22184/1993-8578.2016.67.5.26.34>
- Kretschmann E and Raether H (1968) Radiative decay of nonradiative surface plasmons excited by light. *J. Naturforsch.* A23:2135–2136.
- Kurosawa S, Park JW, Aizawa H, Wakida S, Tao H, Ishihara K (2006) Quartz crystal microbalance immunosensors for environmental monitoring. *Biosens Bioelectron* 22(4):473–481
- Leca-Bouvier B (2010) Enzyme for biosensing application. In: Leca-Bouvier B, Blum L, Zourob M (eds) *Recognition receptors in biosensors*. Springer, New York, pp 177–220
- Lesniewski A, Los M, Jonsson–Niedziółka M, Krajewska A, Szot K, Los JM, Niedziółka–Jonsson J (2014) Antibody modified gold nanoparticles for fast and selective, colorimetric T7 bacteriophage detection. *Bioconjug Chem* 25:644–648
- Lin B, Blaney KM, Malanoski AP, Ligler AG, Schnur JM, Metzgar D, Russell KL, Stenger DA (2007) Using a resequencing microarray as a multiple respiratory pathogen detection assay. *J Clin Microbiol* 45(2):443–452
- Liu G, Rosa-Bauza YT, Salisbury CM, Craik C, Ellman JA, Chen FF, Lee LP (2007) Peptide-nanoparticle hybrid SERS probes for optical detection of protease activity. *J Nanosci Nanotechnol* 7:2323–2330
- Los M, Los J, Wegrzyn G (2006) Rapid detection of bacteriophage infection and prophage induction using electric biochips. *Microb Cell Factories* 5:S38. <https://doi.org/10.1186/1475-2859-5-S1-S38>
- Mamichev DA, Kuznetsov IA, Maslova NE, Zanaevskii ML (2012) Optical sensors based on surface plasmon resonance for high-sensitive biochemical analysis. *Mol Med* 6. [in Russian]
- Matatagui D, Fontecha JL, Fernández MJ, Gràcia I, Cané C, Santos JP, Horrillo MC (2014) Love-wave sensors combined with microfluidics for fast detection of biological warfare agents. *Sensors* 14:12658–12669. <https://doi.org/10.3390/s140712658>
- Mehlmann M, Bonner AB, Williams JV, Dankbar DM, Moore CL, Kuchta RD, Podsiad AB, Tamerius JD, Dawson ED, Rowlen KL (2007) Comparison of the MChip to viral culture, reverse transcription-PCR, and the QuickVue influenzaA+B test for rapid diagnosis of influenza. *J Clin Microbiol* 45(4):1234–1237
- Monzon-Hernandez D, Villatoro J (2006) High-resolution refractive index sensing by means of a multiple-peak surface plasmon resonance optical fiber sensor. *Sensors Actuators B Chem* 115(1):227–231
- Moreira F, Dutra R, Noronha J, Sales G (2014) Novel sensory surface for creatine kinase electrochemical detection. *Biosens Bioelectron* 56:217–222
- Muñoz-Berbel X, García-Aljaro C, Muñoz FJ (2008) Impedimetric approach for monitoring the formation of biofilms on metallic surfaces and the subsequent application to the detection of bacteriophages. *Electrochim Acta* 53:5739–5744
- Muramatsu H, Tamiya E, Suzuki M, Karube I (1989) Quartz-crystal gelation detector for the determination of fibrinogen concentration. *Anal Chim Acta* 217:321–326
- Nikoobakht B, El-Sayed M (2003) Surface-enhanced Raman scattering studies on aggregated gold Nanorods. *J Phys Chem A* 107:3372–3378
- Noh JY, Yoon S-W, Kim Y, Lo TV, Ahn M-J, Jung M-C, Le TB, Na W, Song D, Le VP, Haam S, Jeong DG, Kim HK (2019) Pipetting-based immunoassay for point-of-care testing: application for detection of the influenza A virus. *Sci Rep* 9:16661. <https://doi.org/10.1038/s41598-019-53083-8>

- Panferov VG, Safenkova IV, Zherdev AV, Dzantiev BB (2017) Setting up the cut-off level of a sensitive barcode lateral flow assay with magnetic nanoparticles. *Talanta* 164:69–76. <https://doi.org/10.1016/j.talanta.2016.11.025>
- Razo SC, Panferov VG, Safenkova IV, Varitsev YA, Zherdev AV, Dzantiev BB (2018) Double-enhanced lateral flow immunoassay for potato virus X based on a combination of magnetic and gold nanoparticle. *Anal Chim Acta* 1007:50–60
- Tamarin O, Comeau S, Déjous C, Moynet D, Rebière D, Bezian J, Pistréa J (2003) Real time device for biosensing: design of bacteriophage model using love acoustic waves. *Biosens Bioelectron* 18(5–6):755–763
- Turner APF, Karube I, Wilson GS (1987) *Biosensors: fundamentals and applications*. Oxford University Press, Oxford
- Passi D, Sharma S, Dutta SR, Dudeja P, Sharma V (2015) Ebola virus disease (the killer virus): another threat to humans and bioterrorism: brief review and recent updates. *J Clin Diagn Res* 9:LE01–LE08
- Rojek A, Horby P, Dunning J (2017) Insights from clinical research completed during the West Africa Ebola virus disease epidemic. *Lancet Infect Dis* 17:e280–ee92
- Rossi AM, Wang L, Reipa V, Murphy TE (2007) Porous silicon biosensor for detection of viruses. *Biosens Bioelectron* 23(5):741–745
- Syrmis MW, Whiley DM, Thomas M, Mackay IM, Williamson J, Siebert DJ, Nissen MD, Sloots TP (2004) A sensitive, specific, and cost-effective multiplex reverse transcriptase-PCR assay for the detection of seven common respiratory viruses in respiratory samples. *J Mol Diagn* 6(2):125–131
- Shawky SM, Awad AM, Allam W, Alkordi MH, El-Khamisy SF (2017) Gold aggregating gold: a novel nanoparticle biosensor approach for the direct quantification of hepatitis C virus RNA in clinical samples. *Biosens Bioelectron* 92:349–256
- Templeton KE, Scheltinga SA, Beersma MF, Kroes ACM, Claas ECJ (2004) Rapid and sensitive method using multiplex real-time PCR for diagnosis of infections by influenza A and influenza B viruses, respiratory syncytial virus, and parainfluenza viruses 1, 2, 3, and 4. *J Clin Microbiol* 42:1564–1569
- Timurdogan E, Alaca BE, Kavakli IH, Urey H (2011) MEMS biosensor for detection of hepatitis A and C viruses in serum. *Biosens Bioelectron* 28:189–194
- Uttenhaller E, Schräml M, Mandel J, Drost S (2001) Ultrasensitive quartz crystal microbalance sensors for detection of M13-phages in liquids. *Biosens Bioelectron* 16(9–12):735–743
- Vasan AS, Mahadeo DM, Doraiswami R, Huang Y, Pecht M (2013) Point-of-care biosensor system. *Front Biosci (Schol Ed)* 5:39–71
- Wu Z, Zeng T, Guo W-J, Bai Y-Y, Pang D-W, Zhang Z-L (2019) Digital single virus immunoassay for ultrasensitive multiplex avian influenza virus detection based on fluorescent magnetic multifunctional Nanospheres. *ACS Appl Mater Interfaces* 11(6):5762–5770. <https://doi.org/10.1021/acsami.8b18898>
- Xu S, Ji X, Xu W, Li X, Wang L, Bai Y, Zhao B, Ozak Y (2004) Immunoassay using probe labeling immunogold nanoparticles with silver staining enhancement. *J Therm Anal* 129:63–68
- Zaitsev BD, Kuznetsova IE, Shikhabudinov AM, Ignatov OV, Guliy OI (2012) Biological sensor based on a lateral electric field-excited resonator. *IEEE Trans Ultrason Ferroelectr Freq Control* 59(5):963–969
- Zaitsev BD, Shikhabudinov AM, Teplykh AA, Kuznetsova IE (2015) Liquid sensor based on a piezoelectric lateral electric field-excited resonator. *Ultrasonics* 63:179–183
- Zhou X, Liu L, Hu M, Wang L, Hu J (2002) Detection of hepatitis B virus by piezoelectric biosensor. *J Pharm Biomed Anal* 27:341–345

Chapter 7

Specific Immobilization of Rotaviruses for Atomic Force Microscopy Using Langmuir Antibody Films Based on Amphiphilic Polyelectrolytes



Sergei Georgievich Ignatov, S. Yu. Filippovich, and Ivan Alekseevich Dyatlov

Abstract The Langmuir–Blodgett technique is a useful and suitable tool for fabrication of affinity layers. Langmuir antibody films based on amphiphilic polyelectrolytes have been used for specific immobilization of rotaviruses for atomic force microscopy (AFM) analysis. AFM has been used for structural analysis of virus particles and their identification based on specific interactions of antibodies with rotaviruses. Virus-containing samples were investigated in the atomic force microscope using contact and tapping mode. Monoclonal mouse antibodies against viruses were used for film deposition. Antibodies were deposited on different substrates using Langmuir–Blodgett and Langmuir–Schaeffer techniques. A comparison of the size of virus particles obtained by AFM and electron microscopy has been done.

Keywords AFM · Specific immobilization · Langmuir films · Viruses · Antibodies

Nomenclature

AFM	atomic force microscopy
BSA	bovine serum albumin
COVID-19	coronavirus disease 2019
DNA	deoxyribonucleic acid
MGEs	mobile genetic elements
LB	Langmuir–Blodgett

S. G. Ignatov (✉) · I. A. Dyatlov
State Research Center for Applied Microbiology and Biotechnology,
Obolensk, Moscow Region, Russia
e-mail: ignatov@obolensk.org

S. Y. Filippovich
Bach Institute of Biochemistry, Research Center of Biotechnology of the Russian Academy
of Sciences, Moscow, Russia

MERS-CoV	Middle East respiratory syndrome coronavirus
PHE	public health emergency
PHEIC	public health emergency of international concern external icon
RNA	ribonucleic acid
SARS-CoV	severe acute respiratory syndrome coronavirus
STM	scanning tunneling microscopy

7.1 Introduction

All cellular life-forms, except some intracellular bacterial parasites, host distinct repertoires of viruses and other mobile genetic elements (MGEs). Viruses appear to be the dominant biological entities on our planet, with the total count of virus particles in aquatic environments alone at any given point in time reaching the staggering value of 10^{31} , a number that is at least an order of magnitude greater than the corresponding count of cells (Rohwer 2003; Edwards and Rohwer 2005; Suttle 2005; Rosario and Breitbart 2011; Chow and Suttle 2015). Accordingly, lytic infections of cellular organisms, primarily bacteria, by viruses play a central role in the biological matter turnover in the biosphere (Suttle 2005; Suttle 2007; Rohwer and Thurber 2009; Koonin and Dolja 2013; Chow and Suttle 2015; Cobián Güemes et al. 2016; Danovaro et al. 2016). The genetic diversity of viruses is harder to assess, but beyond doubt, the gene pool of viruses is, in the least, comparable to that of hosts. The estimates of the number of distinct prokaryotes on earth differ widely, in the range of 10^7 to 10^{12} (Curtis et al. 2002; Amann and Rosselló-Móra 2016; Locey and Lennon 2016; Vinatzer et al. 2017), and accordingly, estimation of the number of distinct viruses infecting prokaryotes at 10^8 to 10^{13} is reasonable. Even assuming the lowest number in this range and without attempting to count viruses of eukaryotes, these estimates represent vast diversity. Furthermore, the genomes of most viruses accumulate mutations much faster than genomes of cellular organisms due to both the typically low fidelity of the virus replication machinery that stems, in part, from the absence of proofreading activity in many viruses and the strong selection pressure on virus populations (Holland et al. 1982; Drake et al. 1998; Sanjuán et al. 2010; Sanjuán and Domingo-Calap 2016; Geoghegan and Holmes 2018; Domingo and Perales 2019). Thus, viruses encompass an enormous pool of rapidly evolving genes that appears to continuously contribute to the emergence of new genes in cellular life-forms through the exchange of genetic material between cells and viruses. However, despite the rapid short-term evolution of viruses, the key genes responsible for virion formation and virus genome replication are conserved over the long term due to selective constraints (Szathmáry and Maynard Smith 1997; Takeuchi and Hogeweg 2007; Takeuchi and Hogeweg 2012; Iranzo et al. 2016; Koonin et al. 2017; Berezovskaya et al. 2018).

Generally, viruses are very small living objects with the size from 0.02 to 0.3 μm , although several very large viruses with a length of up to 1 μm (megavirus,

pandoravirus) have recently been detected (Schulz et al. 2020). Living and multiplication of viruses are completely dependent on the host cells (bacterial, plant, or animal). Viruses consist of protein, and sometimes lipid, envelope, RNA or DNA core, and sometimes enzymes necessary for the first stages of virus replication. Viruses are molecular parasites or symbionts that coevolve with nearly all forms of cellular life. The route of virus replication and protein expression is determined by the viral genome type. The single-stranded DNA (ssDNA) viruses are a polyphyletic class, with different groups evolving by recombination between rolling-circle-replicating plasmids, which contributed to the replication protein, and positive-sense RNA viruses, which contributed the capsid protein. The double-stranded DNA (dsDNA) viruses are distributed among several large monophyletic groups and arose via the combination of distinct structural modules with equally diverse replication modules. Phylogenomic analyses reveal the finer structure of evolutionary connections among RNA viruses and reverse-transcribing viruses, ssDNA viruses, and large subsets of dsDNA viruses.

Viruses are classified mainly according to the structure of their genome and the type of their replication, and not depending on the diseases that they cause (Siddell et al. 2020). All viruses were divided into seven distinct classes, based on the structure of the virion's nucleic acid (traditionally called the virus genome) (Baltimore 1971; Agol 1974; Condit 2013):

1. Double-stranded DNA (dsDNA) viruses, with the same replication-expression strategy as in cellular life-forms
2. Single-stranded DNA (ssDNA) viruses that replicate mostly via a rolling-circle mechanism
3. dsRNA viruses
4. Positive-sense RNA [(+)RNA] viruses that have ssRNA genomes with the same polarity as the virus mRNA(s)
5. Negative-sense RNA [(-)RNA] viruses that have ssRNA genomes complementary to the virus mRNA(s)
6. RNA reverse-transcribing viruses that have (+)RNA genomes that replicate via DNA intermediates synthesized by reverse transcription of the genome
7. DNA reverse-transcribing viruses replicating via reverse transcription but incorporating into virions a dsDNA or an RNA-DNA form of the virus genome

Thus, there are DNA viruses and RNA viruses; each type may have single or double chains of genetic material. Single-stranded RNA viruses, in turn, are divided into RNAs with positive polarity and RNAs with negative polarity. Typically, DNA viruses replicate in the nucleus of the host cell, and RNA viruses typically replicate in the cytoplasm. At the same time, some single-stranded RNA viruses of positive polarity, called retroviruses, use a completely different replication method (Koonin and Dolja 2014). Viruses are the causative agents of such dangerous infections as hepatitis C, herpes, and AIDS. Chronic viral infections are characterized by the prolonged, continuous release of the viruses. Viruses are spread through respiratory and intestinal secretions. Clear laboratory diagnosis of viruses is based on detection of the whole virus or viral main antigens or viral DNAs and RNAs or

antigen-specific antibodies, or visualization of viruses and combination of all these detections. It is very difficult to detect and identify viruses because of their size and because they are very small compared with bacterial pathogens. Currently, the definition and identification of viruses are based on three main approaches of polymerase chain reaction (PCR), hybridization, and immunoassays (Delwart 2007; Nicolaisen 2011; Roossinck 2011; Mokili et al. 2012).

However, because these assays depend on the reagents (antibodies, primers, or probes) developed from the characterized viruses and viroids, they are ineffective when the disease is caused by a new pathogen or a mixture of pathogens that share little or no sequence similarity with those described previously. The rapid method was offered in the use of next-generation sequencing technologies for the identification of viruses and viroids (Wu et al. 2015). Serological identification of viruses may be sensitive and specific. Sometimes a histological examination using an electron microscope can help. Viral genomes are small; the genome of RNA viruses ranges from 3.5 up to 27 kb, and the genome of DNA viruses varies from 5 up to 280 kb. Thus, partial and full genome sequencing will become an important component for specific diagnostic for virus detection and identification.

Recently, electron microscopy was used to identify the COVID-19 virus (Kim et al. 2020). As an instrument for nanoscale imaging, atomic force microscopy (AFM) has many benefits over scanning electron microscopy (SEM). While SEM must be carried out in a vacuum, AFM can be undertaken in several different environments, encompassing ambient, liquid, and vacuum. It is ideally suited to the analysis of biological samples due to its ability to image in a liquid environment. This chapter aims to test using AFM for specific visualization of viruses.

7.2 AFM in Virology

Nanobiotechnology is a discipline in which tools from nanotechnology are developed and applied to study biological phenomena. The number of virus particles on Earth is frequently reported in the scientific literature and in general-interest publications as being on the order of 10^{31} (Mushegian 2020). AFM probes surface-adsorbed samples at the nanoscale by using a sharp stylus of nanometric size located at the end of a micro-cantilever. AFM can be used to explore the topography of viruses and protein structures. AFM is not limited to imaging and allows the manipulation of individual viruses with force spectroscopy approaches, such as single indentation and mechanical fatigue assays. These pushing experiments deform the protein structures to get their mechanical information and can be used to monitor the structural changes induced by maturation or the exposure to different biochemical environments, such as pH variation (de Pablo 2019). A characteristic structural element in viruses is the protein capsid, which combines multiple functions, including packaging of the viral genome and recognition of the target cell. These protein cages or shells can be defined as a structure built out of protein subunits enclosing a cavity at the nanometer scale. Although viruses illustrate the definition of a protein

cage, non-viral structures, such as bacterial microcompartments (Cheng et al. 2008), vault particles (Querol-Audi et al. 2009), clathrin cages (Fotin et al. 2004), and artificial virus-like structures (Wimmer et al. 2009; Worsdofer et al. 2011; Lai et al. 2014) are other examples. Virus protein capsids are built up of repeating protein subunits (capsomers) that pack the viral genome (Flint et al. 2004). Viral particles are endorsed with meta-stable properties that permit fulfilling each task of the viral cycle sequentially (Mateu 2013). These capacities have induced using viral capsids as protein containers of artificial cargoes (drugs, polymers, enzymes, minerals) (Douglas and Young 1998) with applications in materials and biomedical sciences. AFM requires the immobilization of the specimen to study on a solid surface (substrate). Viral cages are normally physisorbed on the substrate, using polar, non-polar, and van der Waals forces (Muller et al. 1997). Physisorption traps protein cages on the surface without creating chemical bonds that might alter their structure. Each type of protein shell has individual features such as local charge densities and/or hydrophobic patches (Armanious et al. 2016), which can be employed for adsorption, via electrostatic and/or hydrophobic interactions, on different substrates, such as glass, mica, and HOPG (Highly Oriented Pyrolytic Graphite) (Moreno-Madrid et al. 2017).

AFM has opened a new way regarding the investigation of the physical properties of viruses and virus mechanics. The first imaging attempt regarding viruses was performed using scanning probe microscopy. In scanning tunneling microscopy (STM), imaging the sample has to be electrically conductive, and the particle was covered with a metallic layer that is far from its physiological conditions. This limitation has been overcome using AFM, which does not require electrical conductivity. AFM has been widely used for the topographic property determination of viruses, partially disassembled viruses, viral capsids, nucleic acids, etc. Also, AFM can be used to investigate the viral infection in the live-cell process and for the determination of the interaction forces between viruses and other molecules. A different approach for the determination of the mechanical properties of viruses is based on the consideration of the virus particle and the AFM cantilever. One could say that each type of virus has a preferred substrate since each kind of protein structure exposes different residues (Tetreau et al. 2020). Virus particles and other protein-based supramolecular complexes have vast nanotechnological potential. However, protein nanostructures are “soft” materials prone to disruption by force. Whereas some non-biological nanoparticles (NPs) may be stronger, for certain applications, protein- and virus-based NPs have potential advantages related to their structure, self-assembly, production, engineering, and/or inbuilt functions. Thus, it may be desirable to acquire the knowledge needed to engineer protein-based nanomaterials with a higher strength against mechanical breakage (Medrano et al. 2019).

The characterization of viral structures has required high-resolution techniques such as AFM. AFM has been widely used in the field of biological science. Cells, their structures, and molecules have been extensively studied using this method. The AFM has also been applied within the field of virology. As the structures of many viruses have been determined by electron microscopy and X-ray crystallography, the most appropriate role for AFM is the surface topography of viruses under

many different conditions (in the air and, for the most important biological applications, in solution). The AFM has been used in the high-resolution image of many viruses. Viruses are not easy to characterize, but the capacity to predict the surface charge of viruses opens new possibilities for vaccine purification and making gene therapy too (Michigan Technological University, 2020). Before viruses can be imaged using AFM, they should be immobilized on the surface. There are two methods of immobilization—specific and non-specific. In the non-specific method, samples were put on the surfaces and analyzed after drying. In this case, it is difficult to analyze images, especially in the presence of contaminants. Antibodies are usually used to increase the sensitivity of immobilization. The standard formation of the antibody monolayers for immobilization of viruses is achieved by direct covalent attachment to the surface. It is known that monolayers of pure antibodies or enzymes can lose their specificity and activity (Babitskaya et al. 1997). Amphiphilic polyelectrolytes and lipids have been used to protect antibodies and enzymes from inactivation during the formation of monolayers. In this study, we report on the use of Langmuir films of antibodies based on amphiphilic polyelectrolyte for specific immobilization of rotaviruses for visualization by AFM.

It is possible to analyze the virus morphology in high resolution under physiological conditions (in water medium) (Kuznetsov and McPherson 2011). AFM can be used for nano-sized manipulation using cantilever (Rief et al. 1997; Muller et al. 2002; Schaap et al. 2006). Using cantilever, it is possible to analyze the packing of the genome (Carrasco et al. 2006, 2008; Roos et al. 2009; Hernando-Perez et al. 2012; Snijder et al. 2013; Zeng et al. 2017), virus maturation (Carrasco et al. 2011; Roos et al. 2012; Ortega-Esteban et al. 2013), site-directed mutagenesis (Carrillo et al. 2017), and protein engineering of capsids (Llauro et al. 2016). AFM can be used for the study of phage genome translocation into the bacterial cell (Purohit et al. 2003; Gonzalez-Huici et al. 2004). In addition, protein shells of non-viral origin, encapsulin, and the internal pressure of phages can be measured by AFM (Smith et al. 2001; Hernando-Perez et al. 2012; Llauro et al. 2014; Snijder et al. 2016).

7.3 Specific AFM Visualization

Rotavirus is a very contagious virus that causes diarrhea. It's the most common cause of diarrhea in infants and children worldwide, resulting in over 215,000 deaths annually. Before the development of a vaccine, most children in the United States had been infected with the virus at least once by age 5. Although rotavirus infections are unpleasant, you can usually treat this infection at home with extra fluids to prevent dehydration. Occasionally, severe dehydration requires intravenous fluids in the hospital. Dehydration is a serious complication of rotavirus and a major cause of childhood deaths in developing countries. Good hygiene, such as regular washing hands, is important, but vaccination is the best way to prevent rotavirus

infection <https://www.mayoclinic.org/diseases-conditions/rotavirus/symptoms-causes/syc-20351300>.

Rotaviruses SA 11 (obtained from Chumakov Institute of Poliomyelitis and Viral Encephalites of Russian Academy of Medical Sciences) were grown in rhabdomyosarcoma cells in Dulbecco's modified Eagle's medium supplemented with 10% fetal bovine serum (Sigma-Aldrich, USA). After cultivation, these cells with viruses were destroyed by 3-time freezing/thawing cycles for rotaviruses isolation. Then the suspension was centrifuged to remove cell fragments. The supernatant was transferred with a syringe to clean test-tubes containing 10% sucrose. After the centrifugation, the virus particles were suspended in the phosphate buffer containing NaCl. Formalin was added to the suspension for virus disinfection.

The Langmuir–Blodgett (LB) technique is a way of making ultrathin nanostructured films with a controlled layer structure and crystal parameter, which have many envisioned applications in technology for optical and molecular electronic devices as well as in signal processing and transformation. LB films have a unique potential for controlling the structure of organized matter on the ultimate scale of miniaturization, and must surely find a niche where this potential is fulfilled. The LB technique, a unique bottom-up approach, can produce ultrathin films on a monomolecular level (Bashar et al. 2019). Glass and gold were used as substrates for films. Before deposition, the surfaces were washed by ethyl alcohol and rinsed with distilled water. Antibody films were deposited by the following method. On the first stage, suspension of antibodies was mixed with Tris-HCl buffer. The buffer solution was poured Langmuir–Blodgett trough. Then alkylated polyethyleneimine was added to the surface of the air–water interface. It is believed that polyethyleneimine-based sorbents containing numerous positively charged amine groups (Vasilieva et al. 2018) are electrostatically attracted to the surface structures of the substrate providing steady attachment of cells. In the first stage, polymer macromolecules form a monolayer on the surface of the interface. At the second stage, protein molecules come closer to the surface due to electrostatic interactions. Different substance concentrations and conditions were tested for polymer monolayer film formation on the surface of the air/water interface. The roughness of the resulting films served as criteria for the fabrication of the optimum films. In the case of poly-benzyl-histidine, it became possible to fabricate films with a 1.5–2 nm thickness and a 0.2 nm roughness, which can increase the affinity of the fabricated polymer/antibodies films. This film is formed on the surface of a drying drop due to the self-assembly of polymer macromolecules on the surface of the interface. After 15 min, antibody–polymer complex monolayers were compressed using a compression barrier until the pressure reached 40 mN/m. Then the obtained film of antibody–polymer complexes was transferred to the surface of the substrate using Langmuir–Schaeffer technique (Lafuente et al. 2019). The value of the surface pressure was tested to obtain a maximal density of antibodies. The obtained films of antibodies were stored in a refrigerator at +5° C in a phosphate buffer.

Samples of antibody films were deposited on freshly cleaved mica or glass or gold. Imaging was performed using a Nanoscope IIIa (Digital Instruments, Santa Barbara CA, USA), operating in contact and tapping modes. Commercially

available tips (Veeco NanoProbe tips RTESP7 for tapping mode and NP-S20 for contact mode) were used. Data were analyzed using soft programs for Digital Instruments and NanoScale Explorer program developed in the Institute of Theoretical and Experimental Physics (Moscow, Russia).

The adsorption and binding of biomolecules and microorganisms to the surfaces is a central problem in fundamental studies, but also in biotechnological applications. AFM is a useful tool for such type of analysis. In this study, viruses were specifically immobilized using Langmuir antibody films based on amphiphilic polyelectrolytes for AFM studies. Antibodies on the basis of amphiphilic polymers were used to produce films for specific immobilization of rotaviruses. Amphiphilic polyelectrolytes were used to stabilize the protein conformation of antibodies to improve their affinity. Application of amphiphilic polymers protects the conformation of a protein globule from inactivating effects on the surface of the air/water interface and leads to the magnification of interactions between components of Langmuir film. Alkylated polyethyleneimine was used as an amphiphilic polyelectrolyte.

Immobilization of antibodies is a crucial step for fabricating high-quality affinity surfaces since after immobilization the activity of antibodies should remain high and binding of antigen should occur in a manner that reduces interference. The conventional methods for immobilization of biocomponents and antibodies include physical adsorption, covalent binding, entrapment, etc.; however, they suffer from a poor spatially controlled deposition. Comparing to these methods, Langmuir–Blodgett (LB) technique is considered as a desirable immobilization method owing to the following advantages: making uniform, ordered, and ultra-thin organic films; controlling the number of bio components by the number of deposited layers; and, in addition, preserving the activities and specific recognition properties of biocomponents. The stability of the mixed monolayer is very important because it is related to the transfer efficiency and the quality of deposited LB films. The pure amphiphile monolayer is unstable because of its partial solubility in the subphase. To prepare stable antibody monolayer, we used amphiphilic polyelectrolyte. The electrostatic force between antibodies and amphiphile molecules is expected to be an important factor for the adsorption process and increasing sensitivity and stability of affine surfaces.

The obtained films of antibodies were studied in contact mode AFM using the permissible minimal force of tip–sample interaction to avoid possible damage to the sample surface. Images of films of antibodies on the surface of gold and glass after blocking with bovine serum albumin (BSA) (Fig. 7.1) were obtained. In immunological detection, blocking is used to inhibit non-specific binding reactions. To determine the thickness of the antibody film, a relatively small surface region ($1500 \times 1500 \text{ nm}^2$) was scanned with a large force of tip–sample interaction several times, which resulted in the destruction of the antibodies film in this region (Fig. 7.1). The obtained height difference between damaged and undamaged surfaces was interpreted as the thickness of the film. It varied from 8 to 12 nm depending on the selected region and the substrate material. The obtained films of antibodies were

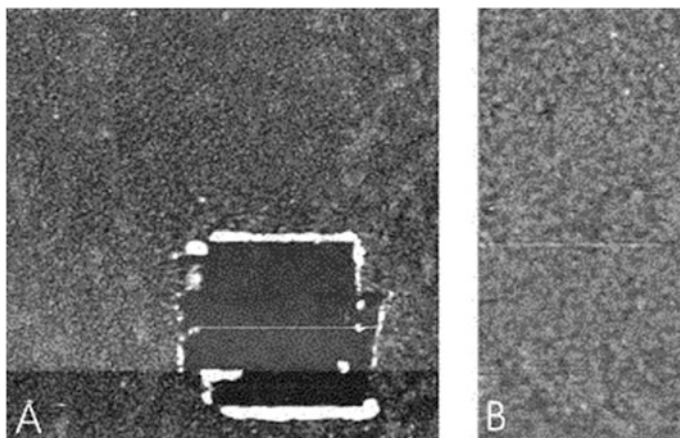
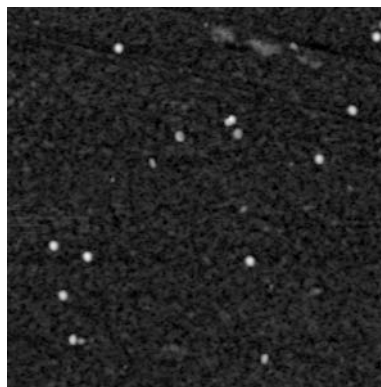


Fig. 7.1 Films of antibodies on the surface of glass (a) and gold (b) after the BSA blocking. On the left image, the surface of the film was specially destroyed to evaluate the thickness of the film. Scan size is $3000 \times 3000 \text{ nm}^2$

Fig. 7.2 Rotaviruses specifically bound to the film of correspondent antibodies formed on the basis of amphiphilic polyelectrolyte. Scan size is $3500 \times 3500 \text{ nm}^2$



stored in a refrigerator at $+5^\circ \text{C}$ in the phosphate buffer for 1 month without change of their immune activity.

AFM images of rotaviruses have been received using Langmuir films of antibodies formed on the basis of amphiphilic polymer (Fig. 7.2). The apparent diameter of rotaviruses ranged from 100 to 120 nm. These results have been compared with the real diameter of virus particles which can be obtained by electron microscopy (70 nm). Analysis of the data revealed that the diameter of viral particles received by AFM is bigger in comparison with results obtained by electron microscopy. Those distortions universally exist in AFM images due to geometrical interaction between the sample surface and the limited size tip. The distortions can cause bigger images than the real sizes using commercial pyramidal tips. The distortions of the images are affected by the shape of the AFM tip and the circumstance of the

particles. Previously, the ability to analyze specific binding of bacterial fragments with the affine surface has been shown (Dubrovin et al. 2012).

7.4 Conclusion and Future Perspectives

In conclusion, a method based on Langmuir antibody films using amphiphilic polyelectrolytes has been developed to specific immobilization of rotaviruses for AFM analysis. AFM is the only method that is presently capable of non-destructive continuous imaging with nanometric resolution. However, it is often difficult to know which object is located on the surface under investigation. From this point of view, we used antibodies for specific immobilization of viruses on the surface for AFM analysis. The new type of Langmuir antibodies films has been used for specific visualization of rotaviruses. The apparent diameters obtained by AFM of these viruses were compared with data obtained by electron microscopy.

A novel method of specific visualization of viruses is very important now. Recently, the charge-coupled device is responding for an outbreak of respiratory disease caused by a new coronavirus that was first detected in China and which has now been detected in almost 70 locations internationally, including in the United States. The virus has been named “SARS-CoV-2,” and the disease it causes has been named “coronavirus disease 2019” (abbreviated “COVID-19”) (www.cdc.gov). On January 30, 2020, the International Health Regulations Emergency Committee of the World Health Organization declared the outbreak a “public health emergency of international concern external icon” (PHEIC). On January 31, 2020, Health and Human Services Secretary Alex M. Azar II declared a public health emergency (PHE) for the United States to aid the nation’s healthcare community in responding to COVID-19 (www.who.int). In December 2019, a cluster of patients with pneumonia of unknown cause was linked to a seafood wholesale market in Wuhan, China. A previously unknown betacoronavirus was discovered through the use of unbiased sequencing in samples from patients with pneumonia. Human airway epithelial cells were used to isolate a novel coronavirus, named 2019-nCoV, which formed a clade within the subgenus sarbecovirus, Orthocoronavirinae subfamily. Different from both MERS-CoV and SARS-CoV, 2019-nCoV is the seventh member of the family of coronaviruses that infect humans. Enhanced surveillance and further investigation are ongoing. Coronaviruses are enveloped non-segmented positive-sense RNA viruses belonging to the family Coronaviridae and the order Nidovirales and broadly distributed in humans and other mammals. Although most human coronavirus infections are mild, the epidemics of the two betacoronaviruses, severe acute respiratory syndrome coronavirus (SARS-CoV) and Middle East respiratory syndrome coronavirus (MERS-CoV), have caused more than 10,000 cumulative cases in the past two decades, with mortality rates of 10% for SARS-CoV and 37% for MERS-CoV. The coronaviruses already identified might only be the tip of the iceberg, with potentially more novel and severe zoonotic events to be revealed.

In December 2019, a series of pneumonia cases of unknown cause emerged in Wuhan, Hubei, China, with clinical presentations greatly resembling viral pneumonia. Deep sequencing analysis from lower respiratory tract samples indicated a novel coronavirus, which was named 2019 novel coronavirus (2019-nCoV). Thus far, more than 800 confirmed cases, including in health-care workers, have been identified in Wuhan, and several exported cases have been confirmed in other provinces in China, and in Thailand, Japan, South Korea, and the USA (Huang et al. 2020).

We suppose that method described in this study may be useful to study other types of viruses including 2019-nCoV.

Acknowledgments The authors wish to thank E.V. Dubrovin and Ignatov D.S. for the help. The work was supported by the Rospotrebnadzor. F.S.Y. was supported by the State Assignment 0104-2019-0024 to Research Center of Biotechnology RAS.

References

- Agol VI (1974) Towards the system of viruses. *Biosystems* 6(2):113–132
- Amann R and Rosselló-Móra R (2016) After all, only millions? *mBio* 7 (4): e00999–e00916. <https://doi.org/10.1128/mBio.00999-16>.
- Armanious A, Aeppli M, Jacak R, Refardt D, Sigstam T, Kohn T, Sander M (2016) Viruses at solid-water interfaces: a systematic assessment of interactions driving adsorption. *Environ Sci Technol* 50:732–743
- Babitskaya JI, Budashov A, Chernov SF, Kurochkin IN, Doroshenko NV, Zubov SV (1997) Langmuir films from antibodies based on amphiphilic polyelectrolytes. *Membrane Cell Biol* 10:689–697
- Baltimore D (1971) Expression of animal virus genomes. *Bacteriol Rev* 35:235–241
- Bashar MM, Ohara H, Zhu H, Yamamoto S, Matsui J, Miyashita T, Mitsuishi M (2019) Cellulose Nanofiber Nanosheet multilayers by the Langmuir–Blodgett technique. *Langmuir* 35(24):8052–8059
- Berezovskaya F, Karev GP, Katsnelson MI, Wolf YI, Koonin EV (2018) Stable coevolutionary regimes for genetic parasites and their hosts: you must differ to coevolve. *Biol Direct* 13:27. <https://doi.org/10.1186/s13062-018-0230-9>
- Carrasco C, Carreira A, Schaap IAT, Serena PA, Gomez-Herrero J, Mateu MG, De Pablo PJ (2006) DNA-mediated anisotropic mechanical reinforcement of a virus. *Proc Natl Acad Sci U S A* 103:13706–13711
- Carrasco C, Castellanos M, De Pablo PJ, Mateu MG (2008) Manipulation of the mechanical properties of a virus by protein engineering. *Proc Natl Acad Sci U S A* 105:4150–4155
- Carrasco C, Luque A, Hernando-Perez M, Miranda R, Carrascosa JL, Serena PA, De Ridder M, Raman A, Gomez-Herrero J, Schaap IAT, Reguera D, De Pablo PJ (2011) Built-in mechanical stress in viral shells. *Biophys J* 100:1100–1108
- Carrillo PJP, Medrano M, Valbuena A, Rodriguez-Huete A, Castellanos M, Perez R, Mateu MG (2017) Amino acid side chains buried along intersubunit interfaces in a viral capsid preserve low mechanical stiffness associated with virus infectivity. *ACS Nano* 11:2194–2208
- Cheng S, Liu Y, Crowley CS, Yeates TO, Bobik TA (2008) Bacterial microcompartments: their properties and paradoxes. *BioEssays* 30:1084–1095
- Chow C-E, Suttle CA (2015) Biogeography of viruses in the sea. *Annu Rev Virol* 2:41–66

- Cobián Güemes AG, Youle M, Cantú VA, Felts B, Nulton J, Rohwer F (2016) Viruses as winners in the game of life. *Annu Rev Virol* 3:197–214
- Condit R (2013) Principles of virology. In: Knipe DM, Howley PM, Cohen JI, Griffin DE, Lamb RA, Martin MA, Racaniello VR, Roizman B (eds) *Fields virology*, vol 1, 6th edn. Lippincott Williams & Wilkins, Philadelphia, pp 21–51
- Curtis TP, Sloan WT, Scannell JW (2002) Estimating prokaryotic diversity and its limits. *Proc Natl Acad Sci U S A* 99:10494–10499. <https://doi.org/10.1073/pnas.142680199>
- Danovaro R, Dell'Anno A, Corinaldesi C, Rastelli E, Cavicchioli R, Krupovic M, Noble RT, Nunoura T, Prangishvili D (2016) Virus-mediated archaeal hecatomb in the deep seafloor. *Sci Adv* 2(10):e1600492. <https://doi.org/10.1126/sciadv.1600492>
- de Pablo PJ (2019) The application of atomic force microscopy for viruses and protein shells: imaging and spectroscopy. *Adv Virus Res* 105:161–187
- Delwart EL (2007) Viral metagenomics. *Rev Med Virol* 17:115–131
- Domingo E, Perales C (2019) Viral quasispecies. *PLoS Genet* 15(10):e1008271. <https://doi.org/10.1371/journal.pgen.1008271>
- Douglas T, Young M (1998) Host-guest encapsulation of materials by assembled virus protein cages. *Nature* 393:152–155
- Drake JW, Charlesworth B, Charlesworth D, Crow JF (1998) Rates of spontaneous mutation. *Genetics* 148:1667–1686
- Dubrovín EV, Fedyukina GN, Kraevsky SV, Ignatyuk TE, Yaminsky IV, Ignatov SG (2012) AFM specific identification of bacterial cell fragments on biofunctional surfaces. *Open Microbiol J* 6:22–28
- Edwards RA, Rohwer F (2005) Viral metagenomics. *Nat Rev Microbiol* 3:504–510
- Fotin A, Cheng Y, Sliz P, Grigorieff N, Harrison SC, Kirchhausen T, Walz T (2004) Molecular model for a complete clathrin lattice from electron cryomicroscopy. *Nature* 432:573–579
- Geoghegan JL, Holmes EC (2018) Evolutionary virology at 40. *Genetics* 210:1151–1162
- Gonzalez-Huici V, Salas M, Hermoso JM (2004) The push-pull mechanism of bacteriophage O29 DNA injection. *Mol Microbiol* 52:529–540
- Hernando-Perez M, Miranda R, Aznar M, Carrascosa JL, Schaap IAT, Reguera D, De Pablo PJ (2012) Direct measurement of phage phi29 stiffness provides evidence of internal pressure. *Small* 8:2366–2370
- Holland J, Spindler K, Horodyski F, Grabau E, Nichol S, VandePol S (1982) Rapid evolution of RNA genomes. *Science* 215:1577–1585. <https://doi.org/10.1126/science.7041255>
<https://www.mayoclinic.org/diseases-conditions/rotavirus/symptoms-causes/syc-20351300>
- Huang C, Wang Y, Li X, Ren L, Zhao J, Hu Y, Zhang L, Fan G, Xu J, Gu X, Cheng Z, Yu T, Xia J, Wei Y, Wu W, Xie X, Yin W, Li H, Liu M, Xiao Y, Gao H, Guo L, Xie J, Wang G, Jiang R, Gao Z, Jin Q, Wang J, Cao B (2020) Clinical features of patients infected with 2019 novel coronavirus in Wuhan, China. *Lancet* 395:497–506
- Iranzo J, Puigbò P, Lobkovsky AE, Wolf YI, Koonin EV (2016) Inevitability of genetic parasites. *Genome Biol Evol* 8:2856–2869
- Kim J-M, Chung Y-S, Jo HJ, Lee N-J, Kim MS, Woo SH, Park S, Kim JW, Kim HM, Han M-G (2020) Identification of coronavirus isolated from a patient in Korea with COVID-19. *Osong Public Health Res Perspect* (1):3–7
- Koonin EV, Dolja VV (2014) Virus world as an evolutionary network of viruses and capsidless selfish elements. *Microbiol Mol Biol Rev* 78(2):278–303
- Koonin EV, Dolja VV (2013) A virocentric perspective on the evolution of life. *Curr Opin Virol* 3:546–557
- Koonin EV, Wolf YI, Katsnelson MI (2017) Inevitability of the emergence and persistence of genetic parasites caused by evolutionary instability of parasite-free states. *Biol Direct* 12(1). <https://doi.org/10.1186/s13062-017-0202-5>
- Kuznetsov YG, McPherson A (2011) Atomic force microscopy in imaging of viruses and virus-infected cells. *Microbiol Mol Biol Rev* 75:268–285

- Lafuente M, Ruiz-Rincón S, Mallada R, Cea P, Pilar Pina M (2019) Towards the reproducible fabrication of homogeneous SERS substrates by Langmuir-Schaefer technique: a low cost and scalable approach for practical SERS based sensing applications. *Appl Surf Sci* 506:144663. <https://doi.org/10.1016/j.apsusc.2019.144663>
- Lai Y-T, Reading E, Hura GL, Tsai K-L, Laganowsky A, Asturias FJ, Tainer JA, Robinson CV, Yeates TO (2014) Structure of a designed protein cage that self-assembles into a highly porous cube. *Nat Chem* 6:1065–1071
- Llauro A, Guerra P, Irigoyen N, Rodriguez JF, Verdaguer N, De Pablo PJ (2014) Mechanical stability and reversible fracture of vault particles. *Biophys J* 106:687–695
- Llauro A, Luque D, Edwards E, Trus BL, Avera J, Reguera D, Douglas T, Pablo PJ, Caston JR (2016) Cargo-shell and cargo-cargo couplings govern the mechanics of artificially loaded virus-derived cages. *Nanoscale* 8:9328–9336
- Locey KJ, Lennon JT (2016) Scaling laws predict global microbial diversity. *Proc Natl Acad Sci U S A* 113:5970–5975
- Mateu MGE (2013) Structure and physics of viruses. Springer. <https://doi.org/10.1007/978-94-007-6552-8>
- Medrano M, Valbuena A, Rodríguez-Huete A, Mateu MG (2019) Structural determinants of mechanical resistance against breakage of a virus-based protein nanoparticle at a resolution of single amino acids. *Nanoscale* 11:9369–9383
- Michigan Technological University. Virus surfaces help engineers study vaccine and gene therapy applications. (2020) *ScienceDaily*, 8 January.
- Mokili JL, Rohwer F, Dutilh BE (2012) Metagenomics and future perspectives in virus discovery. *Curr Opin Virol* 2:63–77
- Moreno-Madrid F, Martin-Gonzalez N, Llauro A, Ortega-Esteban A, Hernando-Perez M, Douglas T, Schaap IA, De Pablo PJ (2017) Atomic force microscopy of virus shells. *Biochem Soc Trans* 45:499–511
- Muller DJ, Amrein M, Engel A (1997) Adsorption of biological molecules to a solid support for scanning probe microscopy. *J Struct Biol* 119:172–188
- Muller DJ, Janovjak H, Lehto T, Kuerschner L, Anderson K (2002) Observing structure, function and assembly of single proteins by AFM. *Prog Biophys Mol Biol* 79:1–43
- Mushegian AR (2020) Are there 10^{31} virus particles on earth, or more, or less? *J Bacteriol*. <https://doi.org/10.1128/JB.00052-20>
- Nicolaisen M (2011) An oligonucleotide-based microarray for detection of plant RNA viruses. *J Virol Methods* 173:137–143
- Ortega-Esteban A, Perez-Berna A, Menendez-Conejero R, Flint S, San Martín C, De Pablo P (2013) Monitoring dynamics of human adenovirus disassembly induced by mechanical fatigue. *Sci Rep* 3(1):1434. <https://doi.org/10.1038/srep01434>
- Purohit PK, Kondev J, Phillips R (2003) Mechanics of DNA packaging in viruses. *Proc Natl Acad Sci U S A* 100:3173–3178
- Querol-Audi J, Casanas A, Uson I, Luque D, Caston JR, Fita I, Verdaguer N (2009) The mechanism of vault opening from the high resolution structure of the N-terminal repeats of MVP. *EMBO J* 28(21):3450–3457
- Rief M, Gautel M, Oesterhelt F, Fernandez JM, Gaub HE (1997) Reversible unfolding of individual titin immunoglobulin domains by AFM. *Science* 276:1109–1112
- Rohwer F (2003) Global phage diversity. *Cell* 113(2):141. [https://doi.org/10.1016/S0092-8674\(03\)00276-9](https://doi.org/10.1016/S0092-8674(03)00276-9)
- Rohwer F, Thurber RV (2009) Viruses manipulate the marine environment. *Nature* 459:207–212
- Roos WH, Gertsman I, May ER, Brooks CL, Johnson JE, Wuite GJL (2012) Mechanics of bacteriophage maturation. *Proc Natl Acad Sci U S A* 109:2342–2347
- Roos WH, Radtke K, Kniesmeijer E, Geertsema H, Sodeik B, Wuite GJL (2009) Scaffold expulsion and genome packaging trigger stabilization of herpes simplex virus capsids. *Proc Natl Acad Sci U S A* 106:9673–9678

- Roossinck MJ (2011) The big unknown: plant virus biodiversity. *Curr Opin Virol* 1:63–67
- Rosario K, Breitbart M (2011) Exploring the viral world through metagenomics. *Curr Opin Virol* 1:289–297
- Sanjuán R, Domingo-Calap P (2016) Mechanisms of viral mutation. *Cell Mol Life Sci* 73:4433–4448
- Sanjuán R, Nebot MR, Chirico N, Mansky LM, Belshaw R (2010) Viral mutation rates. *J Virol* 84:9733–9748
- Schaap IAT, Carrasco C, De Pablo PJ, Mackintosh FC, Schmidt CF (2006) Elastic response, buckling, and instability of microtubules under radial indentation. *Biophys J* 91:1521–1531
- Schulz F, Roux S, Paez-Espino D, Jungbluth S, Walsh D, Denev VJ, McMahon KD, Konstantinidis KT, Eloë-Fadrosh EA, Kyrpides N, Woyke T (2020) Giant virus diversity and host interactions through global metagenomics. *Nature*. <https://doi.org/10.1038/s41586-020-1957-x>
- Siddell SG, Walker PJ, Lefkowitz EJ, Mushegian AR, Dutilh BE, Harrach B, Harrison RL, Junglen S, Knowles NJ, Kropinski AM, Krupovic M, Kuhn JH, Nibert ML, Rubino L, Sabanadzovic S, Simmonds P, Varsani A, Zerbini FM, Davison AJ (2020) Binomial nomenclature for virus species: a consultation. *Arch Virol* 165:519–525
- Smith DE, Tans SJ, Smith SB, Grimes S, Anderson DL, Bustamante C (2001) The bacteriophage phi 29 portal motor can package DNA against a large internal force. *Nature* 413:748–752
- Snijder J, Kononova O, Barbu IM, Uetrecht C, Rurup WF, Burnley RJ, Koay MS, Cornelissen JJ, Roos WH, Barsegov V, Wuite GJ, Heck AJ (2016) Assembly and mechanical properties of the cargo-free and cargo-loaded bacterial nanocompartment encapsulin. *Biomacromolecules* 17:2522–2529
- Snijder J, Uetrecht C, Rose RJ, Sanchez-Eugenia R, Marti GA, Agirre J, Guerin DM, Wuite GJ, Heck AJ, Roos WH (2013) Probing the biophysical interplay between a viral genome and its capsid. *Nat Chem* 5:502–509
- Suttle CA (2005) Viruses in the sea. *Nature* 437:356–361. <https://doi.org/10.1038/nature04160>
- Suttle CA (2007) Marine viruses - major players in the global ecosystem. *Nat Rev Microbiol* 5(10):801–812
- Szathmáry E, Maynard Smith J (1997) From replicators to reproducers: the first major transitions leading to life. *J Theor Biol* 187:555–571
- Takeuchi N, Hogeweg P (2007) The role of complex formation and deleterious mutations for the stability of RNA-like replicator systems. *J Mol Evol* 65:668–686
- Takeuchi N, Hogeweg P (2012) Evolutionary dynamics of RNA-like replicator systems: a bioinformatic approach to the origin of life. *Phys Life Rev* 9:219–263
- Tetreau G, Banneville AS, Andreeva EA, Brewster AS, Hunter MS, Sierra RG, Teulon JM, Young ID, Burke N, Gruenewald TA, Beaudouin J, Snigireva I, Fernandez-Luna MT, Burt A, Park HW, Signor L, Bafna JA, Sadir R, Fenel D, Boeri-Erba E, Rosenthal M, Coquelle N, Burghammer M, Cascio D, Sawaya MR, Winterhalter M, Gratton E, Gutsch I, Federici B, Pellequer JL, Sauter NK, Colletier JP (2020) Serial femtosecond crystallography on in vivo-grown crystals drives elucidation of mosquito-cidal Cyt1Aa bioactivation cascade. *Nat Commun* 11(1):1153. <https://doi.org/10.1038/s41467-020-14894-w>
- Vasilieva SG, Shibzukhova KA, Morozov AS, Lobakova ES (2018) Harvesting of microalgae biomass with Polyethylenimine-based sorbents. *Mosc Univ Biol Sci Bull* 73:36–38
- Vinatzer BA, Tian L, Heath LS (2017) A proposal for a portal to make earth's microbial diversity easily accessible and searchable. *Antonie Van Leeuwenhoek* 110:1271–1279
- Wimmer E, Mueller S, Tumphey TM, Taubenberger JK (2009) Synthetic viruses: a new opportunity to understand and prevent viral disease. *Nat Biotechnol* 27(12):1163–1172
- Worsdofer B, Woycechowsky KJ, Hilvert D (2011) Directed evolution of a protein container. *Science* 331(6017):589–592

Wu Q, Ding S-W, Zhang Y, Zhu S (2015) Identification of viruses and Viroids by next-generation sequencing and homology-dependent and homology-independent algorithms. *Annu Rev Phytopathol* 53:425–444

www.cdc.gov

www.who.int

Zeng C, Moller-Tank S, Asokan A, Dragnea B (2017) Probing the link among genomic cargo, contact mechanics, and nanoindentation in recombinant adeno-associated virus 2. *J Phys Chem B* 121:1843–1853

Chapter 8

Fluorometric and SERS Sensor Systems for Diagnostics and Monitoring of Catecholamine-Dependent Diseases



Irina A. Veselova, Maria I. Makedonskaya, Olga E. Eremina, and Tatiana N. Shekhovtsova

Abstract The developing of the point-of-care sensor systems for sensitive, rapid, available, selective, and at the same time simple methods for detecting neurotransmitters in various biological samples can potentially improve patient care through real-time and remote health monitoring.

The detailed study of literature data and the authors' own experience have demonstrated that fluorescence and surface-enhanced Raman spectroscopy (SERS) are the most actively developing and universal methods for the creation of sensor systems for sensitive, selective, and reproducible determination (including multiplex) of CAs and their metabolites as the markers for the diagnosis of a wide range of diseases associated with the imbalance of neurotransmitters in the human body. One of the most promising approaches to solving the problem of CAs and their metabolites determination consists in utilizing solid-phase fluorescent indicator systems in combination with either the enzymatic derivatization of the analytes (using their interaction with aromatic diamines – benzylamine or 1,2-diphenylethylenediamine in the presence of horseradish peroxidase as a catalyst, and the application of first-order derivative fluorescence spectroscopy for the resolution of their spectra) or the formation of neurotransmitter complexes with metal ions (e.g., a triple complex with europium (III) and tetracycline). Another modern direction of molecular diagnostics is the development of solid-phase nanocomposite fluorescent sensors with a purposefully selected chemical design of both the polymer surface and inorganic nanostructures (e.g., gold and silver nanoparticles, quantum dots), providing *ex vivo* and *in vivo* visualization and determination of neurotransmitter metabolism markers in living tissue and cell structures.

The rapid development of SERS over the past 20 years has been facilitated, firstly, by advances in the targeted synthesis of nanostructured SERS-active materials and, secondly, the elaboration and improvement of Raman spectrometers. SERS opens up new unprecedented possibilities for lowering the detection limits of relevant analytes and their multiplex determination.

I. A. Veselova (✉) · M. I. Makedonskaya · O. E. Eremina · T. N. Shekhovtsova
Department of Chemistry, Lomonosov Moscow State University, Moscow, Russia

Thus, a new promising time-stable SERS indicator system has been proposed. The quantification of neurotransmitters and their metabolites in biological samples at nanomolar and lower-level concentrations was possible due to the formation of complexes with copper (II) on a metallic nanostructured surface followed by measurement of inelastically scattered light. Preliminary results point out the manifest benefits of the future implementation of SERS-sensor systems in clinical medical analysis.

Keywords Fluorescent and SERS sensor systems · Catecholamines and their metabolites · Determination · Biological samples · Diagnostics and monitoring of catecholamine-dependent diseases

Nomenclature

SERS	Surface-enhanced Raman spectroscopy
SERRS	Surface-enhanced resonance Raman spectroscopy
CA	Catecholamine
DA	Dopamine
EP	Epinephrine (adrenaline)
NE	Norepinephrine (noradrenaline)
HVA	Homovanillic acid
VMA	Vanillylmandelic acid
<i>l</i> -DOPA	Dihydroxy-L-phenylalanine
5-HIAA	5-Hydroxyindoleacetic acid
NMN	Normetanephrine
HPLC	High performance liquid chromatography
EC	Electrochemical
MS	Mass spectrometric
FRET	Fluorescence resonance energy transfer
BA	Benzylamine
DPE	1,2-Diphenylethylenediamine
LOD	Limit of detection
CL	Chemiluminescence
SPE	Solid-phase extraction
OTC	Oxytetracycline
4-MPBA	4-Mercaptobenzene boronic acid
RB	Rhodamine B
AgNC	Silver nanocube
AgNF	Silver nanofilm
AuNP	Gold nanoparticle
DBA	Dopamine-binding aptamers

8.1 Introduction

Neurotransmitter exchange is one of the most important processes in the nervous system, mediating both the peripheral and central nervous systems and cardiovascular system regulation of a human body. Abnormalities involving metabolism of neurotransmitters underlie the pathogenesis of some socially significant diseases: neurodegenerative dementia (Kovacs 2016) and neuroendocrine tumors (Kaltsas et al. 2004; Klimstra et al. 2010). Transmission of nerve impulses across synapses happens due to the chemical interactions between the presynaptic and postsynaptic neurons that are, in turn, implemented through special compounds called neurotransmitters (Fig. 8.1). As a rule, neurotransmitters, or neuromediators, are represented by amino acids, peptides, and monoamines that transmit the impulses from a neuron (Vatsadze et al. 2018; Rodan et al. 2015). Currently, more than 100 various biomarkers of socially significant diseases associated with impaired neurotransmitter metabolism are known.

Due to the difference in the levels of neurotransmitters and their metabolites in a healthy person and a patient with a pathology caused by the neuromediation disturbance, these molecules are capable of playing a role of important diagnostic biomarkers. Nowadays the most studied low-molecular-weight markers of the neurotransmitter metabolism are catecholamines (CA), such as dopamine (DA), epinephrine (or adrenaline, EP), norepinephrine (or noradrenaline, NE), and their metabolites: vanillylmandelic acid (VMA), homovanillic acid (HVA), 5-hydroxyindoleacetic acid (5-HIAA), metanephrine (MN), and normetanephrine (NMN). The metabolism of catecholamines drive the regulation of both the

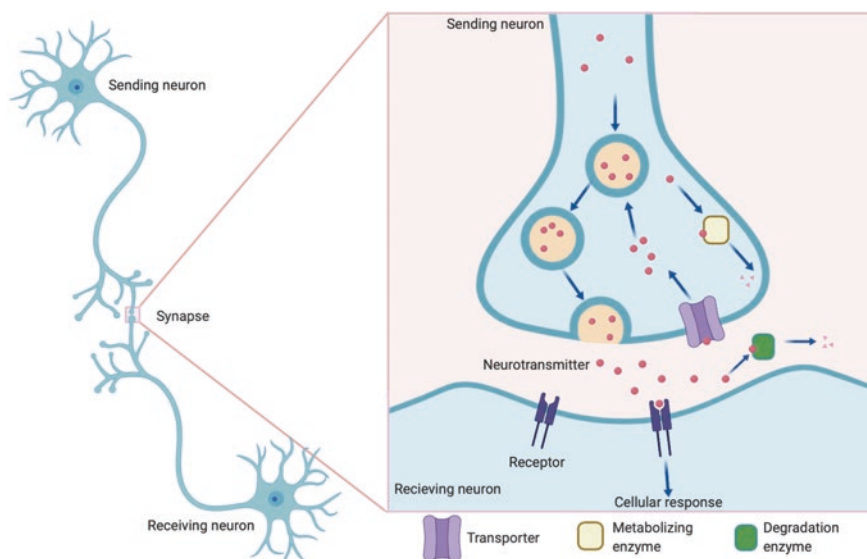


Fig. 8.1 Scheme of neurotransmitter metabolism at a chemical synapse

human mental and physical activity through dopaminergic and adrenergic receptors. Catecholamines are involved in the regulation of the body's response to stress, psychomotor activity, emotional processes, learning, sleep, and memory (Eisenhofer et al. 2004; Ugrumov 2009). The CA level in biological samples (blood plasma, urine, cerebrospinal fluid, different tissue, cells, etc.) of a healthy adult varies within the normal concentrations, thus significant deviations in the concentrations of neuromediators indicate impaired functioning of the body (Barnes et al. 2015).

Diseases associated with the serious disorders of neurotransmitter metabolism can be classified into two main types: (1) neurodegenerative disorders accompanied by a progressive loss of nerve cells and thus a decrease in the concentration of catecholamines and their metabolites (e.g., Alzheimer's and Parkinson's diseases) and (2) neuroendocrine disorders characterized by an excessive synthesis of catecholamines caused by organic lesions or genetic defects in the hypothalamus (such as pheochromocytoma, paraganglioma, carcinoid tumors, neuroblastoma, etc.).

Among the analytical techniques used for the determination of CAs and their metabolites in biological samples, chromatographic (e.g., high performance liquid chromatography – HPLC) methods coupled with electrochemical (EC) (Barco et al. 2014) or mass spectrometric (MS) (Tohmola et al. 2015) detection are the most commonly used. However, all the developed procedures require rather complicated sample preparation steps for biological liquids, including separation and preconcentration of catecholamines and their metabolites. Unfortunately, these methods are time-consuming, expensive and require special bulky equipment and highly qualified personnel. Despite their high selectivity, sensitivity, and availability, electrochemical detectors are known for poor reproducibility at the level of nanomolar concentration of analytes, sensitivity to fluctuations in the mobile phase flow rate, contamination of the electrode, and strict requirements to the nature of the mobile phase (Bicker et al. 2013). HPLC-EC is characterized by low signal-to-noise ratio, the detection sensitivity is not always sufficient enough for the analysis of real biological samples, and the efficiency of chromatographic separation is quite low (Hubbard et al. 2010; Parrot et al. 2011). HPLC-MS/MS is characterized by a significantly higher sensitivity for CAs and their metabolites determination. However, this technique is not rapid enough, there are significant background signals caused by complexity of biological samples which result in ion suppression and ion competition phenomena which drop down the sensitivity (Syslova et al. 2011; Zhu et al. 2011; Nirogi et al. 2013).

The main drawback of immunochemical methods is that all CAs must be susceptible to methylation to transform them into metanephrine and normetanephrine with their subsequent acylation. Moreover, CAs should be pre-extracted from the matrix sample with a borate affinity gel, which greatly complicates the procedure (Wassell et al. 1999).

Despite the problem having been well addressed apparently and the availability of a broad set of methods for CAs determination in plasma and urine, the relatively long analysis time (Zhao and Suo 2008; Nirogi et al. 2013), during which the unstable analytes may degrade, as well as the possibility of errors associated with low

reproducibility and poor peak resolution (Kim et al. 2014) frequently cause numerous diagnostic errors leading to ineffective treatment.

Evidently certain difficulties in the determination of catecholamines in biological samples are caused by their initially very low reference concentrations at the level of 1 nM, with a possible decrease down to 10^{-14} – 10^{-12} M in case of various pathological disorders. In addition, catecholamines in blood are rapidly oxidized by monoamine oxidase, oxygen, and components of biological matrix. Therefore the determination of neurotransmitter metabolism biomarkers circulating in a body (especially in the crisis conditions) should be very rapid (within 15–30 min), simple, and robust in order to be executable at the patient's bedside with portable equipment.

Besides, for the reliable diagnosis of catecholamine-dependent diseases, the possibility of multiplex simultaneous determination of several biomarkers of the neurotransmitter metabolism in one probe is very topical (Veselova et al. 2016). Thus, developing of the point-of-care sensor systems for sensitive, rapid, available, selective, and simple methods for detecting CAs and their metabolites in various biological samples can potentially improve patient care through real-time and remote health monitoring.

Based on the detailed study of literature data, and the authors' own experience, fluorescence and surface-enhanced Raman spectroscopy (SERS) are the most promising and universal methods for the creation of such sensor systems for the determination (including multiplex) of markers for neurotransmitter metabolism.

In the framework of this chapter, the authors tried to generalize, systematize, and present the current state of the development of fluorescent and SERS sensors for catecholamines and their metabolite determination, as well as the prospects of their application for the diagnostics of a number of neurodegenerative diseases and neuroendocrine tumors associated with an imbalance of neurotransmitters in a human body.

8.2 Fluorometric Sensor Systems for the Determination of Catecholamines in Biological Samples

Among various chemical sensor systems, fluorescent ones have several advantages: measurements are usually very sensitive (in some cases it is possible to detect individual molecules), the equipment itself is miniaturized and affordable, while the results are highly reproducible (Geddes et al. 2005; Rodionov et al. 2014; Veselova et al. 2017; Makedonskaya et al. 2018a, b).

The measurement principle of such sensor systems is based either on the fluorescence of neurotransmitter metabolism markers themselves or their fluorescent derivatives, as well as on the use of luminescent labels, e.g., different luminescent dyes.

8.2.1 Determination of Catecholamines Using Their Intrinsic Fluorescence

CA molecules have their own fluorescence with $\lambda_{\text{ex}} = 280$ nm and $\lambda_{\text{em}} = 324$ nm and fluoresce most intensively in acidic medium, when their amino groups are protonated. The strong intrinsic fluorescence of CAs in the UV region may be used for their determination (Hsieh et al. 2002; Hsieh and Chang 2005; Kuo et al. 2005; Cakal et al. 2011; Altun et al. 2015; Fonseca et al. 2017; Ragab et al. 2000; Huang et al. 2019). Xenon lamps (Wang et al. 2002) and especially lasers (Hsieh et al. 2002; Hsieh and Chang 2005; Kuo et al. 2005) are used as excitation sources. To determine CAs, neodymium (Hsieh et al. 2002; Hsieh and Chang 2005), argon (Tong and Yeung 1997), neon (Zhang and Sweedler 2001), and krypton (Paquette et al. 1998) lasers and solid-phase nanolasers (Kuo et al. 2005) are applied. The utilization of high-frequency laser sources is one of the ways to increase the sensitivity of fluorescent determination of CAs.

Unfortunately, it is impossible to use those methods in the analysis of real samples with complicated biological matrixes without a preliminary separation of all components by capillary electrophoresis or HPLC. The majority of organic components of biosamples matrices possess high background signals at the excitation wavelengths of CAs and their metabolites fluorescence (200–300 nm). In addition, the analytes themselves may cause interfering mutual influence.

To enhance the sensitivity and selectivity of the analytes determination in the presence of matrix components, they should be preliminarily separated by capillary electrophoresis (Hsieh et al. 2002; Hsieh and Chang 2005; Kuo et al. 2005) or HPLC (Muzzi et al. 2008; De Benedetto et al. 2014) and additionally pre-concentrated (Cakal et al. 2011; Altun et al. 2015). The detection limits of CAs vary from 2.5 nM to 55 μ M, depending on the excitation source.

8.2.2 Determination of Catecholamines Using Their Fluorescent Derivatives

A promising approach to enhancing the selectivity and sensitivity of CAs and their metabolites determination in biological samples consists in their conversion into corresponding highly fluorescent derivatives. The excitation wavelengths of such derivatives lie in the region of 340–360 nm, depending on the derivatization agent and the analyte. In addition, fluorescence signals of the derivatives are observed in the long-wave region, which provides. This helps to partially eliminate the interfering effect of matrix components in biological materials (blood, urine, etc.) (Tsunoda 2006).

A wide range of derivatization agents is used for CAs and their metabolites derivatization, e.g., aromatic amines such as ethylenediamine (Wang et al. 2003), *o*-phenylenediamine (Jinghe et al. 1998), 1,2-diphenylethylenediamine (Mitsui

et al. 1985), 9-fluorenylmethyl chloroformate (Descombes and Haerdi 1992), naphthalene-2,3-dicarboxaldehyde (Zhang and Gong 2016), glycyglycine (Seki and Yamaguchi 1984) etc.

It was recently demonstrated that the most efficient agents for the derivatization of CAs are benzylamine (BA) and 1,2-diphenylethylenediamine (DPE) in combination with a catalytic system peroxidase–H₂O₂ (with the reaction being performed in polystyrene 96-well plates). Molecules of CAs are oxidized to the CA-o-quinone, which then reacts with the derivatizing agent (BA or DPE) by Michael's reaction. The final derivatization products of the CAs with BA and DPE are 2-phenyl (4,5-dihydropyrrolo) [2,3-f] benzoxazole derivatives that are characterized by more intense fluorescence than the CAs themselves (Rodionov et al. 2014). The pyrocatechol fragment in CA molecules is one of the substrates of horseradish peroxidase (HRP) (Myasnikova et al. 2014). Due to the unique recognizing ability of biocatalysts (oxidoreductase enzymes and proteins), their introduction into the analytical systems significantly improves the selectivity of the CAs determination in the presence of other matrix compounds of different real-world samples, including biological liquids. Derivatizing agents also contribute to improving the selectivity toward the analytes due to the selectivity their interaction (Bratovskaja et al. 2004; Puiu et al. 2008). Using the enzyme provides a significant reduction of the reaction time (down to 5 min) and at the same time enhances the analyte stability by avoiding aggressive organic solvents and heating. Based on the described system, the highly sensitive techniques for the enzymatic determination of CAs by measuring the fluorescence intensity of their reaction mixture were developed (Rodionov et al. 2014).

However, it was especially important to determine several CAs in a mixture simultaneously as well as to be able to determine one analyte in the presence of others in biological samples in order to diagnose a specific tumor disease. To achieve a complete resolution of the analytes in the mixtures, such methods as first- and higher-order derivative fluorescence spectroscopy were used (Makedonskaya et al. 2018a, b). Derivation narrows the spectral bandwidths and enhances minor spectral features, improving the selectivity of multicomponent spectra. The initial (zero-order) fluorescence spectrum of various triple mixtures of CA derivatives, then, the first- and second-order derivative fluorescence spectra were obtained as a result of mathematical processing (Fig. 8.2). It turned out that the limit of detection (LOD) for the techniques using derivative fluorescence spectra was slightly higher than that for the procedures with the initial (zero-order) fluorescence spectra (for instance, LODs for DA were 0.09, 0.10, and 0.11 μM, respectively). However, this difference was insignificant, and the resolution of the first-order derivative spectra was already sufficient for quantitative simultaneous multiplex detection of individual catecholamines in their mixture.

It was demonstrated that all analytes were stable in both plasma and urine samples at room temperature during the analysis and storage at 4 °C within 24 h. Notably, the majority of the matrix components of biological samples, such as uric and ascorbic acids, amino acids (phenylalanine, tyrosine, tryptophan), and various biochemical compounds (urea, creatinine, glucose), did not interfere with the selective determination of CAs, and the proposed technique could be used

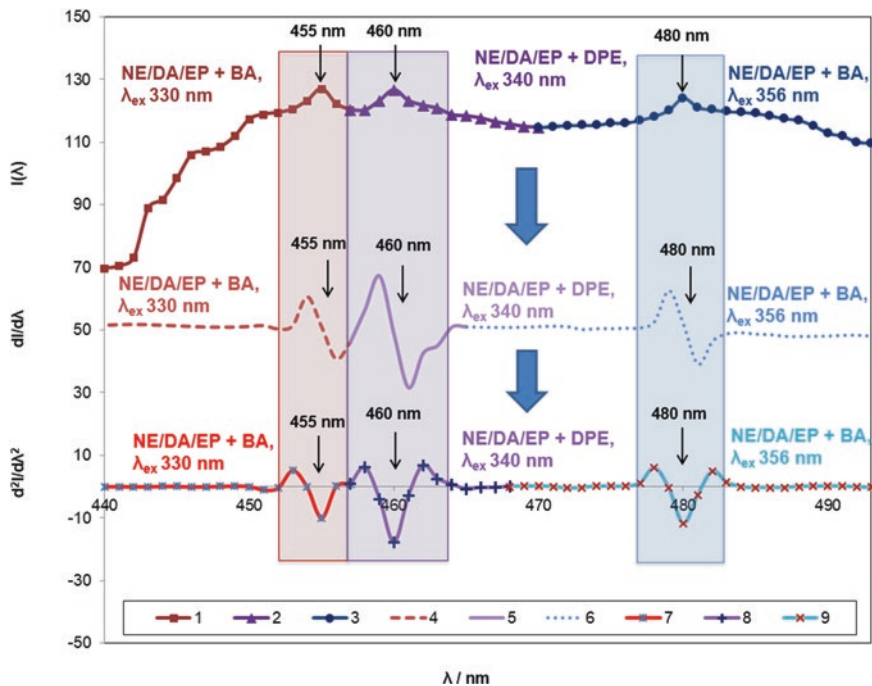


Fig. 8.2 (1–3) The initial (zero-order) fluorescent spectra, (4–6) first-order, and (7–9) second-order derivative fluorescent spectra of the mixtures of the CA derivatives – NE/DA/EP in the ratios similar to the reference concentrations of CAs in the urine of a healthy human (0.1, 1.0, and 0.05 μM for NE, DA, and EP, respectively): (1), (4), (7) NE/DA/EP with BA, $\lambda_{\text{ex}} = 330 \text{ nm}$, $\lambda_{\text{em}} = 455 \text{ nm}$; (2), (5), (8) NE/DA/EP with DPE, $\lambda_{\text{ex}} = 340 \text{ nm}$, $\lambda_{\text{em}} = 460 \text{ nm}$; (3), (6), (9) NE/DA/EP with BA, $\lambda_{\text{ex}} = 356 \text{ nm}$, $\lambda_{\text{em}} = 480 \text{ nm}$

without prior sample preparation steps. These results indicated that the developed approach exhibits good precision, stability, selectivity, and accuracy (Makedonskaya et al. 2018b).

It is expedient to mention here that multiplex analysis is a variant of analysis that provides simultaneous determination of several compounds of the same group in one portion of a sample during one analytical cycle. To provide multiplex analysis, high-throughput techniques based on microchips and sensors, as well as special detection systems under computer control, are applied. Microchips are special matrices with applied molecules of nuclear acids, proteins, or other biomolecules for simultaneous performance of a large number of analyses (Murphy et al. 1992; Kim et al. 2008; Melnikov et al. 2008; Laxman et al. 2008; Kim et al. 2009; Lee et al. 2018). In clinical practice, the application of multiplex analytical techniques improves biochemical examination of patients allowing early diagnosis and controlling of treatment efficiency. In this regard, the above-described method for multiplex determination of CAs and their metabolites based on the measurement of fluorescence of the analyte derivatives and derivative spectra

should significantly facilitate clinical analysis. The developed procedures (Makedonskaya et al. 2018a, b) were applied successfully for rapid, high-throughput (20 samples per 15–30 min) screening of human urine and mice blood plasma. The proposed strategy can be used in the analysis of human urine and blood for rapid diagnosis of neuroendocrine catecholamine-producing diseases.

Importantly, the sensitivity (down to 1.5 nM) (Rodionov et al. 2014; Makedonskaya et al. 2018a, b) and selectivity of the developed methods are much higher than those of electrochemical, immunoassay, fluorescence, and electrophoretic methods and chromatography with electrochemical, fluorescence, chemiluminescence (CL), and UV detection (Wang et al. 2007; Zheng et al. 2011; Seto et al. 2012; Elhag et al. 2014) and are comparable with the analytical characteristics of HPLC-MS. At the same time, the described approach possesses considerable advantages over other methods, including the rapidity and simplicity of analysis and the absence or minimal pretreatment of urine and blood samples (Nichkova et al. 2013).

8.2.3 Determination of Catecholamines Using Fluorescence of Their Metal Complexes

The very high sensitivity of CAs and their metabolites determination (at a level of 1 pM) can be achieved using fluorescence of their complexes with various metal ions, such as Cu(II), Fe(II), Eu(III), Tb(III), etc. For example, the determination of DA (down to 10 μ M) is possible due to its ability to enhance the fluorescence of the calcein blue complex with iron (III), where DA modifies the organic ligand (Seto et al. 2012). In Alam et al. (2012), a method for the determination of EP, DA, and NE with LODs of 0.25, 0.42, and 0.64 nM, respectively, based on fluorescence of their complexes with Tb(III) in the presence of colloidal silver particles, is described. In a paper (Fotopoulou and Ioannou 2002), the sensitivity of EP, NE, and DA determination (LOD 10–70 nM) was enhanced using the fluorescence of their complexes with Tb(III) after preconcentration by solid-phase extraction (SPE). CAs (DA, EP, and NE) could be determined owing to an increase in the fluorescence of their complexes with Tb(III) in micellar medium in the presence of sodium dodecylbenzenesulfonate (Kamruzzamana et al. 2012): fluorescence of the triple complex Tb(III)-CA-DDBS is much higher than that of the double complex Tb(III)-CA. LODs of DA, EP, and NE are in the range 10–100 nM. This procedure allows selective determination of the CAs in blood serum with HPLC without preliminary separation. In addition, triple complexes of CAs with two metal ions (Eu(III)-La(III) or Tb(III)-Gd(III)) were used to enhance the fluorescence intensity of DA (LOD 27 pM) in the presence of sodium dodecylbenzenesulfonate (Si et al. 2013) or EP at pH 10 (LOD 4.5 nM) (Guo et al. 2007).

Recently, a new indicator system based on intensely fluorescing triple complexes of CAs and their metabolites with europium (III) and oxytetracycline (OTC) (hereinafter, the Eu(III)-OTC-CA/metabolite triple complex) has been

proposed (Makedonskaya 2018a). This is a very promising system since it allows the fluorescence intensity of CAs and their metabolites to be increased 200–400-fold in comparison with their intrinsic fluorescence and the fluorescence maximum to be bathochromically shifted, thus minimizing the interfering effect of the biological matrices.

The feasibility of the developed technique of CAs and their metabolites determination in biological samples was preliminarily confirmed by estimating the stability of the formed complexes and the calibration curves for their determination in biological fluids without any competing interactions with the matrix components of samples. The investigated complexes were rather stable (stability constants were $n \times 10^6$). The limits of detection for some model compounds were ultralow (LODs for NMN, NE, HVA, 5-HIAA, EP, DA, VMA, and *l*-DOPA were 0.05, 0.2, 0.3, 0.3, 20.0, 30.0, 40.0 pM, and 0.3 nM, respectively) (Makedonskaya et al. 2018a). Different values of LODs occur apparently due to the different stabilities of the Eu(III)-OTC-analyte complexes, which stems from the differences in the structures of the analyte molecules that affect the strength of their bonding with the Eu(III)-OTC complex (Makedonskaya et al. 2018a). The higher the stability constant of CA/metabolite complex with europium (III) and OTC is, the lower the LOD of a certain analyte should be. The consequence of decreasing the stability constants is: NMN > NE > HVA/5-HIAA > EP > DA/VMA > *l*-DOPA. The results of the paper (Makedonskaya et al. 2018a) revealed the stability of Eu(III)-OTC-CA/metabolite complexes as being one to two orders of magnitude higher than those of the copper(II) complexes with creatinine and amino acids (Karaderi et al. 2007) and one to three orders of magnitude higher than those of some CA complexes with calcium and lanthanum(III) that have long been successfully applied for CA determination in biosamples (Wu et al. 2001).

8.2.4 Solid-Phase and Metal-Dependent Fluorescent Sensor Systems for the Determination of Catecholamines and Their Metabolites

One of the modern areas of molecular diagnostics is the development of solid-phase fluorescent sensor nanocomposite materials with a directionally selected chemical design of the polymer surface and inorganic nanostructures (gold and silver nanoparticles, quantum dots), providing *ex vivo* and *in vivo* visualization and determination of neurotransmitter metabolism markers in living tissue and cell structures (Sancataldo et al. 2019).

Nowadays, the development of such fluorescent sensor systems for the determination of biomarkers of neurotransmitter metabolism is underway at the intersection of materials science, biochemistry, analytical chemistry, optics, and photonics. New fluorescent labels for producing the sensitive and selective analytical signal are nanoparticles and nanosystems (Yao et al. 2014; Hu et al. 2019; Suzuki Yo 2019).

Solid-phase fluorescence in gels, films, membranes, and on other solid surfaces has advantages in comparison with fluorescence in solution, such as simple sample pretreatment, stabilization of analytes in samples, and hence, decrease in analysis errors; in addition, there is a possibility to analyze samples with complicated matrices and decrease the time of analysis due to preliminary immobilization of reaction components. A solid-phase fluorescent biosensor for the determination of phenolic compounds, including CAs, was developed in the paper (Rodionov et al. 2014). The analytical signal was measured directly on the surface of biosensitive layer, consisting of polyelectrolyte complex {horseradish peroxidase-chitosan}.

The investigation of the above-described system based on intensively fluorescing ternary complexes of CAs and their metabolites with europium(III) and oxytetracycline (Makedonskaya et al. 2018a) was continued in micellar media. To stabilize the system, the double complex {Eu(III)-OTC} was immobilized in films containing chitosan, alginate, gelatin, and collagen. LODs of CAs under the optimized conditions varied from 2 to 300 pM. Chitosan seemed to be the most appropriate polymer for the immobilization of the double complex (Eremina et al. 2019): it was stable for at least one month, and the sensitivity of analysis increased up to 40 times with the better reproducibility ($RSD \leq 1.5\%$). Evidently, the reason for such advantage of chitosan is the linearity of its structure and the presence of a large number of amino groups in this polymer that are capable of stabilizing the immobilized complex. These highly sensitive methods were applied for the analysis of rat blood plasma.

The same polymers were used for the development of gel matrixes to determine CAs and their metabolites in 3D cellular structures that closely resemble the live cells and might be applied for solving various biomedical problems. It was found that the cell viability and metrological characteristics of DA determination were the best while using the combination of alginate and collagen gels: the {Eu(III)-OTC} complex was immobilized in alginate gel, and DA (or the neurons producing DA) was introduced into the collagen gel. LOD of DA according to this procedure was 26 pM, $RSD = 0.02\%$. The developed procedure was applied to the determination of DA in PC12 cells of rat pheochromocytoma.

Thus, a novel sensor system for the determination of CAs and their metabolites based on their fluorescent complexes with Eu(III) and OTC immobilized in polymer films and gels have high sensitivity required for the diagnosis of neurodegenerative diseases. They are reproducible, selective in the presence of matrix components of biological samples, rapid, and might be used for early diagnosis of pathological changes in cells and treatment of socially important diseases (Alzheimer's and Parkinson's diseases, cardiovascular and some oncological diseases).

The most promising type of labels for the development of fluorescent nanosensor systems is quantum dots, nanocrystals of inorganic semiconductors, the glow color of which depends on the size and nature of the semiconductor. InP, InAs, GaAs, GaN, ZnS, CdSe, and ZnSe are primarily used as materials for quantum dots.

The fundamental feature of quantum dots consists in their ability to prompt fluorescence of any emission wave upon excitation by a single source of excitation. This capability is the cornerstone for the development of new analytical techniques for the simultaneous detection of several analytes. In bioanalytical applications, this

has resulted in the development of multiplex detection methods designed for multi-parameter analysis of the composition and/or functional properties of biological samples (Barak et al. 2018).

Due to their optical properties (photostability, high quantum fluorescence yield, wide excitation spectrum, and narrow emission band), colloidal quantum dots have attracted increasing attention of analytical chemists.

To obtain a selective analytical signal for each individual analyte, the authors of the paper (Ghasemi et al. 2016) developed fluorescent sensor matrices based on CdTe quantum dots coated with thioglycolic acid. The fluorescent derivatives of EP, *l*-DOPA, and DA obtained by oxidation in the presence of transition metal cations in an alkaline medium were selected as the target compounds. CAs are first oxidized to unstable o-quinone, which can cyclize to form leucoaminochrome. Then leucoaminochrome is oxidized to aminochrome, which transforms into a fluorescent product. The proposed sensor allows one to effectively distinguish between individual catecholamines (DA, EP, and *l*-DOPA) in the concentration range 0.25–30 μM .

In the determination of DA, the effectiveness of quantum dots was demonstrated on the example of CdSe/CdS/ZnS nanoparticles (Mu et al. 2014). The nanoparticles and DA bind to nucleotides (containing amino and hydroxy groups) and DA interacts subsequently with the quantum dots without affecting covalent bonds (e.g., by electrostatic attraction or hydrogen bonds). In this case, DA is oxidized to dopamine ketone, which exhibits electron-acceptor properties concerning NPs leading to fluorescence quench. The proposed dopamine-dopamine ketone fluorescence sensor provides the determination of DA with LOD of 29 nM, demonstrated in the analysis of urine samples, including in the presence of a 100-fold amount of coexisting physiological substances such as amino, ascorbic, and uric acids. An interesting example of a fluorescent sensor is a sensitized layer based on CdS and Ag nanoparticles stabilized with polyamidoamine and persulfate. The high concentration of active functional groups, structural homogeneity, porosity, and biocompatibility of the polymer improve the metrological characteristics of the determination of DA (the LOD of DA in the presence of uric acid is 12 nM) (Sun et al. 2012).

High accuracy, sensitivity, selectivity, and rapidity of the method along with the possibility of using it *ex vivo* and *in vivo*, due to the biocompatibility and low toxicity of the sensor components, are the key features for CAs quantification in practical applications. However, significant disadvantages consist in the need to stabilize the complex with nanoparticles and prevent its oxidation for the reproducibility of fluorescent signals (Sun et al. 2012).

To stabilize catecholamines, such matrices as collagen gel (Gade 1989; Usha et al. 2009), lipid films (Nikolelis et al. 2004), a water-soluble polymer – poly(2,5-bis(3-sulfonatopropoxy)-1,4-phenylethylene) (Huang et al. 2012), triple-phase thin layer (aluminum film, 5-*N,N*-dimethylamino-naphthalene-1-sulfonylated cellulose film, and silica gel) (Nikolelis et al. 2004), and MoS₂ quantum dots functionalized by aptamers and MoS₂ nanofilms (Chen et al. 2018) were used. Some investigations were devoted to CA determination by quenching the fluorescence of quantum dots based on polypyrrole with graphene (Zhou et al. 2015), gold nanoclusters (Tao et al. 2013), CdTe functionalized by thioglycolic acid (Ghasemi et al. 2016), graphene

(Baluta et al. 2017), and CuInS_2 , functionalized by 3-aminophenylboronic acid (Li et al. 2014). Procedures for the CA determination based on the quenching of fluorescence of metal nanostructures in the presence of CAs are known. For example, the approach to determine CAs in cerebrospinal fluid based on their ability to quench fluorescence of gold nanoclusters with bovine serum albumin is described (Govindaraju et al. 2017). For selective determination of DA and EP, fluorescence quenching of fluorescein in the presence of TiO_2 NPs modified with phosphate were used (Wu et al. 2007). LODs of CAs with the use of solid-phase fluorescence varies from 0.05 nM (Chen et al. 2018) to 1 μM (Usha et al. 2009). However, quenching in the presence of CAs decreases the accuracy of the analysis.

One of the promising effects for highly sensitive determination of a wide range of biologically active substances is the effect of metal-enhanced fluorescence, which is not sufficiently studied yet for analytical capabilities. The publications of the last decade have shown the prospects of using silver and gold nanoparticles as fluorescently active materials, providing an increase in the sensitivity of analyte determination by two orders of magnitude and an expansion of the range of samples (Jeong et al. 2018).

The optical properties of noble metal nanoparticles are characterized by the presence of a strong resonance band in the visible light region, called the surface plasmon resonance (SPR) band, that appears due to the formation of surface plasmons, i.e., collective vibrations of metal conduction electrons near the metal/dielectric interface. Gold nanoparticles with a narrow range of SPR wavelengths are more frequently used as an effective fluorescence quencher; however, some examples when gold nanoparticles (AuNPs) enhance the emission of a fluorophore in the long-wavelength region of the spectrum are known. Silver nanoparticles with a wider range of SPR wavelengths are more frequently used to enhance the analytical signal.

A facile aptamer-based sensing strategy was developed for the determination of dopamine through the fluorescence resonance energy transfer (FRET) between rhodamine B (RB) and AuNPs. The different affinities of unbound and bound aptamers toward AuNPs were employed to modulate the FRET efficiency for signal transfer. Dopamine-binding aptamers (DBAs) could protect AuNPs from salt-induced aggregation, resulting in the fluorescence quenching of RB via FRET. Due to specificity of DBA binding, it formed the structured complex with DA, losing the capability to stabilize AuNPs; thus the salt-induced aggregation of AuNPs led to the decrease of fluorescence quenching ability. Correspondingly, the fluorescence intensity of RB recovered along with DA concentration ranging from 26 nM to 2.9 μM with LOD 2 nM. This method was successfully applied for DA determination in chicken liver tissue. Owing to its high sensitivity, excellent selectivity, and convenient procedure, this strategy can provide a promising alternative for dopamine screening (Xu et al. 2015).

To date, metal-enhanced fluorescence is being intensively studied, although there are only a few examples of its application in the analysis of biologically active substances in general (Jeong et al. 2018). Generally, a colloidal solution of spherical

silver nanoparticles (AgNPs) with sizes 20–70 nm stabilized with sodium citrate is used.

The method for the determination of EP, NE, and DA at sub-nanomolar levels was developed. It was found that the luminescence of the complexes formed between the CAs and Tb(III) ion is strongly enhanced in the presence of colloidal AgNPs. The AgNPs cause a transfer of the resonance energy to the fluorophores through the interaction of the excited-state fluorophores and surface plasmon electrons in the AgNPs. Under the optimized conditions, the fluorescence intensity of the system is linearly related to the concentration of the CAs. Linearity is observed in the concentration ranges of EP, NE, and DA 2.5–110, 2.8–240, and 2.4–140 nM, with LOD as low as 0.25, 0.64, and 0.42 nM, respectively. Relative standard deviations determined at 10 nM concentrations (for $n = 10$) gave values of 0.98%, 1.05%, and 0.96% for EP, NE, and DA, respectively (Alam et al. 2012).

Despite the obvious advantages of metallic fluorescent sensor systems, the current problems include a limited range of analytes, low stability and low specificity of nanoparticles, and, accordingly, low accuracy and reproducibility of analyte determination results in biological samples (Jeong et al. 2018).

However, purposeful changing the size, position of surface plasmon resonance band, the nature of the stabilizing shell, and the charge of nanoparticles can allow one to control the intensity of analytical signal and increase the sensitivity, selectivity, and reproducibility of the determination, thereby providing new simple analytical techniques based on fluorescent sensor systems for the determination of markers of neurotransmitter metabolism *in vitro*, *ex vivo*, and *in vivo* for the molecular diagnosis of catecholamine-dependent diseases.

8.3 SERS Sensor Systems for the Determination of Catecholamines and Their Metabolites in Biological Samples

Raman spectroscopy technique does not have many of the limitations of the known techniques for the determination of CAs and their metabolites, primarily related to the lack of selectivity and rapidity of analysis. However, this technique allows one to determine various compounds only at a concentration level of 0.1–0.5 M, which is caused by extremely small cross-sectional area of inelastically scattered light (10^{14} times smaller than the fluorescence cross section and 10^{10} times smaller than the infrared absorption cross section) (Sawa and Snyder 2002). Such low sensitivity of Raman spectroscopy does not satisfy the requirements of the determination of micro- and ultramicro components in various real samples and limits dramatically the number of its practical application.

The most relevant and promising approach to solving the problem of low Raman efficiency is the development of highly sensitive and selective optical sensor systems, whose principle is based on a strong increase in the signal intensity (up to

10^6 – 10^{12} times) due to the effect of plasmon resonance on the surface of noble metals nanostructures. This technique is called SERS: it is promising for nondestructive research of various samples, in recent years gaining popularity as a new highly sensitive express method of analysis (Lee et al. 1988; McGlashen et al. 1990; Schulze et al. 1994; Conway et al. 2001; Sawa and Snyder 2002; Bloom 2004; Dijkstra et al. 2007; Kaya and Volkan 2012; Lim and Kang 2014; Barnes et al. 2015; Garcha and Cohen 2015; Soleymani 2015; Tang et al. 2015; Sergeeva et al. 2017; Eremina et al. 2018; Eremina et al. 2020a, b).

8.3.1 Different Approaches for SERS Determination of Catecholamines and Their Metabolites

The rapid development of SERS over the past 20 years has been facilitated, firstly, by advances in the directed synthesis of nanostructured SERS-active materials (Conway et al. 2001; Sawa and Snyder 2002; Bloom 2004; Barnes et al. 2015; Garcha Cohen 2015; Soleymani 2015; Vatsadze et al. 2018) and, secondly, the development and improvement of Raman spectrometers (Eremina et al. 2018).

SERS spectroscopy opens up new possibilities for reducing the limits of detection of some target analytes to pico- and femtomolar concentrations. The specificity of the analysis is achieved by registering SERS signals in the “fingerprint region” (1500 – 650 cm^{-1}), which are highly informative for the detection of individual compounds in mixtures of complex composition (Schulze et al. 1994). In addition, spectral noise is practically absent in the SERS spectra due to the narrowness of the bands. The indisputable advantages of SERS spectroscopy can also be attributed to its sensitivity to minor changes in the structure and orientation of molecules. Due to all the above characteristics, combined with a weak Raman signal of water, SERS spectroscopy seems to be an ideal method for analyzing complex biological samples without or with minimal sample preparation. Of note, that for applying SERS spectroscopy, one may use a wide range of excitation frequencies that provide the selection of an excitation source with minimal background autofluorescence and photo-destruction of the sample, which is undoubtedly very important for the analysis of real biological samples. Nevertheless, today the use of SERS spectroscopy for determination of the neurotransmitters in practice is very limited and it is still at the initial stage of evaluating the application possibilities (Eremina et al. 2018). It has been reported (Dijkstra et al. 2007) that SERS is already being used in the study of neurotransmitter metabolism by excessive secretion of CAs (DA, EP, and NE) in living cells (pheochromocytoma of rats).

One of the first works in this direction was a paper (Lee et al. 1988), describing the SERS detection of EP, NE, DA, and their metabolites at pH 7.2. The surface of a silver electrode was used as a SERS sensor. A 30 mV laser with a wavelength of 514.5 nm was used for excitation; the accumulation time varied from 10 to 100 s. It was shown that under these conditions, ascorbic acid did not interfere with the

determination. The detection limit was 0.3 μM for each catecholamine. The interfering effect of albumin was studied in the same indicator system. The possibility of analyzing a specific biological sample, 20 μM DA was added to the cerebrospinal fluid, then the sample was analyzed by SERS spectroscopy. The amount of proteins in the test liquid was 0.31 mg/mL, where 65% of their amount was represented by albumin. It was shown that despite maintaining the frequency positions of the main characteristic signals, the signal-to-noise ratio became much lower than that in the SERS spectra of the model solutions. In order to eliminate the interfering effect of proteins containing in biological samples, the authors (McGlashen et al. 1990) proposed the use of polymer-coated electrodes (cellulose acetate or Nafion, a fluorocarbon polymer containing sulfo-groups). It was shown that coating of electrodes significantly increased the signal-to-noise ratio. The concentration dependence of the intensity of the SERS signal for DA in the bilogarithmic coordinates was obtained. This testified to the nonlinearity of the dependence of the analytical signal (at 1479 cm^{-1}) on the concentration of the analyte.

At present, the majority of publications are devoted to attempts to expand the dynamic linear ranges of catecholamines by modifying nanoparticles (Kaya and Volkan 2012). The authors used NPs modified with a complex of iron with nitrilotriacetic acid to better capture dopamine on the silver surface. Thus, it was possible to achieve the LOD 30 fM. The standard deviations of the analytical signal for concentrations of 10^{-8} and 10^{-5} M were not higher than 7%. However, the possibilities for the quantitative determination of CAs by SERS method remain unclear.

Recently, Lim et al. demonstrated the possibility of using SERS spectroscopy to determine DA in the concentration range of 1–10 mM in biological fluids (Lim and Kang 2014). After the development of more advanced surface amplifiers suitable for solving a specific practical problem, the SERS analysis is easy to automate and translate to the point-of-care applications. The literature also describes methods for determining DA in the range 0.01–0.1 fM (LOD 0.006 fM). In this case, the DA concentration was evaluated by a decrease in the intensity of the SERS signal. The feasibility of the determination of DA was demonstrated in the presence of ascorbic acid, glucose, L-cysteine, tyrosine, catechol, phenylethylamine, and serum albumin (Tang et al. 2015).

In another study, a SERS sensor based on a dual molecule recognition for ultrasensitive detection of DA was presented, with LOD 40 fM, without any pretreatment of clinical samples. To implement the sensitive and selective detection of DA in complex samples, the nanoporous silver film (AgNF) surfaces were functionalized with mercaptopropionic acid (MPA) to accurately capture DA, while silver nanocubes (AgNCs) were modified with 4-mercaptopbenzene boronic acid (4-MPBA) as a Raman reporter for the quantitative detection of DA. The nanogaps between AgNCs and the AgNF led to the generation of an abundance of hot spots for the SERS signal and thus effectively improved the sensitivity of DA detection. Measurements of DA concentrations in clinical body fluids such as human serum and urine samples are also demonstrated, showing excellent performance for DA detection in a complex environment (Lu et al. 2020).

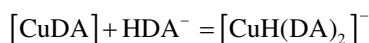
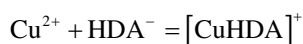
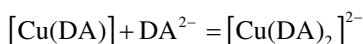
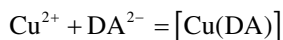
The advantage of SERS spectroscopy consists in its easy combinability with other analytical techniques. For example, the selectivity of the electrochemical determination of neurotransmitters in biological samples is limited by the presence of such components as ascorbic acid, whose redox potential practically coincides with the potential of DA. In addition, large protein molecules are actively adsorbed on the electrode surface. Lee et al. (1988) proposed a combination of the electrochemical accumulation of analytes on the surface of a silver electrode with their SERS selective determination. Thus, when determining CA at the micromolar levels, it was possible to get rid of the interfering effects of ascorbate (0.4 mM), glutathione (1 mM), acetylcholine (1 mM), and some proteins. When using colloidal solutions of silver as a SERS amplifier, the authors were able to decrease the lower limit of the determined concentration to 5 nM (Kneipp et al. 1995; Barreto et al. 2008).

8.3.2 Donor-Acceptor Complexes in SERS Detection and Determination of Catecholamines and Their Metabolites

CAs and their metabolites absorb light in the UV range (270–330 nm), which is far from the plasmon resonance bands of silver (~ 400 nm) and gold (~ 500 nm) nanoparticles, so neurotransmitter molecules give a slight gain in SERS and are almost “invisible” on most bare metallic nanostructures (Goodilin et al. 2018; Manciu et al. 2019). These complexities notwithstanding, a promising approach is the transformation of colorless solutions of CAs to colored ones, i.e., absorbing light in the visible range of the spectrum (Sidorov et al. 2014).

The literature describes examples of the formation of CA donor-acceptor complexes that can contribute to the measurement of a stable and intense SERS signal (Kneipp et al. 1999; Volkan et al. 2000). The formation of complexes with metal ions is characteristic for catechols (in various metastable redox states, such as catecholate, semiquinone, and quinone) (Dei et al. 2004). Particular attention was paid to complexes of catechols with metal cations with variable valency where an intramolecular electron transfer between the metal ion and dioxolane ligands (valence tautomerism) takes place. When a complex of transition metal with catecholates is formed under anaerobic conditions, a band with a high molar coefficient is observed in the range 500–700 nm, which characterizes intramolecular charge transfer (Sever and Wilker 2004). In Fe^{3+} -catecholate complexes, the electron density shifts from the catecholate to the metal ion, and the complex acquires a partially Fe^{2+} -semichinonate character, which ensures rapid oxidation of these complexes by molecular oxygen. At the same time, stabilization of catechols is observed in complexes with Zn^{2+} , Mg^{2+} , and other group II metal cations. M^{2+} -semiquinonates characteristic for Zn^{2+} and Ca^{2+} ions usually have stoichiometry 1:1 and 1:2 (Tipikin et al. 1997).

The available literature on the composition and stability of DA-ion complexes with d-element ions is scarce and contradictory (Walaas et al. 1963). For the complexes formed by DA with Cu^{2+} , the authors (Tipikin et al. 1997) considered various stoichiometric equilibrium schemes, including the formation of the minimum possible number of complexes. The system implements the following five equilibria:



When DA interacts with copper(II) ions, at least five different complexes $\text{Cu}_x\text{H}_y\text{DA}_z$ are formed, where x:y:z may be 1:0:1; 1:0:2; 1:1:1; 1:1:2, and 1: 2: 2. The resulting complexes have a chelate structure.

Mohamed et al. (2004) obtained and isolated solid complexes of a certain composition, which allowed to investigate their structure and properties in detail. Based on the experimental data of the IR and UV-visible spectra and thermal analysis data, CAs behave as bidentate mono- or dibasic ligands upon binding to metal ions. Measurements of the magnetic moment proved the presence of Fe(III) chelates in the octahedral geometry, while Cu(II) chelates are square planar.

Cao et al. (2018) employed surface-enhanced resonance Raman spectroscopy (SERRS) strategy, iron-nitrilotriacetic acid functionalized PVP-AuNPs (Au-Fe(NTA)) as Raman label for rapid and sensitive detection of CA containing DA, NE or EP in complex serum. The presence of AuNPs results in Raman enhancement, and Fe-NTA label can rapidly trap CA molecules adjoining gold core to form NTA-Fe-CA resonant structure, which can amplify the signals of CA. More importantly, the SERS signals of Au-O band from PVP stabilized AuNPs can be utilized as a stable internal calibration standard for quantitative detection of the target analytes. This SERRS strategy is not only capable to offer exciting opportunities to selectively trap the analyte (Sidorov et al. 2014, Eremina et al. 2020b) but also to strongly amplify the Raman signals of CA as well as achieve quantitative measurement.

The reaction of the formation of a complex of CAs with metal ions and additional ligands was also described in Nour El-Dien et al. (2010). Such a complex was used to determine physiologically active CAs in pharmaceutical preparations and urine samples of patients with schizophrenia. The method is based on the reaction of 4-aminoantipyrine with catecholamines in an alkaline medium (pH = 10–11). Importantly, the formed complexes are characterized by absorption maxima at 500,

505, and 480 nm for DA, dobutamine, and vanillylmandelic acid (VMA), respectively. The experimental conditions were optimized: the equilibration time, temperature, pH, and the sequence of reagent addition. Moreover, the stoichiometry of the complexes was determined by the molar ratio method.

The stability constants of mixed ligand complexes of manganese(II), cobalt(II), nickel(II), copper(II), and zinc(II) ions with *l*-DOPA, DA, EP, and NE as the first ligand and *l*-alanine, *l*-histidine, glycylglycine, and ATP as the second ligand were determined pH-metrically at 25 °C in an aqueous KCl solution (Kiss et al. 1984). With UV-vis data, the authors were able to conclude about the binding properties of ambidentate ligands in the studied mixed ligand complexes.

For instance, it was shown that the ambivalent nature of DA allows it to coordinate through the side chain of amino acids (N, O) at lower pH and through ortho-phenolic hydroxy groups (O, O) at higher pH.

The stability of the triple complexes was interpreted by consideration of the differences in the stepwise stability constants of the initial complexes, reverse coordination, charge neutralization, and electrostatic and hydrophobic interactions between ligand pairs.

To determine DA, EP, and NE via SERS spectroscopy, a planar nanostructured sensor, prepared by ultra-sonic silver rain on a glass plate (Sidorov et al. 2016; Goodilin et al. 2018) and further modified by a chitosan layer with copper(II) ions and 4-aminoantipyrine immobilized in the polymer film, was developed. The complexes of catecholamines with copper(II) ions and an additional ligand 4-aminoantipyrine were obtained and characterized.

A planar sensor element was created, consisting of silver nanostructures with SPR band at ~420 nm and capable of amplifying the Raman signal (Eremina et al. 2017). Additionally, AgNPs were coated with an optically transparent chitosan film that acts as a matrix for immobilizing the components of the indicator system for preconcentration of the analyte and protection of silver from photo-destruction and solvent exposure. Methods for the sensitive, multiplex, and rapid determination of DA, NE, and EP by the SERS spectroscopy in the form of the corresponding complexes with copper(II) ions and 4-aminoantipyrine in a concentration range 0.05 nM–100 μM with LODs of 0.01 nM–0.5 μM were developed. The proposed methods were successfully tested in determining catecholamines at the reference levels in the blood plasma of healthy people and rats (Fig. 8.3).

Thus, SERS spectroscopy has significant prospects as a promising analytical tool for samples with complex matrix, since SERS combines high sensitivity and selectivity with minimal sample pretreatment steps, and also it opens up unprecedented possibilities for multiplex determination of various analytes. The practical capabilities of SERS spectroscopy are currently demonstrated in different areas of chemical analysis, connected to medicine, pharmaceutical industry, ecology, fuel and energy industry, etc. However, despite the active development of the theoretical background of this rapidly developing method, as well as successful testing on real samples with various chemical composition and physicochemical properties, the main problems of the SERS spectroscopy include (1) insufficiently wide range of analytes, (2) in some cases unsatisfactory metrological characteristics when analyzing specific

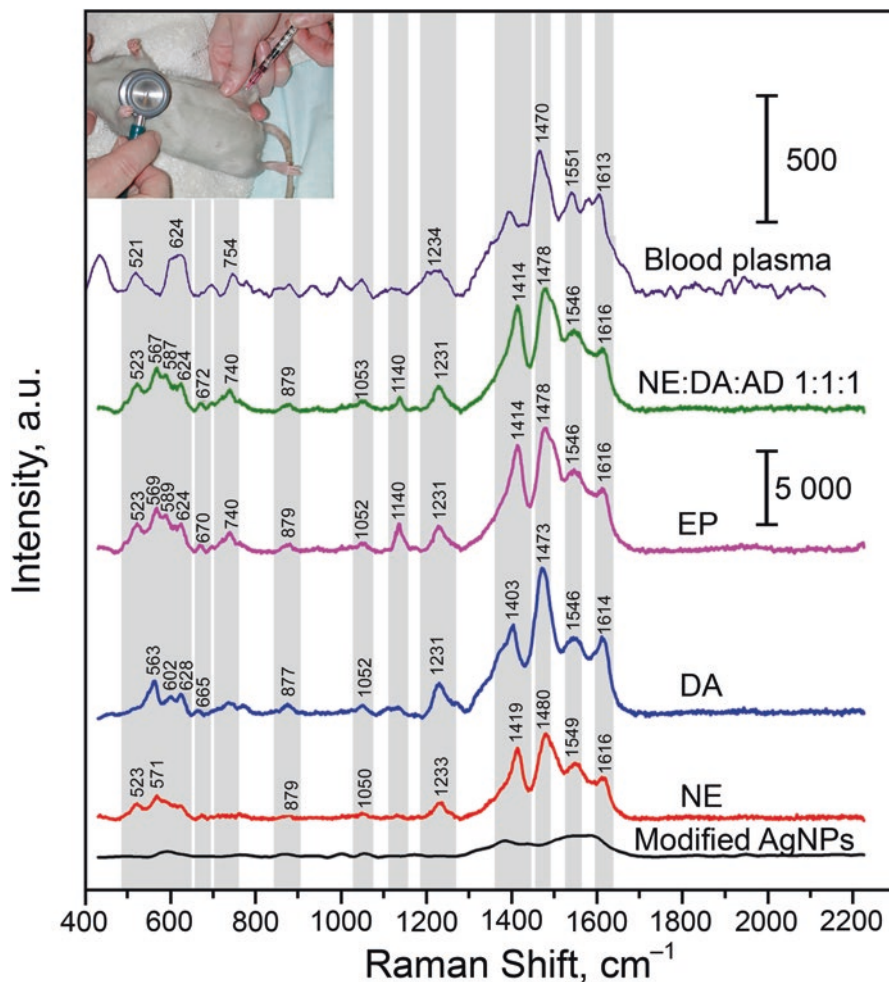


Fig. 8.3 SERS spectra for chemically modified nanostructured silver surface and catecholamines on the described silver surface: norepinephrine, dopamine, epinephrine, their equimolar mixture (1 μM), and blood plasma sample containing 5 nM norepinephrine

samples, which limit the possibilities of its further implementation into the practice of chemical analysis. In addition, for the further development of the use of SERS-active nanostructures in biomedical conditions, it is necessary not only to obtain amplification from individual biomolecules but also to carry out new comprehensive studies aimed at studying the influence of nanostructures on the biological samples under study and assessment of changes in the properties of nanostructures in biological fluids and contact with cells.

Of note, and as discussed earlier, a promising solution of the specific practical problems is, firstly, a purposeful synthesis and “intellectual” functionalization of the

metal nanostructures, taking into account the conditions of the analysis (in the case of biological materials *in vitro*, *ex vivo*, or *in vivo*), and the composition of samples, such as the state of aggregation and polarity, which can be extended to a wide range of relevant analytes and samples. In the future all of these will allow SERS spectroscopy to take a stable niche among other modern analytical techniques.

8.4 Conclusions

We can conclude that the development of approaches to the creation of fluorescent and SERS sensor systems for determining markers of neurotransmitter metabolism in biological samples for diagnostics and monitoring of catecholamines-dependent diseases is an actively developing scientific area. Preliminary results indicate the obvious benefits of the future introduction of such sensor systems into the clinical medical analysis.

One of the most promising approaches to solving the problem of CAs and their metabolite determination consists in utilization of solid-phase fluorescent indicator systems in combination with enzymatic derivatization of the analytes or the formation of their complexes with metal ions. This strategy is capable of providing the stabilization of the sample composition and multiplex, accurate, reproducible, highly sensitive, selective, and rapid determination of CAs and their metabolites without or with minimal sample preparation step.

A novel original biosensing system for the simultaneous multiplex determination of the main markers of catecholamine-producing diseases – CAs (DA, EP, and NE) – and their metabolites (HVA and VMA) in biological liquids without preliminary separation of analytes, without the use of specific antibodies and receptors and with minimum sample pretreatment has been developed. The outstanding features of these system are due to a unique combination of (1) highly fluorescent analyte derivatives obtained by their interaction with two different amines, benzylamine and 1,2-diphenylethylenediamine, in the presence of horseradish peroxidase as a catalyst, and (2) the application of first-order derivative fluorescence spectroscopy for the resolution of their spectra. The proposed procedures provide sensitive (in the range of 3–200 nM), selective, and reproducible (RSDs $\leq 1\%$, $n = 5$) multiplex determination of the CAs and their metabolites in biological liquids and can be successfully applied for the rapid simultaneous (20 samples per 15–30 min) screening of human urine and mice blood plasma (Veselova et al. 2017).

The developed solid-phase indicator system based on the formation of a triple complex of neurotransmitters with europium(III) and tetracycline has unique sensitivity to the same abovementioned markers of neurotransmitter metabolism in biological samples (in some cases at the level of femtomolar concentrations) (Makedonskaya et al. 2018a, b).

A new time-stable SERS-indicator system based on the formation of CA complexes with copper ions with subsequent solid-phase detection using the Raman scattering method has been proposed, which allows one to determine

neurotransmitter metabolism markers in biological samples at nanomolar and lower concentrations (Eremina et al. 2018).

Based on the metal-dependent sensor systems discussed above, nanocomposite hybrid materials were created with purposefully selected chemical design of a microporous polymer surface for measuring the analytical signal by fluorescence and SERS spectroscopic techniques, which provided *ex vivo* determination 3–7 CAs in the PC12 cell line derived from a pheochromocytoma of a rat adrenal medulla.

Acknowledgments This work was supported by the Russian Foundation for Basic Research (grants no. 19-03-00901, 18-33-00827, and 20-33-70264).

References

- Alam A-M, Kamruzzaman M, Lee SH, Kim YH, Kim SY, Kim GM, Jo HJ, Kim SH (2012) Determination of catecholamines based on the measurement of the metal nanoparticle-enhanced fluorescence of their terbium complexes. *Microchim Acta* 176(1–2):153–161
- Altun M, Cakal C, Caglar P (2015) The development of methacrylic acid based monolithic discs used in the microfluidic chips for in the determination of catecholamines. *Sens Actuators B Chem* 208:164–172
- Baluta S, Cabaj J, Malecha K (2017) Neurotransmitter's detection using a fluorescence-based sensor with graphene quantum dots. *Opt Appl* 47(2):225–231
- Barak Y, Meir I, Shapiro A, Jang Y, Lifshitz E (2018) Fundamental properties in colloidal quantum dots. *Adv Mater* 41:e1801442
- Barco S, Alpigiani MG, Ghiggeri GM, Talio M, Maffia A, Tripodi G, Cangemi G (2014) Amoxicillin-associated interference in an HPLC-EC assay for urinary fractionated metanephrines: Potential pitfall in pheochromocytoma biochemical diagnosis. *Clin Biochem* 47(15):119–121
- Barnes MA, Carson MJ, Nair MG (2015) Non-traditional cytokines: how catecholamines and adipokines influence macrophages in immunity, metabolism and the central nervous system. *Cytokine* 72:210–219
- Barreto WJ, Barreto SRG, Ando RA, Santos PS, DiMauro E, Jorge T (2008) Raman, IR, UV–vis and EPR characterization of two copper dioxolene complexes derived from L-DOPA and dopamine. *Spectrochim Acta Part A* 71:1419–1424
- Bicker J, Fortuna A, Alves G, Falcao A (2013) Liquid chromatographic methods for the quantification of catecholamines and their metabolites in several biological samples. *Anal Chim Acta* 768:12–34
- Bloom FE (2004) Neurotransmitters, Overview. // *Encyclopedia of endocrine diseases*. N.Y.: Facts on file, pp 350–356
- Bratovskaja I, Vidzianate R, Kulys J (2004) Oxidation of phenolic compounds by peroxidase in the presence of soluble polymers. *Biochemistry* 69:985–992
- Cakal C, Ferrance JP, Landers JP, Caglar P (2011) Microchip extraction of catecholamines using a boronic acid functional affinity monolith. *Anal Chim Acta* 690(1):94–100
- Cao X, Qinc M, Lia P, Zhouab B, Tanga X, Geab M, Yangab L, Liua J (2018) Probing catecholamine neurotransmitters based on iron-coordination surface-enhanced resonance Raman spectroscopy label. *Sensors Actuators B Chem* 268(1):350–358
- Chen J, Li Y, Huang Y, Zhang H, Chen X, Qiu H (2018) Fluorometric dopamine assay based on an energy transfer system composed of aptamer-functionalized MoS₂ quantum dots and MoS₂ nanosheets. *Microchim Acta* 186(58):1–9
- Conway KA, Rochet JC, Bieganski RM, Lansbury PT (2001) Kinetic stabilization of the α -synuclein protofibril by a dopamine- α -synuclein adduct. *Science* 294:1346–1349

- De Benedetto GE, Fico D, Pennetta A, Malitesta C, Nicolardi G, Lofrumento DD, De Nuccio F, La Pesa V (2014) A rapid and simple method for the determination of 3,4-dihydroxyphenylacetic acid, norepinephrine, dopamine, and serotonin in mouse brain homogenate by HPLC with fluorimetric detection. *J Pharm Biomed Anal* 98:266–270
- Dei A, Gatteshi D, Sangregorio C, Sorace L (2004) Quinonoid metal complexes: Toward molecular switches. *Acc Chem Res* 37:827–835
- Descombes AA, Haerdi W (1992) HPLC Separation of catecholamines after derivatization 9-fluorenylmethyl chloroformate. *Chromatographia* 33(1–2):83–86
- Dijkstra RJ, Scheenen WJJM, Dam N, Roubos EW, ter Meulen JJ (2007) Monitoring neurotransmitter release using surface-enhanced Raman spectroscopy. *J Neurosci Methods* 159(1):43–50
- Eisenhofer G, Kopin IJ, Goldstein DS (2004) Catecholamine metabolism: A contemporary view with implications for physiology and medicine. *Pharmacol Rev* 56(3):331–349
- Elhag S, Ibupoto Z, Nur O, Willander M (2014) Incorporating cyclodextrin with ZnO nanorods: A potentiometric strategy for selectivity and detection of dopamine. *Sensors* 14:1654–1664
- Eremina OE, Sidorov AV, Shekhovtsova TN, Goodilin EA, Veselova IA (2017) Novel multilayer nanostructured materials for recognition of polycyclic aromatic sulfur pollutants and express analysis of fuel quality and environmental health by surface enhanced Raman spectroscopy. *ACS Appl Mater Interfaces* 9(17):15058–15067
- Eremina OE, Semenova AA, Sergeeva EA, Brazhe NA, Maksimov GV, Shekhovtsova TN, Goodilin EA, Veselova IA (2018) Surface enhanced Raman spectroscopy in modern chemical analysis: Achievements and prospects. *Russ Chem Rev* 87(8):741–770
- Eremina OE, Veselova IA, Borzenkova NV, Shekhovtsova TN (2019) Optically transparent chitosan hydrogels for selective sorption and fluorometric determination of dibenzothiophenes. *Carbohydr Polym* 216:260–269
- Eremina OE, Kapitanova OO, Goodilin EA, Veselova IA (2020a) Silver-chitosan nanocomposite as a plasmonic platform for SERS sensing of polyaromatic sulfur heterocycles in oil fuel. *Nanotechnology* 31(22):225503
- Eremina OE, Zatsepin TS, Veselova IA, Zvereva ME (2020b) Detection of damaged DNA sites by surface enhanced Raman spectroscopy. *Mendeleev Commun* 30(1):18–21
- Fonseca BM, Rodrigues M, Cristóvão AC, Gonçalves D, Fortuna A, Bernardino L, Falcão A, Alves G (2017) Determination of catecholamines and endogenous related compounds in rat brain tissue exploring their native fluorescence and liquid chromatography. *J Chromatogr B* 1049–1050:51–59
- Fotopoulou M, Ioannou P (2002) Post-column terbium complexation and sensitized fluorescence detection for the determination of norepinephrine, epinephrine and dopamine using high-performance liquid chromatography. *Anal Chim Acta* 462(2):179–185
- Gade JN (1989) The Mechanism of type I collagen crosslinking with catechol derivatives. Dis. Ph. D. OHSU, 202
- Garcha AS, Cohen DL (2015) Catecholamine excess: Pseudopheochromocytoma and beyond. *Adv Chronic Kidney Dis* 22:218–223
- Geddes CD, Lakowicz JR (2005) Advanced concepts in fluorescence sensing – Part A: Small molecule sensing, vol 9. Springer-Verlag US, N.Y., p 339
- Ghasemi F, Hormozi-Nezhad MR, Mahmoudi M (2016) Identification of catecholamine neurotransmitters using fluorescence sensor array. *Anal Chim Acta* 917:85–92
- Goodilin EA, Semenova AA, Eremina OE, Brazhe NA, Gudilina EA, Danzanova TY, Maksimov GV, Veselova IA (2018) Promising methods for noninvasive medical diagnosis based on the use of nanoparticles: Surface-enhanced Raman spectroscopy in the study of cells, cell organelles and neurotransmitter metabolism markers. *Bull RSMU* 6:57–67
- Govindaraju S, Ankireddy S, Viswanath B, Kim J, Yun K (2017) Fluorescent gold nanoclusters for selective detection of dopamine in cerebrospinal fluid. *Sci Rep* 7:1–12
- Guo Y, Yang J, Wu X, Mao H (2007) Study on the co-luminescence effect of Tb–Gd–epinephrine system and its application to the sensitive determination of epinephrine at nanomol level. *Talanta* 73(2):227–231

- Hsieh M, Chang H (2005) Discontinuous electrolyte systems for improved detection of biologically active amines and acids by capillary electrophoresis with laser-induced native fluorescence detection. *Electrophoresis* 26(1):187–195
- Hsieh M, Hsu C, Tseng W, Chang H (2002) Amplification of small analytes in polymer solution by capillary electrophoresis. *Electrophoresis* 23(11):1633–1641
- Hu F, Xu J, Yi C (2019) Sensing ultra-trace dopamine by restoration of fluorescence on locally acidified gold nanoparticles. *Analyst* 144:4477–4482
- Huang H, Gao Y, Shi F, Wang G, Shah SM, Su X (2012) Determination of catecholamine in human serum by a fluorescent quenching method based on a water-soluble fluorescent conjugated polymer-enzyme hybrid system. *Analyst* 137(6):1481–1486
- Huang X, Guo X-F, Wang H, Zhang H-S (2019) Analysis of catecholamines and related compounds in one whole metabolic pathway with high performance liquid chromatography based on derivatization. *Arab J Chem* 12(7):1159–1167
- Hubbard K, Wells A, Owens T, Tagen M, Fraga C, Stewart C (2010) Determination of dopamine, serotonin, and their metabolites in pediatric cerebrospinal fluid by isocratic high performance liquid chromatography coupled with electrochemical detection. *Biomed Chromatogr* 24:626
- Jeong Y, Kook Y-M, Lee K, Koh W-G (2018) Metal enhanced fluorescence (MEF) for biosensors: General approaches and a review of recent developments. *Biosens Bioelectron* 111:102–116
- Jinghe Y, Guiling Z, Xia W, Fang H, Cunguo L (1998) Fluorimetric determination of epinephrine with o-phenylenediamine. *Anal Chim Acta* 363(1):105–110
- Kaltsas GA, Besser GM, Grossman AB (2004) The diagnosis and medical management of advanced neuroendocrine tumors. *Endocr Rev* 25(3):458–511
- Kamruzzamana M, Alama A-M, Lee SH, Kim YH, Kim SH (2012) A terbium-sensitized spectrofluorimetric method for determination of catecholamines in a serum sample with micelle medium. *Luminescence* 27(1):84–90
- Karaderi S, Bilgic D, Dölen E, Pekin M (2007) Determination of stability constants of mixed ligand complexes of Cu(II) with creatinine and ethylenediamine tetraacetic acid or L-glutamic acid: Potentiometric and spectrophotometric methods. *Rev Inorg Chem* 27:459–472
- Kaya M, Volkan M (2012) New approach for the surface enhanced resonance Raman scattering (SERRS) detection of dopamine at picomolar (pM) levels in the presence of ascorbic acid. *Anal Chem* 84(18):7729–7735
- Kim J, Jeon M, Paeng K-J, Paeng IR (2008) Competitive enzyme-linked immunosorbent assay for the determination of catecholamine, dopamine in serum. *Anal Chim Acta* 619(1):87–93
- Kim J, Park H, Ryu J, Jeon O, Paeng IR (2009) Competitive enzyme-linked immunosorbent assay for a selective and sensitive determination of dopamine in the presence of ascorbic acid and uric acid. *J Immunoassay Immunochem* 31(1):33–44
- Kim JH, Jin S-Y, Hong SS, Lee TH (2014) A carcinoid tumour arising within a tailgut cyst: a diagnostic challenge. *Scott Med J* 59(1):14
- Kiss T, Deak G, Gergely A (1984) Complexes of 3,4-dihydroxyphenyl derivatives. VII. Mixed ligand complexes of L-DOPA and related compounds. *Inorg Chim Acta* 91:269–277
- Klimstra DS, Modlin IR, Coppola D, Lloyd RV, Suster S (2010) The pathologic classification of neuroendocrine tumors. *Pancreas* 39(6):707–712
- Kneipp K, Wang Y, Dasari RR, Feld MS (1995) Near-infrared surface-enhanced Raman scattering (NIR-SERS) of neurotransmitters in colloidal silver solutions. *Spectrochim Acta Part A* 51:481–487
- Kneipp K, Kneipp H, Itzkan I, Dasari RR, Feld MS (1999) Ultrasensitive chemical analysis by Raman spectroscopy. *Chem Rev* 99:2957–2975
- Kovacs G (2016) Molecular pathological classification of neurodegenerative diseases: turning towards precision medicine. *Int J Mol Sci* 17:189–223
- Kuo IT, Huang YF, Chang MT (2005) Silica nanoparticles for separation of biologically active amines by capillary electrophoresis with laser-induced native fluorescence detection. *Electrophoresis* 26(13):2643–2651
- Laxman B, Morris DS, Yu J, Siddiqui J, Cao J, Mehra R, Lonigro RJ, Tsodikov A, Wei JT, Tomlins SA, Chinnaiyan AM (2008) A first-generation multiplex biomarker analysis of urine for the early detection of prostate cancer. *Cancer Res* 68(3):645–649

- Lee NS, Hsieh YZ, Paisley RF, Morris MD (1988) Surface-enhanced Raman spectroscopy of the catecholamine neurotransmitters and related compounds. *Anal Chem* 60(5):442–446
- Lee Y-N, Okumura K, Horio T, Iwata T, Takahashi K, Hattori T, Sawada K (2018) A bioimage sensor for simultaneous detection of multi-neurotransmitters. *Talanta* 179:569–574
- Li H, Wijekoon A, Leipzig N (2014) Encapsulated neural stem cell neuronal differentiation in fluorinated methacrylamide chitosan hydrogels. *Annu Rev Biomed Eng* 42(7):1456–1469
- Lim JW, Kang IJ (2014) Fabrication of chitosan-gold nanocomposites combined with optical fiber as SERS substrates to detect dopamine molecules. *Bull Kor Chem Soc* 35:25–29
- Lu D, Fan M, Cai R, Huang Z, You R, Huang L, Feng S, Lu Y (2020) Silver nanocube coupling with a nanoporous silver film for dual-molecule recognition based ultrasensitive SERS detection of dopamine. *Analyst* 145(8):3009–3016
- Makedonskaya M, Mikhailova A, Veselova I, Fukuda J, Shekhovtsova T (2018a) Fluorescent ternary complexes of some biogenic amines and their metabolites with europium and oxytetracycline for applications in the chemical analysis. *Mendeleev Commun* 28:553–555
- Makedonskaya M, Veselova I, Kalmykov S, Shekhovtsova T (2018b) Novel biosensing system for the simultaneous multiplex fluorescent determination of catecholamines and their metabolites in biological liquids. *J Pharm Biomed Anal* 156:133–144
- Manciu F, Manciu M, Ciubuc J, Sundin E, Ochoa K, Eastman M, Durrer W, Guerrero J, Lopez B, Mahendra S, Bennet K (2019) Simultaneous detection of dopamine and serotonin – A comparative experimental and theoretical study of neurotransmitter interactions. *Biosensors* 9:1:3
- McGlashen ML, Davis KL, Morris MD (1990) Surface-enhanced Raman scattering of dopamine at polymer-coated electrodes. *Anal Chem* 62(8):846–849
- Melnikov AA, Scholtens DM, Wiley EL, Khan SA, Levenson VV (2008) Array-based multiplex analysis of DNA methylation in breast cancer tissues. *J Mol Diagn* 10(1):93–101
- Mitsui A, Nohta H, Ohkura Y (1985) High-performance liquid chromatography of plasma catecholamines using 1,2-diphenylethylenediamine as precolumn fluorescence derivatization reagent. *J Chromatogr* 344:61–70
- Mohamed GG, Zayed MA, Nour El-Dien FA, El-Nahas RG (2004) IR, UV-Vis, magnetic and thermal characterization of chelates of some catecholamines and 4-aminoantipyrene with Fe(III) and Cu(II). *Spectrochim Acta Part A* 60:1775–1781
- Mu Q, Xu H, Li Y, Ma S, Zhong X (2014) Adenosine capped QDs based fluorescent sensor for detection of dopamine with high selectivity and sensitivity. *Analyst* 139(1):93–98
- Murphy JF, Davies DH, Smith CJ (1992) The development of enzyme-linked immunosorbent assays (ELISA) for the catecholamines adrenalin and noradrenalin. *J Immunol Methods* 154(1):89–98
- Muzzi C, Bertocci E, Terzuoli L, Porcelli B, Ciari I, Pagani R, Guerranti R (2008) Simultaneous determination of serum concentrations of levodopa, dopamine, 3-O-methyldopa and a-methyldopa by HPLC. *Biomed Pharmacother* 62(4):253–258
- Myasnikova DA, Polyakov AE, Vashkinskaya OE, Muginova SV, Shekhovtsova TN (2014) The effect of the nature of hydrophilic ionic liquid on the catalytic activity of horseradish and soybean peroxidases. *Mos Univ Chem Bull* 69:97–105
- Nichkova M, Wynveen P, Marc D, Huisman H, Kellermann G (2013) Validation of an ELISA for urinary dopamine: applications in monitoring treatment of dopamine-related disorders. *J Neurochem* 125:724–735
- Nikolelis D, Drivelos D, Simantiraki M, Koinis S (2004) An optical spot test for the detection of dopamine human urine using stabilized in air lipid films. *Anal Chem* 76(8):2174–2180
- Nirogi R, Komarneni P, Kandikere V, Boggavarapu R, Bhyrapuneni G, Benade V, Gorentla S (2013) A sensitive and selective quantification of catecholamine neurotransmitters in rat microdialysates by pre-column dansyl chloride derivatization using liquid chromatography-tandem mass spectrometry. *J Chromatogr B Anal Technol Biomed Life Sci* 913–914:41–47
- Nour El-Dien FA, Frag EYA, Mohamed GG (2010) Coupling reaction and complex formation for the spectrophotometric determination of physiologically active catecholamines in bulk,

- pharmaceutical preparations and urine samples of schizophrenic patients. *Drug Test Anal* 2:234–242
- Paquettea D, Singb R, Banks P, Waldronb K (1998) Capillary electrophoresis with laser-induced native fluorescence detection for profiling body fluids. *J Chromatogr B* 714(1):47–57
- Parrot S, Neuzeret P, Denoroy L (2011) A rapid and sensitive method for the analysis of brain monoamine neurotransmitters using ultra-fast liquid chromatography coupled to electrochemical detection. *J Chromatogr B Anal Technol Biomed Life Sci* 879(32):3871
- Puiu M, Raducan A, Babaligea I (2008) Oxidase-peroxidase reaction: Kinetics of peroxidase-catalysed oxidation of 2-aminophenol. *Bioprocess Biosyst Eng* 31:579–586
- Ragab GH, Nohta H, Zaitso K (2000) Chemiluminescence determination of catecholamines in human blood plasma using 1,2-bis(3-chlorophenyl)ethylenediamine as pre-column derivatizing reagent for liquid chromatography. *Anal Chim Acta* 403(1–2):155–160
- Rodan LH, Gibson KM, Pearl PL (2015) Clinical use of CSF neurotransmitters. *J Pediatr Neurol* 53:277–286
- Rodionov P, Veselova I, Shekhovtsova T (2014) A solid-phase fluorescent biosensor for the determination of phenolic compounds and peroxides in samples with complex matrices. *Anal Bioanal Chem* 406(5):1531–1540
- Sancataldo G, Ludovico S, Mascaro AAA, Sacconi L, Pavone FS (2019) Advanced fluorescence microscopy for in vivo imaging of neuronal activity. *Optica* 6(6):758–765
- Sawa A, Snyder SH (2002) Schizophrenia: diverse approaches to a complex disease. *Science* 296:692–695
- Schulze HG, Blades MW, Bree AV, Gorzalka BB, Greek LS, Turner RFB (1994) Characteristics of backpropagation neural networks employed in the identification of neurotransmitter Raman spectra. *Appl Spectrosc* 48:50–57
- Seki T, Yamaguchi Y (1984) Fluorimetric determination of catecholamines using glycylglycine as the reagent for post-column derivatization. *J Chromatogr A* 287:407–412
- Sergeeva EA, Eremina OE, Sidorov AV, Shekhovtsova TN, Goodilin EA, Veselova IA (2017) Bioprotective polymer layers for surface enhanced Raman spectroscopy of proteins. *Mater Tech Adv Perf Mater* 32(14): 881–887
- Seto D, Maki T, Soh N, Nakano K, Ishimatsu R, Imato T (2012) A simple and selective fluorometric assay for dopamine using a calcein blue–Fe²⁺ complex fluorophore. *Talanta* 94:36–43
- Sever MJ, Wilker JJ (2004) Mechanics of metal-catecholate complexes: The roles of coordination state and metal types. *Dalton Trans* 7:061–1072
- Si H, Zhao F, Cai H (2013) Investigation on the co-luminescence effect of europium (III)–lanthanum (III)–dopamine–sodium dodecylbenzene sulfonate system and its application. *Luminescence* 28(4):510–515
- Sidorov AV, Vashkinskaya OE, Grigorieva AV, Shekhovtsova TN, Veselova IA, Goodilin EA (2014) Entrapment into charge transfer complexes for resonant Raman scattering enhancement. *Chem Commun* 50(49):6468–6470
- Sidorov AV, Grigorieva AV, Goldt AE, Eremina OE, Veselova IA, Savilov SV, Goodilin EA (2016) Chimie douce preparation of reproducible silver coatings for SERS applications. *Funct Mater Lett* 09(01):1650016
- Soleymani J (2015) Advanced materials for optical sensing and biosensing of neurotransmitters. *Trends Anal Chem* 72:27–44
- Sun F, Chen F, Fei W, Sun L, Wu Y (2012) A novel strategy for constructing electrochemiluminescence sensor based on CdS-polyamidoamine incorporating electrodeposited gold nanoparticle film and its application. *Sensors Actuators B* 166-167:702–707
- Suzuki Yo (2019) Development of fluorescent reagent based on ligand exchange reaction for the highly sensitive and selective detection of dopamine in the serum. *Sensors* 19(18):3928
- Syslova K, Rambousek L, Kuzma M, Najmanova V, Bubenikova-Valešova V, Slamberova R, Kačer P (2011) Monitoring of dopamine and its metabolites in brain microdialysates: Method combining freeze-drying with liquid chromatography-tandem mass spectrometry. *J Chromatogr A* 1218(21):3382

- Tang L, Li S, Han F, Liu L, Xu L, Ma W, Kuang H, Li A, Wang L, Xu C (2015) SERS-active Au@Ag nanorod dimers for ultrasensitive dopamine detection. *Biosens Bioelectron* 71:7–12
- Tao Y, Lin Y, Ren J, Qu X (2013) A dual fluorometric and colorimetric sensor for dopamine based on BSA-stabilized Au nanoclusters. *Biosens Bioelectron* 42(1):41–46
- Tipikin DS, Lebedev AV, Rieker A (1997) Effect of calcium cations on acid-base properties and free radical oxidation of dopamine and pyrocatechol. *Chem Phys Lett* 272:399–404
- Tohmola N, Itkonen O, Turpeinen U, Joenvaara S, Renkonen R, Hamalainen E (2015) Preanalytical validation and reference values for a mass spectrometric assay of serum vanillylmandelic acid for screening of catecholamine secreting neuroendocrine tumors. *Clin Chim Acta* 446:206–212
- Tong W, Yeung ES (1997) On-column monitoring of secretion of catecholamines from single bovine adrenal chromaffin cells by capillary electrophoresis. *J Neurosci Methods* 76(2):193–201
- Tsunoda M (2006) Recent advances in methods for the analysis of catecholamines and their metabolites. *Anal Bioanal Chem* 386(3):506–514
- Ugrumov MV (2009) Non-dopaminergic neurons partly expressing dopaminergic phenotype: distribution in the brain, development and functional significance. *J Chem Neuroanat* 38(4):241–256
- Usha R, Rajaram A, Ramasami T (2009) Stability of collagen in the presence of 3,4-dihydroxyphenylalanine (DOPA). *J Photochem Photobiol B* 97(1):34–39
- Vatsadze SZ, Eremina OE, Veselova IA, Kalmykov SN, Nenajdenko VG (2018) 18F-radiopharmaceuticals based on the catecholamine group in the diagnosis of neurodegenerative and neuroendocrine diseases: Approaches to synthesis and development prospects. *Russ Chem Rev* 87:350–373
- Veselova I, Sergeeva E, Makedonskaya M, Eremina O, Kalmykov S, Shekhovtsova T (2016) Methods for determining neurotransmitter metabolism markers for clinical diagnostics. *J Anal Chem* 71:1155–1168
- Veselova I, Malinina L, Barsukova M, Tokareva A, Buslova T, Sokolova L, Pirogov A, Shekhovtsova T (2017) A novel multi-purpose enzymatic system and procedures for the rapid fluorescent determination of flavonoids in herbal pharmaceuticals and plant materials. *Talanta* 171:108–114
- Volkan M, Stokes DL, Vo-Dinh T (2000) Surface-Enhanced Raman of dopamine and neurotransmitters using sol-gel substrates and polymer-coated fiber-optic probes. *Appl Spectrosc* 54:1842–1848
- Walaas E, Walaas O, Haavaldsen S, Pedersen B (1963) Spectrophotometric and electron-spin resonance studies of complexes of catecholamines with Cu (II) ions and the interaction of ceruloplasmin with catecholamines. *Arch Biochem Biophys* 100(1):97–109
- Wang HY, Sun Y, Tang B (2002) Study on fluorescence property of dopamine and determination of dopamine by fluorimetry. *Talanta* 57(5):899–907
- Wang HY, Hui QS, Xu LX, Jiang JG, Sun Y (2003) Fluorimetric determination of dopamine in pharmaceutical products and urine using ethylenediamine as the fluorogenic reagent. *Anal Chim Acta* 497(1–2):93–99
- Wang C, Wang H, Liu Y (2007) Capillary electrophoresis with direct chemiluminescence detection for the analysis of catecholamines in human urine. *Chin Chem Lett* 18:452–454
- Wassell J, Reed P, Kane J, Weinkove C (1999) Freedom from drug interference in new immunoassays for urinary catecholamines and metanephrines. *Clin Chem* 45(12):2216–2223
- Wu Z, Gao F, Wang J, Sweedler J (2001) Ultraviolet native fluorescence detection in capillary electrophoresis using a metal vapor NeCu laser. *Anal Chem* 73(22):5620–5624
- Wu H, Cheng T, Tseng W (2007) Phosphate-modified TiO₂ nanoparticles for selective detection of dopamine, levodopa, adrenaline, and catechol based on fluorescence quenching. *Langmuir* 23(18):7880–7885
- Xu X, Kim K, Liu C, Fan D (2015) Fabrication and robotization of ultrasensitive plasmonic nanosensors for molecule detection with Raman scattering. *Sensors (Basel)* 15(5):10422–10451

- Yao J, Yang M, Duan Y (2014) Chemistry, biology, and medicine of fluorescent nanomaterials and related systems: new insights into biosensing, bioimaging, genomics, diagnostics, and therapy. *Chem Rev* 114(12):6130–6178
- Zhang X, Sweedler JV (2001) Ultraviolet native fluorescence detection in capillary electrophoresis using a metal vapor NeCu laser. *Analyt Chem* 73(22):5620–5624
- Zhang Q, Gong M (2016) On-line preconcentration of fluorescent derivatives of catecholamines in cerebrospinal fluid using flow-gated capillary electrophoresis. *J Chromatogr A* 1450:112–120
- Zhao X, Suo Y (2008) Simultaneous determination of monoamine and amino acid neurotransmitters in rat endbrain tissues by pre-column derivatization with high-performance liquid chromatographic fluorescence detection and mass spectrometric identification. *Talanta* 76(3):690–697
- Zheng Y, Wang Y, Yang X (2011) Aptamer-based colorimetric biosensing of dopamine using unmodified gold nanoparticles. *Sensors Actuators B* 156:95–99
- Zhou X, Ma P, Wang A, Yu C, Qian T, Wu S, Shen J (2015) Dopamine fluorescent sensors based on polypyrrole/graphene quantum dots core/shell hybrids. *Biosens Bioelectron* 64:404–410
- Zhu K, Fu Q, Leung K, Wong Z, Choi R, Tsim K (2011) The establishment of a sensitive method in determining different neurotransmitters simultaneously in rat brains by using liquid chromatography-electrospray tandem mass spectrometry. *J Chromatogr B Anal Technol Biomed Life Sci* 879(1–2):737–742

Chapter 9

Enhanced Sensitivity Rapid Tests for the Detection of Sepsis Marker Procalcitonin



Kseniya V. Serebrennikova, Jeanne V. Samsonova, and Alexander P. Osipov

Abstract Lateral flow immunoassay is a widely used method due to its simplicity and rapidity. However, insufficient sensitivity in the case of a biomarker detection within the clinical ranges when necessary is a limiting factor to implement this method for point-of-care testing and other purposes. This chapter is focused on the approaches to improve the sensitivity (limit of detection) of rapid lateral flow immunoassay on the example of sepsis biomarker procalcitonin. The existing enhancement approaches can be divided into two groups: detectable labels combined with sensitive registration devices and additional signal amplification procedures. The effect of label shape and size (spherical and hierarchical gold nanoparticles) on the detection limit of procalcitonin and additional procedures to enhance the analytical signal of the assay are discussed. The potential of combining lateral flow immunoassay with highly sensitive surface-enhanced Raman spectroscopy is considered. In terms of a simple test for semi-quantitative visual marker detection in several clinically relevant concentration ranges, the one-step gradient lateral flow immunoassay is proposed.

Keywords Lateral flow immunoassay · Immunochromatography · Amplification strategies · Gold nanoparticles · Gold nanoparticle agglomerates · Multi-range gradient lateral flow immunoassay

Nomenclature

ELISA	Enzyme-linked immunosorbent assay
PCT	Procalcitonin
LFIA	Lateral flow immunoassay
GNPs	Gold nanoparticles
GNSs	Gold nanospheres

K. V. Serebrennikova (✉) · J. V. Samsonova · A. P. Osipov
Chemistry Faculty, Lomonosov Moscow State University, Moscow, Leninskiye Gory, Russia
e-mail: ksenijasereb@mail.ru

GNPNs Gold nanopopcorns
GNSTs Gold nanostars

9.1 Introduction

One of the most urgent tasks in the field of analytical biotechnology is the development of new simple methods and portable devices that allow the rapid determination of various compounds in biological fluids, environment, and other objects. The main requirements for them are the simplicity of the assay, high sensitivity, reproducibility of results, stability, cheapness and quickness, and allowance in real time, i.e., within a few minutes to get an answer. Such tests are known in the literature as “rapid tests,” “point-of-care tests” or “POC,” “doctor’s office tests,” or “membrane tests.” The mechanism of such bioanalytical devices is focused on the following general processes: initial “recognition” of the analyte in solution, usually carried out through effective biospecific interaction (e.g., antigen-antibody type), and subsequent signal transformation in the system leading to “visualization” of such specific interactions. The presence of the resulting complexes with analyte can be detected either visually, for example, by staining the solution or solid phase when a special colored label is introduced into the immunocomplex, or using appropriate equipment, for instance, optical reader device. In recent years, rapid methods have been widely used in various fields, such as medical diagnostics, pharmaceutical and food industries, ecology, and veterinary medicine (Ewald et al. 2015; He et al. 2018; Christodouleas et al. 2018; Samsonova et al. 2018).

One of the most common rapid methods for determining target analytes is lateral flow immunoassay (LFIA), which is also called immunochromatographic assay. The advantages of this method include the rapidity (usually 10–15 min) and the simplicity of the assay, as well as the possibility of visual interpretation of the results (Koczula and Gallotta 2016; Sajid et al. 2015). The typical LFIA test strip consists of various materials and each of them performs its specific function (Fig. 9.1). The membrane components of the test strip overlap with one another and are glued to a plastic backing. The principle of LFIA combines immunological and chromatographic methods and is based on the specific interaction between the analyte and recognition element, occurring in different parts of the membrane test strip with pre-immobilized specific reagents and initiated by the applying of a liquid sample. The result of LFIA is the appearance of a colored line in the test zone of the device, the intensity of which corresponds to the analyte level in a sample. The most commonly used labels are metal nanoparticles, such as gold nanoparticles (GNPs) with intense coloration due to the plasmon resonance effect. Quantification of labeled complexes allows the concentration of an analyte in the sample to be calculated using calibration curves. Immunochromatographic tests are often used for diagnostic purposes: confirmation of pregnancy; diagnosing diseases of internal organs (coronary heart disease, renal failure, and diabetes mellitus); identifying

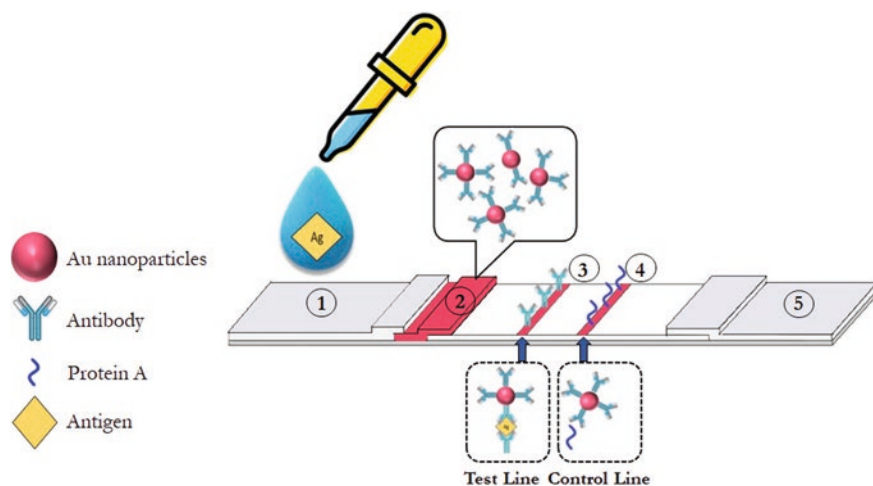


Fig. 9.1 LFIA scheme with gold nanoparticles as a label: (1) sample pad, (2) conjugate pad, (3) test line, (4) control line, (5) absorbent pad

pathogens of infectious diseases, as well as toxic compounds in foods (Tripathi et al. 2018; Hendrickson et al. 2020), feed, or environment (Akter et al. 2019); and others.

The list of LFIA labels is very extensive and includes colloidal gold, latex particles, quantum dots, magnetic particles, liposomes, and others (Edwards et al. 2017; Wilkins et al. 2018; Guteneva et al. 2019; Kim et al. 2019; Zhao et al. 2020). The unique property of metal nanoparticles (for instance, colloidal gold) to generate a recorded signal makes them promising detectable labels for the development of highly sensitive LFIA. Nowadays, GNPs are the most widely used label in rapid tests due to cheapness, simple preparation, and intense color, which can be detected with the naked eye on a test strip. It was postulated that the optimal size of nanoparticles used in LFIA is 30–40 nm since smaller particles do not produce intense color, while larger particles are unstable and form aggregates after several days of storage at 4 °C (Omidfar et al. 2010). Recently, hierarchical GNPs, which are stable due to their complex three-dimensional structure, have been discussed as a promising label to improve the sensitivity of LFIA (Dykman and Khlebtsov 2011). LFIA tests with use of different shaped GNPs were successfully implemented to determine a number of compounds (Lin and Stanciu 2018; Serebrennikova et al. 2018b, 2019; Lai et al. 2019; Hu et al. 2019). Besides, the size-dependent staining of nanoparticles makes it possible to develop a multi-analyte LFIA (Venkataramasubramani and Tang 2009).

In particular cases, conventional LFIA is limited by its sensitivity and reproducibility. In recent years, market trends have led to the development of new materials, labels, and detection systems, the combination of which can significantly improve the analytical characteristics of LFIA (Drygin et al. 2009; Zherdev and Dzantiev 2018; Bishop et al. 2019). Many LFIA signal amplification strategies were

proposed, and most of them include additional steps. Silver enhancement method is widely used in LFIA and carried out by mixing silver salt with a reducing agent followed by silver deposition on GNPs. Changing the red color to black as a result of the silver layer formation on the surface of the particles allows increasing the sensitivity up to 10–15 times (Anfossi et al. 2013; Panferov et al. 2018). Other approaches include enzymatic signal amplification method (Parolo et al. 2013; Samsonova et al. 2015; Zhang et al. 2019); the use of a new “sensitizer,” which is a mixture of labeled primary antibodies and antigen (Nagatani et al. 2006); biotin-streptavidin interaction-based systems (Taranova et al. 2017; Serebrennikova et al. 2018a); modification of LFIA conditions by pre-incubation of the labeled reagent with the sample (Razo et al. 2018); centrifugation-assisted flow control (Shen et al. 2019); and others. These approaches allow achieving up to 100-fold improvement in sensitivity. Thus, overcoming the difficulties in interpretation of the conventional LFIA results associated with individual color perception (age-related effects, innate vision characteristics, psychological factors) by applying new materials, labels, amplification strategies, and registration systems is a challenging task in point-of-care diagnostics.

9.2 Procalcitonin as a Sepsis Marker and Methods of Its Detection

To date, infections and sepsis remain a leading cause of morbidity and mortality in the world. High mortality among septic patients is attributable to the late diagnosis and ineffective supervision and monitoring of the treatment. The most well-studied and common marker in the daily clinical practice for the diagnosis of sepsis and bacterial infections is procalcitonin (PCT) – a peptide precursor of the hormone calcitonin (Meisner 2014). Normally PCT is synthesized in thyroid C cells, and, in the process, the entire PCT turns to calcitonin and practically does not release into the bloodstream. Therefore, PCT concentration in healthy individuals is less than 0.05 ng/ml. When the bacterial infection becomes activated, the PCT level increases in 3–6 h, and the degree of the marker level elevation depends on disease severity (Creamer et al. 2019). A value of $0.25 \leq \text{PCT} < 0.5$ ng/ml indicates the possibility of bacterial infection. A value of $0.5 \leq \text{PCT} < 2$ ng/ml is pathological and refers to systemic infection. High probability of sepsis is associated with $2 \leq \text{PCT} < 10$ ng/ml range, while PCT value above 10 ng/ml indicates severe sepsis or septic shock (Meisner 2014). Therefore, monitoring of PCT concentration over clinically relevant ranges provides the disease management and allows predicting the outcome of sepsis (Vijayan et al. 2017; Sager et al. 2017).

Methods for PCT detection include quantitative (immunoluminometric and enzyme-linked immunofluorescent assays, chemiluminescent, and electrochemiluminescent immunoassays) and semi-quantitative (LFIA) assays that differ in procedure time, detection limit, and reproducibility within clinically relevant ranges

(Schuetz et al. 2017). Quantitative methods for PCT detection are time-consuming and often require specialized equipment. Unlike quantitative methods, immunochromatographic or LFIA tests are used for quick assessment of the biomarker range that is important for early diagnosis of bacteremia and antibiotic use in sepsis. However, the implementation of rapid tests into routine clinical practice is limited by a lack of sensitivity and increased error rate (Manzano et al. 2009; Singh and Anand 2014). Therefore, the integration of new materials and reagents, the development of new formats, signal-enhancement systems, and other techniques are promising approaches for improving LFIA performance.

In this chapter, using PCT as a model system, we consider some ways to improve LFIA sensitivity (limit of PCT detection), including the use of structured GNPs, a range of amplification strategies, and other approaches. In addition, a new design of multi-range gradient LFIA for semi-quantitative visual determination of PCT in serum is proposed.

9.3 Approaches to Decrease the PCT Detection Limit in LFIA

9.3.1 *Spherical and Hierarchical Nanogold Labels and Signal Amplification Strategies*

The protein nature of PCT requires the sandwich format of LFIA (Fig. 9.1). To realize this principle, the capture-specific antibodies were immobilized in the test zone of the analytical membrane, and the conjugate pad was impregnated with paired detection antibodies labeled with GNPs (immunoprobe). When a sample was applied onto the sample pad, its movement along the strip began under capillary forces. Free antigen (PCT) in the sample interacted with immunoprobe, and immunocomplex “antigen-labeled antibody” was formed. In the test zone, specific antibodies bound the immunocomplex, and a triple-colored sandwich complex was visualized. The intensity of the colored test line is directly proportional to the PCT concentration in the sample. The sensitivity of the developing LFIA test should be sufficient to detect the PCT level in the so-called gray area ($0.25 \leq \text{PCT} < 0.5 \text{ ng/mL}$), which corresponds to possible bacterial infection and the initiation of septic conditions.

A comparative study of PCT LFIAs with gold nanospheres (GNSs) and hierarchically structured nanogold labels (nanopopcorns-GNPs and nanostars-GNSTs) of different sizes was performed (Serebrennikova et al. 2018b). The calculated average diameters of obtained GNSs were 20.0 ± 1 , 35.1 ± 2.3 , 50.4 ± 1.6 , 70.2 ± 1.8 , and $100.2 \pm 2.0 \text{ nm}$; GNPNs – $100.1 \pm 5.7 \text{ nm}$; and GNSTs, $64.3 \pm 3.0 \text{ nm}$. The color of GNPs is heavily dependent on their size and shape. Due to the different sizes and shapes of used gold nanolabels, the resulting sandwich complex formed in the test line can be seen as a band with color from red to gray. The study revealed that the

sensitivity of PCT LFIA improves with increasing the size of GNSs up to 40 nm (Serebrennikova et al. 2018b). The use of large GNSs (70 nm and 100 nm) makes the visualization of the analytical and test zones difficult due to the formation of pale-colored lines on the strip. On the other hand, the use of hierarchical large gold nanoparticles (GNPNs and GNSTs) in LFIA allowed detecting lower PCT concentrations. Hierarchical multibranching GNSTs, which are a promising material for bioapplications due to the strong electromagnetic field at the tips, biocompatibility, and stability (Pallavicini et al. 2015), were first used in PCT LFIA (Serebrennikova et al. 2018b). The results of GNST-based LFIA were comparable with conventional GNS-based LFIA that can be attributed to the steric hindrance of large GNSTs preventing interactions between capture antibodies on a strip with “PCT-GNST-labeled antibody” immunocomplex in moving solution. Unlike GNSs and GNSTs, hierarchical large GNPNs combine quasi-spherical structure and strong enhancement of the electromagnetic field near the surface of the particles. GNPNs form a contrast visually detected signal, which tends to improve LFIA sensitivity. Moreover, the quasi-spherical structure of GNPs promotes uniform distribution of antibodies on the surface of gold nanolabels. Thus, the use of GNPNs for PCT LFIA exhibited linearity over the range of 0.5–10 ng/ml with the lowest limit of detection of 0.1 ng/ml which was five times better the sensitivity of 20 nm GNS-based LFIA. Based on the findings it could be concluded that the LFIA sensitivity is affected by the shape of the nanoparticles rather than the size.

In general, LFIA sensitivity can be improved by signal amplification based on different principles. One of the common approaches to improve LFIA sensitivity is the silver enhancement method. This method involves the reduction of silver ions on the GNPs surface followed by color conversion from red to black. Due to its simplicity and achieved high sensitivity, this signal amplification approach has been used in biosensors for over 30 years (Liu et al. 2014). To improve PCT LFIA sensitivity, test strips were immersed in a silver enhancing mixture for 10 min after conventional 20 nm GNS-based LFIA was carried out. The result of the assay was a tenfold improvement in sensitivity with a limit of PCT detection down to 0.05 ng/ml that complies with previous studies (Rodriguez et al. 2016).

The advantage of GNPs is the possibility to use them not merely as a LFIA label but also as a carrier of enzyme label. When used as a direct label, GNPs form red bands in the test and control zones of the strip. When GNPs are bound to horseradish peroxidase-modified antibodies, they exhibit labeling carrier properties. In 2013, Parolo et al. proposed the double GNPs/enzyme label for human IgG LFIA. Thus, the visual signal in the test zone, formed due to the formation of a specific immunocomplex labeled with GNPs, can be further enhanced by the formation of a colored product of the enzymatic reaction. To develop PCT LFIA, a double-labeled conjugate of antibodies with GNPs and horseradish peroxidase was obtained. After applying the sample, two analytical signals were detected, one of which corresponded to the red staining of GNPs and the second to the color of the chromogen resulting from the enzymatic activity of horseradish peroxidase. The limit of visual detection (red color of GNSs) was 1 ng/ml. After incubation with a substrate solution containing 3,3',5,5'-tetramethylbenzidine, a blue color appeared in the

analytical and control zones. Therefore, the approach decreased the limit of PCT detection to 0.1 ng/ml. However, this double GNPs/enzyme label possesses some instability, and the assay time is extended to 30 min due to additional steps to be performed.

The biotin-streptavidin complex has good reaction specificity and high affinity, which explains the widespread use of the system in immunochemistry and immunoassay to enhance specific interactions. A new approach to improve the sensitivity of LFIA through the formation of large stabilized GNP agglomerates was proposed (Serebrennikova et al. 2018a). When streptavidin is added to GNP-labeled biotinylated antibodies, stable GNP agglomerates are formed, consisting of several initial smaller nanoparticles with specific antibodies on their surface (Fig. 9.2). In this case, a streptavidin molecule with four biotin-binding sites plays a role of cross-binding reagent and brings together a few GNSs via streptavidin-biotin interaction with high binding constant. This agglomerate was impregnated onto the conjugate pad and used as the labeled specific anti-PCT reagent. A color change in the test line from red to purple was observed with increasing streptavidin concentration used to form agglomerate with biotinylated antibodies labeled by GNPs. This may be due to the formation of larger complex conjugates, as evidenced by the shift of the plasmon resonance peak to the long-wave region. Given the calibration curves for LFIA with different biotinylated antibodies labeled by GNPs/streptavidin ratios, an increase in streptavidin concentration leads to a slight decrease in the sensitivity of PCT LFIA (Serebrennikova et al. 2018a). This is probably the result of steric hindrance arising in the event of the complex conjugate-antigen capture by the immobilized antibodies. The ratio of 15 parts of biotinylated antibody/GNS immunoprobe to one part of streptavidin was chosen as optimal. The approach allowed five times decreasing in the limit of PCT detection without additional steps and any changes in

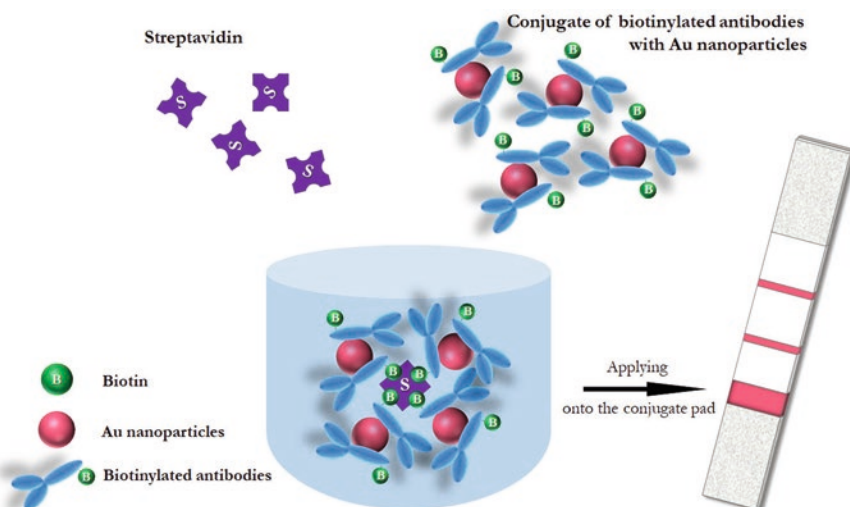


Fig. 9.2 Principle of agglomerate preparation for signal enhancement in LFIA

the strip assembling and assay performance. A similar result was obtained by another research group (Taranova et al. 2017), but in that work the resulting agglomerate formed in reaction mixture while the sample moved through two separate sequential pads with impregnated streptavidin and GNSs/biotinylated antibody conjugate, correspondently.

9.3.2 Another Labels and Signal Registration Systems

Modern analytical trends stimulate researches to look for labels with new interesting properties in terms of signal detection and interpretation. Quantum dots or semiconductor fluorescent nanocrystals over recent years have found broad application in biomedical research (Wagner et al. 2019). They are regarded as a very promising label in LFIA due to their unique properties, namely, the excitation in a wide wavelength range and narrow emission peak increased photostability. However, quantum dots are expensive, and the preparation of conjugates with biomolecules is rather complicated (Foubert et al. 2016). For PCT LFIA a commercial preparation of red quantum dots (CdSe/ZnS) with an emission peak at 655 nm and the carboxylic-functionalized surface was used to prepare labeled specific antibodies. Due to some difficulties associated with low elution of the labeled antibodies from the conjugate pad, an assay was performed by incubating the analytical membrane in a mixture of the quantum dot labeled antibodies and a free PCT solution. After a routine LFIA, the UV laser (340 nm) was used to observe the fluorescence directly in the analytical zone of the strip. To get quantitative data of PCT LFIA, the fluorescent images were processed by special image software. Quantum dot-based LFIA allowed halving the detection limit to 0.25 ng/ml.

One of the promising approaches to improve the sensitivity of LFIA and converting a qualitative “yes/no” result assessment into a quantitative one is the use of surface-enhanced Raman spectroscopy (SERS) as a signal detection method. The popularity of this method is growing due to the possibility of determining biomolecules with a single-molecule-level sensitivity and high selectivity. The advantages of SERS include the capabilities of direct and label-free nondestructive analysis of one or more analytes with minimal requirements for sample preparation, as well as testing of biological fluids or complex sample systems (Pilot et al. 2019). Besides, SERS offers a multiplying amplification of the Raman signal generated by molecules with good stability, convenience, and reproducibility (Jiang et al. 2017; Xiao et al. 2017). As a result, controlled manufacturing of nanostructures led to the widespread use of SERS for biomolecule detection in an immunoassay (Kamińska et al. 2017; Fu et al. 2019).

The principle of the quantitative PCT determination using SERS-based LFIA was implemented by measuring the specific Raman scattering intensities of a reporter molecule within an immunoprobe with double-labeled GNSs concentrated on the test line of the strip after completion of immunorecognition (Fig. 9.3) (Serebrennikova et al. 2017a). The literature indicates that the highest SERS

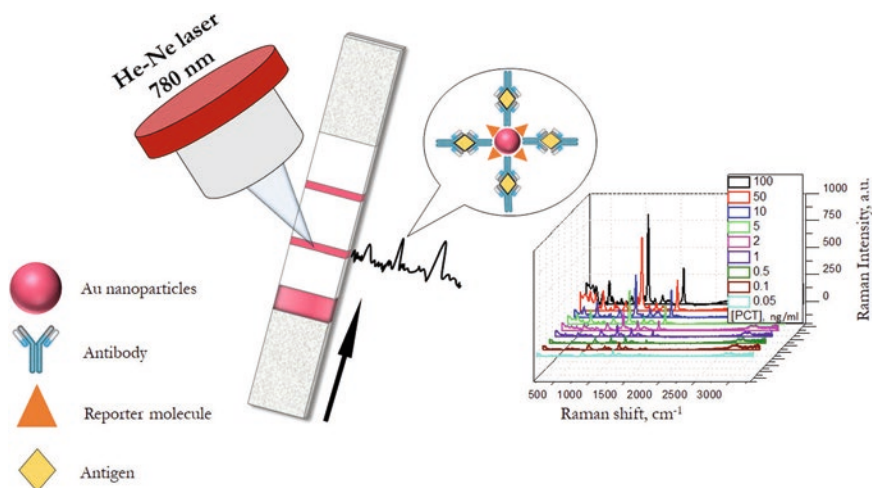


Fig. 9.3 Principle of SERS-based LFIA

intensity is observed for 50 nm GNPs with the same total surface area or concentration of nanoparticles, which is explained by the correlation between amplification and the size of GNP surface area (Hong and Li 2013). In this regard, spherical 50 nm GNPs for the LFIA development were obtained, which ensure the formation of a visually detectable signal during the standard LFIA procedure and sufficient intensity of SERS signal. After completion of the PCT LFIA, the produced colored purple bands (50 nm GNSs) in the test and control zones were first photometrically assessed. Then, the SERS intensity at 1074 cm^{-1} generated from the reporter molecule – mercaptobenzoic acid – in the test zone of the membrane was measured. The limit of PCT detection by SERS and conventional LFIA with GNSs of the same size (50 nm) was comparable and reached a value of 0.5 ng/ml. It should also be emphasized that the SERS-based LFIA demands a special portable registration device for outside laboratory testing.

Summarizing all the abovementioned approaches, it should be concluded that the described methods allowed lowering the limit of PCT detection up to an order (Table 9.1). However, some of them have drawbacks due to the necessity of additional steps or the instability of a label because of its modification (e.g., silver enhancement method, GNS modification with enzyme molecules). All this leads to longer analysis time and is associated with some difficulties of the assay performance under field conditions. Thus, the approbation of silver-enhanced LFIA for the PCT detection in human serum resulted in a high percentage of false-positive results, so this approach is not applicable for the samples of this type (Serebrennikova et al. 2017a). On the contrary, GNS agglomerate-based LFIA and hierarchical gold nanoparticle (GNPN)-based LFIA are user-friendly, ready-to-use, one-step systems (Serebrennikova et al. 2018a, b). Such test strips contain all necessary assay components in dried form, and additional reagents or modification of the assay performance are not required. Thus, while the conventional format of LFIA has insufficient

Table 9.1 Approaches to decrease PCT limit of detection in LFIA

Approach	Label	Detection method	PCT limit of detection, ng/ml	Drawbacks	References
Conventional LFIA	Gold nanospheres	Photometric	0.5		Serebrennikova et al. (2018b)
Label modification	Gold nanospheres/ horseradish peroxidase	Photometric	0.1	Reagent instability, additional analysis step	
Label modification	Gold nanopopcorns	Photometric	0.1		Serebrennikova et al. (2018b)
Label modification	Gold nanosphere agglomerate (35 nm)	Photometric	0.1		Serebrennikova et al. (2018a)
Conventional LFIA with signal enhancement	Silver enhanced gold nanospheres	Photometric	0.05	Reagent instability, additional analysis step, matrix effect	Serebrennikova et al. (2017a)
Another type of label	Quantum dots	Fluorometric	0.25	Expensive label, additional equipment is required	
Another system of signal registration	Gold nanospheres (50 nm)	Surface-enhanced Raman spectroscopy	0.5	Additional equipment is required, longer analysis time	Serebrennikova et al. (2017a)

sensitivity in the required concentration range (PCT “gray zone”), one of the described approaches can be implemented in line with the objective and tasks of the developing method/test. Building upon previous reports, GNPN-based LFIA was proposed to develop a rapid, one-step semi-quantitative visual assay for serum PCT determination in several clinically relevant ranges (Serebrennikova et al. 2018b, 2019).

9.4 Multi-range Gradient PCT LFIA with Semi-quantitative Visual Detection

The conventional LFIA test provides a “yes/no” (qualitative) detection of analyte above or below the cutoff level (Fig. 9.4a), and for the quantitative signal assessment, special readers can be used to register the signal generated by the label. Visual

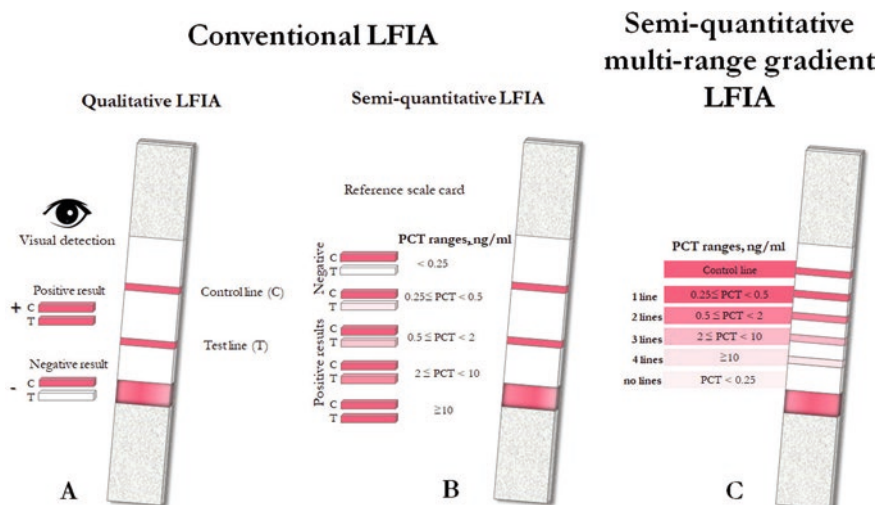


Fig. 9.4 Results assessment in qualitative (a), semi-quantitative, (b) and semi-quantitative multi-range gradient LFIA (c)

semi-quantitative LFIA is carried out by comparing the test line intensity with the reference scale card (Fig. 9.4b). Thus, rapid semi-quantitative detection of PCT in blood serum or plasma with a marker detection limit of 0.5 ng/ml is performed using a commercial semi-quantitative immunochromatographic test B-R-A-H-M-S PCT-Q based on this principle. However, this method involves difficulties in the result interpretation (Singh and Anand 2014). Furthermore, a complex sample matrix may result in false-positive or false-negative results due to the high background color or staining reduction of the test line. Therefore, the improvement in the PCT LFIA visual tests remains relevant.

To address the shortcomings of conventional LFIA, a barcode semi-quantitative LFIA was proposed. The barcode LFIA is based on the formation of multiple test lines by applying capture antibodies at equal concentrations and correlation between the number of revealed test lines with analyte range after the sample is passed through the strip. Due to its simplicity, the barcode LFIA was realized for determination of prostate acid phosphatase (Fang et al. 2011), gliadin (Yin et al. 2016), potato virus X (Panferov et al. 2016), and C-reactive protein (Leung et al. 2008). However, in the barcode LFIA the detected concentration ranges do not always match with the diagnostic cutoff level for a particular marker.

Recently we proposed a multi-range gradient LFIA for semi-quantitative visual determination of serum PCT in five concentration ranges (Fig. 9.4c) (Serebrennikova et al. 2019). The basic difference of multi-range gradient LFIA from barcode LFIA is the possibility to adjust the number of determined concentration ranges and the corresponding analyte cutoffs by changing the concentration of capture antibodies on the particular test line. The gradient distribution of test line staining after assay procedure provides an increase in the capture antibodies concentration from line to

line. As a result, the correlation between the number of colored test lines and the range of biomarker concentrations in the sample is observed. The result of gradient LFIA is a number of colored test lines, which fits to the biomarker concentration range (Fig. 9.4c). By varying the concentration of capture antibodies and the number of test lines formed on the analytical membrane, the number of the biomarker ranges and corresponding cutoffs is regulated depending on the clinical use of a biomarker (Serebrennikova et al. 2017b, 2019).

To validate multi-range gradient PCT LFIA, serum samples were analyzed across five clinically significant concentration ranges (Serebrennikova et al. 2019). A semi-quantitative assessment of the assay results was performed by matching the number of purple (GNSs label) or gray-blue (GNPNs label) test lines (1, 2, 3, or 4) on the analytical membrane to the PCT concentration range (Fig. 9.4c). The data of multi-range gradient visual PCT LFIA and quantitative PCT ELISA showed good concordance for PCT concentrations above 2 ng/ml; however, in the “gray area,” where the diagnosis of sepsis cannot be confirmed, in a few cases a shift in nearby concentration range was observed. According to the PCT guidelines for these doubtful cases, the biomarker measurement should be repeated or monitored after 6–24 h. The purpose of the rapid semi-quantitative multi-range gradient LFIA is biomarker’s blood profile monitoring, i.e., assessment of disease progression or treatment efficacy (in case of antibiotic therapy) over time. The sensitivities of the GNSs-based gradient LFIA and GNPNs-based gradient LFIA were 87.5% and 76.6%, respectively. Replacing GNSs with large, popcorn-like GNPs in gradient PCT LFIA showed comparable assay results. This result can be attributed to the complex shape of the label, which in situ creates steric hindrances to bind labeled antibodies with analyzed antigen in human sera.

Thus, the rapid semi-quantitative multi-range gradient LFIA determines PCT blood level within five clinically significant ranges. The one-step gradient LFIA is carried out by counting the number of colored test lines in 15–20 min without time-consuming sample preparation procedure and subsequent difficulties in interpreting the assay results. To sum up, the proposed multi-range gradient LFIA provides prompt diagnostic results to facilitate clinical decision.

9.5 Conclusion

Despite the advantages of LFIA, the investigation of factors affecting the assay sensitivity remains a matter of great importance. One of these factors is the choice of an effective and easily prepared label for the development of enhanced sensitivity LFIA. A new type of hierarchical nanogold particles was considered, proving that the shape rather than the size of the label affects the sensitivity of the rapid assay. Signal amplification approaches and sensitive systems of the signal registration also need to be evaluated for quantitative analyte detection. The study also showed that advancing to the simple device-free tests, the multi-range gradient LFIA can provide simple, rapid, and effective semi-quantitative visual PCT detection in clinically

relevant concentration ranges. To sum up, the principle of multi-range gradient LFIA can be implemented to develop semi-quantitative immunochromatographic systems for point-of-care testing of diagnostically important markers and for other purposes. Moreover, the application of structured nanogold labels along with the new principles of signal registration opens up new perspectives for the development of easy-to-use portable biosensing devices and rapid tests of wide availability.

References

- Akter S, Kustila T, Leivo J, Muralitharan G, Vehniäinen M, Lamminmäki U (2019) Noncompetitive chromogenic lateral-flow immunoassay for simultaneous detection of microcystins and nodularin. *Biosensors* 9:79
- Anfossi L, Di Nardo F, Giovannoli C, Passini C, Baggiani C (2013) Increased sensitivity of lateral flow immunoassay for ochratoxin A through silver enhancement. *Anal Bioanal Chem* 405:9859–9867
- Bishop JD, Hsieh HV, Gasperino DJ, Weigl BH (2019) Sensitivity enhancement in lateral flow assays: a systems perspective. *Lab Chip* 19:2486–2499
- Christodouleas DC, Kaur B, Chorti P (2018) From point-of-care testing to eHealth diagnostic devices (eDiagnostics). *ACS Cent Sci* 4:1600–1616
- Creamer AW, Kent AE, Albur M (2019) Procalcitonin in respiratory disease: use as a biomarker for diagnosis and guiding antibiotic therapy. *Breathe* 15:296–304
- Drygin YF, Blintsov AN, Osipov AP, Grigorenko VG, Andreeva IP, Uskov AI, Varitsev YA, Anisimov BV, Novikov VK, Atabekov JG (2009) High-sensitivity express immunochromatographic method for detection of plant infection by tobacco mosaic virus. *Biochemistry* 74:986–993
- Dykman L, Khlebtsov N (2011) Gold nanoparticles in biology and medicine: recent advances and prospects. *Acta Nat* 3:34–55
- Edwards KA, Korff R, Baumner AJ (2017) Liposome-enhanced lateral-flow assays for clinical analyses. *Methods Mol Biol* 1571:407–434
- Ewald M, Fechner P, Gauglitz G (2015) A multi-analyte biosensor for the simultaneous label-free detection of pathogens and biomarkers in point-of-need animal testing. *Anal Bioanal Chem* 407:4005–4013
- Fang C, Chen Z, Li L, Xi J (2011) Barcode lateral flow immunochromatographic strip for prostate acid phosphatase determination. *J Pharm Biomed Anal* 56:1035–1040
- Foubert A, Beloglazova NV, Rajkovic A, Sas B, Madder A, Goryacheva IY, De Saeger S (2016) Bioconjugation of quantum dots: Review & impact on future application. *Trends Anal Chem* 83:31–48
- Fu X, Wang Y, Liu Y, Liu H, Fu L, Wen J, Li J, Weic P, Chen L (2019) A graphene oxide/gold nanoparticle-based amplification method for SERS immunoassay of cardiac troponin I. *Analyst* 144:1582–1589
- Guteneva NV, Znoyko SL, Orlov AV, Nikitin MP, Nikitin PI (2019) Rapid lateral flow assays based on the quantification of magnetic nanoparticle labels for multiplexed immunodetection of small molecules: application to the determination of drugs of abuse. *Mikrochim Acta* 186:621
- He W, You M, Wan W, Xu F, Li F, Li A (2018) Point-of-care periodontitis testing: biomarkers, current technologies, and perspectives. *Trends Biotechnol* 36:1127–1144
- Hendrickson OD, Zvereva EA, Popravko DS, Zherdev AV, Xu C, Dzantiev BB (2020) An immunochromatographic test system for the determination of lincosycin in foodstuffs of animal origin. *J Chromatogr B* 1141:122014

- Hong S, Li X (2013) Optimal size of gold nanoparticles for surface-enhanced raman spectroscopy under different conditions. *J Nanomater* 2013: ID 790323
- Hu X, Wan J, Peng X, Zhao H, Shi D, Mai L, Yang H, Zhao Y, Yang X (2019) Calorimetric lateral flow immunoassay detection platform based on the photothermal effect of gold nanocages with high sensitivity, specificity, and accuracy. *Int J Nanomedicine* 14:7695–7705
- Jiang S, Guo J, Zhang C, Li C, Wang M, Li Z, Gao S, Chen P, Si H, Xu S (2017) A sensitive, uniform, reproducible and stable SERS substrate has been presented based on MoS₂@Ag nanoparticles@pyramidal silicon. *RSC Adv* 7:5764–5773
- Kamińska A, Winkler K, Kowalska A, Witkowska E, Szymborski T, Janeczek A, Waluk J (2017) SERS-based immunoassay in a microfluidic system for the multiplexed recognition of interleukins from blood plasma: towards picogram detection. *Sci Rep* 7:10656
- Kim J, Cao XE, Finkelstein JL, Cardenas WB, Erickson D, Mehta S (2019) A two-colour multiplexed lateral flow immunoassay system to differentially detect human malaria species on a single test line. *Malar J* 18:313
- Koczula KM, Gallotta A (2016) Lateral flow assays. *Essays Biochem* 60:111–120
- Lai W, Xiong Z, Huang Y, Su F, Zhang G, Huang Z, Peng J, Liu D (2019) Gold nanoflowers labelled lateral flow assay integrated with smartphone for highly sensitive detection of clenbuterol in swine urine. *Food Agric Immunol* 30:1225–1238
- Leung W, Chan CP, Rainer TH, Ip M, Cautherley GW, Renneberg R (2008) InfectCheck CRP barcode-style lateral flow assay for semi-quantitative detection of C-reactive protein in distinguishing between bacterial and viral infections. *J Immunol Methods* 336:30–36
- Lin L-K, Stanciu LA (2018) Bisphenol A detection using gold nanostars in a SERS improved lateral flow immunochromatographic assay. *Sensors Actuators B Chem* 276:222–229
- Liu R, Zhang Y, Zhang S, Qiu W, Gao Y (2014) Silver enhancement of gold nanoparticles for biosensing: from qualitative to quantitative. *Appl Spectrosc Rev* 49:121–138
- Manzano S, Bailey B, Girodias JB, Cousineau J, Delvin E, Gervais A (2009) Comparison of procalcitonin measurement by a semi-quantitative method and an ultra-sensitive quantitative method in a pediatric emergency department. *Clin Biochem* 42:1557–1560
- Meisner M (2014) Update on procalcitonin measurements. *Ann Lab Med* 34:263–273
- Nagatani N, Tanaka R, Yuhi T, Endo T, Kerman K, Takamura Y, Tamiya E (2006) Gold nanoparticle-based novel enhancement method for the development of highly sensitive immunochromatographic test strips. *Sci Technol Adv Mater* 7:270–275
- Omidfar K, Kia S, Kashanian S, Paknejad M, Besharatie A, Kashanian S, Larijani B (2010) Colloidal nanogold-based immunochromatographic strip test for the detection of digoxin toxicity. *Appl Biochem Biotechnol* 160:843–855
- Pallavicini P, Cabrini E, Borzenkov M, Sironi L, Chirico G (2015) Chapter 3: Applications of gold nanostars: nanosensing, thermal therapy, delivery systems. In: Chirico G, Borzenkov M, Pallavicini P (eds) *Gold nanostars: synthesis, properties and biomedical application*. Springer briefs in materials. Springer, Cham, pp 43–60
- Panferov VG, Safenkova IV, Zherdev AV, Dzantiev BB (2016) Setting up the cut-off level of a sensitive barcode lateral flow assay with magnetic nanoparticles. *Talanta* 164:69–76
- Panferov VG, Safenkova IV, Byzova NA, Varitsev YA, Zherdev AV, Dzantiev BB (2018) Silver-enhanced lateral flow immunoassay for highly-sensitive detection of potato leafroll virus. *Food Agric Immunol* 29:445–457
- Parolo C, de la Escosura-Muñiz A, Merkoçi A (2013) Enhanced lateral flow immunoassay using gold nanoparticles loaded with enzymes. *Biosens Bioelectron* 40:412–416
- Pilot R, Signorini R, Durante C, Orian L, Bhamidipati M, Fabris L (2019) A review on surface-enhanced Raman scattering. *Biosensors* 9:57
- Razo SC, Panferov VG, Safenkova IV, Varitsev YA, Zherdev AV, Pakina EN, Dzantiev BB (2018) How to improve sensitivity of sandwich lateral flow immunoassay for corpuscular antigens on the example of potato virus Y? *Sensors* 18:3975
- Rodríguez MO, Covián LB, García AC, Blanco-López MC (2016) Silver and gold enhancement methods for lateral flow immunoassays. *Talanta* 148:272–278
- Sager R, Kutz A, Mueller B, Schuetz P (2017) Procalcitonin-guided diagnosis and antibiotic stewardship revisited. *BMC Med* 15:15

- Sajid M, Kawde A-N, Daud M (2015) Designs, formats and applications of lateral flow assay: A literature review. *J Saudi Chem Soc* 19:689–705
- Samsonova JV, Safronova VA, Osipov AP (2015) Pretreatment-free lateral flow enzyme immunoassay for progesterone detection in whole cows' milk. *Talanta* 132:685–689
- Samsonova JV, Safronova VA, Osipov AP (2018) Rapid flow-through enzyme immunoassay of progesterone in whole cows' milk. *Anal Biochem* 545:43–48
- Serebrennikova KV, Samsonova JV, Osipov AP (2017a) Gold nanoflowers and gold nanospheres as labels in lateral flow immunoassay of procalcitonin. *Nano Hybrids Composites* 13:47–53
- Serebrennikova KV, Samsonova JV, Osipov AP (2017b) Gradient lateral flow immunoassay of human chorionic gonadotropin. *Mosc Univ Chem Bull* 72:325–327
- Serebrennikova KV, Samsonova JV, Osipov AP (2018a) Enhancement of the sensitivity of a lateral flow immunoassay by using the biotin-streptavidin system. *Mosc Univ Chem Bull* 73:230–234
- Serebrennikova KV, Samsonova JV, Osipov AP (2018b) Hierarchical nanogold labels to improve the sensitivity of lateral flow immunoassay. *Nano-Micro Lett* 10:1–8
- Serebrennikova KV, Samsonova JV, Osipov AP (2019) A semi-quantitative rapid multi-range gradient lateral flow immunoassay for procalcitonin. *Microchim Acta* 186:423
- Shen M, Chen Y, Zhu Y, Zhao M, Xu Y (2019) Enhancing the sensitivity of lateral flow immunoassay by centrifugation-assisted flow control. *Anal Chem* 91:4814–4820
- Schuetz P, Bretscher C, Bernasconi L, Mueller B (2017) Overview of procalcitonin assays and procalcitonin-guided protocols for the management of patients with infections and sepsis. *Expert Rev Mol Diagn* 17:593–601
- Singh M, Anand L (2014) Bedside procalcitonin and acute care. *Int J Crit Illn Inj Sci* 4:233–237
- Taranova NA, Urusov AE, Sadykhov EG, Zherdev AV, Dzantiev BB (2017) Bifunctional gold nanoparticles as an agglomeration-enhancing tool for highly sensitive lateral flow tests: a case study with procalcitonin. *Microchim Acta* 184:4189–4195
- Tripathi P, Upadhyay N, Nara S (2018) Recent advancements in lateral flow immunoassays: A journey for toxin detection in food. *Crit Rev Food Sci Nutr* 58:1715–1734
- Venkataramasubramani M, Tang L (2009) Development of gold nanorod lateral flow test for quantitative multi-analyte detection. In: McGoron AJ, Li CZ, Lin WC (eds) 25th Southern biomedical engineering conference 2009, 15–17 May 2009, Miami, Florida, USA, IFMBE Proceedings, vol 24. Springer, Berlin/Heidelberg, pp 199–202
- Vijayan AL, Vanimaya, Ravindran S, Saikant R, Lakshmi S, Kartik R, Manoj M (2017) Procalcitonin: a promising diagnostic marker for sepsis and antibiotic therapy. *J Intensive Care* 5:51
- Wagner AM, Knipe JM, Orive G, Peppas NA (2019) Quantum dots in biomedical applications. *Acta Biomater* 94:44–63
- Wilkins MD, Turner BL, Rivera KR, Menegatti S, Daniele M (2018) Quantum dot enabled lateral flow immunoassay for detection of cardiac biomarker NT-proBNP. *Sens Bio-Sens Res* 21:46–53
- Xiao G, Li Y, Shi W, Shen L, Chen Q, Huang L (2017) Highly sensitive, reproducible and stable SERS substrate based on reduced graphene oxide/silver nanoparticles coated weighing paper. *Appl Surf Sci* 404:334–341
- Yin HY, Chu PT, Tsai WC, Wen HW (2016) Development of a barcode-style lateral flow immunoassay for the rapid semi-quantification of gliadin in foods. *Food Chem* 192:934–942
- Zhang J, Gui X, Zheng Q, Chen Y, Ge S, Zhang J, Xia N (2019) An HRP-labeled lateral flow immunoassay for rapid simultaneous detection and differentiation of influenza A and B viruses. *J Med Virol* 91:503–507
- Zhao Y, Zhang P, Wang J, Zhou L, Yang K (2020) A novel electro-driven immunochromatography assay based on upconversion nanoparticles for rapid pathogen detection. *Biosens Bioelectron* 152:112037
- Zherdev AV, Dzantiev BB (2018) Ways to reach lower detection limits of lateral flow immunoassays. In: Anfossi L (ed) *Rapid test – advances in design, format and diagnostic applications*, vol 2018. IntechOpen Limited, London, pp 9–43. ISBN 978-1-83881-482-3. Available from: <https://www.intechopen.com/books/rapid-test-advances-in-design-format-and-diagnostic-applications/ways-to-reach-lower-detection-limits-of-lateral-flow-immunoassays>.

Chapter 10

Analytical Capabilities of Some Immunosensors for the Determination of Drugs



Elvina Pavlovna Medyantseva, Daniil Vladimirovich Brusnitsyn,
Elvina Rafailovna Gazizullina, and Herman Constantinovich Budnikov

Abstract At present, biosensors are actively used for the detection of drugs during clinical analyses and medical diagnostics, monitoring of environmental objects, and the quality of food products. Research in the field of biosensors over the past 20 years has been characterized by the study and search for new approaches to enhance the analytical signal by changing the properties of the electrode surface by nanostructures, trying to achieve low limits of detection, and improving other analytical characteristics. Changing the properties of the electrode surface with nanostructured materials in the case of using biosensors (immunosensors) allows achieving higher sensitivity, rapidity, and specificity than using other methods of analysis. This chapter discusses recent advances in the detection of medicinal substances by biosensors modified by various nanomaterials, including carbon nanomaterials, metal nanoparticles, quantum dots, and various types of immunosensors (electrochemical, optical, and piezoelectric), which are the best alternative to the standard analytical methods used.

Keywords Biosensor · Immunosensor · Label · Antigen · Antibody · Nanoparticles · Nanostructured materials · Carbon nanotubes

Nomenclature

HPLC	High-performance liquid chromatography
MS-HPLC	Mass spectrometry with HPLC
Ag	Antigen
Ab	Antibody
NPs	Nanoparticles

E. P. Medyantseva (✉) · D. V. Brusnitsyn · E. R. Gazizullina · H. C. Budnikov
A.M. Butlerov Institute of Chemistry, Kazan (Volga region) Federal University (KFU),
Kazan, Russia
e-mail: Herman.Budnikov@kpfu.ru

HRP	Horseradish peroxidase
LOD	Limit of detection
CV	Cyclic voltammetry
GCE	Glass-carbon electrode
SPGE	Screen-printed graphite electrode
EIS	Electrochemical impedance spectroscopy
MWCNTs	Multiwalled carbon nanotubes
EDC	1-Ethyl-3-(3-dimethylaminopropyl) carbodiimide
NHS	N-Hydroxysuccinimide
IL	Ionic liquid
PBS	Phosphate buffered solution
SPR	Surface plasmon resonance
H2O-NH ₂	Amino derivative on the second-generation polyester polyol platform

10.1 Introduction

Today, there are a huge number of pharmaceutical drugs that are active at very low concentrations and used for the treatment and prevention of diseases. Uncontrolled use, the risk of overdose and side effects, and the study of the effectiveness of the treatment prescribed by the doctor require monitoring of the patient's biological materials in order to quantify drug compounds and their metabolites. The presence of antibiotics in the food of animal origin is possible due to the treatment and feeding of animals with veterinary drugs. Trace amounts of drugs were also found in natural objects (water environments) where they enter as a result of excretion and have a negative impact on living organisms (Sanvicens et al. 2011; Balahura et al. 2019).

The most commonly used methods for drug analysis are chromatographic methods (Berm et al. 2015; Asghari et al. 2017), which have certain disadvantages over biosensor technologies: the specific requirement of sample preparation and the high cost of analysis, as well as a longer analysis time. This uses gas chromatography, liquid chromatography, and high-performance liquid chromatography (HPLC). Tandem methods, such as combined mass spectrometry with HPLC (MS-HPLC), are used to obtain more information about the defined drugs and often to identify it. However, such tandem methods have significant disadvantages: higher cost of analysis compared to HPLC, as well as the requirement of highly qualified staff. If biosensors are used, it is possible to perform analysis in the field and there is practically no sample preparation stage.

A large number of publications have been made on biosensors modified with various types of nanomaterials for determination of drugs, including antibiotics (Lan et al. 2017), adrenomimetics (Wang et al. 2013), anesthetics (Chen et al. 2013), anti-inflammatory (Schirmer et al. 2019), antiviral (Stefan et al. 2003), and anticancer-

cer drugs (Radhapyari et al. 2013). To improve the analytical characteristics of biosensors, various hybrid nanostructured materials are used in their composition (Maduraiveeran and Jin 2017), such as carbon nanomaterials (Merum et al. 2017), quantum dots (Esteve-Turrillas and Abad-Fuentes 2013), and metal nanoparticles. Usually, gold nanoparticles are used among the metal nanoparticles (Wang et al. 2017), but some reports are also available with the use of cerium oxide (Charbgoon et al. 2017) and silicon nanoparticles (Knopp et al. 2009).

The specificity of biosensors allows their use in medical diagnostics, to control the content of drugs in food, environmental objects, as well as for quality control in order to identify falsified products and quantities drugs used in the treatment of diseases, especially depressive disorders. Therefore, biosensors can help to solve a wide range of analytical problems of an applied nature. The use of biosensors contributes to technological progress and improving the quality of human life.

The chapter is devoted to the role, significance, and recent developments in the field of immunosensors for the detection of drugs. The importance and necessity of immunosensors as a special case of biosensors for monitoring the content of drugs in biologically significant objects is shown. The main directions of work in this field are noted, the principles of immunoassay are described, and attention is paid to the nature, structure, and composition of components in immunosensors. The role of various nanomaterials and composites based on their mechanism of functioning in immunosensors has been explained using numerous examples. The possibility of regulating the properties of immunosensors (sensitivity, selectivity) depending on the components included in their composition is shown. Moreover, a special attention has been also given on the analytical capabilities of various immunosensors. In addition, some important challenges in the work of biosensors are discussed.

10.2 Basic Principles of Immunoassay and Research Objects

The principle of immunoassay methods is based on the interaction of an antibody (Ab) with the corresponding antigen (Ag). Abs are proteins of the immunoglobulin class that are produced in the immune system as a result of the manifestation of the body's protective function when a foreign substance – Ag – enters it. Ab has a high affinity and specificity in relation to Ag, due to their molecular complementarity.

Combining the molecular specificity of a biologically recognized object with a transducer expands the analytical capabilities of immunosensors. Recognition of the analyte by an immobilized receptor is accompanied by changes in various properties (physical or chemical nature), which are recorded by the transducer and converted into a measured signal, the value of which is proportional to the concentration of the substance being determined. The most common methods of signal registration are electrochemical, optical, and piezoelectric (Felix and Angnes 2018).

In Table 10.1, the most frequently mentioned in the literature objects of analysis containing various groups of medicinal compounds and immunosensors are given.

Table 10.1 Drugs and medicinal compounds determined by biosensors

Pharmaceutical/drug	Type of immunosensors	Object of analysis
Agonists	Amperometric, impedimetric, surface plasmon resonance	Meat, urine Food for swine Blood serum
Anesthetics	Impedimetric	Blood serum
Antibiotics: aminoglycoside, amphenicol, fluoroquinolone, lactam, nitrofurantoin, penicillin, sulfonamide, tetracycline	Amperometric Impedimetric Piezoelectric Surface plasmon resonance	Animal food Urine, blood serum Pharmaceuticals Pure, surface, and wastewater
Antiviral	Amperometric	Pharmaceuticals
Anticancer	Impedimetric Piezoelectric	Blood serum

It should be noted that the objects of analysis can be not only biological fluids (blood serum, urine) but also water (pure, surface, waste) and food from animal origin.

10.3 Electrochemical Immunosensors

Electrochemical immunosensors are a good alternative to traditional analytical methods for quantifying drugs, due to their high sensitivity and selectivity, and inherent miniaturization. Recently, special attention has been devoted to various methods of modifying the surface of transducers with modern nanostructured materials in order to increase the sensitivity and improve the analytical characteristics of immunosensors for drug detection. Different types of nanomaterials open up new possibilities for electrochemical immunoassay, in terms of improving the electrochemical properties of transducers for better conjugation with biomolecules and using some of them as electrochemical label (Liu and Lin 2007). The most common modifiers are metal nanoparticles (NPs), nanoclusters, nanodendrites, quantum dots (QDs), dendrimers, electrically conductive polymers, and carbon nanomaterials.

10.3.1 Amperometric Immunosensors

Currently, existing developments of amperometric immunosensors are successfully used to determine a wide range of antibiotics, sulfamide, bronchodilators, and drugs against human immunodeficiency. To achieve the required analytical characteristics, modification of the surface of electrodes made of various materials with single-walled and multiwalled carbon nanotubes, graphene, NPs, and metal NCs is used.

Ionic liquids and electron carriers are used. Examples of such amperometric immunosensors are discussed in this section.

The article by Conzuelo et al. (2013) presents a new integrated amperometric immunosensor based on the immobilization of selective Ab on the surface of screen-printed dual carbon electrodes modified by protein-G covalently bound to a 4-aminobenzoic acid film for multiplex determination of sulfonamide and tetracycline antibiotic residues in milk. A direct competitive immunoassay using horseradish peroxidase (HRP)-labeled tracers was carried out. The analytical signal was registered by cyclic voltammetry (CV). The developed method showed very low limit of detection (LOD) for sulfonamide (0.097 ng/ml) and tetracycline (0.858 ng/ml) antibiotics with ranges of detectable concentrations of 0.48–113 ng/ml and 2.84–171 ng/ml, respectively, and good selectivity to other antibiotics found in milk and dairy products.

An electrochemical highly sensitive immunosensor (Zhang et al. 2019) based on Au nanodots (AuNDs), AgNPs, and carbon nanohorns (CNHs) allows to determine sulfonamides of antibacterial effect in water (pure, tap, river, pond, and lake). The indirect competitive interaction involves covering the modified glass-carbon electrode (GCE) coating Ag, the analyte, and the primary antibody (Ab₁), secondary antibody (Ab₂). When Ab₂@ AgNPs@CNHs were captured by the complex covering, Ag-Ab₁, Ag⁺ is released from the electrode in the presence of HNO₃, which significantly amplifies the signal registered by linear sweep voltammetry (LSV). The three-dimensional AuNDs can increase the conductivity of the electrode and the specific activity of the surface. Under optimal conditions, the immunosensor showed a good linear relationship with sulfamethazine in the range of 0.33–63.81 ng/ml with a LOD of 0.12 ng/ml.

Kim et al. (2013) developed an amperometric immunosensor for determination of antibiotic chloramphenicol in meat. Ab against chloramphenicol-acetyltransferases are covalently immobilized on a dendrimer modified by cadmium sulfide (CdS) and bound to an electrically conductive polymer-poly(5,2':5',2"-tertiophene-3'-carboxylic acid). AuNPs, dendrimer, and CdS were applied to the polymer layer to increase the sensitivity of the sensor. Particle sizes were determined using scanning and transmission electron microscopy. The immobilization of nanomaterials and the bio-identifying element was confirmed by quartz microwave and X-ray photoelectron spectroscopy. The detection of chloramphenicol was based on a competitive immune interaction between free and labeled Ag with active Ab centers. Hydrazine was used as a label because it catalyzes the electrochemical reduction of H₂O₂ observed by CV at a potential of -0.35 V. Under optimized conditions, the proposed immunosensor demonstrated a linear response in the range of chloramphenicol concentrations of 50–950 pg/ml with a LOD of 45 pg/ml.

An ultrasensitive label-free amperometric immunosensor has been developed (El-Moghazy et al. 2018) for the detection of chloramphenicol residues in milk using a SPGE coated with a poly(vinyl alcohol-co-ethylene)nanofiber membrane on which anti-chloramphenicol Ab is covalently immobilized. The characteristics of the sensors were studied by electrochemical impedance spectroscopy (EIS). The use of the nanofiber membrane reduced the electron transfer resistance by about four

times compared to a conventional membrane. Cyclic voltammograms were registered in the range of potentials from -1.2 to 0.6 V with a scanning speed of 25 mV/s. Amperometric measurements were performed at -0.66 V. After optimization, the immunosensor demonstrated high sensitivity, selectivity, and stability when an antibiotic was determined in the range of 0.01 – 10 ng/ml, with a LOD of 0.0047 ng/ml.

Determination of penicillin G (Li et al. 2015) in milk was performed using a double lipid membrane and AuNPs as modifiers. Measurements in the CV method were performed on the GCE in a Tris buffer (pH 8.0) in the range of potentials from -0.4 to 0.6 V, the scanning speed of 100 mV/s. According to EIS, when applied to the surface of electrode the Ab against penicillin G, there is a significant increase in the electron transfer resistance. When the Ag-Ab complex is formed, the resistance increases further. The linear range of detectable concentrations is from 3.3×10^{-3} ng/l to 3.3×10^3 ng/l, the LOD of 2.7×10^{-4} ng/l.

According to Zang et al. (2013), an amperometric immunosensor based on double signal amplification by using a biocompatible matrix of a polypyrrole film with AuNCs as a sensor platform and a multi-enzyme-Ab-functionalized Au nanorod as a label allows determining the fluoroquinolone antibiotic ofloxacin in animal food with high sensitivity. The polypyrrole film and NCs were obtained on the GCE surface by electropolymerization and electrochemical deposition, respectively. The ofloxacin-ovalbumin conjugate was immobilized on the modified electrode for subsequent binding to the corresponding Ab. Gold nanorod was synthesized for the deposition of HRP and HRP-Ab₂. The ordered multilayer structure of the immunosensor is characterized by scanning electron microscopy, EIS, and CV methods. Based on the competitive interaction of the corresponding Ab with the captured Ag and free ofloxacin in solution, the immunosensor showed high sensitivity in the range of concentrations from 0.08 to 410 ng/ml with a LOD of 0.03 ng/ml.

A highly sensitive label-free amperometric immunosensor (Yu et al. 2013) was developed to detect an aminoglycoside antibiotic kanamycin in pork using hybrid AgNPs@Fe₃O₄ and graphene mixed with thionine. Thionine was used as an electron transfer mediator. The electrical signal was significantly improved in the presence of graphene due to its high electrical conductivity. Because of the large specific surface area, the NPs used can immobilize more Ab against kanamycin. CV and square-wave voltammetry were used to recognize kanamycin. The proposed immunosensor showed good characteristics, such as LOD of 15 pg/ml, a wide linear range of concentrations from 0.05 to 16 ng/ml, and high stability and selectivity.

It is also proposed to carry out hypersensitive detection of kanamycin in animal products using an amperometric immunosensor (Wei et al. 2012) based on GCE/graphene-nafion/thionin/PtNPs. Ab against kanamycin was immobilized on a modified surface by electrostatic adsorption. The synergistic effect between graphene, thionine, and platinum (Pt) has been studied: the electroactivity of thionine was significantly improved in the presence of graphene and Pt, due to their good electron transferability. The analytical signal was registered by CV. LOD of 5.74 pg/ml, the linearity of the response in the range from 0.01 to 12 ng/ml.

Salbutamol is widely used in the treatment of bronchial asthma and other diseases associated with the respiratory tract. A “sandwich” amperometric

immunosensor (Cui et al. 2012) is described for the detection of salbutamol in serum based on sodium dodecylbenzene sulfonate-functionalized graphene, palladium nanoparticles (PdNPs) in mesoporous silicon oxide of the SBA-15 type (Pd@SBA-15), and ionic liquid (IL). Ab₁ is covalently attached to the graphene sulfone groups in the presence of acyl chloride as a cross-linking reagent. Pd@SBA-15 was obtained by adsorption of H₂PdCl₄ on the surface of SBA-15; then the adsorbed H₂PdCl₄ was reduced to PdNPs by sodium borohydride. Pd@SBA-15 was conjugated with Ab₂ using glutaraldehyde. IL was added to a mixture of Pd@SBA-15 and Ab₂ to stimulate electron transfer. The sensitivity of the immunosensor using Pd@SBA-15/Ab₂/IL to detect salbutamol was significantly higher than those using SBA-15/Ab₂ or Pd@SBA-15/Ab₂. Under optimal conditions, the immunosensor showed a wide operating range of concentrations from 0.02 to 15 ng/ml with a LOD of 7 pg/ml.

Talib et al. (2016) proposed to determine the selective β 2-adrenostimulator clenbuterol with an amperometric immunosensor based on CNTs and poly(3,4-ethylenedioxiophene). GCE, SPGE, and an electrode based on indium and titanium oxide were used. At the same time, the electrode was applied Ab against clenbuterol. There was a competition between the Ag-labeled HRP and the intended one.

10.3.2 Impedimetric Immunosensors

Now the EIS method is actively used to characterize the resistance of the electrodes that form the basis of modern biosensors as part of their comprehensive study. At the same time, the corresponding biosensors can be successfully implemented using the EIS principles. This section presents the most important development of EIS biosensors (immunosensors). The absolute advantages of EIS biosensors include the absence of the need to use special various labels for registering an analytical signal and a simple and understandable mechanism of action.

To determine an antitumor agent from the group of anthracycline antibiotics (doxorubicin) in the blood serum, an impedimetric immunosensor (Rezaei et al. 2011) was developed based on the immobilization of specific monoclonal Ab on the surface of the AuNPs attached to a modified gold electrode using the thiol groups of 1,6-hexanedithiol used as a cross-linking agent. The relative charge transfer resistance of the Ab-coated gold electrode varied linearly with the concentration of doxorubicin. Measurements were carried out in PBS (pH 5.0) containing 0.1 M KCl and 1 mM a mixture of ferricyanide and ferrocyanide (1:1). For LOD of 0.83 pg/ml, the response linearity range was 1–160 pg/ml. The affinity of doxorubicin for immobilized Ab was found to be $1.74 \times 10^{11} \text{ M}^{-1}$.

To determine the β -adrenomimetic (bronchodilator) of salbutamol, Lin et al. (2016) suggest using an impedimetric immunosensor based on AuNPs of different forms. Initially, spherical NPs are electrochemically applied to the surface in the CV mode from -0.5 to 0.5 V at a scanning speed of 50 mV/s for 7 cycles, and then

pyramidal AuNPs are applied at a potential of 620 mV for 10 minutes. The pyramidal structure is achieved due to a kinetically controlled potential and a hydrophilic pre-oxidized surface and a negative reduction potential for nucleotide formation. After applying AuNPs, the surface was treated with mercaptopropionic acid for subsequent application of Ab against salbutamol. Electron transfer resistance was measured by EIS to quantify salbutamol in PBS (pH 7.4) in the presence of 2.5 mM $\text{Fe}(\text{CN})_6^{3-/4-}$. Linear range of detectable concentrations from 0.1 pg/ml to 1 $\mu\text{g}/\text{ml}$, the LOD of 4 fg/ml.

To determine the β -adrenergic agonist ractopamine (Wang et al. 2015) using the EIS method, it was proposed to use an immunosensor based on a gold electrode modified by copper nanoparticles (CuNPs) and $\text{Cu}_2\text{ONPs}@$ reduced graphene oxide (RGO). According to Nyquist diagrams, the electron transfer resistance increases with increasing Ag concentration in the Ag-Ab immunocomplex. Measurements were performed in a PBS (pH 7.4) in the frequency range from 0.01 to 10^5 Hz with an amplitude of 5 mV. The linear range of working concentrations from 0.1 to 10 ng/ml, the LOD of 7.5 pg/ml.

In another study Chen et al. (2013) developed an immunosensor for hypersensitive, and specific detection of the anesthetic ketamine in blood serum by the EIS is reported. Preparation of the sensor includes modification of the gold electrode with a “self-assembling” layer of 3-mercaptopropionic acid, activation using EDC/NHC, and immobilization of the Ab against ketamine to form a sensitive surface. Measurements were performed in PBS (pH 7.4) in the presence of 0.1 M NaCl and 5 M $\text{Fe}(\text{CN})_6^{3-/4-}$. The range of detectable ketamine contents is 1–100 pM with a LOD of 0.41 pM.

A new method for modifying the surface of the gold electrode using functionalized thiols and diazonium salt was used to develop an immunosensor for detecting an antitumor drug methotrexate by EIS (Phal et al. 2018) in blood serum. 4-Carboxybenzenediazonium tetrafluoroborate was synthesized by the diazotization reaction and characterized by infrared spectroscopy and CV. The modified surface of the electrode was immobilized with Ab against methotrexate, the detection of which was carried out with and without the use of a redox marker. EIS analysis with singular decomposition in the absence of $\text{Fe}(\text{CN})_6^{3-/4-}$ showed the best results, since they take into account the dependence on time. A multidimensional regression model on a logarithmic scale demonstrated a linear response in the range from 3×10^{-12} to 3×10^{-4} M with a LOD of 7×10^{-12} M.

10.4 Optical Immunosensors

One of the possible variants to express the quantitative determination of drugs is optical immunosensors. The principle of operation is based on the registration of changes in the optical properties of the medium as a result of the presence of a biological component. Recently, researchers have been interested in immunosensors based on the effects of surface plasmon resonance (SPR) (Utkin et al. 2009).

SPR immunosensors: The examples of immunosensors based on the principles of SPR show that in this case, it is not necessary to label reagents with any special labels or to separate free and bound forms. SPR immunosensors allow to work with a small number of reagents and provide a strong binding of Ab with Ag.

A SPR immunosensor (Fernandez et al. 2012) was proposed for detecting the fluoroquinolone antibiotic enrofloxacin. The study compares the characteristics of sensors that use Ab₁ and Ab₂ in the composition of bioconjugates (anti-IgG and IgG associated with AuNPs). A repeatable procedure was developed for bioconjugation to obtain biohybrid containing AuNPs forming on the surface of the gold electrode mixed “self-assembling” monolayer of polyethylene glycol, functionalized with thiol, with AuNPs, and the subsequent covalent addition of Ab against fluoroquinolones. Thus, for anti-IgG-AuNPs LOD was 0.07 µg/l, and for IgG-AuNPs LOD was 0.11 µg/l.

According to Xia et al. (2017), the determination of gentamicin and chloramphenicol antibiotics can be performed using SPR-based immunosensor. Immobilization of Ag conjugates (activation of the surface of carboxyl groups) was performed using a combination of standard cross-linking reagents (EDC, NHC) on a CM5 microchip. LOD was 5.28 ng/ml for chloramphenicol and 2.26 ng/ml for gentamicin.

Suherman et al. (2015) investigated the possibility of using a SPR immunosensor for determining clenbuterol in urine using an indirect competitive immunoassay based on covalent immobilization of clenbuterol on a monolayer of dithiobis succinimidyl propionate on the surface of the gold electrode. The work used Ab₁ against clenbuterol and polyclonal Ab₂-labeled AuNPs. When removing inhibitors from real samples using silicon dioxide functionalized with carboxyl groups and adjusting the pH of the sample solution by adding PBS (pH 7.5), a linear response was observed in the range of concentrations from 0.01 ppt to 100 ppb with a LOD of 100 fg/ml.

10.5 Piezoelectric Immunosensors

The advantage of piezoelectric immunosensors is the combination of high sensitivity provided by using a quartz resonator as a signal converter and the selectivity of the immunochemical interaction of Ab with the corresponding Ag. To increase the detection sensitivity, surface modification is performed using various substances, including polymers and metal NPs. Sometimes it is a combination of several methods, for example, flow-injection and piezoelectric immunoassay.

The principle of operation of piezoelectric immunosensors is based on the registration of changes in the electrical signal under the action of the mass of the immunocomplex on the quartz plate of the resonator. Such devices allow direct registration of immunochemical interactions without additional labels (fluorescent, enzyme, etc.), which is another advantage (Kalnoy et al. 2014).

Piezoelectric immunosensors (Karaseva and Ermolaeva 2014) based on homologous and group-specific Ab have been developed to determine penicillin G, ampicillin, and the total content of penicillin in milk and meat. To obtain a biosensitive sensor coating, protein conjugates of penicillin G or ampicillin were immobilized on a polypyrrole film obtained by electropolymerization and activated by GA. The obtained values of the affinity constant for polyclonal Ab show high specificity with respect to Ag. Minor cross-reactions have been reported for cephalosporin group antibiotics that share structural fragments with penicillin. Monoclonal group-specific Ab exhibit high specificity in relation to all penicillin group antibiotics, having a β -lactam ring in their structure. Therefore, the use of such Ab provides a determination of the total content of penicillin antibiotics. Calibration curves are linear in the range of concentrations 2.5–250 ng/ml (penicillin G), 2.5–500 ng/ml (ampicillin), and 1–500 ng/ml (penicillin group) with corresponding LOD of 0.8 ng/ml and 3.9 ng/ml.

A piezoelectric immunosensor (Karaseva and Ermolaeva 2012) based on an electro-generated polypyrrole is proposed for detecting residues of the antibiotic chloramphenicol in some food products: meat, milk, honey, and egg. The formation of the receptor layer included electropolymerization of the monomer on the surface of the gold electrode, followed by its activation of GA by amino and carbonyl groups, and covalent binding of the chloramphenicol conjugate on the polymer surface. The determination is based on the competitive interaction of Ab with the drug and protein conjugate. For LOD of 0.2 ng/ml, the calibration curve is linear in the range of concentrations 0.5–100 ng/ml.

Mishra et al. (2015) developed an immunosensor for determination of the antibiotic streptomycin in milk using flow-injection immunoassay in combination with piezo-quartz micro-weighing. The flow system consisted of a flow cell with a volume of 50 μ l, a peristaltic pump, and a six-way crane. The frequency of the crystal was 10 MHz. At the same time, in order to increase the sensitivity, monoclonal Ab was used, which was modified with cysteamine, cysteine, and 11-mercaptoundecanoic acid. The specificity of the interaction was checked in the presence of other drugs: dihydrostreptomycin, kanamycin, and gentamicin. The linear range of detectable concentrations is from 0.3 to 50 ng/ml with a LOD of 0.3 ng/ml.

10.6 Hybrid Nanomaterials in the Composition of the Biosensors

A complex study about the effect of nanostructured materials on the analytical capabilities of amperometric monoamine oxidase biosensors on the example of determination drugs with an antidepressant activity is shown in the works of Medyantseva et al. (2015a) and Brusnitcyn et al. (2016). For the purpose of modification, the surface of SPGE, both carbon nanomaterials (CNTs, graphene oxide) and metal nanoparticles (AuNPs, AgNPs) were used (Medyantseva et al. 2014). The

combination of organic and inorganic nanostructures (hybrid nanostructured materials) as modifiers of the biosensor electrode surface proved to be very promising for improving the analytical capabilities of the developed biosensors.

The study carried out by a complex method of voltammetry, EIS, and atomic force microscopy allowed in each group of modifiers to determine the most suitable nanomaterials for determination antidepressants (imipramine, amitriptyline) with the specified analytical characteristics (Medyantseva et al. 2015b, 2017a).

Comparison of properties of different nanomodifiers in the composition monoamine oxidase biosensors showed that the best hybrid nanostructured modifiers as composites are combinations of MWCNTs in a carboxyl derivative on a second-generation polyester polyol platform and AgNPs stabilized in a third-generation hyperbranched polyester polyol matrix for the determination of antidepressants (tianeptine, moclobemide) (Medyantseva et al. 2017a). This follows from a wider range of working concentrations of 1×10^{-4} – 1×10^{-8} M, reducing the lower limit of the detected concentrations (to the level of 3×10^{-9} M) in comparison with other biosensors.

When using a combination of MWCNTs and AuNPs (Medyantseva et al. 2017b) in chitosan as hybrid nanomaterials as a composite, a linear dependence of the current value on the concentration of an antidepressant is observed in the range from $(1 \times 10^{-4}$ – 5×10^{-9} M) at lower values of the lower limit of the determined contents at the level of 8×10^{-10} M (for moclobemide) and 7×10^{-10} M (for amitriptyline) in comparison with monoamine oxidase biosensors based on electrodes modified only by MWCNTs. The results obtained show that the modification of the electrode surface by hybrid nanocomposites has a positive effect on their analytical capabilities. The same trend is evident in the development of appropriate immunosensors.

The scheme of obtaining and functioning of the immunosensor can be presented as follows (Fig. 10.1). Initially, a hybrid nanocomposite consisting of a combination

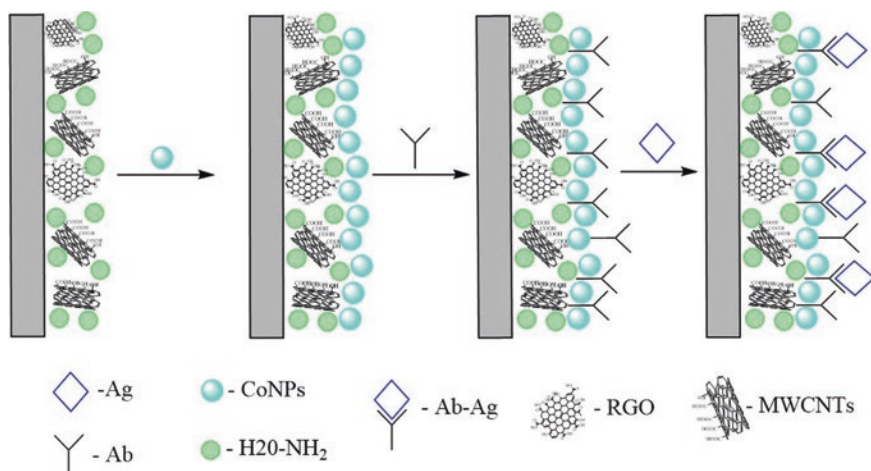


Fig. 10.1 Scheme of obtaining and functioning of the immunosensor

of carbon nanomaterial RGO, MWCNTs and CoNPs in a superbranched polymer (an amino derivative on the second-generation polyester polyol platform-H₂O-NH₂) is applied to the SPGE surface. Then polyclonal Ab against tricyclic antidepressants. When an antidepressant (Ag) is added, it interacts with immobilized Ab on the surface of the SPGE modified with hybrid nanomaterials. The Ag-Ab immune complex is formed, and CoNPs act as a label.

Modification of the biosensor surface by hybrid nanostructures leads to an extension of the range of working concentrations ($1 \times 10^{-4} - 5 \times 10^{-9}$ M) and a decrease in the lower limit of the determined concentrations at the level of $n \times 10^{-10}$ M.

10.7 Conclusion and Future Perspectives

This chapter examines various types of immunosensors for detecting drugs, such as antibacterial, anti-inflammatory, antiviral, anticancer, and veterinary, in biological fluids, animal products, and natural water objects. The most common methods for registering an analytical signal in immunosensory technologies are electrochemical (voltammetry, electrochemical impedance spectroscopy), optical (surface plasmon resonance), and piezoelectric methods.

The combination of a biosensitive and specific receptor with a primary signal converter expands the analytical capabilities of immunosensors. They have a number of advantages in comparison with other methods of determining pharmaceutical products (chromatographic and other physical and chemical methods): high sensitivity and selectivity, fast, miniaturization, minimal pre-processing of the sample, mobility, and low-cost equipment.

Modification of the surface of transducers by various compounds (metal nanoparticles and nanoclusters, quantum dots, carbon nanomaterials, dendrimers, and electrically conductive polymers) leads to its stabilization, increased sensitivity, and improved analytical characteristics of the immunosensors being developed, which makes it possible to determine drugs in residues. Thus, it is promising to use immunosensors as an alternative to the standard analytical methods used.

References

- Asghari A, Saffarzadeh Z, Bazregar M, Rajabi M, Boutorabi L (2017) Low-toxic air-agitated liquid-liquid microextraction using a solidifiable organic solvent followed by gas chromatography for analysis of amitriptyline and imipramine in human plasma and wastewater samples. *Microchem J* 130:122–128
- Balahura LR, Stefan-Van Staden RI, Van Staden JF, Aboul-Enein HY (2019) Advances in immunosensors for clinical applications. *J Immunoassay Immunochem* 40:40–51
- Berm EJJ, Paardekooper J, Brummel-Mulder E, Hak E, Wilffert B, Maring JG (2015) A simple dried blood spot method for therapeutic drug monitoring of the tricyclic antidepressants amitriptyline, nortriptyline, imipramine, clomipramine, and their active metabolites using LC-MS/MS. *Talanta* 134:165–172

- Brusnitsyn DV, Medyantseva EP, Varlamova RM, Sitdikova RR, Fattakhova AN, Konovalova OA, Budnikov GK (2016) Carbon nanomaterials as electrode surface modifiers in development of amperometric monoamine oxidase biosensors. *Inorg Mater* 52:1413–1419
- Charbgoof F, Ramezani M, Darroudi M (2017) Bio-sensing applications of cerium oxide nanoparticles: advantages and disadvantages. *Biosens Bioelectron* 96:33–43
- Chen Y, Yang Y, Tu Y (2013) An electrochemical impedimetric immunosensor for ultrasensitive determination of ketamine hydrochloride. *Sensors Actuators B Chem* 183:150–156
- Conzuelo F, Campuzano S, Gamella M, Pinacho DG, Reviejo AJ, Marco MP, Pingarrón JM (2013) Integrated disposable electrochemical immunosensors for the simultaneous determination of sulfonamide and tetracycline antibiotics residues in milk. *Biosens Bioelectron* 50:100–105
- Cui Z, Cai Y, Wu D, Yu H, Li Y, Mao K, Wang H, Fan H, Wei Q, Du B (2012) An ultrasensitive electrochemical immunosensor for the detection of salbutamol based on Pd@SBA-15 and ionic liquid. *Electrochim Acta* 69:79–85
- El-Moghazy AY, Zhao C, Istamboulie G, Amaly N, Si Y, Noguer T, Sun G (2018) Ultrasensitive label-free electrochemical immunosensor based on PVA-co-PE nanofibrous membrane for the detection of chloramphenicol residues in milk. *Biosens Bioelectron* 117:838–844
- Esteve-Turrillas FA, Abad-Fuentes A (2013) Applications of quantum dots as probes in immunosensing of small-sized analytes. *Biosens Bioelectron* 41:12–29
- Felix FS, Angnes L (2018) Electrochemical immunosensors – a powerful tool for analytical applications. *Biosens Bioelectron* 102:470–478
- Fernandez F, Sanchez-Baeza F, Marco MP (2012) Nanogold probe enhanced Surface Plasmon Resonance immunosensor for improved detection of antibiotic residues. *Biosens Bioelectron* 34:151–158
- Kalnoy SM, Kulichenko AN, Dikova SP, Zharnikova IV, Lyapustina LV, Kovalev DA, Zharnikova TV, Shestopalov KV, Melchenko EA (2014) The technology development for creation of piezoelectric immunosensor for dangerous infectious diseases agents detection. *Modern Problems of Science and Education* 1:61–62
- Karaseva NA, Ermolaeva TN (2012) A piezoelectric immunosensor for chloramphenicol detection in food. *Talanta* 93:44–48
- Karaseva NA, Ermolaeva TN (2014) Piezoelectric immunosensors for the detection of individual antibiotics and the total content of penicillin antibiotics in foodstuffs. *Talanta* 120:312–317
- Kim DM, Rahman MA, Do MH, Ban C, Shim YB (2013) An amperometric chloramphenicol immunosensor based on cadmium sulfide nanoparticles modified-dendrimer bonded conducting polymer. *Biosens Bioelectron* 25:1781–1788
- Knopp D, Tang D, Niessner R (2009) Review: bioanalytical applications of biomolecule-functionalized nanometer-sized doped silica particles. *Anal Chim Acta* 647:14–30
- Lan L, Yao Y, Ping J, Ying Y (2017) Recent advances in nanomaterial-based biosensors for antibiotics detection. *Biosens Bioelectron* 91:504–514
- Li H, Xu B, Wang D, Zhou Y, Zhang H, Xia W, Xu S, Li Y (2015) Immunosensor for trace penicillin G detection in milk based on supported bilayer lipid membrane modified with gold nanoparticles. *J Biotechnol* 203:97–103
- Lin CH, Wu CC, Kuo YF (2016) A high sensitive impedimetric salbutamol immunosensor based on the gold nanostructure-deposited screen-printed carbon electrode. *J Electroanal Chem* 768:27–33
- Liu G, Lin Y (2007) Nanomaterial labels in electrochemical immunosensors and immunoassays. *Talanta* 74:308–317
- Maduraiveeran G, Jin W (2017) Nanomaterials based electrochemical sensor and biosensor platforms for environmental applications. *Trends Environ Anal Chem* 13:10–23
- Medyantseva EP, Brusnitsyn DV, Varlamova RM, Baibatarova MA, Budnikov GK, Fattakhova AN (2014) Determination of antidepressants using monoamine oxidase amperometric biosensors based on screen-printed graphite electrodes modified with multi-walled carbon nanotubes. *Pharm Chem J* 48(7):478–482

- Medyantseva EP, Brusnitsyn DV, Varlamova RM, Beshevets MA, Budnikov HK, Fattakhova AN (2015a) Capabilities of amperometric monoamine oxidase biosensors based on screen printed graphite electrodes modified with multi-wall carbon nanotubes in the determination of some antidepressants. *J Anal Chem* 70(5):535–539
- Medyantseva EP, Brusnitsyn DV, Varlamova RM, Maksimov AA, Fattakhova AN, Konovalova OA, Budnikov GK (2015b) Effect of nanostructured materials as electrode surface modifiers on the analytical capacity of amperometric biosensors. *Russ J Appl Chem* 88(1):40–49
- Medyantseva EP, Brusnitsyn DV, Varlamova RM, Medvedeva OI, Kutyreva MP, Ulakhovich NA, Fattakhova AN, Konovalova OA, Budnikov GK (2017a) Hyperbranched polyesterpolyols as components of amperometric monoamine oxidase biosensors based on electrodes modified with nanomaterials for determination of antidepressants. *Russ J Appl Chem* 90(1):97–105
- Medyantseva EP, Brusnitsyn DV, Varlamova RM, Maksimov AA, Konovalova OA, Budnikov GK (2017b) Surface modification of electrodes by carbon nanotubes and gold and silver nanoparticles in monoaminoxidase biosensors for the determination of some antidepressants. *Russ J Anal Chem* 72(4):362–370
- Merum S, Veluru JB, Seeram R (2017) Functionalized carbon nanotubes in bio-world: Applications, limitations and future directions. *Mater Sci Eng B* 223:43–63
- Mishra GK, Sharma A, Bhand S (2015) Ultrasensitive detection of streptomycin using flow injection analysis-electrochemical quartz crystal nanobalance (FIA-EQCN) biosensor. *Biosens Bioelectron* 67:532–539
- Phal S, Shatri B, Berisha A, Geladi P, Lindholm-Sethson B, Tesfalidet S (2018) Covalently electrografted carboxyphenyl layers onto gold surface serving as a platform for the construction of an immunosensor for detection of methotrexate. *J Electroanal Chem* 812:235–243
- Radhapyari K, Kotoky P, Khan R (2013) Detection of anticancer drug tamoxifen using biosensor based on polyaniline probe modified with horseradish peroxidase. *Mater Sci Eng C* 33:583–587
- Rezaei B, Saghebdoost M, Sorkhe AM, Majidi N (2011) Generation of a doxorubicin immunosensor based on a specific monoclonal antibody-nanogold-modified electrode. *Electrochim Acta* 56(16):5702–5706
- Sanvicens N, Mannelli I, Salvador J, Valera E, Marco MP (2011) Biosensors for pharmaceuticals based on novel technology. *Trends Anal Chem* 30:541–553
- Schirmer C, Posseckardt J, Schroder M, Gläser M, Howitz S, Scharff W, Mertig M (2019) Portable and low-cost biosensor towards on-site detection of diclofenac in wastewater. *Talanta* 203:242–247
- Stefan RI, Bokretson RG, Staden JF, Aboul-Enein HY (2003) Immunosensor for the determination of azidothymidine. Its utilization as detector in a sequential injection analysis system. *Talanta* 59:883–887
- Suherman, Morita K, Kawaguchi T (2015) Highly selective and sensitive detection of β -agonists using a surface plasmon resonance sensor based on an alkanethiol monolayer functionalized on a Au surface. *Biosens Bioelectron* 67:356–363
- Talib NA, Syed Zainol Abidin S, Salam F, Sulaiman Y (2016) Clenbuterol immunosensors based poly(3,4-ethylenedioxythiophene)/ multiwall carbon nanotube (PEDOT/MWCNT) hybrid composite. *Procedia Chem* 20:29–32
- Utkin DV, Ossina NA, Kouklev VE, Erokhin PS, Scherbakova SA, Kutyrav VV (2009) Biosensors: current state and prospects of applying in laboratory diagnostics of particularly dangerous infectious diseases. *Probl Particul Danger Infect* 102(4):11–14
- Wang H, Zhang Y, Li H, Du B, Ma H, Wu D, Wei Q (2013) A silver–palladium alloy nanoparticle-based electrochemical biosensor for simultaneous detection of ractopamine, clenbuterol and salbutamol. *Biosens Bioelectron* 49:14–19
- Wang M, Kang M, Guo C, Fang S, He L, Jia C, Zhang G, Bai B, Zong W, Zhang Z (2015) Electrochemical biosensor based on Cu/Cu₂O nanocrystals and reduced graphene oxide nanocomposite for sensitively detecting ractopamine. *Electrochim Acta* 182:668–675
- Wang P, Lin Z, Su X, Tang Z (2017) Application of Au based nanomaterials in analytical science. *Nano Today* 12:64–97

- Wei Q, Zhao Y, Du B, Wu D, Li H, Yang M (2012) Ultrasensitive detection of kanamycin in animal derived foods by label-free electrochemical immunosensor. *Food Chem* 134(3):1601–1606
- Xia Y, Su R, Huang R, Ding L, Wang L, Qi W, He Z (2017) Design of elution strategy for simultaneous detection of chloramphenicol and gentamicin in complex samples using surface plasmon resonance. *Biosens Bioelectron* 92:266–272
- Yu S, Wei Q, Du B, Wu D, Li H, Yan L, Ma H, Zhang Y (2013) Label-free immunosensor for the detection of kanamycin using Ag@Fe₃O₄ nanoparticles and thionine mixed graphene sheet. *Biosens Bioelectron* 48:224–229
- Zang S, Liu Y, Lin M, Kang J, Sun Y, Lei H (2013) A dual amplified electrochemical immunosensor for ofloxacin: Polypyrrole film-Au nanocluster as the matrix and multi-enzyme-antibody functionalized gold nanorod as the label. *Electrochim Acta* 90:246–253
- Zhang Z, Yang M, Wu X, Dong S, Zhu N, Gyimah E, Wang K, Li Y (2019) A competitive immunosensor for ultrasensitive detection of sulphonamides from environmental waters using silver nanoparticles decorated single-walled carbon nanohorns as labels. *Chemosphere* 225:282–287

Chapter 11

Electrochemical DNA Sensors Based on Nanostructured Polymeric Materials for Determination of Antitumor Drugs



Anna Porfireva, Tibor Hianik, and Gennady Evtugyn

Abstract In this chapter, recent achievements in the development of electrochemical DNA sensors intended for the determination of antitumor drugs have been presented with particular emphasis to the mechanism of signal generation and factors influencing the response of the biosensor toward anthracycline drugs. Besides, the redox properties of electrochemically active polymers as a platform for DNA immobilization and signal generation have been considered and the protocols for voltametric and impedimetric signal recording provided. The possibility to use DNA sensor described for the assessment of commercial medications and biological fluids is discussed together with the prospects of enhancement of the polymers applied in the biosensor assembly.

Keywords DNA sensor · Electropolymerization · DNA intercalator · Anthracycline drugs · Electrochemical impedance spectroscopy

Nomenclature

DNA	Deoxyribonucleic acid
DC	Direct current
EDOT	Ethylenedioxythiophene
EDTA	Ethylenediaminetetraacetic acid
EIS	Electrochemical impedance spectroscopy
EQCM	Electrochemical quartz crystal microbalance
LOD	Limit of detection
PANI	Polyaniline

A. Porfireva · G. Evtugyn (✉)
Analytical Chemistry Department, Kazan Federal University, Kazan, Russia

T. Hianik
Department of Nuclear Physics and Biophysics, Comenius University, Bratislava, Slovakia

PEDOT	Poly(ethylenedioxythiophene)
PSA	Potentiometric stripping amperometry
RNA	Ribonucleic acid

11.1 Introduction

DNA sensors are compact analytical devices involving oligonucleotides or their synthetic analogs as recognition elements (Asal et al. 2018). Many of them were developed for the detection of hybridization of complementary sequences. They are also called genosensor events (Lucarelli et al. 2008). In these sensors, oligonucleotide sequence (strand) related to a gene or other specific parts of the sequence typical for hosting organism is attached to the solid support (polymer film or sensor transducer), and such a hybridization brings dramatic changes in the properties of the reaction area and hence makes the detection of hybridization event more easy. Among many physical methods of hybridization detection, electrochemical approaches prevail due to many advantages, e.g., simple and cost-effective instrumentation, well-elaborated theory, compatibility with commercial equipment, applicability for colored and turbid samples, etc. (Palchetti and Mascini 2008). Electrochemical genosensors described above are widely used for the diagnostics of pathogenic microorganisms and viruses (Simoska and Stevenson 2019), detection of some genetic diseases (Falzarano et al. 2018), genetically modified organism's tissues in the foodstuffs (Manzanarez-Palenzuela et al. 2015), for identification of meat source in food (Azam et al. 2018), and in many other cases. Being compact and easy in production and operation, they offer great opportunities to develop effective devices in medicine or preliminary control of the food outside chemical laboratory (Quesada-González and Merkoçi 2018).

In comparison with hybridization, target interactions of small molecules result in much lower changes in the DNA molecules, which can be hardly detected with conventional techniques described for genosensors. Most of the approaches presently used utilize three strategies: (1) measurements of direct DNA redox activity, mainly oxidation of guanine or adenine, both direct and mediated, and its changes after the analyte binding (Diculescu et al. 2016); (2) application of the DNA molecules as specific sorbent able to accumulate the analyte molecules in a close proximity to the electrode surface followed by their redox reaction (Primo et al. 2014); and (3) recording changes of the electrode interface characteristics resulting from the target interactions with DNA attached to the surface. Besides decreased permeability of the surface layer for low-molecular ions mentioned above, the charge distribution and release of the DNA probes from the surface layer could take place after the contact with analyte molecules (Rozenblum et al. 2019).

In this chapter, main attention is focused on the opportunities offered by electropolymerized materials serving as the DNA carriers and for electric wiring biopolymer involved in target interactions. Appropriate DNA sensors have been

designed for sensitive determination of antitumor drugs specifically interacting with native (double-stranded) DNA and hence influencing the redox properties of the DNA-polymer layer.

11.2 Electropolymerized Materials Used in DNA Sensors

11.2.1 *General Characteristics of Electropolymerization in DNA Sensor Assembling*

Electropolymerization is a reaction of the formation of insoluble products initiated by electron transfer and resulted in deposition of the insoluble product on the electrode surface (Wallace et al. 2003). Monomers which have the ability to undergo electropolymerization include aromatic amines, phenols, and polyheteroaromatic systems, e.g., phenazines and phenothiazines. Although in some cases the electropolymerization reaction starts from reduction of a monomer, the majority of reactions initiating electropolymerization belong to oxidation, i.e., subtraction of an electron from the monomer molecule (Pauliukaite et al. 2007). Radical formed is coupled with the monomer or another radical, and the hydrogen ion is then released from the product to stabilize them and form a dimer. The reactions can continue to oligomeric (polymeric) sequences until their sedimentation, deposition on electrode, or exhaustion of the monomer solution.

The electropolymerization can be performed in different regimes, i.e., multiple cycling of the potential (potentiodynamic regime), at constant polarization potential (potentiostatic regime), or at a constant anodic current (galvanostatic regime) (Nakano et al. 2016). At the beginning of the potential cycling, most of the monomers undergo polymerization and show one pair of redox peaks attributed to their reversible conversion (Topçu and Alanyalıoğlu 2014; Gao et al. 2010). The shape of the peaks is affected by adsorption and pH dependency of redox properties that differ for monomers and polymers. If the potential window is limited by the potentials near these peaks, no polymerization takes place, and minor changes on voltammograms are mostly ascribed by adsorption of the reactants. However, at high anodic potential, an irreversible peak can be found. It corresponds to the formation of reactive radical that starts the reaction chain described above and resulted in formation of the polymeric product. After the first three to five cycles, another pair of peaks appear and continue to increase. It is attributed to the polymeric form. Appropriate peaks are commonly poorly resolved and look as a current plateau. At this moment, the signals of monomers start stabilizing and then decreasing. Changes in the peaks on voltammograms become gradually lower until stabilization after 20–30 cycles. The neutral red polymerization differs from that described because of the equal potentials of redox conversion of polymeric and monomeric dyes (Soltani et al. 2018; Pauliukaite et al. 2007).

Electropolymerization is also affected by the nature of counter ions compensating for the positive charge of the polymer chain (Palma-Cando et al. 2019), pH

(Chen et al. 2018b; Topçu and Alanyalıoğlu 2014), conductivity of the solution (Holla and Selvakumar 2018), surfactant additives (Chen et al. 2018a; Zhou et al. 2019), etc. Thus, the addition of polyionic species like polystyrene sulfonate (Ji et al. 2019) or native DNA (Azadmehr and Zarei 2019) promotes polymerization due to formation of polyionic complexes.

The regime of electrolysis, morphology of the film obtained, and surface charge distribution affect the properties of the polymer particles and could intensify their role in the signal generation (Ćirić-Marjanović 2013a). Besides, other materials are easily implemented in the polymer film. Au (Dehghani et al. 2019; Rahim et al. 2018; Mo et al. 2018), Ag (Khesuoe et al. 2016), Pt (Zheng et al. 2018), carbon nanotubes (Koluçak et al. 2018; Syugaev et al. 2018; Ates and Sarac 2009), and graphene particles (Tang et al. 2020; Sun et al. 2020) are often used for such purposes. They accelerate the electron exchange in the thick polymer films and simplify anchoring of biopolymers and artificial receptors in the close proximity to the electrode. Besides, they increase surface area and establish electric wiring of the redox active sites in the biomolecules.

11.2.2 *Electroconductive Polymers*

All the polymers obtained by electropolymerization for (bio)sensor application can be divided into electroconductive polymers and electroactive polymers.

Electroconductive polymers are mostly presented by polyaniline (PANI), polythiophene, and polypyrrole as well as their derivatives (Peng et al. 2009). They show polaron type of conductivity, in which cation radical is dissociated into vacancies that are transferring along the main polymer chain. For PANI, semi-oxidized form called as emeraldine salt is involved in the charge transfer and offers electroconductivity properties. As the formation of emeraldine salt required strong acids, PANI exerts electroconductivity at $\text{pH} < 3.0$. In other conditions, PANI can exist in the forms of leuco-emeraldine, emeraldine, and pernigraniline (Ćirić-Marjanović 2013b). All the redox equilibria mentioned are pH-dependent.

PANI can form various nanostructures different from each other in size, shape, electrocatalytic activity, and conductivity (Stejskal et al. 2003). Polymerization in strong mineral acids and electropolymerization result in the formation of granules with globular structure. The agglomeration is mostly guided by stacking of the aromatic planes in the oligomers formed by homogeneous nucleation. Nanofibers (“nanowires”) have a high aspect ratio and diameter of 10 nanometers. The formation of nanofibers over granules requires either fast dilution of the reaction media after formation of first nucleates or a slow growth of the seeds on the solid surface. High-current pulse voltammetry can promote preferable formation of the nanofibers in electroconductive form. Other forms, e.g., microspheres or PANI nanotubes, are mostly synthesized by chemical polymerization in certain conditions (Gangopadhyay et al. 2012).

Polypyrrole and polythiophene are obtained by oxidation of appropriate monomer followed by coupling of the electron transfer products. Granulation of polypyrrole as well as formation of nanofibers, nanohorns, and other elongated particles can be performed by application of pulse regimes of electrolysis. Thus, the use of potentiostatic current pulses resulted in formation of a kind of sponge and brush with regularly oriented fibers grown orthogonally to the electrode surface (Karami and Nezhad 2013; Daryakenari et al. 2015; Alam et al. 2019). Nano-ordered polythiophene derivatives are prepared in a similar manner (Fusco et al. 2018).

For polypyrrole and polythiophene, substituents can be introduced either in the monomer molecule or after polymerization by polymer modification. The 3- and 4-positions of the heterocycles are accessible for such modification. In case of polypyrrole, the nitrogen atom of the ring can be quaternized. Normally, derived monomers are mixed with unsubstituted pyrrole or thiophene molecules to decrease the density of the substituents in the polymer structure. This makes it possible to decrease spatial limitation of the binding of the reagents or biomolecules to the substituent's groups necessary for biosensor operation. Oxidation of thiophene requires potential higher than that required for the formation of sulfones. For this reason, the polymer formed is always contaminated with such products. To avoid that and to decrease the potential of electropolymerization, terthiophene and its derivatives are used instead of unsubstituted thiophene. Among derivatives of polypyrrole and polythiophene, PEDOT (poly(ethylene dioxythiophene)) should be mentioned. Its monomer (i.e., EDOT) is water soluble and hence can be easily electropolymerized with formation of conductive layer applicable for covalent modification with biomolecules.

The modification of polypyrrole and polythiophene affects conductivity of the polymer but to a lower extent than in the case of polyaniline. For this reason, they are mostly used as carriers of biopolymers including DNA, while PANI can respond on DNA interactions by changes in its conductivity and redox properties (Tahir et al. 2005; Shoaie et al. 2019).

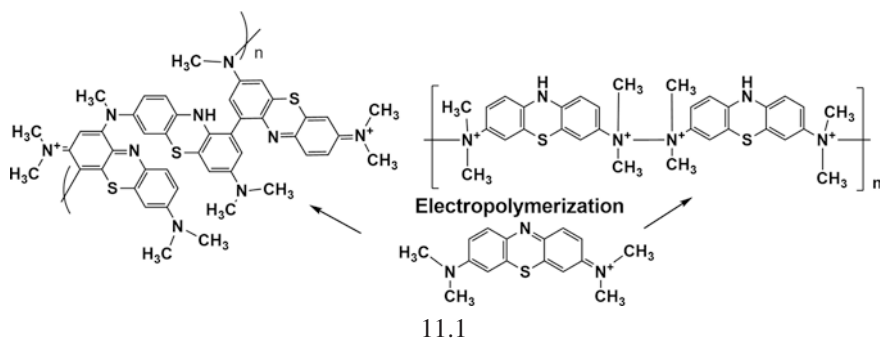
All of the electroconductive polymers mentioned are also obtained by chemical synthesis using strong oxidants, e.g., $(\text{NH}_4)_2\text{S}_2\text{O}_8$, FeCl_3 , or $\text{K}_2\text{Cr}_2\text{O}_7$. The products of chemical synthesis have the structure similar to that of electrosynthesized analogs but can be contaminated with the products of oxidant reaction. For all the electroconductive polymers, low solubility in water and most organic solvents complicate their implementation in the sensor assembly. The solubility can be increased by addition of strong organic acids insoluble in water and phenol as plasticizer.

11.2.3 Electroactive Polymers

Electrochemically active (“*electroactive*”) polymers mediate electron exchange like heterogeneous modifiers commonly used in the electrochemical biosensors, e.g., Prussian blue or Co phthalocyanine. The electroactive polymers can be formed by two approaches, i.e., (1) by electropolymerization of appropriate monomers

exerting reversible redox conversion in a desired range of the potentials and (2) by modification of the polymer with redox active units like ferrocene (Jirimali et al. 2019) or Os bipyridine complex (Bennett et al. 2018). Implementation of redox centers in the polymer chain increases stability of the mediator on the electrode surface and improves even distribution of the redox centers. Besides, polymers of this group are quite effective as redox mediators especially due to their possibility to establish close contact with biomolecules within the polymerization step. Similar effect can be obtained by non-covalent self-assembling of polyelectrolyte complexes containing mediators of electron exchange or redox active components that are entrapped in the complex via multiple electrostatic interactions (Liu et al. 2005). DNA as polyanionic substance with numerous phosphate groups in the skeleton is well compatible with many polycations like poly(l-lysine) (Yabuki et al. 2006). Such assembling protocols are mainly based on electrostatic interactions, which offer a simple and repeatable way for the synthesis of biorecognition layers based on intrinsic distribution of the charge and hence sensitive to the interactions affecting such distribution.

Regarding DNA sensor design, an alternative based on electropolymerization of phenazine or phenoxazine dyes has received higher attention. Among them, polymeric forms of methylene blue, methylene green, and neutral red are most often mentioned in description of DNA sensor assembling. All these dyes are involved in head-to-tail coupling assuming *N*-demethylation and *N*-to-ring binding (Scheme 11.1).



For methylene blue, the structure of the tetramer obtained was confirmed by density functional theory calculation (Ajami et al. 2016) and direct detection with the online electrochemistry-electro-spray mass spectrometry (Kertesz and Van Berkel 2001). Alternative ring-to-ring coupling and benzidine rearrangement (Yogeswaran and Chen 2008) seem less probable because of electrostatic repulsion of cationic centers. Reactivity of differently substituted phenothiazine derivatives and their redox behavior were compared by Karyakin et al. (1999a, b) in search of electrocatalysts for NADH electrooxidation.

Neutral red is polymerized in neutral media to form branched polymer. The deposition of the polymerization products can be monitored by electrochemical quartz crystal microbalance (EQCM) technique (Barsan et al. 2008; Kuzin et al.

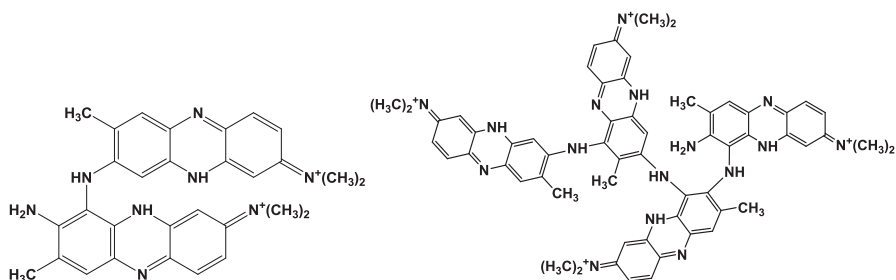


Fig. 11.1 Possible structures of dimer and tetramer of neutral red formed in electropolymerization

2018). Possible structures of neutral red oligomers formed in electropolymerization are presented in Fig. 11.1 (Pauliukaite et al. 2007). Besides, neutral red is the only polymer for which redox potentials of monomeric and polymeric forms are the same (Soltani et al. 2018); hence, no additional pair of peak appears in potential cycling; however, it appears in case of methylene blue or methylene green (Kuzin et al. 2018).

11.3 DNA-Drug Interaction

DNA is one of the most important targets for anticancer drugs that interact with this biomolecule in different manners, e.g., intercalation (implementation in-between pairs of complementary nucleobases), non-covalent binding at minor grooves, DNA strand cleaving and chemical modification of nucleobases (Rauf et al. 2005), etc. Because of such interactions, DNA molecules change their stable conformation and functional properties. Among the consequences of DNA-drug binding, the following processes are most important for antitumor activity: transcription factors and polymerases should be controlled, triple helixes with RNA interfering with transcriptional activity can be formed, and small aromatic ligands should be bind to the double-stranded DNA molecules.

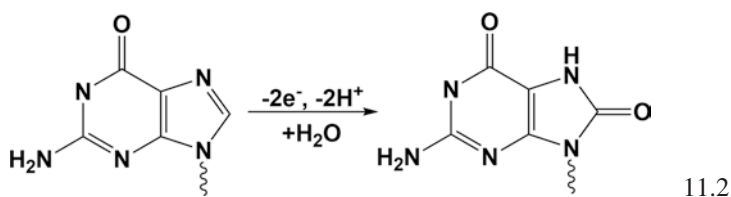
Intercalation It is the mechanism of interaction between small molecules including drugs and native DNA, which is monitored with appropriate biosensor. The antitumor drugs have specific binding site, e.g., certain base pair (commonly guanine-cytosine). Intercalators should have planar aromatic core to stack between the DNA base pairs and anchoring polar groups with an ability of electrostatic interaction with phosphate residues. The DNA intercalation can lengthen and stiffen DNA helix but do not disrupt base pairing or form covalent bonds. Phenothiazine, acridine dyes, and anthracycline antibiotics belong to the intercalators.

Groove Binding It is mostly guided by electrostatic interactions and is limited by the dimensions of guest molecules and minor and major grooves of the DNA helix.

Spatial factors presume higher selectivity of binding against intercalation, even though the efficiency of the binding might be insufficient for serious consequences for the DNA structure (Ma et al. 2011). Groove binding is also considered as a first step and additional stabilization factor for typical DNA intercalators.

Alkylation It is an irreversible addition of alkyl groups to the DNA bases, preferably guanine (N7) and adenine (N3 atoms) (Sirajuddin et al. 2013). DNA alkylating agents are frequently used in cancer chemotherapy (benzimidazoles, pyrrolizidines, and pyrrolobenzodiazepines).

DNA Cleavage It is mostly observed in sugar-phosphate bonds and can also involve removal of the terminal nucleotide or splitting of double strand of DNA (Hasanzadeh and Shadjou 2016). The monitoring of the DNA cleavage as well as other mechanisms of the DNA damage can be performed with biosensors. They record intrinsic signals of guanine oxidation (Scheme 11.2) or changes in the redox activity of the drugs or redox probes responding to accessibility of the nucleobases for small molecules. The approaches to the signal recording are considered in more details in the following chapters.



It should be mentioned that most of the changes in the native DNA structure usually result from complicated mechanisms, which can be indirectly related to initial DNA-drug contact, but also depend on neighboring media and specific processes like metabolic oxidation of some drugs, native DNA repair mechanisms, or changes in the agglomeration and assembling of biopolymers with proteins and lipids. Being common in living beings, such processes are hardly modeled on the biosensor level and hence can complicate the transfer of the phenomena observed on the biosensor interface to the whole organism of potential patient (Campuzano et al. 2018).

Among many complications, oxidative DNA damage should be considered. The reactive oxygen species normally present in the living cells are mostly resulted from the biochemical reactions of oxidoreductases yielding hydrogen peroxide and some anthropogenic pollutants like NO (Patel et al. 2019) or peroxyacetyl nitrate (Zhang et al. 2012; Tang et al. 2014). However, oxidative damage of DNA is enhanced by intercalation of the biopolymer with some drugs, e.g., anthracyclines (Mizutani et al. 2017). They increase the distance between complementary bases in the double-stranded DNA helix and hence allow easy access of radicals to the functional groups, which later cause oxidation (Bernalte et al. 2017).

Electrochemical measurements performed with DNA biosensor can provoke similar consequences. Thus, reactive oxygen species are generated from dissolved

dioxygen present in the cathodic (formation of the anion radical) and anodic reaction solution (formation of OH radical or hydrogen peroxide) (Oliveira and Oliveira-Brett 2012). The efficiency of generation of reactive oxygen species is increased by addition of iron salts (electro-Fenton reaction (Qiu et al. 2015)). As a result, additional peaks attributed to the primary products of oxidative damage, e.g., 8-oxoguanine (Oliveira-Brett et al. 2002), appear on voltammograms even though the drugs themselves do not damage DNA in natural conditions (Oliveira-Brett et al. 2002; Piedade et al. 2002). On one hand, such a behavior can overestimate drug's efficiency tested for cancer cell treatment. On another hand, additional peaks of 8-oxoguanine improve the reliability of the DNA sensor response where two parameters, i.e., peak currents related to guanine and 8-oxoguanine, are changing with the intensity of the external factor (drug concentration or incubation period) in opposite directions.

11.4 DNA Immobilization

Immobilization of biochemical component is an indispensable part of biosensor development, which is necessary to provide essential operational, metrological, and analytical performance of biosensor. The term *immobilization* means transfer of the DNA (protein, antibody, nucleic acid) in insoluble form on the solid support that is in intimate contact with the sensing part of a transducer. In modern electrochemical biosensors, the electrode itself or a thin cover of modifier necessary for signal generation can serve as such support (Jalit et al. 2013). In immobilization, the recognition of an analyte mostly takes place in heterogeneous conditions so that maximal changes of the environment and DNA are located near the electrode. This increases the sensitivity of appropriate signal measurements against homogeneous conditions. However, immobilization is necessary even for preliminary incubation of the DNA with drug. It simplifies following steps of the signal recording and improves metrological characteristics of the DNA sensor. It should be also noted that immobilization always enhances storage period of biosensor because the biopolymers used in biosensors stabilize their structure and recognition abilities by multiple interaction with underlying surface.

Three protocols of DNA immobilization are described in the literature (Fig. 11.2):

- *Physical immobilization* on the solid support by multiple non-covalent interactions.
- *Covalent immobilization* of DNA oligonucleotides via formation of covalent bond between terminal functional groups of the biopolymer and substituents of the carrier (electrode material).
- *Affine immobilization* utilizing natural or artificial receptor-substrate pairs. Avidin-biotin interactions are mostly mentioned among natural reagents and chelate immobilization via nitrilotriacetic acid residues and histidine tags of biopolymers amalgamated with central copper cation among artificial systems.

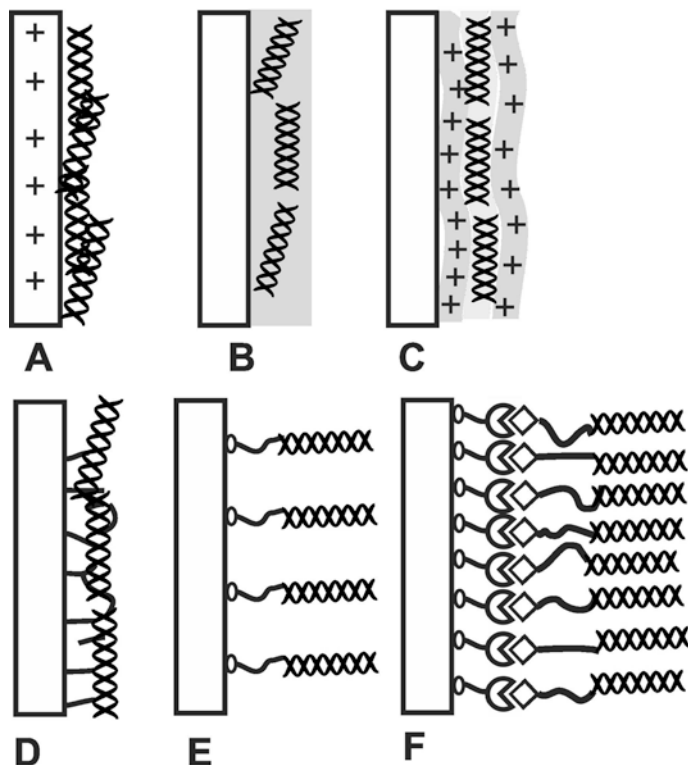


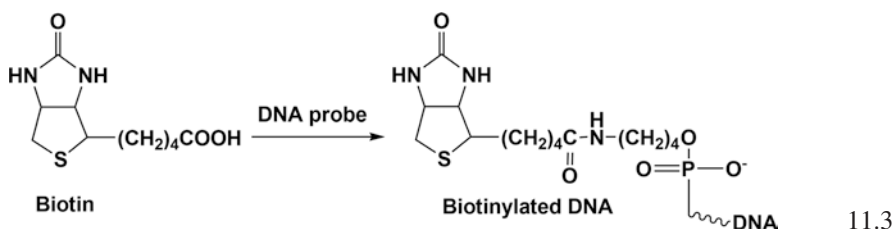
Fig. 11.2 Schematic outlines of various immobilization protocols: (a) physical (electrostatic) adsorption on the electrode surface; (b) entrapment in the polymer film; (c) inclusion in polyelectrolyte complex; (d) covalent attachment with glutaraldehyde; (e) covalent attachment to Au nanoparticles via terminal thiol groups; (f) affine immobilization via avidin-biotin binding

From the very beginning of the DNA biosensors' investigations, *electrostatic accumulation* of the DNA molecules on positively charged surface of carbon electrode becomes very popular due to simple protocol and reproducible results (Mascini et al. 2001). The carbon electrode was first polarized with a high anodic voltage and then put in the DNA solution. The interaction of DNA with the electrode resulted in partial unwinding of the helix and changes of native double-stranded DNA configuration so that the nucleobases became more accessible for electron transfer. The signals mostly related to the guanine and adenine oxidation were recorded using differential pulse voltammetry and potentiometric stripping amperometry (PSA). Entrapment of the DNA in the growing polymer film during the electropolymerization procedure also refers to the physical immobilization of the DNA molecules. It was briefly considered above.

Covalent Immobilization It assumes modification of the DNA molecule that is required for the formation of a new covalent bond between the DNA functional group and carrier. This protocol became popular when DNA sensors were intended

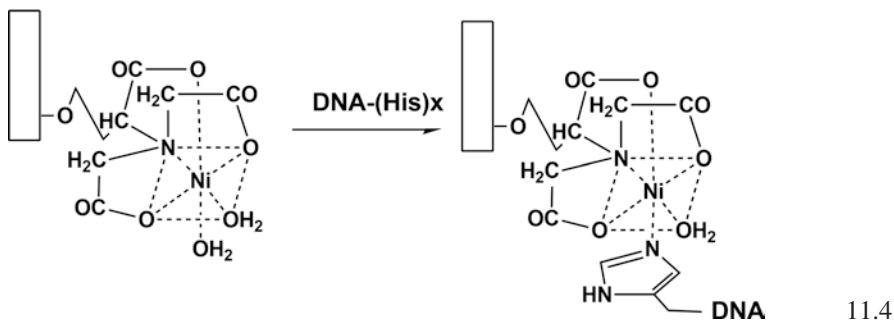
mostly for hybridization of complementary DNA sequences. Comparable size of the DNA target and the probe attached to the electrode required a high steric accessibility of the immobilized sequence. For this purpose, amino, carboxylate, or thiol groups were introduced at the end of the sequence, and various standard techniques of covalent immobilization were used. Thus, carboxylic and amino groups were convenient for carbodiimide binding, while SH groups reacted with golden surface or Au nanoparticles. In case of small drug molecules, such immobilization seems exhausting and complicated as far as signal recording is concerned. Indeed, the attachment of the drug to the DNA binding site insignificantly changes the charge distribution or DNA configuration in comparison with initial DNA molecule. Thus, the sensitivity of the DNA-drug interactions becomes lower than in case of other immobilization protocols. Nevertheless, covalent modification of the DNA molecules is used for introduction of labels and auxiliary molecules enhancing the signal or increasing sensitivity of its recording. Covalent immobilization is based on the use of bifunctional reagents that form one bond with target DNA and another with the carrier. Besides carbodiimides mentioned above, glutaraldehyde can also be used. It preferably reacts with amino groups present in the nucleobases or proteins and forms Schiff bases, which can be then reduced to increase their stability toward hydrolysis. The reaction with glutaraldehyde can form a 3D rigid structure of inert proteins that entraps the DNA molecules and hence preserves them near the electrode surface.

Affine Immobilization It is mostly based on the use of receptor pairs designed by nature and being very effective and specific in binding biopolymers. Thus, avidin-biotin interaction is comparable with that of antigen with antibody by binding ability and can be used for immobilization of biotinylated DNA molecules (Scheme 11.3), which are now commercially available. Secondly avidin or streptavidin can be placed on the electrode and immobilized via glutaraldehyde or carbodiimide binding.



Each avidin molecule can form up to four bonds with the biotin counterparts, and this offers opportunities to assemble 3D structures with predetermined positions of the DNA binding sites. In chelate immobilization, specific interaction is performed with derivatives of nitrilotriacetic acid that can bind to transient metal cations (Scheme 11.4). The complex formed involves histidine residue. It can be implemented as terminal tag in the structure of DNA sequences. As a result, a stable complex is formed near the solid support. Cu^{2+} and Ni^{2+} ions are mostly used in the

assembly of such complexes. They are easily removed by treating with EDTA. This makes it possible to substitute biopolymer after analyte binding. Chelate immobilization can be easily combined with electropolymerization as shown for polypyrrole derivative (Baur et al. 2010).



11.5 Electrochemical DNA Sensors for Drug Determination

Various aspects of drug determination based on principles of biochemical assay and biosensor approaches are summarized in recent reviews published by different authors (Lima et al. 2018; Campuzano et al. 2018; Kurbanoglu et al. 2016; Hasanzadeh and Shadjou 2016). These reviews confirm a high attention is devoted to the drug determination and demonstrate recent progress in the above area.

11.5.1 Anthracyclines and PANI-DNA Sensors

Anthracycline antibiotics were introduced as antitumor drugs about 50 years ago but are still used as a part of composite medications. The necessity in auxiliary components of such forms is related to modest cardiotoxicity of the drugs, limiting their dose and efficiency of application. In DNA biosensors, a representative of anthracyclines, doxorubicin (known also as Adriamycin), was used as an indicator of hybridization of complementary DNA strands and oxidative DNA damage because of its ability to intercalate the DNA helix at guanine-cytosine pairs. The intercalation promotes oxidation of guanine residues and formation of 8-oxoguanine detected by specific peak on voltammograms.

The determination of anthracycline drugs can be performed using the principles described above, i.e., using changes in the redox signals of $[\text{Fe}(\text{CN})_6]^{3-/4-}$ redox probe and those of PANI. It is interesting to see how the involvement of native DNA in the electropolymerized films affects the analytical characteristics of drug determination.

As mentioned above, electropolymerization of aniline in the presence of strong mineral acids can damage native DNA molecules added to the reaction media. To smoothen this effect, it was proposed that electropolymerization should be performed in the presence of oxalic acid (Shamagsumova et al. 2015). The atomic force microscopy indicated a high granulation of the growing PANI film covered the glassy carbon electrode after four cycles of the potential. In the presence of 0.1–2.0 mg/L DNA from salmon sperm, the peaks of the redox reactions responsible for the formation of emeraldine salt enormously increased. This indicated stabilization of conductive form of the polymer. Both electrochemical impedance spectroscopy (EIS) and direct current (DC) voltammetry indicated suppression of the PANI activity in the presence of anthracycline drugs within the concentration range from 10 μM to 0.1 nM (semi-logarithmic scale, LOD 10 pM). Selectivity of the response was estimated by similar experiments in the presence of sulfonamide drugs, which weakly interact with native DNA by minor grooves. The similar effect of sulfamethoxazole was observed at concentrations 1000 times higher. Besides, the DNA sensor was tested on artificial samples of blood serum (recovery 91–93%).

Indirect evidence of the DNA entrapment in the growing PANI film has been obtained using competition effect (Kulikova et al. 2018). In this series of experiments, DNA was saturated with methylene blue, which lost its redox activity in intercalation of the DNA helix. Incubation in doxorubicin solution resulted in the substitution of intercalated methylene blue and its involvement in the electron transfer chain. The more the number of cycles on the step of electropolymerization, the more is the DNA quantities entrapped. Thus, the accumulation of higher amounts of doxorubicin decreased its limit of detection (LOD) from 30 nM (9 cycles) to 0.1 nM (30 cycles). What is more interesting is that the DNA can be removed from the PANI matrix by concentrated HCl and then replaced with a fresh preparation similar to that used in molecular imprinting of the polymers, and such a replacement did not affect the response toward new portions of doxorubicin.

Alternative assembling of surface layer with the DNA drop casted onto the PANI layer did not result in improvement of analytical characteristics of anthracycline determination (on the example of doxorubicin). Even the attempts to protect the biopolymer molecules from the acidic media required on the stage of signal measurement did not allow improving the sensitivity of the EIS response (Porfir'eva et al. 2019). For this reason, the following progress in the biosensor assembling was achieved by layered deposition of the surface components based on combination of electropolymerization and self-assembling (Kulikova et al. 2019). The assembling of the active layers of the DNA sensors mentioned is schematically outlined in Fig. 11.3. Both layers of PANI, i.e., underlying and coating ones, have been obtained in four cycles of potential cycling with no DNA in reaction media. In between two electropolymerization stages, DNA was physically adsorbed on the PANI support followed by careful washing of unbound molecules. The incubation was performed in neutral media to avoid acidic maturation of native DNA. Although the second PANI deposition required acidic conditions, DNA adsorbed is protected from low pH of the environment due to weak multiple interactions with the underlying polymer film. Voltametric detection of doxorubicin with $[\text{Fe}(\text{CN})_6]^{3-}$ redox

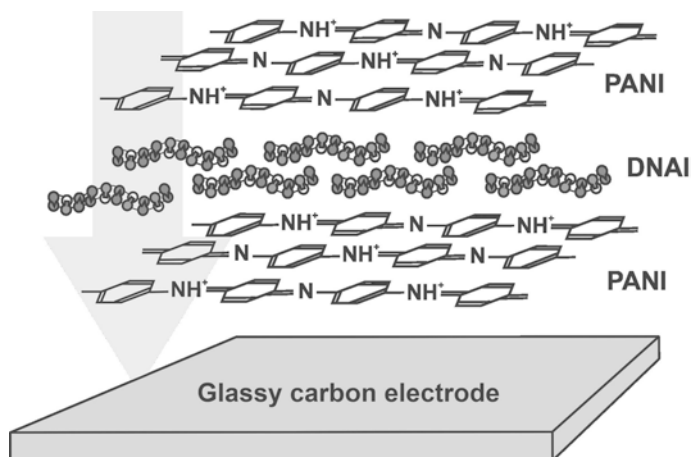


Fig. 11.3 Schematic outline of layer-by-layer assembling of DNA sensor for anthracycline determination

probe showed regular decrease of the cathodic peak current with the thickness of PANI layers and DNA quantities applied. In optimal conditions, LOD of 2 nM and concentration range from 1 mM to 10 nM were achieved. Impedimetric mode allowed decreasing the LOD to 0.6 pM, which is the lowest one for doxorubicin determination based on biosensing approaches.

11.5.2 Other DNA Sensors

Other electroactive polymers were also tested in the assembly of DNA sensors for drug determination. Thus, electropolymerized methylene green and methylene blue were deposited on the glassy carbon electrode in multiple cycling of the potential. DNA was drop casted onto the polymer layer, and then the peak potentials of the phenothiazine dyes were measured before and after the contact of the biosensor with the anthracyclines (Kuzin et al. 2018). The DNA implementation was proved by electrochemical quartz crystal microbalance (EQCM) and EIS. Unfortunately, the working concentrations of doxorubicin affecting the peak potentials exceeded 10 nM.

Polyelectrolyte complexes formed by poly(neutral red) and DNA have been assessed in the detection of doxorubicin by DC and EIS experiments (Porfir'eva et al. 2019). As in the case of the PANI-based biosensors, target interaction increased charge transfer resistance measured in the presence of ferricyanide redox probe. On the contrary, capacitance of the electrode interface was quite stable in the whole range of the drug concentrations tested. Protection of the DNA layer deposited on the polymer with electrochemically inactive polyions (polystyrene sulfonate and polyallylamine hydrochloride) decreased sensitivity of doxorubicin determination.

For a three-layered coating of the above electrolytes, an LOD of 0.2 nM was reported. It was interesting that the formation of the molecular complex between the DNA adsorbed on the electrode and tetraaminated thiacalix[4]arene decreased the LOD twice against naked DNA layer probably due to partial shielding of negative charge of phosphates and decreased repulsion of anionic redox probe from the electrode interface.

Similar polyelectrolyte complexes assembled on the electrode preliminary covered with poly(methylene blue) or poly(methylene green) were used for discrimination of native, thermally, and chemically damaged DNA that was deposited by layer-by-layer assembling together with poly(styrene sulfonate) and poly(allylamine hydrochloride) (Evtugyn et al. 2014). Introduction of DNA in the polyelectrolyte complex was proved by fluorescence microscopy by adsorption of SYBR Green fluorescent dye. The permeability of the surface layer was dependent on the number of layers and DNA position. Maximum changes of the redox probe DC signal were observed with DNA directly contacted with polyphenothiazine coating.

Azure B (see chemical structure in Fig. 11.1) was immobilized on glassy carbon electrode by multiple cycling of the potential in neutral media. The DNA was loaded on the surface after incubation in the doxorubicin solution (Porfireva et al. 2019). The cathodic peak current of poly(Azure B) layer decreased with the increasing concentration of the drug within 1.0 μM and 10 pM. The response was quantified using a four-parameter logistic curve. The LOD that corresponded to 20% shift of the peak current was equal to 0.25 nM. The DNA sensor was validated using blood serum of healthy volunteers, artificial blood plasma, and commercial medications Doxorubicin-LANS® and Doxorubicin-TEVA®. The recovery of about 90% was reported for serum samples containing 1.0–10 nM doxorubicin and 97–105% for artificial plasma.

Poly(proflavine) was obtained in a similar manner, coated with physically adsorbed DNA and treated with doxorubicin (Porfireva et al. 2020). The changes in the cathodic peak current of immobilized dye made it possible to determine from 1 nM to 0.1 μM of doxorubicin and 1 pM–10 nM of daunorubicin (LODs 0.3 and 0.001 nM, respectively). The biosensor was tested on pharmaceutical preparations and spiked solution simulating the plasma electrolytes and possible interference of serum proteins.

11.6 Conclusion

All the reports available confirmed that electrosynthesis provides simple and cost-effective route for the assembling of DNA sensors for small molecule determination. The success in the DNA sensor assembling is mainly associated with application of PANI. Its redox activity and electric conductivity make simpler signal generation and allow using traditional DC voltammetry and EIS. The pulse technique and modification of monomers with hydrophilic substituents that extend the opportunities of electrosynthesis have not yet found broad application in DNA sensors. Nevertheless,

the collected experience in the area of electropolymerization in the presence of DNA allows fabrication of effective and simple in operation biosensors useful for point-of-care applications in chemotherapy and pharmacokinetics. Besides PANI, phenothiazines and neutral red have been found of particular interest because they do not need strong mineral acids for polymerization and respond on the specific DNA interactions by appropriate changes of electron exchange equilibria. Though the sensitivity of response toward drugs was found lower than that of PANI, the LODs achieved were lower for the biosensors utilizing polymeric forms of phenothiazine dyes. Variation in the layer thickness and content by selection of the electrolysis regime and way for DNA implementation allow varying the analytical performance of the DNA sensors produced. This offers new opportunities for the application of recent achievements of DNA sensor design in medicine and new drug screening.

Acknowledgments GE acknowledges financial support of Russian Foundation for Basic Research (RFBR), grant no. 20-03-00207. TH acknowledges the financial support of Scientific Grant Agency VEGA, project no. 1/0419/20.

References

- Ajami N, Ehsani A, Babaei F, Safari R (2016) Electrochemical properties, optical modeling and electrocatalytic activity of pulse-electropolymerized ternary nanocomposite of poly(methylene blue) in aqueous solution. *J Mol Liq* 215:24–30
- Alam I, Guiney LM, Hersam MC, Chowdhury I (2019) Application of external voltage for fouling mitigation from graphene oxide, reduced graphene oxide and molybdenum disulfide functionalized surfaces. *Environ Sci Nano* 6:925–936
- Asal M, Özen Ö, Şahinter M, Poltoğlu İ (2018) Recent developments in enzyme, DNA and immuno-based biosensors. *Sensors* 18:1924. <https://doi.org/10.3390/s18061924>
- Ates M, Sarac S (2009) Conducting polymer coated carbon surfaces and biosensor applications. *Prog Org Coat* 66:337–358
- Azadmehr F, Zarei K (2019) An imprinted polymeric matrix containing DNA for electrochemical sensing of 2,4-dichlorophenoxyacetic acid. *Microchim Acta* 186:814
- Azam NFN, Roy S, Lim SA, Ahmed MU (2018) Meat species identification using DNA-luminol interaction and their slow diffusion onto the biochip surface. *Food Chem* 248:29–36
- Barsan MM, Pinto EM, Brett CMA (2008) Electrosynthesis and electrochemical characterisation of phenazine polymers for application in biosensors. *Electrochim Acta* 53:3973–3982
- Baur J, Gondran C, Holzinger M, Defrancq E, Perrot H, Cosnier S (2010) Label-free femtomolar detection of target DNA by impedimetric DNA sensor based on poly(pyrrrole-nitilotriacetic acid) film. *Anal Chem* 82:1066–1072
- Bennett R, Osadebe I, Kumar R, Ó Conghaile P, Leech D (2018) Design of experiments approach to provide enhanced glucose-oxidising enzyme electrode for membrane-less enzymatic fuel cells operating in human physiological fluids. *Electroanalysis* 30:1438–1445
- Bernalte E, Carroll M, Banks CE (2017) New electrochemical approach for the measurement of oxidative DNA damage: voltammetric determination of 8-oxoguanine at screen-printed graphite electrodes. *Sensors Actuators B Chem* 247:896–902
- Campuzano S, Pedrero M, Pingarron JM (2018) Electrochemical nucleic acid-based biosensing of drugs of abuse and pharmaceuticals. *Curr Med Chem* 25:4102–4118

- Chen C, Han Z, Lei W, Ding Y, Lv J, Xia M, Wang F, Hao G (2018a) A sensitive electrochemical sensor based on polypyrrole/electrochemically reduced graphene oxide for the determination of imidacloprid. *J Electrochem Sci Eng* 9:143–152
- Chen S, Liu S, Wen A, Zhang J, Nie H, Chen J, Zeng R, Long Y, Jin Y, Mai R (2018b) New insight into electropolymerization of melamine. I: chloride promoted growth of polymelamine in different pH medium. *Electrochim Acta* 271:312–318
- Ćirić-Marjanović R (2013a) Recent advances in polyaniline composites with metals, metalloids and nonmetals. *Synth Met* 170:31–56
- Ćirić-Marjanović G (2013b) Recent advances in polyaniline research: polymerization mechanisms, structural aspects, properties and applications. *Synth Met* 177:1–47
- Daryakenari AA, Apostoluk A, Aradilla D, Sadki S, Delaunay J-J (2015) Pulse electropolymerization synthesis of PPy(DBS) nanoparticle layers. *J Solid State Electrochem* 19:655–661
- Dehghani D, Nasirizadeh N, Yazdanshenas ME (2019) Determination of cefixime using a novel electrochemical sensor produced with gold nanowires/graphene oxide/electropolymerized molecular imprinted polymer. *Mater Sci Eng C Mater Biol Appl* 96:654–660
- Diculescu VC, Chiorcea-Paquim AM, Oliveira-Brett AM (2016) Applications of a DNA-electrochemical biosensor. *TrAC Trends Anal Chem* 79:23–36
- Evtugyn GA, Stepanova VB, Porfireva AV, Zamaleev AI, Fakhrullin RR (2014) Electrochemical DNA sensors based on nanostructured organic dyes/DNA/polyelectrolyte complexes. *J Nanosci Nanotechnol* 14:6738–6747
- Falzarano MS, Flesia C, Cavalli R, Guiot C, Ferlini A (2018) Nanodiagnostics and nanodelivery applications in genetic alterations. *Curr Pharm Des* 24:1717–1726
- Fusco G, Göbel G, Zanoni R, Bracci MP, Favero G, Mazzei F, Lisdat F (2018) Aqueous polythiophene electrosynthesis: a new route to an efficient electrode coupling of PQQ-dependent glucose dehydrogenase for sensing and bioenergetic applications. *Biosens Bioelectron* 112:8–17
- Gangopadhyay R, Chowdhury DA, De A (2012) Functionalized polyaniline nanowires for biosensing. *Sensors Actuators B Chem* 171–172:777–785
- Gao Q, Sun M, Peng P, Qi H, Zhang C (2010) Electro-oxidative polymerization of phenothiazine dyes into a multilayer-containing carbon nanotube on a glassy carbon electrode for the sensitive and low-potential detection of NADH. *Microchim Acta* 168:299–307
- Hasanzadeh M, Shadjou N (2016) Pharmacogenomic study using bio- and nanobioelectrochemistry: drug-DNA interaction. *Mater Sci Eng C* 61:1002–1017
- Holla W, Selvakumar M (2018) Effect of different electrolytes on the supercapacitor Behavior of single and multilayered electrode materials based on multiwalled carbon nanotube/polyaniline composite. *Macromol Chem Phys* 219:1800213. <https://doi.org/10.1002/macp.201800213>
- Jalit Y, Moreno M, Gutierrez FA, Arribas AS, Chicharro M, Bermejo E, Zapardiel A, Parrado Z, Rivas GA, Rodríguez MC (2013) Adsorption and electrooxidation of nucleic acids at glassy carbon electrodes modified with multiwalled carbon nanotubes dispersed in polylysine. *Electroanalysis* 25:1116–1121
- Ji J, Li M, Chen Z, Wang H, Jiang X, Zhuo K, Liu Y, Yang X, Gu Z, Sang S, Shu Y (2019) In situ fabrication of organic electrochemical transistors on a microfluidic chip. *Nano Res* 12:1943–1951
- Jirimali HD, Nagarale RK, Saravanakumar D, Shin W (2019) Ferrocene tethered polyvinyl alcohol/silica film electrode for electrocatalytic sulfite sensing. *Electroanalysis* 30:828–833
- Karami H, Nezhad AR (2013) Investigation of pulse-electropolymerization of conductive polypyrrole nanostructures. *Int J Electrochem Sci* 8:8905–8921
- Karyakin AA, Karyakina EE, Schmidt H-L (1999a) Electropolymerized azines: a new group of electroactive polymers. *Electroanalysis* 11:149–155
- Karyakin AA, Karyakina EE, Schuhmann W, Schmidt H-L (1999b) Electropolymerized azines. P.II. In a search of the best electrocatalyst of NADH oxidation. *Electroanalysis* 11:553–557
- Kertesz V, Van Berkel GJ (2001) Electropolymerization of methylene blue investigated using on-line electrochemistry-electrospray mass spectrometry. *Electroanalysis* 13:1425–1430

- Khesuoe M, Matoetoe M, Okumu F (2016) Potential of silver nanoparticles functionalized polyaniline as an electrochemical transducer. *J Nano Res* 44:21–34
- Kolucaçık E, Karabiberöglü ŞU, Dursun Z (2018) Electrochemical determination of serotonin using pre-treated multi-walled carbon nanotube-polyaniline composite electrode. *Electroanalysis* 30:2977–2987
- Kulikova TN, Porfireva AV, Shamagsumova RV, Evtugyn GA (2018) Voltammetric sensor with replaceable polyaniline-DNA layer for doxorubicin determination. *Electroanalysis* 30:2284–2292
- Kulikova T, Porfireva A, Evtugyn G, Hianik T (2019) Electrochemical DNA sensors with layered polyaniline – DNA coating for detection of specific DNA interactions. *Sensors* 19:469. <https://doi.org/10.3390/s19030469>
- Kurbanoglu S, Dogan-Topal B, Rodriguez EP, Bozal-Palabiyik B, Ozkan SA, Uslu B (2016) Advances in electrochemical DNA biosensors and their interaction mechanism with pharmaceuticals. *J Electroanal Chem* 775:8–26
- Kuzin Y, Kappo D, Porfireva A, Shurpik D, Stoikov I, Evtugyn G, Hianik T (2018) Electrochemical DNA sensor based on carbon black – poly(Neutral red) composite for detection of oxidative DNA damage. *Sensors* 18:3489. <https://doi.org/10.3390/s18103489>
- Lima HRS, da Silva JS, Farias EAO, Teixeira PRS, Eiras C, Nunes LCC (2018) Electrochemical sensors and biosensors for the analysis of antineoplastic drugs. *Biosens Bioelectron* 108:27–37
- Liu AH, Anzaib J, Wang J (2005) Multilayer assembly of calf thymus DNA and poly(4-vinylpyridine) derivative bearing [Os(bpy)2Cl]2+: redox behavior within DNA film. *Bioelectrochemistry* 67:1–6
- Lucarelli F, Tombelli S, Minunni M, Marrazza G, Mascini M (2008) Electrochemical and piezoelectric DNA biosensors for hybridisation detection. *Anal Chim Acta* 609:139–159
- Ma D-L, Chan DS-H, Lee P, Kwan MH-T, Leung C-H (2011) Molecular modeling of drug–DNA interactions: virtual screening to structure-based design. *Biochimie* 93:1252–1266
- Manzanarez-Palenzuela CL, Martín-Fernandez B, Lopez MS-P, Lopez-Ruiz B (2015) Electrochemical genosensors as innovative tools for detection of genetically modified organisms. *TrAC Trends Anal Chem* 66:19–31
- Mascini M, Palchetti I, Marrazza G (2001) DNA electrochemical biosensors. *Fresenius J Anal Chem* 369:15–22
- Mizutani H, Hotta S, Nishimoto A, Ikemura K, Miyazawa D, Ikeda Y, Maeda T, Yoshikawa M, Hiraku Y And Kawanishi S (2017) Pirarubicin, an Anthracycline anticancer agent, induces apoptosis through generation of hydrogen peroxide. *Anticancer Res* 37: 6063–6069
- Mo X, Zhao G, Dou W (2018) Electropolymerization of stable leucoemeraldine base polyaniline film and application for quantitative detection of *Escherichia coli* O157:H7. *J Electron Mater* 47:6507–6517
- Nakano H, Hayashi K, Oue S, Kobayashi S (2016) Effects of electrolysis conditions on the morphologies and corrosion resistances of polyaniline films formed on Fe by electropolymerization. *Mater Trans* 57:1319–1326
- Oliveira SCB, Oliveira-Brett AM (2012) In Situ DNA oxidative damage by electrochemically generated hydroxyl free radicals on a boron-doped diamond electrode. *Langmuir* 28:4896–4901
- Oliveira-Brett AM, Vivan M, Fernandes IR, Piedade JA (2002) Electrochemical detection of in situ adriamycin oxidative damage to DNA. *Talanta* 56:959–970
- Palchetti I, Mascini M (2008) Electroanalytical biosensors and their potential for food pathogen and toxin detection. *Anal Bioanal Chem* 391:455–471
- Palma-Cando A, Rendón-Enríquez I, Tausch M, Scherf U (2019) Thin functional polymer films by electropolymerization. *Nanomaterials* 9:1125
- Patel MK, Pandey S, Burritt DJ, Tran L-SP (2019) Plant responses to low-oxygen stress: interplay between ROS and NO signaling pathways. *Environ Exp Bot* 161:134–142
- Pauliukaite R, Ghica ME, Barsan M, Brett CMA (2007) Characterisation of poly(neutral red) modified carbon film electrodes; application as a redox mediator for biosensors. *J Solid State Electrochem* 11:899–908

- Peng H, Zhang L, Soeller C, Travas-Sejdic J (2009) Conducting polymers for electrochemical DNA sensing. *Biomaterials* 30:2132–2148
- Piedade JA, Fernandes IR, Oliveira-Brett AM (2002) Electrochemical sensing of DNA-adriamycin interactions. *Bioelectrochemistry* 56:81–83
- Porfir'eva AV, Shibaeva KS, Evtugyn VG, Yakimova LS, Stoikov II, Evtugyn GA (2019) An electrochemical DNA sensor for doxorubicin based on a polyelectrolyte complex and aminated thiacalix[4]arene. *J Anal Chem* 74:707–714
- Porfireva A, Vorobev V, Babkina S, Evtugyn G (2019) Electrochemical sensor based on poly(Azure B)-DNA composite for doxorubicin determination. *Sensors* 19:2085
- Porfireva AV, Goida AI, Rogov AM, Evtugyn GA (2020) Impedimetric DNA sensor based on poly(proflavine) for determination of anthracycline drugs. *Electroanalysis* 32:827. submitted. <https://doi.org/10.1002/elan.201900653>
- Primo EN, Oviedo MB, Sánchez CG, Rubianes MD, Rivas GA (2014) Bioelectrochemical sensing of promethazine with bamboo-type multiwalled carbon nanotubes dispersed in calf-thymus double stranded DNA. *Bioelectrochemistry* 99:8–16
- Qiu S, He D, Ma J, Liu T, Wait TD (2015) Kinetic modeling of the electro-Fenton process: quantification of reactive oxygen species generation. *Electrochim Acta* 176:51–58
- Quesada-González D, Merkoçi A (2018) Nanomaterial-based devices for point-of-care diagnostic applications. *Chem Soc Rev* 47:4697–4709
- Rahim MZA, Govender-Hondros G, Adeloju SB (2018) A single step electrochemical integration of gold nanoparticles, cholesterol oxidase, cholesterol esterase and mediator with polypyrrole films for fabrication of free and total cholesterol nanobiosensors. *Talanta* 189:418–428
- Rauf S, Gooding JJ, Akhtar K, Ghauri MA, Rahman M, Anwar MA, Khalid AM (2005) Electrochemical approach of anticancer drugs–DNA interaction. *J Pharm Biomed Anal* 37:205–217
- Rozenblum GT, Pollitzer IG, Radrizzani M (2019) Challenges in electrochemical aptasensors and current sensing architectures using flat gold surfaces. *Chemosensors* 7:57
- Shamagsumova R, Porfireva A, Stepanova V, Osin Y, Evtugyn G, Hianik T (2015) Polyaniline-DNA based sensor for the detection of anthracycline drugs. *Sensors Actuators B Chem* 220:573–582
- Shoafie N, Daneshpour M, Azimzadeh M, Mahshid S, Khoshfetrat SM, Jahanpeyma F, Gholaminejad A, Omidfar K, Foruzandeh M (2019) Electrochemical sensors and biosensors based on the use of polyaniline and its nanocomposites: a review on recent advances. *Microchim Acta* 186:465. <https://doi.org/10.1007/s00604-019-3588-1>
- Simoska O, Stevenson KJ (2019) Electrochemical sensors for rapid diagnosis of pathogens in real time. *Analyst* 144:6461–6478
- Sirajuddin S, Ali S, Badshah A (2013) Drug–DNA interactions and their study by UV–Visible, fluorescence spectroscopies and cyclic voltammetry. *J Photochem Photobiol B Biol* 124:1–19
- Soltani S, Davarnejad R, Rahimi F, Matin T, Ahmadi E (2018) Copper nanoparticles/poly-neutral ted modified pencil graphite electrode for electroanalysis of folic acid. *J Chem Pharm Res* 10:99–109
- Stejskal J, Omastová M, Fedorova S, Prokeš J, Trchová M (2003) Polyaniline and polypyrrole prepared in the presence of surfactants: a comparative conductivity study. *Polymer* 44:1353–1358
- Sun T, Li M, Zhou S, Liang M, Chen Y, Zou H (2020) Multi-scale structure construction of carbon fiber surface by electrophoretic deposition and electropolymerization to enhance the interfacial strength of epoxy resin composites. *Appl Surf Sci* 499:143929
- Syugaev AV, Lyalina NV, Maratkanova AN, Shakov AA (2018) Effect of sodium dodecyl sulfate and carbon particles/nanotubes on electrodeposition of polyaniline from oxalic acid solution. *J Solid State Electrochem* 22:931–942
- Tahir ZM, Alocilja EC, Grooms DL (2005) Polyaniline synthesis and its biosensor application. *Biosens Bioelectron* 20:1690–1695
- Tang Y, Guo Y, Zhang L, Cai J, Yang P (2014) A novel electrochemical biosensor for monitoring protein nitration damage affected by NaNO_2 /hemin/ H_2O_2 . *Biosens Bioelectron* 54:628–633

- Tang X, Raskin J-P, Kryvutsa N, Hermans S, Slobodian O, Nazarov A, Debliquy M (2020) An ammonia sensor composed of polypyrrole synthesized on reduced graphene oxide by electropolymerization. *Sensors Actuators B Chem* 305:127423
- Topçu E, Alanyalıoğlu M (2014) Electrochemical formation of poly(thionine) thin films: the effect of amine group on the polymeric film formation of phenothiazine dyes. *J Appl Polym Sci* 131:39686. <https://doi.org/10.1002/app.39686>
- Wallace GG, Spinks GM, Kane-Maguire IAP, Teasdale PR (2003) *Conductive electroactive polymers. Intelligent materials systems*. CRC Press, Boca Raton
- Yabuki S, Fujii S, Mizutani F, Hirata Y (2006) Permeation regulation of charged species by the component change of polyion complex membranes. *Anal Biochem* 375:141–143
- Yogeswaran U, Chen S-M (2008) Multi-walled carbon nanotubes with poly(methylene blue) composite film for the enhancement and separation of electroanalytical responses of catecholamine and ascorbic acid. *Sensors Actuators B Chem* 130:739–749
- Zhang Y, Liu H, Hu N (2012) Electrochemical detection of natural DNA damage induced by in situ peroxidase-generated reactive nitrogen species in DNA layer-by-layer films. *Bioelectrochemistry* 86:67–71
- Zheng H, Wang M, Chen J, Liu M, Ye Y, Yan Z (2018) Improved sensitivity and selectivity glucose biosensor based on PANI-GRA nanocomposite film decorated with Pt nanoparticles. *Int J Electrochem Sci* 13:6272–6285
- Zhou H, Zhi X, Zhang W, Zhai H-J (2019) A simple strategy to prepare polyaniline nanorods by surfactant-assisted electropolymerization for remarkably improved supercapacitive performances. *Org Electron* 69:98–105

Chapter 12

Variants of Amperometric Biosensors in the Determination of Some Mycotoxins: Analytical Capabilities



Elvina Pavlovna Medyantseva, Regina Markovna Beylinson,
Adelina Ildarovna Khaybullina, and Herman Constantinovich Budnikov

Abstract The chapter is devoted to amperometric biosensors for the determination of various mycotoxins that are contaminants of food, animal feed, and grain crops having toxic and carcinogenic properties. The analytical capabilities of various biosensors based on cholinesterase, tyrosinase, horseradish peroxidase, and aflatoxin oxidase were evaluated. Their advantages and disadvantages over other methods are noted. Immunochemical (immunoenzyme) methods of mycotoxin analysis and development of immunosensors with horseradish peroxidase and tyrosinase as labels are focused. Separate aptasensors for determining mycotoxins are considered. The influence of nanomaterials and composites based on these nanomaterials on the analytical characteristics of biosensors is shown. The advantages of using biosensors in comparison with the other methods of analysis, problems, and disadvantages of their application in practice are noted.

Keywords Amperometric biosensor · Immunosensor · Aptasensor · Mycotoxin · Enzyme · Cholinesterase · Tyrosinase · Horseradish peroxidase · Aflatoxin oxidase · Label · Nanoparticles · Nanostructured materials · Carbon nanotubes · Enzyme immunoassay

Nomenclature

Ab	Antibody
AFB1	Aflatoxin B1
AFM1	Aflatoxin M1
OTA	Ochratoxin A
ZEN	Zearalenone
T-2 toxin	Trichothecenes T2

E. P. Medyantseva (✉) · R. M. Beylinson · A. I. Khaybullina · H. C. Budnikov
A.M. Butlerov Institute of Chemistry, Kazan Federal University (KFU), Kazan, Russia

CNTs	Carbon nanotubes
ELISA	Enzyme immunoassay
CE	Cholinesterase
HRP	Horseradish peroxidase
LOD	Limit of detection
MWCNTs	Multiwalled carbon nanotubes
GO	Graphene oxide
Au NPs	Gold nanoparticles
GCE	Glassy-carbon electrodes
MAC	Maximum allowable concentration

12.1 Introduction

The mycotoxins encompass a wide group of compounds that are very different in their chemical structure and, consequently, in their toxic effects. There are more than 250 species of microscopic fungi that can produce several hundred mycotoxins. Mycotoxins (from the Greek *mykes* (mushroom) and *toxikon* (poison)) are secondary metabolites of microscopic fungi that have pronounced toxic properties. Mycotoxins are produced mainly by fungi of the genera *Aspergillus*, *Fusarium*, and *Penicillium*. The most common mycotoxins that are distinguished by their toxic and carcinogenic properties, as well as foods that may be infected with mycotoxins, are shown in Table 12.1 (Haque et al. 2020).

Biosensors represent technology that can be applied to several sectors of the food industry for the storage of grains and raw materials, food production/processing, security and protection, and packaging of food. Diverse biosensors have emerged in the last decade as an alternative for analyzing microorganisms and toxins in food due to the capability for fast analysis, reproducibility, stability, and accuracy. A wide variety of transducers can be explored for mycotoxin and spoilage, and fungi detection, where optical (surface plasmon resonance – SPR and fluorescence), piezoelectric (quartz crystal microbalance – QCM), and electrochemical (impedimetric, potentiometric, and amperometric) spectroscopies stand out as main biosensing method (Oliveira et al. 2019).

Biosensors are one of the most effective tools to identify the fungi and mycotoxins. They are extremely sensitive and easy to operate, facilitating quick and reproducible analysis, followed by the advantage of low-cost tools, miniaturization, and the development of portable devices. The research work in this direction continues in different laboratories (Medyantseva et al. 2014; Varlamova et al. 2016).

Another widely used approach for the detection of mycotoxins is based on immunoassays, such as enzyme immunoassay (ELISA), which mainly examines the signal produced by chromogenic substrates after the formation of the antigen-antibody complex. Immunochemical tests are easy to use due to their simplicity, multiple reading of samples, and low cost. Oliveira et al. (2019) reviewed some

Table 12.1 The main representatives of mycotoxins and their brief characteristics

Mycotoxin	Fungal species	Pathological effects and toxicities	Food commodity
Aflatoxins (AFB1, AFB2, AFG1, AFG2, AFM1, AFM2)	<i>Aspergillus flavus</i> , <i>Aspergillus parasiticus</i> , <i>Aspergillus nomius</i>	Carcinogenic, mutagenic, hepatotoxic, teratogenic, nephrotoxic, immunosuppressive	Maize, wheat, rice, spices, sorghum, ground nuts, tree nuts, almonds, oilseeds, dried fruits, cheese, spices, milk and dairy products, eggs, meat
Ochratoxin A (OTA)	<i>Aspergillus ochraceus</i> , <i>Penicillium viridicatum</i>	Nephrotoxic, hepatotoxic, neurotoxic, mutagenic, teratogenic, immunodepressants, carcinogenic, inhibition of protein synthesis	Cereals, barley, wheat, dried vine fruit, wine, coffee, oats, spices, rye, raisins, grape juice
Zearalenone (ZEN)	<i>Fusarium graminearum</i> , <i>Fusarium culmorum</i>	Carcinogenicity, immunotoxicity, genotoxicity, reproductive and developmental toxicity	Barley, oats, wheat rice, sorghum, sesame, soybeans, cereal-based products
Patulin (PAT)	<i>Penicillium expansum</i> , <i>Aspergillus byssochlamys</i>	Neurotoxicity, embryotoxicity, teratogenicity, immunotoxicity, convulsions,	Apples, apple juice, cherries, cereals, apricots, grapes, pears, peaches, olives, bilberries
Trichothecenes T2 (T-2)	<i>F. tricinatum</i> , <i>F. sporotrichiella</i> , <i>F. solani</i>	Cytotoxicity, immunodepressants, mutagenic, neurotoxic, anorexia, dermatitis, infertility	Corn, peanuts, rice
Fumonisin (FB1, FB2, FB3)	<i>F. moniliforme</i> , <i>F. anthophilum</i> , <i>F. dlamini</i> , <i>F. globosum</i> , <i>F. napiforme</i> , <i>F. nygamai</i> , <i>F. subglutinans</i>	Hepatotoxic, immunotoxic, cytotoxicity, carcinogenic, apoptosis, pulmonary edema, immunodepressants	Maize, maize products, corn-based products, sorghum, asparagus, rice, milk

types of bio- and immunosensors used for the detection of mycotoxins in detail. The aim of this chapter is to discuss the recent achievements in the development of amperometric biosensors for the determination of mycotoxins. Moreover, the role of modern nanomaterials and composites in changing the analytical capabilities of biosensors (immunosensors) has been also discussed.

12.1.1 *Enzyme Sensors*

Biosensors using enzymes, whole cells, and artificial receptors (molecular printed polymers, MIP), along with affine biosensors, provide high selectivity for binding mycotoxins. Among a sufficiently large number of enzymes known to date, only a limited number have found application in the development of biosensors. This is due to a number of reasons which mainly include the high cost of purified enzymes, as well as the difficulties associated with the choice of systems that record the result of biospecific interactions. The need for the electrochemical activity of the products of the enzymatic reaction or the substrates themselves is one of the conditions for the development of amperometric biosensors. These are the properties of compounds associated with the activity of esterases, hydrolases, and oxidoreductases. Therefore, enzymes of these classes are most often used for the development of amperometric biosensors.

Biosensors Based on Cholinesterase

Over the course of 9 years (from 2001 to 2010), as reviewed by Grieshaber et al. (2008), more than 100 research papers related to the creation of cholinesterase biosensors (CE biosensors) were published. At the same time, the possibilities of CE biosensors were considered by the example of determining irreversible inhibitors (organophosphorus insecticides and nerve poisons), pseudo-irreversible inhibitors (carbamic pesticides, insecticides, toxins), and reversible inhibitors, for example, aflatoxin B1 (AFB1).

One of the major concerns is the contamination of food products, grains, and feed by mycotoxins, which are usually produced by various fungi, has forced researchers to turn to CE again. It was shown that cholinesterase BSs based on printed graphite electrodes have the necessary sensitivity in determining one of the most toxic mycotoxins – AFB1. The detection of AFB1 is more profitable than the detection of insecticides by the CE biosensor, since reversible inhibition usually results in a complete recovery of the enzyme activity after measuring the inhibitory effect by simply washing the biosensor even with water.

The potentiometric biosensor based on AChE was developed for inhibition determination of AFB1, and a possibility in principle of the real samples analysis using the developed biosensor was shown. The working parameters of AChE biosensors for inhibition determination of AFB1 were studied and optimized. The bioselective membrane contained 1% AChE, and 4 mM AChCl was chosen as a working substrate concentration. Dynamic range of AFB1 determination was 0.2–40 µg/ml. The developed biosensor was characterized by sufficient signal reproducibility over 1 working day and could be stored for a month. An influence of the sample preparation on the biosensor operation and the matrix effect were also studied. A possibility to measure AFB1 in real samples by the biosensor developed is stated (Stepurska et al. 2015)

Biosensors Based on Horseradish Peroxidase (HRP)

Immobilized HRP biosensors can be used primarily to determine the peroxidase substrate –hydrogen peroxide. This task is very relevant: there is a need for analyses of biological fluids and other solutions for determining hydrogen peroxide due to its key role in various processes in the human body and in the environment.

Alonso-Lomillo et al. (2011) summarized the process of developing biosensors based on HRP for the determination of OTA. Biosensors were manufactured using a single screen-printing technology. Ink containing HRP was directly applied to carbon electrodes by screen printing, which ensures high speed and simplicity of the process of manufacturing biosensors for determining OTA. The change in the formal redox potential of the Fe (III)/Fe (II) pair was used to demonstrate the efficiency of the process of loading HRP as a fragment of ink. Chrono-amperometrically detected oxidation current associated with the concentration of OTA in various beer samples. Under optimal conditions, the range of working concentrations is 23.85–203.28 nmol/L. Reproducibility, expressed in relative standard deviation, was 10%. Regarding stability, the biosensor retained 30% of the initial sensitivity even after the third calibration. The LOD was 26.77 ± 3.61 nmol/L.

An amperometric biosensor based on HRP for determining the content of citrine mycotoxin in rice samples was described in Zachetti et al. (2013). The biosensor is based on the use of a carbon-paste electrode modified with carbon nanotubes included in mineral oil, HRP, and ferrocene as a redox mediator. The biosensor is coated externally with a dialysis membrane, which is fixed on the electrode. Reproducibility was 70%. The linear region of the determined contents is from 1 to 11.6 nmol/L, LOD 0.75 nmol/L. To confirm the results, a fluorimetric determination of citrine was carried out in the same rice samples. A very good correlation was obtained between electrochemical and spectrophotometric methods.

The combination of the two enzymes was very successful, which was reported in the study by Puiu et al. (2012). A kinetic approach is described for studying the interaction of AChE of electric eel and AFB1 or its protein conjugate (e.g., AFB1-HRP-) to develop a simple and sensitive method for the detection of these compounds. The dissociation constant K_d of the AChE/AFB1-HRP interaction (0.4 mM), obtained using surface plasma resonance, is very close to the inhibition constant obtained by amperometry ($K_i = 0.35$ mM). This proves that the conjugation of AFB1 with a carrier protein does not significantly affect the affinity of AFB1 for AChE. Thus, the AChE/AFB1-HRP pair can be used as a system simulating the binding of AChE to other AFB1 protein adducts and then can be used to develop biosensors for determining AFB1 bound to plasma proteins. The immobilization protocol suggested minimizing nonspecific adsorption on a self-organizing monolayer of the functionalized surface of the surface plasma resonance chip without additional hydrophilic components. At the same time, the immobilization process was developed in such a way as to prevent the possible occurrence of mass transfer restriction effects during the operation of the biosensor. The LOD was 0.008 mM for AFB1-HRP (2.5 ng/ml) and 0.94 ng/ml for AFB1 itself, which is lower than for spectrophotometric and amperometric analyses.

Biosensors Based on Aflatoxin Oxidase

Li et al. (2011) first developed an amperometric biosensor for determining AFB1 based on immobilized aflatoxin oxidase incorporated in a sol-gel, which was deposited on a platinum electrode modified by multilayer carbon nanotubes (MLCNs). The covalent bond between aflatoxin oxidase and MLCNs made it possible to maintain enzyme activity and sensitive response to the oxidation of AFB1. The apparent Michaelis-Menten constant for AFB1 is 7.03 mmol/L. The sensor allowed us to obtain a linear dependence in the concentration ranges from 3.2 nmol/L to 721 nmol/L (from 1 ng/ml to 225 ng/ml) with a LOD of 1.6 nmol/L (signal-to-noise ratio is 3), average response time of 44 s (at a concentration of AFB1 greater than 45 ng/ml – in less than 30 s.), and a high sensitivity coefficient. The activation energy was 18.8 kJ/mol, which indicates a large value of the catalytic effect of aflatoxin oxidase during the oxidation of AFB1 for this biosensor. Aflatoxin oxidase covalently attached to multiwalled CNTs has been successfully used to detect AFB1, which turns into an oxidized form with oxygen consumption and the formation of H₂O₂.

Thus, amperometric biosensors are a very successful application for the analysis of objects infected with mycotoxins. It can be noted that today the process of sensitivity and selectivity of determinations can be controlled using different options for immobilizing enzymes on the surfaces of various detectors, including those modified with various nanomaterials. The combination of the two enzymes also contributes to the improvement of mycotoxin determination methods. And finally, the use of narrowly targeted enzymes (using aflatoxin oxidase as an example) improves the selectivity of determinations.

Medyantseva et al. (2012, 2014) proposed new amperometric biosensors for the determination of mycotoxins based on modified multiwalled carbon nanotubes (MLCNs), planar platinum electrodes, and immobilized enzymes: CE, cysteine desulphydrase, alkaline phosphatase, and tyrosinase. Mycotoxins have shown to exhibit the properties of reversible inhibitors: OTA and ZEN-ChE, AFB1, OTA, and ZEN-alkaline phosphatase and CDG-patulins-alkaline phosphatase-ZEN-tyrosinase, which allows their determination using appropriate modified MLCN biosensors in the concentration range from $n \times 10^{-(5-6)}$ to $n \times 10^{-(9-12)}$ mol/L. The use of a modifier allows you to expand the range of detectable concentrations; reduce LOD, by no less than an order of magnitude; increase the sensitivity coefficient; improve the correlation coefficient; and obtain more reproducible results compared to the unmodified version of biosensors.

The kinetic parameters of the reactions of the enzymatic conversion of substrates in the presence of enzyme sensors and mycotoxins in the corresponding concentration ranges for each case are estimated. It would be necessary to specify. The proposed biosensors were tested in the analysis of grain crops (wheat, barley, corn) and animal feed (bran of cereal crops) in Russia and Vietnam, and food products (peanut kernels, buckwheat, apples, apple juice) allowed to detect mycotoxins at and below maximum allowable concentration (MAC) with relative standard deviation no more than 0.076.

Amperometric biosensors based on planar platinum electrodes modified with multilayer carbon nanotubes, gold nanoparticles, and an immobilized enzyme (tyrosinases) are designed to detect patulin mycotoxin in the concentration range of 1×10^{-6} – 8×10^{-12} mol/L with an error of no more than 0.063. The results were used to control the content of patulin in foods (Fig. 12.1) (Varlamova et al. 2016).

New amperometric biosensors have been proposed for the determination of AFM1 based on modified CNTs, graphene oxide (GO), and gold nanoparticles (Au NPs) in chitosan of planar platinum electrodes and an immobilized tyrosinase enzyme. It has been established for the first time that AFM1 exhibits the properties of a reversible tyrosinase inhibitor, which allows its determination using biosensors modified with nanomaterials in the concentration range of 1×10^{-6} – 1×10^{-11} mol/L, with c_{H} 5×10^{-12} mol/L. The kinetic parameters of the enzymatic conversion of phenol in the presence of a tyrosinase biosensor modified with CNT, GO, AuNPs, and mycotoxin M1 were estimated. The proposed enzyme sensors based on tyrosinase have been used to test methods for determining AFM1 in food products (Varlamova et al. 2019).

12.1.2 Enzyme-Linked Immunosorbent Assay (ELISA) for the Determination of Mycotoxins

For the determination of mycotoxins, various variants of the highly sensitive enzyme-linked immunosorbent assay (ELISA) are widely used. They allow you to get accurate results and use minimally purified and even untreated extracts. It should be noted that recently a number of review articles have appeared on the problems of

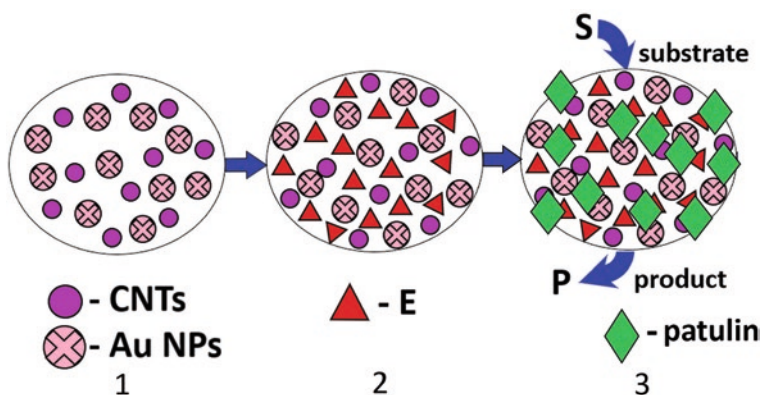


Fig. 12.1 Scheme of the action of a biosensor based on immobilized tyrosinase includes graphite screen-printed electrode with CNTs and AuNPs (1), with immobilized enzyme (tyrosinase) (2), with patulin in solution (3). *E* enzyme, *CNTs* carbon nanotubes, *AuNPs* gold nanoparticles, *S* substrate, *P* product of the enzymatic reaction

mycotoxin ICA, which summarize the relevant literature on this issue (Gogin 2005), which is presented in this section.

A new amperometric immunosensor for supersensitive detection of ZEN based on mesoporous carbon (MC) and trimetallic nanograys (core/shell particles with moving cores enclosed in shells) is proposed. MC improves the sensitivity of the immunosensor due to its extremely large specific surface area, corresponding pore location, and good conductivity. Rattles are composed of an Au core and an imperfect (defective) AgPt-shell structure (Au/AgPt) and are retained in the MC by physical adsorption. The method of X-ray spectroscopy confirmed the composition of the synthesized nanopowders. Compared to monometallic and bimetallic nanoparticles (NPs), Au/AgPt nanopowders show a higher electron transfer rate due to the synergistic effect of NPs of Ag and Pt. Ab to ZEN was immobilized on nanorotations through Ag-NH₂ and Pt-NH₂ groups. An immunosensor based on cyclic and square-wave voltammetry makes it possible to determine ZEN with a LOD of 1.7 µg/ml and has a wide linear range of detectable concentrations from 0.005 to 15 ng/ml, as well as good stability, reproducibility, and selectivity of results. It is possible to use the sensor in clinical analysis (Liu et al. 2014).

An electrochemical immunosensor consisting of magnetic balls and disposable printed electrodes was used to determine the ZEN in baby food samples. The number of paramagnetic balls is limited by the surface of the modified printed electrode, where electrochemical detection is achieved by the participation of the substrate and the mediator for HRP LOD is 0.007 µg/L (Hervas et al. 2010).

Another variant of immunoassay was developed by Mai (2013). Since AFB1 is one of the most dangerous toxins causing aflatoxicosis, an enzyme-linked immunosorbent sensor was developed to detect AFB1 using tyrosinase as an enzyme label. The range of working concentrations of the developed immunosensor for determining AFB1 was 1×10^{-6} – 1×10^{-12} mol/L. Low percent cross-reactivity for other mycotoxins indicates a high selectivity for the determination of AFB1. The binding constants of the formed immune complexes Ab-AFB1: $K_{a1} = (6.9 \pm 0.2) \times 10^{10}$ mol/L and $K_{a2} = (2.7 \pm 0.1) \times 10^9$ mol/L. The developed immunosensors were used to

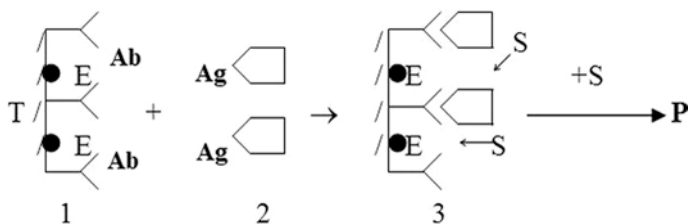


Fig. 12.2 Scheme of the action of an immunosensor based on immobilized Ab against AFB1 and tyrosinase includes co-immobilized enzyme (tyrosinase) and Ab (1), Ag in solution - AFB1 (2), the formed immune complex and options for approaching the substrate to the active surface of the enzyme (3). *T* transducer, *E* enzyme, *Ab* antibody, *Ag* antigen, *S* substrate, *P* product of the enzymatic reaction

control the content of AFB1 in food (nuts), which made it possible to determine this mycotoxin at and below the MAC (Fig. 12.2).

Immunosensors for Detecting Mycotoxins with Horseradish Peroxidase as a Label

Peroxidase is one of the most studied enzymes and is most often used as a label for one of the biocomponents in biosensors based on the principles of immunochemical recognition. The use of the enzyme significantly increases the sensitivity of the method. Due to the relatively low cost of peroxidase in comparison with fluorescent or radioactive labels, peroxidase biosensors are widely used.

Istamboulié et al. (2016) reported the development of an electrochemical immunosensor for detecting ultra-trace amounts of AFM1 in food products. The sensor was based on competitive immunoassay using HRP as a label. Ab-coated magnetic NPs were used to separate bound and unbound fractions. Samples containing AFM1 were incubated with a certain amount of Ab and HRP conjugate. The resulting mixture was applied to the surface of a planar graphite electrode, and, in the presence of an organic mediator [5-methylphenazinium methyl sulfate], the electrochemical response was evaluated chronoamperometrically. Such an immunosensor has a LOD of 0.01 ppb, which is below the maximum allowable concentration for milk.

To determine OTA in wine samples, an electrochemical immunosensor was developed using a printed gold working electrode and the Ag/AgCl system as a pseudo-comparison electrode (Heurich et al. 2011). A competitive enzyme-linked immunosorbent assay was carried out with an immobilized OTA conjugate, which was achieved by passive adsorption or covalent immobilization using an amine bond with a carboxymethylated dextran hydrogel onto a gold working electrode. Electrochemical detection was carried out using TMB and H₂O₂ and HRP as the enzyme label. Chronoamperometry at -150 mV was used to register the generated signal. As a result, the immunosensor for OTA reached a LOD of 0.5 µg/L with a linear range of detectable concentrations of 0.1–10 µg/L for passive adsorption of toxin conjugants, while for covalent immobilization on a gold electrode modified with a hydrogel of carboxymethylated dextran, the LOD was 0.05 mcg/l with a linear range of concentrations of 0.01–100 µg/L. The modified gold immunosensor was tested in the analysis and affinity-purified wine samples. LOD in buffer solutions amounted to 0.05 µg/L.

12.1.3 Aptasensors for Detecting Mycotoxins

Aptamers are short oligonucleotide sequences obtained by combinatorial chemistry and selected against the target analyte. They offer a wide range of functions, including an affinity for mycotoxins and modifications necessary for implementation in the assembly of biosensors, also called aptasensors (Evtugyn and Hianik 2020).

Yang et al. (2020) successfully constructed a novel electrochemical aptasensor for sensitive and selective detection of AFB1. The thiolated complementary strand (cDNA) of the AFB1 aptamer was immobilized on the surface of the GCE modified with AuNPs through Au-S bond. The aptamer was attached on the surface of GCE via by specific base pairing. In the presence of AFB1, the aptamer was detached from the electrode surface by specific recognition between the AFB1 and aptamer, forming aptamer-AFB1 conjugates in solution. The conjugates were digested by exonuclease I to trigger AFB1 recycling. DNA-AuNPs-HRP nanoprobe were bound with cDNA on the surface of electrode by specific base pairing. HRP could catalyze the oxidation of hydroquinone (HQ) to benzoquinone (BQ) by H_2O_2 for producing a strong electrochemical signal. The electrochemical signals increased with increasing concentrations of AFB1 in a range from 10^{-3} ng/ml $^{-1}$ to 200 ng/ml $^{-1}$ with a low detection limit of 3.3×10^{-4} ng/ml $^{-1}$. The aptasensor has been applied for the determination of AFB1 in peanuts and corn samples and the recoveries were 88.5%–110.2%.

An electrochemical aptasensor based on competitive immunoassay for the determination of OTA was described by Bonel et al. (2011). The OTA-specific aptamer was functionalized with magnetic beads and competed with mycotoxin conjugated to HRP (HRP-OTA) and free OTA. After the separation and purification step for magnetic separation, the aptamers modified with paramagnetic beads were immobilized on disposable graphite-printed electrodes in a magnetic field, and the product of the enzymatic reaction with the substrate was detected by differential-pulse voltammetry. Magnetic separation results were previously tested, optimized, and compared with other competitive immunoassay schemes (direct/indirect with the aid of an aptasensor immobilized on the surface of disposable printed graphite electrodes or with the participation of an aptamer functionalized using gold nanoparticles). The magnetic immunosensor showed a linear response to OTA in the range of 0.78–8.74 ng/ml, with LOD of 0.07 ± 0.01 ng/ml, and was accurately applied to extracts of certified wheat ears with a relative standard deviation of at least 8%.

Prabhakar et al. (2011) developed a highly sensitive impedimetric aptasensor based on a Langmuir-Blodgett film (polyaniline-stearic acid) containing a DNA aptamer specific for OTA supported on the indium-tin-oxide electrode for determining OTA. It has been proven that the aptasensor operates in a linear concentration range from 0.0001 μ g/ml (0.1 ng/ml) to 0.01 μ g/ml (10 ng/ml) and 1 μ g/ml–25 mg/ml with a LOD of 0.1 ng/ml. Analysis time does not exceed 15 min. The aptasensor can be reused about 13 times. The binding constant of the aptamers with OTA, calculated using the Langmuir adsorption isotherm, was 1.21×10^7 M $^{-1}$.

For a sensitive determination of OTA, Barthelmebs et al. (2011) formed a new electrochemical aptasensor based on disposable printed electrodes. Two strategies for determining OTA were investigated: using indirect and direct competitive analysis based on the use of superparamagnetic nanoparticles. The characteristics of modified aptasensors, such as reproducibility, stability, sensitivity, and analysis time, were studied. The best characteristics were obtained by implementing a direct competitive analysis format. In this case, free OTA competed with labeled alkaline phosphatase OTA; in this case, magnetic beads were immobilized to bind OTA to

the DNA aptamer. For electrochemical detection due to the conversion of the corresponding substrate for the alkaline phosphatase enzyme, differential pulse voltammetry was used. The developed aptasensor made it possible to achieve LOD of 0.11 ng/ml. The range of working concentrations is from 0.11 to 0.15 ng/ml.

12.2 Conclusion and Future Perspectives

The chapter is devoted to issues related to the analytical capabilities of some types of amperometric biosensors (immunosensors) for the determination of mycotoxins in various objects – food, animal feed, and cereals. The prevalence and high toxicity have led to the fact that the focus on the development of appropriate biosensors is given to the determination of aflatoxins (AFB1 and M1), ZEN, and OTA. The most common transducers (primary converters) in such biosensors (immunosensors) are printed graphite electrodes, although GCE continues to be used successfully in these devices (biosensors).

For the development of amperometric biosensors, enzymes of the esterase, hydrolase, and oxidoreductase class are most often used, due to the electrochemical activity of the products of the enzymatic reaction or the substrates themselves. A separate section is devoted to the use of HRP as a label, which helps to reduce the LOD of mycotoxins.

Another technique that is currently widely used to improve analytical characteristics is the modification of the surface of electrodes with various carbon materials, metal nanoparticles, and composites based on them in combination with various matrix materials. All this contributes to an increase in the working area of the electrodes and, as a result, to an increase in the analytical signal. All this leads to an improvement in the sensitivity of determinations and determination of mycotoxins at and below the MAC.

Thus, modern analytical needs for the determination of mycotoxins can be successfully implemented using amperometric biosensors. The goal is to bring research results to consumers, i.e., in the commercialization of related developments. Despite the excellent analytical characteristics in many cases, it should be noted that the problem remains the preservation of immunological and catalytic properties of biocomponents in the composition of biosensors over time.

References

- Alonso-Lomillo MA, Domínguez-Renedo O, Torno-de Romón L, Arcos-Martínez MJ (2011) Horseradish peroxidase-screen printed biosensors for determination of Ochratoxin A. *Anal Chim Acta* 688:49–53
- Barthelmebs L, Hayat A, Limiadi A, Marty J, Nogue T, Barthelmebs L (2011) Electrochemical DNA aptamer-based biosensor for OTA detection, using superparamagnetic nanoparticles. *Sensors Actuators B* 54:2180–2218

- Bonel L, Vidal JC, Duato P, Castillo JR (2011) An electrochemical competitive biosensor for ochratoxin A based on a DNA biotinylated aptamer. *Biosens Bioelectron* 26:3254–3259
- Evtugyn G, Hianik T (2020) Aptamer-based biosensors for mycotoxin detection. In: *Nanomycotoxicology: treating mycotoxins in the nano way*. Elsevier, London, pp 35–70
- Gogin A (2005) Mycotoxins: effective control effective production. *Compound Feed J* 2:68–70
- Grieshaber D, MacKenzie R, Voros J, Reimhult E (2008) Electrochemical biosensors – sensor principles and architectures. *Sensors* 8(3):1400–1458
- Haque MA, Wang Y, Shen Z, Li X, He C (2020) Mycotoxin contamination and control strategy in human, domestic animal and poultry: a review. *Microb Pathog* 142:104095. <https://doi.org/10.1016/j.micpath.2020.104095>
- Hervas M, Lypez AM, Escarpa A (2010) Simplified calibration and analysis on screen-printed disposable platforms for electrochemical magnetic bead-based immunosensing of zearalenone in baby food samples. *Biosens Bioelectron* 25:1755–1760
- Heurich M, Kadir M, Tothill IE (2011) An electrochemical sensor based on carboxymethylated dextran modified gold surface for ochratoxin A analysis. *Sensors Actuators* 156:162–116
- Istamboulié G, Paniel N, Zara L, Granados LR, Barthelmebs L, Noguer T (2016) Development of an electrochemical biosensor for the detection of Aflatoxin M1 in milk. *Talanta* 146:464–469
- Li S, Chen J, Cao H, Yao D, Liu D (2011) Amperometric biosensor for aflatoxin B1 based on aflatoxin-oxidase immobilized on multiwalled carbon nanotubes. *Food Control* 22:43–49
- Liu LA, Chao Y, Cao W, Wang Y, Luo C, Pang X, Fan D, Wei Q (2014) Label-free amperometric immunosensor for detection of zearalenone based on trimetallic Au-core/AgPt-shell nanorattles and mesoporous carbon. *Anal Chim Acta* 847:29–36
- Mai TTH (2013) Amperometric biosensors for the detection of some mycotoxins. PRhD dissertation. Kazan Federal University. Kazan:148
- Medyantseva EP, Mai TTH, Varlamova RM, Tarasova EY, Sahapova GR, Budnikov HC (2012) Amperometric biosensors for determining ochratoxin A. *Kazan Univ Ser Nat Sci* 154:92–104
- Medyantseva EP, Mai TTH, Tarasova EY, Sahapova GR, Nikolaeva OV, Budnikov HK (2014) Amperometric biosensors based on alkaline phosphatase and carbon nanotubes for the detection of certain mycotoxins. *Factory laboratory diagnostics of materials*. 80:5–12
- Oliveira IS, Junior AGS, Andrade CAS, Oliveira MDL (2019) Biosensors for early detection of fungi spoilage and toxigenic and mycotoxins in food. *Curr Opin Food Sci* 29:64–79
- Prabhakar N, Matharu Z, Malhotra BD (2011) Polyaniline Langmuir–Blodgett film based aptasensor for ochratoxin A detection. *Biosens Bioelectron* 26:4006–4011
- Puiu M, Istrate O, Rotariu L, Bala C (2012) Kinetic approach of aflatoxin B1–acetylcholinesterase interaction: a tool for developing surface plasmon resonance biosensors. *Anal Biochem* 421:587–594
- Stepurska KV, Soldatkin OO, Arkhypova VM, Lagarde F, Jaffrezic-Renault N, Dzyadevych SV (2015) Development of novel enzyme potentiometric biosensor based on pH-sensitive field-effect transistors for aflatoxin B1 analysis in real samples. *Talanta* 144:1079–1084
- Varlamova RM, Medyantseva EP, Hamidullina RR, Budnikov HC (2016) Determination of patulin by amperometric tyrosinase biosensors based on electrodes modified with carbon nanotubes and gold nanoparticles. *Sci Notes Kazan Univ Ser Nat Sci* 158:351–368
- Varlamova RM, Medyantseva EP, Hamidullina RR, Budnikov HC (2019) Amperometric tyrosinase biosensors based on modified nanomaterials electrodes for the determination of aflatoxin M1. *J Anal Chem* 74:71–80
- Yang H, Zhang Q, Liu X, Yang Y, Yang Y, Liu M, Li P, Zhou Y (2020) Antibody-biotin-streptavidin-horseradish peroxidase (HRP) sensor for rapid and ultra-sensitive detection of fumonisins. *Food Chem* 316:126356. <https://doi.org/10.1016/j.foodchem.2020.126356>
- Zachetti VGL, Granero AM, Robledo SN, Zon MA, Fernández H (2013) Development of an amperometric biosensor based on peroxidases to quantify citrinin in rice samples. *Bioelectrochemistry* 91:37–43

Chapter 13

The New Class of Diagnostic Systems Based on Polyelectrolyte Microcapsules for Urea Detection



Sergey A. Tikhonenko, Alexey V. Dubrovskii, Aleksandr L. Kim,
and Egor V. Musin

Abstract The chapter describes new diagnostic systems for analysis of urea concentration based on polyelectrolyte microcapsules containing urease. In the first case, urea concentration was determined using both loose microcapsules (microdiagnosticum) and fixed on a solid surface (diagnostic plate). The multiple uses of the microdiagnosticum and the diagnostic plate were shown; the results obtained have deviations that do not exceed the threshold value of 9.6%. The concentration of urea in blood serum was determined by the modified Berthelot method using a diagnostic plate instead of a free enzyme. We also determined urea in the urine using microdiagnostics. The next diagnostic system was a microdiagnostic with an encapsulated enzyme, the functioning of which was recorded by the sedimentation method. The method consisted in changing the mass of polyelectrolyte microcapsules depending on the urea content in the medium. The possibility of multiple use of the created microdiagnosticum for the analysis of urea solutions is shown. An ionic precipitant is selected, which forms an insoluble carbonate inside the microcapsule, and a microcapsule titer is established, which is optimal for the functioning of the microdiagnosticum. The third diagnostic system option was a biosensor based on a pH-sensitive field-effect transistor (FT). Polyelectrolyte microcapsules with embedded paramagnetic Fe_3O_4 particles and a urease enzyme capable of biotransformation of urea were used as bioreceptors. The bioreceptor was formed on the gate surface of the transistor using a constant magnetic field. The deposition of microcapsules in the gate area was due to the presence of paramagnetic particles in the bioreceptor. This method of biosensor formation took several seconds and did not require additional chemicals to treat the electrode surface before and after the measurement. The biosensor has been tested on real milk samples.

Keywords Microdiagnosticum · Encapsulated enzyme · Diagnostic system · Urea diagnostic · Field-effect transistor · Biosensor · Magnetic field immobilization

S. A. Tikhonenko (✉) · A. V. Dubrovskii · A. L. Kim · E. V. Musin
Institute of Theoretical and Experimental Biophysics, Russian Academy of Science,
Moscow, Russia

Nomenclature

CDL	Clinical diagnostic laboratories
PMC	Polyelectrolyte Microcapsules
FET	field-effect transistor
EDTA	Ethylenediaminetetraacetic Acid
PSS	Polystyrenesulfonate
PAH	Polyallylamine
PEI	Polyethyleneamine
QP	Quartz Plate
I _c	drain current
U _z	gate voltage

13.1 Introduction

Clinical biochemistry is an integral part of modern medicine. The most important determined substrates are urea, lactate, creatinine, glucose, and others. The most common among substrates is urea, the nitrogen containing the end product of protein catabolism. An increased level of urea in the blood is associated with hyperuricemia caused, for example, by dehydration, increased protein catabolism, decreased renal perfusion, and with other pathologies.

At the moment, the most widespread are enzymatic methods of analysis based on the use of free enzymes (Dolgov and Selivanova 2006; Menshikov et al. 2009). Enzymological methods of analysis are based on the use of chemical reactions involving enzymes. The content of the component to be determined is detected either by the quantity of the end product of the enzymatic reaction (end-point method) or by the initial speed of the process (enzymatic kinetics method). However, there are a few drawbacks inherent in these methods: the ambiguity of the analysis in the presence of high molecular weight compounds that are aggressive to the enzyme, the relatively short storage time, a single use of the enzyme, etc.

One way to remedy these deficiencies is to immobilize enzymes (Mohamad et al. 2015). So, the technology on the inclusion of enzymes in the gel has become widely used, since it is quite simple and allows coping with the tasks set. For example, the hybrid alginate–gelatin–calcium matrix has high sealability, which allows reducing the yield of the enzyme in the analyzed medium and providing a higher degree of mechanical stability (Shen et al. 2011). The inclusion of lipase in κ -carrageenan increased its thermal stability and resistance to organic solvents (Tümtürk et al. 2007; Jegannathan et al. 2010). Berdnikov with co-authors in 2004 suggested immobilizing urease on the surface of a glass electrode with a gelatin membrane or an acrylamide gel layer. This electrode can detect ammonium ions, which are formed as a result of catalytic decomposition of urea. The electrode determines their

level in the thickness of the gel, and as a result, the urea concentration can be calculated from the measured potential.

In addition, polymer coatings obtained by successive adsorption of oppositely charged polyelectrolytes and intended for use as coatings of hard surfaces of arbitrary shape are known (Decher and Hong, 1993). The attachment of enzyme molecules having a corresponding electrostatic charge between polyelectrolyte layers is described by Lvov and Sukhorukov (1997). The disadvantage of this technology is the close contact of the molecules of the immobilized enzyme with the surrounding layers of the polyelectrolyte film, which is able to inactivate the enzyme-sensor and the relatively low content of molecules of the immobilized enzyme per unit area of the coating, which can be increased only by increasing the number of layers of the enzyme in the multilayer coating.

Further development of this technology is polyelectrolyte microcapsules (PMC), which are used to immobilize enzymes (Bobreshova et al. 1999). Such capsules are obtained by alternately adsorbing the oppositely charged polyelectrolytes onto a colloidal particle, followed by its removal (Donath et al. 1998). These microcapsules have a diameter of 0.5–10 μm , with a semipermeable shell, the composition and thickness of which can be controlled (Mayya et al. 2003; Shenoy et al. 2003; Sukhorukov et al. 2005).

In the final version, the technology for producing polyelectrolyte microcapsules consists of three stages. The first stage is the preparation of CaCO_3 -core containing the enzyme. The second stage is the sequential layering of selectively selected oppositely charged polyelectrolytes on the core particles and the formation of a multilayer shell. The third stage is the destruction and removal of the core particle. Schematically, this technology is presented in Fig. 13.1.

An important property of the PMC shell is its semipermeability—permeability to low molecular weight compounds and impermeability to high molecular weight substances and large particles. Due to this property of the polyelectrolyte shell, the microcapsule containing the enzyme and placed in a multicomponent medium

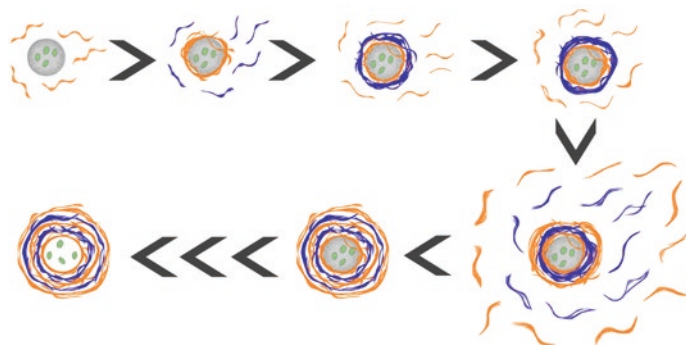


Fig. 13.1 Technology to produce polyelectrolyte microcapsules. Stage 1—Formation of CaCO_3 core containing enzyme; stage 2—layering of polyelectrolytes on the core; stage 3—dissolution of the core particle

becomes an analyzer of low molecular weight substances—substrates, inhibitors, or activators of the encapsulated enzyme.

The use of encapsulated enzymes in PMC has several advantages over the use of native enzyme. Sukhorukov et al. (2007) have shown that the encapsulated urease retains its activity for more than six months, while the native enzyme is only a week; in addition, the protein was not affected by the negative effects of proteases in solution.

Kazakova et al. (2011) used microcapsules containing a pH-sensitive fluorescent probe (SNARF-1) and urease, and this system was used to develop a urea sensor capable of determining the local pH of the medium. In the works of Reshetilov et al. (2015, 2016), a potentiometric sensor based on PMC containing urease was described for the determination of urea in milk and blood.

Despite the advantages of diagnostic systems based on polyelectrolyte microcapsules, such as protecting encapsulated enzymes from unfavorable external influences and preserving their enzymatic activity for a long time, there are disadvantages. The main disadvantage is the difficulty of conducting the analysis with the help of microcapsules, as well as fluorescent recording systems, which are not common in the modern clinical diagnosis of low molecular weight compounds. In connection with these, there is a need to modify existing clinical and diagnostic analyses without significantly complicating the procedure for their conduct. In this chapter, several such modifications are showed, which make it possible to carry out analyses in clinical diagnostic laboratories.

In this chapter, a diagnostic system for low molecular weight compounds based on enzymes encapsulated in polyelectrolyte microcapsules, microdiagnostics, is demonstrated.

One of the main advantages of the proposed microdiagnostics is multiple use by extracting microcapsules from the reaction medium and their subsequent practice. Encapsulation of enzyme-sensor increases the stability of the enzyme in solution and longer storage of diagnostic systems.

So, Kim et al. (2019) suggest using a filtering method to extract microcapsules from a reaction medium for reuse.

It was found that measurements carried out using microcapsules recovered by the filtration method give reproducible results when they are reused. The spread of values between repetitions did not exceed 3%, which fully meets the requirements for this type of diagnostic reagents.

Similarly, we studied the possibility of multiple use of PMC containing urease to determine the concentration of urea in the analyzed liquid in a wide range of its concentrations. We studied the dependence of the microdiagnosticum response on the urea concentration in the solution over a wide range of measurements with repeated use. It was found that the measurements are linear in nature, and the deviation from linearity is 7%. The measurements were carried out using the same capsules (more than 50 times).

13.2 Practical Use of Microdiagnosticum as Diagnostic System

The possibility of using polyelectrolyte microcapsules with the enzyme included for the analysis of biological fluids was demonstrated. For this, the urinary content of the urine of two volunteers was determined using a microdiagnosticum with encapsulated urease. The urea concentration in the biological fluid of each volunteer was measured at least 8 times using the same capsules, removing the capsules by filtration. The obtained data were compared with the results of measuring the urea concentration in the urine of the same subjects using the “Urea EP DDS” kit of Diakon-DS (Kit for measuring the urea concentration in the urine).

It can be seen from the Table 13.1 that the data obtained using the microdiagnosticum and the “Urea EP DDS” kit are practically the same; the spread of the data does not exceed 3%, which indicates the reliability of the results obtained and the possibility of using a microdiagnosticum in clinical and biochemical analysis.

Despite the obvious advantages of the proposed microdiagnosticum, its main disadvantage is the laboriousness of use its extraction from the analyzed medium. To eliminate this drawback, we propose fixing microcapsules with the included proteins—sensors on a solid surface and the creation on their basis of a diagnostic plate.

Table 13.1 Comparative results of application of microdiagnosticum and a kit of the “Diakon” company for determination of urea concentration in biological fluid (urine)

	Microdiagnosticum (average of n measurements.)		“Diakon” kit	
	Optical density, 540 nm	Urea concentration, mM	Optical density, 540 nm	Urea concentration, mM
Calibrator (E_k)	0.14	8.3	0.065	8.3
1 volunteer (E_0) ($n = 10$)	0.093 ± 0.004	540 ± 20	0.043	549
2 volunteer (E_0) ($n = 8$)	0.107 ± 0.0045	621 ± 23	0.049	625.7

The concentration of urea (C) in daily urine was determined by the formula:

$$C \text{ (mmol/day)} = \frac{E_0 \times V \times 100}{E_k} * 8.3$$

V – the amount of urine collected per day, L;

100 – coefficient of dilution of urine;

8.3 – urea concentration in the calibrator, mmol/L.

13.2.1 Fixing Polyelectrolyte Microcapsules on a Quartz Plate

To fix the microcapsules on the quartz plate, a method was developed to apply polymer layers to the quartz plate (QP). To make its surface electrostatic properties, the polyethylene imine (PEI) mesh polymer was used. Later, using the technology of alternate adsorption, polymers were applied to the quartz plate, the fact of fixing of which was registered spectrophotometrically using the absorption peak of the PSS (wavelength 225 nm).

Subsequently, the polyelectrolyte microcapsules of the composition (PSS/PAH)₂ were fixed on the resulting polymer film, the surface charge of which is the opposite of the charge of the capsules. In the last step, the microcapsules were fixed with additional layers of polyelectrolytes, and the CaCO₃ cortex was removed from the PMC using an EDTA solution (the scheme of this technology is shown in Fig. 13.2).

It can be seen from the above that this method allows fixing polyelectrolyte microcapsules on the surface of a solid carrier, which opens the possibility for creating a diagnostic plate based on the encapsulated enzyme, which retains its activity, and due to the semipermeability of the coating, the substrate from the solution can freely penetrate to the enzyme.

13.2.2 Multiple Uses of the Diagnostic Plate

Multiple uses of the diagnostic plate which happens due to extracting of sensor component of it from analyze middle is the main advantage of the diagnostic plate. Apportunity of Multiple extraction of the diagnostic plate from analyze middle is the main advantage of this diagnostic system.

The spectrophotometric Berthelot method was modified by replacement of urease to the diagnostic plate, which contained on its surface polyelectrolyte microcapsules with encapsulated urease for using.

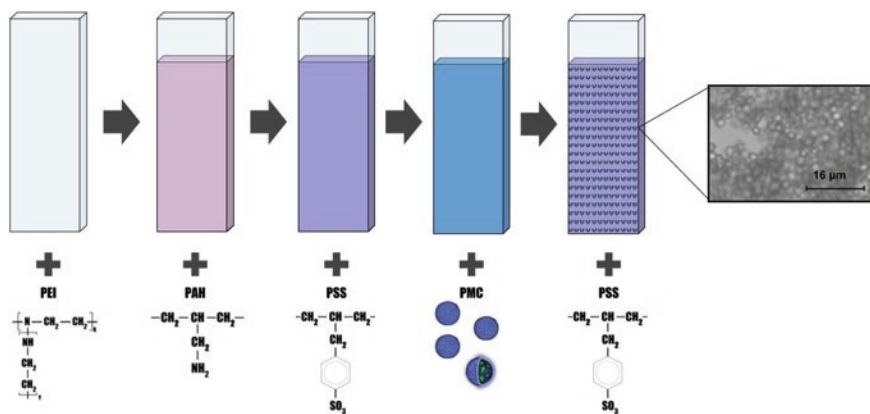


Fig. 13.2 The technology of fixing PMC on a quartz plate

The optical densities of different concentration of urea were obtained using the only diagnostic plate with fixed PMC with encapsulated urease. When the diagnostic plate is reused, the deviations do not exceed the threshold value of 9.6%.

Similarly, the possibility reusing a diagnostic plate containing urease was studied to determine the urea concentration in the analyzed liquid over a wide range of its concentrations. Based on these data, a calibration curve has been constructed, which allows us to further determine the concentration of urea in solutions with multiple use of the diagnostic plate.

13.2.3 *Detection of Urea Concentration in Blood Serum*

In addition, work was carried out to study the possibility of using diagnostic plates for the analysis of biological fluids. To do this, blood serum was taken from five volunteers, and the urea concentration was determined according to the standard urease method of Berthelot using both a free enzyme and a diagnostic plate, and these results are shown in Table 13.2. From Table 13.2, the measurement data with free enzyme and diagnostic plate differ by no more than 4.26%.

13.2.4 *Development of Polyelectrolyte-Based Enzymatic Diagnosticum with Precipitation Detection System for Urea Assay in Solution*

We have proposed yet another original diagnostic system for the detection and quantitative analysis of biologically active substances in various aqueous media based on polyelectrolyte microcapsules (Dubrovsky et al. 2017). The essence of this technique is to change the sedimentation rate of microcapsules with the enzyme included in them, depending on the concentration of an analyte in the diagnosed solution.

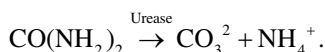
Polyelectrolyte capsules with urease incorporated in them were prepared on CaCO_3 -urease composite spherulites by sequential adsorption of PSS and PAH. To solve this problem, capsules of the form $(\text{PSS} / \text{PAH})_3 / \text{PSS}$ were obtained.

Table 13.2 Comparison of the results of using the standard urease method of Berthelot using a free enzyme and a diagnostic plate

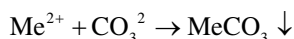
Sample	Diagnostic plate, mM	Standard deviation, %	Enzyme, mM	Standard deviation, %
1	16.2	3.14	15.9	1.73
2	10.9	4.19	11.3	2.21
3	19.3	2.2	20.1	1.43
4	15.4	1.5	15.9	3.62
5	38.2	3.75	39.9	2.1

A study of the catalytic ability of urease included in microcapsules showed that although its activity is significantly reduced, this does not significantly affect the possibility of using these capsules as sensors. The activity of the encapsulated enzyme remains almost unchanged for several months.

In aqueous solutions, urease catalyzes degradation of urea to CO_3^{2-} and NH_4^+ :



In the presence of divalent metals (Me^{2+}), for example Ca^{2+} or Ba^{2+} , carbonic acid, arising within capsules with urease, forms an insoluble precipitate of MeCO_3 :



If urease is in polyelectrolyte capsules, then the catalytic decomposition of urea and the formation of carbonate will occur directly inside the capsules (Antipov et al. 2003). The interaction of the resulting carbonate anion with the metal cation from the surrounding solution leads to the formation of a MeCO_3 precipitate.

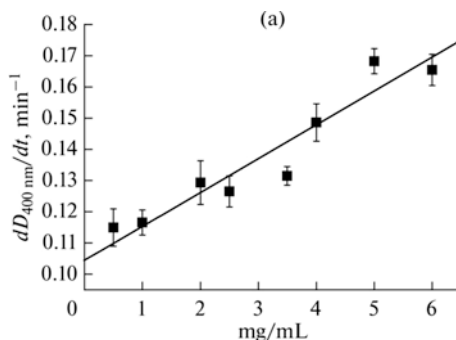
Since the polyelectrolyte shells of the capsules are well permeable to low molecular weight compounds, it is necessary that the concentration of metal cations inside the capsule be high, which will lead to almost complete binding of the carbonate inside the capsule and will not allow it to escape through the shell and form a precipitate in the solution.

The capsules (2×10^7 titre) were placed in 1 M barium chloride and incubated for 15 min. After the capsules were saturated with the Ba^{2+} ions, urea was introduced, and the mixture was incubated for another 30 min at 25 °C. Next, the capsules were removed from the reaction by centrifugation at 1500 g, the supernatant was decanted, and the precipitate was resuspended in a 0.05 M tris-HCl buffer (pH 6.2). Furthermore, the precipitated microcapsules saturated with barium carbonate were analyzed in this dispersion system to evaluate the dependence of the optical density on time. The measurements were carried out at 400 nm. The dependence of the suspension optical density on the urea concentration 5 min after the start of precipitation is shown in the Fig. 13.3. The linearity of this dependence made possible to use it as a calibration plot for measurements of urea contents in solutions.

13.2.5 Reuse of Microdiagnosticum

One of the advantages of the developed microdiagnosticum is the reutilization of the urease polyelectrolyte capsules. The microcapsules used for the calibration plot (Fig. 13.3) were centrifuged, suspended in 0.2 M EDTA, and incubated for 12 h until all barium carbonate was dissolved. Next, the capsules were washed with water three times and used to build another calibration plot.

Fig. 13.3 Dependence of optical density of the microcapsule suspension on urea content



The linear nature of this curve allows us to conclude that it is possible to reuse urease-containing polyelectrolyte microcapsules as a microdiagnosticum.

13.2.6 Polyelectrolyte Microcapsules with Urease and Paramagnetic Particles as a Basis for a Potentiometric Biosensor for Determining Urea

Further, we proposed a potentiometric diagnostic system developed on the basis of microcapsules with urease and paramagnetic particles (Reshetilov et al. 2015).

The biosensor for determining urea is a pH-sensitive field-effect transistor, coupled using a constant magnetic field with a bioreceptor, which is a polyelectrolyte capsule with encapsulated urease and paramagnetic particles Fe_3O_4 .

The production of polyelectrolyte capsules with an enzyme and magnetic particles is carried out separately from the field-effect transistor (Fig. 13.4A).

All stages of obtaining polyelectrolyte microcapsules with an enzyme were carried out according to the technology presented in Fig. 13.1. Further, these microcapsules were located directly on the surface of the magnet pole. Microcapsules were sedimented onto the gate using a constant magnetic field; its strength at the magnet poles was 12,000 Oe. This magnetic field did not lead to a change in the chemical sensitivity of the field-effect transistor and to a change in the mutual position of the current–voltage curves in the coordinates “ I_c (drain current) - U_z (gate voltage).” According to the test visual assessment, the settling time of the microcapsules on the gate of the field-effect transistor in a magnetic field did not exceed 2–3 s. After measuring the sample, the magnet was removed from the transistor zone in order to eliminate the attraction of microcapsules and not violate the conditions for washing the FET.

A schematic representation of the relative position of the FET, a permanent magnet, and polyelectrolyte microcapsules with built-in urease and paramagnetic particles is shown in Fig. 13.4B.

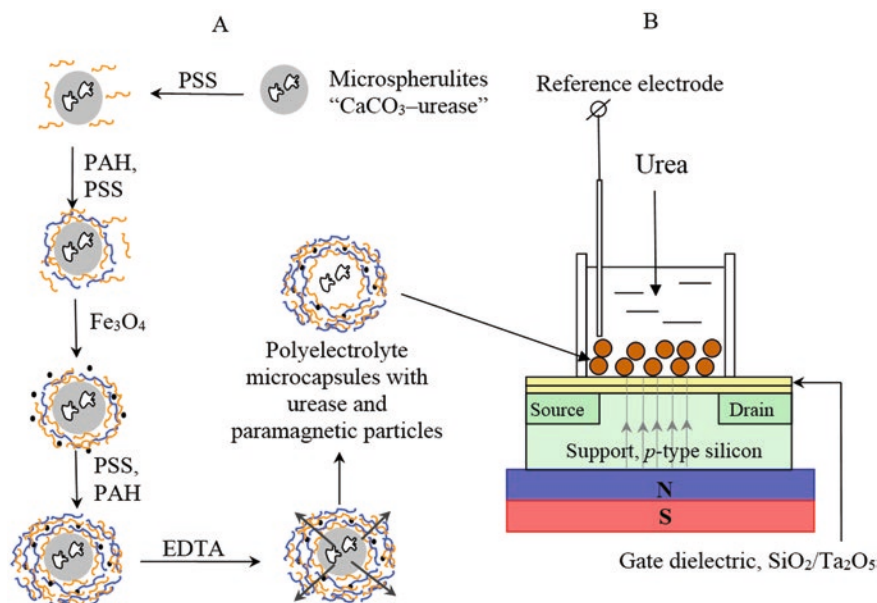


Fig. 13.4 Schemes of (a) the formation of microcapsules with urease and paramagnetic particles and (b) bioreceptor immobilization on the surface of a field-effect transistor under the action of a constant magnetic field

Subsequently, using the developed biosensor, the urea concentration in milk samples was measured. The results of this measurement are shown in Table 13.3.

The proposed method for the formation of a bioreceptor element on the transducer immediately before measurement allows one to significantly reduce and simplify the analysis procedure. The bioreceptor was removed from the electrode surface after measurements in the absence of a magnet, without using special reagents to restore the surface after analysis. The biosensor described in the work allows determining urea in samples in the range 0.03–100 mM and can compete with other models of biosensors for determining urea in milk.

13.2.7 Biosensors Based on Polyelectrolyte Microcapsules Containing Fluorescent Dyes

Diagnostic systems based on fluorescence of sensor molecules are common and easy to measure. The use of these fluorescent labels with enzymes will expand the list of diagnosed compounds, the concept base on use of fluorescent markers to detect the products of an enzymatic reaction (Kobayashi et al. 2010). Joint encapsulation of enzyme and the fluorescent dye will allow to determine quantitatively and qualitatively substances locally, within the same microcapsule. The main advantage

Table 13.3 Measurement of milk samples

Sample	Biosensor readings, a ± S.D., mM	Injected, mM	Found		a ± S.D., mM	The coefficient of variation, %
			mM	% of injected		
1	0.04 ± 0.0019	0.01	0.05	500	0.05 ± 0.00245	4.9
		0.05	0.09	180	0.09 ± 0.00405	4.5
		0.1	0.12	120	0.12 ± 0.00564	4.7
		0.5	0.60	120	0.60 ± 0.0288	4.8
		1	1.20	120	1.20 ± 0.054	4.5
		5	5.30	106	5.30 ± 0.2226	4.2
2	0.08 ± 0.0035	0.01	0.07	700	0.07 ± 0.0035	5
		0.05	0.10	200	0.10 ± 0.0045	4.5
		0.1	0.14	140	0.14 ± 0.00658	4.7
		0.5	0.60	120	0.60 ± 0.0276	4.6
		1	1.10	110	1.10 ± 0.0539	4.9
		5	5.20	104	5.20 ± 0.2496	4.8

a – the average value of measurements taken in 3–5 repetitions; S.D. – standard deviation

of using these capsules with optical recording is the possibility of building single capsule-based sensors.

Fluorescent dyes are mainly used to detect the basic ions of physiological relevance, notably Na⁺, K⁺, Cl⁻, Ca²⁺, and H⁺ (Gomez-Hens and Valarcel 1982; Donoso et al. 1992; Takahashi et al. 1999), although other metabolites, particularly glucose (Pickupa et al. 2005), have also been investigated. Enzymes, which, as a result of their activity, change the concentration of these ions in the medium, can be used in conjunction with these labels, which will make it possible to determine more complex compounds in solution. For example, in the work of Kazakova et al. (2011), the possibility of joint encapsulation of urease and pH-sensitive dye SNARF-1 was shown. Encapsulated urease catalyzed urea hydrolysis, which resulted in a change in the pH of the analyzed medium. The pH-sensitive label changes its fluorescence intensity, which allows estimating the urea concentration in the medium. As a result, a diagnostic system was obtained that is able to determine the concentration of urea by the intensity of the fluorescence label.

This technology allows you to determine the concentration of low molecular weight compounds using one such capsule, containing an enzyme and a fluorescent label. This technology was demonstrated in an article by Kazakova et al. (2012). The confocal microscopy allows observing the fluorescence from individual capsule on addition of lactate at millimolar concentrations.

The application of sensory nano and microparticles for metabolite control in the human body is of growing importance in the biomedical sciences. Packaging of sensing elements within micron and submicron structures enables investigation of local environmental tissue changes in close proximity to a positioned sensing surface. The micron-sized multicomponent capsules could be further optimized for in-situ intracellular sensing and metabolite monitoring on the basis of fluorescence reporting (Goldys 2009).

13.3 Conclusion and Perspectives

The chapter describes the possibility of using microcapsules with urease loaded in them as diagnostic systems for urea. The possibility of their repeated use is shown. Comparative characteristics of clinical and biochemical analyses were carried out using both free (standard methods) and encapsulated enzyme. From the obtained data, it can be seen that the clinical diagnostic methods of analysis based on microcapsules with the protein included in them are not inferior in their diagnostic characteristics to the modern analysis methods used in clinical diagnostic laboratories, and their advantages, such as repeated use, longer storage, and ease of analysis, talk about their competitive advantages and open up prospects not only for the successful implementation of this new class of diagnostic systems, but also about the transition in the future, all CDLs on microdiagnostics.

References

- Antipov A, Shchukin D, Fedutik Y, Zaneskina I, Klechkovskaya V, Sukhorukov G, Mohwald H (2003) Urease-catalyzed carbonate precipitation inside the restricted volume of polyelectrolyte capsules. *Macromol Rapid Commun* 24:274–277
- Berdnikov A, Semko M, Yu S (2004) Medical devices, apparatus, systems and complexes. Part I. technical methods and apparatus for express diagnostics: manual. Kazan state technical University, Kazan
- Bobreshova M, Sukhorukov GB, Saburova EA, Elfimova LI, Shabarchina LI, Sukhorukov BI (1999) Lactate dehydrogenase in the interpolyelectrolyte complex. Function and stability, *Biofizika* 44:813–820
- Decher G, Hong J-D. (1993) One- or multi-layered layer elements applied to supports and their production. United States Patent 5208111.
- Dolgov V, Selivanova A (2006) Biochemical studies in clinical diagnostic laboratories of primary health care institutions, Vital Diagnostics, St. Petersburg.
- Donath E, Sukhorukov G, Caruso F, Davis S, Möhwald H (1998) Novel hollow polymer shells by colloid-templated assembly of polyelectrolytes. *Angew Chem* 16:2202–2205
- Donoso P, Mill J, O'Neill S, Eisner D (1992) Fluorescence measurements of cytoplasmic and mitochondrial sodium concentration in rat ventricular myocytes. *J Physiol* 448:93–509
- Dubrovsky A, Shabarchina L, Tikhonenko S (2017) Polyelectrolyte-based enzymatic diagnosticum with precipitation detection system for urea assay in solution. *Appl Biochem Microbiol* 53:427–432
- Goldys E (2009) Fluorescence applications in biotechnology and life sciences. Wiley–Blackwell, London
- Gomez-Hens A, Valarcel M (1982) Spectrofluorimetric determination of inorganic anions: a review. *Analyst* 107:465–465
- Jegannathan K, Jun-Yee L, Chan E, Ravindra P (2010) Production of biodiesel from palm oil using liquid core lipase encapsulated in κ -carrageenan. *Fuel* 89:2272–2277
- Kazakova L, Shabarchina L, Sukhorukov G (2011) Co-encapsulation of enzyme and sensitive dye as a tool for fabrication of microcapsule based sensor for urea measuring. *Phys Chem Chem Phys* 13:11110–11117

- Kazakova L, Shabarchina L, Salzitsa S, Pavlov A, Vadgama P, Skirtach A, Sukhorukov G (2012) Chemosensors and biosensors based on polyelectrolyte microcapsules containing fluorescent dyes and enzymes. *Anal Bioanal Chem* (5):1559–1568
- Kim A, Musin E, Dubrovskii A, Tikhonenko S (2019) Determination of urea concentration using urease-containing polyelectrolyte microcapsules. *Anal Methods* 11:1585–1590
- Kobayashi H, Ogawa M, Alford R, Choyke P, Urano Y (2010) New strategies for fluorescent probe design in medical diagnostic imaging. *Chem Rev* 110:2620–2640
- Lvov Y, Sukhorukov G (1997) Protein architecture: assembly of ordered films by means of alternated adsorption of oppositely charged macromolecules. *Membrane Cell Biol* 3:277–303
- Mayya K, Schoeler B, Caruso F (2003) Preparation and organisation of nanoscale polyelectrolyte-coated gold nanoparticles. *Adv Funct Mater* (3):183–188
- Menshikov VV (2009) *Methods of clinical laboratory research*, Labora, Moscow
- Mohamad N, Marzuki N, Buang N, Huyop F, Wahab R (2015) An overview of technologies for immobilization of enzymes and surface analysis techniques for immobilized enzymes. *Biotechnol Biotechnol Equip* (2):205–220
- Pickupa J, Hussaina F, Evansa N, Rolinskib O, Birch D (2005) Fluorescence-based glucose sensors. *Biosens Bioelectron* 20:2555–2565
- Reshetilov A, Plekhanova Y, Tikhonenko S, Dubrovsky A (2015) Polyelectrolyte microcapsules with urease and paramagnetic particles as a basis for a potentiometric biosensor for determining urea. *J Anal Chem* 70:1186–1190
- Reshetilov A, Plekhanova Y, Dubrovskii A, Tikhonenko S (2016) Detection of urea using urease and paramagnetic Fe₃O₄ particles incorporated into polyelectrolyte microcapsules. *Process Biochem* (2):277–281
- Shen Q, Yang R, Hua X, Ye F, Zhang W, Zhao W (2011) Gelatin-templated biomimetic calcification for β -galactosidase immobilization. *Process Biochem* 46:1565–1571
- Shenoy D, Antipov A, Sukhorukov G, Mohwald H (2003) Layer-by-layer engineering of biocompatible, decomposable Core-Shell structures. *Biomacromolecules* (2):265–272
- Sukhorukov G, Fery A, Mohwald H (2005) Intelligent micro- and nanocapsules. *Prog Polym Sci* 8:885–897
- Sukhorukov B, Tikhonenko S, Saburova E, Dubrovsky A, Dybovskaia Y, Shabarchina L (2007) Encapsulation of proteins and polyelectrolyte nano- and microcapsules and the problems of developing an enzyme microdiagnosticum. *Biofizika* 6:1041–1048
- Takahashi A, Camacho P, Lechleiter JD, Herman B (1999) Measurement of intracellular calcium. *Physiol Rev* 79:1089–1125
- Tümtürk H, Karaca N, Demirel G, Sahin F (2007) Preparation and application of poly(N,N-dimethylacrylamide-co-acrylamide) and poly(N-isopropylacrylamide-co-acrylamide)/kappa-Carrageenan hydrogels for immobilization of lipase. *Int J Biol Macromol* (3):281–285

Chapter 14

Bioluminescent Nano- and Micro-biosensing Elements for Detection of Organophosphorus Compounds



Elena Efremenko, Ilya Lyagin, Olga Senko, Olga Maslova,
and Nikolay Stepanov

Abstract Organophosphorus compounds (OPC) are capable of interaction with various biological targets. At the same time, some enzymes can modify these OPC, mainly by hydrolysis. In total, both those and other enzymes can be involved in determining the presence and concentration of various OPC. This review presents recent scientific developments in the area of enzymatic (nano) and cell (micro) biosensing elements, used for the luminescent analysis of OPC in various environmental objects. For these purposes, various immobilized forms of enzymes and different cells of microorganisms can be used, as well as their various combinations. Modern methods of analysis make it possible to detect OPC in pg/l concentrations, which opens up enormous prospects for their practical application. Some examples of commercially available enzymatic and cell recognition elements for OPC determination in real environmental samples are performed.

Keywords Bioluminescence · Fluorescence · Biosensor · Biorecognition element · Organophosphorus compounds · Cholinesterase · Organophosphate hydrolase · Immobilization · Living cells · Enzymes

Nomenclature

2D PSPC	Two-dimensional poly(styrene) photonic crystal
AChE	Acetylcholinesterase
ADI	Allowable daily intake
AgNPs	Silver nanoparticles
ALP	Alkaline phosphatase
AuNCs	Gold nanoclusters
BE	Biosensitive elements

E. Efremenko (✉) · I. Lyagin · O. Senko · O. Maslova · N. Stepanov
Faculty of Chemistry, Lomonosov Moscow State University, Moscow, Russia

BSPOTPE@MnO ₂ /SiO ₂ NPs	SiO ₂ nanoparticles covered by 1,2-bis[4-(3-sulfonatopropoxy) phenyl]-1,2-diphenylethene and capped by MnO ₂ nanosheets
BTB	Bromothymol blue
BTE	Brake thermal efficiency
Ccg2-EPSPS	5-Enolpyruvylshikimate-3-phosphate synthase fused to the hydrophobin Ccg2
ChE	Cholinesterase
ChOx	Choline oxidase
DACM	<i>N</i> -(7-Dimethylamino-4-methylcoumarin-3-yl) maleimide
DCC/HDA	<i>N,N'</i> -Dicyclohexylcarbodiimide and hexaethylenediamine
DFP	<i>O,O</i> -Diisopropyl fluorophosphate
EDC	1-Ethyl-3-(3-dimethylaminopropyl)carbodiimide
EST2	Esterase 2 from <i>Alicyclobacillus acidocaldarius</i>
FITC	Fluorescein 5(6)-isothiocyanate
GG/FB	Guinea green B and basic fuchsin dyes
GFP	Green fluorescent protein
grQD/AuNPs	AuNPs capped by graphene QDs
His ₆ -MPH	Methylparathion hydrolase containing His ₆ -tag at N-terminus
His ₆ -OPH	OPH containing His ₆ -tag at N-terminus
HRP	Horseradish peroxidase
LOD	Limit of detection
Lum-Cu-Cys-AuNPs	Composite of luminol with AuNPs covered by Cys and Cu ²⁺
MPH-GST	Methylparathion hydrolase containing GST-tag
MPT	Methylparathion
MRL	Maximum residue levels
NTA	Nitrilotriacetic acid
OPC	Organophosphorus compounds
OPH	Organophosphorus hydrolase
OPH-His ₆	Organophosphorus hydrolase containing His ₆ -tag at C-terminus
OPP	Organophosphorus pesticides
PAAM	Poly(acrylamide)
PAH@PSS/CdTe QDs	Multilayer composite of poly(allylamine hydrochloride) and poly(styrenesulfonate) on the surface of CdTe QDs
PAM	Photosynthetic apparatus of microalgae
PT	Parathion
PVA	Poly(vinyl alcohol)
PVDF	Poly(vinylidene fluoride)
PX	Paraoxon

rGO@AuNPs/GCE	Reduced graphene oxide and Au nanoparticles on the surface of glassy carbon electrode
sNHS	<i>N</i> -Hydroxysuccinimide
Tb-BTC MOF	Metal-organic framework of Tb and benzene-1,3,5-tricarboxylic acid
UiO-66-NH ₂	Metal-organic framework of Zr and aminoterephthalic acid

14.1 Introduction

The widespread use of organophosphorus pesticides (OPP) is an integral part of modern agriculture. This necessitates careful monitoring of their presence in a wide variety of objects (in natural water sources, soil extracts, food products, agricultural raw materials, etc.) using a variety of detection methods (Amine et al. 2016; Samsidar et al. 2018; Li et al. 2018), which provide a fast, selective, and effective (quantitative) determination of pesticides (Van Dyk and Pletschke 2011). The most promising methods are those based on the use of biosensitive elements (BE) with enzymatic activity, which guarantee a highly sensitive detection of pesticides to be analyzed as specific substrates or inhibitors acting under certain conditions (temperature, pH, the chemical composition of media) typical for real objects and processes occurring *in vivo* (Lyagin et al. 2017). The generated analytical signal can be reliably detected as a result of the enzymatic process. The creation of BE with certain characteristics (Yan et al. 2018) that satisfy the existing regulatory requirements for the content of determined OPP (Table 14.1) is the main task for science in this area. For these purposes, both the BE used and the signal amplification and registration method can vary. A successful combination of these components (biosensitive, amplifying, and recording) of biosensors allows achieving a high level of analysis sensitivity (up to ng/l).

The development of biosensors designed to solve specific analytical problems associated with the discovery of OPP has become possible owing to the accumulated empirical data and the development of modern physicochemical methods for the study of enzymatic biocatalysts while accumulating fundamental knowledge about the features of OPP and enzymes effectively interacting (through hydrolysis, inhibition, modifications, etc.) with such organophosphorus compounds (Varfolomeev and Efremenko 2020).

Today, many variants of cellular biosensor systems for detecting OPP are known. The use of living cells as BE allows both the determination of specific concentrations of individual OPP and the assessment of the overall toxicity of analyzed samples containing several pollutants. Thus, in the case of cell-based BE, it is possible to track not only the actual concentration of toxins (Ismailov et al. 2019) but also the biosafety of various environments.

Now, various approaches developed for the detection of different target compounds (Hicks et al. 2020) are currently under applied investigation in the area of

Table 14.1 Examples of some OPP and their norms in various foodstuffs^a

Pesticide ^b MRL; ADI/PTDI	Structure	Pesticide ^b MRL; ADI/PTDI	Structure
Cadusafos 0.01 mg/kg 0–0.5 µg/d/kg		Glyphosate 0.05–15 mg/kg 0–1000 µg/d/kg	
Chlorpyrifos 0.01–20 mg/kg 0–10 µg/d/kg		Glufosinate 0.02–3 mg/kg 0–10 µg/d/kg	
Diazinon 0.01–2 mg/kg 0–5 µg/d/kg		Fenamiphos 0.005–0.05 mg/kg 0–0.8 µg/d/kg	
Ethephon 0.01–7 mg/kg 0–50 µg/d/kg		Malathion 0.01–13 mg/kg 0–300 µg/d/kg	
Ethoprophos 0.01–0.2 mg/kg 0–0.4 µg/d/kg		Methylparathion 0.05–5 mg/kg 3 µg/d/kg	

^aThe maximum residue levels (MRL) and allowable daily intake (ADI) (or provisional tolerable daily intake, PTDI) are revealed for various eatable foods according to *Codex Alimentarius* of FAO WHO (<http://www.fao.org/fao-who-codexalimentarius/>)

^bGlyphosate (*N*-(phosphonomethyl)-glycine), glufosinate (2-amino-4-[hydroxy(methyl)phosphono]butanoic acid), diazinon (*O,O*-diethyl-*O*-(4-methyl-6-(propan-2-yl)pyrimidin-2-yl) phosphorothioate), cadusafos (*O*-ethyl *S,S*-bis(1-methylpropyl) phosphorodithioate), malathion (*O,O*-dimethyl-*S*-(1,2-dicarbetoxyethyl) phosphorodithioate), methylparathion (*O,O*-dimethyl-*O*-(4-nitrophenyl) phosphorothioate), fenamiphos (*N*-[ethoxy-(3-methyl-4-methyl sulfanyl phenoxy) phosphoryl]propan-2-amine), chlorpyrifos (*O,O*-diethyl-*O*-(3,5,6-trichloropyridine-2-yl) phosphorothioate), ethephon (2-chloroethylphosphonic acid), ethoprophos (*O*-ethyl *S,S*-diisopropyl phosphorodithioate)

OPP analysis. In this regard, the new genetically modified cells of various microorganisms are tested as BE for the application in OPC detection.

According to recent publications, the general sum of modern BE based on different enzymes or various cells taken in a free (soluble/suspended) or immobilized forms is presented in Figs. 14.1 and 14.2. It is obvious that all the developed variants of the BE can be characterized by some advantages and limitations for their practical use. However, the information about recent achievements in the development of BE for OPP analysis testified to a high popularity of the optical (luminescent) meth-

ods of signal registration since exactly these analytical methods are supported with equipment accessible to the most consumers.

The aim of the chapter is the analysis of the main recent scientific achievements in the development of various bioanalytical systems capable of determining the widely used OPP. Particular attention has been paid on new interdisciplinary researches and luminescent methods for their practical implementation. It should be noted that this chapter did not specifically address the enzyme-linked immunosorbent assay methods of OPP, as well as analytical systems based on aptamers (Duan et al. 2016, Che Sulaiman et al. 2020) and molecularly imprinted polymers (Boulanour et al. 2018) since such reviews are already published.

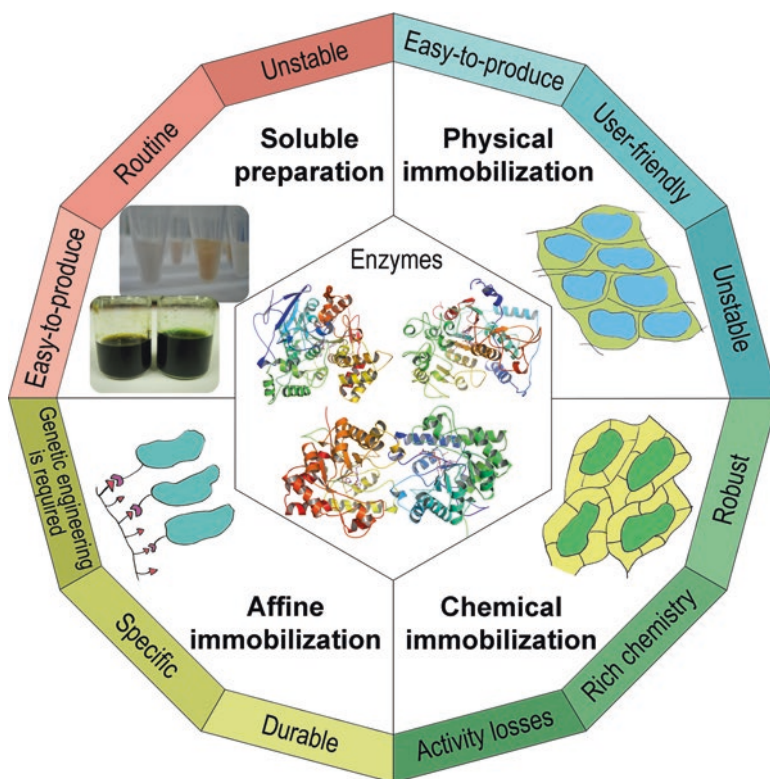


Fig. 14.1 The main approaches used to obtain enzyme BE for OPP detection, the key features of which are represented on the outer edge

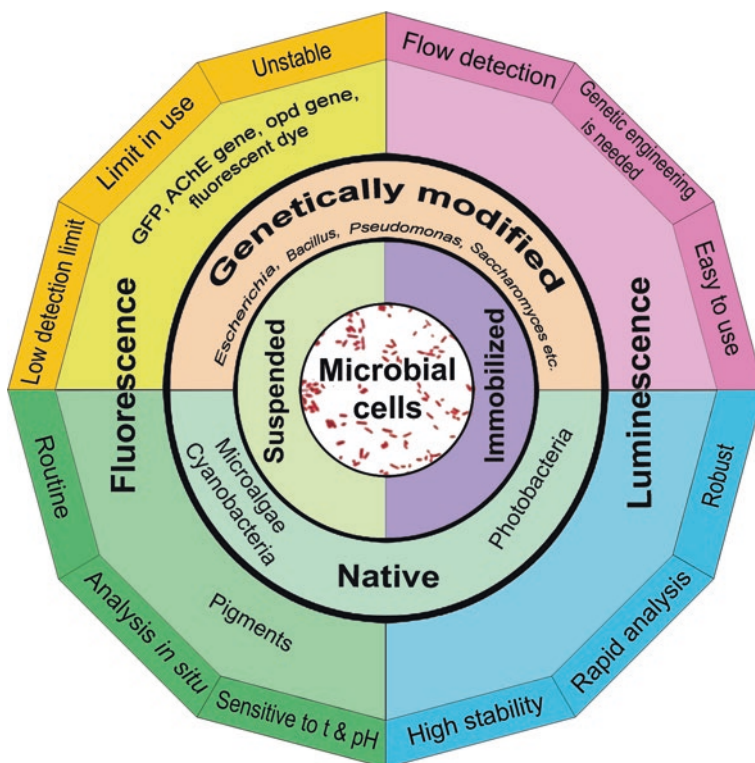


Fig. 14.2 Generalized scheme of approaches used in the development of BE for the detection of OPP based on the use of whole living cells of various microorganisms. The typical features of the BE are represented on the outer edge

14.2 Enzyme Biosensors for Organophosphorous Compounds (OPC)

The mechanism of action of many OPC is the inactivation of various enzymes from different biological sources (Lyagin et al. 2017, Mangas et al. 2017), which forms the basis for their use as pesticides. Based on this, appropriate enzymes are used to determine the presence of OPP. An analysis of the structure of these enzymes allows using the rational design of biosensitive elements for specific tasks, for example, by site-directed chemical modifications of protein molecules, due to their additional stabilization, etc. All OPC to one degree or another inhibit acetyl- and butyrylcholinesterase (Eldufani and Blaise 2019). These enzymes belong to serine hydrolases and contain in their active center the amino acid residue of serine, the phosphorylation of which in reactions with OPC leads to practically irreversible inhibition of the enzymes. The high affinity of binding of cholinesterase (ChE) to OPC, coupled with

the highly sensitive methods used to determine its enzymatic activity, makes it possible to determine extremely low concentrations of inhibitors, which made this enzyme an excellent object for research and development of a large number of different biosensors based on it (Table 14.2).

Other examples of enzymes being inhibited by OPP are acidic and alkaline phosphatases (Ghosh et al. 2013). Monoesters of phosphates are natural substrates for these enzymes; therefore, di- and tri-esters of phosphates are often playing the role of competitive phosphatase inhibitors. Like ChE, phosphatases act simultaneously as a BE and signal enhancer, but since reversible inhibition of enzymes occurs in this case, the sensitivity of OPC determination using phosphatases in biosensing systems will always be significantly lower than in the ChE variants.

In addition, the enzymes (Lyagin et al. 2017) hydrolyzing OPC are widely used in the development of various BE. The OPC decomposition products are determined, forming a signal of a certain magnitude. For example, the hydrolysis products of methylparathion (4-nitrophenol) or chlorpyrifos (3,5,6-trichloropyridine-2-ol) can be determined using optical methods. However, there are very few substances with such absorption among the hydrolysis products of various OPC, or it is difficult to discriminate the products in the analyzed media containing other compounds that interfere with the target determination analyte. In this regard, other methods for recording the analytical signal are often involved. Enzymatic hydrolysis of OPC is typically accompanied by the formation of charged molecules and a change in the pH of the reaction medium, which can be detected directly or using a pH-sensitive probe or tracer. In order to further improve the analytical characteristics, such hydrolases can be used in combination with other enzymes, for example, ChEs (Lyagin et al. 2017).

A wide variety of optical methods can be used today to convert the analytical signal of enzyme BE into a result accessible for registration and interpretation: classical – spectrophotometric, fluorescent, and chemiluminescent – as well as more modern ones, fluorescent quantum dots and surface plasmon resonance. By combining various enzymes and recording systems, it is possible to create biosensors with the required sensitivity, performance, and cost. Among the optical methods, the most sensitive are fluorescent ones (Table 14.2). To realize this, fluorescent substrates are widely used, or substrates that, under the action of enzymes, turn into fluorescent products or enzymes containing specially introduced fluorescent labels. Recently, the use of nano-objects and, in particular, quantum dots (Chungchai et al. 2020; Hu et al. 2019; Korram et al. 2019; Wang et al. 2019; Zhang et al. 2019) has become increasingly popular for such bioanalytical systems, which can interact with the substrate or product, giving an analytical signal. This significantly increases the sensitivity of OPC determination in real samples by two to three orders of magnitude (up to ng/l) (Hu et al. 2019; Wang et al. 2019; Yang et al. 2019) as compared with similar systems without quantum dots.

Table 14.2 Examples of enzyme biosensors used to determine OPC

Enzyme ^a	Method of detection	Limits of detection ^{b,c} (References)
<i>Soluble enzymes</i>		
AChE	Absorbance/fluorescence of rhodamine B probe	0.1 µg/l diazinon, 0.3 mg/l malathion, 1 µg/l phorate (Liu et al. 2012)
»	Absorbance of reaction product (indophenol)	0.8 mg/l chlorpyrifos, 0.4 mg/l phoxim, 1.3 mg/l triazophos, 1.4 mg/l methamidophos (in real samples: from 0.8 mg/kg, recovery 75–108%) (Jin et al. 2020)
»	Absorbance of grQD/AuNPs	0.7 µg/l chlorpyrifos (in real samples: from 30 µg/l, recovery 93–105%) (Chungchai et al. 2020)
»	Absorbance of PtNPs	20 µg/l dichlorvos (in real samples, recovery 85–97%) (Cao et al. 2019)
»	Fluorescence of tetraphenylethene probe	8 µg/l dimethoate (in real samples: from 50 µg/l, recovery 98–112%) (Cai et al. 2019)
»	Fluorescence of DACM probe	1.5 ng/l PX (in real samples: from 4 ng/l, recovery 94–110%) (Wang et al. 2011)
»	Fluorescence of FITC label	0.6 µg/l chlorpyrifos (in real samples, (recovery – n/a) (Silletti et al. 2015)
»	Fluorescence of fluorescein label	1.4 µg/l omethoate, 1 µg/l dichlorvos (in real samples: from 5 µg/l, recovery 100–102%) (Huang et al. 2019a)
»	Fluorescence of NaGdF ₄ :Yb,Tm NPs	50 ng/l diazinon (in real samples: from 0.5 µg/l, recovery 84–107%) (Wang et al. 2019)
»	Fluorescence of NaYF ₄ :Yb,Er NPs	2 ng/l MPT (in real samples: from 30 ng/l, recovery 96–110%) (Long et al. 2015)
»	Fluorescence of carbon QDs	14 µg/l PX, 33 µg/l malathion, 17 µg/l methamidophos (in real samples: from 0.3 µg/l, recovery 93–110%) (Korram et al. 2019)
»	Fluorescence of N,Cl-doped carbon QDs	30 ng/l PX (in real samples: from 1 µg/l, recovery 92–109%) (Yang et al. 2019)
»	Fluorescence of BSPOTPE@MnO ₂ /SiO ₂ NPs	1 µg/l paraoxon (10 µg/l on paper with naked eye) (in real samples: from 5 µg/l, recovery 98–104%) (Wu et al. 2019)
ALP	Fluorescence of reaction product (2-naphthol)	1.34 mg/l fenitrothion (in real samples: from 10 mg/l, recovery 96–100%) (Diaz et al. 2015)
EST2	Fluorescence of reaction product (4-methylumbelliferol)	6 µg/l PX (in real samples: from 72 µg/l, recovery – n/a) (Cetrangolo et al. 2019)

(continued)

Table 14.2 (continued)

Enzyme ^a	Method of detection	Limits of detection ^{b,c} (References)
HRP	Absorbance/fluorescence of reaction product	2 mg/l (UV/Vis) and 4 µg/l (FL) glyphosate (Ibarra Bouzada et al. 2019)
OPH	Fluorescence of CdTe QDs	18 µg/l MPT (in real samples: from 50 mg/kg, recovery 96–117%) (Yan et al. 2015a)
»	Fluorescence of CuInS ₂ QDs	15.8 µg/l MPT (in real samples: from 100 µg/kg, recovery 90–105%) (Yan et al. 2015b)
»	Fluorescence of Mn-ZnS QDs	5 µg/l MPT (in real samples: from 50 µg/l, recovery 81–99%) (Zhang et al. 2019)
»	Absorbance of F-sensitive film	18.4 µg/l DFP (Ramanathan et al. 2010)
OPH-His ₆	Fluorescence of pyranine label	2 µg/l PX, 10 µg/l MPT (Thakur et al. 2013)
»	Fluorescence of pyranine label	20 µg/l PX, 50 µg/l MPT, 50 µg/l coumaphos (in real samples: from 50 µg/l, recovery 90–125%) (Thakur et al. 2012)
Trypsin	Fluorescence of CdTe QDs	40 ng/l MPT (in real samples: from 0.2 µg/kg, recovery 95–110%) (Yan et al. 2015c)
AChE with ChOx	Fluorescence of CdTe QDs	1 µg/l dichlorvos (in real samples: from 170 mg/l, recovery 97–101%) (Meng et al. 2013)
»	Fluorescence of graphene QDs	172 µg/l dichlorvos, 84 µg/l MPX (in real samples: 2 mg/l, recovery 101–112%) (Sahub et al. 2018)
AChE with HRP	Fluorescence of N-doped carbon QDs with 2,3-diaminophenazine	3.2 µg/l dichlorvos, 13 µg/l MPT (in real samples: from 0.1 mg/kg dichlorvos, recovery 93–106%; and from 0.1 mg/kg MPT, recovery 93–106%) (Huang et al. 2019c)
<i>Physical immobilization</i>		
AChE included between layers of PAH in composite PAH@PSS/CdTe QDs on glass or quartz substrate	Fluorescence of CdTe QDs	2.9 ng/l PX, 1.3 ng/l PT, 0.24 µg/l dichlorvos, 12.6 ng/l omethoate (in real samples: from 2.3 µg/l, recovery 105–115%) (Zheng et al. 2011)
AChE included in cryostructure of CdTe QDs	Fluorescence of CdTe QDs	0.33 ng/l PX, 0.27 ng/l PT, 2.6 ng/l dichlorvos (in real samples: from 1.1 µg/l, recovery 99–109%) (Hu et al. 2019)
ChE adsorbed on cellulose or glass nanofiber paper	Absorbance of GG/FB probe	0.1 mg/l diethylchlorophosphate (Matějovský and Pitschmann 2019)

(continued)

Table 14.2 (continued)

Enzyme ^a	Method of detection	Limits of detection ^{b,c} (References)
AChE and ChOx included into Cu ₃ (PO ₄) ₂ nanoflowers	Absorbance of reaction end-product	10 ng/l PX or 0.5 mg/l by naked eye (in real samples: from 5 µg/l, recovery 83–112%) (Jin et al. 2019)
EST2 adsorbed on nitrocellulose membrane	Absorbance of reaction end-product	2.75 mg/l PX (in real samples with soluble enzyme: from 2.75 mg/l, recovery – n/a) (Febbraio et al. 2011)
MPH-GST ^b adsorbed on PVDF membrane (Immobilon™-P ⁵⁰)	Absorbance of BTB probe	1 mg/l MPT (by naked eye, in real samples: from 10 mg/l, recovery 75–93%) (Anh et al. 2011)
OPH adsorbed on AgNPs coated by silica	Fluorescence of pyranine label	1 µg/l PX (Tuteja et al. 2014)
<i>Chemical immobilization</i>		
AChE attached by epichlorohydrin to chitosan on cellulose paper	Absorbance of fast blue B probe	200 mg/l chlorpyrifos, 10 mg/l diazinon, 4 mg/l fenamiphos, 500 mg/l malathion, 25 mg/l profenofos, 50 mg/l temephos (Badawy and Taktak 2018)
AChE attached by EDC to PAAM on 2D PSPC	Light scattering on 2D PSPC	0.02 pg/l dipterex (Qi et al. 2018)
»	Light scattering on 2D PSPC	0.01 pg/l sarin (Qi et al. 2019)
AChE and ChOx attached by glutaraldehyde to rGO@AuNPs/GCE with Lum-Cu-Cys-AuNPs	Electro-chemiluminescence of Lum-Cu-Cys-AuNPs	85 ng/l glyphosate (in real samples: from 1 µg/l, recovery 99–105%) (Liu et al. 2020)
His ₆ -OPH attached by DCC/HDA to UiO-66-NH ₂	Fluorescence of coumarin 1 probe	10 µg/l MPT (in real samples: from 1 mg/l, recovery 95–105%) (Mehta et al. 2019a)
His ₆ -OPH attached by EDC/sNHS to BTC of Tb-BTC MOF	Absorbance of reaction product (4-nitrophenol)	0.6 µg/l MPT (Mehta et al. 2019b)
<i>Affine immobilization</i>		
His ₆ -MPH on agarose modified by NTA and loaded with Ni ²⁺	Absorbance of reaction product (4-nitrophenol)	1 mg/l MPT (Lan et al. 2012)
Ccg2–EPSPS on polystyrene or SiO ₂ glass	Absorbance of reaction end-product	8.5 µg/l glyphosate (Döring et al. 2019)

^aAbbreviations: *AChE* acetylcholinesterase, *grQD/AuNPs* AuNPs capped by graphene QDs, *DACM N-(7-dimethylamino-4-methylcoumarin-3-yl)maleimide*, *FITC* fluorescein 5(6)-isothiocyanate, *BSPOTPE@MnO₂/SiO₂ NPs* SiO₂ nanoparticles covered by 1,2-bis[4-(3-sulfonatopropoxyl) phenyl]-1,2-diphenylethene and capped by MnO₂ nanosheets, *ALP* alkaline phosphatase, *EST2* esterase 2 from *Alicyclobacillus acidocaldarius*, *HRP* horseradish peroxidase, *OPH* organophosphorus hydrolase, *OPH-His₆* organophosphorus hydrolase containing His₆-tag at C-terminus, pyranine – trisodium 8-hydroxyppyrene-1,3,6-trisulfonate, *ChOx* choline oxidase,

(continued)

Table 14.2 (continued)

MPH-GST methylparathion hydrolase containing GST-tag, *PVDF* poly(vinylidene fluoride), *BTB* bromothymol blue, *AgNPs* nanoparticles of Ag, *PAH@PSS/CdTe QDs* multilayer composite of poly(allylamine hydrochloride) and poly(styrenesulfonate) on the surface of CdTe QDs, *GG/FB* guinea green B and basic fuchsin dyes, *His₆-OPH* OPH containing His₆-tag at N-terminus, *DCC/HDA* *N,N'*-dicyclohexylcarbodiimide and hexaethylenediamine, *UiO-66-NH₂* metal-organic framework of Zr and aminoterephthalic acid, *EDC* 1-ethyl-3-(3-dimethylaminopropyl)carbodiimide, *sNHS* *N*-hydroxysuccinimide, *Tb-BTC MOF* metal-organic framework of Tb and benzene-1,3,5-tricarboxylic acid, *PAAM* poly(acrylamide), *2D PSPC* two-dimensional poly(styrene) photonic crystal, *rGO@AuNPs/GCE* reduced graphene oxide and Au nanoparticles on the surface of glassy carbon electrode, *Lum-Cu-Cys-AuNPs* composite of luminol with AuNPs covered by Cys and Cu²⁺, *His₆-MPH* MPH containing His₆-tag at N-terminus, *NTA* nitrilotriacetic acid, *Ccg2-EPSPS* 5-enolpyruvylshikimate-3-phosphate synthase fused to the hydrophobin Ccg2

^bIn the case of real samples, limit of detection or minimal concentration used during analysis are presented together with their recovery as compared to one determined by reference method of analysis (HPLC, GC/MS, etc.) or to a spiked quality. n/a – not available

^cDetected compounds: chlorpyrifos (*O,O*-diethyl-*O*-(3,5,6-trichloropyridine-2-yl) phosphorothioate), coumaphos (*O,O*-diethyl-*O*-(3-chloro-4-methyl-2-oxo-2*H*-chromen-7-yl) phosphorothioate), diazinon (*O,O*-diethyl-*O*-(4-methyl-6-(propan-2-yl)pyrimidin-2-yl) phosphorothioate), dichlorvos (*O,O*-dimethyl-*O*-(2,2-dichlorovinyl) phosphate), DFP (*O,O*-diisopropyl fluorophosphate), dimethoate (*O,O*-dimethyl *S*-methylcarbamoylmethyl phosphorodithioate), fenitrothion (*O,O*-dimethyl-*O*-(3-methyl-4-nitrophenyl) phosphorothioate), glyphosate (*N*-(phosphonomethyl)-glycine), malathion (*O,O*-dimethyl-*S*-(1,2-dicarbetoxyethyl) phosphorodithioate), methamidophos (*O,S*-dimethyl phosphoramidothioate), *MPT* methylparathion (*O,O*-dimethyl-*O*-(4-nitrophenyl) phosphorothioate), omethoate (*O,O*-dimethyl *S*-methylcarbamoylmethyl phosphorothioate), *PT* parathion (*O,O*-diethyl-*O*-(4-nitrophenyl) phosphorothioate), *PX* paraoxon (*O,O*-diethyl-*O*-(4-nitrophenyl) phosphate), phorate (*O,O*-diethyl-*S*-[(ethylsulfanyl)methyl] phosphorodithioate), profenofos (*O*-(4-bromo-2-chlorophenyl) *O*-ethyl *S*-propyl phosphorothioate), temephos (*O,O,O',O'*-tetramethyl *O,O'*-sulfanediybis(1,4-phenylene) diphosphorothioate), triazophos (*O,O*-diethyl *O*-(1-phenyl-1*H*-1,2,4-triazol-3-yl) phosphorothioate)

The typical analysis sensitivity in model systems (up to ng/l) is better than in real systems (up to µg/l). However, such sensitivity is already completely consistent with the requirements for OPC control in compliance with their maximum permissible content in the tested environmental objects (Table 14.1) and various commercial products (Ibarra Bouzada et al. 2019).

Today, the trend toward the development of “reagentless” optical biosensors for OPC detection, for example, in the form of microfluidic chips or strips (Chungchai et al. 2020; Hu et al. 2019; Matějovský and Pitschmann 2019), is popular. For this, a substrate with a tracer is often immobilized together with the enzyme. Under the influence of microfluidic forces from the solvent in the applied sample, they are set in motion and mixed with the immobilized enzyme, giving an analytical signal visible to the naked eye. This approach has composed the basis for a large number of commercially available strips for the rapid and simple determination of OPC with limits of detection down to µg/l (Lyagin et al. 2017).

14.3 Microbial Sensing Elements in the Detection of OPC

14.3.1 Biosensors Based on Whole Cells of Photoluminescent Bacteria for OPC Detection

It has been shown that it is possible to simply, quickly, and efficiently detect OPP in water, air, soil, and other media in a discrete or flow mode using optical whole-cell biosensors (Ma et al. 2014; Zhang et al. 2014). Among them, those options in which cellular BE are used to record changes in luminescence and fluorescence are of particular interest and practical importance.

Luminescent microbial photobiosensors often include photobacterial cells (*Photobacterium phosphoreum*, *Vibrio fischeri*, *Vibrio harveyi*, etc.) which are sensitive to a wide range of OPP and provide a simple technical implementation of the method of analysis and recording of the analytical signal using existing equipment (luminometer), which is widely available today including the portable version (Lopez-Roldan et al. 2012; Ismailov and Aleskerova 2015). Such photobiosensors are based on two successive energy converters: chemical, transforming chemical energy into light, and photoelectronic, converting light into an electrical signal (Ismailov and Aleskerova 2015; Efremenko 2018). Examples of commercial implementation of such test systems are known: Microtox (Azur Environmental, USA), Toxalert (Merck, Darmstadt, Germany), BioFixLumi (Macherey-Nagel, Duren, Germany), ToxTracer (Skalar, Breda, Netherlands), LUMISTox (Hach-Lange, Düsseldorf, Germany), DeltaTox (SDI, Newark DE, USA), Mutatox (USA), Vitotox (GENTAUR Molecular Products, Belgium), BioTox (Aboatox Oy, Helsinki, Finland), and others (Halmi 2016; Bilal and Iqbal 2019; Gheorghie et al. 2019). In particular, using Microtox®, the photodegradation process of dichlorvos (2,2-dichlorovinyl dimethyl phosphate) by simulated sunlight and UV-254 irradiation (Bustos et al. 2019) was studied, and the presence of OPP in apple juice was determined (Mossa et al. 2017) (Table 14.3).

The mechanism of toxicity and inhibition in light emitted from bacteria is a result of the interaction of the luciferase, reduced flavin, and a long-chain aldehyde in the presence of oxygen. The metabolic energy produced in this pathway changes to chemical energy, through the electron transport system, into visible light (Efremenko et al. 2014; Mossa et al. 2017).

To assess the presence of OPP using luminescent bacteria based on quenching of luminescence in the presence of a toxicant, a median effective concentration (EC50) is used, which causes a decrease in the level of the initial bioluminescence signal by 50% (Zhang et al. 2008). Limit of detection (LOD) can be determined from calibration curves as the ecotoxicant concentration resulting in the drop of baseline bioluminescence by three standard deviations, i.e., by 15%, to 85%: $(I/I_0)_{\min} = 100\% - 3\sigma = 85\%$ (Efremenko et al. 2016).

Widely and narrowly specific biotests are being developed with the expression of the bacterial luciferase gene induced in the presence of the OPP analyzed in various cells: *Vibrio* sp., *Escherichia coli*, *Pseudomonas aeruginosa*, *Ralstonia eutropha*,

Table 14.3 Examples of microbial luminescent sensing systems used for OPC detection

Biosensing element	OPC	LOD	Analysis [References]	
<i>Luminescent whole-cell photobiosensing elements</i>				
<i>Vibrio fischeri</i> Microtox™	Chlorpyrifos	–	Discrete mode of luminescent analysis of water samples (Mossa et al. 2017; Bustos et al. 2019)	
	Dichlorvos	–		
	Fenitrothion	1.2 mg/l		
<i>Vibrio qinghaiensis</i> sp. Q67	Fenitrothion	1 µM	Discrete mode of luminescent analysis of water samples (Zhang et al. 2008)	
	Malathion			
	Dicapthon			
	Chlormephos			
	Methylparathion			
	Famphur			
	Monocrothophos	1.92 mM	Discrete mode of luminescent analysis of water samples (Zhou et al. 2010)	
Phosphamidon	0.13 mM			
<i>P. phosphoreum</i> Immobilized in poly(vinyl alcohol) (PVA) cryogel	Coumaphos	91 mg/l	Discrete mode of luminescent analysis of water samples (Efremenko 2018)	
	Parathion	15 mg/l		
	Malathion	18 mg/l		
	Coumaphos	18 µg/l	Flow mode of luminescent analysis of water samples (Efremenko et al. 2016)	
	Parathion	11 µg/l		
	Malathion	3.3 µg/l		
	Methylparathion	12 µg/kg	Discrete mode of luminescent analysis of soil extracts (Efremenko 2018)	
	Malathion	320 µg/kg		
	Dimethon-S-methyl	29 µg/kg		
	Coumaphos	0.32 mg/kg		
	Methylparathion	0.45 mg/kg		Flow mode of luminescent analysis of soil extracts (Efremenko 2018)
	Malathion	0.012 mg/kg		
	Dimethon-S-methyl	1.4 µg/kg		
	Coumaphos	0.011 mg/kg		
Chlorpyrifos	2.1 mg/kg	Discrete mode of luminescent analysis of soil extracts (Senko et al. 2017)		
<i>Microalgae whole-cell biosensing elements</i>				
<i>Chlorella vulgaris</i>	Quinalphos, chlorfenvinphos, dimethoate, phorate	1–500 µM	Control of PAM in detection of OPP in rice growing (Jena et al. 2012)	

(continued)

Table 14.3 (continued)

Biosensing element	OPC	LOD	Analysis [References]
<i>Spirulina (Arthrospira) platensis</i>	Chlorpyrifos	0–40 mg/l	Control of PAM (Bhuvanewari et al. 2018)
<i>Fluorescence</i>			
<i>E. coli</i> XL1-Blue was used as a host for co-displaying of OPH, MPH, and GFP	Parathion, Methylparathion	0.6 mg/l 0.5 mg/l	Fluorescence (50 mM PBS buffers with pH 4–8), very sensitive analysis to natural pH change (Liu et al. 2013)
<i>E. coli</i> cells carrying a chpR expression vector and a chpA promoter–atsBA transcriptional fusion plasmid encoding sulfatase (atsA) and formylglycine generating enzyme (atsB) from <i>Klebsiella sp.</i>	Chlorpyrifos	87.7 µg/l	Fluorescent biosensor was used for analysis of real water samples from a pond (Whangsuk et al. 2016)
AuNCs/yeast-AChE-E69Y/F330L (AChE wild-type and mutants (E69Y and E69Y/F330L) from <i>Drosophila</i> were displayed on the surface of yeast (<i>Saccharomyces cerevisiae</i> EBY100) through a-aggglutinin-mediated microbial surface display system)	Paraoxon	9.1 pg/l	Fluorescence (50 mM PBS buffer (pH 7.4), low matrix effect on the signal (Liang and Han 2020)
Hydrogel beads containing <i>E. coli</i> (plasmid pJK33) (40% (w/w) Poly(ethylene glycol) diacrylate and 0.4% (w/w) 2-hydroxy-2-methylpropiophenone	Paraoxon	0.83 mg/l	Fluorescent <i>E. coli</i> -containing beads and 1.3 µM of SNAFL dye were used at 40 °C. The sensor can not be reused. (Fleischauer and Heo 2014)

Staphylococcus aureus, *Bacillus subtilis*, etc. (Axelrod et al. 2016). It has been shown that such cells can be used to estimate the toxicity of media containing some individual OPC (fenitrothion, malathion, dicapthion, chlormephos, methylparathion, and famphur) or their mixture (Zhang et al. 2008) (Table 14.3).

The use of cells as BE in an immobilized form, when different gel matrices (agar, agarose, Ca²⁺ and Sr²⁺ alginate gels, and cryogels of polyvinyl alcohol (PVA)) are applied, turned out to be more effective as compared to using suspension cells of photobacteria. The BE based on immobilized cells have a long shelf life (more than 60 weeks), increased stability of the analytical signal, and the ability to determine OPP in the analysis of flow mode at a rate of 180 ml/h (Efremenko et al. 2016). These characteristics open up the possibility and prospects for the use of this BE in monitoring OPC in aquatic environments. The successive OPC determining in soil extracts during flow analysis using immobilized photobacterial cells

also was shown (Efremenko 2018) (Table 14.3). It has been established that immobilized cells of photobacteria quantitatively react with many ecotoxicants. This allows the use of BE developed for the determination of low OPC concentrations in natural systems. However, today the number of studies on OPC monitoring in soils using bioluminescent cells is significantly less than the number of similar studies related to the environmental monitoring of water bodies. Most likely, analytical studies of soil samples, the process of creating BE, and methods for assessing ecotoxicity are more difficult tasks than for water sources. Yet, the development of new ecomonitoring systems based on immobilized cells of luminous bacteria useful for OPP detection in a variety of natural and commercial objects remains relevant. The systems should provide effective OPC detection at concentrations lower or at the level of MRL values (Table 14.1).

14.3.2 Microalgae and Cyanobacteria as Biosensing Elements in OPC Fluorescent Detection

The active use of microalgae and cyanobacteria cells as BE to detect the presence of OPC exists because they are the first in the trophic chains responding to the presence of ecotoxicants without accumulating OPC in significant concentrations (Ettajani et al. 2001; Correa-Reyes et al. 2007). Portable biosensors using fluorescence of microalgae cells were developed to detect various xenobiotics in natural environments (Gosset et al. 2018; Zamora-Sequeira et al. 2019).

The fluorimetric methods used to estimate the functional activity of the photosynthetic apparatus of microalgae (PAM) (Nikolaou et al. 2014), fluorescence transient type, PSII quantum yields, the photochemical quenching (qP(REL)), and the electron transport rate per reaction center (ET0/RC) (Sun et al. 2015) make it possible to obtain data on presence or absence of OPP and interpret them as revealed concentrations of these xenobiotics. These methods enable rapid analysis of the state and process dynamics of aquatic ecosystems and have a relatively high sensitivity (Brayner et al. 2011; Nikolaou et al. 2014).

The OPC has different effects on PAM of phototrophic microorganisms; some inhibit and some, on the contrary, cause an increase in the level of fluorescence (Jena et al. 2012). This is probably because some OPC in small concentrations can be used by microalgae and cyanobacteria cells as sources of nutrients, in particular phosphorus (Chen et al. 2016). For cyanobacteria *Microcystis wessenbergii*, for example, the different concentrations of OPC can cause both a decrease and an increase in fluorescence, and this dependence changes with increasing cell cultivation time (Sun et al. 2015). Similar trends were observed with the use of freshwater green microalgae *Pseudokirchneriella subcapitata* and *Nannochloris oculata* (Martinez et al. 2015). That is why, in the process of creating BE, it is important to regulate such parameters as the age and concentration of the cells. Based on this, it is especially advisable to use

immobilized cells as a base of such BE (Jena et al. 2012). According to Jena et al. (2012) and Bhuvanewari et al. (2018), the effect of OPP on microalgae and cyanobacteria using chlorophyll fluorescence analysis of the tested microorganisms can be most effectively studied with *Chlorella vulgaris* and *Spirulina platensis* cells as BE (Table 14.3).

14.3.3 Other Cell-Based Approaches to OPC Fluorescent Detection

Among the optical biosensors that determine OPP (Yan et al. 2018) and use cells as BE, the most promising ones due to the simplicity of their creation, use, high sensitivity, selectivity, and fast response (Gui et al. 2017) are those based on the use of fluorescent protein (Rajkumar et al. 2017), which can emit a detectable signal in cells of genetically modified microorganism when OPP appears as an inducer of the protein synthesis. As a result of the metabolic activity of the microorganism, a change in the environment occurs, which causes electronic excitation in the exogenous element and the emission of fluorescence. So, many OPC were detected using similar microbial fluorescent BE (Table 14.3).

“Artificial” BE based on yeast cells (*Saccharomyces cerevisiae*) with surface-displayed AChE mutants were constructed for the ultra-trace paraoxon assay with aggregation-caused fluorescence quenching of gold nanoclusters (AuNCs) (Liang and Han 2020). The electropositive thiocholine can not only bind with AuNCs by Au-S bond but also absorb AuNCs by the electrostatic interaction, leading to the aggregation of AuNCs and corresponding fluorescence quenching. Fluorescence analysis using such BE showed hypersensitivity to the detection of paraoxon in concentration 9.1 pg/l (Table 14.3). In addition, this BE was used to detect pesticides in tap and seawater, sewage, and cucumber juice with recoveries in the range of 96.4–106.8%.

Another BE was obtained by co-displaying of organophosphorus hydrolase (OPH) and methylparathion hydrolase (MPH)-green fluorescent protein (GFP) fusion on the cell surface of *Escherichia coli* using the truncated ice nucleation protein (INPNC) and Lpp-OmpA as the anchoring motifs (Liu et al. 2013). The resulting recombinant strain was capable of determining the OPP in concentrations up to 2 μM (0.5–0.6 mg/l). However, this BE was highly sensitive to pH change. Fluorescence at pH 6 decreased by 45% from the level that was determined at pH 7.5 and almost completely disappeared at pH 4.

The BE for the detection of chlorpyrifos is known (Whangsuk et al. 2016). It contains *Escherichia coli* cells carrying a chpR expression vector and a chpA promoter-atsBA transcriptional fusion plasmid encoding sulfatase (atsA) and formylglycine-generating enzyme (atsB) from *Klebsiella* sp. The sulfatase is activated by formylglycine-generating enzyme and then converts 4-methylumbelliferyl

to the fluorescent 4-methylumbelliferone. Chlorpyrifos detection by genetic-based cell BE has low LOD of the pesticide 87.7 $\mu\text{g/l}$ (Table 14.3).

Interesting BE was obtained by immobilization of *E. coli* (OPH)-expressed cells in photocross-linked hydrogel beads containing 40% (w/w) poly(ethylene glycol) diacrylate and 0.4% (w/w) 2-hydroxy-2-methylpropiophenone (Fleischauer and Heo 2014). The detection of paraoxon with the BE was carried out using pH-sensitive fluorescence dye (SNAFL, Life Technologies Co., Eugene, OR) that responds to photons produced from the intracellular OPH reaction with the paraoxon. This sensor could detect the paraoxon with LOD=0.83 mg/l (Table 14.3). A long analysis time (more than 0.5 h) is the main disadvantage of this BE. The activity of the used entrapped cells decreased by 80% of their native OPH activity, and this BE cannot be reused.

Thus, it was shown that the use of fluorescent cellular BE allows the determination of various OPC with high enough sensitivity. However, these BE show serious flaws that limit their use in OPP detecting. In this regard, the development of new effective BE allowing a quick determination of OPC presence is still relevant.

14.4 Conclusion and Future Perspectives

BE for OPC analysis has come a long way from its first appearance to modern commercial products. They can be combined with different methods of signal registration and contain various enzymes and cells in an immobilized and non-immobilized form. The most existing developments completely satisfy the requirements for sensitivity in determining the OPC content in various objects (Table 14.1) and are also extremely easy to use for consumers. However, many researchers are striving to further improve OPC detection limits with the new BE. Thus, the transition to different nano-objects and modern nanomechanical detectors and signal converters (Muenchen et al. 2018, Pundir et al. 2019) can provide breakthrough achievements, as it was 8 years ago with the development of “reagentless” optical detection of AChE enzyme activity inhibitors (Febbraio et al. 2011), which became the basis for a large number of commercially available “strips” (test strips) for the rapid and simple determination of OPC (Lyagin et al. 2017). Combining enzymatic BE with aptasensors (Huang et al. 2019a) may be also very interesting.

Another promising approach is surface-enhanced Raman spectroscopy (Schlücker 2014), which can be more sensitive than other surface plasmon resonance options, due to the possibility of recognizing different compounds directly in the test sample (without preliminary sample preparation), and which uses gold or silver nanoparticles (El Alami et al. 2016). In addition, other optical methods that have found so far limited use, such as the Rayleigh scattering technique (Huang et al. 2019b), may find a wider application. Flow and microfluidic enzyme biosensors have significant potential for further development. Sure, they can be successfully adapted to classical chromatographic determination

methods, for example, with a calorimetric detector (Yuan et al. 2016), which can be easily replaced by some optical (luminescent) variant.

The most important among the objects for continuous monitoring of OPP are raw materials and products of agriculture and/or food industry, light industry products, water, and soil resources since OPC are widely used in many fields of our life and are highly toxic compounds for animals and humans (Sidhu et al. 2019). Today, biomedicine (Li et al. 2019), including strip biosensors (Bagheri et al. 2019) and minimally invasive transdermal detection (Mishra et al. 2017), is showing great interest in such BE, but so far the introduction of BE for daily OPC monitoring in environmental objects in practice is absent. Further development of the achievements of science in this area and the cheapening of BE will make it possible to change the situation by spreading practical analysis of OPC.

Acknowledgments This research was funded by the Russian Science Foundation [Grant No. 16-14-00061].

References

- Amine A, Arduini F, Moscone D, Palleschi G (2016) Recent advances in biosensors based on enzyme inhibition. *Biosens Bioelectron* 76:180–194
- Anh DH, Cheunrungsikul K, Wichitwechkarn J, Surareungchai W (2011) A colorimetric assay for determination of methyl parathion using recombinant methyl parathion hydrolase. *Biotechnol J* 6:565–571
- Axelrod T, Eltzov E, Marks RS (2016) Bioluminescent bioreporter pad biosensor for monitoring water toxicity. *Talanta* 149:290–297
- Badawy MEI, Taktak NEM (2018) Design and optimization of bioactive paper immobilized with acetylcholinesterase for rapid detection of organophosphorus and carbamate insecticides. *Curr Biotechnol* 7:392–404
- Bagheri N, Cinti S, Caratelli V, Massoud R, Saraji M, Moscone D, Arduini F (2019) A 96-well wax printed Prussian Blue paper for the visual determination of cholinesterase activity in human serum. *Biosens Bioelectron* 134:97–102
- Bhuvanewari GP, Purushothaman CS, Pandey PK, Gupta S, Kumar HS, Shukla SP (2018) Toxicological effects of chlorpyrifos on growth, chlorophyll a synthesis and enzyme activity of a cyanobacterium *Spirulina (Arthrospira) platensis*. *Int J Curr Microbiol App Sci* 7:2980–2990
- Bilal M, Iqbal HM (2019) Microbial-derived biosensors for monitoring environmental contaminants: recent advances and future outlook. *Process Saf Environ Prot* 124:8–17
- Boulanouar S, Mezzache S, Combès A, Pichon V (2018) Molecularly imprinted polymers for the determination of organophosphorus pesticides in complex samples. *Talanta* 176:465–478
- Brayner R, Couté A, Livage J, Perrette C, Sicard C (2011) Micro-algal biosensors. *Anal Bioanal Chem* 401:581–597
- Bustos N, Cruz-Alcalde A, Iriel A, Cirelli AF, Sans C (2019) Sunlight and UVC-254 irradiation induced photodegradation of organophosphorus pesticide dichlorvos in aqueous matrices. *Sci Total Environ* 649:592–600
- Cai Y, Fang J, Wang B, Zhang F, Shao G, Liu Y (2019) A signal-on detection of organophosphorus pesticides by fluorescent probe based on aggregation-induced emission. *Sensors Actuators B Chem* 292:156–163
- Cao J, Wang M, She Y, Abd El-Aty AM, Hacımüftüoğlu A, Wang J, Yan M, Hong S, Lao S, Wang Y (2019) Rapid colorimetric determination of the pesticides carbofuran and dichlor-

- vos by exploiting their inhibitory effect on the aggregation of peroxidase-mimicking platinum nanoparticles. *Microchim Acta* 186:390
- Cetrangolo GP, Gori C, Rusko J, Terreri S, Manco G, Cimmino A, Febbraio F (2019) Determination of picomolar concentrations of paraoxon in human urine by fluorescence-based enzymatic assay. *Sensors* 19:4852
- Che Sulaiman IS, Chieng BW, Osman MJ, Ong KK, Rashid JIA, Wan Yunus WMZ, Noor SAM, Kasim NAM, Halim NA, Mohamad A (2020) A review on colorimetric methods for determination of organophosphate pesticides using gold and silver nanoparticles. *Microchim Acta* 187:131
- Chen S, Chen M, Wang Z, Qiu W, Wang J, Shen Y, Wang Y, Ge S (2016) Toxicological effects of chlorpyrifos on growth, enzyme activity and chlorophyll a synthesis of freshwater microalgae. *Environ Toxicol Pharmacol* 45:179–186
- Chungchai W, Amatongchai M, Meelapsom R, Seebunrueng K, Suparsorn S, Jarujamrus P (2020) Development of a novel three-dimensional microfluidic paper-based analytical device (3D- μ PAD) for chlorpyrifos detection using graphene quantum-dot capped gold nanocomposite for colorimetric assay. *Int J Environ Anal Chem* 100:1160–1178.
- Correa-Reyes G, Viana MT, Marquez-Rocha FJ, Licea AF, Ponce E, Vazquez-Duhalt R (2007) Nonylphenol algal bioaccumulation and its effect through the trophic chain. *Chemosphere* 68:662–670
- Diaz AN, Sanchez FG, Aguilar A, de Vicente ABM, Bautista A (2015) Fast stopped-flow enzymatic sensing of fenitrothion in grapes and orange juice. *J Food Compos Anal* 42:187–192
- Döring J, Rettke D, Rödel G, Pompe T, Ostermann K (2019) Surface functionalization by hydrophobin-EPSPS fusion protein allows for the fast and simple detection of glyphosate. *Biosensors* 9:104
- Duan N, Wu S, Dai S, Gu H, Hao L, Ye H, Wang Z (2016) Advances in aptasensors for the detection of food contaminants. *Analyst* 141:3942–3961
- Efremenko EN (ed) (2018) Immobilized cells: biocatalysts and processes: monograph. RIOR, Moscow. <https://doi.org/10.29039/02004-3>
- Efremenko EN, Senko OV, Aleskerova LE, Alenina KA, Mazhul MM, Ismailov AD (2014) Biosensors based on the luminous bacteria *Photobacterium phosphoreum* immobilized in polyvinyl alcohol cryogel for the monitoring of ecotoxicants. *Appl Biochem Microbiol* 50:477–482
- Efremenko EN, Maslova OV, Kholstov AV, Senko OV, Ismailov AD (2016) Biosensitive element in the form of immobilized luminescent photobacteria for detecting ecotoxicants in aqueous flow-through systems. *Luminescence* 31:1283–1289
- El Alami A, Lagarde F, Tamer U, Baitoul M, Daniel P (2016) Enhanced Raman spectroscopy coupled to chemometrics for identification and quantification of acetylcholinesterase inhibitors. *Vib Spectrosc* 87:27–33
- Eldufani J, Blaise G (2019) The role of acetylcholinesterase inhibitors such as neostigmine and rivastigmine on chronic pain and cognitive function in aging: a review of recent clinical applications. *Alzheimers Dement Translat Res Clin Interv* 5:175–183
- Ettajani H, Berthet B, Amiard JC, Chevolut L (2001) Determination of cadmium partitioning in microalgae and oysters: contribution to the assessment of trophic transfer. *Arch Environ Contam Toxicol* 40:209–221
- Febbraio F, Merone L, Cetrangolo GP, Rossi M, Nucci R, Manco G (2011) Thermostable esterase 2 from *Alicyclobacillus acidocaldarius* as biosensor for the detection of organophosphate pesticides. *Anal Chem* 83:1530–1536
- Fleischauer V, Heo J (2014) An organophosphate sensor based on photo-crosslinked hydrogel-entrapped *E. coli*. *Anal Sci* 30:937–942
- Gheorghe S, Lucaciu I, Paun I, Vasile G, Petre J, Iancu V, Stoica C, Mitru D, Nita-Lazar M (2019) Anthropogenic pollutants: 10 years of progress in ecotoxicological studies and aquatic risk assessment. *Rom J Ecol Environ Chem* 1:26–38
- Ghosh K, Mazumder Tagore D, Anumula R, Lakshmaiah B, Kumar PP, Singaram S, Matan T, Kallipatti S, Selvam S, Krishnamurthy P, Ramarao M (2013) Crystal structure of rat intestinal

- alkaline phosphatase – role of crown domain in mammalian alkaline phosphatases. *J Struct Biol* 184:182–192
- Gosset A, Durrieu C, Renaud L, Deman AL, Barbe P, Bayard R, Chateaux JF (2018) Xurography-based microfluidic algal biosensor and dedicated portable measurement station for online monitoring of urban polluted samples. *Biosens Bioelectron* 117:669–677
- Gui Q, Lawson T, Shan S, Yan L, Liu Y (2017) The application of whole cell-based biosensors for use in environmental analysis and in medical diagnostics. *Sensors* 17:1623
- Halmi MIE (2016) Rapid ecotoxicological tests using bioassay systems—a review. *J Biochem Microbiol Biotechnol* 4:29–37
- Hicks M, Bachmann TT, Wang B (2020) Synthetic biology enables programmable cell-based biosensors. *ChemPhysChem* 21(2):132–144
- Hu T, Xu J, Ye Y, Han Y, Li X, Wang Z, Sun D, Zhou Y, Ni Z (2019) Visual detection of mixed organophosphorous pesticide using QD-AChE aerogel based microfluidic arrays sensor. *Biosens Bioelectron* 136:112–117
- Huang N, Qin Y, Li M, Chen T, Lu M, Zhao J (2019a) A sensitive fluorescence assay of organophosphorus pesticides using acetylcholinesterase and copper-catalyzed click chemistry. *Analyst* 144:3436–3441
- Huang Y, Yang J, Cheng J, Zhang Y, Yuan H (2019b) A novel spectral method for determination of trace malathion using EryB as light scattering probe by resonance Rayleigh scattering technique. *Spectrochim Acta A Mol Biomol Spectrosc* 213:104–110
- Huang S, Yao J, Chu X, Liu Y, Xiao Q, Zhang Y (2019c) One-step facile synthesis of nitrogen-doped carbon dots: a ratiometric fluorescent probe for evaluation of acetylcholinesterase activity and detection of organophosphorus pesticides in tap water and food. *J Agric Food Chem* 67:11244–11255
- Ibarra Bouzada LME, Hernández SR, Kergaravat SV (2019) Glyphosate detection from commercial formulations: comparison of screening analytic methods based on enzymatic inhibition. *Int J Environ Anal Chem* 149:1–15. <https://doi.org/10.1080/03067319.2019.1691176>
- Ismailov AD, Aleskerova LE (2015) Photobiosensors containing luminescent bacteria. *Biochem Mosc* 80:733–744
- Ismailov A, Aleskerova L, Alenina K, Efremenko E (2019) Biosensors using free and immobilized cells of luminous bacteria. In: Suzuki H (ed) *Analytical Applications and Basic Biology 2019*. IntechOpen London, United Kingdom, pp.39–59. <https://doi.org/10.5772/intechopen.85624>
- Jena S, Acharya S, Mohapatra PK (2012) Variation in effects of four OP insecticides on photosynthetic pigment fluorescence of *Chlorella vulgaris* Beij. *Ecotoxicol Environ Saf* 80:111–117
- Jin R, Kong D, Zhao X, Li H, Yan X, Liu F, Sun P, Du D, Lin Y, Lu G (2019) Tandem catalysis driven by enzymes directed hybrid nanoflowers for on-site ultrasensitive detection of organophosphorus pesticide. *Biosens Bioelectron* 141:111473
- Jin L, Hao Z, Zheng Q, Chen H, Zhu L, Wang C, Liu X, Lu C (2020) A facile microfluidic paper-based analytical device for acetylcholinesterase inhibition assay utilizing organic solvent extraction in rapid detection of pesticide residues in food. *Anal Chim Acta* 1100:215–224
- Korram J, Dewangan L, Nagwanshi R, Karbhal I, Ghosh KK, Satnami ML (2019) A carbon quantum dot–gold nanoparticle system as a probe for the inhibition and reactivation of acetylcholinesterase. *New J Chem* 43:6874–6882
- Lan W, Chen G, Cui F, Tan F, Liu R, Yushupjiang M (2012) Development of a novel optical biosensor for detection of organophosphorus pesticides based on methyl parathion hydrolase immobilized by metal-chelate affinity. *Sensors* 12(7):8477–8490
- Li X, Cui H, Zeng Z (2018) A simple colorimetric and fluorescent sensor to detect organophosphate pesticides based on adenosine triphosphate-modified gold nanoparticles. *Sensors* 18:4302
- Li S, Zhao J, Huang R, Santillo MF, Houck KA, Xia M (2019) Use of high-throughput enzyme-based assay with xenobiotic metabolic capability to evaluate the inhibition of acetylcholinesterase activity by organophosphorous pesticides. *Toxicol in Vitro* 56:93–100

- Liang B, Han L (2020) Displaying of acetylcholinesterase mutants on surface of yeast for ultra-trace fluorescence detection of organophosphate pesticides with gold nanoclusters. *Biosens Bioelectron* 148:111825
- Liu D, Chen W, Wei J, Li X, Wang Z, Jiang X (2012) A highly sensitive, dual-readout assay based on gold nanoparticles for organophosphorus and carbamate pesticides. *Anal Chem* 84:4185–4191
- Liu R, Yang C, Xu Y, Xu P, Jiang H, Qiao C (2013) Development of a whole-cell biocatalyst/biosensor by display of multiple heterologous proteins on the *Escherichia coli* cell surface for the detoxification and detection of organophosphates. *J Agric Food Chem* 61:7810–7816
- Liu H, Chen P, Liu Z, Liu J, Yi J, Xia F, Zhou C (2020) Electrochemical luminescence sensor based on double suppression for highly sensitive detection of glyphosate. *Sensors Actuators B Chem* 304:127364
- Long Q, Li H, Zhang Y, Yao S (2015) Upconversion nanoparticle-based fluorescence resonance energy transfer assay for organophosphorus pesticides. *Biosens Bioelectron* 68:168–174
- Lopez-Roldan R, Kazlauskaitė L, Ribo J, Riva MC, González S, Cortina JL (2012) Evaluation of an automated luminescent bacteria assay for in situ aquatic toxicity determination. *Sci Total Environ* 440:307–313
- Lyagin IV, Efremenko EN, Varfolomeev SD (2017) Enzymatic biosensors for determination of pesticides. *Russ Chem Rev* 86:339–355
- Ma XY, Wang XC, Ngo HH, Guo W, Wu MN, Wang N (2014) Bioassay based luminescent bacteria: interferences, improvements, and applications. *Sci Total Environ* 468:1–11
- Mangas I, Estevez J, Vilanova E, França TC (2017) New insights on molecular interactions of organophosphorus pesticides with esterases. *Toxicology* 376:30–43
- Martínez RS, Di Marzio WD, Sáenz ME (2015) Genotoxic effects of commercial formulations of chlorpyrifos and tebuconazole on green algae. *Ecotoxicology* 24:45–54
- Matějovský L, Pitschmann V (2019) A strip biosensor with guinea green B and fuchsin basic color indicators on a glass nanofiber carrier for the cholinesterase detection of nerve agents. *ACS Omega* 4:20978–20986
- Mehta J, Dhaka S, Paul AK, Dayananda S, Deep A (2019a) Organophosphate hydrolase conjugated UiO-66-NH₂ MOF based highly sensitive optical detection of methyl parathion. *Environ Res* 174:46–53
- Mehta J, Dhaka S, Bhardwaj N, Paul AK, Dayananda S, Lee S-E, Kim K-H, Deep A (2019b) Application of an enzyme encapsulated metal-organic framework composite for convenient sensing and degradation of methyl parathion. *Sensors Actuators B Chem* 290:267–274
- Meng X, Wei J, Ren X, Ren J, Tang F (2013) A simple and sensitive fluorescence biosensor for detection of organophosphorus pesticides using H₂O₂-sensitive quantum dots/bi-enzyme. *Biosens Bioelectron* 47:402–407
- Mishra RK, Vinu Mohan AM, Soto F, Chrostowski R, Wang J (2017) A microneedle biosensor for minimally-invasive transdermal detection of nerve agents. *Analyst* 142:918–924
- Mossa ATH, Mohafrash SMM, Shalaby AR (2017) Toxicity assessment of chlorpyrifos, malachite green and tetracyclines by Microtox® assay: detoxification by ultrasonic. *Sci Technol* 10(2):68–79
- Muenchen DK, Martinazzo J, Brezolin AN, de Cezaro AM, Rigo AA, Mezarroba MN, Manzoli A, de Lima Leite F, Steffens J, Steffens C (2018) Cantilever functionalization using peroxidase extract of low cost for glyphosate detection. *Appl Biochem Biotechnol* 186:1061–1073
- Nikolaou A, Bernardi A, Bezzo F, Morosinotto T, Chachuat B (2014) A dynamic model of photo-production, photoregulation and photoinhibition in microalgae using chlorophyll fluorescence. *IFAC Proc* 47:4370–4375
- Pundir CS, Malik A, Preety (2019) Bio-sensing of organophosphorus pesticides: a review. *Biosens Bioelectron* 140:111348
- Qi F, Lan Y, Meng Z, Yan C, Li S, Xue M, Wang Y, Qiu L, He X, Liu X (2018) Acetylcholinesterase-functionalized two-dimensional photonic crystals for the detection of organophosphates. *RSC Adv* 8:29385–29391

- Qi F, Yan C, Meng Z, Li S, Xu J, Hu X, Xue M (2019) Acetylcholinesterase-functionalized two-dimensional photonic crystal for the sensing of G-series nerve agents. *Anal Bioanal Chem* 411:2577–2585
- Rajkumar P, Ramprasath T, Selvam GS (2017) A simple whole cell microbial biosensors to monitor soil pollution. In: Grumezescu A (ed) *New pesticides and soil sensors*. Academic Press, Cambridge, pp 437–481
- Ramanathan M, Wang L, Wild JR, Meyerhoff ME, Simonian AL (2010) Monitoring of diisopropyl fluorophosphate hydrolysis by fluoride-selective polymeric films using absorbance spectroscopy. *Anal Chim Acta* 667:119–122
- Sahub C, Tuntulani T, Nhujak T, Tomapatanaget B (2018) Effective biosensor based on graphene quantum dots via enzymatic reaction for directly photoluminescence detection of organophosphate pesticide. *Sensors Actuators B Chem* 258:88–97
- Samsidar A, Siddiquee S, Md Shaarani S (2018) A review of extraction, analytical and advanced methods for determination of pesticides in environment and foodstuffs. *Trends Food Sci Technol* 71:188–201
- Schlücker S (2014) Surface-enhanced Raman spectroscopy: concepts and chemical applications. *Angew Chem Int Ed* 53:4756–4795
- Senko O, Maslova O, Efremenko E (2017) Optimization of the use of His₆-OPH-based enzymatic biocatalysts for the destruction of chlorpyrifos in soil. *Int J Environ Res Public Health* 14:1438
- Sidhu GK, Singh S, Kumar V, Dhanjal DS, Datta S, Singh J (2019) Toxicity, monitoring and biodegradation of organophosphate pesticides: a review. *Crit Rev Environ Sci Technol* 49:1135–1187
- Silletti S, Rodio G, Pezzotti G, Turemis M, Dragone R, Frazzoli C, Giardi MT (2015) An optical biosensor based on a multiarray of enzymes for monitoring a large set of chemical classes in milk. *Sensors Actuators B Chem* 215:607–617
- Sun KF, Xu XR, Duan SS, Wang YS, Cheng H, Zhang ZW, Zhou GJ, Hong YG (2015) Ecotoxicity of two organophosphate pesticides chlorpyrifos and dichlorvos on non-targeting cyanobacteria *Microcystis wessenbergii*. *Ecotoxicology* 24:1498–1507
- Thakur S, Reddy MV, Siddavattam D, Paul AK (2012) A fluorescence based assay with pyranine labeled hexa-histidine tagged organophosphorus hydrolase (OPH) for determination of organophosphates. *Sensors Actuators B Chem* 163:153–158
- Thakur S, Kumar P, Reddy MV, Siddavattam D, Paul AK (2013) Enhancement in sensitivity of fluorescence based assay for organophosphates detection by silica coated silver nanoparticles using organophosphate hydrolase. *Sensors Actuators B Chem* 178:458–464
- Tuteja SK, Kukkar M, Kumar P, Paul AK, Deep A (2014) Synthesis and characterization of silica-coated silver nanoprobe for paraoxon pesticide detection. *BioNanoSci* 4:149–156
- Van Dyk JS, Pletschke B (2011) Review on the use of enzymes for the detection of organochlorine, organophosphate and carbamate pesticides in the environment. *Chemosphere* 82:291–307
- Varfolomeev SD, Efremenko EN (2020) Organophosphorus neurotoxins: monograph. RIOR, Moscow. <https://doi.org/10.29039/02026-5>
- Wang K, Wang L, Jiang W, Hu J (2011) A sensitive enzymatic method for paraoxon detection based on enzyme inhibition and fluorescence quenching. *Talanta* 84:400–405
- Wang P, Li H, Hassan MM, Guo Z, Zhang ZZ, Chen Q (2019) Fabricating an acetylcholinesterase modulated UCNP-Cu²⁺ fluorescence biosensor for ultrasensitive detection of organophosphorus pesticides-diazinon in food. *J Agric Food Chem* 67:4071–4079
- Whangskuk W, Thiengmag S, Dubbs J, Mongkolsuk S, Loprasert S (2016) Specific detection of the pesticide chlorpyrifos by a sensitive genetic-based whole cell biosensor. *Anal Biochem* 493:11–13
- Wu X, Wang P, Hou S, Wu P, Xue J (2019) Fluorescence sensor for facile and visual detection of organophosphorus pesticides using AIE fluorogens-SiO₂-MnO₂ sandwich nanocomposites. *Talanta* 198:8–14
- Yan X, Li H, Wang X, Su X (2015a) A novel fluorescence probing strategy for the determination of parathion-methyl. *Talanta* 131:88–94

- Yan X, Li H, Yan Y, Su X (2015b) Selective detection of parathion-methyl based on near-infrared CuInS₂ quantum dots. *Food Chem* 173:179–184
- Yan X, Li H, Han X, Su X (2015c) A ratiometric fluorescent quantum dots based biosensor for organophosphorus pesticides detection by inner-filter effect. *Biosens Bioelectron* 74:277–283
- Yan X, Li H, Su X (2018) Review of optical sensors for pesticides. *TrAC Trends Anal Chem* 103:1–20
- Yang M, Liu M, Wu Z, He Y, Ge Y, Song G, Zhou J (2019) Carbon dots co-doped with nitrogen and chlorine for “off-on” fluorometric determination of the activity of acetylcholinesterase and for quantification of organophosphate pesticides. *Microchim Acta* 186:585
- Yuan M, Yu J, Cao H, Xu F (2016) Effective improvement in performance of a miniature FIA-calorimetric biosensing system via denoising column addition and flow rate optimization. *Sensors Actuators B Chem* 229:492–498
- Zamora-Sequeira R, Starbird-Pérez R, Rojas-Carillo O, Vargas-Villalobos S (2019) What are the main sensor methods for quantifying pesticides in agricultural activities? A review. *Molecules* 24:2659
- Zhang YH, Liu SS, Song XQ, Ge HL (2008) Prediction for the mixture toxicity of six organophosphorus pesticides to the luminescent bacterium Q67. *Ecotoxicol Environ Saf* 71:880–888
- Zhang W, Asiri AM, Liu D, Du D, Lin Y (2014) Nanomaterial-based biosensors for environmental and biological monitoring of organophosphorus pesticides and nerve agents. *Trends Anal Chem* 54:1–10
- Zhang F, Liu Y, Ma P, Tao S, Sun Y, Wang X, Song D (2019) A Mn-doped ZnS quantum dots-based ratiometric fluorescence probe for lead ion detection and “off-on” strategy for methyl parathion detection. *Talanta* 204:13–19
- Zheng Z, Zhou Y, Li X, Liu S, Tang Z (2011) Highly-sensitive organophosphorous pesticide biosensors based on nanostructured films of acetylcholinesterase and CdTe quantum dots. *Biosens Bioelectron* 26:3081–3085
- Zhou X, Sang W, Liu S, Zhang Y, Ge H (2010) Modeling and prediction for the acute toxicity of pesticide mixtures to the freshwater luminescent bacterium *Vibrio qinghaiensis* sp.-Q67. *J Environ Sci* 22:433–440

Part III
Features of the Determination of Glucose

Chapter 15

Nano- and Microelectrochemical Biosensors for Determining Blood Glucose



Sergei Evgenyevich Tarasov, Yulia Victorovna Plekhanova, Mahendra Rai, and Anatoly Nikolaevich Reshetilov

Abstract Blood glucose analysis is currently an important issue both for ordinary people wishing to monitor their health and for patients suffering from various diseases, especially diabetes mellitus. This chapter considers nano- and micro-sized devices based on biological receptors for glucose level measurements. As attention is largely paid to non-invasive techniques, we also touch upon the existing glucose assays for other fluids of the organism that require no skin-cover integrity to be disturbed. We present data on the development of continuous blood glucose level monitoring to provide a true picture of glycemic changes over large periods of time. The advantages and limitations of using enzyme electrochemical biosensors for glucose detection are discussed. A part of the work deals with specific features of using carbon and metal nanoparticles in biosensors to improve their properties. The current fundamental research in the development of biosensors and available commercial devices is also discussed.

Keywords Blood glucose · Diabetes · Glucose biosensors · Microsensors · Nanosensors · Non-invasive glucose analysis · Continuous monitoring of glucose · Electrochemical biosensors · Nanomaterials

Nomenclature

AuNPs	gold nanoparticles
FAD	flavin adenine dinucleotide
GDH	glucose dehydrogenase

S. E. Tarasov · Y. V. Plekhanova · A. N. Reshetilov (✉)
Laboratory of Biosensors, G.K. Skryabin Institute of Biochemistry and Physiology of Microorganisms, Pushchino Center for Biological Research of the Russian Academy of Sciences, Pushchino, Moscow Region, Russian Federation
e-mail: anatol@ibpm.pushchino.ru

M. Rai
Nanobiotechnology Laboratory, Department of Biotechnology, Sant Gadge Baba Amravati University, Amravati, Maharashtra, India

GOx	glucose oxidase
LOD	limit of detection
MPtNT	one-dimensional platinum nanotubes
MWCNTs	multiwalled carbon nanotubes
PQQ	pyrroloquinoline quinone
PtNPs	platinum nanoparticles
TTF-TCNQ	tetrathiafulvalene tetracyanoquinodimethane

15.1 Introduction

According to the data by the World Health Organization, an estimated 422 million people in the world suffer from diabetes, and by 2030, the disease will become the cause of each seventh death on the planet (Global report on diabetes 2018). The global level of the disease has doubled over the last 35 years, from 4.7 up to 8.5%. In Russia, 4,498,955 patients with this diagnosis have been registered by 2018 (Dedov et al. 2018). The causes of the disease have not been yet fully understood, which requires the fast and efficient quantitative determination of glucose.

There are three different types of diabetes:

1. Type 1 diabetes usually affects the young and is a disease characterized by the loss of β -pancreatic cell ability to produce and secrete insulin. Approximately 10% of diabetics have Type 1 (Rodriguez et al. 2020).
2. Type 2 diabetes commonly affects older patients and occurs when the pancreas does not produce enough insulin or when the body does not use the produced insulin effectively. Type 2 diabetes makes up more than 90% of all cases of diabetes in adults, according to the Centers for Disease Control and Prevention (Kim et al. 2019).
3. Sometimes gestational diabetes is singled out as the third type. It is a temporary condition that occurs during pregnancy and affects 2–4% of all pregnancies with a further increased risk of developing diabetes (Stewart 2020).

Excess of glucose in blood plasma causes a hyperglycemic state that leads to numerous complications such as blindness, cardiovascular diseases, and renal failure (Lee et al. 2018). Due to severe medical consequences of diabetic complications, patients critically require continuous personal monitoring and control of blood glucose level.

Most personal sensors developed to date are based on electrochemical devices with an enzyme as a receptor element and are associated with invasive blood taking techniques. Biosensor models are developed in several major directions. As invasive techniques are inconvenient for the user and may cause a discomfort, patients may fail to observe the control of glucose level. For this reason, one of the directions of glucose biosensor research is associated with the development of non-invasive diagnostic monitoring methods (Sadana and Sadana 2015). There are numerous papers that are investigating a relation between the level of glucose in human blood and

other physiological fluids (sweat, tears, saliva) and the possibility of developing wearable non-invasive devices for glucose measurements. Another direction of research aims to improve the parameters of biosensors themselves—to enhance the accuracy of the assay, to preserve the activity of the receptor elements at a high level for a prolonged period of time. Yet another important direction is related to the research and development of totally autonomous self-powered devices that require no external power supply sources and are capable of transmitting information to the user wirelessly.

The chapter briefly reviews the general state of the art in electrochemical biosensors for blood glucose determination. A brief history of the development of glucose biosensors is given, and they are compared with other standard glucose assay techniques. Emphasis is made on the assessment of the possibility of continuous and non-invasive glucose measurements in blood and other biological fluids, as well as on the use of various nanomaterials as glucose biosensors' elements.

15.2 Standard Methods of Glucose Determination in Clinical Laboratories

There are numerous methods that enable quantitative determination of glucose in the model and the organism (Galant et al. 2015; Wang and Lee 2015). The following trends of assay are singled out: optical (spectrophotometric, spectrofluorimetric, diffraction), electrochemical (amperometric, potentiometric, conductometric), chromatographic, titrimetric, and calorimetric. Clinical diagnostic laboratories mainly use enzymatic spectrophotometric and amperometric glucose determination methods. Outside clinical laboratories, photometric techniques with test strips are additionally used. Chromato-mass spectrometric procedures are frequently used to certify standard blood serum samples. Spectrofluorimetric, diffraction, and chromatographic methods are widespread in biomedical research. Such methods as non-enzymatic spectrophotometry and electrochemistry, titrimetric and calorimetric procedures, as well as a number of enzymatic spectrophotometric procedures are not used in most cases in modern clinical and diagnostic practice (Buzanovskii 2015).

The earliest methods of glucose detection are titrimetric. They are based on the ability of glucose to reduce copper salts or potassium ferricyanide at one of the stages of its detection. The method is not applicable for assaying glucose in biological objects due to a high error of manual measurement (Simon et al. 1968).

More modern chromatographic methods include gas chromatography–mass spectrometry, which enables analyses of complex–composition mixtures (Gladilovich and Podolskaya 2010). This method is highly sensitive; however, the assays of glucose and other sugars require preliminary stages of sample preparation (Andreis et al. 2014) due to the extraction of initial samples and their transfer to sublimable forms mainly by ester formation.

A more widespread method is high-performance liquid chromatography using UV, fluorescence, or refraction-index detectors (Yuh et al. 1998). The main

advantage of this method is the simplicity of sample preparation, because the components to be determined are separated in an aqueous medium. For glucose detection processes, the method also requires preionization of sugars in solution by increasing pH of the medium.

A highly popular group of glucose detection techniques in aqueous media are colorimetric methods. They can be divided into non-enzymatic and enzymatic. Spectrophotometric enzymatic methods of glucose determination that possess an exceptional selectivity, fast assay rate, and sufficient accuracy are a good alternative for assays of manufactured foods but are insufficiently effective for blood assays (Moodley et al. 2015).

In recent years, most clinical measurements have been based on electrochemical biosensors. They contain a specific enzyme glucose oxidase (GOx) immobilized on the surfaces of various types of electrodes. Glucose breaks down as the result of the operation of the enzyme, and the amount of the formed hydrogen peroxide or consumed oxygen is registered. New-generation biosensors have also emerged, which register the direct transfer of electrons from the active site of the enzyme, which catalyzes the glucose breakdown reaction, to the electrode (Yu et al. 2014).

15.3 History of the Research and Development of Glucose Biosensors

Over 15,000 original articles, reviews, and monographs on the development of enzymatic glucose biosensors have been published since 1962 up to the present. Initially, 40 years ago, about one article per year was published on the subject of biosensors; to date, their number reaches 4500 articles (Turner 2013; Olson and Bae 2019), and the world market of (bio)sensors has grown from 5 million to 17 billion US dollars (Biosensors Market Report 2019–2026). These rapid growth rates are largely due to the colossal demand in personal analyzers, for example, glucometers. By the data of the World Health Organization, about 4.5 million diabetes patients in Russia and more than 200 thousand in Moscow need constant (no less than twice a day) blood glucose assays. On the other hand, interest in personified medicine as well as in various smart diagnostic personal devices based on biosensors is high today as never before. The milestones achieved in the development of commercially available glucose biosensors are presented in Table 15.1.

The idea of the glucose enzymatic electrode, the first-generation biosensor, was proposed in 1962 (Clark and Lyons 1962). The first device was based on a thin layer of GOx, trapped on the surface of an oxygen electrode (by means of a semi-transparent dialysis membrane), and monitoring the oxygen consumed in the reaction presented in Fig. 15.1.

The Clark technology was subsequently passed on to Yellow Spring Instrument Company, which in 1975 launched the first special biosensor for glucose (the YSI 23 analyzer) for direct measurement of glucose in 25-ml blood samples. Though it

Table 15.1 History of commercially available electrochemical glucose biosensors

Year	Device name	Company	Sample volume, μL	Measurement time, s	Features
1973 (re-launched in 1975)	YSI 23 analyzer	Yellow spring instrument company, USA	25		Glucose enzyme electrode that monitors hydrogen peroxide, which occurs during the oxidation of glucose in the body GOx; Fast glucose assay in blood samples; High price of Pt electrode could be used exclusively in clinical laboratories
1987	ExacTech	MediSense, USA	10–50	30	Second-generation biosensor using mediator electron transfer to the electrode; The first pocket-sized home glucose meter
1991	Glucocard GT-1610	Arkray, Japan	5	60	Second-generation biosensor using mediator electron transfer to the electrode; Compact, small sample size; Ascorbic and uric acid are interfering with the measurements
1992	i-STAT portable clinical analyzer	i-STAT Corp., USA	65	120	Glucose is measured amperometrically via the product (H_2O_2) of the glucose oxidase reaction; Measures the level Na^+ , K^+ , Cl^- и NH_4^+ ions and glucose simultaneously
1997	Precision QID	Abbott, USA	3,5	20	Based on ExacTech technology, has built-in memory, remembers the last 10 patient results

(continued)

Table 15.1 (continued)

Year	Device name	Company	Sample volume, μL	Measurement time, s	Features
1998	OneTouch FastTake	LifeScan, Switzerland	1,5	15	LifeScan's first electrochemical sensor; Automatically drags the blood drop into the tip of the test strip on contact; 150 results in memory, automatic average results from 14 days
2000	FreeStyle blood glucose monitoring system	Therasense, USA	0,3	15	Glucose dehydrogenase is used instead of glucose oxidase; The system allows samples to be taken from multiple sites including the fingertips, forearm, upper arm, thigh, calf, and fleshy part of the hand; Has PC connectivity
2001	Sof-tact	MediSense, USA	2–3	20	Based on ExacTech technology; First instrument with automated testing, ease of operation, 450 results in memory, an average of 7.14 or 28 days; High price (\$ 200 for the device and \$ 50 for a set of test strips); Limitations of this device include a poorer than predicted uptake of alternate site testing, the considerable size of the instrument, and the restriction to a single measurement
2001	Precision Xtra	Abbott, USA	0.6 (1.5 for ketones)	5 (10 for ketones)	First device for measuring glucose and ketones simultaneously

(continued)

Table 15.1 (continued)

Year	Device name	Company	Sample volume, μL	Measurement time, s	Features
2001	GlucoWatch	Cygnus Inc., USA	–	Up to 3 measurements per hour for 12 hours	The first wearable continuous glucose meter to measure extracellular fluid glucose; Takes up to 3 hours to warm up, false alarm, inaccuracy, skin irritation and sweating, discontinued in 2008
2002	MiniMed	Sylmar, USA	–	Measurements once a minute	First commercial in vivo glucose biosensor contains an automated insulin pump; 1–2 years of work until replacement
2002	Accu-Chek advantage	Roche, Switzerland	3–3.5	15	Glucose dehydrogenase is used instead of glucose oxidase; Features 17 test strips in a single drum that is fully integrated into the meter, which avoids the need for handling of individual strips; Automatic selection and removal of test strips at the touch of a button
2003	Ascensia contour	Bayer, Germany	0.6	5	Glucose dehydrogenase is used instead of glucose oxidase; Needs no coding; Device was calibrated by plasma, in which the concentration of sugar is 11% higher than in blood
2006	STS continuous glucose monitoring system	Dexcom, USA	–	–	Second FDA-approved continuous glucose monitoring system; Can be used within 3 days before replacement

(continued)

Table 15.1 (continued)

Year	Device name	Company	Sample volume, μL	Measurement time, s	Features
2009	Countour USB	Bayer, Germany	–	–	The first and only blood glucose monitor that plugs directly into a computer, providing instant access to software that can help optimize diabetes management by analyzing blood glucose readings
2009	DIDGET	Bayer, Germany	–	–	The first device for children with diabetes, integrated with a game console
2011	AgaMatrix nugget + iBGStar app	Sanofi Aventis, France	–	–	The first meter combined with a mobile application for the iPhone
2015	G4 platinum CGM system	Dexcom, USA	–	–	First FDA-approved glucose monitoring mobile app
2016 – For use in clinics (2017 – For personal use)	FreeStyle libre	Abbott, USA	–	–	First CGM that does not require calibration with fingerstick measurement; Can be worn up to 10 days without replacement (up to 14 days with the pro version); 12 hours of warm-up before measurements in the first version of the device (then reduced to 1 h)

was not the first commercial device for glucose measurement. Slightly earlier, in the late 1960s, the Ames Reflectance Meter (ARM) was developed, which combined Dextrostix dry test strips with photometry for measuring glucose in blood. Several more devices based on reflectance measurements and standard test strips, such as Reformat (Boehringer Mannheim, Germany) and Eyetone (Arkray, Japan), were launched on the market in the early 1970s (Clarke and Foster 2012). These devices were successfully used in hospitals for a decade; still, most commercial devices for personified measurements of blood glucose levels are based on the ideas of Clark and Lyons. In 1973, Guilbault and Lubrano (1973) described an enzyme electrode

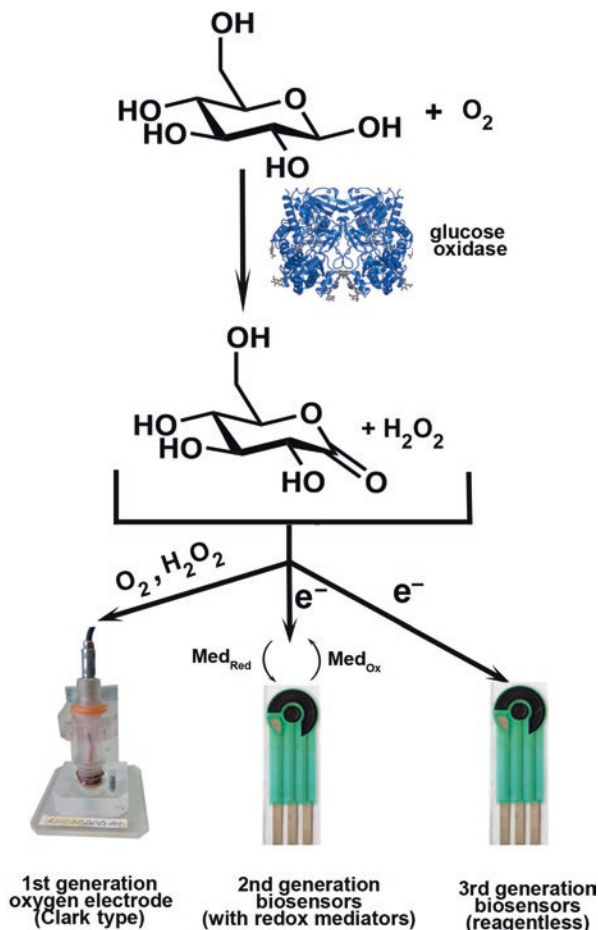
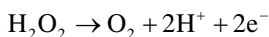


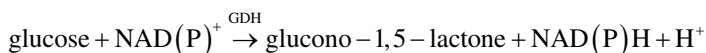
Fig. 15.1 The biochemical reaction underlying the first-, second-, and third-generation electrochemical glucose biosensors

for determination of glucose in blood based on the amperometric monitoring of oxygen peroxide released in the glucose oxidase-catalyzed reaction:



Updike and Higgs, in 1967, first successfully immobilized GOx in polyacrylamide gel, which enabled stabilizing the enzyme and simplifying measurements by the biosensor in biological fluids (Updike and Hicks 1967a, b). Since then, numerous variants of enzyme-based electrochemical sensors, differing by the design of the electrode, material of the membrane, or method of immobilization, have been described in the literature. It is also worth noting that not only GOx but also other

enzymes, for example, glucose dehydrogenase (GDH), can be used as a biological element:



Further improvements were related to the replacement of oxygen as a natural electron acceptor for a synthetic mediator. They laid the foundation of second-generation biosensors (Liu and Wang 2001). GOx is not capable of directly transferring electrons to the surface of traditional electrodes, because the FAD redox center is enclosed by a thick protein layer, and this blocks the direct transfer of electrons. Therefore, the use of a non-physiological electron acceptor for electron transfer and for solving the problem of oxygen deficit is the main approach in this generation of sensors. Mediators in these biosensors should oxidize the enzyme complex faster than oxygen, be insoluble and non-toxic. First- and second-generation biosensors have a number of drawbacks. Their commercial implementations are invasive or semi-invasive and require reference calibration; also, they are not able to serve as a part of an autonomous glucose-concentration regulation system (Hovorka 2006).

Third-generation biosensors are reagentless and are based on the direct transfer between the enzyme and the electrode without mediators. To provide for the direct transfer of electrons to the electrode, organic conducting materials can be used instead of mediators with high toxicity (Guo and Li 2010). Nevertheless, only a few enzymes, including peroxidases, demonstrate the direct transfer of electrons on the surface of standard electrodes (Teng et al. 2009). Providing for the direct transfer from other enzymes requires additional modification of electrodes (e.g., by nanomaterials, conducting gels). In particular, conducting organic compounds, such as tetrathiafulvalene tetracyanoquinodimethane (TTF-TCNQ), are capable of being carriers both for PQQ-dependent GDH and for GOx (Yoo and Lee 2010). For this reason, third-generation glucose biosensors possess a greater potential for creating needle-type implantable devices for continuous monitoring of blood glucose level.

Today, biosensor devices successfully compete with traditional methods routinely used in clinical diagnostics and assuming the use of expensive equipment, special premises, and qualified personnel. The development strategy of bioanalytical assay methods is shifted toward conducting the initial examination outside the healthcare facility within the framework of personified medicine approach. Research is aimed at the development and fabrication of inexpensive, sensitive, selective, and handy devices, convenient for an unsophisticated user.

15.4 Application of nanomaterials in Glucose Biosensors

The characteristics of glucose biosensors are often improved by nanomaterials (Fig. 15.2). They can be used to enhance the catalytic properties of electrodes by increasing the sensor surface area, to change the physical parameters of the

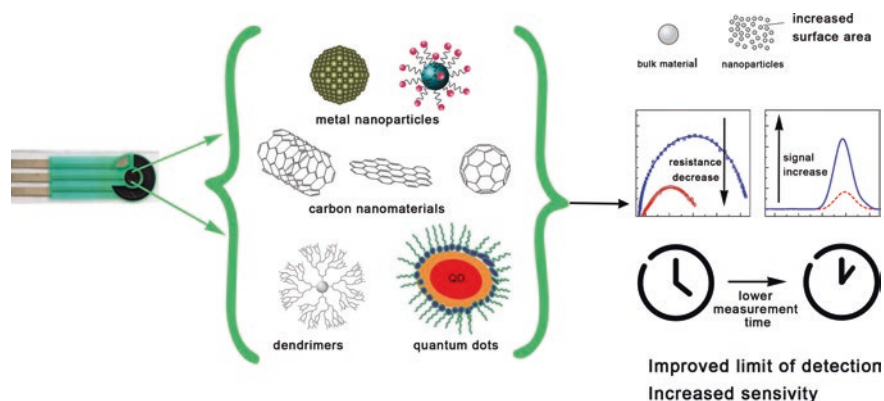


Fig. 15.2 Changes in the characteristics of electrochemical glucose biosensors when using nanomaterials

electrode (flexibility, elasticity, strength, etc.), and to enable the development of nanosized sensors (Cash and Clark 2010). Such nanomaterials as carbon nanotubes (Cosnier et al. 2014; Reshetilov et al. 2019), graphene (Karimi et al. 2015), electroformed nanofibers (Sapountzi et al. 2017), gold nanoparticles (Zhou et al. 2020), and quantum dots (Wang et al. 2018) are included into biosensors to increase their sensitivity, response time, and limit of detection (LOD) (Noah and Ndangili 2019). Such biosensors can be used to measure glucose both *in vitro* and *in vivo* (Taguchi et al. 2014).

Graphene and carbon nanotubes are used the most often among carbon nanomaterials (Zhu et al. 2012). Application of carbon nanomaterials enables reducing the resistance of charge transfer from enzyme's active site to the electrode surface, owing to which the biosensor signal, its sensitivity, and operation speed increase.

Valentini et al. (2013) used the one-stage application of polypyrrole film with GOx by electrophoresis to a gold microelectrode coated with single-walled carbon nanotubes. The linear range of concentrations was 4 up to 100 M, which covers the range of hypo- and hyperglycemia.

Tang et al. (2014) applied multiwalled carbon nanotubes (MWCNTs) in a composite with chitosan and polythionine. Owing to the use of conductive wires from MWCNTs, the authors achieved a higher amperometric signal and an LOD of 5 μM . The biosensor response time was a mere 15 s; the linear detection range, 0.04 to 2.5 mM.

Kang et al. (2009) were the first to develop in their work a glucose biosensor based on graphene and chitosan by fixing the mixture on a glassy carbon electrode. Their biosensor had an LOD of 20 μM and a linear range from 80 μM up to 12 mM. Alwarappan et al. (2010) used polypyrrole instead of chitosan; polypyrrole encapsulated nanolayers of graphene and GOx and was sedimented on the glassy carbon electrode. Their biosensor was capable of detecting glucose with an LOD of 3 μM and detection linear range of 3 to 40 μM . Sometimes investigators do not use pure graphene but the one modified with additional nanoparticles. In particular,

Norouzi et al. (2011) in their work used a nanographene support alloyed with zinc oxide nanoparticles immobilized in GOx. Their biosensors showed a high sensitivity to glucose with an LOD of 0.02 μM and linear range of 0.1 to 20 μM . Another biosensor based on graphene and metal nanoparticles was developed by Rafighi et al. (2016). They sedimented a thin layer of GOx on the surface of a composite from graphene, polyethyleneimine, and gold particles (GNS-PEI-AuNPs). Their biosensor was found to have a lower LOD (0.32 μM) and a broader linear range (1–100 μM) than biosensors without nanoparticle modification (Alwarappan et al. 2010). In another study, Gupta et al. (2017) used graphene quantum dots, which are zero-dimensional materials with quantum confinement and edge site effects. The developed GOx–GQD biosensor responded efficiently and linearly to the presence of glucose over concentrations ranging between 10 μM and 3 mM with an LOD of 1.35 μM .

Metal nanoparticles, as we mentioned above, are also used to improve biosensors' parameters (Nenkova et al. 2017; Lee et al. 2019). For instance, dissolved suspensions of nanoparticles are applied to detect glucose by electrochemical and optical methods (Taguchi et al. 2014).

In a study, Rassas et al. (2019) used gold nanoparticles as glucose biosensor components. A polyelectrolyte complex from chitosan–kappa-carrageenan coated with AuNP was used to immobilize GOx on the surface of a gold electrode. The obtained biosensor possessed a good reproducibility and stability with an LOD of 5 μM and a linear detection range of 10 μM to 7 mM. Silver nanoparticles were used by Hsu et al. (2011) as a matrix for immobilization of GOx. A graphite electrode coated with a complex of nanoparticles, GOx, nafion, and chitosan provided for a linear detection range of 0.5 to 6 mM. Zhang et al. (2015) reported the use of magnetic Fe_3O_4 nanoparticles for the purpose of enhanced enzyme immobilization, electrochemical activity, and additional magnetic properties. The LOD of glucose for the biosensor was 16 μM ; the linear range, from 16 μM up to 26 mM.

One more form of nanoparticles used as a component of biosensors for glucose assays includes platinum nanoparticles (PtNPs). Liu et al. (2013) developed a biosensor based on PtNPs synthesized on the surface of the eggshell membrane and GOx; the biosensor was capable of detecting glucose within the linear range of 10–225 μM in blood serum samples with recoveries between 93.6 and 102.8%. Yang et al. (2017) also developed an amperometric biosensor from one-dimensional platinum nanotubes (MPtNT) for glucose assays. The LOD of the MPtNT-based biosensor is calculated to be 0.2 μM ; the linear range, from 0.025 to 2.20 mM.

As can be seen from the above discussion, in recent years investigators have frequently combined various types of nanomaterials to obtain the best possible biosensor parameters. On the whole, nanotechnologies contributed to improving the sensitivity and linear ranges of detection of various glucose biosensors to sufficient levels for continuous monitoring of glucose in blood both in healthcare facilities and under conditions of home use.

15.5 Continuous Monitoring of Glucose

Continuous monitoring of glucose is based on the measurement of glucose concentration not less than each 5 min for a prolonged period of time (more than 24 h). Continuous monitoring provides a more detailed information on the character and tendencies of glucose-level change and makes it possible to identify periods of nocturnal hypoglycemia and postprandial hyperglycemia, to adjust sugar-reducing therapy, and to introduce changes to the diet and physical-activity schedule. Continuous monitoring of the glucose level in blood *ex vivo* was proposed by Albisser et al. in 1974, and in 1982, a system for *in vivo* monitoring was developed (Shichiri et al. 1982). At present, two types of continuous glucose monitoring systems are used: continuous subcutaneous glucose monitoring and continuous monitoring of glucose in blood. Still, due to a possible contamination of the electrode with proteins, a risk of thromboembolism, and coagulation factors, most of these systems do not measure blood glucose directly. For this reason, subcutaneously implantable needle-type electrodes were developed to measure the concentration of glucose in extracellular fluid (Yoo and Lee 2010). Extracellular fluid contains glucose at a concentration similar to that in blood (McGarraugh 2009). Sensors for glucose concentration measurements in extracellular fluid use either subcutaneous microdialysis probes or microneedles (Lucarelli et al. 2012; Corrie et al. 2015); microneedles are more popular and are used on the market more often. These devices continuously monitor glucose levels, and using the trackable glucose profile, automatically inject insulin at hyperglycemic peaks and glucagon at hypoglycemic troughs. A low concentration of O₂ (required for operation of GOx) in extracellular fluid causes problems with long-time stability of the biosensor. The problems were overcome by using a special membrane for modulating the inflow of glucose and uptake of O₂. Based on this technology, a device named GlucoWatch was developed (Cygnus, Inc., USA). Its operation, however, was fraught with some problems: application of an electric field caused skin irritations, and additional calibrations were necessary using blood tests with fingerprick, and the measurement accuracy was disturbed by patient sweating (Vashist 2012). On top of that, GlucoWatch could not monitor glucose in short periods of time, because glucose was extracted and measured at different times. For this reason, the device was discontinued soon after its launch in 2002, and in 3 years after that the company closed down.

The first needle-type enzyme electrode for subcutaneous implantation was described by Shichiri et al. (1982). The first commercial needle-type glucose biosensor began to be sold by Minimed (Sylmar, CA, USA). Nevertheless, it did not provide real-time data, and the results of every 72-h monitoring should be obtained via a technician (Gross et al. 2000). Later, its analogues appeared: SEVEN and G4 Platinum of Dexcom (San-Diego, CA, USA), iPro2 of Medtronic MiniMed (Dublin, Ireland), Freestyle Navigator and Libre of Abbott (Abbott Park, Illinois, USA). These devices display updated concentrations of glucose in real-time mode

approximately each 3–5 min. The sensor is disposable and can be used from 3 to 14 days (Boscari et al. 2018; Dungan and Verma 2018).

Thus, the continuous glucose monitoring systems are convenient for outpatient, inpatient, and home use. At present, investigators test novel types of continuous glucose monitoring systems and try to overcome the shortcomings of the existing devices (Sola-Gazagnes et al. 2019). This technology is a step forward on the way to creating implantable devices for automated human health monitoring, for example, artificial pancreas, which can simulate the natural insulin control process in the organism.

15.6 Non-invasive Methods of Glucose Analysis

As we mentioned above, invasive methods of research are inconvenient for the end user; for this reason, many investigators have focused on the development of non-invasive glucose monitoring sensors. The first developed non-invasive sensors were based on optical methods of analysis (Oliver et al. 2009) and measured the change of the physical properties of light in extracellular fluid or in the ocular anterior chamber. Nevertheless, to date those developments have not found broad commercial application.

Many investigations focus on the search for a relation between glucose levels in blood and in other biological fluids that require no invasive sampling, such as tears, saliva, and sweat (Corrie et al. 2015). Glucose sensors in the form of contact lenses were developed for monitoring glucose levels in lacrimal fluid (Chu et al. 2011; Yao et al. 2011). The essence of the method is that an electrochemical sensor with immobilized GOx is screen-printed on the plastic surface of the lens. The sensors demonstrated a high signal speed, high sensitivity to glucose, and a good reproducibility within the range of low concentrations of glucose. However, it is necessary still to overcome such problems as a more efficient suppression of interference, total biocompatibility for wearable contact lenses, and integration of sensors with readout and communication chains.

Saliva is yet another attractive object of research, because its samples are easy to obtain. Besides, simultaneously with glucose level measurements, one can have information on other significant compounds, such as lactate or cholesterol. Still, accurate measurement of glucose concentration can be prevented by the occurrence of various postprandial impurities in saliva. As a rule, the assessment of glucose in saliva requires it to be filtered to discard large biomolecules. Such sensors can be incorporated into, for example, mouthguards (Kim et al. 2014). In Arakawa et al. (2016), a system of a platinum electrode coated with a GOx membrane and an Ag/AgCl electrode was incorporated into plastic mouthguards to measure the level of glucose in artificial saliva for 5 h. However, contact lenses and mouthguards are inconvenient for long-term use due to their unfavorable impact on the eyes and mouth cavity. Besides, the volume of these biological fluids is limited, which does

not make it possible to use them for continuous monitoring of glucose levels in the organism.

The use of sweat is promising in this respect. Sweat glands are distributed all over the body, and the level of glucose in sweat changes rapidly enough to reflect the physiological conditions in the main part of the body (Sakaguchi et al. 2013). Various sorts of sensors have been developed for convenient glucose-level monitoring in sweat during training. Wearable wristbands (Gao et al. 2016) and disposable sensors (Lee et al. 2017) can continuously monitor glucose level changes in sweat, remaining attached to the skin for long periods of time. Such devices offer a simple monitoring of the level of glucose in sweat, because the fluid's capillary channel in the sensing strip efficiently adsorbs sweat. Devices in the form of plasters have also been developed (Cho et al. 2017); they include not only a biosensor but also an enzyme fuel cell to feed the entire device at the expense of the endogenous substrates of the organism. The fully integrated and self-powered smartwatch for continuous sweat glucose monitoring is an even more complex device (Zhao et al. 2019). It includes a GOx-based biosensor, a signal processor, and a display to output information about the level of glucose.

Depending on the sweat generation conditions, its parameters, such as temperature and acidity, may vary, which has a negative effect on measurement accuracy. For instance, during physical exercises, the pH of sweat drops down from 6.3 to 4–5 depending on the amount of lactic acid released, and the temperature of sweat directly depends on ambient temperature (Jadoon et al. 2015). To eliminate distortions, temperature and pH sensors are integrated with glucose sensors, which increases the accuracy of glucose monitoring by providing corrections based on precalibrated data. A temperature increase leads to enhance bioreceptor's enzymatic activity and to overrate the readings of the device. For a more accurate assessment of glucose in blood via sweat, it is necessary to introduce individual correlation coefficients for glucose concentrations for each person under different measurement conditions (Lee et al. 2017). Besides, under ordinary conditions sweat is not released by itself in amounts required for measurements. Its release should be stimulated by either physical exercises or by additional chemical agents, which can be inconvenient or unrealizable for many potential users. Also, the section of skin in the vicinity of the biosensor requires to be cleaned periodically, because residual glucose and exogenous contaminants may negatively affect the measurement accuracy.

15.7 Conclusion

Over the almost 60 recent years since the development of the first glucose-assay biosensor, significant changes have occurred both in the requirements to these devices and the technology of their production. The newest achievements in the fields of medicine, biotechnology, chemistry, physics, and cybernetics are used to create modern glucose monitoring devices. Various sorts of nanomaterials and nanoparticles that enable increasing the sensors' sensitivity and enhancing their

long-term stability are combined in the receptor element of the biosensor. Biosensor supports from flexible polymer materials enable continuous monitoring of glucose by means of wearable devices with wireless data transfer. Non-invasive methods are potentially more in demand but are still less accurate as compared with direct blood glucose monitoring methods and often require individual adjustments for each patient. As the number of diabetics constantly increases, and there is no efficient treatment yet, the demand for glucose monitoring systems shall remain invariably high. The most important tasks for investigators in the near future are to increase the biosensor's lifetime and to overcome the physical/physiological factors that affect the accurate registration of glucose concentration in the human organism.

Acknowledgments The authors are grateful for the support by the Russian Foundation for Basic Research (RFBR) within the framework of the project "Study of bioelectrochemical properties of the PEDOT/TEG/biocatalyst composite for Microbial fuel cell" No 19-58-45011.

References

- Albisser AM, Leibel BS, Ewart TG, Davidovac Z, Botz CK, Zingg W, Schipper H, Gander R (1974) Clinical control of diabetes by the artificial pancreas. *Diabetes* 23:397–404
- Alwarappan S, Liu C, Kumar A, Li C-Z (2010) Enzyme-doped graphene nanosheets for enhanced glucose biosensing. *J Phys Chem C* 114(30):12920–12924
- Andreis E, Küllmer K, Appel M (2014) Application of the reference method isotope dilution gas chromatography mass spectrometry (ID/GC/MS) to establish metrological traceability for calibration and control of blood glucose test systems. *J Diabetes Sci Technol* 8(3):508–515. <https://doi.org/10.1177/1932296814523886>
- Arakawa T, Kuroki Y, Nitta H, Chouhan P, Toma K, Sawada S, Takeuchi S, Sekita T, Akiyoshi K, Minakuchi S, Mitsubayashi K (2016) Mouthguard biosensor with telemetry system for monitoring of saliva glucose: a novel cavitas sensor. *Biosens Bioelectron* 84:106–111. <https://doi.org/10.1016/j.bios.2015.12.014>
- Biosensors Market Size, Share and Trends Analysis Report by Application (Agriculture, Medical), by Technology (Thermal, Electrochemical, Optical), by End Use (PoC testing, Food Industry), And Segment Forecasts, 2019–2026.
- Boscari F, Galasso S, Facchinetti A, Marescotti MC, Vallone V, Amato AML, Avogaro A, Bruttomesso D (2018) FreeStyle libre and Dexcom G4 platinum sensors: accuracy comparisons during two weeks of home use and use during experimentally induced glucose excursions. *Nutr Metab Cardiovasc Dis* 28(2):180–186. <https://doi.org/10.1016/j.numecd.2017.10.023>
- Buzanovskii VA (2015) Methods for the determination of glucose in blood. Part 1. *Rev J Chem* 5:30–81
- Cash KJ, Clark HA (2010) Nanosensors and nanomaterials for monitoring glucose in diabetes. *Trends Mol Med* 16(12):584–593
- Cho E, Mohammadifar M, Choi S (2017) A self-powered sensor patch for glucose monitoring in sweat. 2017 IEEE 30th International Conference on Micro Electro Mechanical Systems (MEMS). <https://doi.org/10.1109/memsys.2017.7863417>.
- Chu MX, Miyajima K, Takahashi D, Arakawa T, Sano K, Sawada S, Kudo H, Iwasaki Y, Akiyoshi K, Mochizuki M, Mitsubayashi K (2011) Soft contact lens biosensor for in situ monitoring of tear glucose as non-invasive blood sugar assessment. *Talanta* 83(3):960–965
- Clark LC Jr, Lyons C (1962) Electrode systems for continuous monitoring in cardiovascular surgery. *Ann New York Acad Sci* 102:29–45

- Clarke SF, Foster JR (2012) A history of blood glucose meters and their role in self-monitoring of diabetes mellitus. *Br J Biomed Sci* 69(2):83–92
- Corrie SR, Coffey JW, Islam J, Markey KA, Kendall MAF (2015) Blood, sweat, and tears: developing clinically relevant protein biosensors for integrated body fluid analysis. *Analyst* 140(13):4350–4364. <https://doi.org/10.1039/c5an00464k>
- Cosnier S, Holzinger M, Le Goff A (2014) Recent advances in carbon nanotube-based enzymatic fuel cells. *Front Bioeng Biotechnol* 2:45. <https://doi.org/10.3389/fbioe.2014.00045>
- Dedov II, Shestakova MV, Vikulova OK, Zheleznyakova AA, Isakov MA (2018) Diabetes mellitus in Russian Federation: prevalence, morbidity, mortality, parameters of glycaemic control and structure of hypoglycaemic therapy according to the Federal Diabetes Register, status 2017. *Diabetes Mellitus* 21(3):144–159. <https://doi.org/10.14341/DM9686>
- Dungan K, Verma N (2018) Monitoring technologies – continuous glucose monitoring, mobile technology, biomarkers of glycemic control. In: Feingold KR, Anawalt B, Boyce A et al. (editors), *Endotext* [Internet]. South Dartmouth (MA): [MDText.com, Inc.](https://www.ncbi.nlm.nih.gov/books/NBK279046/) 2018; 2000-. Available from: <https://www.ncbi.nlm.nih.gov/books/NBK279046/>
- Galant AL, Kaufman RC, Wilson JD (2015) Glucose: detection and analysis. *Food Chem* 188:149–160
- Gao W, Emaminejad S, Nyein H, Challa S, Chen K, Peck A, Fahad HM, Ota H, Shiraki H, Kiriya D, Lien D-H, Brooks GA, Davis RW, Javey A (2016) Fully integrated wearable sensor arrays for multiplexed in situ perspiration analysis. *Nature* 529:509–514. <https://doi.org/10.1038/nature16521>
- Gladilovich VD, Podolskaya EP (2010) Possibilities of using the method of GC–MS (a review). *Nauchnoye Priborostroyeniye* 20(4):36–49. (in Russian)
- Global Report on Diabetes (2018) Geneva, World Health Organization, Licence CC BY-NC-SA 3.0 IGO.
- Gross TM, Bode BW, Einhorn D, Kayne DM, Reed JH, White NH, Mastrototaro JJ (2000) Performance evaluation of the MiniMed continuous glucose monitoring system during patient home use. *Diabetes Technol Therapeutics* 2:49–56
- Guilbault G, Lubrano G (1973) An enzyme electrode for the amperometric determination of glucose. *Anal Chim Acta* 64:439–455
- Guo CX, Li CM (2010) Direct electron transfer of glucose oxidase and biosensing of glucose on hollow sphere-nanostructured conducting polymer/metal oxide composite. *Phys Chem Chem Phys* 12:12153–12159
- Gupta S, Smith T, Banaszak A, Boeckl J (2017) Graphene quantum dots electrochemistry and sensitive electrocatalytic glucose sensor development. *Nano* 7(10):301. <https://doi.org/10.3390/nano7100301>
- Hovorka R (2006) Continuous glucose monitoring and closed loop systems. *Diabet Med* 23(1):1–12
- Hsu FY, Yu DS, Chang JC, Chuang CL (2011) Silver nanoparticles as a glucose oxidase immobilization matrix for Amperometric glucose biosensor construction. *J Chin Chem Soc* 58(6):756–760
- Jadoon S, Karim S, Akram MR, Kalsoom Khan A, Zia MA, Siddiqi AR, Murtaza G (2015) Recent developments in sweat analysis and its applications. *Int J Analyt Chem* 164974. <https://doi.org/10.1155/2015/164974>
- Kang X, Wang J, Wu H, Aksay IA, Liu J, Lin Y (2009) Glucose oxidase-graphene-chitosan modified electrode for direct electrochemistry and glucose sensing. *Biosens Bioelectron* 25(4):901–905
- Karimi A, Othman A, Uzunoglu A, Stanciu L, Andreescu S (2015) Graphene based enzymatic bioelectrodes and biofuel cells. *Nanoscale* 7:6909–6923. <https://doi.org/10.1039/c4nr07586b>
- Kim J, Valdés-Ramírez G, Bandodkar AJ, Jia W, Martínez AG, Ramírez J, Mercier P, Wang J (2014) Non-invasive mouthguard biosensor for continuous salivary monitoring of metabolites. *Analyst* 139(7):1632–1636. <https://doi.org/10.1039/c3an02359a>
- Kim JU, Ku YS, Kim HJ, Trinh NT, Kim W, Jeong B, Heo TH, Lee MK, Lee KE (2019) Oral diabetes medication and risk of dementia in elderly patients with type 2 diabetes. *Diabetes Res Clin Pract* 154:116–123

- Lee H, Song C, Hong YS, Kim MS, Cho HR, Kang T, Shin K, Choi SH, Hyeon T, Kim D-H (2017) Wearable/disposable sweat-based glucose monitoring device with multistage transdermal drug delivery module. *Sci Adv* 3(3):e1601314. <https://doi.org/10.1126/sciadv.1601314>
- Lee H, Hong YJ, Baik S, Hyeon T, Kim D-H (2018) Enzyme-based glucose sensor: from invasive to wearable device. *Adv Healthc Mater* 7:1701150. <https://doi.org/10.1002/adhm.201701150>
- Lee W-C, Kim K-B, Gurudatt NG, Hussain KK, Choi CS, Park D-S, Shim Y-B (2019) Comparison of enzymatic and non-enzymatic glucose sensors based on hierarchical Au-Ni alloy with conductive polymer. *Biosens Bioelectron* 130:48–54
- Liu J, Wang J (2001) Improved design for the glucose biosensor. *Food Technol Biotechnol* 39:55–58
- Liu W, Wu H, Li B, Dong C, Choi MMF, Shuang S (2013) Immobilization of platinum nanoparticles and glucose oxidase on eggshell membrane for glucose detection. *Anal Methods* 5(19):5154. <https://doi.org/10.1039/c3ay40327k>
- Lucarelli F, Ricci F, Caprio F, Valgimigli F, Scuffi C, Moscone D, Palleschi G (2012) GlucoMen day continuous glucose monitoring system: a screening for enzymatic and electrochemical interferences. *J Diabetes Sci Technol* 6(5):1172–1181. <https://doi.org/10.1177/193229681200600522>
- McGarraugh G (2009) The chemistry of commercial continuous glucose monitors. *Diabetes Technol Therapeutics* 11(1):17–24. <https://doi.org/10.1089/dia.2008.0133>
- Moodley N, Ngxamngxa U, Turzyniecka MJ, Pillay TS (2015) Historical perspectives in clinical pathology: a history of glucose measurement. *J Clin Pathol* 68:258–264
- Nenkova RD, Ivanov YL, Godjevargova TI (2017) Influence of different nanoparticles on electrochemical behavior of glucose biosensor. *AIP Conf Proc* 1809:020037. <https://doi.org/10.1063/1.4975452>
- Noah NM, Ndagili PM (2019) Current trends of nanobiosensors for point-of-care diagnostics. *J Analyt Methods Chem*:1–16. <https://doi.org/10.1155/2019/2179718>
- Norouzi P, Ganjali H, Larijani B, Ganjali MR, Faridbod F, Zamani HA (2011) A glucose biosensor based on nanographene and ZnO nanoparticles using FFT continuous cyclic voltammetry. *Int J Electrochem Sci* 6:5189–5199
- Oliver NS, Toumazou C, Cass AEG, Johnston DG (2009) Glucose sensors: a review of current and emerging technology. *Diabet Med* 26(3):197–210. <https://doi.org/10.1111/j.1464-5491.2008.02642.x>
- Olson N, Bae J (2019) Biosensors – publication trends and knowledge domain visualization. *Sensors* 19(11):2615. <https://doi.org/10.3390/s19112615>
- Rafiqi P, Tavahodi M, Haghghi B (2016) Fabrication of a third-generation glucose biosensor using graphene-polyethyleneimine-gold nanoparticles hybrid. *Sensors Actuators B Chem* 232:454–461. <https://doi.org/10.1016/j.snb.2016.03.147>
- Rassas I, Braiek M, Bonhomme A, Bessueille F, Raffin G, Majdoub H, Jaffrezic-Renault N (2019) Highly sensitive voltammetric glucose biosensor based on glucose oxidase encapsulated in a chitosan/kappa-carrageenan/gold nanoparticle bionanocomposite. *Sensors* 19(1):154. <https://doi.org/10.3390/s19010154>
- Reshetilov A, Plekhanova Y, Tarasov S, Tikhonenko S, Dubrovsky A, Kim A, Kashin V, Machulin A, Wang G-J, Kolesov V, Kuznetsova I (2019) Bioelectrochemical properties of enzyme-containing multilayer polyelectrolyte microcapsules modified with multiwalled carbon nanotubes. *Membranes* 9(4):53. <https://doi.org/10.3390/membranes9040053>
- Rodriguez AK, Melo AE, Domingueti CP (2020) Association between reduced serum levels of magnesium and the presence of poor glycemic control and complications in type 1 diabetes mellitus: a systematic review and meta-analysis. *Diabetes Metabol Syndrome Clin Res Rev* 14:127–134
- Sadana A, Sadana N (2015) Biomarkers and biosensors. Detection and binding to biosensor surfaces and biomarkers applications. Elsevier Science, Amsterdam
- Sakaguchi K, Hirota Y, Hashimoto N, Ogawa W, Hamaguchi T, Matsuo T, Miyagawa J-I, Namba M, Sato T, Okada S (2013) Evaluation of a minimally invasive system for measuring glucose

- area under the curve during oral glucose tolerance tests: usefulness of sweat monitoring for precise measurement. *J Diabetes Sci Technol* 7:678–688
- Sapountzi E, Braiek M, Chateaux JF, Jaffrezic-Renault N, Lagarde F (2017) Recent advances in electrospun nanofiber interfaces for biosensing devices. *Sensors* 17(8):1887. <https://doi.org/10.3390/s17081887>
- Shichiri M, Kawamori R, Yamasaki Y, Hakui N, Abe H (1982) Wearable artificial endocrine pancreas with needle-type glucose sensor. *Lancet* 2:1129–1131
- Simon RK, Christian GD, Purdy WC (1968) The coulometric determination of glucose in human serum. *Clin Chem* 14(5):463–476
- Sola-Gazagnes A, Faucher P, Jacqueminet S, Ciangura C, Laforgue DD, Monsier-Pudar H, Roussel R, Larger E (2019) Disagreement between capillary blood glucose and flash glucose monitoring sensor can lead to inadequate treatment adjustments during pregnancy. *Diabetes Metab.* <https://doi.org/10.1016/j.diabet.2019.08.001>
- Stewart ZA (2020) Gestational diabetes. *Obstetr Gynaecol Reproduct Med.* <https://doi.org/10.1016/j.ogrm.2019.12.005>
- Taguchi M, Ptitsyn A, McLamore ES, Claussen JC (2014) Nanomaterial-mediated biosensors for monitoring glucose. *J Diabetes Sci Technol* 8(2):403–411
- Tang W, Li L, Wu L, Gong J, Zeng X (2014) Glucose biosensor based on a glassy carbon electrode modified with polythionine and multiwalled carbon nanotubes. *PLoS One* 9(5):e95030. <https://doi.org/10.1371/journal.pone.0095030>
- Teng YJ, Zuo SH, Lan MB (2009) Direct electron transfer of horseradish peroxidase on porous structure of screen-printed electrode. *Biosens Bioelectron* 24(5):1353–1357
- Turner A (2013) Biosensors: then and now. *Trends Biotechnol* 31(3):119–120
- Updike SJ, Hicks GP (1967a) The enzyme electrode. *Nature* 214:986–988
- Updike SJ, Hicks GP (1967b) Reagentless substrate analysis with immobilized enzymes. *Science* 158:270–272
- Valentini F, Fernandez G, Tamburri E, Palleschi G (2013) Single walled carbon nanotubes/polypyrrole-GOx composite films to modify gold microelectrodes for glucose biosensors: study of the extended linearity. *Biosens Bioelectron* 43:75–78. <https://doi.org/10.1016/j.bios.2012.11.019>
- Vashist SK (2012) Non-invasive glucose monitoring technology in diabetes management: a review. *Anal Chim Acta* 750:16–27
- Wang H-C, Lee A-R (2015) Recent developments in blood glucose sensors. *J Food Drug Anal* 23(2):191–200
- Wang B, Shen J, Huang Y, Liu Z, Zhuang H (2018) Graphene quantum dots and enzyme-coupled biosensor for highly sensitive determination of hydrogen peroxide and glucose. *Int J Mol Sci* 19(6):1696. <https://doi.org/10.3390/ijms19061696>
- Yang H, Shi Q, Song Y, Li X, Zhu C, Du D, Lin Y (2017) Glucose biosensor based on mesoporous Pt nanotubes. *J Electrochem Soc* 164(6):B230–B233. <https://doi.org/10.1149/2.1421706jes>
- Yao H, Shum AJ, Cowan M, Lähdesmäki I, Parviz BA (2011) A contact lens with embedded sensor for monitoring tear glucose level. *Biosens Bioelectron* 26(7):3290–3296. <https://doi.org/10.1016/j.bios.2010.12.042>
- Yoo EH, Lee SY (2010) Glucose biosensors: an overview of use in clinical practice. *Sensors (Basel, Switzerland)* 10(5):4558–4576. <https://doi.org/10.3390/s100504558>
- Yu Y, Chen Z, He S, Zhang B, Li X, Yao M (2014) Direct electron transfer of glucose oxidase and biosensing for glucose based on PDDA-capped gold nanoparticle modified graphene/multiwalled carbon nanotubes electrode. *Biosens Bioelectron* 52:147–152. <https://doi.org/10.1016/j.bios.2013.08.043>
- Yuh Y-S, Chen J-L, Chiang C-H (1998) Determination of blood sugars by high pressure liquid chromatography with fluorescent detection. *J Pharm Biomed Anal* 16(6):1059–1066. [https://doi.org/10.1016/s0731-7085\(97\)00052-6](https://doi.org/10.1016/s0731-7085(97)00052-6)
- Zhang W, Li X, Zou R, Wu H, Shi H, Yu S, Liu Y (2015) Multifunctional glucose biosensors from Fe₃O₄ nanoparticles modified chitosan/graphene nanocomposites. *Sci Rep* 5:11129. <https://doi.org/10.1038/srep11129>

- Zhao J, Lin Y, Wu J, Nyein HYY, Bariya M, Tai L-C, Chao M, Ji W, Zhang G, Fan Z, Javey A (2019) A fully integrated and self-powered smartwatch for continuous sweat glucose monitoring. *ACS Sensors* 4(7):1925–1933. <https://doi.org/10.1021/acssensors.9b00891>
- Zhou F, Jing W, Liu S, Mao Q, Xu Y, Han F, Wei Z, Jiang Z (2020) Electrodeposition of gold nanoparticles on ZnO nanorods for improved performance of enzymatic glucose sensors. *Mater Sci Semicond Process* 105:104708. <https://doi.org/10.1016/j.mssp.2019.104708>
- Zhu Z, Garcia-Gancedo L, Flewitt AJ, Xie H, Moussy F, Milne WI (2012) A critical review of glucose biosensors based on carbon nanomaterials: carbon nanotubes and graphene. *Sensors (Basel, Switzerland)* 12(5):5996–6022. <https://doi.org/10.3390/s120505996>

Chapter 16

Microstructured Electrochemical SMBG Biosensor Chip Design Development for Sustainable Mass Production Based on the Strategic Platform Patent Map



Hideaki Nakamura

Abstract An environmentally and user-friendly biosensor chip design for self-monitoring of blood glucose (SMBG) is a basic need. Moreover, the biosensor chip design is required for sustainable mass production. In order to satisfy this requirement, the streamlined manufacturing of biosensor chips is required. This chapter presents representative examples of the platform patents registered for future sustainable mass production of the electrochemical SMBG biosensor chips which were designed to satisfy the abovementioned requirements. Furthermore, for user-friendly, several examples of needle-integrated biosensor chip designs are explained as parts of distinctive platform designs. As new analytical tools applying unique capillary actions, examples of biosensor array chips are also explained.

Keywords Platform patent map · Sustainable designs · Electrochemical SMBG biosensor chip · Minimally invasive · Array chip · Environmentally-friendly · User-friendly

Nomenclature

DO	Dissolved oxygen
FFE	Face-to-face electrode
GOD	Glucose oxidase
IP	Intellectual property
QOL	Quality of life
SMBG	Self-monitoring of blood glucose

H. Nakamura (✉)

Department of Liberal Arts, Tokyo University of Technology, Hachioji, Japan

e-mail: nakamurahd@stf.teu.ac.jp

© Springer Nature Switzerland AG 2021

M. Rai et al. (eds.), *Macro, Micro, and Nano-Biosensors*,

https://doi.org/10.1007/978-3-030-55490-3_16

16.1 Introduction

The demand for biosensor chips is increasing year after year (Bahadır and Sezginturk 2015), especially widespread are self-monitoring of blood glucose (SMBG) biosensors for clinical use in diabetes (Yoo and Lee 2010). The World Health Organization (WHO) reported that the number of people with diabetes has risen from 108 million in 1980 to 422 million in 2014 (WHO 2018). WHO projects that diabetes will be the seventh leading cause of death in 2030 (Mathers and Loncar 2006). Such a demand for biosensor chips will further increase toward the realization of personalized medicine (Turner 2017) and healthcare (Sekretaryova et al. 2016; Nakamura 2018).

Since the first biosensor was invented by Updike and Hicks (1967), development for SMBG biosensors has spread worldwide (Nakamura and Karube 2003). The development of SMBG biosensor chips for practical use has been divided into two types, i.e., optical systems and electrochemical systems. In this chapter, the history of the development of the electrochemical biosensor chip is described as follows.

In 2003, various types of SMBG biosensors were already on the market in Japan. Table 16.1 shows the characteristics of the practical SMBG biosensors which included two types as electrochemical and optical systems. In the electrochemical SMBG biosensor, glucose oxidase (GOD) or glucose dehydrogenase (GDH) was used. Most of these SMBG biosensors require three steps, setting up a biosensor chip to a measurement device, blood sampling using a lancet (needle), and automatic measurement by the introduction of a blood sample to the biosensor chip. Only GlucoWatch, produced by Cygnus Co. (USA), had a different system that applied reverse iontophoresis for sampling through intact skin. The electrochemical SMBG biosensors that should be noted here are rationally designed biosensor chip which was manufactured by Matsushita Kotobuki Co. (Japan) and minimally invasive designed biosensor chip which was manufactured by Therasense Co. (USA). By this product, the sample volume was drastically reduced from 30 to 0.3 μL . The reduction techniques of sample volume are described later.

Each company must carefully handle whether it will obtain a patent for intellectual property (IP) associated with the product (Sherkow 2016). At that time, various types of SMBG biosensors as described above were already commercialized. Some of these technologies were publicized by patent applications, and these are introduced as notable inventions in the next section.

16.2 Technological Backgrounds in Notable Inventions

In the present section, the technological backgrounds that led to the mass production of electrochemical SMBG biosensor chips are described. Table 16.2 shows the features of the first literature about the biosensor and subsequent notable patents for the production of electrochemical sensor chips.

Table 16.1 Practical SMBG biosensors in 2003 (Nakamura and Karube 2003)

Sold in Japan	Product	Maker	Country	Principle	Biosensor chip	Centesis	Sample volume (μL)	Measurement	
								time (sec)	range (mg dL^{-1})
1997.3	Medisafe reader	Terumo	Japan	CM	GOD-POD, color coupler	Finger	4	18	20–600
1998.1	Precision QID	Abbott lab	USA	EM	GOD, mediator	Finger	3.5	20	20–600
1998.5	NovoAssist plus	Lifescan	USA	CM	GOD-POD, color coupler	Finger	10	30	0–500
2000.4	Dexter Z II	Bayer	USA	EM	GOD, mediator	Finger	3	30	10–600
2000.4	Glucocard diameter α	Matsushita Kotobuki	Japan	EM	GOD, mediator	Finger	2	15	20–600
2001.4	Sof-tact	Abbott lab	USA	EM	GDH, mediator	Arm etc	3	20	30–450
2002.3	Free style	Therasense	USA	EM	Enzyme	Arm etc	0.3	ca.15	20–500
2002.4 (USA)	GlucoWatch biographer	Cygnus	USA	EM	GOD	Arm	Slight	–	40–400
2002.6	Medisafe EZ Voice	Terumo	Japan	CM	GOD-POD, color coupler	Finger	4	18	20–600
2002.7	Accucheck active	Roche diagnostic	Germany	CM	GDH, mediator, color coupler	Arm etc	2	5	10–600
2003.1	OneTouch ultra	Lifescan	USA	CM	Enzyme	Arm etc	1	5	20–600

CM Colorimetry, EM Electrochemical method

16.2.1 Inventions of the First Biosensor

The first biosensor known as an enzyme electrode was invented for the measurement of glucose by Updike and Hicks (1967). The enzyme electrode was fabricated using a Clark-type dissolved oxygen (DO) electrode. A gel immobilized enzyme, GOD was put onto the surface of the DO electrode. By utilizing the specificity of GOD catalysis reaction to glucose, the glucose concentration in biological solutions and in the tissues in vitro was successfully determined. This technique became the basis for the development of electrochemical SMBG biosensor chips. The technologies required for mass production of sensors are shown below.

Realization of

- Disposable sensor chip and storage stability of loading reagents.
- Glucose measurement that does not rely on blood oxygen.

Table 16.2 Features of notable inventions that led to the mass-production technology of electrochemical SMBG biosensor chips

Publication		Inventor (Author)	Assignee (Affiliation)	Title of invention	Feature
Year	Number				
1967	Nature	(Updike SJ, Hicks GP)	(University of Wisconsin)	The enzyme electrode	DO electrode, glucose sensor
1972	JPS47500	Rogers RW	Miles	Detector of specific chemical substance	Disposable sensor, dry reagent
1973	JPS4837187 (US3838033A) ^a	Mindt W, Racine P, Schlapfer P	Roche	Enzyme electrode	Enzyme, mediator
1977	JPS52142584 (US4053381A)	Bata Greer CJ, Chilian J, Daniel DS et al.	Kodak	Ion selective electrode	Disposable sensor
1979	JPS5450396 (US4224125A)	Nakamura K, Nankai S, Iijima T, Fukuda M	Matsushita	Enzyme electrode	Enzyme, mediator
1981	JPS5679242 (US4301412A)	Hill JR, Meyer AE	United	Liquid conductivity measurement system and its sample card	Capillary
1986	JPS61502419 (US4810658A)	Shanks IA, Smith AM, Nylander CI	Unilever	Specific reactive sample collection and test device and method for producing the same	Capillary, spacer
1989	JPH01291153 (US5120420A)	Nankai S, Kawaguri M, Fujita M, Iijima T	Matsushita	Biosensor	Basic structure, sample inlet port, multi- detection sensor
1991	JPH03202764	Kawaguri M, Ohtani M, Nankai S	Matsushita	Biosensor and manufacturing method thereof	Basic structure, blood cell and protein filtration membrane

(continued)

Table 16.2 (continued)

Publication		Inventor (Author)	Assignee (Affiliation)	Title of invention	Feature
1995	JPH07248306	Toyama T, Karube I	Casio, Karube I	Biosensor	Porous spacer, face-to-face electrode (FFE) structure
1996	JPH08285814	Toyama T	Casio	Biosensor	FFE structure, sample-inlet port, bead spacer
1997	JPH09264870	Toyama T	Casio	Biosensor	FFE structure, sample-inlet port, bead spacer
2000	(US6071391A)	Gotoh M, Mure H, Shirakawa H	NOK	Enzyme electrode structure	FFE structure, sample-inlet port, adhesive spacer
2001	WO2001033216	Liamos CT, Feldman BJ, Krishnan R, et al.	Therasense	Small volume in vitro analyte sensor and related	FFE structure, sample-inlet port, thin spacer

^aUSP registration number

- Sample uptake at less volume.
- Elimination of interfering substances.
- Effective electrochemical reaction.
- Reduction of sample volume.
- Calibration-free biosensor chip.

They were required for mass production of the electrochemical SMBG biosensor chips. The present section describes how these requirements by any technological backgrounds as notable inventions were being met.

16.2.2 Inventions of Disposable Sensor Chips and Dry Reagents

In 1972 (JPS47500), ideas for a detector of specific chemical substances using a disposable sensor chip and dry reagents were publicized by Miles Co. As an example, a pattern of the two-electrode system was made by the printing of metal thin film onto the surface of a ceramic substrate. A terminal of the small electrode chip to a connector was formed at the opposite of the electrochemical detector part. The

electrode chip was easy to make, remove from the measurement device, and discard after use.

As another feature, the biosensor chip was coated with semipermeable membrane immobilized reagents which were able to detect specific chemical substances. By the invention, the biosensor chip was enabled to stock under the dry condition and use it without any preparation for the measurement. This small electrode chip employed metal as the electrode material. For biosensor, GOD can be immobilized on the chip as a dry reagent, and hydrogen peroxide (H_2O_2) generated by catalyzing glucose can be measured through the metal electrodes.

Another disposable sensor chip, Kodak Co. also publicized an ion-selective electrode in 1977 (JPS52142584); therefore, the ion-selective electrode was used not only as a chemical sensor but also as a biosensor by immobilization of enzyme.

16.2.3 Limitation of Glucose Biosensor Chip Based on H_2O_2 Detection

The concentration of oxygen containing in the whole blood is around 20 mL dL^{-1} (WHO 2002). However, oxygen containing in the blood plasma is used for the glucose measurement and the concentration is only 0.3 mL dL^{-1} (as a value of oxygen partial pressure: $p\text{O}_2$). In addition, this oxygen concentration is calculated as 0.13 mmol L^{-1} for molar concentration and $4.3 \text{ mg O}_2 \text{ L}^{-1}$ for mass concentration. For reference, the oxygen concentration in pure water is $8.84 \text{ mg O}_2 \text{ L}^{-1}$ (1 atm at 20°C) for mass concentration. It can be seen that the oxygen in the plasma contains only about half of the pure water.

On the other hand, blood glucose levels of a healthy person change before and after meals, and the blood glucose levels are approximately $70\text{--}100 \text{ mg dL}^{-1}$ without taking a meal (fasting blood sugar) (WHO 1999). Diabetes is diagnosed when the fasting blood glucose concentration is above 126 mg dL^{-1} (7 mmol L^{-1}) or blood glucose concentration after eating (blood glucose at any time) is above 200 mg dL^{-1} . Blood glucose concentrations for preventing disease complications are based on fasting blood glucose concentrations of less than 130 mg dL^{-1} and blood glucose concentrations less than 180 mg dL^{-1} at 2 hours after meals. On the other hand, warning symptom appears due to autonomic nerve reaction (attempts to increase blood glucose levels) when blood glucose concentrations fall below 70 mg dL^{-1} . The hypoglycemic symptom occurs when the brain is in a glucose-deficient state and appears when the blood glucose concentration is less than 50 mg dL^{-1} . Therefore, the SMBG biosensor chip is required to determine the wide linear range of glucose concentration.

When hydrogen peroxide is employed as an indication for electrochemical glucose measurement, the same molar DO with glucose is required. For example, to determine 180 mg dL^{-1} blood glucose accurately, over 10 mmol L^{-1} DO is suitable for the measurement. However, oxygen in whole blood is only enabled to dissolve

0.13 mmol L⁻¹ in the plasma as mentioned above. This was the technological limitation in the electrochemical SMBG biosensor chip development basing on the hydrogen peroxide detection. As a result, the response to glucose tends to saturate on the high concentration side, so that the linear range of the calibration curve tends to narrow. In addition, for the practical development of the electrochemical SMBG biosensor chip, responses to blood glucose must be in a safety zone (zone A) of the Clarke Error Grid Analysis (Clarke et al. 1987).

16.2.4 Inventions of Electrochemical Mediator Methods for Biosensor Chip

Under such technological backgrounds, there has been a strong demand for glucose measurement that does not rely on blood oxygen. Then, Roche Co. publicized an enzyme electrode employing an electrochemical mediator in 1973 (JPS4837187). The enzyme electrode chip was fixed enzyme and electrochemical mediator into the semipermeable membrane. Subsequently, in 1979 (JPS5450396), Matsushita Co. publicized an enzyme electrode which was co-immobilized both enzyme and mediator to the polymer to prevent leakage of a mediator.

In general, electrochemical mediator enables to make a calibration curve at a wide-linear range of analyte concentration due to its high solubility to the water-soluble sample. For example, potassium ferricyanide is widely used in the glucose biosensor as an electrochemical mediator and the solubility to water is 46 g dL⁻¹ (140 mmol L⁻¹). The solubility of the electrochemical mediator to water is much higher than that of DO. Thus, the electrochemical mediator method has become one of the indispensable technologies for the practical application of the electrochemical SMBG biosensor.

On the other hand, these enzyme electrode chips had to be dipped in the sample solution at the measurement. However, blood collection is required every time for blood glucose measurement. Therefore, to reduce the sample volume was one of the issues to be solved for practical use of the electrochemical SMBG biosensor.

16.2.5 Inventions of Chip Designs Employing Capillary Action

To reduce the sample volume, United Co. publicized a groundbreaking idea applying capillary action in 1981 (JPS5679242). They developed a liquid conductivity measurement system and its sensor chip. The sensor chip equipped an electrochemical reaction cell with electrodes placed in a semicircular narrow channel as a sample-feeding pass, and the sample solution was spontaneously pulling from a sample-inlet port into the cell by the capillary action. To realize the capillary action in the sensor chip, an air-discharge port was also made. As a result, this sensor chip

did not need to dip the detection part into the sample solution. In addition, the sample volume requiring the measurement was spontaneously and accurately taken into the electrochemical reaction cell by the capillary action and was drastically reduced.

On the other hand, Unilever Co. in 1986 publicized different sensor chip designs employing capillary action which act by walls in only three directions (JPS61502419). To realize the sensor chip design, they employed for the first time a spacer plate to sandwich between the electrode substrate and the cover plate. In general, the capillary action has a strong impression that the liquid is drawn into the narrow tube so that the entire inner wall surface of the capillary is swollen. However, if there are plural or curved wall surfaces on which the surface tension of the liquid acts, the liquid has a property of being drawn into the inside. Thus, they employed the physical property of the liquid sample to the sensor chip design.

Subsequently, Matsushita Co. in 1989 publicized the rational design of a biosensor chip applying the capillary action for mass production (JPH01291153). The biosensor chip is fabricated by stacking three plates, i.e., a cover plate, a spacer plate, and an electrode substrate, and had a sample-inlet port, a sample-feeding path, and an air-discharge port. The electrochemical reaction cell was formed in a part of the sample-feeding path. A similar design was commercialized (Table 16.1). In this chip design, to apply a multi-detection system was also claimed.

16.2.6 Inventions of Chip Designs Eliminating Interference Substances

Matsushita Co. further developed an electrochemical SMBG biosensor chip employing blood cell and protein filtration membranes (JPH03202764, 1991). The membrane coated on the electrode surfaces. In electrochemical measurement, the influences of both blood cells and protein containing in whole blood on the signal were one of the problems in the development of the electrochemical SMBG biosensor chips. To solve the problem, Casio Co. also developed several types of electrochemical biosensor chips (JPH07248306, 1995). They employed a porous spacer to eliminate both blood cells and proteins contained in the whole blood. Thus, it can be considered that these biosensor chips applied capillary action to remove blood components.

16.2.7 Inventions of Chip Designs Enhancing Electrochemical Reaction

In addition, Casio Co. carried out the impressive invention in the electrochemical SMBG biosensor chip design which was a face-to-face electrode (FFE) structure. The FFE structure enabled to enhance the efficiency of the electrochemical reaction

and to reduce sample volume by reducing the thickness of the spacer. In the case of Matsushita Co., they employed a plate and two adhesive layers as the spacer (JPH01291153). However, the adhesive layers could cause the thickness of the spacer to vary.

On the other hand, Casio Co. in 1996 employed uniform insulating beads as the spacer, the uniform insulating beads dispersed in the FFE structure (JPH08285814). Then, the electrochemical reaction cell was located in the structure, and the thickness was accurately fixed with the diameter of the beads. However, the electrode responses had a possibility that varied depending on the arrangement of the beads for each chip. To solve the problem, the beads were included in the ink used as the adhesive layer (JPH09264870, 1997).

16.2.8 Inventions of Chip Designs Reducing Sample Volume

In 2000, NOK Co. publicized an electrochemical SMBG biosensor chip which had the FFE structure (US6071391A). The sample was pulling into the electrochemical reaction cell by the capillary action which acts by walls in only three directions, i.e., there was no air-discharge port. The spacer was just made by an adhesive layer. By this invention, the sample volume was drastically reduced.

In addition, they applied screen-printing techniques to form conductive carbon ink electrodes on the insulating substrate. Namely, the electrode was formed from carbon instead of a noble metal to achieve low production costs. The screen-printed electrode does not require polishing of the electrode surfaces like metal electrodes which were formed by such as plating or vacuum vapor deposition (JPH01291153). Therefore, the application of the screen-printing techniques to make the electrochemical SMBG biosensor chip became one of the indispensable technologies for subsequent mass production.

In 2001, Therasense Co. publicized an electrochemical SMBG biosensor chip to reduce the sample volume by reducing the thickness of the spacer as much as possible (WO/2001/033216). This biosensor chip had also the FFE structure; therefore, the volume of the electrical reaction cell was effectively reduced. In addition, the biosensor chip had an air-discharge port as a different point with the chip publicized from NOK Co.

16.2.9 Calibration-Free Biosensor Chip

For practical use of the electrochemical or optical SMBG biosensor chip, the development of the calibration-free biosensor chip was required to simplify measurement operations. In other words, the mass production of the biosensor chips with a high yield that does not require calibration was required. However, in general, this technique is not disclosed and has become the know-how of each manufacturer. In this

way, each company should carefully consider whether to obtain IP patents related to the product as described above (Sherkow 2016). Thus, in the next section, I will partially introduce what we have made public about the mass production of the calibration-free biosensor chips.

In the present section, the technological backgrounds relating to the mass production of the electrochemical SMBG biosensor chips are described based on the invention history.

16.3 Our Chip Designs for Sustainable Mass Production

Because of technical limitations, at that time, I considered the challenges to be addressed to achieve future sustainable mass production of the electrochemical SMBG biosensor chips. The solutions to the challenges are described in this section. A part of the solutions was evolved in the joint research (including me) of Sumitomo Electric Industries, Ltd. (SEI) and the National Institute of Advanced Industrial Science and Technology (AIST), which was conducted in parallel with my own project at that time. Therefore, it is not directly related to the contents of this chapter. The solutions obtained by the joint research are clearly shown in the relevant literature. Thus, the most of ideas presented here were independently invented by me (I wrote most parts of each patent specification applied and drew the figures myself) and patented by us (a total of 59 applications and publications in 45 patents registered in Japan). As the evidence, even though the contents of an individual patent could be understood by the co-inventors, however the whole flow of these sustainable developments based on the platform patent map shown in this chapter was created only in my thoughts, and, no one would have been able to expect it until today unless it was presented in this way. For reference, all of the patents I was involved in had 173 applications, of which 63 were registered in Japan (Appendix Tables 1 and 2). Of these patents, the ideas of the platform that will lead to future sustainable mass production are presented here.

16.3.1 *What Is Sustainable Mass Production and What Is Required of Chip Design?*

For future practical use, the sustainable mass production of the electrochemical SMBG biosensor chips is ideal when considered comprehensively. Here,

What is the sustainable mass production for the electrochemical SMBG biosensor chips?

It is to be streamlined manufacturing, i.e.

- Saving costs by reduction of materials and fabrication processes.
- Keeping high yield and reducing defective chips.

- Reducing variation between lots.

What is required of chip design to realize such sustainable mass production?

It is the “chip design” in pursuit of accuracy that can be reached because it is simple.

Further, designing sustainable chips is also necessary to realize sustainable mass production in the future. For this purpose, what is required of chip designs?

- Chip designs for simple and accurate assembly, i.e., realizing 3D assembling with few parts and without positioning between the parts and calibration-free measurement.
- Environmentally-friendly chip designs, i.e., other than the above, employing biodegradable materials and simple packaging or no packaging and enabling long-term storing.
- User-friendly chip designs, i.e., being disposable, realizing highly visible sample introduction by transparent chip (as a universal design), minimally invasive measurement by highly precise detection, few step measurement by needle integration, and multi-sensing, etc.
- New development of chip design as analytical tools, i.e., improving chip utility, employing the advanced application of capillary action, or new sample introductions instead of the capillary action (vacuum and electrowetting), non-conductive lancet, self-sterilizing lancet, and array chips, etc.

Thus, the requirements for the chip design for sustainable mass production are described. From the next section, the details of the requirements for the chip designs are explained according to the patents and other literature which we publicized. Appendix Table 1 shows a patent list that our patents registered in Japan.

16.3.2 Chip Designs for Simple and Accurate Assembly

In 2003, the biosensor chip was mainly assembled by stacking multiple plates as described in the Sect. 16.2 (Fig. 16.1a). However, I thought such a stacking method would be a disadvantage for assembling a small-sample biosensor chip in the case of mass production. The reasons were as follows:

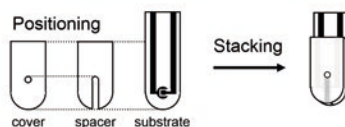
- Difficulty in increasing the accuracy of positioning multiple plates.
- Difficulty to reduce a small-sample volume by using a plate as a spacer.

To solve these two issues, I sought a way to easily assemble a biosensor chip with a small number of parts and a 3D structure without positioning between parts. Then, I inspired a biosensor chip design for sustainable mass production in 2003. From the inspiration, I invented two platform methods which were the simplest 3D assembly methods I could think of. These were the mass production methods of biosensor chips by:

- Deforming a single substrate (JP4036384 and JP4038575, registered in 2007).

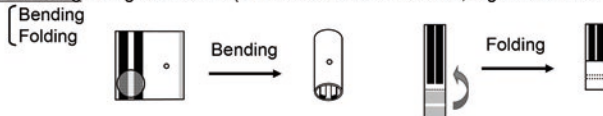
a) One of the conventional methods

Stacking multiple plates (JPH01291153, Matsushita Co. publicized in 1989)



b) Our platform methods

i) Deforming a single substrate (JP4036384 and JP4038575, registered in 2007)



ii) Continuously bonding two long substrates together (JP4277104, 2009)

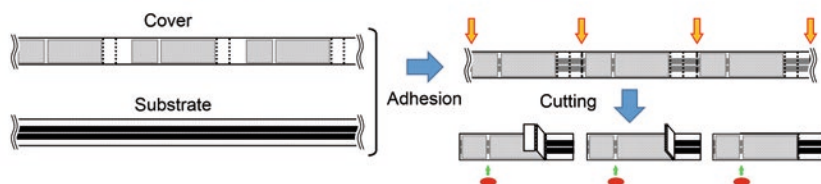


Fig. 16.1 Comparison between conventional stacking method and our platform methods for mass production of electrochemical SMBG biosensor chip. All these drawings were diverted from Japan Patent Office (JPO) Public Relations

- Continuously bonding two long substrates together (JP4277104, 2009).

The former platform idea was finally divided into two patents, and the original idea was a 3D structured biosensor chip formation by deforming a single substrate. The difference was in the way of deformation. In other words, one method was to bend the single substrate, and the other was to fold the single substrate. In both methods, the 3D chip structure was assembled by deforming the substrate so that the surface-formed electrodes were on the inside (Fig. 16.1b-i). Of these methods, the most suitable method for mass production was the folding method.

Fig. 16.2 shows an example of the process of the folding method. The biosensor chip could be assembled without positioning by folding the corners of the substrate so that they overlap. By employing the adhesive layer as a spacer, the 3D structure of the biosensor chip could assemble without a spacer plate and reduce the sample volume by reducing the thickness of the spacer. However, when trying to reduce the sample volume by reducing the thickness of the adhesive layer, a slight variation in the thickness of the adhesive layer caused a large variation in the measured value. The factors that caused the variation in the thickness of the adhesive layer include warping of the folded substrate, the type of adhesive, and the temperature and humidity during assembly. To avoid the warping of the folded substrate, various folding ways to fix the 3D structure of the biosensor chip were considered (Fig. 16.3). As the other way of mass production, the continuous bonding method was able to

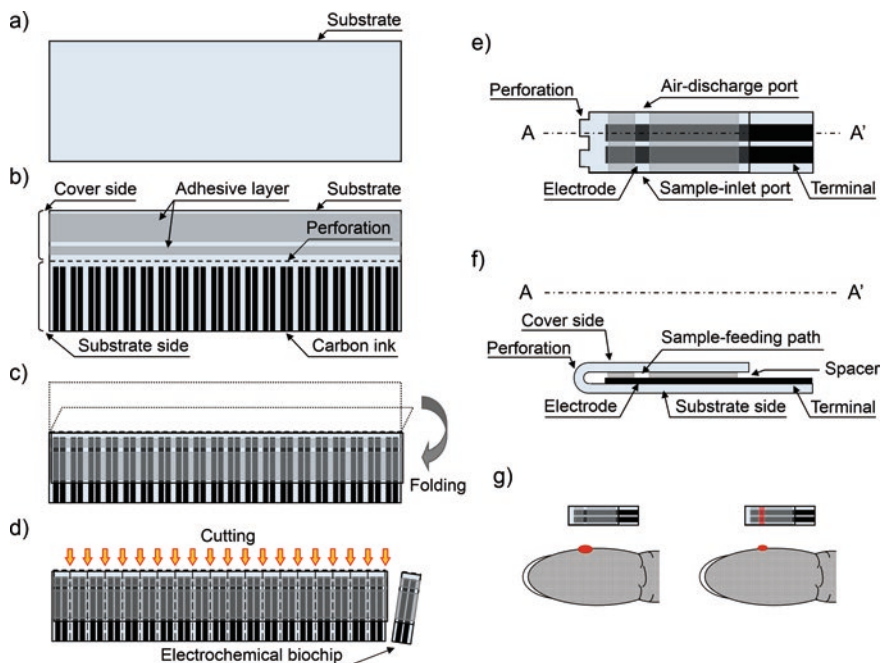


Fig. 16.2 Detail process of sustainable mass production by employing folding method. (a) Substrate, (b) printing of adhesive layer as a spacer and carbon ink as an electrode pattern on a substrate, formation of perforation, (c) folding of the cover side, (d) cutting to each electrochemical biochip, (e) electrochemical biochip and A-A' cross section, (f) cross-sectional view from arrow in the overview of (e), and example of clinical use. For biochip production, biochemical reagents are printed on the substrate or carbon ink surface between the adhesive layers. Diverted from JPO Public Relations

adhere to two long substrates together accurately without the need for special alignment (Fig. 16.1b-ii). About the type of adhesive and the assemble conditions were also investigated by the joint research of SEI and AIST in detail (Kaimori et al. 2006).

Further accurate assembly of the biosensor chip, the resist layer was employed and covered on the carbon ink to form the electrode surface (Fig. 16.4). Originally, in the case of measuring an analyte in a sample solution, only the electrochemically active substance existing at the interface between the electrode surface and the sample solution can be measured. Therefore, if there is an amount of sample solution necessary to cover the electrode surface, the measurement can be performed. In other words, the volume of the sample solution away from the electrode surface is wasted for measurement, and it can be seen that the thinner the spacer, the better. In addition, the resist layer was able to define the electrode area more accurately than the adhesive layer, thereby suppressing variation in measured values and increasing the possibility of mass production of highly precise biosensor chips that do not require calibration. As a result, we realized the world's smallest blood sample volume as small as 200 nL in the joint research of SEI and AIST (Kaimori et al. 2006).

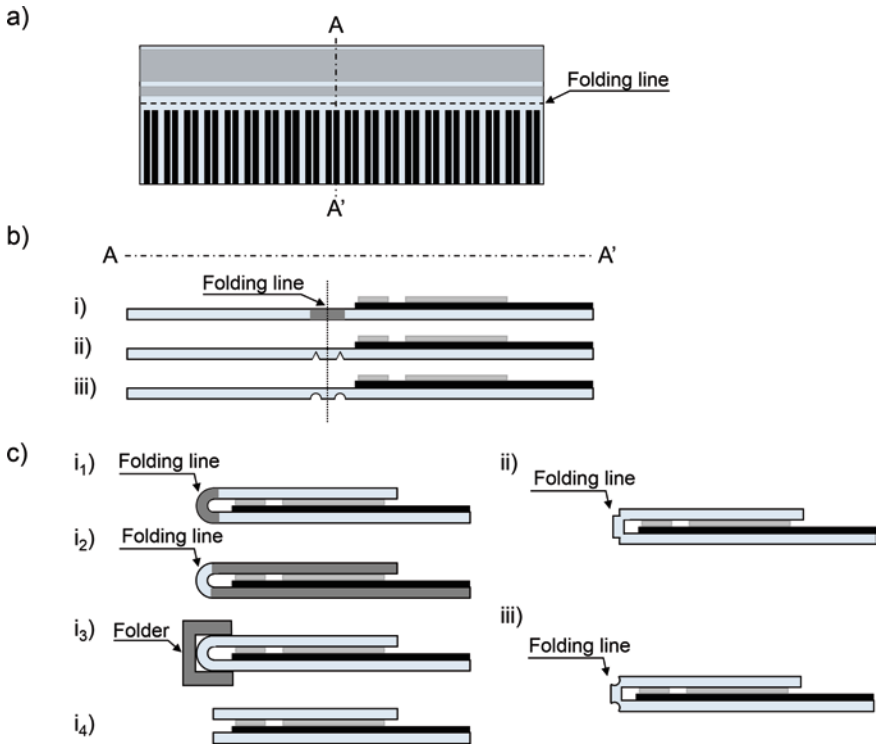


Fig. 16.3 Examples in folding methods. (a) Substrate and A-A' cross section, (b) cross-sectional view from arrow in the overview of (a), and folding line, (i) perforation, (ii) triangular grooves, and (iii) fan-shaped grooves, (c) various folding ways (i₁) hardening of substrate (JP4649594, 2010), (i₃) fixing by using a folder, (i₄) cutting of folding point, (ii) folding of triangular grooves, and (iii) folding of fan-shaped grooves. Diverted from JPO Public Relations

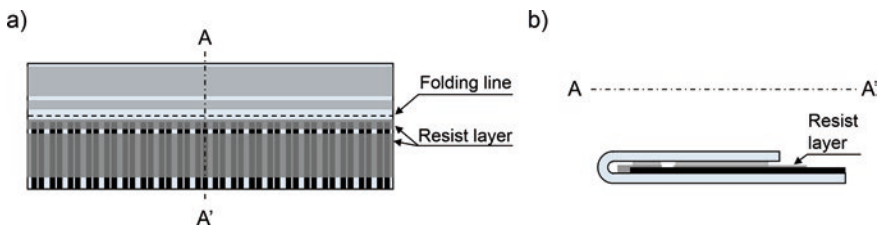


Fig. 16.4 Example of folding method employing resist layer. (a) Substrate and A-A' cross section, (b) cross-sectional view from arrow in the overview of a. Diverted from JPO Public Relations

Thus we were able to make the platform designs that could meet the requirement of the simple and accurate biosensor chip assembly for sustainable mass production. Based on these chip designs to lead the sustainable mass production, I have further designed the biosensor chips and we have studied to meet further requirements.

16.3.3 *Environmentally-Friendly Chip Designs*

As the second requirement for sustainable mass production, I invented several types of environmentally-friendly chip designs that solve two issues like plastic waste and waste reduction.

At that time, the problem of plastic waste was taken up by scientists, but it was not so seriously accepted by society (Barnes et al. 2009). However, it was necessary to pay attention to the use of plastic as a material for mass production. Thus, for the substrate, I thought to employ biodegradable materials such as polylactic acid. Eventually, this idea was mentioned in the patent specifications but not implemented.

Like the other issues, waste reduction was required especially in the industry involved in mass production. For sustainable mass production of the electrochemical SMBG biosensor chips, it was considered to reduce the materials relating to the products and to prolong the service life after production. The latter case could reduce overall production.

To solve these issues, I focused on the packaging of biosensor chips. For practical use, the issue related to the packaging of the electrochemical SMBG biosensor chips concerned not only in the environmental aspects but also in both aspects of manufacturing cost and keeping storage stability. To reduce the manufacturing cost, the biosensor chips should not be individually packaged. Rather, a plurality of biosensor chips can be put together and sold in one bottle containing a desiccant. However, in this case, the storage stability of the biosensor chip might be a problem especially in humid countries like Japan.

Because of the above problems, I proposed several ideas about the packaging designs for biosensor chips to reduce the waste, and some of them were assembled and examined to their utility. All of these ideas were finally granted as the patents as follows:

- Biosensor chip design of simple packaging (JP3890417, 2006).
- Biosensor chip design of package-free (Nakamura et al. 2007c, JP4399581, 2009, and JP4469983, 2010).
- Biosensor chip design enabling long-term storing (Nakamura et al. 2007c, JP4399581, 2009, and JP4469983, 2010).

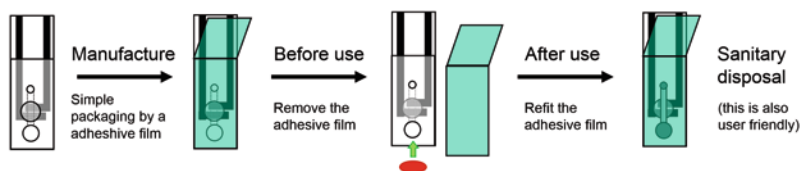
Fig. 16.5 shows several examples of package designs for the biosensor chip. Figure 16.5a shows an example of the simple packaging biosensor chip. By employing a desorption film, both a sample-inlet port and an air-discharge port were simultaneously sealed. Thereby, this biosensor chip was able to prevent blood leakage by reapplying desorption film after use. For this reason, the biosensor chip after use could be sanitized, including the prevention of infectious diseases. In other words, this biosensor chip also met as the user-friendly described in the next section. In addition, for this type of the biosensor chip, a design that allows preservatives such as desiccants to be loaded into the chip, as well as the reagent layer, was also considered.

Figures 16.5b and 16.6 show two examples of the package-free biosensor chips. These biosensor chips were designed so that the sample-feeding path, which had been closed up to that time, was released by deforming the chip structure and the sample inlet port and the air-discharge port appeared at the same time. The biosensor chip was also designed to allow the loading of preservatives into the chip and to measure multiple constituents simultaneously. Further, this biosensor chip design was assembled by screen printing and examined its storage stability (Nakamura et al. 2007c). As a result, the storage stability as the electrochemical SMBG biosensor signals of the chip has kept the biosensor signals for 6 months. Figure 16.6a shows a cap type of the package-free biosensor chip. The sample volume was 550 nL. Figure 16.6b shows a holding type of the simultaneous two-biosensing chip, and the sample volume was 900 nL each. The sample volumes obtained with these designs were comparable to those of SMBG biosensors that were commercially available at that time. Such a reduction of the sample volume was achieved by applying surfactant into the sample-feeding pass. Thus, these package-free biosensor chips could show excellent characteristics in terms of environmentally-friendly and user-friendly.

Introduction of Other Developmental Studies

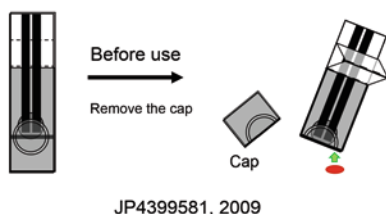
At that time, biosensor chips were designed not only for medical use but also for environmental use. In the development of the environmentally-friendly biosensor chips, a simple packaging disposable microbial biosensor chip for environmental

a) Biosensor chip design with simple packaging (JP3890417, 2006)

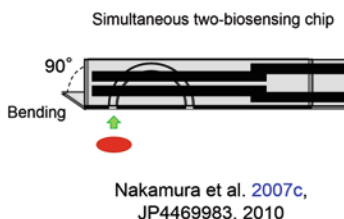


b) Biosensor chip design without packaging and enabling long-term storing (Nakamura et al. 2007c, JP4399581, 2009 and JP4469983, 2010)

i) Cap type



ii) Bending type



Package-free biosensor chips

Fig. 16.5 Examples of environmentally-friendly biosensor chip designs. Diverted from JPO Public Relations. Reprinted from (Nakamura 2007c), Copyright (2020), with permission from Elsevier

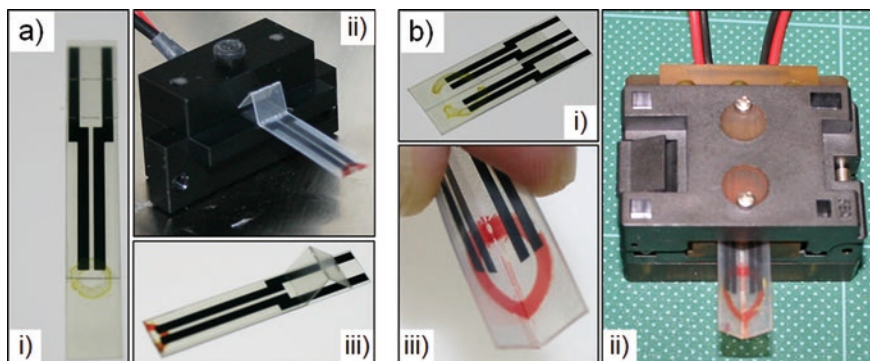


Fig. 16.6 Photographs of package-free biosensor chips. (a) Cap type and (b) folding type with simultaneous two-biosensing chip. (i) Before use, (ii) electrochemical measurement, and (iii) after measurement. Diverted from JPO Public Relations

monitoring has also been designed (Nakamura et al. 2007a, Nakamura 2010). This biosensor chip had a lot of ideas that I had thought about so far. For example, the biosensor chip had a stirrer reactor, had long-term storage of viable microbe cells, and was ready to use when needed. Further, the down-facing electrode was designed to prevent microbial cell deposition, and desorption film was employed to prevent microbial contamination after in situ measurements.

As described above, I designed the environmentally-friendly biosensor chips to realize sustainable mass production. These biosensor chips also had the other properties requiring user-friendly designs, which are explained in the next section.

16.3.4 User-Friendly Chip Designs

As the third requirement for sustainable mass production, I considered that the user-friendly biosensor chip designs should be realized. In the user-friendly biosensor chip designs, universal design is also included. The universal design here refers to the design of a product to make it available to everyone, regardless of age, disability, or other factors (Story et al. 1998). For example, because vision decreases as diabetes progresses, biosensor chip designs need to be easy to use (i.e., user-friendly), to prevent a reduction in quality of life (QOL).

What is the user-friendly biosensor chip designs for diabetics?

It is to be:

- Disposable.
- Transparent.
- Hygienic.
- Minimally invasive.
- Multi-measurable.

- Simple operation.
- Able to store and manage.

Disposable, Transparent, Hygienic

In the case of a specification in which the biosensor is repeatedly used, a user needs a procedure related to regeneration such as washing every time a blood glucose level is measured. This is not only problematic in terms of ease of use but can also be a burden for diabetics with reduced vision. On the other hand, when the biosensor is disposable, the inconvenience associated with use is eliminated. As an example of the disposable biosensor chip, the simple packaging design was already shown in the previous section (Fig. 16.5a). This was not only disposable, but after use, the blood collection could be sealed inside the biosensor chip and hygienically discarded to prevent infection. At the time, there were products on the market where individually packaged biosensor chips could not be opened easily by the grip of elderly users. In that sense, the package design was one of the important issues in putting user-friendly chips into practical use. Further, by assembling with a transparent substrate such as polyethylene terephthalate (PET), it was highly visible and user-friendly as shown in the practical example in Fig. 16.6.

In terms of hygiene, another point of view was considered. It was a lancet used for blood sampling. The lancet must be sterilized before use and hygienically discarded to prevent infection after use. If the lancet has a self-sterilization property, these issues might be improved. Thus, I designed a photocatalytic lancet of which surface was coated with titanium dioxide (TiO_2) nano-layer by vacuum evaporation (JP4469950, 2010). By observation with a field emission scanning electron microscope (FE-SEM; JSM-7700F, JEOL Co., Japan), secondary electron images (SEI) of the TiO_2 layer on the surface of the lancets were obtained, and the TiO_2 layer was crystallized with around 300 nm in thickness. In addition, by observation with energy-dispersive X-ray spectroscopy (EDS), the surface layer of the lancets consisted of TiO_2 . To estimate the self-sterilization property of the TiO_2 nano-layer, Sinohara et al. were developed a device for activating photocatalyst and a method for activating photocatalyst (JP4590586, 2010). Applying the knowledge patented, we estimated the antibacterial properties of the photocatalytic lancet employing *E. coli* K-12. Then, lancing resistances were also estimated (Naemura and Saito 2005). As a result, the practical properties of this lancet were shown (Nakamura et al. 2007b).

Minimally Invasive

To be minimally invasive was one of the important requirements to realize the user-friendly biosensor chip. As mentioned earlier, this requirement was more successful in joint research of SEI and AIST (realized a measurement at 200 nL sample) than in the efforts of my laboratory side (550 nL sample).

In addition, minimally invasive blood sampling was also important for the user. When blood sampling is difficult to bleed from the finger, it is better to shake the arm before puncturing and collect blood at the tip of the finger with centrifugal force or warm the puncturing finger. However, the user-friendly lancet had to be developed as an engineer. Therefore, in addition to the photocatalytic lancet, I also designed a non-conductive lancet for this aim that can be used for the needle-integrated sensor described below (JP4873536, 2011).

Multi-Measurable

In order to reduce the burden on the user, it is desirable to be able to perform multiple measurements with a single blood collection. As an example to satisfy the requirement, the simultaneous two-biosensing chip design is already shown in Fig. 16.5b and 16.6b. In this case, multiple measurements could be performed simultaneously. As an example of the multiple measurements, it is also possible in principle to measure the blood glucose level and hematocrit simultaneously employing a three-electrode system (Fig. 16.7). The hematocrit value can be assumed from blood movement speed by capillary action through conductivity measurement between two electrodes. In this principle, salinity value can also be measured. As a practical example, we simultaneously measured glucose and lactate concentration (Nakamura et al. 2007c). In this case, further precise measurement of blood glucose concentration can be performed by duplicate measurements using two sets of the electrode systems.

Applying the folding method, another type of a simultaneous two-biosensing chip was also designed to simplify the chip assembly of the holding type (Fig. 16.8; JP4807493, 2011). By employing two sets of electrode systems, these conductometric measurements can be performed simultaneously with a blood glucose measurement.

Simple Operation

For diabetics, the blood glucose measurement operation should be as simple as possible. To realize the simple procedure, a needle-integrated biosensor chip design should be developed. For this aim, I proposed 11 platform designs of the needle-integrated biosensor chips, and a total of 27 patents were registered in Japan. These platform designs were classified with the positional relationship between the needle and the biosensor chip or electrode and the presence or absence of the suction mechanism so on. Unfortunately, due to space limitations, only the first platform design is introduced here (JP4576624, 2010). As the references, the other two platform designs are introduced in the next section as needle-integrated biosensor chips with distinctive-electrochemical detector designs.

The measurement procedure consists of only two steps: cartridge installation and subsequent measurement after puncturing. This cartridge employs a backflow prevention valve to draw blood into the biosensor when the air in the cartridge is exhausted (Fig. 16.9). Also, the breathable film is fixed to the end of the air-discharge port to prevent unnecessary blood sampling by suction. As a user-friendly property, the cartridge is simply packaged with a desorption film, and after measurement, the

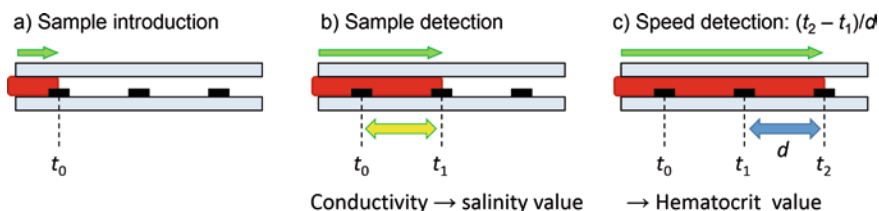


Fig. 16.7 Application examples of conductivity measurements using a three-electrode system (JP4448940, paragraph 0012)

desorption film is reapplied and the cartridge is discarded. As further user-friendly property, the spotlight guiding system is also adapted to be used in the dark.

In the development of the needle-integrated biosensor chip, the needle placed in the vicinity of the biosensor detection unit must be kept hygienic until it is used, preventing contamination with measurement reagents. As a countermeasure, in addition to the adoption of the photocatalytic needle (JP4469950, 2010) and the non-conductive needle (JP4873536, 2011), it was considered the adoption of a soft material (published as JP2007-014646 and rejected) or a bulkhead (JP4576628, 2010) to protect the needle tip from the reagent layer. However, the example of the first design (Fig. 16.9) had required complicated assembly processes and was far from sustainable mass production and the environmentally-friendly design. To solve the problem, I designed the remaining ten platforms.

Able to Store and Manage

Storage and management of the biosensor chips or needle-integrated biosensor chips are some of the important issues to obtain accurate results. Therefore, several patents that were registered also proposed biosensor chip storage. However, until then, the IP about the management of biosensor chips was not held down in our developmental study, so we devised a management method for biosensor chips equipped with IC tags (JP4631027, 2010). In this patent, the biosensor chip is equipped with an IC tag that stores information about manufacturing conditions, expiration date, storage conditions, and analytes. As shown in Fig. 16.10, the biosensor chip, a chip stocker, and a measurement device can be connected by radio waves, etc., and the sound for guiding the user can be played from the measurement machine.

As described above, I designed the user-friendly biosensor chips to realize both the sustainable mass production (except for the example of the needle-integrated biosensor chip) and the enhancement of QOL for diabetics. Based on the know-how cultivated in biosensor research and development, the next section describes the challenges of new chip design as analytical tools.

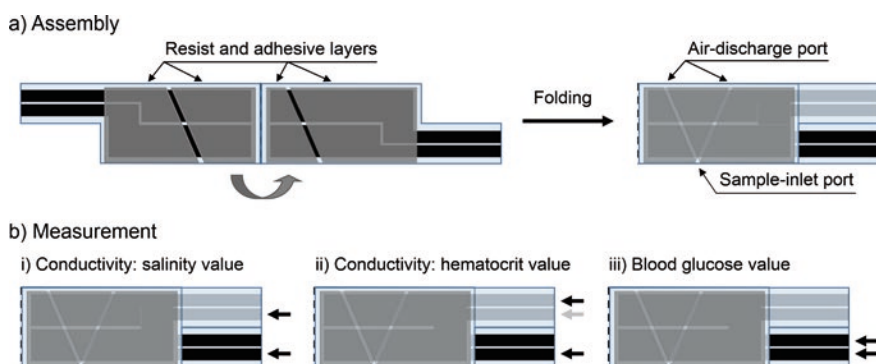


Fig. 16.8 Application of the folding method to a simultaneous two-biosensing chip. This is the result of joint research of SEI and AIST (JP4807493, 2011). Diverted from JPO Public Relations

a) An example of a simple packaging biosensor chip and its needle-integrated cartridge

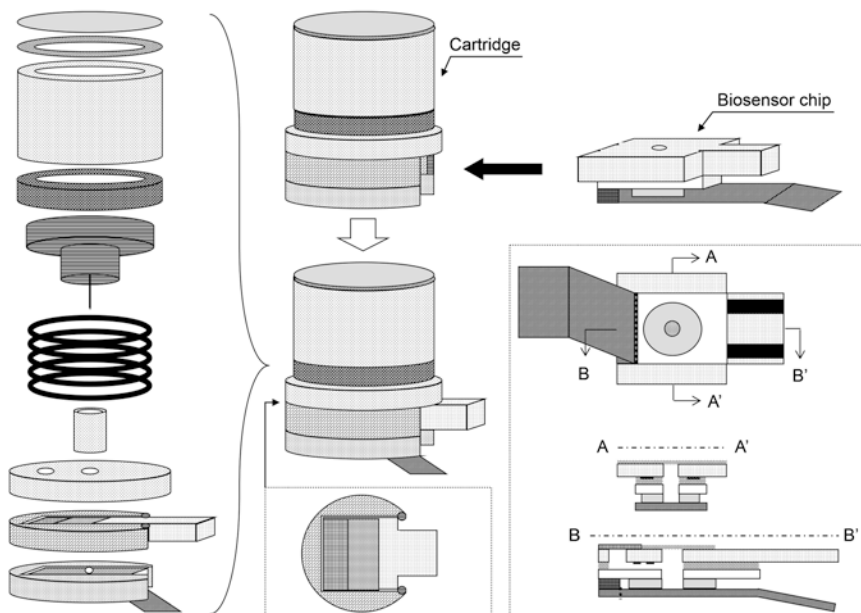


Fig. 16.9 An example of the first platform design of a needle-integrated biosensor chip (JP4576624, 2010). Diverted from JPO Public Relations

b) Mechanism inside cartridge during puncturing

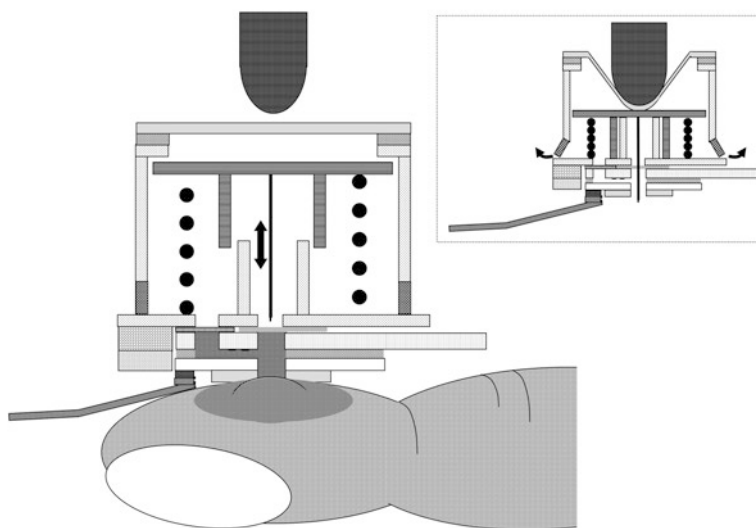


Fig. 16.9 (continued)

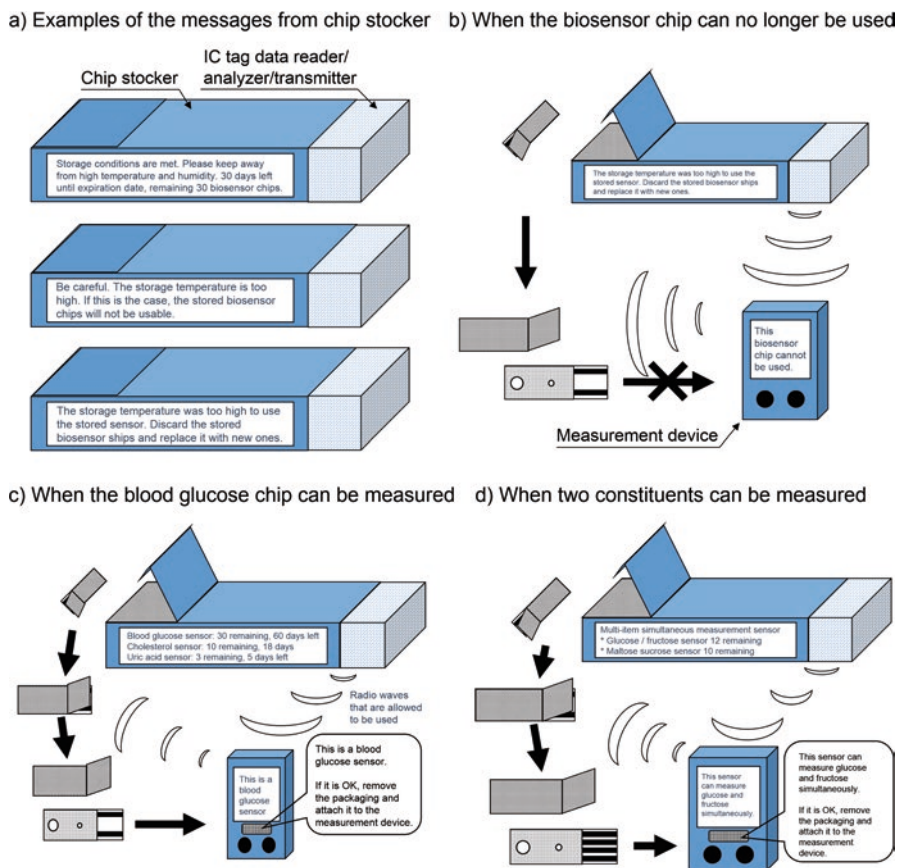


Fig. 16.10 An example of storage and management for the biosensor chips equipped with IC tags (JP4631027, 2010). Diverted from JPO Public Relations

16.3.5 New Development of Chip Designs as Analytical Tools

In this section, of the content that has not yet been described biosensor chip development, it describes the contents that should be noted. Here, two new concept electrochemical detector designs applying the capillary action, a sample transfer system applying the capillary action and the electrowetting technique, and biosensor array chips designed based on various platform techniques are explained.

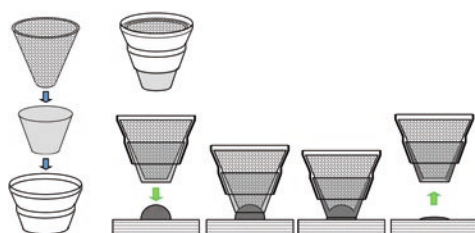
New Concept for Electrochemical Detector Design I (A Two-Hollow Cone Structure)

The capillary actions can be observed that the diameter of the tube is sufficiently small. Then, the combination of surface tension and adhesive forces between the liquid and container wall acts to propel the liquid without the need for external force. Then, the surface tension is caused by cohesion within the liquid. This action can also be observed in narrow spaces.

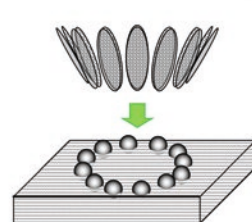
For example, the liquid can be propelled in a narrow space between two plates. Similarly, the liquid can be filled in a narrow space between two hollow cones lacking the top. According to this principle, I came up with the design of a biosensor chip with a unique sample-inlet port. The biosensor chip design is as follows. These two hollow cones lacking the top are electrically conductive, a non-conductive spacer is installed between them, and each is connected to an electrochemical measurement device. Thus, one of the new concept chip structures was designed (JP4631028, 2010). Several examples of this idea are shown in Fig. 16.11.

Because there is no upper part of the two hollow cones in this design, the central portion of the electrode system is hollow (Fig. 16.11a). Therefore, the puncture needle can be penetrated through the central portion. As a result, a needle-integrated biosensor chip that can be easily assembled was designed. Further, the sample volume can be reduced as much as possible by narrowing the distance between the electrodes and reducing the diameter of the electrode tip to the limit of the puncture needle. Based on this distinctive electrode design, a multi-detection system could easily be assembled as shown in Fig. 16.11b and c. In Fig. 16.11d, another design of the needle-integrated biosensor chip was shown in Fig. 16.11a. The design is too elaborate for a disposable chip and it is not easy to assemble, but it can also be equipped with an IC tag, an LED light, and a puncture depth adjustment mechanism.

a) The 1st example of electrochemical detector design and its needle-integrated biosensor chip



b) The 2nd example of multiple electrochemical detector design



c) The 3rd example of multiple electrochemical detector design and its measurement device

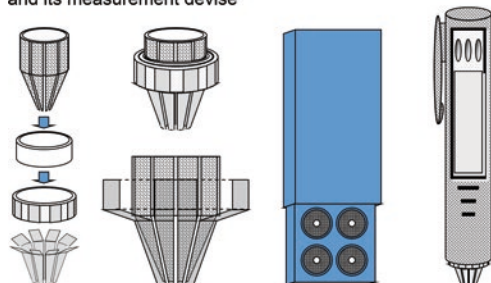


Fig. 16.11 Examples of new concept electrochemical detector design I (a) two hollow cone structures lacking the top; JP4650314, 2010). Diverted from JPO Public Relations

d) The 1st example of electrochemical detector design and other design of its needle-integrated biosensor chip

i) Internal structure I

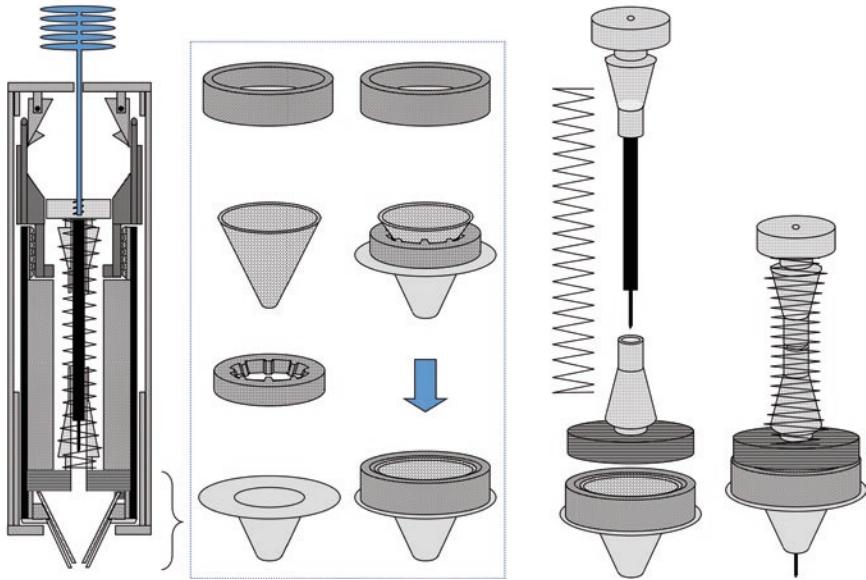


Fig. 16.11 (continued)

ii) Internal structure II

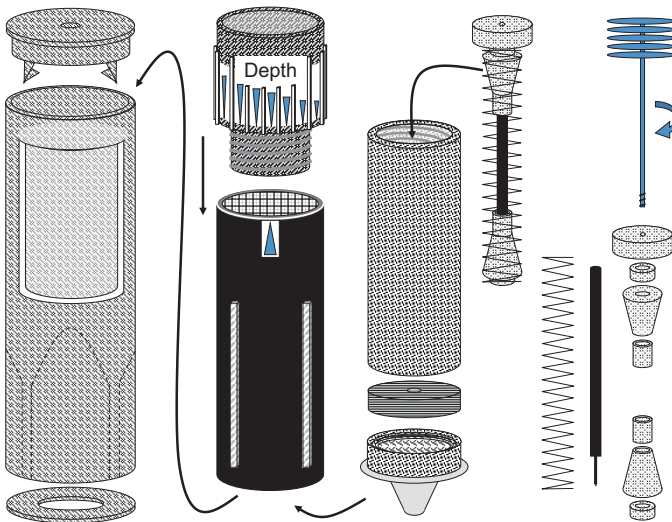


Fig. 16.11 (continued)

New Concept of Electrochemical Detector Design II (Multiple Columnar Structures)

Thatched roof prevents leaking of the rain by gathering vegetation such as stems or branches. The reason why rain does not leak from the thatched roof is because of the capillary action that works between the columnar structures such as the stems and branches. By applying this principle, an electrochemical detection unit comprising a plurality of columnar structures was designed as a new concept chip structure (JP4650314, 2010). Several examples are shown in Fig. 16.12.

Figure 16.12a shows the basic design of a three-electrode system. By the capillary action, the sample solution can come into contact with the surface of three electrodes. Figure 16.12b shows a two-electrode system. An electrochemical detector design shown in Fig. 16.12c can reduce the sample volume by reducing the areas of each electrode. Figure 16.12d shows an example of the needle-integrated biosensor chip. The puncture needle moves to penetrate the center of the three electrodes. After puncturing the skin, the tip of the needle moves to a higher position than the electrode, so that the conductive puncture needle does not affect the electrochemical reaction. The invention of non-conductive needles was born from this background (JP4873536, 2011). This type of needle-integrated biosensor chip was designed to be that the disposable needle and the biosensor chip can fit in the same simple packaging. The simple package can hygienically be discarded by reapplying the desorption film after use.

On the other hand, the multiple columnar electrode structure can also be applied as a new liquid transfer technique by employing electrowetting (JP2005199231,

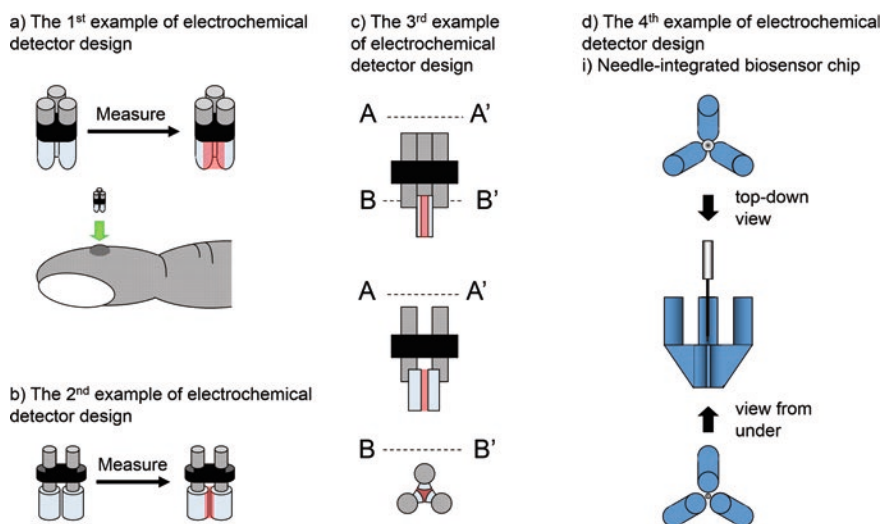


Fig. 16.12 Examples of new concept electrochemical detector design II (a) multiple columnar structure; JP4650314, 2010). Diverted from JPO Public Relations

ii) Puncturing and blood introduction

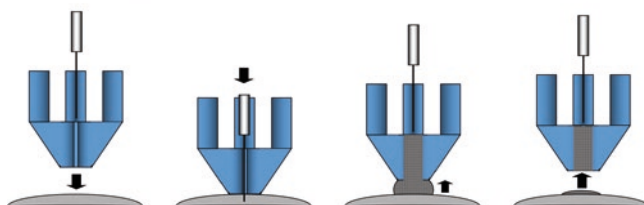


Fig. 16.12 (continued)

2005; Tsukuba Technology Seed Co.). In this technique, the liquid can be moved smoothly by causing a potential difference between the electrodes without the use of any surfactants. This electrowetting technique is an epoch-making liquid delivery technique that does not use tubes, capillaries, or pumps and can be applied as a new analytical tool (Fig. 16.12e).

Biosensor Array Chip Designs

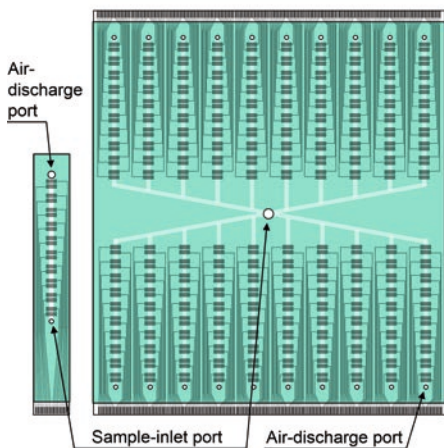
Many of the platform chip designs introduced so far have applied to biosensor array chips. Here, distinctive biosensor array chips that can be applied as new analytical tools are described. Figure 16.13 shows examples of the biosensor array chips, and these employed the capillary action for sample feeding to the electrochemical reaction cells. Figure 16.13a shows simple packaging biosensor array chips (JP3890417, 2006). These three chips are provided with sample-inlet port(s) and air-discharge port(s) on the same plane plate so that simple packaging with desorption film. The array chip after use can be hygienically discarded after reapplying the desorption film. Figure 16.13a-i shows single-sample inlet port array chips which can measure multiple measurements simultaneously from one drop of the sample solution. Figure 16.13a-ii shows a multiple-sample inlet port array chip which can measure multiple samples simultaneously using a spotter.

Figure 16.13b shows an example of a holding-type package-free biosensor array chip (JP4469983, 2010). Both sample-inlet ports and air-discharge ports are opened after holding the array chip. Therefore, reagents in each electrochemical reaction cell can be stored until use.

Figure 16.13c shows an example of a FFE structured biosensor array chip (JP4635258, 2010). This biosensor array chip has two key points: the assembly method and the electrode structure. In fact, this array chip is designed to be able to assemble a simple and accurate chip structure. For this aim, buttons are employed instead of position holes which are used for stacking plates. In the electrode structure, there are two major points. (1) By the thickness of each electrode, the sample solution is difficult to move outside the space between the two facing electrodes. (2) The distance between electrodes can be reduced as much as possible without using

a) Examples of simple-packaging biosensor array chips (JP3890417, 2006)

i) Single-sample inlet port array chip



ii) Multiple-sample inlet port array chip

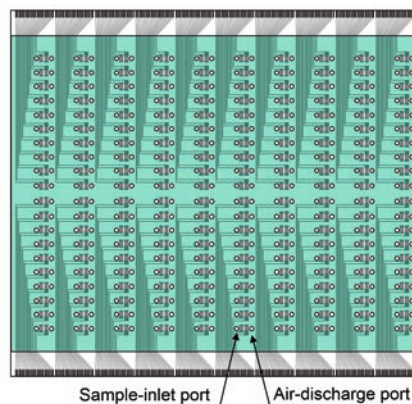


Fig. 16.13 Examples of biosensor array chip designs. Diverted from JPO Public Relations

b) Examples of bending type package-free biosensor array chip (JP4469983, 2010)

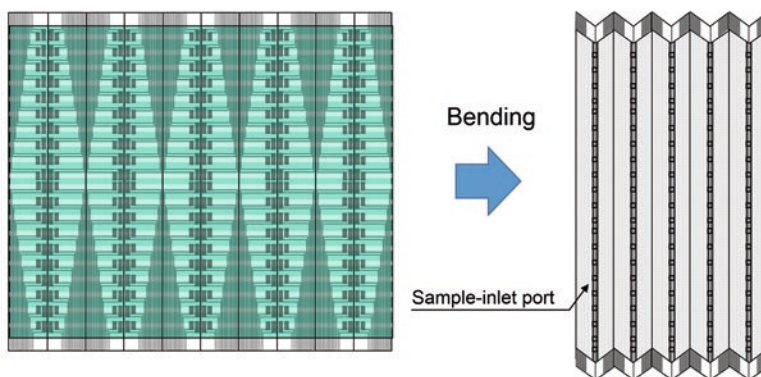


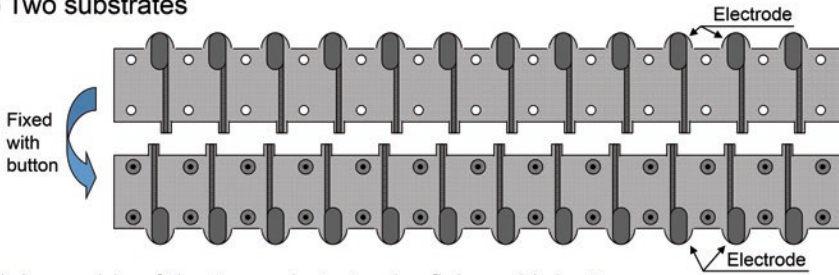
Fig. 16.13 (continued)

a spacer such as a plate. By these effects, this array chip can perform the electrochemical measurement efficiently with a small sample.

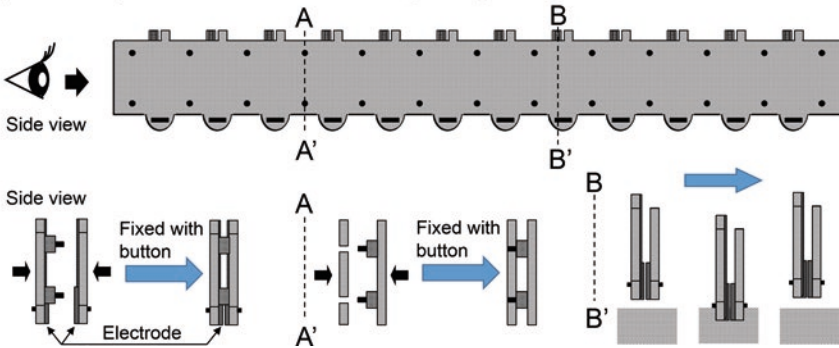
Figure 16.13d shows examples of the multiple columnar biosensor array chips (JP4650314, 2010). When this array chip system is used, the number and volume of samples, the number of electrodes in each reaction cell, electrode materials, etc. can

c) Examples of FFE structured biosensor array chip (JP4635258, 2010)

i) Two substrates

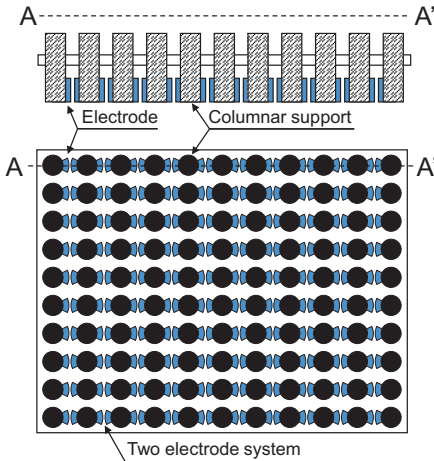


ii) Assembly of the two substrates by fixing with buttons



d) Examples of multiple columnar biosensor array chips (JP4650314, 2010)

i) Two electrode system (10 x 10 detectors)



ii) Three electrode system (75 detectors)

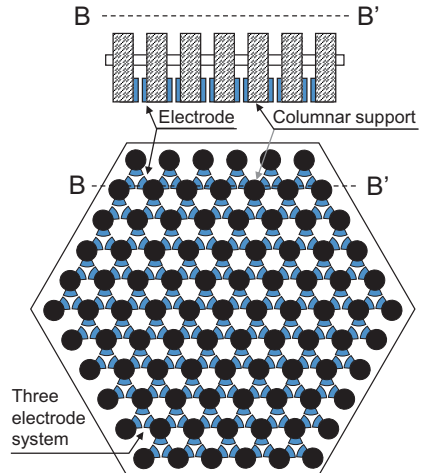


Fig. 16.13 (continued)

be freely combined according to the purpose. As shown here, the possibilities of capillary action to biosensor chips or biosensor array chips are infinite.

At that time, I was working on biosensor chip designs from the widest possible perspective. The present section described strategic approaches to achieve future sustainable mass production of the electrochemical SMBG biosensor chips based on my original patent map. In these approaches, the biosensor chips were simply and accurately assembled and designed. Based on the chip assembly method, both the environmentally and user-friendly biosensor chips were designed for practical use. In the environmentally-friendly section, the microbial biosensor chip for environmental monitoring also introduced an example of other developmental chip studies. Finally, new concept biosensor chips and biosensor array chips were designed employing a new application method of the capillary action.

The current status of both the biosensor chips and the biosensor array chips are drastically changed by the advent of new printing techniques such as 3D printers and by the advance of nanotechnologies compared with about one decade ago (Loo et al. 2019). In addition, the United Nations raised the sustainable development goals (SDGs) in 2015 (United Nations, 2015). For people to reach these goals, I hope that our efforts will be applied to such new technology areas.

16.4 Conclusion

In the present chapter, I presented new designs for the electrochemical SMBG biosensor chips because of user QOL, environment, and economic efficiency. These designs are based on my strategic patent map for technological platform constructions. Finally, I sincerely hope there will be an opportunity to explain in detail the developmental strategy trajectory based on my platform patent map.

Acknowledgments The author cordially thanks Dr. Isao Karube for allowing me to apply for many patents and Dr. Masao Gotoh for teaching me how to write the patent of my first invention (JP4036384 and JP4038575). Finally, the author also thanks Dr. Anatoly Reshetilov and Dr. Mahendra Rai for allowing me to publish the present chapter.

Conflict of Interest The author has no conflicts of interest to disclose.

Appendix

Appendix Table 1 A list of patent applications to Japan Patent Office (JPO)

No.	Registration		Application Date	Title	IPC ¹	Claims	Inventors			Applicants	Worldwide Applications	Remarks
	Number	Year					Principal	Others				
1	JP3890417	2006	27/8/2003	Biosensor having adhesive and separable protective film	G01N 27/28	24	Nakamura et al.	2	AIST ²	PCT/JP2004/011451	Figs. 16.5a and 16.13a	
2	JP3914992	2007	9/12/2003	Urine component detecting device	G01N 27/28	5	Gotoh et al.	2	AIST	PCT/JP2004/017850		
3	JP4036384	2007	15/11/2006	Biosensor and manufacturing method therefor	G01N 27/327	16	Nakamura et al.	2	AIST	PCT/JP2004/005436	JP4038575, Fig. 16.1bi ~ 4	
4	JP4038575	2007	4/3/2004	Biosensor and method for manufacturing the same	G01N 27/327	41	Nakamura et al.	2	AIST	PCT/JP2004/005436	JP4036384, Fig. 16.1bi ~ 4	
5	JP4247844	2009	17/2/2005	Urinary glucose biosensor	G01N 27/416	9	Gotoh et al.	4	AIST	PCT/JP2005/002391		
6	JP4277104	2009	20/2/2004	Manufacturing method for biosensor adjacent-bonded sheet	G01N 27/327	17	Nakamura et al.	2	AIST		Figure 16.1bii	
7	JP4374464	2009	21/2/2005	Biosensor	G01N 27/30	27	Gotoh et al.	4	AIST	PCT/JP2005/002699		
8	JP4399581	2009	21/1/2005	Biosensor	G01N 27/28	25	Nakamura et al.	3	AIST		Nakamura et al. (2007c), Figs. 16.5bi, 16.6a	
9	JP4448940	2010	28/7/2005	Needle-integrating biosensor	A61B 5/151	21	Nakamura et al.	2	AIST	PCT/JP2006/312818	JP4547535 ⁴ , Fig. 16.7	
10	JP4469950	2010	23/2/2005	Puncturing needle	A61B 5/151	10	Nakamura et al.	3	AIST		Nakamura et al. (2007b)	

(continued)

No.	Registration		Application Date	Title	IPC ¹	Claims	Inventors		Applicants	Worldwide Applications	Remarks
	Number	Year					Principal	Others			
11	JP4469983	2010	21/1/2005	Biosensor for multichannel simultaneous measurement and usage of it	G01N 27/28	16	Nakamura et al.	3	AIST	(US20050247573)	Figs. 16.5bii, 16.6b and 16.13b
12	JP4518846	2010	22/6/2004	Sensor chip manufacturing method and sensor chip	G01N 27/327	9	Hosoya et al.	7	AIST&SEF ³		
13	JP4547535	2010	27/6/2005	Needle-integrated biosensor	A61B 5/151	14	Nakamura et al.	2	AIST	PCT/JP2006/312818	JP4448940
14	JP4568879	2010	12/5/2005	Biosensor for diagnosing soil, and soil diagnostic method using the same	G01N 27/416	16	Nakamura et al.	2	AIST		
15	JP4576624	2010	2/3/2005	Biosensor integral with needle	A61B 5/157	58	Nakamura et al.	2	AIST	PCT/JP2006/303908	JP4595064, Fig. 16.9
16	JP4576626	2010	5/7/2005	Biosensor integrated with puncturing instrument	A61B 5/157	3	Nakamura et al.	2	AIST		
17	JP4576627	2010	5/7/2005	Biosensor integrated with puncturing instrument	A61B 5/157	22	Nakamura et al.	2	AIST		
18	JP4576628	2010	13/7/2005	Needle-integrated biosensor	A61B 5/157	8	Nakamura et al.	2	AIST		
19	JP4586210	2010	27/6/2005	Needle-integrated biosensor	A61B 5/157	5	Nakamura et al.	2	AIST	PCT/JP2006/312820	JP4595070, JP4893921
20	JP4590586	2010	31/1/2006	Device for activating photocatalyst and method for activating photocatalyst using it	B01J 35/2	14	Sinohara et al.	3	AIST		Nakamura et al. (2007b)
21	JP4595064	2010	19/4/2005	Needle-integrated biosensor	A61B 5/157	11	Nakamura et al.	2	AIST	PCT/JP2006/303908	JP4576624

22	JP4595070	2010	27/6/2005	Needle-integrated biosensor	A61B 5/157	5	Nakamura et al.	2	AIST	PCT/JP2006/312820	JP4893921, JP4586210
23	JP4631027	2010	29/3/2005	IC tag-mounted biosensor, and package thereof	G01N 27/327	16	Nakamura et al.	2	AIST		Figure 16.10
24	JP4631028	2010	4/4/2005	Detection part of biosensor	G01N 27/28	54	Nakamura et al.	2	AIST		Figure 16.11
25	JP4631029	2010	27/6/2005	Needle-integrated biosensor	A61B 5/151	18	Nakamura et al.	2	AIST		
26	JP4631030	2010	27/6/2005	Needle-integrated biosensor	A61B 5/151	22	Nakamura et al.	2	AIST		
27	JP4631031	2010	5/7/2005	Integrated needle type biosensor	A61B 5/151	12	Nakamura et al.	2	AIST		
28	JP4635258	2010	2/3/2006	Biosensor	G01N 27/327	9	Nakamura et al.	2	AIST		Figure 16.13c
29	JP4635260	2010	16/3/2006	Biosensor and manufacturing method therefor	G01N 27/327	13	Nakamura et al.	2	AIST		
30	JP4649594	2010	3/2/2006	Biosensor and its manufacturing method	G01N 27/327	12	Nakamura et al.	2	AIST		Figure 16.3
31	JP4650314	2010	23/3/2006	Biosensor	G01N 27/30	11	Nakamura et al.	2	AIST		Figure 16.12 and 16.13d
32	JP4665135	2011	3/2/2006	Biosensor and its manufacturing method	G01N 27/327	9	Nakamura et al.	2	AIST		
33	JP4670013	2011	3/2/2006	Biosensor and its manufacturing method	G01N 27/327	20	Nakamura et al.	2	AIST		
34	JP4677642	2011	26/9/2008	Method of manufacturing biosensor connection sheet	G01N 27/327	13	Nakamura et al.	2	AIST		

(continued)

No.	Registration		Application Date	Title	IPC ¹	Claims	Inventors		Applicants	Worldwide Applications	Remarks
	Number	Year					Principal	Others			
35	JP4682360	2011	5/7/2005	Integrated needle type biosensor	A61B 5/15	18	Nakamura et al.	2	AIST		
36	JP4682361	2011	5/7/2005	Biosensor integrated with puncturing instrument	A61B 5/151	18	Nakamura et al.	2	AIST		
37	JP4686763	2011	31/1/2006	Needle unitary type biosensor	A61B 5/157	12	Nakamura et al.	2	AIST		
38	JP4706063	2011	31/1/2006	Needle unitary type biosensor	A61B 5/157	17	Nakamura et al.	2	AIST		
39	JP4706070	2011	6/7/2009	Ink	G01N 27/30	1	Gotoh et al.	4	AIST		
40	JP4752044	2011	27/2/2006	Blood component measuring device	A61B 5/157	15	Gotoh et al.	2	AIST		
41	JP4766430	2011	31/1/2007	Ethanol measuring method	G01N 33/98	10	Nakamura et al.	1	AIST		
42	JP4798502	2011	31/1/2007	Method of measuring BOD	G01N 27/416	11	Nakamura et al.	2	AIST		Nakamura et al. (2007a) and Nakamura (2010)
43	JP4798503	2011	31/1/2007	Glucose measuring method	G01N 27/416	10	Nakamura et al.	1	AIST		
44	JP4807493	2011	6/10/2005	Sensor chip and manufacturing method therefor	G01N 27/416	12	Nakamura et al.	7	AIST & SEI		Figure 16.8
45	JP4822511	2011	9/2/2006	Needle-integrated biosensor	G01N 27/416	9	Nakamura et al.	2	AIST		
46	JP4853947	2011	14/3/2006	Biosensor	G01N 27/28	17	Nakamura et al.	2	AIST		

47	JP4862195	2011	8/9/2006	Bio-sensor measuring device, bio-sensor measuring system, and bio-sensor measuring method	G01N 27/416	6	Kaimori et al.	7	AIST & SEI	PCT/JP2006/317897
48	JP4868405	2011	1/2/2007	Method for measuring activity of microorganism	G01N 33/18	12	Nakamura et al.	1	AIST	
49	JP4873536	2011	7/2/2006	Non-conductive needle	A61B 5/157	8	Nakamura et al.	2	AIST	
50	JP4893921	2011	14/2/2006	Biosensor	G01N 27/28	12	Nakamura et al.	2	AIST	PCT/JP2006/312820 JP4595070, JP4586210
51	JP4894038	2012	1/11/2006	Biosensor cartridge	A61B 5/157	4	Fujimura et al.	8	AIST & SEI	
52	JP4894039	2012	21/11/2006	Biosensor cartridge and biosensor device	A61B 5/151	5	Fujimura et al.	9	AIST & SEI	PCT/JP2007/063466
53	JP4899156	2012	1/2/2007	Method for measuring activity of eukaryotic microorganism	C12Q 1/06	15	Nakamura et al.	1	AIST	
54	JP4953139	2012	17/4/2007	Biosensor chip	A61B 5/157	6	Kitamura et al.	8	AIST & SEI	PCT/JP2007/058368
55	JP4958275	2012	16/2/2007	Needle-integrated sensor	G01N 27/28	7	Fujimura et al.	9	AIST & SEI	PCT/JP2007/074246
56	JP4958276	2012	24/2/2007	Needle integrated type sensor	A61B 5/151	5	Fujimura et al.	9	AIST & SEI	PCT/JP2007/066195 JPA2006/224993
57	JP4958291	2012	9/7/2007	Sensor chip measurement apparatus	G01N 27/28	7	Fujimura et al.	9	AIST & SEI	
58	JP4979005	2012	28/5/2007	Biosensor measuring instrument	G01N 27/28	2	Nakamura et al.	7	AIST & SEI	

(continued)

No.	Registration		Application Date	Title	IPC ¹	Claims	Inventors		Applicants	Worldwide Applications	Remarks
	Number	Year					Principal	Others			
59	JP4986290	2012	31/7/2007	Sensor device	G01N 27/327	5	Fujimura et al.	8	AIST & SEI		
60	JP4997583	2012	17/3/2005	Sensor	C01B 31/02	16	Gotoh et al.	6	AIST		
61	JP5126755	2012	3/2/2010	Method of manufacturing biosensor integrated with puncture device	A61B 5/151	14	Nakamura et al.	2	AIST		
62	JP5126756	2012	3/2/2010	Method of manufacturing biosensor integrated with puncture device	A61B 5/151	2	Nakamura et al.	2	AIST		
63	JP5289666	2013	24/1/2005	Sensor chip connecting body and its manufacturing method	G01N 27/327	2	Kaimori et al.	7	AIST & SEI		

¹ International Patent Classification. ² National Institute of Advanced Industrial Science and Technology. ³Sumitomo Electric Industries Ltd. ⁴ other included patent(s). Detail information of the Japanese patents are available from World Intellectual Property Organization (<https://patentscope2.wipo.int/search/en/structuredSearch.jsf>). In that case, search for the grant number and English version of the document is available here

Appendix Table 2 A list of patent applications to PCT

No.	Application Number		Date	Publication number	Title	IPC	Claims	Inventors		Applicants	Grant number in Japan (Application)		
	No.							Principal	Others		1	2	3
1	PCT/IP2004/005436		15/4/2004	WO/2005/010519	Biosensor and production method therefor	C12M 1/00	59	Nakamura et al.	2	AIST	JP4038575		
2	PCT/IP2004/011451		10/8/2004	WO/2005/022140	Biosensor with adhesive and peelable protective film	B65D 77/00	25	Nakamura et al.	2	AIST	JP3890417		
3	PCT/IP2004/017850		1/12/2004	WO/2005/057210	Urine component detecting system and detector	A61B 5/00	12	Gotoh et al.	4	AIST	JP3914992		
4	PCT/IP2004/018193		7/12/2004	WO/2005/056824	Method of detecting sulfate-conjugated bile acid and test paper and biosensor to be used therein	C12N 11/00	23	Gotoh et al.	4	AIST	(JPA2003/408930)		
5	PCT/IP2005/000828		24/1/2005	WO/2005/073399	Method of qualitatively/quantitatively determining phosphate ion and phosphate ion sensor	C12Q 1/68	21	Nakamura et al.	2	AIST	(JPA2004/019230)		
6	PCT/IP2005/002391		17/2/2005	WO/2005/080953	Urinary glucose biosensor	G01N 27/327	9	Gotoh et al.	4	AIST	JP4247844		
7	PCT/IP2005/002699		21/2/2005	WO/2005/088288	Carbon nanotube biosensor	C09D 11/00	27	Gotoh et al.	4	AIST	JP4374464		
8	PCT/IP2006/300941		23/1/2006	WO/2006/078010	Sensor chip	G01N 27/327	12	Hosoya et al.	7	AIST & SEI	(JPA2005/015310)		
9	PCT/IP2006/300966		23/1/2006	WO/2006/078016	Sensor chipconcatenated body of sensor chips and manufacturing method thereof	G01N 27/327	10	Kaimori et al.	7	AIST & SEI	(JPA2005/015644)		
10	PCT/IP2006/300982		23/1/2006	WO/2006/078022	Sensor chip manufacturing method and sensor chip	G01N 27/327	9	Kaimori et al.	7	AIST & SEI	(JPA2005/015994)		

(continued)

11	PCT/IP2006/503908	3/1/2006	WO/2006/093206	Biosensor coupled with needle	A61B 5/157	41	Nakamura et al.	2	AIIST	JP4576624	JP4595064
12	PCT/IP2006/512818	27/6/2006	WO/2007/001001	Needle integrating biosensor	A61B 5/157	24	Nakamura et al.	2	AIIST	JP4547535	JP44448940
13	PCT/IP2006/512820	27/6/2006	WO/2007/001003	Biosensor	A61B 5/157	14	Nakamura et al.	2	AIIST	JP4586210	JP4595070 JP4893921
14	PCT/IP2006/517897	8/9/2006	WO/2007/032286	Bio-sensor measuring device, bio-sensor measuring system, and bio-sensor measuring method	G01N 27/327	6	Kainoni et al.	7	AIIST & SEI	JP4562195	
15	PCT/IP2006/520569	16/10/2006	WO/2007/046334	Biosensor chip and process for producing the same	G01N 27/327	6	Kitamura et al.	7	AIIST & SEI	(JPA2005/302330)	
16	PCT/IP2006/520570	16/10/2006	WO/2007/046335	Sensor chip and method for producing the same	G01N 27/327	17	Nakamura et al.	6	AIIST & SEI	(JPA2005/301307)	
17	PCT/IP2006/521279	25/10/2006	WO/2007/049646	Sensor chip and sensor system	G01N 27/327	4	Nakamura et al.	6	AIIST & SEI	(JPA2005/312326)	
18	PCT/IP2007/058368	17/4/2007	WO/2007/119853	Sensor chip	A61B 5/151	7	Kitamura et al.	8	AIIST & SEI	JP4953139	
19	PCT/IP2007/058370	17/4/2007	WO/2007/123135	Bio sensor system	A61B 5/151	5	Fujimura et al.	8	AIIST & SEI	(JPA2006/113916)	
20	PCT/IP2007/058880	24/4/2007	WO/2007/123243	Bio sensor chip	A61B 5/157	4	Fujimura et al.	8	AIIST & SEI	(JPA2006/119885)	
21	PCT/IP2007/059391	2/5/2007	WO/2007/129671	Holder for measuring instrument and biosensor measuring instrument	A61B 5/157	6	Kitamura et al.	8	AIIST & SEI	(JPA2006/131948)	
22	PCT/IP2007/063466	5/7/2007	WO/2008/004623	Biosensor cartridge and method for manufacturing the same	A61B 5/151	7	Kaimori et al.	8	AIIST & SEI	JP4594039	

23	PCT/JP2007/063817	11/7/2007	WO/2008/007702	Biosensor chip and process for manufacturing the same	G01N 27/327	7	Kaimori et al.	9	AIIST & SEI	(JPA2006/193886)	
24	PCT/JP2007/066195	21/8/2007	WO/2008/023703	Biosensor cartridge	A61B 5/157	11	Fujimura et al.	10	AIIST & SEI	JP4958276 (JPA2006/224993)	
25	PCT/JP2007/071331	1/11/2007	WO/2008/056598	Biosensor cartridge, biosensor device, specimen sampling method, manufacturing method for biosensor cartridge, and needle-integrated sensor	A61B 5/151	18	Fujimura et al.	10	AIIST & SEI	(JPA2006/304972, 2006/313466, 2007/043034)	
26	PCT/JP2007/071332	1/11/2007	WO/2008/062648	Biosensor cartridge and biosensor apparatus	A61B 5/157	6	Fujimura et al.	9	AIIST & SEI	JP4894039	
27	PCT/JP2007/074246	17/12/2007	WO/2008/075651	Biosensor cartridge, method of using biosensor cartridge, biosensor device and needle-integrated sensor	A61B 5/157	19	Fujimura et al.	9	AIIST & SEI	JP4958275 (JPA2006/341792)	
28	PCT/JP2008/050240	11/1/2008	WO/2008/084840	Biosensor cartridge	A61B 5/157	5	Fujimura et al.	8	AIIST & SEI	(JPA2007/003909)	
29	PCT/JP2008 052313	13/2/2008	WO/2008/099837	Biosensor cartridge and method of producing the same	A61B 5/157	7	Fujimura et al.	7	AIIST & SEI	(JPA2007/033122)	
30	PCT/JP2008/053198	25/2/2008	WO/2008/105373	Sensor device	A61B 5/151	10	Fujimura et al.	9	AIIST & SEI	(JPA2007/046327, 2007/191904)	
31	PCT/JP2008/053199	25/2/2008	WO/2008/114576	Biosensor cartridge	A61B 5/157	6	Fujimura et al.	9	AIIST & SEI	(JPA2007/073872)	

^aUnited States patent application

References

- Bahadır EB, Sezgingurk MK (2015) Applications of commercial biosensors in clinical, food, environmental, and bioterror/biowarfare analyses. *Anal Bioanal Chem* 478:107–120
- Barnes DKA, Galgani F, Thompson RC, Morton Barlaz M (2009) Accumulation and fragmentation of plastic debris in global environments. *Philos Trans R Soc Lond Ser B Biol Sci* 364:1985–1998
- Clarke WL, COXD, Linda A et al (1987) Evaluating clinical accuracy of system for self-monitoring of blood glucose. *Diabetes Care* 10:622–628
- Kaimori S, Kitamura T, Ichino M et al (2006) Structural development of a minimally invasive sensor chip for blood glucose monitoring. *Anal Chim Acta* 573:104–109
- Loo JFC, Ho AHP, Turner APF, Mak WC (2019) Integrated printed microfluidic biosensors. *Trends in Biotech*, in press
- Mathers CD, Loncar D (2006) Projections of global mortality and burden of disease from 2002 to 2030. *PLoS Med* 3:e442
- Naemura K, Saito H (2005) Precise positioning of the epidural anesthesia needles by puncture force. *Micromechatronics* 49:38–44
- Nakamura H (2010) Recent organic pollution and its biosensing methods. *Anal Meth* 2:430–444
- Nakamura H (2018) Biosensors: monitoring human health for the SDGs sustainable development goals. *Biomed J Sci Tech Res* 9:1–4
- Nakamura H, Karube I (2003) Current research activity in biosensors. *Anal Bioanal Chem* 377:446–468
- Nakamura H, Suzuki K, Ishikuro H et al (2007a) A new BOD estimation method employing a double-mediator system by ferricyanide and menadione using the eukaryote *Saccharomyces cerevisiae*. *Talanta* 72:201–216
- Nakamura H, Tanaka M, Shinohara S et al (2007b) Development of a self-sterilizing lancet coated with a titanium dioxide photocatalytic nano-layer for self-monitoring of blood glucose. *Biosens Bioelectron* 22:1920–1925
- Nakamura H, Tohyama K, Tanaka M et al (2007c) Development of a package-free transparent disposable biosensor chip for simultaneous measurements of blood constituents and investigation of its storage stability. *Biosens Bioelectron* 23:621–626
- Sekretaryova AN, Eriksson M, Turner APF (2016) Bioelectrocatalytic systems for health applications. *Biotechnol Adv* 34:177–197
- Sherkow JS (2016) Protecting products versus platforms. *Nature Biotechnol* 34:462–465
- Story MF, Mueller JL, Mace RL (1998) The universal design file: designing for people of all ages and abilities. Education Resources Information Center Retrieved from <https://files.eric.ed.gov/fulltext/ED460554.pdf>
- Turner APF (2017) Enabling mobile health. *Procedia Technol* 27:4–5
- United Nations (2015) The sustainable development goals (SDGs) consisting of 17 global goals. Transforming our world: the 2030 agenda for sustainable development (2030 Agenda). Retrieved from <https://www.un.org/sustainabledevelopment/>
- Urdike SJ, Hicks GP (1967) The enzyme electrode. *Nature* 214:986–988
- WHO (2002) Blood, oxygen and the circulation. In: WHO (ed) *The clinical use of blood in general medicine, obstetrics surgery & anaesthesia trauma & burns*, Geneva, pp 20–37
- WHO (2018) Diabetes. WHO. Retrieved from <https://www.who.int/news-room/fact-sheets/detail/diabetes>
- World Health Organization (1999) Definition, diagnosis and classification of diabetes mellitus and its complications. In: Report of a WHO consultation. WHO. Retrieved from https://www.staff.ncl.ac.uk/philip.home/who_dmc.htm
- Yoo EH, Lee SY (2010) Glucose biosensors: an overview of use in clinical practice. *Sensors* 10:4558–4576

Part IV
Biofuel Elements and Self- Powered
Biosensors for Human Health

Chapter 17

Biological Fuel Cells: Applications in Health and Ecology



Ivan Alexeevich Kazarinov and Mariia Olegovna Meshcheryakova

Abstract Biological fuel cells (BFCs) in the long term are a promising form of genuine fuel cells. Unlike conventional fuel cells that use hydrogen, ethanol, and methanol as fuel, biofuel cells use organic products of metabolic processes or organic electron donors as a fuel to generate current. In BFCs, biological redox reactions are controlled enzymatically, while in chemical fuel cells, the catalyst kinetics are determined by noble metals, most often by platinum.

A fuel cell is an electrochemical device that continuously converts chemical energy into electrical energy, as long as there are fuel and an oxidizing agent. Despite their high efficiency, the advantages of chemical fuel cells are partially offset by the high cost of the catalysts, high operating temperatures, and the corrosiveness of the electrolytes used in them. In this regard, biofuel elements are attractive and promising. They work in moderate conditions, that is, at ambient temperature and pressure. They also use neutral electrolyte and low-cost platinum-free catalysts. In biofuel elements, the catalyst is either microorganisms or enzymes.

This chapter discusses the principles of operation of microbial and enzymatic fuel cells and some of their applications in healthcare and in the conversion of wastewater organic substances into electrical energy using microbial fuel cells.

Keywords Biological fuel cells · Microbial fuel cells · Enzyme fuel cells · Microbial electrochemical technology · Bioanode · Biocathode · Mediator · Conversion of organic waste into bioenergy · Implantable biofuel cell

Nomenclature

BFCs	biological fuel cells
EFCs	enzyme fuel cells
MFCs	microbial fuel cells
DTA	ethylenediaminetetraacetic acid

I. A. Kazarinov (✉) · M. O. Meshcheryakova (✉)
Department of Physical Chemistry, Saratov State University, Saratov, Russia
e-mail: kazarinovia@mail.ru; mno24@mail.ru

NAD+	nicotinamide adenine dinucleotide
NADP+	nicotinamide adenine dinucleotide phosphate
FAD	flavin adenine dinucleotide
PQQ	pyrroloquinoline quinone
LDH	lactate dehydrogenase
Cytc	cytochrome c
MP-11	microperoxidase-11
DMRB	dissimilative metal-reducing bacterium
IMD	implantable medical devices
EBFC	enzymatic biofuel cell
BAC	blood alcohol content

17.1 Introduction

Biological fuel cells (BFCs) are devices that use biological components as catalysts to generate electricity (Tanisho and Kamiya 1985; Katz 2003; Shukla et al. 2004; Davila et al. 2008; Kazarinov 2012). In BFC, either whole microorganisms or enzyme preparations are used as catalysts. In this regard, BFCs are divided into enzyme fuel cells (EFCs) and microbial fuel cells (MFCs). In addition, unlike chemical fuel cells that use hydrogen, ethanol, and methanol as fuel, very expensive catalysts that usually work in corrosive electrolytes, BFCs can use energy-intensive, but electrochemically passive substances (carbohydrates, organic acids, alcohols, as well as many organic wastes). This opens up the possibility of simultaneously solving environmental and energy problems. BFCs operate in moderate conditions such as at ambient temperature and pressure.

Currently, research in the field of BFCs is being intensively developed in many world scientific centers. A large number of original works have been published on various problems of MFCs and EFCs. Among several reviews devoted to this issue, some of the important reviews include Katz (2003), Shukla et al. (2004), and Kazarinov (2012).

Given the close symbiotic relationship between humans and microorganisms, MFCs can be a continuous, long-lasting, and safe power source for implantable medical devices (IMD). Implantable medical devices (IMD) can be divided into two categories: devices to support functional operations of a body and devices for in vivo measurements. The first category includes pacemakers, cochlear implants, drug pumps, and biochips, and the second includes blood meters, blood glucose meters, and temperature sensors. A common feature of IMD is that they require a stable and efficient power source that can be obtained using biofuel elements.

Huge economic and environmental prospects for microbial fuel cells come from the conversion of industrial wastewater containing high levels of easily degradable organic material into electrical energy. Recovery of energy and valuable products could partially offset the cost of wastewater treatment and somewhat reduce our dependence on fossil fuels.

In this chapter, we aimed to discuss the principles of operation of MFCs and EFCs and some of their applications in healthcare and in the conversion of wastewater organic substances into electrical energy using bioelectrochemical technologies.

17.2 MFCs

17.2.1 *The Anodes of MFCs*

The use of microorganisms in biofuel elements eliminates the need to isolate individual enzymes, thereby providing cheaper catalysts for biofuel elements. The main problem of MFC is the transfer of a charge from a cell of the microorganism to an electrode. Therefore, microorganisms for generating electricity can be used in four types of MFCs (Kazarinov 2012):

1. For the purpose of generating energy, fuels are produced in individual reactors and transported to the anode of a conventional fuel cell. In them, the microbial bioreactor is separated from the actual fuel cell. These are indirect MFCs.
2. In MFC, the process of microbiological fermentation proceeds directly in the anode compartment of the fuel cell. These are direct-acting MFCs.
3. Mediator MFCs are also type of direct-acting MFCs. In them, electron transfer mediators transfer electrons between the microbial biocatalytic system and the electrode. The mediator molecules take electrons from the biological transfer chain of electrons of microorganisms and transfer them to the anode of the bio-fuel element.
4. Mediator-free MFCs: In these, metal-reducing bacteria having cytochromes in the outer membrane and capable of electrically contacting the electrode surface directly ensure the operation of the MFCs.

Indirect MFCs

As an example of indirect type of MFCs, a microbial system that produces hydrogen as a fuel for chemical fuel cells has been discussed. Various bacteria and algae, such as *Escherichia coli*, *Enterobacter aerogenes*, *Clostridium butyricum*, *Clostridium acetobutylicum*, and *Clostridium perfringens*, are known to produce hydrogen under anaerobic conditions (Lewis 1966; Raeburn and Rabinowitz 1971; Thauer et al. 1972, 1977; Jungermann et al. 1973).

The conversion of carbohydrate to hydrogen is achieved through a multi-enzyme system. In practice, however, the yield of H₂ is only ~25% of theoretical (Suzuki et al. 1983).

In microbial systems producing electrochemically active metabolites in the anode compartment of a biofuel cell, the fermentation process takes place directly

on the electrode surface, delivering fuel (H_2) to the anode. Additional by-products of the fermentation process (formic, acetic, and lactic acids) are also used as fuels (Karube et al. 1977; Liu et al. 1978).

Mediator MFCs

Since the reduced particles resulting from metabolic processes inside microbial cells are isolated by a microbial membrane, the contact of the microbial cells with the electrode is poor and usually leads only to poor electron transfer through the membrane, with the exception of some special cases described below. The electroactive groups responsible for the redox activity of enzymes in microbial cells are located in the depths of their prosthetic groups, which leads to poor electrical contact between the cells and the electrode surface. Low molecular weight redox particles can help electron transfer between the intracellular bacterial space and the electrode, and they are called mediators.

The mediator molecules must satisfy the following requirements (Kazarinov 2012):

1. the oxidized mediator should easily penetrate through the bacterial membrane to the reduced particles inside the bacteria;
2. the redox potential of the mediator should correspond to the potential of the recovered metabolite;
3. the mediator in no degree of oxidation should not interfere with other metabolic processes;
4. the restored mediator should easily leave the cell through the bacterial membrane;
5. mediators in both oxidized and reduced states must be chemically stable in an electrolyte solution, readily soluble, and should not be adsorbed on bacterial cells and electrode surfaces;
6. the electrochemical kinetics of the oxidation process of the restored state of the mediator on the electrode should be fast.

A number of organic compounds were studied in combination with bacteria to test the efficiency of electron transfer by a mediator between microorganisms and the anode surface. Neutral red, methylene blue, gallocyanin (Kazarinov et al. 2011), and some organic dyes were often used as mediators in biofuel elements. The redox potentials and structures of some of the electronic mediators are presented in Table 17.1.

However, exogenous mediators are too expensive for practical use, toxic to the biocatalyst at the concentrations that are required to obtain good MFC characteristics, and are destroyed during prolonged operation. Under certain conditions, electrochemically active microorganisms in MFCs are capable of producing their own mediator compounds that are involved in extracellular electron transfer processes (Rabaey and Verstraete 2005). This can happen in two ways: through the production of secondary and primary metabolites (Schröder 2007).

Table 17.1 The structure and redox potentials of some exogenous mediators

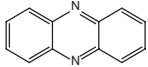
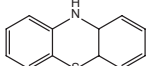
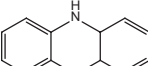
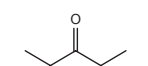
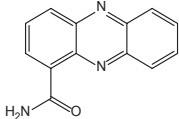
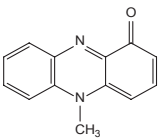
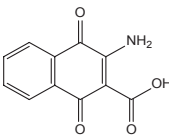
Class	Structure	Redox-mediator	E, V (n.a.)
Substances		Neutral red	-0.32
		Safranin	-0.29
		Phenazine ethosulfate	0.06
Phenazines		New methylene blue	-0.02
		Toluidine Blue Oh	0.03
		Thionine	0.06
		Phenothiazinone	0.13
Phenothiazines		Resorfin	-0.05
		Gallocyanin	0.02
Phenoxazines		2-hydroxy-1,4-naphthoquinone	-0.14
		Anthraquinone-2,6-disulfonate	-0.18

Table 17.2 The structure and redox potentials of endogenous mediators

Redoxmediator	Structure	E, V
Phenazine-1-carboxamide		-0,115
Pyocyanin		-0,03
2-amino-3-carboxy-1,4-naphthoquinone		-0,071

Secondary metabolites (endogenous mediators) are redox-active substances and serve as reversible terminal electron acceptors transporting electrons from a bacterial cell to a solid oxidizer (MFC anode) or to aerobic layers of a biofilm where they are oxidized and can again participate in redox processes. Examples of endogenous redox mediators are presented in Table 17.2.

The overall efficiency of electron transfer mediators depends on many parameters, especially the rate constant of the electrochemical reoxidation of the mediator, which depends on the electrode material (Davis and Yarbrough 1962; Kano and Ikeda 2000). The effectiveness of exogenous redox mediators in the bioelectrochemical system “substrate-bacterial cell-mediator” can be estimated only by studying the kinetics of biocatalytic processes in similar systems, as proposed in many previous reports (Gradskov et al. 2001; Kuz'micheva et al. 2007; Kazarinov et al. 2011, 2014; Naumova et al. 2015).

A mixture of two mediators may be useful for optimizing effectiveness. Two mediators—thionine and Fe (III)-EDTA—are used with the *Escherichia coli* biocatalyst for the oxidation of glucose (Tanaka et al. 1983). The electrodes should be designed to facilitate electrical contact between the biocatalytic system and the anode. Mediators can be connected with microorganisms in three ways (Sell et al. 1989; Park et al. 2000):

1. a diffusion mediator mediating between the microbial suspension and the anode surface;
2. a diffusion mediator mediating between the anode and microbial cells covalently connected to the electrode. For the connection of microbial cells with the surface, standard organic reagents (cyanamide and acetyl chloride) are used;
3. a mediator adsorbed on microbial cells and providing electronic transfer from them to the anode.

Mediator-Free MFCs

Some types of microorganisms in MFCs can directly transfer electrons to the anode. These include metal-reducing bacteria, such as *Geobacter sulfurreducens* (Methé 2003; Bulter 2004), *Rhodospirillum rubrum* (Rabaey 2007), and *Shewanella putrefaciens* (Myers 1992, 2001; Kim 1999, 2002; Lovley 2006), which are found in sediments where they use insoluble electron acceptors, for example, iron oxide (III) or manganese oxide (IV). The direct transfer of electrons is due to the presence of cytochromes in their outer membrane or due to the ability to develop electron-conducting molecular pills (nanowires).

Thus, the work of MFC depends on the maximum cell density in the first monolayer on the anode surface. Nanowires can provide structural support for the formation of thick electroactive biofilms and, thus, increase the performance of MFCs. The development of mediator-free microbial fuel cells using *Shewanella putrefaciens* IR-1 is described in the article by Kim (2002). Table 17.3 shows the characteristics of the mediator and mediator-free MFCs that are currently achieved.

Thus, a comparison of the data presented shows that, in terms of power characteristics, mediator-free fuel cells do not yet surpass mediator systems. However, due to their advantage over mediator fuel cells in cost, the absence of toxic mediators is obvious. In non-mediator fuel cells, there are also many possibilities for increasing the efficiency of electronic transfer.

Table 17.3 Power densities of some mediator and mediator-free microbial fuel cells (Vega 1987; Zhang 1995; Kim 1999; Tender 2002; Choi 2003; Park 2003; Bond 2003)

Electronic transfer mechanism	Microorganisms	Substrate	Electrode	P, mW/m ²
Mediator Electronic Transfer	<i>Proteus vulgaris</i>	Glucose	Glassy carbon	4.5
	<i>Proteus vulgaris</i>	Glucose	Glassy carbon	85
	<i>Escherichia coli</i>	Lactate	Graphite fabric	1.2
		Lactate	Smooth graphite	91
	<i>Pseudomonas aeruginosa</i>	Glucose	Smooth graphite	88
	Mixed culture	Sulfide/acetate	Graphite	32
Direct electronic transfer	<i>Shewanella putrefaciens</i>	Lactate	Graphite fabric	0.19
	<i>Geobacter sulfurreducens</i>	Acetate	Smooth graphite	13
	<i>Rhodofexax ferrireducens</i>	Glucose	Smooth graphite	8
		Glucose	Graphite fabric	17.4
		Glucose	Porous graphite	33

17.2.2 Cathodes for MFCs

The operation of the cathode significantly affects the generation of electricity in the MFCs. Cathodic reactions can be both chemical and biochemical. Oxygen is the most suitable electronic acceptor for MFC, due to its high redox potential, low price, availability, sustainability, and the absence of chemical waste (water is the only final product). However, the low rate of oxygen reduction on the surface of graphite electrodes is one of the limiting factors for optimal MFC operation. Therefore, platinum is usually used as a catalyst for dissolved oxygen or air cathodes. However, its use is limited due to the high cost and possible poisoning by components present in the solution (Liu et al. 2004).

Efficient cathode operation requires catalysts or electronic picks, which are expensive to use. In this regard, biocathodes that use microorganisms as catalysts to promote cathodic reactions are a very promising alternative (He and Largus 2006). Biocathodes can be aerobic and anaerobic depending on the final electron acceptor at the cathode. For aerobic biocathodes with oxygen as the final electron acceptor, electronic mediators, such as iron or manganese, are first reduced at the cathode and then re-oxidized by microorganisms. Anaerobic biocathodes directly restore final electron acceptors, such as nitrate and sulfate ions. Significant difficulties are the choice and service life of the ion-exchange membrane separating the anode and cathode spaces.

The Nafion membrane is widely used as a proton exchange membrane for MFCs (Bond et al. 2002, Logan et al. 2005). This membrane is highly selective for protons, but low in stability since it is sensitive to contamination (for example, ammonium).

The best results were obtained using the Ultrex cation exchange membrane. This membrane is less selective but more stable and able to work for 3 months (Rabaey et al. 2003). The proton exchange membrane increases the internal resistance of the system, so in some studies, it is removed to increase the power of the MFC; however, due to the diffusion of oxygen into the anode chamber, the Coulomb efficiency of the element decreases.

17.3 EFCs

Enzymes have a complex structure, including proteins. An electron-carrying enzyme block (an apoenzyme or a cofactor) is deeply hidden inside its complex structure. Therefore, an effective electrical connection between the electrode substrate and the enzyme biocatalyst is difficult. Mediated bioelectrocatalysis is useful for studying the kinetics of electronic transfer of enzymes and is a key reaction in the use of enzymes in biofuel cells (Turner et al. 1987). In the case of quinogemoproteins, direct and mediated electron transfer between the enzyme and the electrode is possible, where the heme in the protein functions as a built-in mediator in the enzymatic electrochemical reaction.

17.3.1 *Enzymes for Anodic Reactions of Biofuel Elements*

Coenzyme forms of vitamins are pyridine nucleotides. In accordance with the recommendations of the International Biochemical Union Enzyme Commission, coenzyme-1 is called NAD⁺ (nicotinamide adenine dinucleotide), and coenzyme-2 is called NADP⁺ (nicotinamide adenine dinucleotide phosphate). Pyridine nucleotides are coenzymes for the dehydrogenase group of enzymes responsible for the catalysis of some biological redox reactions. As examples of some redox reactions involving pyridine nucleotides, we can consider the action of the enzyme dehydrogenase ethyl alcohol, which oxidizes ethanol to acetaldehyde. In alcohol biofuel cells, this reaction serves as the basis for electron generation.

Flavoproteins are enzymes that catalyze redox reactions in biological systems. The enzyme contains FAD (flavin adenine dinucleotide) as a prosthetic group. Flavoprotein enzymes are also commonly found in redox systems, including pyridine nucleotides. Figure 17.1 explains the participation of these coenzymes in biological redox processes. It shows a number of redox reactions used to oxidize nucleotides of flavin and pyridine again. Molecular oxygen is the ultimate electron acceptor. Such electron transfer chains are associated with the respiratory processes of microorganisms. In the case of biofuel cells, the electrode acts as the final electron acceptor, and the electrons are sent to the anode to generate current.

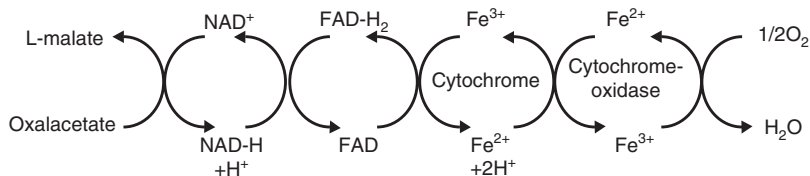


Fig. 17.1 A simplified chain of electron transport for the oxidation of pyridine and flavin nucleotides with molecular oxygen

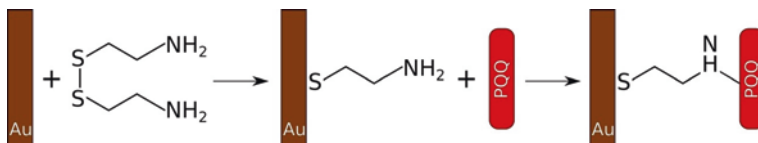
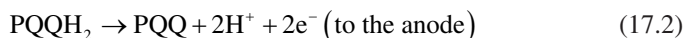
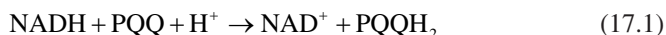


Fig. 17.2 The configuration of the gold electrode modified by PQQ (pyrroloquinoline quinone)

Anodes Based on NADH Bioelectrocatalysis

The process of electrochemical oxidation of NADH/NAD⁺ is deeply irreversible and proceeds with great overvoltage. Strong adsorption of NAD⁺ and NADH poisons the electrode surface and inhibits the oxidation process. Therefore, the non-catalyzed electrochemical oxidation of NAD(F)H is not suitable for use in practical fuel cells; mediated bioelectrocatalysis is required. Mediated bioelectrocatalysis proceeds through the mediator of pyrroloquinoline quinone (PQQ), covalently connected to a gold electrode via a self-assembled cystamine monolayer in the presence of Ca²⁺ ions as promoters:



The assembly of the gold electrode modified with PQQ is shown schematically in Fig. 17.2. The covalent bond of the redox mediator with self-assembled cystamine monolayers on the surface of the gold electrode is important in the preparation of multi-component organized systems (Willner and Riklin 1994). The resulting electrode shows good electrocatalytic activity in the oxidation reaction of NAD(F)H, especially in the presence of Ca²⁺ cations as promoters (Katz et al. 1994). The electrocatalytic anode current and quasi-reversible redox wave in the presence of NADH observed by the researchers indicate the effective electrocatalytic oxidation of the cofactor by reactions (17.1) and (17.2).

Based on these observations, two anode reactions of the fuel cell were standardized, including electrocatalytic regeneration of NAD. In the first case, methanol electrooxidation occurs via NAD⁺-dependent dehydrogenase. Diaphorase catalyzes

the oxidation of NADH to NAD⁺ using benzylviologen as an electron acceptor on a graphite anode (Fig. 17.3) (Palmore et al. 1998). The graphite anode thus releases electrons to reduce oxygen at the platinum cathode. An effective electrode acting as an anode in the presence of NAD(F)-dependent enzyme should include three integrated, electrically contacting components: the NAD (F)⁺ cofactor associated with the corresponding enzyme, and a catalyst that allows efficient cofactor regeneration.

The biocatalytic anode was connected to the oxygen cathode to form a biofuel cell. The complete reaction in a biofuel cell is the oxidation of methanol with oxygen. The biofuel cell produced a voltage of 0.8 V and a maximum power density of 0.68 mW/cm² at 0.49 V. However, this multi-enzyme system was used in an unorganized configuration where all biocatalysts exist as diffusion components in the cell.

In the second case, the electrooxidation of lactate was carried out by assembling an integrated lactate dehydrogenase (LDH) monolayer electrode made by affinity crosslinking of components (Bardef et al. 1997; Katz et al. 1998; Kharitonov et al. 2000). These complexes at the interface can be further crosslinked to form integrated bioelectrocatalytic matrices consisting of electronic relay blocks, cofactor, and enzyme molecules (Fig. 17.4).

The resulting monolayer-functionalized electrode binds NAD-dependent enzymes (e.g., L-lactate dehydrase (LDH)) with affinity interactions between the cofactor and the biocatalyst (Fig. 17.4). These enzyme electrodes electrocatalyze the oxidation of the corresponding substrates (e.g., lactate) (Davis et al. 2002). Crosslinking the enzyme layer using glutaraldehyde provides a stable, electrically contacting electrode.

This system illustrates a fully integrated, rigid biocatalytic matrix consisting of an enzyme, cofactor, and catalyst. The complex between the cofactor NAD⁺ and LDH levels the enzyme on the electrode substrate, thereby providing an effective electrical connection between the enzyme and the electrode, and at the same time, PQQ is involved in the regeneration of NAD⁺.

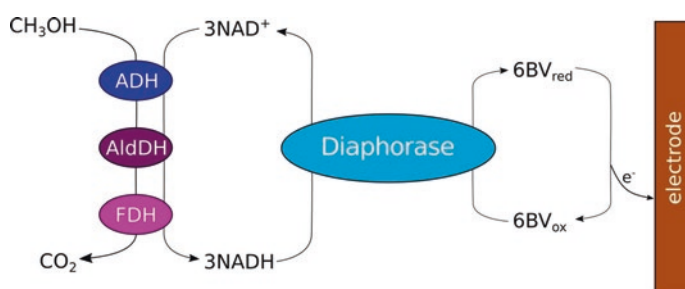


Fig. 17.3 The anode configuration of the methanol-dioxygen biofuel cell: NAD-dependent dehydrogenases oxidize CH₃OH to CO₂; diaphorase catalyzes the oxidation of NADH to NAD⁺ using N, N'-dibenzyl-4,4-bipyridine (benzylviologen, BV²⁺) as an electron acceptor. BV⁺ oxidizes to BV²⁺ on the graphite anode and releases electrons to reduce oxygen at the platinum cathode. ADH alcohol dehydrogenase, AldDH aldehyde dehydrogenase, FDH formate dehydrogenase

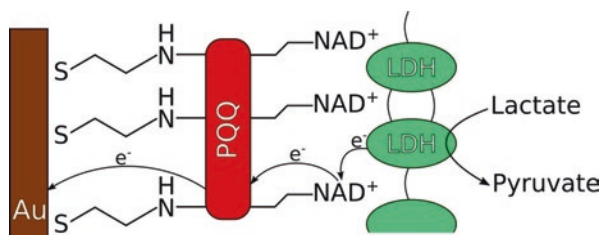


Fig. 17.4 Configuration of the lactate dehydrogenase (LDH) monolayer gold electrode by cross-linking the affinity complex formed between LDH and the gold electrode functionalized with the PQQ/NAD⁺ monolayer

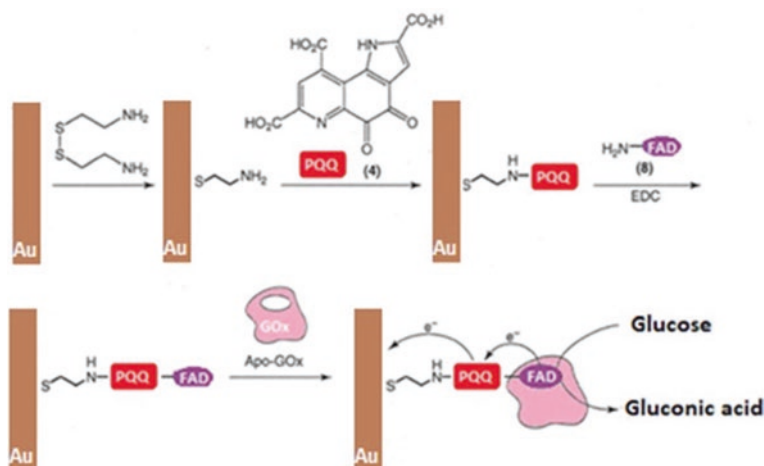
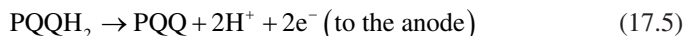


Fig. 17.5 The configuration of the glucose oxidase enzyme electrode (apo-GOx) on a PQQ-FAD monolayer on a gold electrode. (Willner et al. 1996)

Anodes Based on Bioelectrocatalysis of FAD Blocks

Bioelectrocatalysis of flavoenzymes can also be used as an anode reaction in a bio-fuel cell. Recently, a new method for establishing electrical contact between the redox center of flavoenzymes and their environment has been demonstrated, based on the reconstruction of the surface layer when PQQ is connected covalently with the main cystamine monolayer on the Au electrode, and then N6-(2-aminoethyl)-FAD is attached to the PQQ blocks (Fig. 17.5). Subsequently, apoglucose oxidase was reconstituted on the FAD blocks of the PQQ/FAD monolayer architecture, giving a structurally aligned, immobilized biocatalyst on the electrode surface, leading to a high current density of glucose oxidation (Riklin et al. 1995; Willner et al. 1996; Katz et al. 1999a):





The electrode constantly oxidizes the PQQ sites located on the periphery of the protein, and the PQQ-mediated oxidation of the FAD centers includes bioelectrocatalytic oxidation of glucose (Eqs. (17.3), (17.4), and (17.5)). The resulting electric current is controlled by the recycling rate of the restored FAD substrate.

Control experiments showed that without the PQQ component, the system does not detect electronic communication with the electrode surface, that is, the PQQ electronic relay block is indeed a key component in the electrooxidation of glucose (Bardef et al. 1997; Katz et al. 1998).

17.3.2 *Enzyme Cathodes in Biofuel Cells*

The biocatalytic reduction of oxidizing agents (e.g., oxygen, hydrogen peroxide) has attracted much less attention than the biocatalytic oxidation of fuels. However, in order to create an element of a biofuel cell, it is important to design a functional cathode for reducing an oxidizing agent, which is connected to the anode and ensures the flow of an electrically balanced current. Conventional O₂ reducing cathodes used in chemical fuel cells are not compatible with biocatalytic anodes due to the high temperatures and pressures used to operate them. Thus, biocatalytic reduction processes at the cathode should be considered as a design strategy for all functional fuel cells based on biomaterials. As an example, consider an enzymatic oxygen electrode as a cathode for a biofuel cell.

Bioelectrocatalytic Cathodes Based on Oxygen

Direct electrochemical reduction of oxygen proceeds with a very high overvoltage (approximately -0.3 V on a pure Au electrode at pH 7). Thus, in order to utilize oxygen reduction in fuel cells, catalysts are required. The reduction of O₂ with the transfer of four electrons to water, with or without the formation of peroxide, is a big problem for the future development of biofuel cells, since such reactive intermediates would lead to the degradation of biocatalysts in the system.

Biocatalytic systems composed of enzymes and corresponding electron transfer mediators (e.g., bilirubin oxidase (Tsujimura et al. 2001) or mushroom laccase (Tayhas et al. 1999) with 2,2'-azino-bis-(3-ethylbenzothiazolin-6-sulfonate as a mediator)) are able to efficiently biocatalyze the electroreduction of O₂ to H₂O at ~ 0.4 V (relative to BCE), significantly reducing overvoltage. These systems, however, are composed of dissolved enzymes and mediators working diffusely, which is

unacceptable for technological applications. Organized layered enzyme systems are much more promising for use in biocatalytic cathodes.

Cytochrome *c* (Cyt c), which includes the only thiol group in the 102-cysteine residue (iso-2-cytochrome *c* yeast from *Saccharomyces cerevisiae*), was deposited as a monolayer on an Au electrode by covalent bonding of thiol groups to an electrode modified with a maleimide monolayer (Fig. 17.6) (Katz et al. 1999b; Pardo-Yissar et al. 2000). A monolayer Cyt c -electrode interacted with COx to form an affinity complex on the surface, which was then cross-linked with glutaraldehyde. A similar structure of Cyt c /COx was organized on the surface of crystalline Au-quartz microbalances. Microgravimetric studies show that the surface coating of COx based on the Cyt c monolayer with $\sim 2 \cdot 10^{-12}$ mol/cm 2 . This surface density corresponds to an almost tightly packed COx monolayer.

On the cyclic voltammogram of a pure Au electrode in the presence of O $_2$ (the background electrolyte is in equilibrium with air), a cathode wave of electroreduction of O $_2$ is observed at ~ -0.3 V relative to n.c. This recovery wave shifts to the negative region in the presence of a monolayer Cyt c electrode. This implies that the heme/protein layer is inactive as a biocatalyst for O $_2$ reduction. In fact, the Cyt c monolayer increases the overvoltage of oxygen reduction due to hydrophobic blocking of the electrode surface.

On the cyclic voltammogram of a layered Cyt c /COx crosslinked electrode in the presence of O $_2$, an electrocatalytic wave was observed at ~ -0.07 V, indicating that the Cyt c /COx layer works as a biocatalytic interface during oxygen reduction. Thus, the effective bioelectrocatalizable reduction of O $_2$ by the Cyt c /COx interface is due to the direct electrical connection between Cyt and the electrode and the electrical contact in the crosslinked Cyt c /COx structure. The electron transfer to Cyt c is accompanied by the electron transfer to COx, which acts as an electron storage biocatalyst for the joint four-electron reduction of O $_2$ according to Eqs. (17.6), (17.7), and (17.8) (two-electron reduction of O $_2$ gives H $_2$ O $_2$, and the joint four-electron reduction of O $_2$ –H $_2$ O):

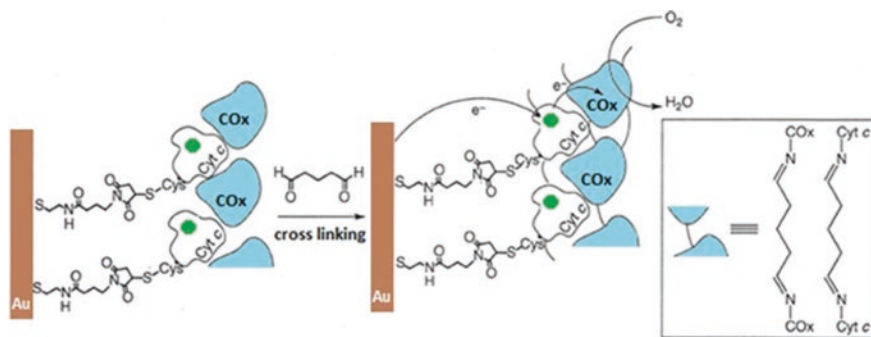
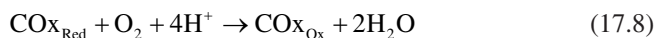
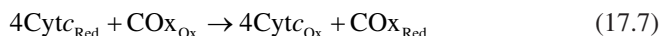
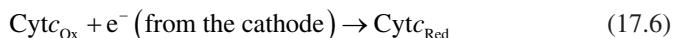


Fig. 17.6 Assembly of the integrated bioelectrocatalytic electrode Cyt c /COx. (Pardo-Yissar et al. 2000)



To estimate the electron transfer rate constant for the complete bioelectrocatalytic process corresponding to the reduction of O_2 , experiments were performed with a rotating disk electrode (Katz et al. 1999a). From the construction of Koutetskii–Levich, the calculated number of electrons involved in O_2 reduction ($n = 3.9 \pm 0.2$) and the electrochemical rate constant ($k = 5.3 \cdot 10^{-4}$ cm/s) were obtained. The total electron transfer rate constant was calculated ($K_{\text{full}} = 6.6 \cdot 10^5 \text{ M}^{-1} \text{ s}^{-1}$), taking into account the surface density of the bioelectrocatalyst $2 \cdot 10^{-12} \text{ mol/cm}^2$. Since, it is only slightly higher than the experimental value, it can be accepted that the primary process of electron transfer from the electrode to the Cyt c monolayer is a limiting stage of the complete bioelectrocatalytic reduction of O_2 .

17.3.3 Biofuel Cells Based on Layered Enzyme Electrodes

Previous sections covered electrode development and the assembly of separate biocatalytic anodes and cathodes. When designing biofuel cells, it is important to connect the cathode and anode blocks into integrated devices. Block integration is not free of restrictions. The oxidizing agent should not interact with the biocatalyst relay, nor with the cofactor blocks on the anode interface, since this would reduce or inhibit the biocatalyzed oxidation of the fuel substrate. In addition, for the synchronous operation of the biofuel cell, it is necessary to achieve charge compensation between these two electrodes, and the electron flux in the external circuit must be compensated by the transfer of cations in the electrolyte solution. To overcome these limitations, solutions of catholyte and anolyte can be placed in separate compartments.

Biofuel Cell Based on PQQ and MP-11 Monolayer Functionalized Electrodes

Figure 17.7 is a diagram of a biofuel cell in which bioelectrocatalizable reduction of H_2O_2 is carried out using microperoxidase-11 (MP-11), and NADH is oxidized using PQQ (Willner et al. 1998). In this biofuel cell, H_2O_2 and NADH were used by cathode and anode substrates, respectively.

The electrode potentials exhibit Nernst behavior, reaching a limiting value at high substrate concentrations ($\sim 1 \cdot 10^{-3} \text{ M}$). From the limit values of the potentials of

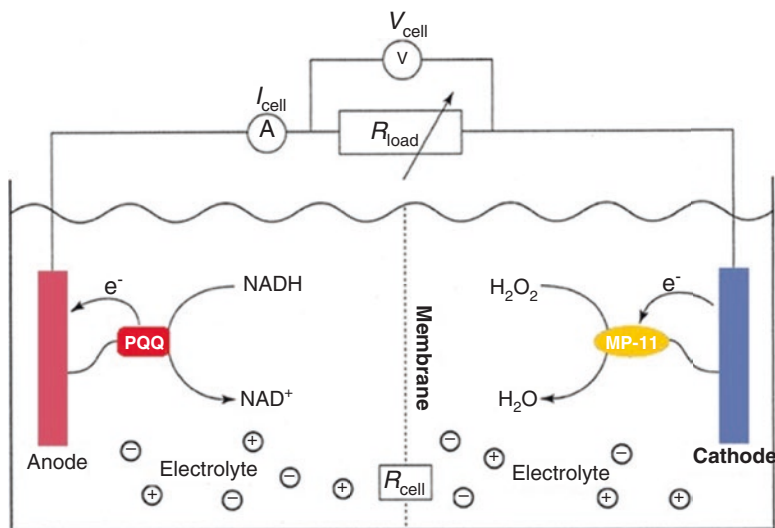


Fig. 17.7 A configuration diagram of a biofuel cell using NADH and H_2O_2 as substrates of fuel and an oxidizing agent, and electrodes functionalized by PQQ and MP-11 as a catalytic anode and cathode, respectively. (Willner et al. 1998)

the PQQ and MP-11 functionalized electrodes, the open-circuit voltage of the cell was estimated to be ~ 0.3 V. The cell gives a short circuit current (I_{sc}) and an open-circuit voltage (V_{oc}): ~ 100 μA and 310 mV, respectively. The power received from the biofuel cell ($P = V \cdot I$) reaches a maximum of 8 μW with an external load of 3 $\text{k}\Omega$.

17.4 Conversion of Organic Waste into Electrical Energy Using MFCs

Reducing dependence on fossil fuels and reducing pollution are the main trends that are forcing humanity to seek new sources of energy. Wastewater treatment is an area in which these two goals can be combined.

The problem of wastewater treatment, starting from the second half of the twentieth century, is relevant for all countries of the world. In the United States, about 15 gW of electric power (3% of all electricity produced in the country) is spent on the treatment of organic-rich wastewater, while the wastewater itself contains 17 gW of electric power (Logan and Rabaey 2012). From a colloidal chemical point of view, wastewater is a heterogeneous mixture of organic, inorganic, dissolved, colloidal, and suspended in water impurities. Organic matter, which is now wasted or lost in wastewater processes, is rich in energy. The utilization of part of this energy would provide a new source of electricity. Or we could release this hidden energy in production processes to get other useful chemicals, such as biofuels or industrial

chemicals, which currently require energy or organic substrates. Industrial wastewater, for example, from food and brewing factories, sugar industries, agricultural wastewater from livestock farms, and wastewater from the pulp and paper industries are ideal raw materials for bioprocessing because they contain high levels of easily degradable organic material, which leads to economic benefit even when fluid heating is required.

In addition, they already have a high water content, which eliminates the need to add it. Such wastewater is a potential processing facility from which bioenergy and biochemicals can be obtained. Recovery of energy and valuable products could partially offset the cost of wastewater treatment and somewhat reduce our dependence on fossil fuels. There are several biological strategies for treating industrial and agricultural wastewater (Largus et al. 2004):

1. Wastewater treatment using MFCs
2. Methanogenic anaerobic enzymatic degradation of organic matter in the wastewater
3. Enzymatic production of hydrogen from wastewater
4. Biological chemical production

Three of these strategies lead to the production of bioenergy (electricity, methane, hydrogen), and the fourth to the enzymatic production of biochemicals.

Consider the current scientific and technical conditions and problems of bioelectrochemical technologies for the treatment of wastewater using MFCs.

Figure 17.8 shows the general scheme of MFC operation in the case of wastewater treatment. Anaerobic microorganisms oxidize the organic material in the anode chamber and transfer the resulting reduced equivalents (electrons) to the cathode. For example, the dissimilative metal-reducing bacterium (DMRB) *Geobacter* spp. establishes direct physical contact with solid electron acceptors and uses the periplasmic proteins of *c*-type cytochrome as a metal reductase (Nevin and Lovley 2000; Magnuson et al. 2001); therefore, these organisms must grow as a biofilm on the surface of the electrode (Bond 2003). Other types of DMRB, such as *Shewanella*

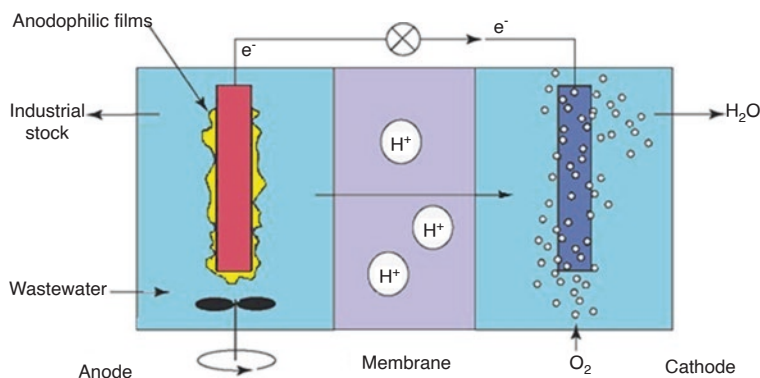


Fig. 17.8 Diagram of a two-chamber microbial fuel cell (MTE) used in wastewater treatment

spp., can transfer electrons to solid acceptors either through direct contact or by generating soluble quinones acting as electron shuttles (Nevin and Lovley 2002; Newman and Kolter 2000). For organisms of this type, direct contact with the electrode surface is not required. In addition to microorganisms transferring electrons to the anode, the presence of other organisms may be conducive to MFC. Park and Zeikus (2002) demonstrated that a mixed culture produced current that was six times higher than that produced by a pure culture.

Consequently, microbial communities developing in the anode chamber may have a function similar to that found in methanogenic anaerobic boilers, except that microorganisms, those can transfer electrons to the electrode surface, replace methanogens. Rabaey (2007) called such microbial communities adapted anodophilic consortia.

Typical maximum power densities in MFCs are from ~ 2 to 3 W/m^2 of the design electrode (usually the cathode) under optimal conditions of $\sim 30^\circ\text{C}$, solution conductivity of $\sim 20 \text{ mS/cm}$, and well-buffered solutions at neutral or slightly alkaline pH. The power densities of MFCs are much lower than in hydrogen fuel cells, which yield about 1 W/cm^2 , but these power densities are due to chemical fluxes in biofilms based on a similar flux in terms of equivalent electrons (e.g., 24 mol electrons per glucose molecule) (Logan 2008). The upper limits of $17\text{--}19 \text{ W/m}^2$ were predicted for MFCs based on estimates, assuming minimal internal resistance or taking first-order kinetics typical of microorganisms in biofilms (Logan 2009; Fan et al. 2008). An increase in the electrode packing density (electrode area per reactor volume) gives up to 1.55 kW per 1 m^3 of reactor volume (2.77 W/m^2) under optimal conditions (Fan et al. 2007), which is much higher than, as a rule, obtained from wastewater ($<0.5 \text{ W/m}^2$) (Hays et al. 2011; Ahn and Logan 2010). The lower power densities obtained from wastewater are explained by the slower biodegradation kinetics of complex substrates, lower solution conductivity, and lower buffer capacity.

The complex nature of many sources of biomass waste requires that a diverse microbial community degrade the various components of the organic matter. Although many bacteria can generate an electric current, high power densities from complex sources of organic matter are usually associated with the presence of member of Geobacteraceae family in the anode community (Logan 2009; Kiely et al. 2011). These microbes use a limited number of substrates with acetate, which is the most common among various strains, although lactate and others are also possible substrates (Call and Logan 2011; Speers and Reguera 2012). Therefore, syntrophic interactions may be required to convert complex organic matter into simpler substrates, which can then be used by exoelectrogens (Kiely et al. 2011).

The nature of syntrophic associations is very similar to anaerobic digestion, where a variety of substrates are decomposed into simple molecules that are used to produce methane by members of the genus *Methanosarcinales* (Lettinga 1995). Associations in communities in MFC with certain microbes are not well understood, and they affect the power disproportionately to individual contributions (Rabaey et al. 2004). For example, power was increased by 30–70% by adding gram-positive *Enterococcus faecium* to gram-negative cultures of *Pseudomonas*

aeruginosa, even though pure *E. faecium* cultures produced little power (Read et al. 2010). Further studies have shown that *Enterococcus aerogenes* can produce 2,3-butanediol, resulting in increased production of the electronic shuttle (phenazine) by *P. aeruginosa* microbes (Venkataraman et al. 2011).

The ability to directly convert organic material from wastewater to bioelectricity is exciting but requires a fundamental understanding of microbiology and the further development of technology (Kazarinov et al. 2016; Meshcheryakova et al. 2018). Low specific characteristics (specific energy, specific power) of MFCs are the main constraint in the implementation of this microbial electrochemical technology. So, the maximum power densities produced in MFC using domestic wastewater alone (without other energy sources) reached 12 W/m³ (Reshetilov et al. 2005), which is equivalent to 0.07 kW/m³ produced within 6 h (comparable to the times of activated treatment sludge). This energy recovery is low, given that domestic wastewater contains ~2 kW/m³ (Heidrich et al. 2011).

17.5 The Use of Biofuel Elements in the Field of Medicine

In recent years, studies of fuel cells have intensified in areas other than energy, including in the field of medicine (Calabrese et al. 2004). In accordance with various aspects in the field of medicine, fuel cell applications are divided into implantable medical devices and non-implantable medical devices.

17.5.1 The Use of Fuel Cells in Implantable Medical Devices

Implantable medical devices (IMD) can be divided into two categories: devices with functional support (Fernández et al. 2004) and in vivo measurement devices (Chen et al. 2006). The first includes pacemakers (Wessels 2002), cochlear implants (Dong et al. 2004), drug pumps (Cao et al. 2000), and biochips (Guisseppi-Elie 2011), and the second includes a blood meter, glucometers (Yuhashi et al. 2005), and temperature sensors. A common feature of IMD is that they require a stable and efficient power supply (Jia 2012). Traditional implantable medical devices are powered by lithium-ion batteries, which require replacement from time to time. This replacement process leads to high medical costs and causes an unbearable pain to patients.

The biofuel element demonstrates high energy conversion efficiency, mild operating conditions, simple structure, and, most importantly, excellent biocompatibility and long service life without periodic refueling, since organic compounds and oxygen in the human body can be used as fuel and oxidizing agent. Integrating fuel cells into in vivo implantable devices (as the implantable power of a medical device or an implantable medical sensor) will significantly reduce medical costs and alleviate the suffering of patients.

Modern studies of biofuel elements used in implantable medical devices are mainly focused on the use of microorganisms and biological enzymes as catalysts. The use of the microbial layer in the human body as a catalyst is the most attractive prospect for a fuel cell supplying implantable medical devices because of its simple setup and low cost. At the same time, the high selectivity of microorganisms and the low power output of MFCs limit their wide application possibilities. On the other hand, the use of the enzyme as a catalyst demonstrates excellent compatibility and significant power, but it suffers from a short duration of the enzyme, which leads to a rapid deterioration of the characteristics of the fuel cell. Therefore, the development of biofuel elements with stable performance, as well as its low cost, used in implantable medical devices, is still ongoing.

The Use of Microorganisms as Catalysts

The earliest use of a fuel cell in the medical field is a microbial fuel cell received electrical energy using MFC containing *E. coli* and human leukocytes (Cooney et al. 1996; Justin et al. 2004, 2011; Sun et al. 2006). The results showed that voltage and current were associated with the ability to oxidize glucose by *E. coli*. In another experiment using human leukocytes as a catalyst, the generated current was less than the recorded value for the *E. coli* catalyst. Their research shows the possibility of using human cells and fluids to generate energy for implantable medical devices in the future.

Given the symbiotic relationship between humans and microorganisms, Liu et al. (2010) reported the creation of a microbial fuel cell in the transverse colon of the body. An anode made of biocompatible material was spirally attached to the intestinal wall. The cathode was located in the middle of the intestine, where oxygen was present in high concentration. Due to this arrangement, the cell can continuously and stably generate electricity as a result of mobility in the intestines of microorganisms and intestinal contents. This system revolutionized the concept and prospects of implantable medical devices, demonstrating a fundamentally new approach to providing them with electricity.

The use of MFCs implanted in the human colon has been proposed. Due to a large number of anaerobic microorganisms naturally present in the intestinal mucosa, and at the same time, many aerobic microorganisms in the lumen flowing with the fecal mass, the proposed idea is exciting, and the risk of infection will not cause serious concern. In particular, a tubular MFC design with a microbial anode designed to adhere to the colon mucosa was developed. The low output power was limited by the cathode, due to the small electrode surface area and low O₂ concentration (Han et al. 2010).

As an alternative to using whole cells in an MFC construct, some of the authors studied the possibility of using mitochondria as biocatalysts (Arechederra and Minter 2008; Bhatnagar et al. 2011). Mitochondria offer a compromise between high MFCs efficiency and high volume catalytic activity. Without any pre-treatment, the use of the microbial layer as a catalyst for a fuel cell demonstrates excellent

biocompatibility and also reduces the capital cost of implantable medical devices. However, the high selectivity of microorganisms prevents the widespread use of this technology. Some reviews of this technology can be found in the literature (Yang et al. 2011; Ren et al. 2012; Katz and MacVittie 2013).

The Use of Enzymes as Catalysts

An enzymatic biofuel cell (EBFC) for medical applications can use glucose oxidase, bilirubin oxidase, laccase, and other enzymes extracted from a living organism as catalysts (Karyakin et al. 2002). With its small size and good biocompatibility, EBFC has an attractive prospect for implantation or microdevices in vivo (Kang et al. 2005).

Mano et al. (2002, 2003a, b) studied the generation of electricity by high-pressure biofuel cells using body fluids and subcutaneously actuated medical sensors on implants. The fuel cell consisted of two carbon fiber electrodes with a diameter of 7 μm , which protruded from the inside. The entire fuel cell was packaged in composite resin. Glucose was oxidized by an enzyme deposited on the anode, while oxygen molecules decomposed at the cathode and additionally formed water upon enzymatic coating of *Coriolus hirsutus*. It was found that the fuel cell generates a power of 0.6 μW . When the battery is operated at human body temperature with an output voltage of 0.78 V, it can power the implanted silicon chip. Researchers expected biofuel cells to supply electricity to a subcutaneous implant glucometer, where changes in blood glucose concentration can be monitored.

Sato et al. (2005) developed a fuel cell for generating electricity using glucose in the blood. The fuel cell was attached to a vitamin K3 polymer acting as an electronic conductor, bovine serum was used as the electrolyte, and carbon on which glucose oxidase was applied was used as the electrode. The EBFC during glucose decomposition had a maximum power of 12.8 $\mu\text{W}/\text{cm}^2$.

Recently, the same group reported a microfuel cell with a needle anode and gas diffusion cathode as direct energy generation with natural organisms in the epidermis (Miyake et al. 2011). They inserted it into fresh grapes and received a maximum power of 26.5 mW, which can be used as an indicator of glucose levels. At the same time, a needle anode was inserted into the blood vessel of the rabbit ear, where the output was stabilized. In the near future, thanks to the development of micro/nanotechnology, it is expected that an even thinner anode of a microneedle matrix will be implemented in biofuel cell systems for minimally invasive repairs.

In addition, Lin et al. (2009) have recently developed a prototype implantable biofuel cell (BFC) using physiological fluid. The fuel cell used carbon materials like electrodes and contained anode and cathode surface modified with glucose oxidase and bilirubin oxidase, respectively. In vitro experiments on bovine serum to simulate the human physiological environment confirmed the effect of glucose concentration, temperature, and pH of the reaction solution on the output current of the biofuel cell.

In studies of Zebda et al. (2011) and Cinquin et al. (2010), glucose EBFC was implanted inside two mice. The battery consisted of a graphite disk containing glucose oxidase and polyphenol oxidase and was wrapped in a dialysis bag. In vivo enzymes in the mice oxidized glucose and produced a power of $6.5 \mu\text{W}$, which lasted for 4 h, suggesting that such an element is based on glucose can provide current for implantable medical devices (Cinquin et al. 2010).

Katz et al. successfully introduced biofuel cells into snails, which were much smaller than rats (Halámková et al. 2012). Enzyme-coated electrodes were introduced through the sheath into the cochlea's body. When the cochlea crawled, the fuel cell generated electric power of $7.45 \mu\text{W}$ as a result of the oxidation of glucose in the cochlea's body. The authors also implanted an enzymatic biofuel element into a lobster (MacVittie et al. 2013), and they received a constant output voltage of 1.2 V, which can support the operation of an electronic clock. The same authors focused on biomedical studies of biological fuel cells used in rats and laid the foundation for the development of a fuel cell system for implantable medical devices (Castorena-Gonzalez et al. 2013).

In another experiment, five enzyme biofuel elements were sequentially connected and placed them in a human serum solution to simulate human blood circulation (MacVittie et al. 2013). A battery pack with enzymatic bioelements can produce a voltage of 3 V, sufficient to power a pacemaker. Rasmussen et al. (2012) and Schwefel et al. (2015) successfully implanted a similar fuel cell in cockroaches and mushrooms. More recently, the concept of biological intelligence has been expanded by a Japanese research team (Shoji et al. 2014a, b), which installed a fuel cell in a living cockroach.

Membrane-Free Biofuel Cell Based on GOx and Cyt c /COx Monolayer Electrodes

The next generation of biofuel cells can use a complex ordered enzyme or multi-enzyme system immobilized on both electrodes, which can eliminate the need to compartmentalize the anode and cathode. The use of effective electron transfer in enzyme-modified electrodes can provide specific biocatalytic transformations that kinetically compete with any chemical reaction of the electrode, and exclude the reactions of biocatalysts with interfering substrates transferred from the back of the compartment, including oxygen. This would allow the development of biofuel cells without compartments, where the biocatalytic anode and cathode are immersed in the same phase without separation by a membrane.

In the considered example (Fig. 17.9), an anode consisting of GOx reduced to a PQQ-FAD monolayer (see Fig. 17.5) for biocatalyzed glucose oxidation was connected to a cathode composed of an aligned Cyt c /COx pair that catalyzes the reduction of O_2 to water (see Fig. 17.6) (Park and Zeikus 2002).

Since reduced GOx provides an extremely effective biocatalytic oxidation of glucose that is not affected by oxygen, the anode can function in the presence of oxygen. Thus, a biofuel cell uses O_2 as an oxidizing agent and glucose as a fuel

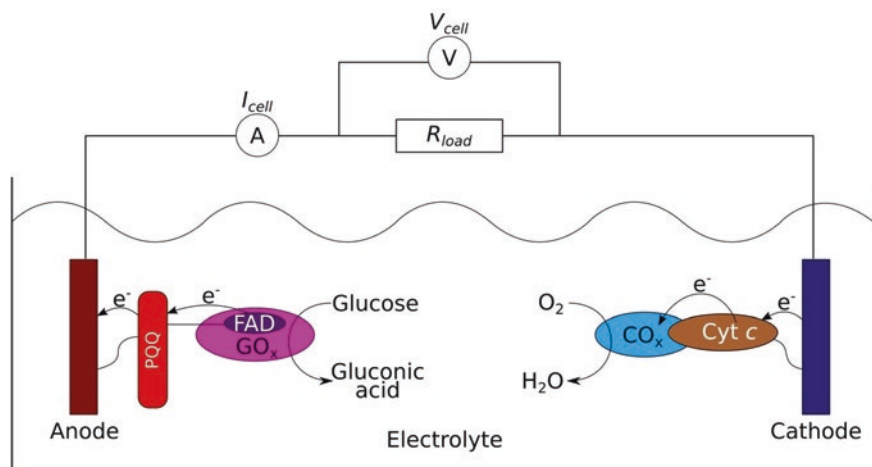


Fig. 17.9 Schematic configuration of a cell-less biofuel cell using glucose as fuel and oxygen as an oxidizing agent, and gold electrodes functionalized with PQQ-FAD/GOx and Cyt c /CO x as a biocatalytic anode and cathode, respectively

without the need to separate the compartments by a membrane. The operation of such a cell was studied at various external loads (Park and Zeikus 2002), and a coefficient of efficiency of $\sim 40\%$ was achieved with a maximum output power of $4 \mu\text{W}$ and an external load of $0.9 \text{ k}\Omega$. The relatively low power removed from the cell is mainly due to the small potential difference between the anode and cathode. Bioelectrocatalyzed oxidation of glucose occurs at the redox potential PQQ-electronic mediator $E^\circ = -0.125 \text{ V}$ (at pH 7), while the redox potential of Cyt c is $E^\circ = 0.03 \text{ V}$. This gives a potential difference between the anode and cathode of only 155 mV .

Using electronic picks with more negative potentials, the power diverted from the cell can be increased. The main advantage of this system is its operation in a non-cutoff configuration. This suggests that the electrodes can be used as *in vivo* power generation devices using glucose and O_2 from the blood as fuel and oxidizing agents. Such power generation devices can power implantable devices, such as electrical stimulators or insulin pumps.

17.5.2 The Use of Fuel Cells in Medical Equipment *In Vitro*

Fuel cells have attractive prospects not only in implanted medical devices but also in a wide range of non-implantable medical applications. Currently, various technologies of fuel cells used in medical equipment are constantly used.

At the beginning of this century, Heller and co-workers developed an accurate and painless glucometer that can continuously monitor blood glucose levels using

fuel cell technology (Feldman et al. 2000; Heller 2005, 2006; Heller and Feldman 2008). The main element of the glucometer is a fast and accurate microtone coulometer. The results were accurately measured due to the short diffusion distance of the reagent, the fast oxidation time, and the independence of the kinetic parameters of coulometry (such as temperature, viscosity, and activity). More importantly, the instrument requires only 300 nl of blood (less than a blood-sucking mosquito sample), eliminating the pain caused by a puncture of the skin. TheraSense is planning to build fuel cells for a one-time surface-mounted sensor with a volume of less than 1 mm³. Sensor electrodes were inserted into subcutaneous users, and because of their thin and flexible design, pain was not felt. Battery life was limited to a few days, after which people can replace it with a new one.

Li et al. (2004) developed a glucose oxidase electrode, combining a stable blue film electrode with a modified sol-gel-immobilized enzyme technology. The glucose concentration is in the range of 0.05–4.75 mmol/L and varies linearly with the reaction current. The enzyme electrode does not interact with ascorbic and uric acids present in the system, or with other electrically active fungi, exhibiting stable behavior. The proposed cell is simple and convenient to use, and also does not require much time, and on its basis, it is possible to implement a reliable method for determining the level of glucose in the blood to meet clinical needs.

In addition, a fuel cell was used to test alcohol in expired air (Workman 2014). The main elements of the fuel cell sensor consist of two platinum electrodes and intermediate layers of a porous acidic electrolyte. Alcohol in the exhaled air is oxidized to acetic acid and water through the fuel cell, creating a voltage proportional to the concentration of alcohol. A commercial alcohol tester called BAC track (blood alcohol content (BAC)) should appear on the market with technologically compatible functions since it can be combined with smartphones via Bluetooth. This product can not only check whether it is safe to drive a car, but also indicate how long it will take to get rid of alcohol. Therefore, it is expected that it will have great market prospects.

Currently, fuel cells can also be used to measure the concentration of oxygen in a mixed gas from a clinic respirator. Thus, they became known as medical oxygen batteries or oxygen sensors (Feng 2009). At constant temperature and pressure, the voltage of the fuel cell is directly proportional to the concentration of oxygen. There are currently alternative oxygen fuel cells for fans on the market. Ruo-Ming Hu et al. (2012, 2013a, b) developed a portable micro-oxygen generator using direct and reverse fuel cell technology. The principle of reverse fuel cell technology involves the use of oxygen in the air with an increased concentration (>98% of pure oxygen).

Hu's group developed a portable tool for treating chronic wounds that is the same size as a mobile phone. The device gave a microstream of pure oxygen at a rate of 3 ml/h, continuously supplied to the wound surface, and obtained promising results in clinical trials. The purpose of this device is chronic wound healing. The group's recent goal is also to use a wound healing tool for treating psoriasis. Scherson et al. (2014) have developed a similar oxygen microgenerator showing the same characteristics.

17.6 Conclusion

Biofuel cells for generating electricity from energy-intensive organic substrates can be created with various approaches. One of them involves using microorganisms as bioreactors to ferment raw materials into fuel, for example, hydrogen, which is then fed to the anode of a conventional fuel cell. The second approach to the use of microorganisms in biofuel cells involves an in situ electrical connection of metabolites generated in microbial cells with the electrode substrate using diffusion electron mediators. A further methodology for the development of biofuel cells includes the use of redox enzymes for the targeted oxidation and reduction of substrates of a specific fuel and oxidizer on electrode substrates and the generation of electricity.

To achieve this, it is important to create integrated enzyme electrodes that provide electrical contact between the enzyme system and the conductive substrate. A detailed study of the electron transfer rates through the interface, biocatalytic rate constants, and cell resistance is important for the development of biofuel cells. The identification of the limiting stage will then allow the development of a strategy for improving and increasing cell yield. Chemical modification of redox enzymes with synthetic blocks that improve electrical contact with electrodes provides a general way to improve the electrical output of biofuel cells. Site-specific modification of redox enzymes and reconstruction of the surface of enzymes represent a new promising tool for aligning and orienting biocatalysts on electrode surfaces. The effective electrical contact of aligned proteins with electrodes suggests that future efforts should focus on the development of structural mutants of redox proteins to improve their electrical contact with electrodes. Step-by-step nanoengineering of electrode surfaces with relay-cofactor-biocatalyst blocks through organic synthesis allows controlling electron transfer cascades in structures. By “tuning” the redox potentials of synthetic relays or biocatalytic mutants, it is possible to improve the energy performance of biofuel cells.

The configurations of the biofuel cells described in this chapter can theoretically be extended to other redox enzymes and fuel substrates with numerous technological applications. Generating electricity from biomass substrates using biofuels could supplement energy sources from chemical fuel cells. An important potential use of biofuel cells is in situ assembly in human body fluids, such as blood. The generated electricity can be used to power implanted devices such as electrical stimulators, pumps (e.g., insulin pumps), sensors, and prosthetic modules.

Further research in this direction should be focused on the development of compact in vivo medical devices with high safety, durability, ease of replacement, and low cost. As soon as the use of a fuel cell in the human body is successful, humanity will face a new medical revolution.

References

- Ahn Y, Logan BE (2010) Effectiveness of domestic wastewater treatment using microbial fuel cells at ambient and mesophilic temperatures. *Bioresour Technol* 101:469–475
- Arechederra R, Minteer SD (2008) Organelle-based biofuel cells: immobilized mitochondria on carbon paper electrodes. *Electro Acta* 53(23):6698–6703
- Bardef A, Katz E, Buckmann AF, Willner I (1997) NAD⁺-dependent enzyme electrodes: electrical contact of cofactor-dependent enzymes and electrodes. *J Am Chem Soc* 119:9114–9119
- Bhatnagar D, Xu S, Fischer C, Arechederra RL, Minteer SD (2011) Mitochondrial biofuel cells: expanding fuel diversity to amino acids. *Phys Chem Chem Phys* 13(1):86–92
- Bond DR (2003) Electricity production by *Geobacter sulfurreducens* attached to electrodes. *Appl Environ Microbiol* 69:1548–1555
- Bond DR, Holmes DE, Tender LM, Lovely DR (2002) Electrode-reducing microorganisms that harvest energy from marine sediments. *Science* 295:483–485
- Bulter JI (2004) A diheme c-type cytochrome involved in Fe (III) reduction by *Geobacter sulfurreducens*. *J Bacteriol* 186:4042–4045
- Calabrese BS, Gallaway J, Atanassov P (2004) Enzymatic biofuel cells for implantable and microscale devices. *Chem Rev* 104(10):4867–4886
- Call DF, Logan BE (2011) Lactate oxidation coupled to iron or electrode reduction by *Geobacter sulfurreducens* PCA. *Appl Environ Microbiol* 77:8791–8794
- Cao L, Mantell S, Polla D (2000) Implantable medical drug delivery systems using microelectromechanical systems technology. *Microtechnologies*. In: *Medicine and biology 1st annual international conference 2000 IEEE*, p 487–490
- Castorena-Gonzalez JA, Foote C, MacVittie K, Halánek J, Halámková L, Martinez-Lemus LA, Katz E (2013) Biofuel cell operating in vivo in rat. *Electroanalysis* 25(7):1579–1584
- Chen L, Wang HN, Zhong Y (2006) Advance in power supply of the medical implantable electronic device. *Biomed Eng Res* 4:285–289
- Choi Y (2003) Dynamic behaviors of redox mediators within the hydrophobic layers as an important factor for effective microbial fuel cell operation. *Bull Kor Chem Soc* 24(4):437–440
- Cinquin P, Gondran C, Giroud F, Mazabrard S, Pellissier A, Boucher F, Alcaraz JP, Gorgy K, Lenouvel F, Mathé S, Porcu P, Cosnier S (2010) A glucose biofuel cell implanted in rats. *PLoS One* 5(5):10476
- Cooney MJ, Roschi E, Marison IW, Comminellis C, von Stockar U (1996) Physiologic studies with the sulfate-reducing bacterium *Desulfovibrio desulfuricans*: evaluation for use in a biofuel cell. *Enzym Micro Technol* 18(5):358–365
- Davila D, Esquivel J, Vignes N (2008) Development and optimization of microbial fuel cells. *J New Mater Electroch Systems* 11:99–103
- Davis JB, Yarbrough JHF (1962) Preliminary experiments on a microbial fuel cell. *Science* 137:615–616
- Davis G, Hill HAO, Aston WJ, Higgins IJ, Turner APF (2002) Ferrocene-mediated enzyme electrode for amperometric determination of glucose. *Enzyme Microbiol Technol* 30:145–148
- Dong M, Zhang C, Wang Z, Li D (2004) A neuro-stimulus chip with telemetry unit for cochlear implant. In: *Biomedical circuits and systems IEEE international workshop IEEE, S1/3/ INV-S1/39-12*.
- Fan Y, Hu H, Liu H (2007) Sustainable power generation in microbial fuel cells using bicarbonate buffer and proton transfer mechanisms. *Environ Sci Technol* 41:8154–8158
- Fan Y, Sharbrough E, Liu H (2008) Quantification of the internal resistance distribution of microbial fuel cells. *Environ Sci Technol* 42:8101–8107
- Feldman B, McGarraugh G, Heller A, Bohannon N, Skyler J, DeLeeuw E (2000) FreeStyle: a small-volume electrochemical glucose sensor for home blood glucose testing. *Diabetes Technol Ther* 2(2):221–229
- Feng LJ (2009) Working principle and performance testing of oxygen battery in ventilator. *China Med Equip* 24(7):57–58

- Fernández JL, Mano N, Heller A, Bard AJ (2004) Optimization of “Wired” enzyme O₂-Electroreduction catalyst compositions by scanning electrochemical microscopy. *Angew Chem Int Ed* 43(46):6355–6357
- Gradskov DA, Ignatov VV, Kazarinov IA (2001) Bioelectrochemical oxidation of glucose using bacteria *Escherichiacoli*. *Russ J Electrochem* 37(11):1397–1400
- Guiseppi-Elie A (2011) An implantable biochip to influence patient outcomes following trauma-induced hemorrhage. *Anal Bioanal Chem* 399(1):403–419
- Halámková L, Haláček J, Bocharova V, Katz E (2012) Implanted biofuel cell operating in a living snail. *J Am Chem Soc* 134(11):5040–5043
- Han Y, Yu C, Liu H (2010) A microbial fuel cell as power supply for implantable medical devices. *Biosens Bioelectron* 25(9):2156–2160
- Hays S, Zhang F, Logan BE (2011) Performance of two different types of anodes in membrane electrode assembly microbial fuel cells for power generation from domestic wastewater. *J Power Sources* 196:8293–8300
- He Z, Largus T (2006) Application of bacterial biocathodes in microbial fuel cells. *Electroanalysis* 18(19–20):2009–2015
- Heidrich ES, Curtis TP, Dolfing J (2011) Determination of the internal chemical energy of wastewater. *Environ Sci Technol* 45:827–832
- Heller A (2005) Integrated medical feedback systems for drug delivery. *J AIChE* 51(4):1054–1066
- Heller A (2006) Potentially implantable miniature batteries. *Anal Bioanal Chem* 385(3):469–473
- Heller A, Feldman B (2008) Electrochemical glucose sensors and their applications in diabetes management. *Chem Rev* 108(7):2482–2505
- Hu RM, Ogasawara L, Cao GY (2012) A self-breathing electrochemical oxygen generator machine: China Patent CN202626304U, 2012.12.26
- Hu RM, Ogasawara L, Cao GY (2013a) A preservation and use method of self-breathing electrochemical oxygen generator machine: China Patent CN103205771A, 2013.07.17
- Hu RM, Ogasawara L, Cao GY (2013b) A self-breathing electrochemical oxygen system: China Patent CN203159721U, 2013.08.28
- Jia JW (2012) Experimental research on blood fuel cell using carbon fiber electrodes. PhD thesis, Jilin University, China
- Jungermann KA, Thauer RK, Leimenstoll G, Decker K (1973) Function of reduced pyridine nucleotide-ferredoxin oxidoreductase in saccharolytic clostridia. *Biochim Biophys Acta* 305:268–280
- Justin GA, Zhang Y, Sun M, Sclabassi R (2004) Biofuel cells: a possible power source for implantable electronic devices. In: Engineering in medicine and biology society IEMBS'04. 26th annual international conference of the IEEE. IEEE 2004; 2:4096–4099
- Justin GA, Zhang Y, Cui XT, Bradberry CW, Sun M, Sclabassi RJ (2011) A metabolic biofuel cell: conversion of human leukocyte metabolic activity to electrical currents. *J Biol Eng* 5(1):5–9
- Kang F, Wu YH, Li TM (2005) Research progress in biofuel cell. *J Power Technol* 28(11):723–727
- Kano K, Ikeda T (2000) Fundamentals and practices of mediated bioelectrocatalysis. *Anal Sci* 16:1013–1021
- Karube I, Matsunaga T, Tsuru S, Suzuki S (1977) Biochemical fuel cell utilizing immobilized cells of *Clostridium butyricum*. *Biotechnol Bioeng* 19:1727–1733
- Karyakin AA, Morozov SV, Karyakina EE, Varfolomeyev SD, Zorin NA, Cosnier S (2002) Hydrogen fuel electrode based on bioelectrocatalysis by the enzyme hydrogenase. *Electrochem Commun* 4(5):417–420
- Katz E (2003) Biochemical fuel cells. In: Katz E, Shipway AN, Wilner I (eds) *Handbook of fuel cells – fundamentals, Technology and Application*, vol 1. Wiley, Hoboken, pp 2–27
- Katz E, MacVittie K (2013) Implanted biofuel cells operating in vivo—methods, applications and perspectives—feature article. *Energy Environ Sci* 6(10):2791–2803
- Katz E, Lotzbeyer T, Schlereth DD, Schuhmann W, Schmidt HL (1994) Electrocatalytic oxidation of reduced nicotinamide coenzymes at gold and platinum electrode surfaces modified with a monolayer of pyrroloquinoline quinone. Effect of Ca²⁺cations. *J Electroanal* 373:189–200

- Katz E, Heleg-Shabtai V, Bardea A, Willner I, Rau HK, Haehnel W (1998) Fully integrated biocatalytic electrodes based on bioaffinity interactions. *Biosens Bioelectron* 13:741–756
- Katz E, Riklin A, Heleg-Shabtai V, Willner I, Buckmann AF (1999a) Glucose oxidase electrodes via reconstitution of the apoenzyme: tailoring of novel glucose biosensors. *Anal Chim Acta* 385:45–48
- Katz E, Willner I, Kotlyar AB (1999b) A non-compartmentalized glucose/O₂ biofuel cell by bioengineered electrode surfaces. *J Electroanal Chem* 479:64–68
- Kazarinov IA (2012) Vvedenie v biologicheskujuelektrohimiju (Introduction to biological electrochemistry). Izd-voSarat.un-ta, Saratov
- Kazarinov IA, Kuz'micheva EV, Ignatova AA (2011) The estimation of performance of exogenous redox mediators in the bioelectrochemical system glucose–*Escherichia coli* cells-mediator. *J ElektrokhimicheskayaEnergetica (Electrochemical Energetics)* 11(2):60–64
- Kazarinov IA, Ignatova AA, Naumova MN (2014) Kinetics of the Electrocatalytic oxidation of glucose by *Escherichia coli* bacterial cells in the presence of exogenous mediators. *Russ J Electrochem* 50(1):87–91
- Kazarinov IA, Meshherjakova MO, Karamysheva LV (2016) Conversion of wastes into electrical energy through microbial electrochemical technologies. *J ElektrokhimicheskayaEnergetica (Electrochemical Energetics)* 16(4):207–225
- Kharitonov AB, Alfonta L, Katz E, Willner I (2000) Probing of bioaffinity interactions at interfaces using impedance spectroscopy and chronopotentiometry. *J Electroanal Chem* 487:133–141
- Kiely PD, Regan JM, Logan BE (2011) The electric picnic: synergetic requirements for exoelectrogenic microbial communities. *Curr Opin Biotechnol* 22:378–385
- Kim BH (1999) Direct electrode reaction of Fe (III)-reducing bacterium, *Shewanellaputrefaciens*. *J Microbiol Biotechnol* 9:127–131
- Kim HJ (2002) A mediator-less microbial fuel cell using a metal reducing bacterium, *Shewanellaputrefaciens*. *Enzym Microb Technol* 30:145–152
- Kuz'micheva EV, Stepanov AN, Kazarinov IA, Ignatov OV (2007) Studying kinetics of oxidation of glucose by bacterial cells *Escherichia Coli* by means of a method of a rotating disk electrode. *J ElektrokhimicheskayaEnergetica (Electrochemical Energetics)* 7(4):200–204
- Largus T, Karim K, Al-Dahhan MH, Wrenn BA, Domiguez-Espinosa R (2004) Production of bioenergy and biochemicals from industrial and agricultural wastewater. *Trends Biotechnol* 22(9):478–485
- Lettinga G (1995) Anaerobic digestion and wastewater treatment systems. *Antonie Van Leeuwenhoek* 67:3–28
- Lewis K (1966) Symposium on bioelectrochemistry of microorganisms, IV. Biochemical fuel cells. *Bacteriol Rev* 30:101–113
- Li T, Yao ZH, Zhao ZHDL (2004) A novel oxidize electrode for clinical assay of glucose in human serum. *J Instrum Anal* 23(3):67–69
- Lin JQ, Zhou XQ, Ma L (2009) Experiments in vitro of biofuel cell for implantable medical devices. *J Southwest Jiaotong Univer* 44(4):600–603
- Liu CC, Carpenter NA, Schiller JG (1978) Role of platinum black in a bio-fuel cell using glucose or hydrogen as fuel source. *Biotechnol Bioeng* 20:1687–1689
- Liu H et al (2004) Production of electricity during wastewater treatment using a single chamber microbial fuel cell. *Environ Sci Technol* 38:2281–2285
- Liu H, Yu CL, Xie BZ (2010) An electrode device for forming microbial fuel cells in the human colon: China Patent CN102354760A, 2010.02.15
- Logan BE (2008) *Microbial fuel cells*. Wiley, Hoboken
- Logan BE (2009) Exoelectrogenic bacteria that power microbial fuel cells. *Nat Rev Microbiol* 7:375–381
- Logan E, Rabaey K (2012) Conversion of wastes into bioelectricity and chemicals by using microbial electrochemical technologies. *Science* 337:686–690
- Logan BE, Murano C, Scott K, Gray ND, Head IM (2005) Electricity generation from cysteine in a microbial fuel cell. *Water Res* 39:942–952

- Lovley DR (2006) Microbial energizers: fuel cells that keep on going. *Microbe* 1:323–329
- MacVittie K, Halámek J, Halámková L, Southcott M, Jemison WD, Lobel R, Katz E (2013) From cyborg lobsters to a pacemaker powered by implantable biofuel cells. *Energy Environ Sci* 6(1):81–86
- Magnuson TS et al (2001) Isolation, characterization and gene sequence analysis of a membrane-associated 89 kDa Fe (III) reducing cytochrome c from *Geobacter sulfurreducens*. *J Biochem* 359:147–152
- Mano N, Mao F, Heller A (2002) A miniature biofuel cell operating in a physiological buffer. *J Am Chem Soc* 124(44):12962–12963
- Mano N, Mao F, Shin W, Chen T, Heller A (2003a) A miniature biofuel cell operating at .78 V. *Chem Commun* 4:518–519
- Mano N, Mao F, Heller A (2003b) Characteristics of a miniature compartment-less glucose-O₂ biofuel cell and its operation in a living plant. *J Am Chem Soc* 125(21):6588–6594
- Meshcheryakova MO, Karamysheva LV, Kazarinov IA (2018) Modelling of the wastewater treatment process using microbial bioelectrochemical technologies. *J ElektrokhimicheskayaEnergetica* (Electrochemical Energetics) 18(4):199–210. <https://doi.org/10.1850/1608-4039-2018-18-4-199-210>
- Methe BA (2003) Genome of *Geobacter sulfurreducens*: metal reduction in subsurface environments. *Science* 302:1967–1969
- Miyake T, Haneda K, Nagai N, Yatagawa Y, Onami H, Yoshino S, Abec T, Nishizawa M (2011) Enzymatic biofuel cells designed for direct power generation from biofluids in living organisms. *Energy Environ Sci* 4(12):5008–5012
- Myers CR (1992) Localization of cytochromes to the outer membrane of anaerobically grown *Shewanella putrefaciens* MR-1. *J Bacteriol* 194:3429–3438
- Myers CR (2001) Role of outer membrane cytochromes OmcA and OmcB of *Shewanella putrefaciens* MR-1 in reduction of manganese dioxide. *Appl Environ Biotechnol* 67:260–269
- Naumova MN, Meshcheryakova MO, Turkovskaja OV, Kazarinov IA (2015) Comparative studying of kinetics of bioelectrochemical oxidation of glucose in neutral environments by means of the microorganisms *Escherichia coli* and *Enterobacter cloacae*. *J ElektrokhimicheskayaEnergetica* (Electrochemical Energetics) 15(3):130–135
- Nevin KP, Lovley DR (2000) Lack of production of electronshuttling compounds or solubilization of Fe (III) during reduction of insoluble Fe (III) oxide by *Geobactermetallireducens*. *Appl Environ Microbiol* 66:2248–2251
- Nevin KP, Lovley DR (2002) Mechanisms for accessing insoluble Fe (III) oxide during dissimilatory Fe (III) reduction by *Geothrixfermentans*. *Appl Environ Microbiol* 68:2294–2299
- Newman DK, Kolter R (2000) A role for excreted quinones in extracellular electron transfer. *Nature* 405:94–97
- Palmore GTR, Bertschy H, Bergens SY, Whitesides GM (1998) A methanol/dioxygen biofuel cell 6 that uses NAD(+)- dependent dehydrogenases as catalysts: application of an electro7 enzymatic method to regenerate nicotinamide adenine dinucleotide at low 8 overpotentials. *J Electroanal Chem* 443:155–161
- Pardo-Yissar V, Katz E, Willner I, Kotlyar AB, Sanders C, Lill H (2000) Biomaterial engineered electrodes for bioelectronics. *Faraday Discuss* 116:119–134
- Park DH (2003) Improved fuel cell and electrode designs for producing electricity from microbial degradation. *Biotechnol Bioeng* 81:348–355
- Park DH, Zeikus JG (2002) Impact of electrode composition on electricity generation in a single-compartment fuel cell using *Shewanella putrefaciens*. *Appl Microbiol Biotechnol* 59:58–61
- Park DH, Kim SK, Shin IH, Jeong Y (2000) Electricity production in biofuel cell using modified graphite electrode with neutral red. *J Biotechnol Lett* 22:1301–1304
- Rabaey K (2007) Microbial ecology meets electrochemistry: electricity driven and driving communities. *ISME J* 1:9–18

- Rabaey K, Verstraete W (2005) Microbial fuel cells: novel biotechnology for energy generation. *Trends Biotechnol* 435(6):291–298
- Rabaey K, Lissens G et al (2003) A microbial fuel cell capable of converting glucose to electricity at high rate and efficiency. *Biotechnol Lett* 25:1531–1535
- Rabaey K, Boon N, Siciliano SD, Verhaege M, Verstraete W (2004) Biofuel cells select for microbial consortia that self-mediate electron transfer. *Appl Environ Microbiol* 70:5373–5382
- Raeburn S, Rabinowitz JC (1971) Pyruvate: ferredoxin oxidoreductase. I. The pyruvate-CO₂ exchange reaction. *Arch Biochem Biophys* 146:9–20
- Rasmussen M, Ritzmann RE, Lee I, Pollack AJ, Scherson D (2012) An implantable biofuel cell for a live insect. *J Am Chem Soc* 134(3):1458–1460
- Read ST, Dutta P, Bond PL, Keller J, Rabaey K (2010) Initial development and structure of biofilms on microbial fuel cell anodes. *BMC Microbiol* 10:98
- Ren H, Lee HS, Chae J (2012) Miniaturizing microbial fuel cells for potential portable power sources: promises and challenges. *Microfluid Nanofluidics* 13(3):353–381
- Reshetilov AN, Ponamoreva ON, Reshetilova TA, Bogdanovskaya VA (2005) Generacijaj električeskoj jenergii v biotoplivnom jelemente na osnovе kletok mikroorganizmov [Generation of electrical energy in a biofuel cell based on microorganism cells]. *Vestnik biotehnologii* 1(2):54–62
- Riklin A, Katz E, Willner I, Stocker A, Buckmann AF (1995) Improving enzyme–electrode contact redox modifications cofactors. *Nature* 376:672–675
- Sato F, Togo M, Islam MK, Matsue T, Kosuge J, Fukasaku N, Kurosawac S, Nishizawaa M (2005) Enzyme-based glucose fuel cell using vitamin K 3-immobilized polymer as an electron mediator. *Electrochem Commun* 7(7):643–647
- Scherson D, Cali L, Sarangapani S (2014) A Portable oxygen concentrator for wound healing applications. *Meet Abstr Electrochem Soc MA2014-02:16:862*
- Schröder U (2007) Anodic electron transfer mechanisms in microbial fuel cells and their energy efficiency. *Phys Chem Chem Phys* 9:2619–2629
- Schwefel J, Ritzmann RE, Lee IN, Pollack A, Weeman W, Garverick S, Willisa M, Rasmussena M, Schersona D (2015) Wireless communication by an autonomous self-powered cyborg insect. *J Electrochem Soc* 161(13):3113–3116
- Sell D, Kramer P, Kreysa G (1989) Use of an oxygen gas diffusion cathode and a three-dimensional packed bed anode in a bioelectrochemical fuel cell. *Appl Microbiol Biotechnol* 31:211–213
- Shoji K, Akiyama Y, Suzuki M, Nakamura N, Asano T, Nakamura N, Ohno H, Morishima K (2014a) Trehalose biofuel cells using insect hemolymph for insect robots. *Micro-NanoMechatronics and human science (MHS)*. *Int Symp IEEE* 2014:1–2
- Shoji K, Akiyama Y, Suzuki M, Nakamura N, Ohno H, Morishima K (2014b) Diffusion refueling biofuel cell mountable on insect. In: *Micro Electro Mechanical System (MEMS)*, IEEE 27th international conference. 2014, p 163–166
- Shukla AK, Suresh P, Berchmans S, Rajendran A (2004) Biological fuel cells and their applications. *Curr Sci* 87(4):455–468
- Speers AM, Reguera G (2012) Electron donors supporting growth and electroactivity of *Geobacter sulfurreducens* anode biofilms. *Appl Environ Microbiol* 78:437–444
- Sun M, Justin GA, Roche PA, Zhao J, Wessel BL, Zhang Y, Sclabassi RJ (2006) Passing data and supplying power to neural implants. *Eng Med Biol Mag IEEE* 25(5):39–46
- Suzuki S, Karube I, Matsuoka H, Ueyama S, Kawakubo H, Isoda S, Murahashi T (1983) Biochemical energy conversion by immobilized whole cells. *Ann N Y Acad Sci* 413:133–143
- Tanaka K, Vega CA, Tamamushi R (1983) Thionine and ferric chelate compounds as coupled mediators in microbial fuel cells. *Bioelectrochem Bioeng* 11:289–297
- Tanisho S, Kamiya N (1985) Microbial fuel cell using *Enterobacter aerogenes*. *Bioelectrochem Bioenerg* 21:25–32
- Tayhas G, Palmore R, Kim HH (1999) Electro enzymatic reduction of dioxygen to water in the cathode compartment of a biofuel cell. *J Electroanal Chem* 464:110–117

- Tender LM (2002) Harnessing microbially generated power on the seafloor. *Nat Biotechnol* 20:821–825
- Thauer RK, Kirchner FH, Jungermann KA (1972) Properties and function of the pyruvate formate lyase reaction in clostridia. *Eur J Biochem* 27:282–290
- Thauer RK, Jungermann KA, Decker K (1977) Energy conservation in chemotrophic anaerobic bacteria. *Bacteriol Rev* 41:100–180
- Tsujimura S, Tatsumi H, Ogawa J, Shimizu S, Kano K, Ikeda T (2001) Bioelectrocatalytic reduction of dioxygen to water at neutral pH using bilirubin oxidase as an enzyme and 2,2'-azino-bis (3-ethylbenzothiazolin-6-sulfonate) as an electron transfer mediator. *J Electroanal Chem* 496:69–75
- Turner APF, Karube I, Wilson GS (1987) *Biosensors fundamentals and applications*. Oxford University Press, New York
- Vega CA (1987) Mediating effect of ferric chelate compounds in microbial fuel cells with *Lactobacillus planetarium*, *Streptococcus lactis* and *Erwinia dissolvens*. *Bioelectrochem Bioenerg* 17:217–222
- Venkataraman A, Rosenbaum MA, Perkins SD, Werner JJ, Angenent LT (2011) Metabolite-based mutualism between *Pseudomonas aeruginosa* PA14 and *Enterobacter aerogenes* enhances current generation in bioelectrochemical systems. *Energy Environ Sci* 4:4550–4559
- Wessels D (2002) Implantable pacemakers and defibrillators: device overview & EMI considerations. In: *Electromagnetic Compatibility EMC 2002 IEEE International Symposium IEEE*, 2:911–915.
- Willner I, Riklin A (1994) Electrical communication between electrodes and NAD(P)⁺-dependent enzymes using Pyrroloquinolinequinone-enzyme electrodes in a self-assembled monolayer configuration: Design of a new Class of Amperometric biosensors. *Anal Chem* 66:1535–1539
- Willner I, Heleg-Shabtai V, Blonder R, Katz E, Tao G, Buckmann AF, Heller A (1996) Electrical wiring of glucose oxidase by reconstitution of FAD modified monolayers assembled onto Au electrodes. *J Am Chem Soc* 118:10321–10322
- Willner I, Arad G, Katz E (1998) A biofuel cell based on pyrroloquinoline quinone and microperoxidase-11 monolayer functionalized electrodes. *Bioelectrochem Bioeng* 44:209–214
- Workman JTE (2014) *The science behind breath testing for ethanol*. University of Massachusetts. *Law Rev* 7(1):4–11
- Yang Y, Sun G, Xu M (2011) Microbial fuel cells come of age. *J Chem Technol Biotechnol* 86(5):625–632
- Yuhashi N, Tomiyama M, Okuda J, Igarashi S, Ikebukuro K, Sode K (2005) Development of a novel glucose enzyme fuel cell system employing protein engineered PQQ glucose dehydrogenase. *Biosens Bioelectron* 20(10):2145–2150
- Zebda A, Gondran C, LeGoff A, Holzinger M, Cinquin P, Cosnier S (2011) Mediatorless high-power glucose biofuel cells based on compressed carbon nanotube-enzyme electrodes. *Nat Commun* 2:370
- Zhang X (1995) Modelling of a microbial fuel cell process. *Biotechnol Lett* 17:809–812

Chapter 18

Recent Trends in Fabrication and Applications of Wearable Bioelectronics for Early-Stage Disease Monitoring and Diagnosis



Ramila D. Nagarajan and Ashok K. Sundramoorthy

Abstract Modern technology has offered many ways to use chemical and biosensors effectively in detecting various analytes in environmental, medical, and food samples. Recently, people have started to use wearable devices to track various kinds of information about their health and fitness level. The market of wearable devices in 2015 was \$5 billion which showed 25% enhancement over 2014, and it is further expected to grow for the next 5 years. The primary focus of this chapter is to bring the latest developments on nanofabricated wearable devices which integrated on the epidermis, thereby analyzing by a non-invasive and non-obtrusive fashion. We have given more emphasis on the recent developments in the fabrication methodologies toward the chemical and biosensor for physical parameter measurements of heart rate, glucose, temperature, and pressure levels. To prepare wearable devices, nanomaterials such as 2D graphene, 1D carbon nanotubes, conducting polymers, and noble metal nanoparticles have been used as transducers. There are various challenges in recording the real-time measurements on human body during physical movements when there are drastic changes in the temperature, pressure, and humidity of the device, so these parameters have to be taken into account during flexible sensor device manufacturing. There are further developments on wearable devices which can track the health of patients, and also depending on the need, it can release drug into the body in a controlled manner for a timely diagnosis. We have also discussed the need of wearable devices and their use as temperature/motion sensor, respiration rate analyzer, heart rate and blood pressure monitoring, detecting the level of glucose, lactate, pH, etc. In addition, therapeutic applications and future hopes of wearable sensors have been discussed.

R. D. Nagarajan · A. K. Sundramoorthy (✉)
Department of Chemistry, SRM Research Institute, SRM Institute of Science and Technology,
Kattankulathur, Tamil Nadu, India
e-mail: ashokkus@srmist.edu.in

Keywords Electrochemical sensor · Flexible wearable device · Non-invasive method · Early stage analyzes · Cost-effective and therapy applications

Nomenclature

SERS	Surface Enhanced Raman Spectroscopy
PEDOT:PSS	Poly(3,4-ethylenedioxythiophene):polystyrene sulfonate
PDMS	Polydimethylsiloxane
CNTs	Carbon nanotubes
GO	Graphene oxide
rGO	Reduced graphene oxide
BN	Boron nitride
MoS ₂	Molybdenum disulfide
WS ₂	Tungsten disulfide
RFID	Radio-frequency identification
PTC	Positive temperature coefficient
NTC	Negative temperature coefficient
Ag NWs	Silver nanowires
Ag NPs	Silver nanoparticles
PET	Polyethylene terephthalate
SEBS	Styrene-ethylene-butadiene-styrene
SWCNTs	Single-walled carbon nanotubes
PU	Polyurethane
FSSF	Free-standing stretchable fiber
b.p.m	Beats per minute
HR	Heart rate
ECG	Electrocardiography
PVDF	Poly(vinylidene fluoride)
PVDF-TrFE	poly(vinylidene fluoride-co-trifluoroethylene)
PEIE	Ethoxylatedpolyethylenimine
MWCNTs	multiwalled carbon nanotubes
VS	vinylsiloxane
PFTs	Pulmonary function tests
wPt	Wrinkled platinum
IC	Inspiratory capacity
ESMF	Etched single mode fiber
CB	Carbon black
MLGs	Multilayer graphene platelets
Au NW	Gold nanowire
ROA	Reflectance oximeter array
H ₂ O ₂	Hydrogen peroxide
LED	Light emitting diode
OCET	Organic electrochemical transistor
Na ⁺ ion	Sodium ion

18.1 Introduction

The word “sensor” is derived from the Latin word *Sentire*, which means the recognition of particular molecules/analyte/compound. Initially, the sensing process arises from the human body by reflecting various forms of signals. In humans, the sensing mechanisms are based on touch, hearing, taste, and pain. These functions are mainly depending on the input signal and the transformation to the final receptor through where the output signal will be assessed. Chemical and biosensors which are the devices used to generate the electrical signal from the chemical or biomolecules transformation processes (Yogeswaran and Chen 2008). Briefly, chemical sensor is a device that converts concentration of target analyte into a measurable analytical signal through transducers. The analytical signal can be correlated to the quantity of the material/compound/molecule (Compagnone et al. 2017) present in the sample. The measurable signal may be in the form of electric current or potential, thermal resistance, thermal conductivity, and optical properties (Hulanicki et al. 1991). In the electrochemical sensor, the measured output signal should be in the form of current, voltage, resistance, or capacitance. The electrochemical sensors are broadly classified into two categories namely chemical sensors and biosensors. If the active element of the sensor is a biomolecule, converting or catalyzing the (bio) chemical reactions into a measurable signal is known as an electrochemical biosensor (Mehrotra 2016). Electrochemical sensors are more suitable for health care monitoring than the other sensors (e.g. Chemosensors, Surface Enhanced Raman Spectroscopy (SERS), etc.) because it offers high selectivity, sensitivity, good repeatability, reproducibility, and stability at relatively low cost. Additionally, the preparation of electrochemical sensors is simple, provides easy handling, and the catalyst material can be reused multiple times (Coelho et al. 2016).

However, the biosensor may not give accurate results in the complex samples. For example, when applied to the target nucleotides and tissues interaction, the electrode surface modified with biocatalyst may get damaged or adsorbed by other biomolecules (fouling) or unbounded molecules could further affect or change the electrode response. To overcome the above problems, biosensors can be applied specifically to the target area of human body, so it may avoid unnecessary complexity associated with the sample matrix (Bizzotto et al. 2018).

In this chapter, we have highlighted the recent trends on developing wearable bio(chemical) sensors for direct monitoring of human activity and corresponding changes in their body such as temperature, heart rate, blood pressure, and biomarkers levels (glucose, lactate, pH, etc.) in body fluids (sweat, tears, etc.). Specifically, wearable sensors made of using 2D graphene, 1D carbon nanotubes (CNTs), and conducting polymers poly(3,4-ethylenedioxythiophene) polystyrene sulfonate (PEDOT:PSS) with flexible Polydimethylsiloxane (PDMS) substrate are highlighted. The advantages of wearable sensors and associated challenges in maintaining sensitivity, repeatability, reliability, and stability of the devices are discussed under normal and flexible conditions. Also, wearable devices can do monitoring of glucose levels in hyperglycemia patients, and at the same time, it was designed to deliver the drug activated by thermally actuated needles present on the same fabricated device. Further challenges and the future scope of wearable devices are described.

18.1.1 Development of Wearable Devices for Various Applications

Electronic sensor devices are mainly developed with more portability options to integrate with wireless communication to enable easy health monitoring, environmental monitoring, weather forecast, food analysis, etc. (Heikenfeld et al. 2018). Wearable devices have gained more attention in the past few years to use in commercial products (e.g. barcode scanners). Nowadays, the use of barcode scanner is more attractive and simple compared to the manual entry. As we can see, many advertisements have been showcased to encourage the use of wearable devices to improve the habit of eating healthy and medical diagnosis of labors and the athletes (Aroganam et al. 2019; Mardonova and Choi 2018). In recent years, scientists have developed devices to control the operation process of mining industry and carefully monitor the environmental condition in underground of the deep mines. Wearable safety helmets are also produced to detect methane and carbon monoxide gases when working in deep underground at a particular region (Hazarika 2016). Similarly, the children activities are monitored in the class room while studying the case reports through the wearable devices (Geršak et al. 2020).

18.1.2 Advantage of Wearable Devices

Applications of chemical and biosensors are playing important role in health care monitoring. Wearable electronic devices can be used as an alternative tool to do health monitoring (through a mobile device) without using expensive analytical instruments. These devices are based on non-invasive methodology to analyze the individual's pathophysiology (Godfrey et al. 2018). The common laboratory analytical instruments are not flexible, and more steps are involved in the sample extraction and analysis. Wearable sensors can be prepared by using interdisciplinary knowledge from chemistry, biology, and micromechanical engineering systems to do selective and sensitive detection of target analytes in environmental, biomedical, and food samples. The main advantage of these devices is that they can be easily miniaturized as simple body attachable tools for medical diagnosis and treatment.

18.1.3 Challenges in Wearable Devices

Wearable devices such as sweat sensors can be used for a variety of applications. However, there are challenges that remain to overcome during the usage on the surface of the epidermis. The device performance can be altered by various parameters. For example, the device can give wrong results due to problems associated

with the improper adherence on the skin, handling of fluid (sweat, tears, etc.), incubation time, and concentration levels of target analyte that may pose challenges to accurately detect and report. Another important hurdle is the point of stretchability of wearable devices. Because of human activity or body movements, the wearable sensor may produce more noise and changes in the temperature, humidity, and pH level of sweat. This problem of the wearable devices can be improved by fabricating the device with a strain-dependent material with high flexibility. If the wearable devices are made with more accurate measurements under mechanical stress and strain (tactile sensor) (Wu et al. 2020), they may be more suitable for commercial applications. Different kinds of wearable devices are available in the market for regular usage in the form of smart watches (Lee et al. 2013), smart contact lens (Rodger et al. 2006), smart bandages (Long et al. 2018), clothing (Lin et al. 2018), etc.

18.2 Materials Used to Prepare Flexible Devices

Previously, organic and inorganic materials have been used to prepare the substrate for flexible devices. For example, inorganic material silicon was used, but it is rigid and easily breakable under stress. To improve the flexibility of the device, flexible carbon nanomaterials such as 2D graphene (Sundramoorthy et al. 2015b) and 1D CNTs have been used (Sundramoorthy et al. 2015a). They had shown outstanding chemical and physical properties with superior intrinsic flexibility compared to the conducting polymers. Although organic electroluminescence molecules had excellent intrinsic flexibility, it shows poor conductivity which is several orders of magnitude lower than the inorganic semiconducting material (Forrest 2004; Zou et al. 2018). 2D graphene-based flexible devices showed outstanding mechanical property with good optical transmittance of 97.7% which is suitable for the optoelectronics. Graphene could be used as good thermos-resistive and piezoelectric material, which makes them suitable for healthcare point of observation using paper-based graphene electrodes (Mohanraj et al. 2020). The large-scale production of graphene film is also possible with the role-to-role printing process and ultra-high vacuum chemical vapor deposition process to produce the flexible wearable devices (Kim and Ahn 2017). Similarly, graphene derivatives (graphene oxide, GO (Choo et al. 2019) and reduced graphene oxide, rGO) (Zhou et al. 2019) and the other 2D materials like boron nitride (BN) (Siddiqui et al. 2017), molybdenum disulfide (MoS_2) (Singh et al. 2019), and tungsten disulfide (WS_2) (Rehman et al. 2017) had also been used to produce flexible wearable devices. In the case of organic molecules, PDMS was used as a substrate to prepare the flexible electronic device. The conducting polymer PEDOT:PSS was also used to prepare a flexible supercapacitor device (Li et al. 2016). The inkjet-printed PEDOT:PSS film was used to fabricate stretchable circuits in the electronics (Kraft et al. 2020).

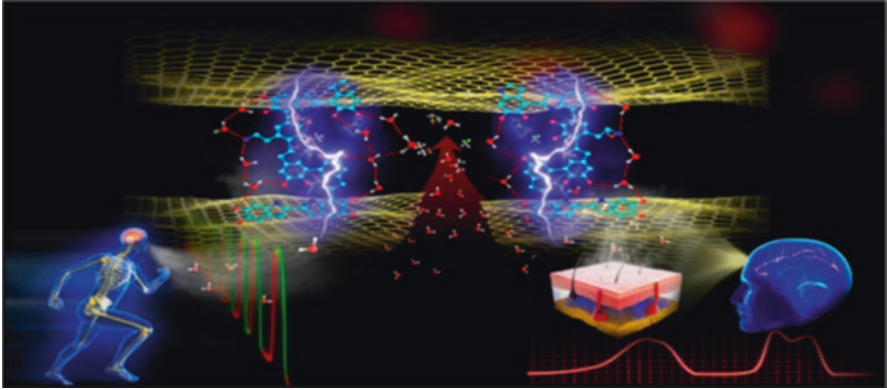


Fig. 18.1 shows graphene-based wearable device for health care monitoring through non-invasive methods and the wireless transmission of data. (Reproduced with permission from He et al. 2018)

18.3 Wearable Devices

18.3.1 Fabrication Technique for Wearable Devices

Flexible devices were fabricated based on chip integration at the micro- and nano-levels. Such fabrication techniques improved the functionality of stretching, adhesion, and decreased the production cost (Li et al. 2019). The wearable devices made by different lithography techniques such as photon-based lithography, charged particle-based lithography, printing-based lithography, tip-based lithography, and thermal tip lithography. Due to user-friendly nature, printing-based lithography was used to print various patterned structures. To have better interaction between human skin and the monitoring (wearable) device, the sensing component has to be flexible and stretchable with good sensitivity when attached. For example, Fig. 18.1 shows a demonstration of graphene-based device in the analysis of humidity level and respiration rate on the skin during breathing and speaking. The response time was 20 ms, and it transformed the signal wirelessly (He et al. 2018; Wang et al. 2016). The requirement for electrode fabrication by conventional technology is expensive. But printing process is scalable for the production of flexible device for different applications. It includes screen printing technology, inkjet printing technology, and roll-to-roll printing technology for large-scale production with low cost (Li et al. 2019).

18.3.2 Flexible Wearable Device for Health Monitoring

Generally, the medical professionals monitor the bio-signals on different parts of the body. Bio-signals are observed on the arm, wrist, chest, and fluids secreted in the body (Khan et al. 2016). Figure 18.2 represents the various monitoring tools used

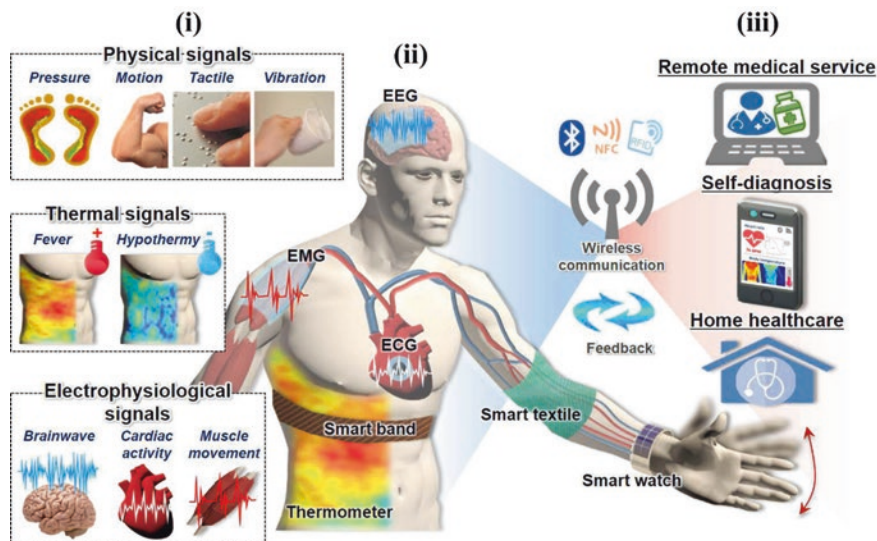


Fig. 18.2 (i) Represents the various sensors associated with health care monitoring to analyze the physical activity and bio-signals. (ii) Flexible material on the sensing location. (iii) The wireless transformation of signal through Bluetooth, RFID, and their application in different places. (Reproduced with permission from Ha et al. 2018)

for recording the changes during physical activity and bio-signals which were recorded in the human body by various wearable devices. These body attachable devices recorded and transmitted the signals wirelessly through the Bluetooth, and Radio-frequency identification (RFID) technology for the point of care applications (Ha et al. 2018).

18.3.3 Wearable Thermal Sensor

To monitor the physiological state of a person, the temperature measurement is required, and if it exceeds the elevated body temperature, it is the symptoms of fever. The internal temperature is about 37°C in the human body, and the core temperature is constant which is related to the heat produced by the body and heat loss to the environment (Olesen 1982). When an organic field-effect transistor prepared using gold or platinum was used as a temperature sensing material for epidermal electronics, it showed poor performance under the stretching condition of the device. To overcome this issue, ceramic materials and transition metal oxide films were used in the making of thermistor, but still, these devices were lacking in mechanical flexibility (Yan et al. 2015). So, wearable devices are fabricated using CNTs, graphene, or metal oxide nanomaterial to improve the stretching and decrease the production cost of fabrication (Kanao et al. 2015).

The temperature sensors were used to record temperature by using the thermistor and thermoelectric effects. For the conventional use, thermistor sensor is a better device by means of the temperature sensing related to the resistance. There are two types of sensors, one is positive temperature coefficient (PTC), where the temperature increases linearly with the resistance increases. In the second case, temperature decreases and the decrease in resistance corresponds to negative temperature coefficient (NTC).

So, the thermistor response is given by the following equation

$$R_t = R_o \exp\beta(1/T - 1/T_o)$$

Where R_t is the resistance of material at temperature T , and T_o is the reference temperature at that point when the resistance was R_o . β is the thermistor constant of the material. It can be obtained by getting the slope value from $\ln R_t$ and $(1/T)$.

Yan et al. (2015) demonstrated a thermistor using graphene as a stretchable material and silver nanowire (Ag NW) as electrode on the PDMS substrate (Fig. 18.3a). This device is stretchable up to 50%, and their relative thermal resistance was measured (Yan et al. 2015). Figure 18.3b was the I–V curves recorded using the thermistor when 0% strain was applied. Kanao et al. (2015) reported a selective temperature sensor with the strain force applied on the substrate, so the flexibility problem was fixed by creating tactile strain sensor with thermal sensor using printed flexible material on the cantilever structure. The fabricated device is used to monitor the temperature along with the strain based on cantilever structure for bending the substrate and application toward the e-skin device.

CNTs with silver nanoparticles (Ag NPs) were printed on polyethylene terephthalate (PET) film to fabricate a strain sensor. For temperature sensing, printed CNTs with PEDOT:PSS on the same PET substrate are used (Kanao et al. 2015). In 2018, Zhu et al. made a stretchable thermal sensor device with strain suppression. The CNT-based fabricated transistors device with strain-dependent circuit modification measures inaccuracy of ± 1 °C for the uniaxial stain-dependent errors up to 0–60%. The output was measured using static and dynamic approach, and in static approach, the circuit design achieves a sensitivity of -24.2 mV°C⁻¹ in the temperature range about 15–55 °C which was in the range of ambient and human body temperature. In dynamic approach, the tunable sensitivity was in the range from -20.2 mV°C⁻¹ to -41.7 mV°C⁻¹, and the sensing resolution was 0.5 °C. CNTs patterned transistor was placed on the epidermis of the wrist. The thermal changes were recorded by the device attached on the prosthetic rubber hand. The flexibility monitored by applying uniaxial strain and the temperature changes was observed when the hair dryer was brought near the fabricated device. The stretchable thin-film transistor device was made with styrene-ethylene-butadiene-styrene (SEBS) as the substrate. Using photolithography, the source-drain and gate electrodes were patterned using unsorted single-walled CNTs (SWCNTs), and supramolecular-polymer-sorted semiconducting SWCNTs were used to bridge the source and drain electrodes. The temperature changes were measured with and without introducing

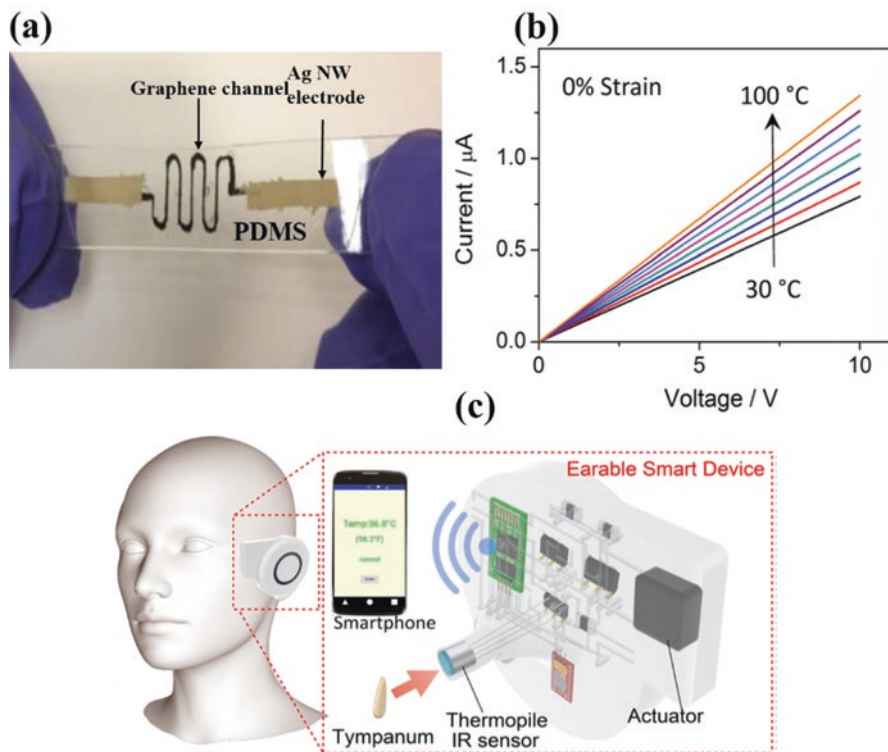


Fig. 18.3 (a) The optical image for the thermistors based on graphene channel on the PDMS substrate with 0% strain, (b) Represents the I–V curves for the graphene integrated channel with 0% induced strain device for monitoring temperature. (Reproduced with permission from Yan et al. 2015). (c) Wearable device for monitoring the internal core body temperature based on the infrared sensor, and microphones are connected for the hearing aid process. (Reproduced with permission from Ota et al. 2017)

strain in the temperature range of 22–55 °C by applying uniaxial strain from as 20, 40, and 60% (Zhu et al. 2018). Trung et al. (2018) demonstrated the strain-free stretchable temperature sensors designed using rGO with polyurethane (PU) composite by simple fiber-spinning method. This stretchable fiber withstands the strain limit up to 50% and the measured inaccuracy of ± 0.37 °C. The fabricated stretchable fiber increased the temperature response of (0.8% / 1 °C), the sensing resolution of the stretchable fiber was 0.1 °C embedded on the PDMS substrate, and its efficiency of stretching tendency shows 90%. The free-standing stretchable fiber (FSSF) sewn on the stretchable bandage attached on the forearm showed the efficiency of measuring temperature in the human skin while doing cycling with the changes and the sensing resolution as 0.1 °C. FSSF-based bandages and fabrics were suitable for monitoring temperature changes and applications in personal health care monitoring (Trung et al. 2018).

The measurement of core temperature is essential for health monitoring. The fabrication of 3D-printed wearable smart device is demonstrated which can be worn on the ear to monitor the temperature changes from the tympanic membrane on the basis of infrared sensor. The earable smart device is fully integrated with the data processing unit through the wireless connection, and it acts as a hearing aid with the design of microphone and actuators (Ota et al. 2017) (Fig. 18.3c). The biocompatible and ultra-flexible temperature sensor was fabricated on a semipermeable PU film. It measured the human body temperature for 24/7. The biocompatible nature of the flexible device was studied in vitro for the temperature measurement, and the obtained results are compared with the mercury thermometer, and it proved the practical application for temperature monitoring in human body. The temperature changes were also observed on the human body by water vapor and flowing air respiration by the device adhered on the forearm (Chen et al. 2015). However, the reported flexible device for temperature sensor is affected by the strain factor due to bending and twisting of the fabricated materials and lacks in the point of care application. This problem was fixed with the elimination of strain induced sensor for measuring temperature resistance.

18.3.4 Flexible Sensor for Heart Rate Monitoring

Monitoring of human pulse and the respiration rate is important for people who suffer from cardiac infarction, arrhythmia, and hypertension. In the final stages, it may lead to heart attack within a few minutes and unexpected death (Ha et al. 2018). The normal function of the human heart is a cyclic sequence of deoxygenated blood through the lungs and pumping oxygenated blood through aorta to the body, and this process is called cardiac cycle. The heart rate (HR) signal was expressed in terms of beats per minute (b.p.m). The HR signal is manually measured at the point of wrist and the neck by radial artery and carotid artery or by directly listening to the heartbeat rate from the stethoscope. The HR can be also measured by optical, pressure, and electrical sensor. The methods can be varied according to the sensing location, and HR can be electrically monitored by placing a sensor on the chest. To use the optical and pressure technique, HR sensor is placed on the wrist. The most important technique is currently used for HR monitoring known as electrocardiography (ECG).

ECG skin electrodes pick the depolarization signal from the heart muscles. ECG system is carried out by 12 leads, but the signal can be detected on the chest by using two electrodes. The ECG signals are conventionally monitored with the gel-assisted Ag/AgCl electrode in clinical measurements, and it causes skin irritation. The problem was fixed by using HR wearable device, and it avoided the gel-assisted process and made direct contact with the skin. Sekine et al. (2018) demonstrated printed ferroelectric polymer-based wearable sensor to monitor the HR on the skin. This flexible printed sensor showed fast response time of 0.2 s with high pressure sensitivity of (~ 0.025 MPa) toward the HR monitoring. The device was printed

using ferroelectric polymer of Poly(vinylidene fluoride) (PVDF) and the derivative of copolymer called poly(vinylidene fluoride-co-trifluoroethylene) [PVDF-TrFE). This material is soluble in polar solvents, so it makes them suitable for the solution-printing process. This ferroelectric polymer-based pressure sensor was adhered on the human wrist and neck and monitored the blood flow through a wireless connection (Sekine et al. 2018). In 2017, Cai and coworkers demonstrated highly stretchable strain-free epidermal sensors for the respiration rate and cardiac cycle monitoring. This device was fabricated by using percolative network of 3D graphene foam and 1D CNTs by chemical vapor deposition. It showed high sensitivity, strain up to 85% with a gauge factor of 20.5 and stability of >5000 cycles. This strain-free device distinguished the normal healthy person and pregnancy person by variation in the artery wrist pulse waveforms. The cracks were observed after applying strain. With the applied strain of 85%, few CNTs are bridged and lost their electrical conductivity. However, after applying of 100% strain, the device got ruptured (Fig. 18.4a). This strain-free sensor has been applied on the epidermis of human skin and eliminated the signal-to-noise ratio for the precise detection of respiration rate and cardiac cycle (Cai et al. 2017). Figure 18.4b and c show the resistance change observed for artery pulse waveform for a healthy and pregnant person, and monitoring before/after the sports activity of a volunteer. Simultaneous thermal and ECG sensors were fabricated to monitor changes in the human body temperature and pulse rate in the real time as shown in Fig. 18.4d. This technique avoids the gel-assisted process for good adhesion to the skin, and the material fabrication was done on the PET substrate. For good adhesion, ethoxylatedpolyethyl- enimine (PEIE) mixed with PDMS was used to enhance the adhesive force on the skin. The multiwalled CNTs (MWCNTs) were mixed with the adhesive material for improving the conductivity.

The ECG sensor was adhered on the chest of the human body before and after running to monitor ECG. It was found that ECG signals got affected slightly due to the generation of sweat after running. However, after wiping the sweat, the device retains its original performance and reached to the original value. This study showed that the wearable device may be suited for the sports application and to monitor the temperature changes on the volunteer chest. The ECG signal can be recorded during the position of sitting, standing, and the running position (Fig. 18.4e).

The results of flexible thermal sensors are verified with the infrared sensor (Fig. 18.4f) (Yamamoto et al. 2017). The other proposed method for bio-inspired composite is the PDMS substrate decorated with the vinyl siloxane (VS) mushroom-shaped tips. This fabricated device had direct adhesion onto the skin surface with the strength of 18 kPa to monitor the respiration rate and HR. The signal-to-noise ratio of the device and strain sensor is improved to 59.7. Due to strong adhesive nature on the chest, it differentiated the normal breath rate from a deep breath by changes in the resistance of the sensor during shrinking and expansion of the chest. The blood flow pressure was also measured as 84 beats per minute, and the sensor waveform was recorded in 10 s. It indicated that the signal of the artery pulse was detectable (Drotlef et al. 2017).

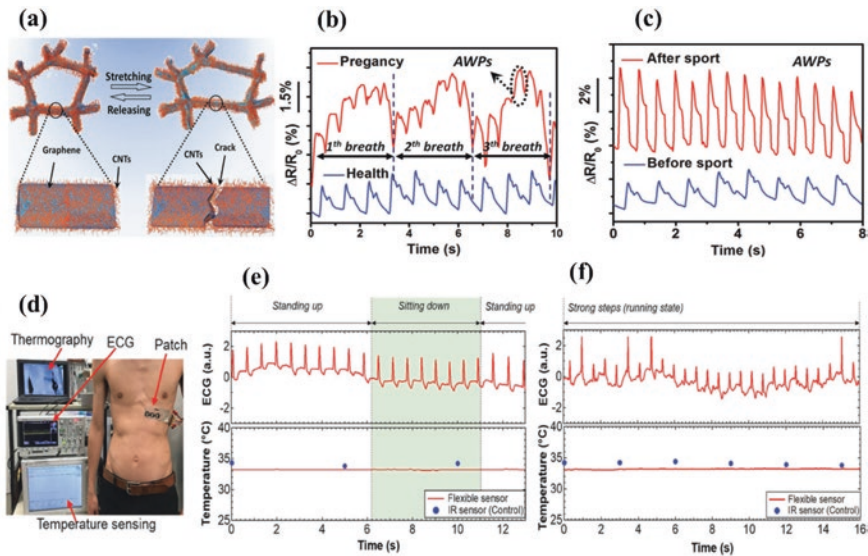


Fig. 18.4 (a) Shows the pulse rate sensor based on the fabricated microstructured 3D graphene foam with CNT to show the variation by cracking the sensing of pulse rate. (b) The graph represents the resistance change recording of healthy and pregnancy person. (c) The graph for recording the resistance for artery wave pulse of a human before and after sport. (Reproduced with permission from Cai et al. 2017). (d) The real-time monitoring of thermal and pulse rate (Electrocardiogram) signals was observed simultaneously. (e & f) show the graph of thermal sensing and ECG recording during the position of standing and sitting and the same observed during running position. (Reproduced with permission from Yamamoto et al. 2017)

18.3.5 Micropatterned Devices for Respiration Rate

For a healthy person, the basic sign indicates the flow of oxygen and exhale of carbon dioxide. The abnormal symptoms of respiration rate lead to asthma and pulmonary disease which is affecting around 435 million people around the world. To measure the flow of breath, sensors are attached on the chest and abdomen. The general method for respiration rate monitoring is use of pulmonary function tests (PFTs) connected with spirometry and diffusion capacity methods. Spirometry is a challenging method because one has to breathe maximally than normal, and it does not ensure accurate reading and is also not suitable for long-term use. Pegan et al. (2016) developed wrinkled platinum (wPt) as sensing material which is placed on the chest with adhesive tape and measured based on the contraction and relaxation of muscles. This sensing material showed 185% strain range with highest gauge factor of 42. It is connected with spirometric measurements and correlated based on the inspiratory capacity (IC) and tidal volume. The digital spirometer showed 95% accurate results when muscles expand during physical activity (Pegan et al. 2016). Moreover, Chu et al. (2019) reported a wearable device with Band-Aid models for respiratory and motion monitoring with the simple fabrication method by using

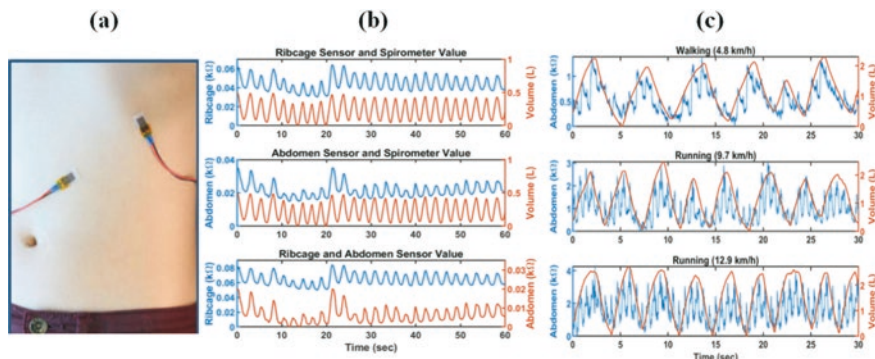


Fig. 18.5 (a) The visual images of flexible wearable sensor bandage on the abdomen and rib cage for monitoring the respiration. (b) The representation of simultaneous strain sensor along with respiration sensing and the sensor location on the abdomen and rib cage and the resistance change was measured. (c) The same respiration changes were observed in the abdomen during the difference in the running speed and the increase in the respiration volume recorded. (Reproduced with permission from Chu et al. 2019)

photo-resistive technique. The wearable devices attached on the abdomen and rib cage were shown in Fig. 18.5a, and further strain relief patterns were designed to adhere on the skin. The simultaneous measurement of strain and respiration rate was recorded on the sensing location of abdomen and ribcage, and corresponding resistance change was observed for respiration of volume (Fig. 18.5b). The measured respiration rate was based on the expansion and contraction during standing and movements such as running and walking. Furthermore, the data were collected through wireless transmission via Bluetooth. A well-calibrated model was developed for measuring changes in resistance of the strain sensor with respect to the volume expansion of breath (breathe exhaled). This can be used to measure the respiration rate and respiration volume by the sensor adhered on the skin. The measured changes are recorded during walking at the speed of 4.8, 9.7, and 12.9 km/h, and the respiration volume was also recorded (Fig. 18.5c). This device was useful for the asthma and pulmonary chronic disease patients (Chu et al. 2019). The fiber optic sensor made with the MoS₂ nanosheets showed 14-fold enhancement for human breath monitoring with quick response time of 0.066 s. This MoS₂-coated etched single mode fiber (ESMF) has to be analyzed with real-time monitoring in human breath (Du et al. 2017).

18.3.6 Flexible Devices to Measure Blood Pressure

Blood pressure monitoring is important for humans. The blood pressure levels can be maximum and minimum which leads to systolic and diastolic disorders. For a normal person, the blood pressure is (above/below) 120/80 for systolic and

diastolic. If the blood pressure is higher than the above-mentioned levels, then it leads to hypertension. Blood pressure is commonly measured by using a sphygmomanometer which is wrapped around the arm and measures the pressure using a manometer. But the usage of a sphygmomanometer has lacked many points in the frequent analysis. People may lose their life in unreasonable condition due to the improper monitoring of the pulse waveform. The research has started to develop wearable pressure sensors by either one of piezo-resistive/capacitive or piezoelective. Mostly, the used techniques were based on capacitive and piezoelectric methods. The flexible sensors made with resistance measurements were also available. In 2014, Zhu et al. (2014) prepared a flexible pressure sensor with the quick response time of 0.2 ms using microstructure graphene arrays on the PDMS substrate. This flexible sensor was tested on the artificial hand by applying temporal and static touch with finger which gives signal in the form of Morse code. It showed high sensitivity of -5.53 kPa^{-1} in low pressure range (Zhu et al. 2014).

Flexible capacitive type sensor is developed based on the robust e-skin to monitor the pressure with the sensitivity of 35 kPa^{-1} in the range of 0–0.2 kPa by using conducting carbon black on the PDMS substrate (CB/PDMS) by applying 1 V bias. These capacitive pressure sensors showed outstanding performance than the other reported sensors. This pressure sensor was applied in the human wrist and recorded three wave forms of signal. To measure blood pressure, the calibration is established between the measured capacitance and the pressure. It clearly showed the difference of systolic and diastolic waves of the arterial pulse (Pruvost et al. 2019). For the piezo-resistive model, the pressure sensor was made with the PDMS foams covered by multilayer graphene platelets (MLGs). After stabilization cycle, this device measured 10 kPa in the applied pressure of 70 kPa with sensitivity of 0.23 kPa^{-1} , and the sensor variation was 1 Pa (Rinaldi et al. 2016). Another model was reported using gold nanowires (Au NWs) for pressure sensing application. The device was made of Au NWs-imprinted design sandwiched between two PDMS sheets. This fabrication method is scalable, and it can be operated at the battery voltage of 1.5 V with low energy consumption. The response time of analysis was $<17 \text{ ms}$ and detects in the pressure range of 13 Pa. This device overcomes the issue of stress, torsion, and bending forces. Interestingly, the real-time monitoring can be performed to detect the vibrations around the device in the distance of millimeter. It measured the vibrations of music, and it was capable of recording the repeated music (Gong et al. 2014).

18.3.7 Wearable Pulse Oxygenation Device

In human body, the hemoglobin process is for transportation of oxygen from lungs to tissue. The process of oxygenation is the measure of concentration of oxyhemoglobin to total oxy- and deoxyhemoglobin concentrations in the blood. The measurement of oxygenation can be different depending on the sensing location of tissue, veins, and peripheral. The measured signals are observed on the pulsatile arterial blood known as pulse oxygenation. Oximetry method determines the

oxygen saturation level in tissue and estimates the concentration of oxy- and deoxy-hemoglobin. The pulse oxygenation reflects the human cardiovascular health condition (Khan et al. 2018). For a normal person, the pulse oxygenation level was greater than 95%; if the level is less than 80%, it may lead the internal organ to lose their activity. The pulse oxygenation can be measured by optical measurements by placing the sensor on finger and wrist. Their transmitted or reflected signal was measured on the basis of concentration of oxy-hemoglobin in the blood. The signals were recorded by a photodetector for the transmittance and reflectance signal (photodetector attached on the same side of the skin). Khan et al. (2018) monitored oxygen saturation level on forehead by using a flexible sensor. They have used a reflectance oximeter array (ROA) which is a flexible and printable device on the silicon-integrated circuits with organic photo-electronics. A flexible device was prepared to monitor pulse oxygenation level in blood and tissue using four red and near infrared red organic light emitting diodes and eight organic photodiodes. Blade coating and screen printing processes were used to fabricate the flexible sensor with organic optoelectronics. Their device differentiated signals of oxyhemoglobin from hemoglobin molar absorptivities. Compared to commercial transmittance oximeters, it showed more accuracy with mean error of 1.1% with the reflectance oximeter. To evaluate the concentration of oxygen tested level in the volunteer through the inhaled air concentration and breathing through facemask, the changes were observed by concentrations of oxygen. The reflection mode sensor on the forehead observed the changes in the concentration of oxygenation, and the commercial finger probe sensor was also attached to it. The oxygenation of volunteers was measured by the reflectance and transmittance probe, and the concentration of oxygen changed from 21% to 15% over the time period of 8 min. Within this time period, the transmission mode falls from 96% to 90.5% and again returns to 94.5%. But in the case of reflectance mode, the oxygen saturation varies from 98% to 90.4%, but the saturation was observed as 93.5%. In the reflectance mode of measurements, 1.1% error is observed during the period of 8 min when compared with the transmittance mode. Similarly, other group is reported a flexible device made of organic and inorganic materials for measuring the heartbeat rate and pulse oxygenation. They used green and red organic materials to fabricate the flexible substrate. The difference in the signal was observed by the appearance of oxyhemoglobin and hemoglobin at the green wavelength (Lochner et al. 2014).

18.3.8 Non-invasive Method for Glucose Sensor

Up to the year of 2000, about 171 million people were affected by diabetes (Group et al. 2009). An elevated level of glucose leads to diabetes, and the secretion of insulin plays a major role in the human body. The monitoring of glucose concentration is critical for the diabetes patients. The abnormal levels of glucose lead to major health problems such as cardiac disease, renal failure, and the cerebral organ failure. To monitor the glucose concentration in the human blood samples, there were

several methods developed through optical (Steiner et al. 2011), fluorescent (Pickup et al. 2005), infrared spectroscopy (Kottmann et al. 2012), chemiluminescence (Duan et al. 2019), electrochemical (Kumar et al. 2010), and field-effect transistors (Shan et al. 2018). Glucose sensor was fabricated by the enzymatic and non-enzymatic methods (Jeevanandham et al. 2020). In the glucose biosensing, glucose oxidase enzyme was used, and it produces the hydrogen peroxide (H_2O_2) as a byproduct. Then, H_2O_2 get decomposed and produced hydrogen, oxygen, and free electrons. This measurement was based on the flow of current. To avoid the classical stationary electrodes, Yoon et al. (2013) used microneedles array technique. They fabricated a device by using platinum nanoparticles/carbon nanotube-modified silicon microstructure as electrode setup to detect the glucose concentration in vitro analysis. It gave better sensitivity ($17.73 \pm 3 \mu\text{A}/\text{mM}\cdot\text{cm}^2$) than other reported noble materials with the detection range from 3 to 20 mM by amperometry (Yoon et al. 2013). For real-time monitoring of glucose concentration in human urine samples, the microfluidic device combined with the screen-printed electrode had been developed for the point of care monitoring (Yang et al. 2013). The glucose sensor was fabricated on the polymer substrate by creating microstructures. Then, it shaped into particular shape as contact lens and glucose oxidase enzyme immobilized on the titanium sol-gel film (Yao et al. 2011).

Glucose sensor was fabricated on the flexible polyimide substrate with rGO and chitosan-glucose oxidase immobilized substrate as a working electrode to detect glucose in sweat. This device detected the glucose concentration in the range of 0–2.4 mM in sweat with fast response time of 20 s. This fabricated sensor was well adhered on the skin for the human sweat analysis of glucose (Xuan et al. 2018). The wireless measurement of glucose concentration is demonstrated using contact lens with 2D graphene aligned with 1D Ag NWs hybrid which showed the excellent stretchability and conductivity.

Similarly, pyrene linker was decorated to immobilize the glucose oxidase to do glucose oxidation process, and the resistance changes were observed by the drain current. This device was tested in phosphate buffer electrolyte solution and also in the artificial tear solution. Obtained results are reproducible, so it may be applied for real applications, and the fabricated contact lens was applied in the eyes of live rabbit for the in vivo application studies. The glucose concentration was monitored based on the light emitting diode (LED), after putting the contact lens on the rabbit, and when the glucose concentration increased above 0.9 mM, the LED turned off. The stability of the sensor was also checked after blinking the eyes of the rabbit, and it did not show any signs of abnormal behavior (Park et al. 2018).

18.3.9 Lactate Sensor

Lactate sensor is important for clinical diagnosis, food analysis, and cell culture. In our human body, the lactate level may differ; when the body was at rest, the concentration of lactate was found to be 0.5–1.5 mM, and during exercise, the

concentration increased up to 25 mM (Rathee et al. 2016). The analysis was carried out through the non-invasive methods in saliva, sweat and tears, etc. The preferred method was based on lactate oxidase immobilized on the substrate. Currano et al. (2018) demonstrated a device based on the organic electrochemical transistor (OECT) which monitors the lactate concentration in the sweat. The commercially available thin-film lithium-ion batteries were fabricated directly on the kapton substrate to power the board, and OECT was used as a transducing element with immobilized lactate oxidase enzyme through the cross-linker of glutaraldehyde. The OECT transistor showed better sensitivity up to 1 mM (Currano et al. 2018).

Similarly, a non-enzymatic lactate sensor was developed using screen-printed electrode with electro-polymerized 3-aminophenylboronic acid to detect the lactate concentration from 3 to 100 mM, and the limit of detection obtained was 1.5 mM with the response time of 2–3 min (Zaryanov et al. 2017). In another study, a wearable gloves sensor was developed using CNTs immobilized with lactate oxidase as working electrode and Ag/AgCl as reference electrode painted on the glove using pipette which showed better results for the detection of lactate. The fabricated wearable glove biosensor detected lactate in the human sweat while doing exercise, running, cycling, and jogging. The lactate concentration was very low during running, and the results were also compared with the reported values. It is further verified by the obtained results from the standard spectrophotometer. This is a new method to fabricate the wearable device for various applications including medicine, defense, and environmental monitoring (Luo et al. 2018).

18.4 Patterned Device for pH Sensor

The acidity or alkalinity of the sample is monitored by the pH measurements. The measurement of pH is necessary in human body to study the hydration level. The Nernst equation depicted the pH sensitivity was 59 mV per pH at room temperature. Nakata et al. (2018) fabricated a temperature and pH sensor using the charge-coupled device, and it was measured as 240 mV/pH. The output signal was four times higher than the theoretical factors, and the sensitivity of pH varies along with the temperature. The real application of the pH sensor was recorded in the human sweat along with the temperature monitoring on the human skin. In the flexible pH sensor, potential changed according to the pH of the solution which was dropped on the device. After confirmation, the real sensing of temperature and pH was done on the human arm with sweat. This time noise was observed due to improper adhesion of sensing membrane on the skin. The observed noise was eliminated by repeating ten continuous measurements and got stabilized. This performance was compared with the commercially available pH sensor and standard infrared radiation sensor. The obtained results are in good agreement with the commercial sensors, so it is suitable for the real application in human sweat.

The integrated microfluidic sweat sensor monitored the concentration of electrolyte (sodium ion, Na⁺), pH, and temperature on the human body. The real

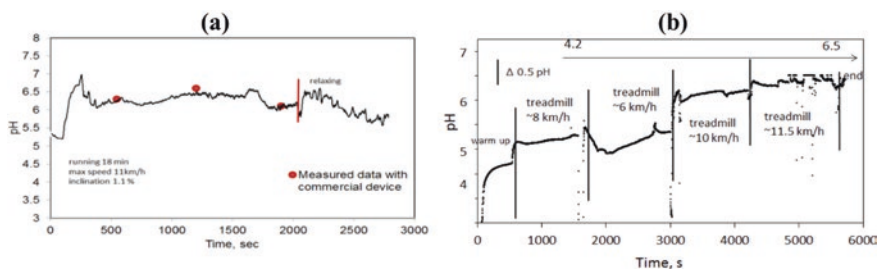


Fig. 18.6 (a) Represents the pH changes with time compared with the commercial sensor during sweat of human subjects during the running speed of 11 km/h. (b) The pH changes were observed in sweat during running in the treadmill with respect to time. (Reproduced with permission from Anastasova et al. 2017)

application of the wearable device adhered on the human skin detected pH changes with the time during cycling of ergometry. The pH changes were recorded during the running with the speed of 11 km/h and obtained data compared with the commercial sensor (Fig. 18.6a). Further, continuous recording of pH during treadmill by varying the speed and the changes was observed with respect to time as shown in Fig. 18.6b. The device for sodium ion detection was fabricated using polyvinyl chloride membrane and electrochemically depositing PEDOT. For measuring pH, iridium oxide and the special modification for metabolites with enzyme were made and used to test in human saliva (Anastasova et al. 2017).

18.4.1 Flexible Devices for Monitoring Body Movements

A low-cost fabrication method based on MoS_2 is developed as wearable device and integrated on the eraser as substrate to monitor human body movements. This device is placed on the knee which monitored and reported the number of steps taken, distance travelled, and the walking speed. Furthermore, it calculated the breath rating and monitored the hydration level. The sensing response was increased up to 56.8% on the MoS_2 flexible device when the strain is applied under the level of 16%. Finally, the recorded data can be transferred directly to our mobile phones via wireless connection (Shinde et al. 2019).

18.5 Wearable Device for Therapeutic Applications

The wearable devices fabricated for the analysis of biosignals from the human body. The analytical improvement was observed when the fabricated device was directly attached on the skin to monitor the biosignals, and at the same time, it can deliver

drug based on the need to the person simultaneously for the therapeutic application. It is not possible with the traditional methods where we have to analyze the samples and then recommend the drug to inject manually. Lee and colleagues demonstrated a graphene/gold/gold mesh composite which had the excellent electrochemical sensitivity toward glucose, and the fabricated patch also can release the drug based on the control measurements. The microneedle based device monitored each change such as pH, humidity, and temperature along with the patch which delivers the drug metformin to control the high glucose level in human skin. The fabricated device was experimentally demonstrated in diabetic mice through thermally actuated system. The microneedle-fabricated patch was monitored the glucose level—hyperglycemia triggers the drug delivery thermally and transfers the data of observation wirelessly. The fabricated wireless device was adhered on the human skin, and it is a promising for the future applications toward the chronic disease and diabetic therapeutic applications (Lee et al. 2016).

18.5.1 Future Aspects of Wearable Sensor

We have discussed some of the reported wearable sensors which could be applied for monitoring the bio-signals of human subjects. The device fabrication was done through different methods/approaches to transmit the recorded data through wireless communication. Even though there is the availability of wearable devices for monitoring the pulse rate, blood pressure, and respiration rate, treatment cannot be done directly by controlled devices. These kinds of problems can be rectified by having controlled release of drugs wherever needed depending on the measurements/or analysis. It is expected that the fabricated device could simultaneously monitor the unusual signs of human body and releases the drug for therapeutic applications on demand. Also, wearable biosensor devices could only monitor the bio-signals but may not monitor or analyze the presence of microbes such as bacteria and viruses and related infections. Similarly, the circulating tumor cell detection is demonstrated on the microelectrodes. But, it is not in the form of wearable devices for early-stage detection, so they followed the traditional method by using antibodies and identified the circulating tumor cell in the final stages. So it may not be helpful for early-stage detection, and it leads to fatal death. If the wearable devices can identify the circulating tumor cell in the early stage and supply the drug automatically at controlled fashion, it could be a potential tool or opportunity for the entire world to save a lot of people. The researchers could bring out different ideas and solutions to challenges various existing problems by adopting the non-invasive methodology to identify the cancer tumors and do immediate therapeutic treatments and save lives.

18.6 Challenges

Before clinical research, the fabricated wearable device may face several challenges in order to adapt it in the point of care application (Izmailova et al. 2018). Some of the serious issues are regarding the practical application such as resiliency of the device, reusability, biocompatibility, and long-term stability (Bandodkar and Wang 2014). After the device is undergone, the mechanical deformation by body movements and specifically the challenges were observed for textile-based sensor products where washing takes place under different temperatures and chemicals. These parameters have to be taken care of during the developmental stage of the sensors to overcome extreme and withstand high stresses. Also, the main issues came such as reliability and viability during the recording of instruments. To effectively do health monitoring at home, we need smart technology through mobile phones—wireless connection and data transfer which are better than the traditional methods. When we target some of the analytes (pathogens and proteins), the difficulty arises with the issue of preparing the protocol for monitoring. The regeneration of the wearable devices faces another challenge under continuous monitoring, and the problem was fixed *in vitro* by using extreme pH conditions, but the same idea did not work for analysis on human body condition due to variation in pH. Sometimes, the sensitivity of the device may be not suitable for the detection of a very low-level concentration of analyte present *in vivo* on human body monitoring. The standard methods such as those that are immunoassay based are used to detect the pathogens and proteins by involving multiple steps. The sandwich-type immunoassay may not be suitable to prepare the wearable device for the continuous monitoring of biosignals on human body condition. The analysis of the pathogen with antimicrobial coatings on the teeth is developed to overcome the issue and enhance the performance of wearable device (Mannoor et al. 2012). The important requirements of the wearable devices are that they should be calibration free and user-friendly, and the measurements must be accurate and comparable with the standard devices available in the market. Finally, the critical point is to develop the wearable devices in minimum size (miniaturized sensor), reusable, easy storage, high stability of the device, and no toxic effect due to materials used to fabricate the sensor. These parameters should be considered before manufacturing any wearable biosensor devices for health care monitoring.

18.7 Conclusions

The importance (need) of wearable sensors in day-to-day life for different applications to reduce the man power and improve safety measures (helmets with sensors), and of gas sensors to monitor the poisonous gases in underground mining industries, cancer cell detection, etc. has been widely known. These wearable sensors play a vital role in health care applications by recording bio-signals in the human

body such as monitoring temperature, pressure and respiration rate, the pulse oxygenation level, oxyhemoglobin and deoxyhemoglobin in blood, analysis of glucose, pH, and lactate levels for fitness applications. The multinational companies (e.g. Google, Apple, noviosense and orsense, etc.) have already developed wearable smart devices such as apple watch to monitor the human heart rate while running, and are expected to introduce many new innovative devices for health analysis. They will introduce many such valuable health care/biomedical products in the commercial market. The upcoming technology may provide low-cost solution for continuous monitoring of elder people having chronic diseases at home. The non-invasive device methodology to estimate catecholamine concentration in human bio-fluids such as antioxidant level in tears and the pathogens identification in saliva/or sweat will be realized in the near future. The transmission of data will be based on integration with radiofrequency identification and Bluetooth device which could directly transfer the data to the computer or cell phone in a friendly accessible fashion. The wearable devices can be applied for real-time monitoring of health condition and analysis using e-skin (electronic skin) or through epidermal skin – in vivo analysis. It is believed that details discussed in the present chapter will help to give basic knowledge to the reader and to understand the facts about wearable sensor and their advantages in health care.

Acknowledgements This work was financially supported by the Science and Engineering Research Board, India (Ref. No.: ECR/2016/001446). We also thank DST (International Bilateral Cooperation Division) for financial support through “INDO-RUSSIA Project (File No.: INT/RUS/RFBR/385).” RDN thanks SRM IST for Ph.D. student fellowship.

References

- Anastasova S, Crewther B, Bemnowicz P, Curto V, Ip HMD, Rosa B, Yang G-Z (2017) A wearable multisensing patch for continuous sweat monitoring. *Biosens Bioelectron* 93:139–145
- Aroganam G, Manivannan N, Harrison D (2019) Review on wearable technology sensors used in consumer sport applications. *Sensors* 19:1983
- Bandodkar AJ, Wang J (2014) Non-invasive wearable electrochemical sensors: a review. *Trends Biotechnol* 32:363–371
- Bizzotto D, Burgess IJ, Doneux T, Sagara T, Yu H-Z (2018) Beyond simple cartoons: challenges in characterizing electrochemical biosensor interfaces. *ACS Sens* 3:5–12
- Cai Y, Shen J, Dai Z, Zang X, Dong Q, Guan G, Li L, Huang W, Dong X (2017) Extraordinarily stretchable all-carbon collaborative Nanoarchitectures for epidermal sensors. *Adv Mater* 29:1606411
- Chen Y, Lu B, Chen Y, Feng X (2015) Breathable and stretchable temperature sensors inspired by skin. *Sci Rep* 5:11505
- Choo DC, Bae SK, Kim TW (2019) Flexible, transparent patterned electrodes based on graphene oxide/silver nanowire nanocomposites fabricated utilizing an accelerated ultraviolet/ozone process to control silver nanowire degradation. *Sci Rep* 9:5527
- Chu M, Nguyen T, Pandey V, Zhou Y, Pham HN, Bar-Yoseph R, Radom-Aizik S, Jain R, Cooper DM, Khine M (2019) Respiration rate and volume measurements using wearable strain sensors. *NPJ Digit Med* 2:8

- Coelho M, Giarola J, da Silva A, Tarley C, Borges K, Pereira A (2016) Development and application of electrochemical sensor based on molecularly imprinted polymer and carbon nanotubes for the determination of carvedilol. *Chemosensors* 4:22
- Compagnone D, Di Francia G, Di Natale C, Neri G, Seeber R, Tajani A (2017) Chemical sensors and biosensors in Italy: a review of the 2015 literature. *Sensors* 17:868
- Currano LJ, Sage FC, Hagedorn M, Hamilton L, Patrone J, Gerasopoulos K (2018) Wearable sensor system for detection of lactate in sweat. *Sci Rep* 8:15890
- Drotlef D, Amjadi M, Yunusa M, Sitti M (2017) Bioinspired composite microfibers for skin adhesion and signal amplification of wearable sensors. *Adv Mater* 29:1701353
- Du B, Yang D, She X, Yuan Y, Mao D, Jiang Y, Lu F (2017) MoS₂-based all-fiber humidity sensor for monitoring human breath with fast response and recovery. *Sensors Actuators B Chem* 251:180–184
- Duan Y, Huang Y, Chen S, Zuo W, Shi B (2019) Cu-doped carbon dots as catalysts for the Chemiluminescence detection of glucose. *ACS Omega* 4:9911–9917
- Forrest SR (2004) The path to ubiquitous and low-cost organic electronic appliances on plastic. *Nature* 428:911
- Geršak V, Vitulić HS, Prosen S, Starc G, Humar I, Geršak G (2020) Use of wearable devices to study activity of children in classroom; case study—learning geometry using movement. *Comput Commun* 150:581–588
- Godfrey A, Hetherington V, Shum H, Bonato P, Lovell NH, Stuart S (2018) From A to Z: wearable technology explained. *Maturitas* 113:40–47
- Gong S, Schwalb W, Wang Y, Chen Y, Tang Y, Si J, Shirinzadeh B, Cheng W (2014) A wearable and highly sensitive pressure sensor with ultrathin gold nanowires. *Nat Commun* 5:1–8
- Group, D.P.P.R, Knowler WC, Fowler SE, Hamman RF, Christophi CA, Hoffman HJ, Brenneman AT, Brown-Friday JO, Goldberg R, Venditti E, Nathan DM (2009) 10-year follow-up of diabetes incidence and weight loss in the diabetes prevention program outcomes study. *Lancet* 374:1677–1686
- Ha M, Lim S, Ko H (2018) Wearable and flexible sensors for user-interactive health-monitoring devices. *J Mater Chem B* 6:4043–4064
- Hazarika P (2016) Implementation of smart safety helmet for coal mine workers. In: 2016 IEEE 1st international conference power electronics, intelligent control and energy systems (ICPEICES), p 1–3
- He J, Xiao P, Shi J, Liang Y, Lu W, Chen Y, Wang W, Théato P, Kuo S-W, Chen T (2018) High performance humidity fluctuation sensor for wearable devices via a bioinspired atomic-precise tunable graphene-polymer heterogeneous sensing junction. *Chem Mater* 30:4343–4354
- Heikenfeld J, Jajack A, Rogers J, Gutruf P, Tian L, Pan T, Li R, Khine M, Kim J, Wang J (2018) Wearable sensors: modalities, challenges, and prospects. *Lab Chip* 18:217–248
- Hulanicki A, Glab S, Ingman F (1991) Chemical sensors: definitions and classification. *Pure Appl Chem* 63:1247–1250
- Izmailova ES, Wagner JA, Perakslis ED (2018) Wearable devices in clinical trials: hype and hypothesis. *Clin Pharmacol Ther* 104:42–52
- Jeevanandham G, Jerome R, Murugan N, Preethika M, Vediappan K, Sundramoorthy AK (2020) Nickel oxide decorated MoS₂ nanosheet-based non-enzymatic sensor for the selective detection of glucose. *RSC Adv* 10:643–654
- Kanao K, Harada S, Yamamoto Y, Honda W, Arie T, Akita S, Takei K (2015) Highly selective flexible tactile strain and temperature sensors against substrate bending for an artificial skin. *RSC Adv* 5:30170–30174
- Khan Y, Ostfeld AE, Lochner CM, Pierre A, Arias AC (2016) Monitoring of vital signs with flexible and wearable medical devices. *Adv Mater* 28:4373–4395
- Khan Y, Han D, Pierre A, Ting J, Wang X, Lochner CM, Bovo G, Yaacobi-Gross N, Newsome C, Wilson R (2018) A flexible organic reflectance oximeter array. *Proc Natl Acad Sci* 115:E11015–E11024
- Kim H, Ahn J-H (2017) Graphene for flexible and wearable device applications. *Carbon N Y* 120:244–257

- Kottmann J, Rey JM, Luginbühl J, Reichmann E, Sigrist MW (2012) Glucose sensing in human epidermis using mid-infrared photoacoustic detection. *Biomed Opt Express* 3:667–680
- Kraft U, Molina-Lopez F, Son D, Bao Z, Murmann B (2020) Ink development and printing of conducting polymers for intrinsically stretchable interconnects and circuits. *Adv Electron Mater* 6:1900681
- Kumar SA, Cheng H-W, Chen S-M, Wang S-F (2010) Preparation and characterization of copper nanoparticles/zinc oxide composite modified electrode and its application to glucose sensing. *Mater Sci Eng C* 30:86–91
- Lee Y-H, Kim J-S, Noh J, Lee I, Kim HJ, Choi S, Seo J, Jeon S, Kim T-S, Lee J-Y (2013) Wearable textile battery rechargeable by solar energy. *Nano Lett* 13:5753–5761
- Lee H, Choi TK, Lee YB, Cho HR, Ghaffari R, Wang L, Choi HJ, Chung TD, Lu N, Hyeon T (2016) A graphene-based electrochemical device with thermoresponsive microneedles for diabetes monitoring and therapy. *Nat Nanotechnol* 11:566
- Li Y, Ren G, Zhang Z, Teng C, Wu Y, Lu X, Zhu Y, Jiang L (2016) A strong and highly flexible aramid nanofibers/PEDOT: PSS film for all-solid-state supercapacitors with superior cycling stability. *J Mater Chem A* 4:17324–17332
- Li Q, Zhang J, Li Q, Li G, Tian X, Luo Z, Qiao F, Wu X, Zhang J (2019) Review of printed electrodes for flexible devices. *Front Mater* 5(77)
- Lin C-C, Yang C-Y, Zhou Z, Wu S (2018) Intelligent health monitoring system based on smart clothing. *Int J Distrib Sens Netw* 14:1550147718794318
- Lochner CM, Khan Y, Pierre A, Arias AC (2014) All-organic optoelectronic sensor for pulse oximetry. *Nat Commun* 5:5745
- Long Y, Wei H, Li J, Yao G, Yu B, Ni D, Gibson ALF, Lan X, Jiang Y, Cai W (2018) Effective wound healing enabled by discrete alternative electric fields from wearable Nanogenerators. *ACS Nano* 12:12533–12540
- Luo X, Shi W, Yu H, Xie Z, Li K, Cui Y (2018) Wearable carbon nanotube-based biosensors on gloves for lactate. *Sensors* 18:3398
- Mannoor MS, Tao H, Clayton JD, Sengupta A, Kaplan DL, Naik RR, Verma N, Omenetto FG, McAlpine MC (2012) Graphene-based wireless bacteria detection on tooth enamel. *Nat Commun* 3:763
- Mardonova M, Choi Y (2018) Review of wearable device technology and its applications to the mining industry. *Energies* 11:547
- Mehrotra P (2016) Biosensors and their applications—a review. *J Oral Biol Craniofacial Res* 6:153–159
- Mohanraj J, Durgalakshmi D, Rakkesh RA, Balakumar S, Rajendran S, Karimi-Maleh H (2020) Facile synthesis of paper based graphene electrodes for point of care devices: a double stranded DNA (dsDNA) biosensor. *J Colloid Interface Sci* 566:463–472
- Nakata S, Shiomi M, Fujita Y, Arie T, Akita S, Takei K (2018) A wearable pH sensor with high sensitivity based on a flexible charge-coupled device. *Nat Electron* 1:596
- Olesen BW (1982) Thermal comfort. *Tech Rev* 2:3–37
- Ota H, Chao M, Gao Y, Wu E, Tai L-C, Chen K, Matsuoka Y, Iwai K, Fahad HM, Gao W (2017) 3d printed “earable” smart devices for real-time detection of core body temperature. *ACS Sens* 2:990–997
- Park J, Kim J, Kim SY, Cheong WH, Jang J, Park YG, Na K, Kim YT, Heo JH, Lee CY (2018) Soft, smart contact lenses with integrations of wireless circuits, glucose sensors, and displays. *Sci Adv* 4:eaap9841
- Pegan JD, Zhang J, Chu M, Nguyen T, Park S-J, Paul A, Kim J, Bachman M, Khine M (2016) Skin-mountable stretch sensor for wearable health monitoring. *Nanoscale* 8:17295–17303
- Pickup JC, Hussain F, Evans ND, Rolinski OJ, Birch DJS (2005) Fluorescence-based glucose sensors. *Biosens Bioelectron* 20:2555–2565
- Pruvost M, Smit WJ, Montoux C, Poulin P, Colin A (2019) Polymeric foams for flexible and highly sensitive low-pressure capacitive sensors. *NPJ Flex Electron* 3:7

- Rathee K, Dhull V, Dhull R, Singh S (2016) Biosensors based on electrochemical lactate detection: a comprehensive review. *Biochem Biophys Rep* 5:35–54
- Rehman MM, Siddiqui GU, Doh YH, Choi KH (2017) Highly flexible and electroforming free resistive switching behavior of tungsten disulfide flakes fabricated through advanced printing technology. *Semicond Sci Technol* 32:95001
- Rinaldi A, Tamburrano A, Fortunato M, Sarto M (2016) A flexible and highly sensitive pressure sensor based on a PDMS foam coated with graphene nanoplatelets. *Sensors* 16:2148
- Rodger DC, Weiland JD, Humayun MS, Tai Y-C (2006) Scalable high lead-count parylene package for retinal prostheses. *Sensors Actuators B Chem* 117:107–114
- Sekine T, Sugano R, Tashiro T, Sato J, Takeda Y, Matsui H, Kumaki D, Dos Santos FD, Miyabo A, Tokito S (2018) Fully printed wearable vital sensor for human pulse rate monitoring using ferroelectric polymer. *Sci Rep* 8:4442
- Shan J, Li J, Chu X, Xu M, Jin F, Wang X, Ma L, Fang X, Wei Z, Wang X (2018) High sensitivity glucose detection at extremely low concentrations using a MoS₂-based field-effect transistor. *RSC Adv* 8:7942–7948
- Shinde A, Sahatiya P, Kadu A, Badhulika S (2019) Wireless smartphone-assisted personal healthcare monitoring system using a MoS₂-based flexible, wearable and ultra-low-cost functional sensor. *Flex Print Electron* 4:25003
- Siddiqui GU, Rehman MM, Yang Y-J, Choi KH (2017) A two-dimensional hexagonal boron nitride/polymer nanocomposite for flexible resistive switching devices. *J Mater Chem C* 5:862–871
- Singh E, Singh P, Kim KS, Yeom GY, Nalwa HS (2019) Flexible molybdenum disulfide (MoS₂) atomic layers for wearable electronics and optoelectronics. *ACS Appl Mater Interfaces* 11:11061–11105
- Steiner M-S, Dürkop A, Wolfbeis O (2011) Optical methods for sensing glucose. *Chem Soc Rev* 40:4805–4839
- Sundramoorthy AK, Wang Y-C, Gunasekaran S (2015a) Low-temperature solution process for preparing flexible transparent carbon nanotube film for use in flexible supercapacitors. *Nano Res* 8:3430–3445
- Sundramoorthy AK, Wang Y, Wang J, Che J, Thong YX, Lu ACW, Chan-Park MB (2015b) Lateral assembly of oxidized graphene flakes into large-scale transparent conductive thin films with a three-dimensional surfactant 4-sulfocalix [4] arene. *Sci Rep* 5:10716
- Trung TQ, Dang TML, Ramasundaram S, Toi PT, Park SY, Lee N-E (2018) A stretchable strain-insensitive temperature sensor based on free-standing elastomeric composite fibers for on-body monitoring of skin temperature. *ACS Appl Mater Interfaces* 11:2317–2327
- Wang S, Chinnasamy T, Lifson MA, Inci F, Demirci U (2016) Flexible substrate-based devices for point-of-care diagnostics. *Trends Biotechnol* 34:909–921
- Wu C, Zhang T, Zhang J, Huang J, Tang X, Zhou T, Rong Y, Huang Y, Shi S, Zeng D (2020) A new approach for an ultrasensitive tactile sensor covering an ultrawide pressure range based on the hierarchical pressure-peak effect. *Nanoscale Horiz* 5:541–552
- Xuan X, Yoon HS, Park JY (2018) A wearable electrochemical glucose sensor based on simple and low-cost fabrication supported micro-patterned reduced graphene oxide nanocomposite electrode on flexible substrate. *Biosens Bioelectron* 109:75–82
- Yamamoto Y, Yamamoto D, Takada M, Naito H, Arie T, Akita S, Takei K (2017) Efficient skin temperature sensor and stable gel-less sticky ECG sensor for a wearable flexible healthcare patch. *Adv Healthc Mater* 6:1700495
- Yan C, Wang J, Lee PS (2015) Stretchable graphene thermistor with tunable thermal index. *ACS Nano* 9:2130–2137
- Yang J, Yu J-H, Strickler JR, Chang W-J, Gunasekaran S (2013) Nickel nanoparticle–chitosan-reduced graphene oxide-modified screen-printed electrodes for enzyme-free glucose sensing in portable microfluidic devices. *Biosens Bioelectron* 47:530–538
- Yao H, Shum AJ, Cowan M, Lähdesmäki I, Parviz BA (2011) A contact lens with embedded sensor for monitoring tear glucose level. *Biosens Bioelectron* 26:3290–3296

- Yogeswaran U, Chen S-M (2008) A review on the electrochemical sensors and biosensors composed of nanowires as sensing material. *Sensors* 8:290–313
- Yoon Y, Lee G, Yoo K, Lee J-B (2013) Fabrication of a microneedle/CNT hierarchical micro/nano surface electrochemical sensor and its in-vitro glucose sensing characterization. *Sensors* 13:16672–16681
- Zaryanov NV, Nikitina VN, Karpova EV, Karyakina EE, Karyakin AA (2017) Nonenzymatic sensor for lactate detection in human sweat. *Anal Chem* 89:11198–11202
- Zhou HP, Ye X, Huang W, Wu MQ, Mao LN, Yu B, Xu S, Levchenko I, Bazaka K (2019) Wearable, flexible, disposable plasma-reduced graphene oxide stress sensors for monitoring activities in Austere environments. *ACS Appl Mater Interfaces* 11:15122–15132
- Zhu B, Niu Z, Wang H, Leow WR, Wang H, Li Y, Zheng L, Wei J, Huo F, Chen X (2014) Microstructured graphene arrays for highly sensitive flexible tactile sensors. *Small* 10:3625–3631
- Zhu C, Chortos A, Wang Y, Pfattner R, Lei T, Hinckley AC, Pochorovski I, Yan X, To JW-F, Oh JY (2018) Stretchable temperature-sensing circuits with strain suppression based on carbon nanotube transistors. *Nat Electron* 1:183
- Zou M, Ma Y, Yuan X, Hu Y, Liu J, Jin Z (2018) Flexible devices: from materials, architectures to applications. *J Semicond* 39:11010

Chapter 19

Self-Powered Biosensors in Medicine and Ecology



Yulia Victorovna Plekhanova, Sergei Evgenyevich Tarasov, Anna Evgenievna Kitova, Mikhail Alexandrovich Gutorov, and Anatoly Nikolaevich Reshetilov

Abstract Self-powered biosensors use the principle of a; an assayed substance in them also serves as the source of electric energy required for the device to operate. This makes it possible to simplify the design and avoid using external power supply sources. Self-powered biosensors were developed for medical analysis of compounds such as lactate, ethanol, glucose, thrombin, acetylcholine, and others. These devices can find wide application not only in medicine but also in fields like ecological monitoring. This will solve several tasks simultaneously: the cleanup of the environment, assessment of the number of contaminants, and generation of electric energy. This chapter considers the recent achievements in the field of autonomous power-supply biosensors and their advantages/drawbacks as compared with other types of biosensors.

Keywords Self-powered biosensors · Biofuel cell · Medicine · Ecological monitoring

19.1 Introduction

The development of modern biosensors requires a number of conditions to be fulfilled. In particular, devices should be compact and simple to use and ensure high sensitivity and speed of assay. Besides, they should be equipped with autonomous portable power supply sources to provide for the operation not only in the labora-

Y. V. Plekhanova (✉) · S. E. Tarasov · A. E. Kitova · A. N. Reshetilov (✉)
Laboratory of Biosensors, G.K. Skryabin Institute of Biochemistry and Physiology of Microorganisms, Pushchino Center for Biological Research of the Russian Academy of Sciences, Pushchino, Moscow Region, Russian Federation
e-mail: plekhanova@ibpm.pushchino.ru; anatol@ibpm.pushchino.ru

M. A. Gutorov
Gamma-DNA LLC, Territory of Skolkovo Innovation Centre, Moscow, Russia

tory but also on the sampling site. One of the solutions to this problem could be the use of self-powered biosensors. Energy sources, in this case, are part of the biosensor and are represented by biofuel cells. A device with an autonomous power supply source is an instrument operated without the use of an external storage battery or wireless energy transfer. Under ideal conditions, such a device is fully functional for a prolonged period (Reid and Mahbub 2020). The concept of biosensor devices based on electrochemical energy conversions in biofuel cells was first proposed by Katz et al. (2001). In such devices, the output power of the biofuel cells is directly proportional to the concentration of the analyte. Subsequently, it has been shown that this technology can also be introduced as an early warning system of biologically active compounds in aqueous systems (Kim et al. 2007; Liu et al. 2014). The current generated by the biofuel cells is a direct indication of the metabolic activity of electroactive bacteria at the anode. When the system is in a stable state determined as a constant electrical signal, any violations of the metabolism and bacterial growth evoke changes of current. If the working parameters, such as pH, temperature, and conductivity of the supplied solution are maintained constant, this change of current can correlate with the occurrence of a particular substance in the sample. This is the main principle of using biofuel cells as electrochemical microbial biosensors. The anodic biofilm of the biofuel cells acts as a recognition component (bioreceptor). Its reaction to specific stress (e.g., a toxicant in the feeding flow) affects the rate of electron flow to the anode and is converted to a change of current. In the biofuel cells, the excitation voltage is provided for the oxidation of fuel on the anode surface and a related reduction of the oxidant on the cathode surface, whereas other types of amperometric biosensors require an external voltage to oxidize the analyte (Lovley 2008). No external converters are required in the case of the biofuel cells because the presence of a contaminant in the supplied flow is immediately detected by a certain change of current in the system.

In medicine, the source of fuel for powering these biosensors can be metabolites in blood and other human fluids. The use of human fluids simultaneously solves several problems: (1) providing data about the content of compounds for diagnosing human health and (2) providing for energy to power biosensors and other devices required to maintain life activities (cardiac stimulators, pacemakers, neurostimulators, hearing and low-vision aids, implantable diagnostic, etc. systems).

Self-tolerant metabolic energy sources are an extremely promising power supply for autonomous bioelectronic devices that function in an implantable mode as well as without implantation. It is the absence of a highly efficient supply source that largely restricts the development of a technology for the fabrication of adaptive contact lenses, neurostimulators and hearing aids, and their entry into a market. A good deal of research showed a relationship between the content of analyzed substances in the blood and other fluids of the organism, which makes it possible, among other things, to stop using invasive methods of assay and to use other fluids, such as sweat, tears, etc. (Makaram et al. 2014; Nery et al. 2016) for assessing the human health status using biosensors, which can be fed by substances present in the assayed sample. The biofuel cell constituents are readily renewable – the environment is not contaminated at the replacement of spent anode and cathode; no com-

plex procedures are required to be carried out. Yet another advantage of biofuel cells as a source of energy is the use of biological and organic materials, which are practically inapplicable in any other industry.

This chapter examines recent developments of self-powered biosensors for the determination of a wide variety of compounds. Variants of using such devices are presented for assessment of human health (medicine, sports) and life standards (ecological monitoring) (Fig. 19.1). Special emphasis is made on the use of modern materials of electrodes and nanomaterials for improving the parameters of self-powered biosensors.

19.2 Materials Used for Modification of Biosensors

The modification of biosensors by various nanomaterials such as nanotubes (Cosnier et al. 2014), graphene (Karimi et al. 2015), gold nanoparticles (Ratautas and Dagsys 2019), etc. is widely used at present. This makes it possible to improve the characteristics of sensors: to increase the effective area of the surface, to enhance the sensitivity of electrodes, as well as to improve the kinetics of electron transport. Thus, for instance, a self-powered microRNA biosensor device based on enzymatic biofuel cells and cruciform DNA was presented by Wang et al. (2020). The basis of the cathode and anode were nanoparticles of graphene and gold in combination with sulfur and selenium. On the anode, glucose oxidase was immobilized. Potassium ferricyanide was immobilized on the biocathode as an electron transport mediator; cruciform DNA bioconjugate was used as a signal amplifier. The addition of microRNA evoked the reaction of hybridization between microRNA and DNA probe on the biocathode. The linear range of microRNA detection was 0.5–10,000 fM. Detection of microRNA in blood serum samples using a self-powered biosensor can be of great significance in clinical studies for early diagnosis of cancer diseases.

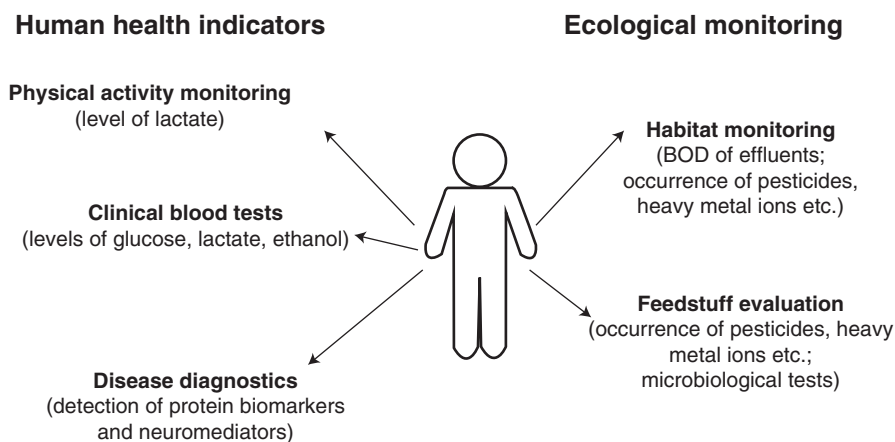


Fig. 19.1 Possible fields of application of self-powered biosensors

Han et al. (2015) proposed to use a self-powered biosensor based on a carbon nanotubes/Meldola's blue glucose dehydrogenase composite for the detection of p53 wild-type protein. In the presence of this protein, the biofuel cells' total power and level of current were observed to decrease, which enabled its detection in normal and cancer cell lysates without any extensive sample pretreatment/separation or specialized instruments.

Self-powered biosensors can utilize not only electrochemical signal converters. For instance, owing to the unique characteristics of piezoelectric materials, rapid response-time piezoelectric sensors are capable of efficiently measuring high-frequency dynamic signals and be rather promising for devices with autonomous power supply sources (Gu et al. 2019). Selvarajan et al. (2017) described the direct detection of cysteine by a self-powered device based on a film with BaTiO₃ nanoparticles possessing semiconductor and piezoelectric properties. The properties of the film's surface charge change depending on the concentration of cysteine. The linear range of detection was 10 μM–1 mM. The self-powered cysteine sensor based on an agarose/BaTiO₃ nanoparticle composite can be used for the diagnosis of chronic diseases, such as rheumatoid arthritis, Parkinson's disease, Alzheimer's disease, and even adverse pregnancy outcomes.

19.3 Practical Application of Self-Powered Biosensors in Medicine

Self-powered biosensors can be used in several fields of medical research. Such devices are used for laboratory studies of particular substances, for monitoring of physical activity indices (e.g., in sportspersons) and as implantable sensors. Here we wish to discuss in detail on the use of self-powered biosensors for assaying the concentrations of some important substances and biomarkers. Some examples of the developed self-powered biosensors are given in Table 19.1.

Wearable self-powered biosensors can be incorporated into articles of clothing, contact lenses, mouthguards, as well as plasters with microneedle arrays (Reid and Mahbub 2020). One of the directions in the development of wearable sensors is that of collectors of energy produced in the oxidation of various biological fluids' components (Bandodkar and Wang 2014). The use of biological fluids (in particular, human sweat) for the generation of electricity by wearable biofuel cells presents a wide range of possibilities and conditions for such tasks to be solved. However, progress in this field is limited by rather low power of supply sources, as well as by the lack of safe, thin, and elastic materials for providing the contact of the skin with wearable biofuel cells. Besides, analysis of, e.g., sweat, adds another task – volumes of sweat are, as a rule, rather insignificant, which requires miniature sensors for its analysis to be developed (Heikenfeld 2016). The recent achievements in the field of biosensors for analysis of the composition of sweat can be found in the reviews (Gao et al. 2016; Rocchitta et al. 2016; Neethirajan 2017).

Table 19.1 Applications of self-powered biosensors

Analyte	Recognition element	Power supply source	References
MicroRNA	Glucose oxidase	Biofuel cell and cruciform DNA	Fu-Ting Wang et al. (2020)
DNA in blood serum	Au-thiol binding the ssDNA probe on the surface of a cathode	Microbial fuel cell	Asghary et al. (2016)
Cysteine	BaTiO ₃ nanoparticles/agarose	Piezoelectric nanogenerator	Selvarajan et al. (2017)
Human immunoglobulin G	ZnO nanowire nanogenerator	Piezoelectric nanogenerator	Zhao et al. (2014)
Carcinoembryonic antigen	Conductive glass substrate with (PEDOT) layer/ molecularly imprinted polymer of polypyrrole	Photovoltaic cell	Tavares et al. (2019)
Lacrimal fluid/ lactate	Lactate dehydrogenase, NAD ⁺ cofactor, poly(methylene green)	Lactate-based biofuel cells	Reid et al. (2015)
Lactate	Lactate oxidase, dimethylferrocene-modified linear poly(ethyleneimine) hydrogel	Lactate-based biofuel cells	Hickey et al. (2016)
Ethanol in sweat	Alcohol oxidase, Prussian blue	Anodic enzyme reaction	Kim et al. (2016)
Thrombin	DNA bioconjugate containing glucose oxidase and aptamer	(glucose/O ₂) biofuel cells glucose-based biofuel cells	Wang et al. (2020)
Glucose in blood	Glucose oxidase and Prussian blue	Glucose-based biofuel cells	Aller-Pellitero et al. (2020)
Glucose	Glucose oxidase and Co ₃ O ₄ as electron acceptors (electron accepting material)	Photoelectrochemical detection	Çakıroğlu and Özacar (2018)
Glucose in interstitial fluid	Glucose oxidase and ferricyanide	Microneedle-based transdermal biosensor	Strambini et al. (2015)
Acetylcholine in plasma	Acetylcholinesterase	Anodic enzyme reaction	Moreira et al. (2017)
Chlorpyrifos	Acetylcholinesterase	Photoelectrochemical detection	Cheng et al. (2019)
BOD analysis	Microorganisms isolated from activated sludge	Microbial fuel cell	Pasternak et al. (2017)
Heavy metal ions	Activated sludge	Microbial fuel cell	Yu et al. (2017)
<i>Vibrio parahaemolyticus</i>	Aptamer/glucose dehydrogenase	Enzymatic biofuel cell	Yu et al. (2020)
	Aptamer/glucose dehydrogenase/polythionine/ carbon nanotubes/gold nanoparticle bioanode		

(continued)

Table 19.1 (continued)

Analyte	Recognition element	Power supply source	References
Ascorbic acid	ITO electrodes/carbon nanomaterials/Prussian blue electrochromic display	Ascorbic acid/O ₂ biofuel cells	Zloczewska et al. (2014)
Bisphenol	Laccase/MWCNTs	Enzymatic biofuel cell	Li et al. (2020)
Herbicides	Thylakoid membranes at the bioanode/platinum air cathode	Biosolar cell	Rasmussen and Minteer (2013)

Reid et al. (2015) reported biofuel cells in which lacrimal fluid serves as a fuel. The developed biofuel cells are the basis for the development of self-powered electronic contact lenses and ophthalmological devices with an integrated power supply source. Recent developments in this field are also presented in Reid et al. (2016) and Rasmussen et al. (2016).

19.3.1 Detection of Glucose

This section considers the application of self-powered biosensors for clinical diagnosis of particular human metabolites. Determination of glucose in physiological fluids is attributed to widespread clinical analyses and is of special importance at the diagnosis and monitoring of diabetes mellitus and some other diseases.

Recently, electrochromic materials are gaining great importance in the development of self-powered biosensors owing to their optoelectronic properties. Aller-Pellitero et al. (2020) presented a glucose biosensor based on glucose oxidase and Prussian blue. Thin layers of electrochromic material based on semiconducting antimony and tin oxide particles coated with Prussian blue were applied by screen printing onto the electrodes. The glucose biosensor was connected to an electrochromic display, and the system operated as a galvanic cell. The special co-planar design of the device and the use of a polyelectrolyte gel provided for an efficient separation between the sample and the electrochromic component, which made it possible to avoid interference in the operation of the device even when using color samples, e.g., blood. Polymer electrolyte gel was printed on top of the display, replacing the conventional aqueous supporting electrolytes used in most electroanalytical experiments and thus allowing the fabrication of a fully printed solid-state analytical device. In the presence of glucose (within the range of 2.5–10 mM), the device provides a visual readout that can be read by the naked eye.

Glucose biosensors are the most in-demand and maximally commercialized type of sensors at present, so the development of self-powered glucose sensors have attracted the attention of many investigators. Thus, Slaughter and Kulkarni (2019) presented a miniature bioelectrochemical device, based on direct electron transfer, for monitoring of glucose level in blood plasma (Fig. 19.2). Lv et al. (2018)

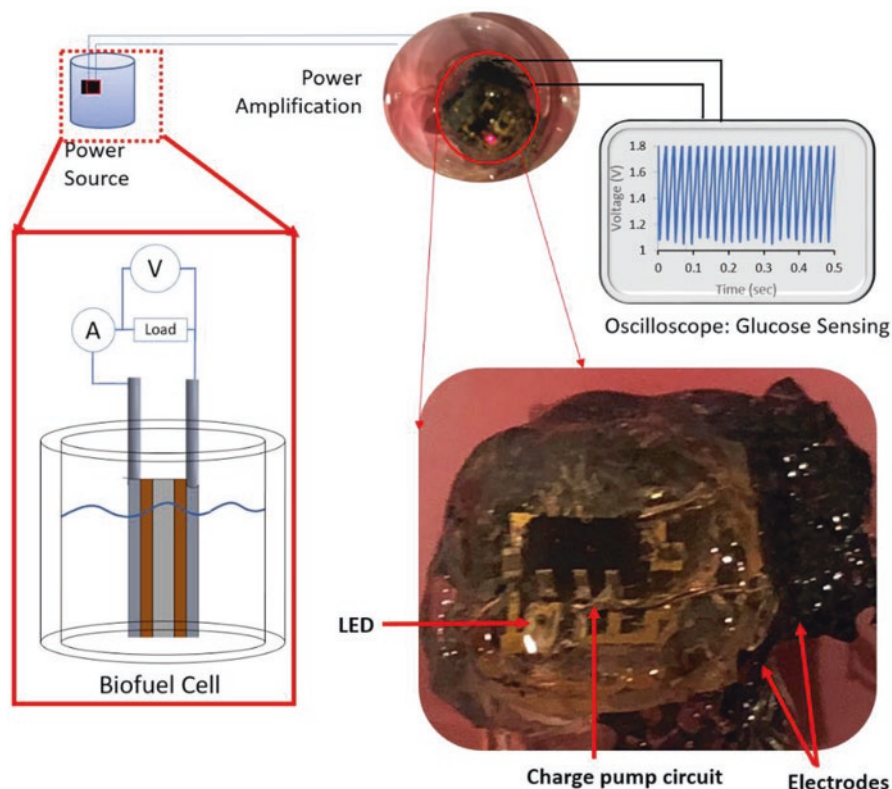


Fig. 19.2 Experimental setup of glucose biofuel cell and glucose sensing. Charge pump circuit consisting of a $0.1 \mu\text{F}$ capacitor functioning as a transducer, where the charge pump circuit is powered by the electrical power generated by the glucose biofuel cell. (Reproduced from Slaughter and Kulkarni 2019 under a Creative Commons Attribution 4.0 License. Published by Multidisciplinary Digital Publishing Institute)

described a biosensor cathode additionally modified by a composite of laccase, gold nanoparticles, and carbon nanotubes. For the detection of glucose in physiological fluids, Kim et al. (2018) used light sources from daily life environments such as fluorescent light and sunlight. On the whole, improvements of glucose sensors are aimed to simplify the assaying techniques and to develop wearable devices, using which the levels of glucose in the organism can be measured noninvasively.

19.3.2 Detection of Lactate

Detection of lactate is of great importance both in clinical research and for sports medicine. The level of lactate in human blood at rest is within the range of $0.5\text{--}1.5 \text{ mM}$ (Phypers and Pierce 2006); at physical exercises, it reaches much

higher values (20–25 mM) (Stanley et al. 1985), which is important in sports medicine for tracking the athlete's fitness level. The content of lactate in blood is a health indicator because a lactate level increase under normal conditions is a cause of a number of pathologies (Valenza et al. 2005). This makes evident the importance of this detection in medical analyses.

Hickey et al. (2016) presented a self-powered amperometric lactate biosensor containing dimethyl ferrocene-modified linear poly(ethyleneimine) hydrogel; it performed the function of an immobilization matrix as well as that of a mediator providing for electron transfer to the cathode containing bilirubin oxidase and from lactate oxidase at the anode. The linear range of this biosensor was 0–5 mM lactate at a sensitivity of $45 \mu\text{A cm}^{-2} \text{mM}^{-1}$. The specific power of the biosensor was $122 \mu\text{W cm}^{-2}$ and current density, $657 \mu\text{A cm}^{-2}$. Open circuit voltage was 0.57 V, which is sufficient to provide for the operation of the biosensor and acts as a supplemental power supply source for external electronic devices with small power consumption.

Baingane and Slaughter (2017) described an electrochemical lactate biosensor in which the anode and cathode are modified by D-lactate dehydrogenase and bilirubin oxidase, respectively. A 10 pF capacitor was integrated via a charge pump circuit to the biofuel cell to realize the self-powered lactate biosensor with a footprint of $1.4 \text{ cm} \times 2 \text{ cm}$. The charge pump enabled the boosting of the biofuel cell voltage in bursts of 1.2–1.8 V via the capacitor. By observing the burst frequency of a 10 pF capacitor, the exact concentration of lactic acid was deduced. The authors demonstrated a lactate self-powered biosensor capable of noninvasive real-time monitoring of a key metabolite of stress or trauma (Fig. 19.3).

19.3.3 *Detection of Ethanol*

Exceeding the blood alcohol concentration is the cause of road accidents and constitutes a danger for human health. In this regard, there is a need to create exact and simple-to-use devices for its detection. Yet, only a few works have dealt with the development of self-powered biosensors for the detection of ethanol. Possibly, this is because concentrations of alcohol in biological fluids are, as a rule, insufficient to provide for continuous generation of electric energy and the operation of a biosensor.

Kim et al. (2016) developed a wearable tattoo biosensor for noninvasive monitoring of alcohol in induced sweat. The wearable platform for monitoring was an iontophoretic biosensor system in the form of a temporary tattoo on flexible support equipped with a wireless communication system. Perspiration is stimulated by pilocarpine iontophoresis, and the amperometric detection of ethanol in induced sweat is provided for by the operation of alcohol dehydrogenase and Prussian blue.

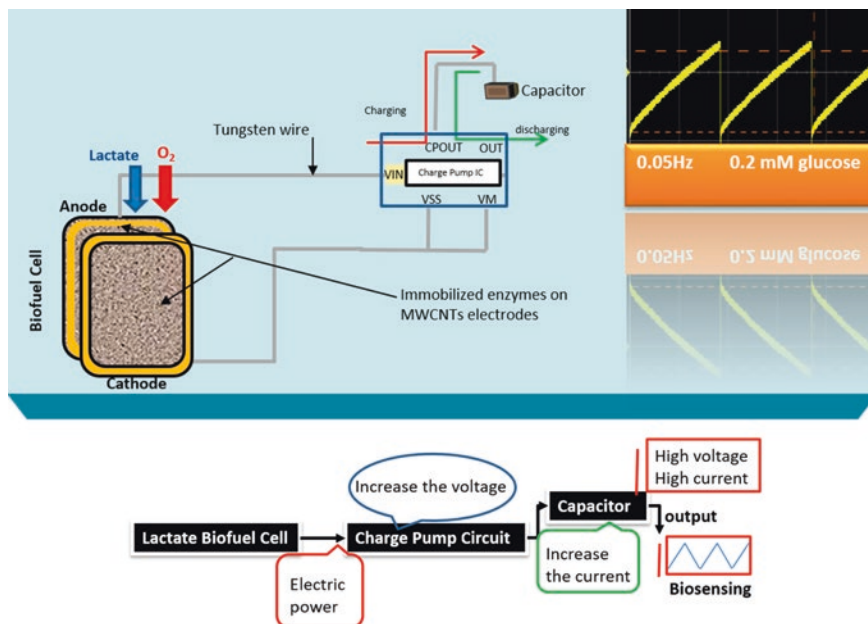


Fig. 19.3 The self-powered electrochemical lactate biosensor based on the integration of enzymatic lactate biofuel cell with a charge pump and capacitor circuits. (Reproduced from Baingane and Slaughter 2017 under a Creative Commons Attribution 4.0 License. Published by Multidisciplinary Digital Publishing Institute)

19.3.4 Detection of Proteins

Early diagnoses of various diseases make it necessary to register protein biomarkers with very low levels of concentration in the patient's biological fluid, of the order of 10^{-13} M and lower. Aptamers are represented by small (usually from 20 up to 60 nucleotides) single-stranded RNA or DNA molecules capable of binding the target molecule with high affinity and specificity. To date, a large number of aptamers to various targets have been obtained, ranging from simple inorganic molecules to large protein complexes and entire cells (Lakhin et al. 2013). Aptamers are widely used as a recognizing component in biosensors, as they have high stability and specificity while being reasonably cheap (Song et al. 2012).

Thrombin (a specific serine protease) plays an important role in the coagulation cascade by splitting fibrinogen to form fibrin and stimulating the aggregation of thrombocytes (Crawley et al. 2007). Low concentrations of thrombin have a protective effect for cells; however, its higher concentrations may damage them. For this reason, thrombin is considered to be the most important biomarker of cardiovascular diseases, inflammations, and tissue regeneration. These studies are basic for the creation of self-powered biosensors. Thus, Wang et al. (2020a) developed an electrochemical sensor platform with an autonomous power supply for detecting throm-

bin based on a single-chamber enzymic (glucose / O₂) biofuel cell. Carbon paper was modified by nanoparticles of tin sulfide (SnS₂ nanoflowers) and gold and a DNA-carbon nanotube conjugate. The sandwich structure of the bioanode made it possible to considerably increase the open-circuit voltage evoked by combining the protein with DNA bioconjugate that contains glucose oxidase and the aptamer. The enzymic biofuel cell-based aptasensor catalyzed the oxidation of glucose in the presence of thrombin. The range of detected thrombin concentrations was 0.02–5 ng/mL. This hybrid device, in which a storage element based on a capacitor and a biofuel cell is used, can be also used for assaying other proteins if the aptamer is replaced by another suitable aptamer, which is of importance in clinical research.

Wang et al. (2020b) developed a self-powered biosensor for the detection of platelet-derived growth factor-BB (PDGF-BB), which is considered to be an important biomarker of neoplasms. Ultra-thin nitrogen-doped carbon shell/gold nanoparticles (N-UHCS/AuNPs) were coated with bilirubin oxidase to form a biocathode. As a bioanode, a SiO₂@gold nanoparticle-aptamer (SiO₂@AuNPs-ssDNA) composite was used. In the absence of PDGF-BB, the open-circuit voltage (E_{OCV}) is low due to the effect of steric hindrance. When PDGF-BB is added, SiO₂@AuNPs-ssDNA falls away from the bioanode because of the recognition of PDGF-BB by the DNA. Thus, glucose can reach the active sites of glucose oxidase, and much bigger E_{OCV} is achieved. This bioassay needs no external power supply and shows high sensitivity and selectivity, exhibiting a great promise as a powerful tool for sensitive detection of tumor markers.

19.3.5 Detection of Acetylcholine

Diseases caused by brain disorders are due to a drop in the level of important neurotransmitters. Monitoring of their biomarkers is important for the diagnosis and therapy of such diseases (Si and Song 2018). Moreira et al. (2017) reported a hybrid (acetylcholine/oxygen) self-powered biofuel cell based on an enzymatic anode and a platinum cathode for detection of acetylcholine in plasma. Acetylcholinesterase was immobilized on a nanostructured electrode from porous gold on the surface of platinum. The anode produced in this way was used in a miniature membrane-free flow-through biofuel cell. The peak power generated by the biofuel cell was 4 nW at a voltage of 260 mV and a current density of 9 $\mu\text{A cm}^{-2}$. The response time was 3 min. The obtained results are promising for the diagnosis of Alzheimer's disease and present an alternative approach to the existing methods.

Other neuromodulators such as glutamate as well as their precursors, e.g., l-3,4-dihydroxyphenylalanine (the dopamine precursor), can also serve as possible sources for electric energy generation (Gonzalez-Solino and Lorenzo 2018).

19.4 Self-Powered Biosensors in Ecological Monitoring

Biofuel cells have enormous analytical potential as biosensors, including for assaying the quality of water. Some examples of the developed self-powered biosensor models used for ecological monitoring are presented in Table 19.1. The main parameter of effluent water contamination is biochemical oxygen demand (BOD). The traditional BOD determination methods require a prolonged procedure of the analysis, whereas biosensors can determine the BOD level in mere minutes. Microbial biofuel cells (MFC) are promising tools for the analysis of effluents. If the MFC functions at an unsaturated concentration of fuel, a change of organic substance fed to the system evokes a change in the amount of generated electrons and, therefore, a change of the output current. Thus, the current generated by the MFC correlated with the BOD of the supplied solution (Lorenzo et al. 2009). The first MFC-based BOD sensor was described by Karube and coauthors in 1977. As easily oxidizable organic compounds are always present in effluents, they can serve as the basis for feeding the biosensors that assay the concentrations of contaminants. Pasternak and coauthors reported a self-powered autonomous BOD biosensor for online water quality measurement based on signal frequency (Pasternak et al. 2017). Contamination of water with urine can be detected using this sensor. As electroactive microorganisms are used to produce this biosensor, it is self-powered and can operate autonomously for 5 months.

Compounds analyzed in water can be pesticides, heavy metal ions, surfactants, and petroleum products. For instance, Cheng et al. (2019) presented a visible-light-driven self-powered photoelectrochemical biosensor for the detection of organophosphate pesticides. The biosensor was fabricated from indium oxide and titanium components, which were its basis. The anode included titanium dioxide nanoparticles as photoactive material, nitrogen-doped carbon quantum dots as photosensitizer, and acetylcholinesterase as a biorecognition element. Acetylcholinesterase catalyzed the hydrolysis of acetylcholine chloride followed by the generation of thiocholine, as the result of which the biosensor response as a photocurrent increased significantly. The bioactivity of acetylcholinesterase is inhibited by organophosphorus pesticides, as the result of which the concentration of thiocholine decreases leading to a decrease of photocurrent. Chlorpyrifos was chosen as a model compound; the linear range of its detection was 0.001–1.5 $\mu\text{g mL}^{-1}$.

Rasmussen and Minter (2013) developed a self-powered biosensor for the detection of herbicides in water. This sensor was able to detect several commercial herbicides, including atrazine, bromacil, and diuron with a linear response up to concentrations of 15 mg L^{-1} and limits of detection below 0.5 mg L^{-1} , which are below the EPA limits. This biosensor does not require large instrumentation, which allows for its easy use in the field and requires no sample preparation to concentrate the desired compounds.

Yu et al. (2017) proposed to use a self-powered microbial fuel cell-based biosensor for the detection of heavy metal ions in aqueous environments. The presence of heavy metals in water inhibited the respiratory activity of electroactive bacteria at

the bioanode and made it possible to determine the concentrations of Cu^{2+} , Hg^{2+} , Zn^{2+} , Cd^{2+} , Pb^{2+} , and Cr^{3+} ions by the decrease of the level of current generated by the fuel cell.

Another important parameter of water quality is microbiological indices. Yu et al. (2020) proposed an enzymatic self-powered biosensor with the visual self-checking function for the ultrasensitive detection of *Vibrio parahaemolyticus* with a low detection limit of 2 CFU mL^{-1} . The proposed biosensor was composed of the aptamer/glucose dehydrogenase/polythionine/carbon nanotubes/gold nanoparticles bioanode, the mediated Prussian blue/Prussian white electrode with the visual self-checking function, and the bilirubin oxidase/carbon nanotubes biocathode.

19.5 Conclusion

Autonomous power-supply modules operated continuously without external power sources should become an integral part of future wearable bioelectronics. The developed self-powered systems will help in filling this niche of devices. Besides, the real application of wearable bioelectronics in the monitoring of important health-status information requires a wireless digital system for processing and transmission of signals to large distances.

The advantages of wearable biosensors are their miniature size, highly accurate analysis, and inexpensive production. Wearable biosensors open new possibilities for the diagnosis and therapy of a number of diseases in medicine and can be used for monitoring the health status of both sportspeople in training and healthy individuals wishing to monitor their health in their daily lives. Self-powered biosensors also open broad prospects of their use in ecological monitoring. Despite the progress in this field of research, several problems remain unsolved. This is the integration of biosensors into wearable devices, their miniaturization and autonomous operation, the reduction of interference in the operation of these devices, simplicity of use, etc. In all these tasks, self-powered biosensors, which possess unique characteristics and enormous potential, make it possible to find solutions or approach them.

References

- Aller-Pellitero M, Santiago-Malagón S, Ruiz J, Alonso Y, Lakard B, Hihn J-Y, Guirado G, del Campo FJ (2020) Fully-printed and silicon free self-powered electrochromic biosensors: towards naked eye quantification. *Sensors Actuators B Chem* 306:127535
- Asghary M, Raouf JB, Rahimnejad M, Ojani R (2016) A novel self-powered and sensitive label-free DNA biosensor in microbial fuel cell. *Biosens Bioelectron* 82:173–176
- Baingané A, Slaughter G (2017) Self-powered electrochemical lactate biosensing. *Energies* 10(10):1582

- Bandodkar AJ, Wang J (2014) Non-invasive wearable electrochemical sensors: a review. *Trends Biotechnol* 32(7):363–371
- Çakıroğlu B, Özacar M (2018) A self-powered photoelectrochemical glucose biosensor based on supercapacitor Co_3O_4 -CNT hybrid on TiO_2 . *Biosens Bioelectron* 119:34–41
- Cheng W, Zheng Z, Yang J, Chen M, Yao Q, Chen Y, Gao W (2019) The visible light-driven and self-powered photoelectrochemical biosensor for organophosphate pesticides detection based on nitrogen doped carbon quantum dots for the signal amplification. *Electrochim Acta* 296:627–636
- Cosnier S, Holzinger M, Le Goff A (2014) Recent advances in carbon nanotube-based enzymatic fuel cells. *Front Bioeng Biotechnol* 2:45
- Crawley JTB, Zanardelli S, Chion CKNK, Lane DA (2007) The central role of thrombin in hemostasis. *J Thromb Haemost* 5:95–101
- Di Lorenzo M, Curtis TP, Head IM, Scott K (2009) A single-chamber microbial fuel cell as a biosensor for wastewaters. *Water Res* 43:3145–3154
- Gao W, Nyein HYY, Shahpar Z, Tai L-C, Wu E, Bariya M, Ota H, Fahad HM, Chen K and Javey A (2016) Wearable sweat biosensors. *IEEE Int Electron Devices Meeting (IEDM)*, San Francisco: 6.6.1–6.6.4
- Gonzalez-Solino C, Lorenzo M (2018) Enzymatic fuel cells: towards self-powered implantable and wearable diagnostics. *Biosensors* 8(1):11
- Gu Y, Zhang T, Chen H, Wang F, Pu Y, Gao C, Li S (2019) Mini review on flexible and wearable electronics for monitoring human health information. *Nanoscale Res Lett* 14:263–278
- Han Y, Chabu JM, Hu S, Deng L, Liu Y-N, Guo S (2015) Rational tuning of the electrocatalytic nanobiointerface for a “turn-off” biofuel-cell-based self-powered biosensor for p53 protein. *Chem Eur J* 21(37):13045–13051
- Heikenfeld J (2016) Technological leap for sweat sensing. *Nature* 529:475–476
- Hickey DP, Reid RC, Milton RD, Minter SD (2016) A self-powered amperometric lactate biosensor based on lactate oxidase immobilized in dimethylferrocene-modified LPEI. *Biosens Bioelectron* 77:26–31
- Karimi A, Othman A, Uzunoglu A, Stanciu L, Andreescu S (2015) Graphene based enzymatic bioelectrodes and biofuel cells. *Nanoscale* 7:6909–6923
- Karube I, Matsunaga T, Mitsuda S, Suzuki S (1977) Microbial electrode BOD sensors. *Biotechnol Bioeng* 19(10):1535–1547
- Katz E, Bückmann AF, Willner I (2001) Self-powered enzyme-based biosensors. *J Am Chem Soc* 123:10752–10753
- Kim M, Hyun MS, Gadd GM, Kim HJ (2007) A novel biomonitoring system using microbial fuel cells. *J Environ Monit* 9:1323–1328
- Kim J, Jeeran I, Imani S, Cho TN, Bandodkar A, Cinti S, Mercier PP, Wang J (2016) Noninvasive alcohol monitoring using a wearable tattoo-based iontophoretic-biosensing system. *ACS Sensors* 1:1011–1019
- Kim K, Kim H, Jang H, Park J, Jung GY, Kim M-G (2018) Self-powered biosensors using various light sources in daily life environments: integration of p-n heterojunction photodetectors and colorimetric reactions for biomolecule detection. *ACS Appl Mater Interfaces* 10(46):39487–39493
- Lakhin AV, Tarantul VZ, Gening LV (2013) Aptamers: problems, solutions and prospects. *Acta Nat* 5(4):34–43
- Li X, Li D, Zhang Y, Lv P, Feng Q, Wei Q (2020) Encapsulation of enzyme by metal-organic framework for single-enzymatic biofuel cell-based self-powered biosensor. *Nano Energy* 68:104308. <https://doi.org/10.1016/j.nanoen.2019.104308>
- Liu B, Lei Y, Li B (2014) A batch-mode cube microbial fuel cell based “shock” biosensor for wastewater quality monitoring. *Biosens Bioelectron* 62:308–314
- Lovley DR (2008) The microbe electric: conversion of organic matter to electricity. *Curr Opin Biotechnol* 19:564–571

- Lv P, Zhou H, Mensah A, Feng Q, Wang D, Hu X, Wei Q (2018) A highly flexible self-powered biosensor for glucose detection by epitaxial deposition of gold nanoparticles on conductive bacterial cellulose. *Chem Eng J* 351:177–188
- Makaram P, Owens D, Aceros J (2014) Trends in nanomaterial-based non-invasive diabetes sensing technologies. *Diagnostics* 4(2):27–46
- Moreira FTC, Sale MGF, Di Lorenzo M (2017) Towards timely Alzheimer diagnosis: a self-powered amperometric biosensor for the neurotransmitter acetylcholine. *Biosens Bioelectron* 87:607–614
- Neethirajan S (2017) Recent advances in wearable sensors for animal health management. *Sens Bio-Sens Res* 12:15–29
- Nery EW, Kundys M, Jeleń PS, Jönsson-Niedziółka M (2016) Electrochemical glucose sensing: is there still room for improvement? *Anal Chem* 88(23):11271–11282
- Pasternak G, Greenman J, Ieropoulos I (2017) Self-powered, autonomous biological oxygen demand biosensor for online water quality monitoring. *Sensors Actuators B Chem* 244:815–822
- Phyers B, Pierce JT (2006) Lactate physiology in health and disease. *Continuing Edu Anaesthesia, Critical Care Pain* 6(3):128–132
- Rasmussen M, Minteer SD (2013) Self-powered herbicide biosensor utilizing thylakoid membranes. *Anal Methods* 5(5):1140
- Rasmussen M, Abdellaoui S, Minteer SD (2016) Enzymatic biofuel cells: 30 years of critical advancements. *Biosens Bioelectron* 76:91–102
- Ratautas D, Dagys M (2019) Nanocatalysts containing direct electron transfer-capable oxidoreductases: recent advances and applications. *Catalysts* 10(1):9
- Reid RC, Mahbub I (2020) Wearable self-powered biosensors. *Curr Opin Electrochem* 19:55–62
- Reid RC, Minteer SD, Gale BK (2015) Contact lens biofuel cell tested in a synthetic tear solution. *Biosens Bioelectron* 68:142–148
- Reid RC, Jones SR, Hickey DP, Minteer SD, Gale BK (2016) Modeling carbon nanotube connectivity and surface activity in a contact lens biofuel cell. *Electrochim Acta* 203:30–40
- Rocchitta G, Spanu A, Babudieri S, Latte G, Madeddu G, Galleri G, Nuvoli S, Bagella P, Demartis MI, Fiore V, Manetti R, Serra PA (2016) Enzyme biosensors for biomedical applications: strategies for safeguarding analytical performances in biological fluids: a review. *Sensors* 16:780
- Selvarajan S, Alluri NR, Chandrasekhar A, Kim S-J (2017) Direct detection of cysteine using functionalized BaTiO₃ nanoparticles film based self-powered biosensor. *Biosens Bioelectron* 91:203–210
- Si B, Song E (2018) Recent advances in the detection of neurotransmitters. *Chemosensors* 6(1):1
- Slaughter G, Kulkarni T (2019) Detection of human plasma glucose using a self-powered glucose biosensor. *Energies* 12(5):825
- Song K-M, Lee S, Ban C (2012) Aptamers and their biological applications. *Sensors* 12:612–631
- Stanley WC, Gertz EW, Wisneski JA, Morris DL, Neese RA, Brooks GA (1985) Systemic lactate kinetics during graded exercise in man. *Am J Physiol* 249(6):E595–E602
- Strambini LM, Longo A, Scarano S, Prescimone T, Palchetti I, Minunni M, Giannesi D, Barillaro G (2015) Self-powered microneedle-based biosensors for pain-free high-accuracy measurement of glycaemia in interstitial fluid. *Biosens Bioelectron* 66:162–168
- Tavares APM, Truta LAANA, Moreira FTC, Carneiro LPT, Sales MGF (2019) Self-powered and self-signalled autonomous electrochemical biosensor applied to cancer embryonic antigen determination. *Biosens Bioelectron* 140:111320
- Valenza F, Aletti G, Fossali T, Chevallard G, Sacconi F, Irace M, Gattinoni L (2005) Lactate as a marker of energy failure in critically ill patients: hypothesis. *Crit Care* 9(6):588–593
- Wang F-T, Wang Y-H, Xu J, Huang K-J, Liu Z-H, Lu Y-F, Wang S-Y, Han Z-W (2020) Boosting performance of self-powered biosensing device with high-energy enzyme biofuel cells and cruciform DNA. *Nano Energy* 68:104310
- Wang Y, Wang F, Han Z, Huang K, Wang X, Liu Z, Wang S, Lu Y (2020a) Construction of sandwiched self-powered biosensor based on smart nanostructure and capacitor: toward multiple signal amplification for thrombin detection. *Sensors Actuators B Chem* 304:127418

- Wang F-T, Wang Y-H, Xu J, Huang K-J (2020b) High-energy sandwiched-type self-powered biosensor based on DNA bioconjugates and nitrogen doped ultra-thin carbon shell. *J Mater Chem B*. <https://doi.org/10.1039/c9tb02574j>
- Yu D, Bai L, Zhai J, Wang Y, Dong S (2017) Toxicity detection in water containing heavy metal ions with a self-powered microbial fuel cell-based biosensor. *Talanta* 168:210–216
- Yu W, Kong X, Gu C, Gai P, Li F (2020) Ultrasensitive self-powered biosensors with visual self-checking function for pathogenic bacteria detection. *Sensors Actuators B Chem* 307:127618
- Zhao Y, Deng P, Nie Y, Wang P, Zhang Y, Xing L, Xue X (2014) Biomolecule-adsorption-dependent piezoelectric output of ZnO nanowire nanogenerator and its application as self-powered active biosensor. *Biosens Bioelectron* 57:269–275
- Zloczewska A, Celebanska A, Szot K, Tomaszewska D, Opallo M, Jönsson-Niedziolka M (2014) Self-powered biosensor for ascorbic acid with a Prussian blue electrochromic display. *Biosens Bioelectron* 54:455–461

Chapter 20

Self-Powered Implantable Biosensors: A Review of Recent Advancements and Future Perspectives



Pavel M. Gotovtsev, Yulia M. Parunova, Christina G. Antipova,
Gulfia U. Badranova, Timofei E. Grigoriev, Daniil S. Boljshin,
Maria V. Vishnevskaya, Evgeny A. Konov, Ksenia I. Lukanina,
Sergei N. Chvalun, and Anatoly Nikolaevich Reshetilov

Abstract Biosensors became one of the promising technologies in recent years. Wide applications and active development of related technologies lead to rising number of biosensors-related publications. A lot of them focused on the implantable biosensors that can help to operate future implantable medical devices. One of the main issues for implantable biosensors became power supply. In this chapter, several perspective approaches for the development of self-power biosensors are discussed. We have presented an overview of power generation approaches that can be applied in the case of implantable biosensors applications. It is worth mentioning that bioelectrochemical systems can be very powerful, but their influence on the organism is still not fully clear. Also, an overview of recent research in the field of electroconductive materials for implantable bioelectrochemical systems, with both biofuel cells and biosensors application, is presented. Moreover, a variety of approaches for material development from carbon nanomaterials to the polymeric systems have been described; and finally, some novel approaches for self-powered implantable systems are discussed.

Keywords Biosensors · Bioelectronics · Implantable devices · Energy harvesting · Flexible electronics · Biocompatible materials

P. M. Gotovtsev (✉) · Y. M. Parunova · C. G. Antipova · G. U. Badranova · T. E. Grigoriev ·
M. V. Vishnevskaya · E. A. Konov · K. I. Lukanina · S. N. Chvalun
National Research Centre “Kurchatov Institute”, Moscow, Russia

D. S. Boljshin
Physical Faculty, Lomonosov Moscow State University, Moscow, Russia

A. N. Reshetilov
Laboratory of Biosensors, G.K. Skryabin Institute of Biochemistry and Physiology of
Microorganisms, Pushchino Center for Biological Research of the Russian Academy of
Sciences, Pushchino, Moscow Region, Russian Federation

Nomenclature

BFC	biofuel cell
CND	carbon nanodots
CNT	carbon nanotubes
GO	graphene oxide
PDMS	polydimethylsiloxane
PEDOT PSS	poly-(3,4-ethylene dioxothiophene) poly- styrene sulfonate
PI	polyimide
PTFE	polytetrafluoroethylene
PVDF	polyvinylidene fluoride

20.1 Introduction

The development of different implantable medical devices became common today. There are a number of different sensors, pacemakers, neuroimplants, and micro-pumps presented in the scientific literature (Ko 2012; Joung 2013; Meng and Sheybani 2014; Li et al. 2019). Several limitations are slowing the wide application of such devices particularly the absence of constant lifelong power supply. Figure 20.1 illustrates the recent approaches for the power supply of implantable devices. Those approaches can be divided into three:

1. Different types of batteries
2. Energy transfer system both wireless and through contact surface electrodes
3. Implantable energy generators

The first two approaches can be combined—energy transfer systems widely used for recharging implanted batteries. But significant interest today is focused on energy generators due to the possibility to provide lifelong implantation (Vostrikov et al. 2019). In this chapter, we will focus on the electrical generation system for implantable biosensors. Such generators can be operated as a joint system with biosensors solving both and power supply and signal processing operations.

Implantable energy generators became an object of significant interest in recent years (Halámková et al. 2012; Mano and De Poulpiquet 2018). This interest is based on the active development of the different active devices and sensors both implantable (Jandial and Hoshide 2017; Karagkiozaki et al. 2013; Musk 2019) and non-implantable (Clement et al. 2011; Kay and Wilks 2015). Such electrical generators can be of different types (Dagdeviren et al. 2017):

1. Generators based on the use of the mechanical energy of organs, tissues, and liquids;
2. Different thermoelectric generators;

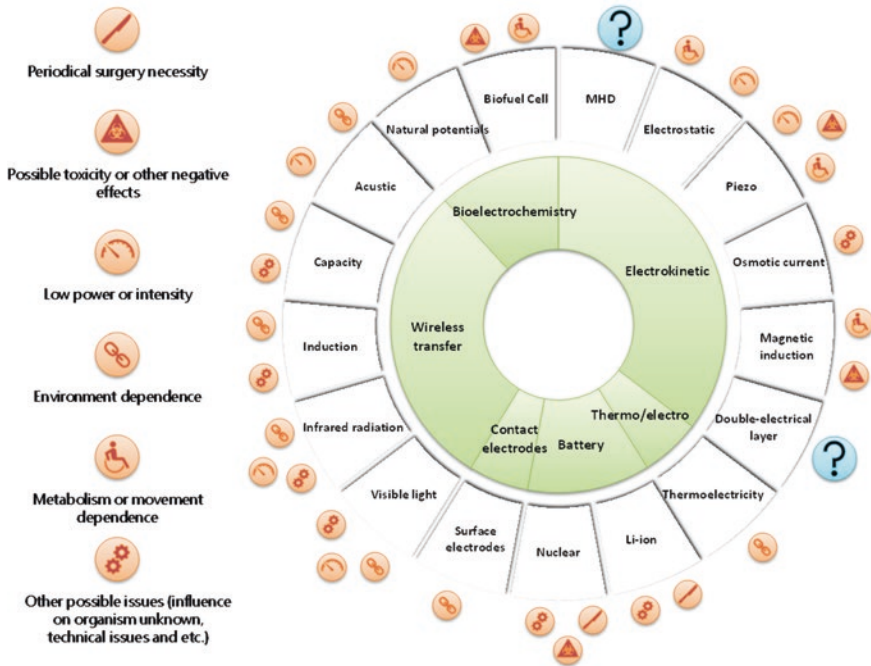


Fig. 20.1 Recent approaches for power supply of implantable devices

3. Generators based on the use of the chemical energy to generate electricity by application of fuel cells with different catalyzers.

There are a number of different generators developed in laboratories in recent years (Fan et al. 2012; Dagdeviren et al. 2017). Enzyme biofuels cells (BFC) are most discussed in recent decades (Dagdeviren et al. 2017). Those devices can generate electrical energy by consumption of energy-rich chemicals like glucose and oxygen (Gotovtsev et al. 2018). Different physiological liquids are discussed as possible glucose source for enzyme BFC. The most popular one is the blood where glucose concentration can be as high as several mM in normal conditions (Ben Amar et al. 2015). Also, liquids in abdominal cavities (Cosnier et al. 2014), secreted liquids like sweat (Lv et al. 2018) and tears (Rasmussen et al. 2015), and cerebrospinal fluid (Rapoport et al. 2012) are under consideration. The cerebrospinal fluid became the object of high interest due to the intensive development of neuroimplants (Rizea et al. 2019). The feature of neuroimplants maintenance is related to the minimization of neurosurgical procedures that lead in turn to the interest to lifelong implantation (Koch et al. 2019; Zhao et al. 2019), with lifelong power source operation. In this case, cerebrospinal fluid with glucose concentration about 2.8–3.9 mM (Clifford Schold et al. 1980; Whitehead 2019) seems to be a very perspective substrate for enzyme BFC.

Today there is no data concerning BFC influence of the nearby organs and tissues via local glucose consumption (Dagdeviren et al. 2017). Recent experiments showed that in the case of laboratory rats, 100-day implantation does not provide any sufficient negative influence (Zebda et al. 2013). Also, to predict the operation of BFC, several approaches in mathematical modeling were used in recent years (Korth et al. 2015; Pankratova and Gorton 2017; Reshetilov et al. 2017b). Those approaches can give a possibility at least to calculate glucose consumption by BFC for further discussion of its influence on the tissues. Thus, it is possible to combine glucose biosensor and generator in one system.

Thermoelectric generators are interesting for implantable devices power supply because electric generation does not correlate with metabolism directly (Vostrikov et al. 2019). But thermoelectric generators utilize temperature difference between the entire body and ambient air that leads to the necessity to implant one part of the generator very close to the skin.

Generators based on the use of the mechanical energy of organs, tissues, and liquids include a very wide range of different approaches (see Fig. 20.1). Usually, such generators do not influence metabolism or other biological processes in the organism for energy generation, instead of the harvesting energy. As a thermoelectric generator, they produce low energy output but can be discussed as a somehow stable generator in comparison with biofuel cells.

Next, we will focus on biofuel cells due to the possibility of its combination with biosensors and discuss perspective electroconductive materials and finally describe the possible concepts of electricity generation systems to enhance power output and thus decrease energy limitation for different implantable devices.

20.2 Electroconductive Materials for Biofuel Cells Electrodes

Today the field of nanotechnology has become an integral part of biofuel cells as an applied science. Different nanomaterials are used to modify the biotic–abiotic interface for better direct bioelectrocatalysis. Since practicality is important for medical applications, implantable enzymatic biofuel cells must operate without a classical separator between anodic and cathodic chambers containing oxygen. So there are three general requirements for biofuel cell electrodes: biocompatibility, high specific surface area, high level of adhesion and penetration of cells and enzymes into the volume of material. Considering these conditions, there is a huge variety of carbon-based nanomaterials such as carbon nanotubes (CNT), CNT sponges, carbon nanodots (CND), 3D graphene, graphene oxide (GO) nanosheets, etc. (Ji et al. 2020; Huang et al. 2020). However, in the scientific literature at the moment, there is no clear understanding of the pharmacokinetics of nanodispersed carbon in the body, especially for long periods of stay in the body—the fact is that nanosized particles are not detected by the immune system, freely pass through cell membranes, and are not excreted during natural metabolism. Because of this and also to make flexible devices, a wide diversity of nanomaterials such as gold nanoparticles

and different composite fillers for porous polymer systems has been extensively utilized in the development of improved bioelectrodes.

Carbon materials are mostly biocompatible and own superior conductivity and good mechano-thermal stability (Reshetilov et al. 2017a, b). Moreover, they are considered as a good tool for electron transmission and electrical wiring promotion of enzymes due to their high specific surface area (Reshetilov et al. 2017b). Lately, buckypaper continues to be explored in a broad spectrum of applications. It is a thin film-like structure that consists of a CNT grid cluster. Buckypaper possesses the characteristics of flexibility, lightweight, and ease of processing. The scope of application includes the fabrication of electrodes for sensors, biofuel cells, supercapacitors, etc., although loose films of Buckypaper are quite fragile and complex to be modified.

Carbon nanodots have a discrete and quasispherical shape. CND are characterized by the large specific surface area and outstanding adsorption capacity. CND efficiently acted as electron senders and promoted the electron transfer process. Eventually, the enzymatic biofuel cells resulted in maximum power output as high as 40.8 mWcm^{-2} at 0.41 V with the open circuit potentials of 0.93 V (Babadi et al. 2016).

Self-assembly of GO nanosheets has been widely applied to prepare monolithic 3D graphene structures. For example, 3D graphene hydrogel has been prepared through the one-step hydrothermal treatment of GO suspension (Kang et al. 2019). GO nanosheets are finely dispersed owing to the electrostatic repulsions from the functional groups in a stable GO suspension (Liu et al. 2018).

Sensor materials meet differences from electrode materials property set: at the present level of sensor technology, the use of sensors with high porosity is not so necessary, more important is the affinity for a detectable molecule (Qiu et al. 2017). So, a significant part of the biosensor research area is made up of polymer devices that sense and transmit information about a biological process, like blood pressure or individual physiological parameters. Long-term applicable biosensors should induce minimal damage in contact with tissues and maintain full functionality. Thus, biocompatibility and anti-fouling are essential requirements for the sensor materials. Depending on the intended application device, lifetimes vary from a couple of minutes to several months. Polymeric materials are extensively studied as coating layers due to its non-toxicity and non-inflammatory properties. In the literature, plenty of sensor types using different composite or polymer-based materials with diverse architecture and morphology are presented. For instance, a nanopolytetrafluoroethylene (PTFE) film was used as triboelectric layer in an endocardial pressure sensor. The device showed fine results during *in vitro* and *in vivo* experiments, good blood compatibility, and long-time reliability (Babadi et al. 2016). Another polymer cardiac monitoring system was based on triboelectric layer-contained nanostructured PTFE also. Biocompatible, hermetic, and flexible pack for the device was obtained employing PTFE, polydimethylsiloxane (PDMS), and parylene. The cardiac sensor was successfully implanted in a male adult Yorkshire porcine model which demonstrated good results in blood pressure monitoring and long-time reliability (Mansouri et al. 2017).

It should be noted that a key requirement for a reference electrode in flexible biosensors is the ability to maintain a constant potential under mechanical tension (Gong and Cheng 2017). A commercial approach to creating a flexible electrode is to coat commonly used polymer substrate (PTFE, PDMS) with a layer of Ag/AgCl by screen printing or drop-casting (Nyein et al. 2016). PDMS with percolation networks of AU-based nanomaterials (nanowires and nanotubes) on the surface is used for fabricating flexible electrochemical biosensors due to its good stretchability. The increase in resistance is 47% at 50% tension (Jeerapan et al. 2016; Liu et al. 2016; Xuan et al. 2018). Another method is to cover the surface of the base electrode with a layer of silver with further chlorination. The disadvantage of these electrodes is that slight displacement of the potential might occur (about 80 mV) (Zheng et al. 2014).

In a study, Nasar and Perveen (2019) designed a flexible respiratory sensor based on a PDMS film. The biosensor was implanted into the left chest skin of rats for an *in vivo* experiment, which revealed a high correlation between breathing rate and a number of “paired peak groups.”

Polyvinylidene fluoride (PVDF) films encapsulated by polyimide (PI) were used as blood pressure sensors in an ascending aorta of a male domestic porcine (Qiu et al. 2017). After adopting the design, the present sensor was utilized as a real-time blood pressure monitoring system (Liu et al. 2018). To monitor bladder pressure, the device based on PDMS sponge fixed between flexible polyvinylchloride and polyethylene terephthalate sheets was used (Zheng et al. 2016).

Electroconductive poly-(3,4-ethylene dioxythiophene) poly-styrene sulfonate (PEDOT PSS) is widely used as an implantable material. In the paper, Gotovtsev et al. (2019) presented 3D structure material that can be biocompatible and showing conductivity close to 0,01 S/cm.

Ion-selective membranes are used to obtain a good selectivity and quick response. Depending on the target, different materials can be utilized to fabricate the ion-selective membrane, that is, polyaniline suitable for pH detecting, poly (vinyl chloride) in the mixture with Na-ionophore can be employed as the Na⁺ selective membrane (Zhang et al. 2015; Cheng et al. 2016).

The literature provides information on the use of polyurethane, polyethylene glycol (PEG), and zwitterionic polymers in fabricating biosensors (Jin et al. 2017; Hassani et al. 2018; Solaimuthu et al. 2020).

As mentioned above, there is a huge variety of different approaches for electrode materials for bioelectrochemical biosensors and BFC. From carbon nanomaterials to the conductive polymeric systems, everything is under consideration now. The main focus of the research is to enhance the conductive properties of the material with respect to the effective immobilization of sensing enzymes and biocompatibility.

20.3 Self-Powered Biosensors Approaches

The main basis of many of the self-powered biosensors is the bioelectrochemical process—the electricity generates via bioelectrochemical reactions and the next current and/or voltage measuring. The value of current and/or voltage corresponds to the concentration of measuring substances. This can be both single-enzyme systems and multienzyme systems (Grattieri and Minteer 2018).

Today, the most common biosensors are glucose sensors (Fang et al. 2017; Oh et al. 2018). They are widely used for diabetes monitoring (Dautta et al. 2020; Bennett and Leech 2020). Examples of using sensors combining with drug delivery systems are presented in the literature (Rahimi et al. 2017). Lee et al. (2017) developed a device consisting of an ultra-thin and flexible substrate that incorporates sensors for glucose concentration, temperature, humidity, and pH. It also includes microneedle arrays for controlled drug delivery. The working electrode is made of Au and modified with a mixture of glucose oxidase enzyme, chitosan, graphene, and bovine serum albumin. This system permits the detection of glucose in the concentration range from 10 μ M to 1 mM.

Also, an interesting combination of sensors can be electrical generation sensing combined with electrical consumption sensing in case of enough energy availability (Zhou and Dong 2011). Such flexible monitoring devices were presented in several publications (Gao et al. 2016; Wang et al. 2017). The biosensor can detect glucose, lactose, and electrolytes (K^+ , Na^+) in perspiration (Gao et al. 2016). Enzymes are used for metabolites detection and ion-selective electrodes for electrolytes. Enzymatic sensors are also based on Au-electrode coated with a mixture of chitosan, single-walled carbon nanotubes, and enzymes (glucose and lactose oxidases).

The cascades of bioelectrochemical reactions can be built in the logic circuit that can be used for preliminary control of biosensor applications (Katz 2015; Grattieri and Minteer 2018). This approach can lead to decreasing the energy consumption of the whole system.

As mentioned, the above combination of different sensors in one device can be an effective platform for health monitoring, but such a platform requires flexibility in terms of power supply and effective power supply approach. Figure 20.2 illustrates the concept of such a flexible system. To stabilize energy generation, there are several different generators used: BFC as the most powerful and others like thermoelectric as more stable and do not influence the metabolism. Control unit consists of two subunits: one provides data transfer and the second one provides energy management. Basic principles and some technical ideas are already under study for different applications like the Internet of Things systems (Gotovtsev and Dyakov 2016), and today additional research to transfer such approaches to the implantable devices is required. It is necessary to mention that some research in the field of ultra-low-power electronics is already done (Sarpeshkar 2013). Those systems can operate with low currents and voltages with appropriate energy efficiency.

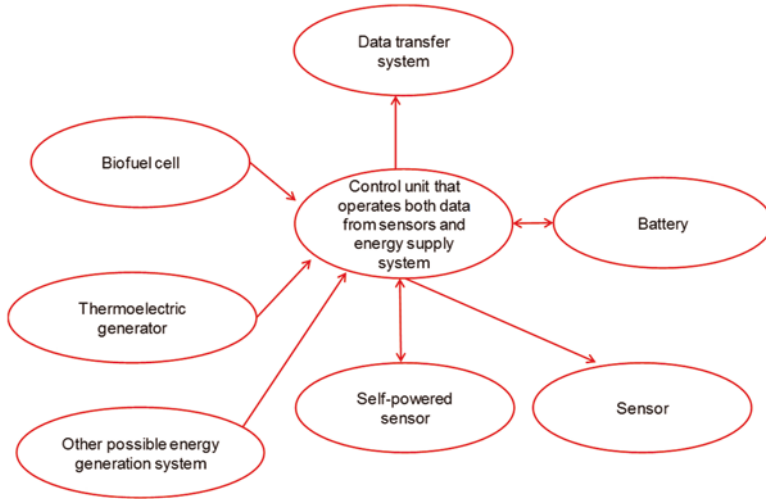


Fig. 20.2 Concept of multigenerators and multisensors system

20.4 Conclusion

Self-power implantable systems are actively developing today. There are a number of different possible applications and different approaches. In this chapter, we focused on the electrode material part of the research and some perspective concepts. From a material science point of view, there is a huge variety of materials in order to develop electrodes for bioelectrochemical systems. Different research groups try different approaches, and all of them have some perspective and efficiency.

Finally, it can be said that a combination of different sensors and generators can be the perspective approach for further research.

Acknowledgments This work was supported by RFBR in the form of research project No. 18-29-23024mk.

References

- Amar AB, Kouki AB, Cao H (2015) Power approaches for implantable medical devices. *Sensors (Basel)* 15:28889–28914. <https://doi.org/10.3390/s151128889>
- Babadi AA, Bagheri S, Hamid SBA (2016) Progress on implantable biofuel cell: nano-carbon functionalization for enzyme immobilization enhancement. *Biosens Bioelectron* 79:850e60. <https://doi.org/10.1016/j.bios.2016.01.016>
- Bennett R, Leech D (2020) Improved operational stability of mediated glucose enzyme electrodes for operation in human physiological solutions. *Bioelectrochemistry* 133:107460

- Cheng X, Xue X, Ma Y, Han M, Zhang W, Xu Z, Zhang H, Zhang H (2016) Implantable and self-powered blood pressure monitoring based on a piezoelectric thinfilm: simulated, in vitro and in vivo studies. *Nano Energy* 22:453–460
- Clement RGE, Bugler KE, Oliver CW (2011) Bionic prosthetic hands: a review of present technology and future aspirations. *Surgeon* 9:336–340. <https://doi.org/10.1016/J.SURGE.2011.06.001>
- Cosnier S, Le Goff A, Holzinger M (2014) Towards glucose biofuel cells implanted in human body for powering artificial organs: review. *Electrochem Commun* 38:19–23. <https://doi.org/10.1016/j.elecom.2013.09.021>
- Dagdeviren C, Li Z, Wang ZL (2017) Energy harvesting from the animal/human body for self-powered electronics. *Ann Rev Biomed Eng* 19:85–108. <https://doi.org/10.1146/annurev-bioeng-071516>
- Dautta M, Alshetaiwi M, Escobar J, Tseng P (2020) Passive and wireless, implantable glucose sensing with phenylboronic acid hydrogel-interlayer RF resonators. *Biosens Bioelectron* 151:112004
- Fan F-R, Tian Z-Q, Lin WZ (2012) Flexible triboelectric generator. *Nano Energy* 1:328–334. <https://doi.org/10.1016/j.nanoen.2012.01.004>
- Fang L, Liang B, Yang G, Hu Y, Zhu Q, Ye X (2017) A needle-type glucose biosensor based on PANI nanofibers and PU/E-PU membrane for long-term invasive continuous monitoring. *Biosens Bioelectron* 97:196–202
- Gao W, Emaminejad S, Nyein HYY, Challa S, Chen K, Peck A, Fahad HM, Ota H, Shiraki H, Kiriya D, Lien D-H, Brooks GA, Davis RW, Javey A (2016) Fully integrated wearable sensor arrays for multiplexed in situ perspiration analysis. *Nature* 529:509–514
- Gong S, Cheng W (2017) One-dimensional nanomaterials for soft electronics. *Adv Electron Mater* 3:1600314
- Gotovtsev PM, Dyakov AV (2016) Biotechnology and internet of things for green smart city application. In: 2016 IEEE 3rd world forum internet things, IEEE, p 542–546. <https://doi.org/10.1109/WF-IoT.2016.7845476>
- Gotovtsev P, Vorobiev V, Migalev A, Badranova G, Gorin K, Dyakov A, Reshetilov A (2018) Bioenergy based power sources for mobile autonomous robots. *Robotics* 7:2–18. <https://doi.org/10.3390/ROBOTICS7010002>
- Gotovtsev PM, Badranova GU, Zubavichus YV, Chumakov NK, Antipova CG, Kamyshinsky RA, Presniakov MY, Tokaev KV, Grigoriev TE (2019) Electroconductive PEDOT:PSS-based hydrogel prepared by freezing-thawing method. *Heliyon* 5:e02498. <https://doi.org/10.1016/J.HELİYON.2019.E02498>
- Grattieri M, Minter SD (2018) Self-powered biosensors. *ACS Sens* 3:44–53. <https://doi.org/10.1021/acssensors.7b00818>
- Halámková L, Halámek J, Bocharova V, Szczupak A, Alfonta L, Katz E (2012) Implanted bio-fuel cell operating in a living snail. *J Am Chem Soc* 134:5040–5043. <https://doi.org/10.1021/ja211714w>
- Hassani FA, Mogan RP, Gammad GG, Wang H, Yen S-C, Thakor N, Lee C (2018) Toward self-control systems for neurogenic underactive bladder: a triboelectric nanogenerator sensor integrated with a bistable micro-actuator. *ACS Nano* 12:3487–3501
- Huang H, Li T, Jiang M, Wei C, Ma S, Chen D, Tong W, Huang X (2020) Construction of flexible enzymatic electrode based on gradient hollow fiber membrane and multi-wall carbon tubes meshes. *Biosens Bioelectron* 152:112001
- Jandial R, Hoshide R (2017) Bionic-brain: controlling a prosthetic hand. *World Neurosurg* 105:980–982. <https://doi.org/10.1016/j.wneu.2017.07.092>
- Jeeran I, Sempionatto JR, Pavinatto A, You J-M, Wang J (2016) Stretchable biofuel cells as wearable textile-based self-powered sensors. *J Mater Chem* 4(47):18342–18353
- Ji J, Woo J, Chung Y, Joo SH, Kwon Y (2020) Membraneless enzymatic biofuel cells using iron and cobalt co-doped ordered mesoporous porphyrinic carbon based catalyst. *Appl Surf Sci* 511:145449

- Jin Z-H, Liu Y-L, Chen J-J, Cai S-L, Xu J-Q, Huang W-H (2017) Conductive polymer-coated carbon nanotubes to construct stretchable and transparent electrochemical sensors. *Anal Chem* 89(3):2032–2038
- Joung YH (2013) Development of implantable medical devices: from an engineering perspective. *Int Neurorol J* 17:98–106. <https://doi.org/10.5213/inj.2013.17.3.98>
- Kang Z, Zhang Y-HPJ, Zhu Z (2019) A shriveled rectangular carbon tube with the concave surface for high-performance enzymatic glucose/O₂ biofuel cells. *Biosens Bioelectron* 132:76e83. <https://doi.org/10.1016/j.bios.2019.02.044>
- Karakiozaki V, Karagiannidis PG, Gioti M, Kavatzikidou P, Georgiou D, Georarakis E, Logothetidis S (2013) Bioelectronics meets nanomedicine for cardiovascular implants: PEDOT-based nanocoatings for tissue regeneration. *Biochim Biophys Acta* 1830:4294–4304. <https://doi.org/10.1016/j.bbagen.2012.12.019>
- Katz E (2015) Biocomputing – tools, aims, perspectives. *Curr Opin Biotechnol* 34:202–208. <https://doi.org/10.1016/j.copbio.2015.02.011>
- Kay S, Wilks D (2015) Bionic hand transplantation: linking the cortex to the hand. *Lancet* 385:2130–2132. [https://doi.org/10.1016/S0140-6736\(14\)61989-9](https://doi.org/10.1016/S0140-6736(14)61989-9)
- Ko WH (2012) Early history and challenges of implantable electronics. *ACM J Emerg Technol Comput Syst* 8: <https://doi.org/10.1145/2180878.2180880>
- Koch J, Schuettler M, Pasluosta C, Stieglitz T (2019) Electrical connectors for neural implants: design, state of the art and future challenges of an underestimated component, *J Neural Eng* <https://doi.org/10.1088/1741-2552/ab36df>
- Korth B, Rosa LFM, Harnisch F, Picioreanu C (2015) A framework for modeling electroactive microbial biofilms performing direct electron transfer. *Bioelectrochemistry* 106:194–206. <https://doi.org/10.1016/j.bioelechem.2015.03.010>
- Lee H, Song C, Hong YS, Kim MS, Cho HR, Kang T, Shin K, Choi SH, Hyeon T, Kim D-H (2017) Wearable/disposable sweat-based glucose monitoring device with multistage transdermal drug delivery module. *Sci Adv* 3:e1601314
- Li K, Cheng X, Zhu F, Li L, Xie Z, Luan H, Wang Z, Ji Z, Wang H, Liu F, Xue Y, Jiang C, Feng X, Li L, Rogers JA, Huang Y, Zhang Y (2019) A generic soft encapsulation strategy for stretchable electronics. *Adv Funct Mater* 29:1806630. <https://doi.org/10.1002/adfm.201806630>
- Liu YL, Jin ZH, Liu YH, Hu XB, Qin Y, Xu JQ, Fan CF, Huang WH (2016) Stretchable electrochemical sensor for real-time monitoring of cells and tissues. *Angew Chem Int Ed* 55(14):4537–4541
- Liu Z, Ma Y, Ouyang H et al (2018) Transcatheter self-powered ultrasensitive endocardial pressure sensor. *Adv Funct Mater* 29:1807560
- Lv J, Jeeran I, Tehrani F, Yin L, Silva-Lopez CA, Jang J-H, Joshua D, Shah R, Liang Y, Xie L, Soto F, Chen C, Karshalev E, Kong C, Yang Z, Wang J (2018) Sweat-based wearable energy harvesting-storage hybrid textile devices. *Energy Environ Sci* 11:3431–3442. <https://doi.org/10.1039/C8EE02792G>
- Mano N, De Poulpique A (2018) O₂ reduction in enzymatic biofuel cells. *Chem Rev* 118:2392–2468. <https://doi.org/10.1021/acs.chemrev.7b00220>
- Mansouri N, Babadi AA, Bagheri S, Hamid SBA (2017) Immobilization of glucose oxidase on 3D graphene thin film: novel glucose bioanalytical sensing platform. *Int J Hydrog Energy* 42:1337e43. <https://doi.org/10.1016/j.ijhydene.2016.10.002>
- Meng E, Sheybani R (2014) Insight: implantable medical devices. *Lab Chip* 14:3233–3240. <https://doi.org/10.1039/c4lc00127c>
- Musk E (2019) An integrated brain-machine interface platform with thousands of channels. *J Med Internet Res* 21(10):e16194
- Nasar A, Perveen R (2019) Applications of enzymatic biofuel cells in bioelectronic devices. A review. *Hydrogen Energy* 44:15287–15312
- Nyein HYY, Gao W, Shahpar Z, Emaminejad S, Challa S, Chen K, Fahad HM, Tai L-C, Ota H, Davis RW (2016) A wearable electrochemical platform for noninvasive simultaneous monitoring of Ca²⁺ and pH. *ACS Nano* 10(7):7216–7224

- Oh SY, Hong SY, Jeong YR, Yun J, Park H, Jin SW, Lee G, Oh JH, Lee H, Lee S-S (2018) Skin-attachable, stretchable electrochemical sweat sensor for glucose and pH detection. *ACS Appl Mater Interfaces* 10(16):13729–13740
- Pankratova G, Gorton L (2017) Electrochemical communication between living cells and conductive surfaces. *Curr Opin Electrochem* 5:193–202. <https://doi.org/10.1016/j.coelec.2017.09.013>
- Qiu H-J, Guan Y, Luo P, Wang Y (2017) Recent advance in fabricating monolithic 3D porous graphene and their applications in biosensing and biofuel cells. *Biosens Bioelectron* 89:85–95
- Rahimi R, Ochoa M, Tamayol A, Khalili S, Khademhosseini A, Ziaie B (2017) Highly stretchable potentiometric pH sensor fabricated via laser carbonization and machining of carbon-polyaniline composite. *ACS Appl Mater Interfaces* 9(10):9015–9023
- Rapoport BI, Kedzierski JT, Sarpeshkar R (2012) A glucose fuel cell for implantable brain-machine interfaces. *PLoS One* 7:e38436. <https://doi.org/10.1371/journal.pone.0038436>
- Rasmussen M, Abdellaoui S, Minter SD (2015) Enzymatic biofuel cells: 30 years of critical advancements. *Biosens Bioelectron* <https://doi.org/10.1016/j.bios.2015.06.029>
- Reshetilov AN, Plekhanova JV, Tarasov SE, Bykov AG, Gutorov MA, Alferov SV, Tenchurin TK, Chvalun SN, Orekhov AS, Shepelev AD, Gotovtsev PM, Vasilov RG (2017a) Evaluation properties of bioelectrodes based on carbon superfine materials containing model microorganisms *Gluconobacter*. *Nanotechnol Russia* 12:107–115. <https://doi.org/10.1134/S1995078017010098>
- Reshetilov AN, Plekhanova YV, Tarasov SE, Arlyapov VA, Kolesov VV, Gutorov MA, Gotovtsev PM, Vasilov RG (2017b) Effect of some carbon nanomaterials on ethanol oxidation by *Gluconobacter oxydans* bacterial cells. *Appl Biochem Microbiol* 53:123–129. <https://doi.org/10.1134/S0003683817010161>
- Rizea RE, Gheorghita KL, David G, Ciurea AV (2019) Neuromodulation devices nowadays. *Rom Neurosurg* 33:31–33. <https://doi.org/10.33962/roneuro-2019-005>
- Sarpeshkar R (2013) Ultra energy efficient systems in biology, engineering, and medicine. In: 2013 Third Berkeley symposium on energy efficient electronic systems, IEEE, p 1–1. <https://doi.org/10.1109/E3S.2013.6705873>
- Schold CS, Wasserstrom WR, Fleisher M, Schwartz MK, Posner JB (1980) Cerebrospinal fluid biochemical markers of central nervous system metastases. *Ann Neurol* 8:597–604. <https://doi.org/10.1002/ana.410080609>
- Solaimuthu A, Vijayan AN, Murali P, Korrapati PS (2020) Nano-biosensors and their relevance in tissue engineering. *Curr Opin Biomed Eng* 13:84–93
- Vostrikov S, Somov A, Gotovtsev P (2019) Low temperature gradient thermoelectric generator: modelling and experimental verification. *Appl Energy* 255:113786. <https://doi.org/10.1016/J.APENERGY.2019.113786>
- Wang S, Wu Y, Gu Y, Li T, Luo H, Li L-H, Bai Y, Li L, Liu L, Cao Y (2017) Wearable sweatband sensor platform based on gold nanodendrite array as efficient solid contact of ion-selective electrode. *Anal Chem* 89(19):10224–10231
- Whitehead WE (2019) Cerebrospinal fluid shunting. In: *Cerebrospinal Fluid Disorders*. Springer, Cham, pp 281–295. https://doi.org/10.1007/978-3-319-97928-1_16
- Xuan X, Yoon HS, Park JY (2018) A wearable electrochemical glucose sensor based on simple and low-cost fabrication supported micro-patterned reduced graphene oxide nanocomposite electrode on flexible substrate. *Biosens Bioelectron* 109:75e82
- Zebda A, Cosnier S, Alcaraz J-P, Holzinger M, Le Goff A, Gondran C, Boucher F, Giroud F, Gorgy K, Lamraoui H, Cinquin P (2013) Single glucose biofuel cells implanted in rats power electronic devices. *Sci Rep* 3:1516. <https://doi.org/10.1038/srep01516>
- Zhang H, Zhang XS, Cheng XL et al (2015) A flexible and implantable piezoelectric generator harvesting energy from the pulsation of ascending aorta: in vitro and in vivo studies. *Nano Energy* 12:296–304
- Zhao Z, Li X, He F, Wei X, Lin S, Xie C (2019) Parallel, minimally-invasive implantation of ultra-flexible neural electrode arrays. *J Neural Eng* 16:035001. <https://doi.org/10.1088/1741-2552/ab05b6>

- Zheng Q, Shi BJ, Fan FR et al (2014) In vivo powering of pacemaker by breathing- driven implanted triboelectric nanogenerator. *Adv Mater* 26:5851–5856
- Zheng Q, Zhang H, Shi BJ et al (2016) In vivo self-powered wireless cardiac monitoring via implantable triboelectric nanogenerator. *ACS Nano* 10:6510–6518
- Zhou M, Dong S (2011) Bioelectrochemical interface engineering: toward the fabrication of electrochemical biosensors, biofuel cells, and self-powered logic biosensors. *Acc Chem Res* 44:1232–1243. <https://doi.org/10.1021/ar200096g>

Index

A

Acetylcholine, 390, 391
Acetylcholinesterase, 39, 41–43
AChE-biotest, 41–43
Acoustic biosensors, 95
Activity, 19–33, 241, 245, 253–255
Aflatoxin B1 (AFB1), 216–223
Aflatoxin M1 (AFM1), 219, 221
Agglomerates, 167
Alkaloids, 49
Allelopathy, 51
Allium test, 44
Amperometric, 99
Amperometric biosensor, 213–223
Amplification procedures, 161
Analytical characteristics, 178, 180, 187
Anode, 327–336, 338, 340, 341, 343–345, 348
Anthracycline drugs, 204, 205
Antibiotic-resistant, 22, 24, 25
Antibody (Ab), 63, 64, 66, 69, 70, 97, 99, 101, 105, 107, 108, 110, 111, 117–127, 179, 181–186, 188
Antigen (Ag), 63, 65, 68, 70, 179, 181–186, 188
Aptamer, 389, 390, 392
Aptasensor, 221–223
Artificial, 59
Atomic, 59, 117–127
Atomic force microscopy (AFM), 59, 62–70, 120–126

B

Bacteria, 21, 22, 24, 58–63, 67, 75–87
Bactericidal, 21–25, 27, 28, 33
Bacteriophages, 98, 99, 102, 105, 107, 108, 111, 112
Bioanalytical, 78, 79
Biocathodes, 331
Biochemical oxygen demand (BOD), 391
Biochip, 4
Biocompatibility, 278
Biocompatible, 401, 402
Bioelectrocatalysis, 332–336, 400
Bioelectrochemical technologies, 327, 340
Bioenergy, 340
Biofilm, 21
Biofuel cell, 5, 9, 327, 334–336, 338, 339, 344–346, 382, 387–390
Biofuel element, 327, 342, 345
Biofuel systems, 3
Biological fluids, 267, 273, 278
Biological fuel cells (BFCs), 326
Biological samples, 136–154
Bioluminescence, 250
Biosafety, 50, 51
Biosensor, 5–10, 12, 98–112, 178, 179, 183, 186–188, 214–219, 221, 223, 233, 234, 241, 381–392
Biosensor array chips, 306, 310, 311, 313
Biotin-streptavidin interaction-based systems, 164
Blood glucose, 266–268, 272, 274, 277, 280
Blood pressure monitoring, 367
Butyrylcholinesterase (BChE), 75, 76

C

Cantilever sensor, 109–111
Capillary action, 291–293, 295, 303, 306, 309, 310, 313
Carbon-based nanomaterials, 400
Carbon nanotubes, 217–219, 275
Cardiac monitoring system, 401
Catecholamines and their metabolites, 136, 137, 142–147, 149
Catecholamines-dependent diseases, 133–154
Cell, 57–70
Charge transfer complexes, 149–153
Chip, 9, 11
Cholinesterase, 244
Chromatographic, 267
Colloidal, 75
Colorimetric biosensors, 103
Columnar electrode structure, 309
Commercial devices, 272
Components, 59
Conductometric sensors, 99
Continuous bonding method, 296
Conversion, 326, 327, 342
COVID-19, 120, 126
Cyanobacteria, 253, 254
Cyclic voltammetry (CV), 181–184

D

Densitometric biosensors, 103
Detection, 58–60, 67, 68, 70, 77–81, 83–87, 179–185, 239–256
Detection of analytes, 358, 374
Determination, 177–188, 241, 245, 249, 253, 255
Diabetes, 266, 268
Diagnostic, 133–154, 228–236
Diagnostic plate, 229–231
Disposable biosensor chip, 302
DNA damage, 200, 204
Dopamine, 40
Doxorubicin, 204–207
Drugs, 177–188

E

Electroactive polymers, 196, 197, 206
Electrochemical, 382, 384, 388, 389
Electrochemical biosensors, 267, 268
Electrochemical impedance spectroscopy (EIS), 181–184, 187
Electrochemical sensor, 357
Electroconductive, 400–402

Electroconductive polymers, 196, 197
Electrode, 180–187
Electronic skin, 375
Electropolymerization, 195–199, 202, 204, 205, 208
Electrostatic accumulation, 202
Elodea leaf, 46
Encapsulated, 228–233, 236
Energy sources, 382
Enhancement approaches, 161
Environmental, 249, 253, 256
Environmental-friendly biosensor chip, 300, 301, 313
Enzymatic signal amplification method, 164
Enzyme, 83–85, 214, 216–221, 223, 226–236, 241, 242, 244, 245, 255, 327, 328, 332, 334, 336, 343–345, 348
Enzyme biofuels cells, 399
Enzyme fuel cells (EFCs), 326
Eserin, 42
Ethanol, 388
Europium (III), 141, 142

F

Field-effect transistor (FET), 4, 5, 7–9
Films, 117–127
Fish electric organs, 43
Flexible devices, 359, 360, 364, 367–369, 372
Fluorescence, 250, 253–255
Fluorescent derivatives, 137–139, 141, 144
Fluorimetric, 135–154
Fluorometric, 133–154
Folding method, 296–298, 303, 304
Food analysis, 358, 370
Force, 59, 117–127
Fragments, 59, 62–65, 67–70
Fungicidal, 19–33

G

Generators, 398–400, 404
Glassy carbon electrode, 205–207
Glucose, 383, 384, 386, 387, 390, 392
Glucose detection, 267, 268
Glucose in blood, 266, 272, 276, 277, 279
Glucose oxidase (GOD), 5–12
Glucose sensors, 369, 370
Glycated albumin (GA), 85, 86
Gold nanoparticles, 161, 174, 175
Gold nanospheres (GNSs), 165
Gradient lateral flow immunoassay, 161, 175
Graphene, 359–363, 368, 373

H

Health monitoring, 358, 360, 361, 364, 374
Heart rate monitoring, 364, 365
Heavy water, 45
Hierarchical gold nanoparticles, 169
Horseradish peroxidase (HRP), 217, 220–223
Human activity, 357, 359
Hydrolysis, 241, 245

I

Immobilization, 201–204
Immobilized, 256, 257
Immunoassay, 214, 219–222
Immunomodulating, 19–33
Immunosensor, 99, 177–188, 214, 215, 220–223
Implantable biosensors, 397–404
Implantable energy generators, 398
Implantable medical devices (IMD), 326, 342–346
Implants, 20, 21, 23, 33
Infections, 21–23, 25, 26, 28, 33
Inhibitors, 241, 245, 255
Intellectual property (IP), 286, 294, 304
Invasive techniques, 266

L

Label, 180–182, 185, 188, 220, 221, 223
Label-free, 78–80, 82, 85
Lactate, 387–389
Lactate sensor, 370, 371
Langmuir, 117–127
Lateral flow immunoassay (LFIA), 162
Limit, 58
Limit of detection (LOD), 275
Linear detection range, 275, 276
Liver mitochondrial homogenate, 39
Low limit of detection (LOD), 181–186, 276

M

Macrosensors, 5
MAO-biotest, 39–41
Mediator, 327, 328, 330, 332, 333, 336, 346
Medicine, 20, 22, 23, 25, 33, 381–392
Metal complexes, 141, 142
Metal-dependent, 142–146, 154
Metal-enhanced fluorescence, 145
Metal nanoparticles, 276
Methotrexate, 44
Methylene blue, 198, 199, 205–207

Methylene green, 198, 199, 206, 207
Microbial fuel cells (MFCs), 326, 330, 391
Microdiagnosticum, 228–235
Microorganisms, 326–328, 330–332, 340, 341, 343, 344, 348
Microscopy, 58, 59, 62, 117–127
Microspores, 49, 50
Microwave resonator, 109, 111
Minimally-invasive blood sampling, 302
Molecular electronics, 4
Monitoring, 133–154
Monoamine oxidase (MAO), 39
Monolayer, 123, 124
Multi-channel, 6
Multiple uses, 230, 231
Multi-range gradient LFIA, 165, 171, 172
Multiwalled carbon nanotubes (MWCNTs), 7
Mycotoxin, 213–223

N

Nano, 19–33
Nanobiochip, 6
Nanomaterials, 178–181, 186–188, 267, 274–276, 279, 359, 361, 383
Nanoparticles (NPs), 22–25, 27, 29–31, 33, 77, 79, 80, 82, 180–188, 255, 275, 276, 279
Nanosensors, 3–14
Nanostructured, 179, 180, 186, 187
Nanotechnology, 22, 25, 33, 400
Nanowire, 9, 11
Needle-integrated biosensor chip, 303–305, 307, 309
Neostigmine, 42, 48–50
Neurotransmitter exchange, 135
Neutral red, 198, 199, 206, 208
Non-invasive, 278–280
Non-invasive methods, 358, 360, 369–371, 373
Nose, 59, 61–62

O

Ochratoxin A (OTA), 217, 218, 221–223
Optical fiber sensors, 103
Optical sensors, 102
Organic, 57
Organophosphorus compounds (OPC), 242, 244, 245, 249–256
Oxidation process, 328, 333
Oxytetracycline, 141, 143
Ozone, 49

P

- Package-free biosensor chips, 300, 301
- Parameters, 267, 274, 276, 279
- Pathogens, 62, 70
- Peacemakers, 398
- Peroxides, 49
- Pesticides, 241, 244, 254
- Photobacteria, 252
- Photocatalytic needle, 304
- Photon-based lithography, 360
- pH sensor, 371, 372
- Piezoelectric resonators, 107
- Planar technology, 6, 10
- Plate acoustic wave, 107
- Platform chip designs, 310
- Platform patent map, 286–313
- Point-of-care, 137
- Polyallylamine (PAH), 230, 231
- Polyaniline (PANI), 196, 197, 204–207
- Polydimethylsiloxane (PDMS), 357, 359, 362, 363, 365, 368
- Polyelectrolyte microcapsules (PMC), 227–231, 233–235
- Polyelectrolytes, 117–127
- Poly(3,4-ethylenedioxythiophene) polystyrene sulfonate (PEDOT:PSS), 7, 8
- Polymers, 121, 124
- Polypyrrole, 196, 197, 204
- Polystyrenesulfonate (PSS), 230, 231
- Polythiophene, 196, 197
- Potentiometric biosensor, 233, 234
- Potentiometric sensors, 99
- Power, 381, 382, 384, 386–390, 392
- Principal component analysis (PCA), 78, 82, 86
- Procalcitonin, 161–173
- Pulse oxygenation device, 368, 369

Q

- Quantum dots, 163, 168

R

- Raman, C.V., 77, 81, 83–87
- Redox reactions, 332
- Refractometric biosensors, 103
- Respiration rate, 360, 365–367, 373, 375
- Response time, 275

S

- Screen printing, 300
- Sedimentation, 231
- Self-assembly, 401
- Self-monitoring of blood glucose (SMBG), 286–313
- Self-powered, 381–392, 403
- Sensor, 227, 228, 230, 234
- Sensor systems, 133–154
- Sepsis, 161–173
- Serotonin, 39, 40
- Silver, 77–80, 82–87
- Silver enhancement method, 166, 169
- Simultaneous multiplex determination, 153
- Smart watches, 359
- Solid-phase, 142–146
- Spectra, 78, 79, 81, 82, 84–87
- Surface, 19–33, 122–124, 180–188
- Surface-enhanced Raman scattering/spectroscopy (SERS), 75–87, 133–154, 168
- Surface plasmon resonance (SPR), 103, 104
- Sustainable mass production, 286–313
- Sweat sensors, 358, 371

T

- Targeted molecules, 357, 359
- Tear Sensors, 357, 359, 370, 371, 375
- Therapeutic applications, 372, 373
- Thermal sensors, 361, 362, 364, 365
- Thermoelectric generators, 398, 400
- Thiocholine, 83–85
- 3D assembling, 295
- Thrombin, 389
- Tissue bioindicators, 39
- Tissue biosensor, 38, 39
- Tissue sections, 38
- Toxicity, 241, 250, 252
- Tradescantia* stamen filament cells, 46
- Traditional methods, 274
- Transparent biosensor chip, 295, 301
- Tryptamine, 39, 40
- Tuberculosis (TB), 22, 24–28, 30
- Turbidimetric biosensors, 103
- Tyramine, 39, 40
- Tyrosinase, 218–220

U

Urease, 226, 228–236

User-friendly biosensor chip, 301, 302, 304, 313

VViral particles, 96, 98, 102, 105, 107, 110,
111, 113

Virus, 80, 81, 118–123, 125, 126

Virus detection, 95–113

Volatile, 57, 71

Volatile organic components (VOCs), 60, 69

WWastewater treatment, 326,
339, 340

Wearable, 384, 387, 388, 392

Wearable devices, 357–362,
364–366, 371–374**Z**Zearalenone (ZEN), 218,
220, 223